



UNIVERSITAT<sub>DE</sub>  
BARCELONA

## Exploring adamantine-like scaffolds for a wide range of therapeutic targets

Elena Valverde Murillo



Aquesta tesi doctoral està subjecta a la llicència **Reconeixement- Compartiqual 3.0. Espanya de Creative Commons.**

Esta tesis doctoral está sujeta a la licencia **Reconocimiento - Compartiqual 3.0. España de Creative Commons.**

This doctoral thesis is licensed under the **Creative Commons Attribution-ShareAlike 3.0. Spain License.**

UNIVERSITAT DE BARCELONA

FACULTAT DE FARMÀCIA

EXPLORING ADAMANTANE-LIKE SCAFFOLDS FOR A WIDE RANGE OF  
THERAPEUTIC TARGETS

Elena VALVERDE MURILLO  
2015



UNIVERSITAT DE BARCELONA

FACULTAT DE FARMÀCIA

PROGRAMA DE DOCTORAT de Química Orgànica Experimental i Industrial

EXPLORING ADAMANTANE-LIKE SCAFFOLDS FOR A WIDE RANGE OF  
THERAPEUTIC TARGETS

Memòria presentada per Elena VALVERDE MURILLO per optar al títol de  
Doctor per la Universitat de Barcelona

Co-Director i Tutor:  
Dr. Santiago Vázquez Cruz

Co-Director:  
Dr. Manuel Vázquez Carrera

Doctoranda:  
Elena Valverde Murillo

Elena VALVERDE MURILLO  
2015



*A mi familia*

*Al meu petit estimat*



*“La lluna és bella com tu, nineta meva  
Mira’m amb els teus ulls verds  
i jo seré el teu sant que va cap al cel  
Vine amb mi,  
a veure la lluna brillant i blanca, com la teva ànima  
Vine amb mi, amor meu,  
fes que et pugui estimar i besar cada dia”*

*-Àngela Hitos Murillo-*





El treball experimental recollit en aquesta Memòria s'ha realitzat al Departament de Farmacologia i Química Terapèutica de la Facultat de Farmàcia de la Universitat de Barcelona.

Aquest treball ha estat finançat pel Ministerio de Ciencia e Innovación (Projectes CTQ2008-03768, CTQ2011-22433 i SAF2014-57094-R). Per la realització de la present Tesi Doctoral he gaudit d'una beca predoctoral D'Ajuts de Tercer Cicle atorgada per l'Institut de Biomedicina de la Universitat de Barcelona (2011-2015).



## Agraïments

Després de moltes hores d'escriptura i llesta per enquadernar aquesta tesi, arriba un dels moments més esperats però que a l'hora resulta el més difícil d'escriure. Són moltes les persones les que han contribuït d'alguna manera en la realització d'aquesta tesi, directament o indirecta, i des d'aquestes pàgines voldria expressar el meu més sincer agraïment a totes elles, i a les que segur se'm passen d'anomenar.

Primero de todo, a mi co-director y tutor de tesis el Dr. Santiago Vázquez Cruz, Profesor agregat del Departament de Farmacologia i Química Terapèutica. Ha sido largo el viaje desde que me abriste las puertas del laboratorio hace ya más de 8 años. Tu dedicación y pasión por la química, así como la buena persona que eres, me han empujado siempre a ser mejor y seguir aprendiendo. Muchas gracias por haber pensado en mí al escoger estudiante para la beca predoctoral, por estar siempre dispuesto a escucharme y ayudarme en lo necesario, y por haberme dado la suficiente libertad a la hora de llevar a cabo la tesis. Se me va hacer raro eso de que no seas mi jefe a partir de ahora, pero aun así espero que sigas siendo mi consejero y amigo. Gracias Santi!

En segona posició, però no per això menys important, al meu co-director de tesi el Dr. Manel Vázquez Carrera, Professor titular del Departament de Farmacologia i Química Terapèutica. Ha estat més curt el temps que he estat al teu laboratori, però suficient per veure el gran professional i encara millor persona que ets. Gràcies per ajudar-me quan ho he necessitat, i per acceptar-me en el teu grup de treball sense pràcticament conèixer-me. Et desitjo molta sort a tu i a la teva família.

Quisiera agradecer también al Dr. Pelayo Camps, Profesor emèrit del Departament de Farmacologia i Química Terapèutica. Gracias por acogerme en su grupo de investigación y por poner toques de cordura cuando ésta faltaba en el laboratorio.

Voldria agrair al grup de científics que han col·laborat en aquest treball. Al Dr. Francesc X. Sureda, de la Universitat Rovira i Virgili (Reus), per la determinació de l'activitat antagonista contra el receptor de l'NMDA dels compostos sintetitzats. Al Dr. David Soto, de la Universitat de Barcelona, pels estudis electrofisiològics i per explicar-me amb molta paciència els seus experiments. Al grup de recerca del Dr. Scott Webster, de la University of Edinburgh (Regne Unit), per la determinació de la inhibició dels nostres compostos contra l'enzim 11 $\beta$ -HSD1. Al grup de recerca del Professor Dr. Francisco J. Luque, per la realització dels càlculs de docking i dinàmiques moleculars. Al grup de recerca del Professor Dr. Bruce Hammock i al Dr. Christophe Morisseau pels seus consells en quant a la realització dels assajos enzimàtics i de solubilitat.

A l'Institut de Biomedicina de la Universitat de Barcelona, i especialment a la Judit Agustí, per l'ajuda prestada en quant a la beca predoctoral. També, a la M<sup>a</sup> Àngels Barceló de la Secretaria d'Estudiants i Docència de la Facultat de Farmàcia per la paciència mostrada durant el dipòsit de la tesi.

Al personal Científico-Tècnic de la Universitat de Barcelona, concretament a la Dra. Ana Linares, a la M<sup>a</sup> Antònia Molins i a la Vicky Muñoz-Torrero de la Unitat de RMN, per la realització dels espectres de RMN, i a la Dra. Asunción Marín i a la Laura Ortiz per la realització dels espectres de masses. També a la Pilar Domènech, del Servei de Microanàlisi del Centre d'Investigació i Desenvolupament (CID, CSIC) de Barcelona, per la realització dels anàlisis elementals.

Al Dr. Diego Muñoz-Torrero, Professor titular del Departament de Farmacologia i Química Terapèutica, por su amabilidad y cordialidad, y su disposición de aconsejar a los doctorandos cuando es necesario. A la Dra. Carmen Escolano por amenizar los mediodías, por ser una gran anfitriona en sus fiestas de la piscina, y por prestarme su ayuda en el HPLC.

A la Maite, per la seva eficàcia en el tema administratiu i per resoldre'ns els dubtes de paperassa. A la Pilar per mantenir el laboratori net i polit i pels "bon dies" tan agradables cada matí. A Javier por llenar el agua destilada, llevar la muestras al PCB, CSIC y químicas, realizar los pedidos y hacer los partes. A Armando por ser el manitas más eficiente del laboratorio, y probablemente de toda la facultad. Y al Josep Galdón per mantenir la facultat en ordre i estar sempre alerta.

A tota la gent que ha passat i estat pel laboratori de Química Farmacèutica durant aquest temps i que sense ells no hagués estat lo mateix. Als que considero els mestres del lab, que han ensenyat a les generacions venidores les "bones" practiques de laboratori. A Loli, porque fuiste tú quien me enseñó cómo trabajar en el laboratorio de la mejor forma posible. A l'Eva, per ser un exemple a seguir de constància i per les teves ganex contagioses de saber-ne més i més. Ara tens un nou repte, el petit Marc, segur que ho faràs increïblement bé! A la Tània, pel teu saber fer i per ajudar-nos als més despistats en la recerca de material i reactius. A l'Eli, per ensenyar que el temps és relatiu i que es pot treballar molt més ràpid que la resta. Al Carles, per confirmar que el temps és relatiu i que el dia dona per molt, per parlar, cotillejar, ensenyar i, també, treballar ;). Als dos, per rebre'm tan bé a Dundee, i per acollir-me a Cambridge al vostre mega-super sofà!

Als que les nostres tesis han coincidit més temps i amb els que també hem compartit moments molt divertits. A l'Ane, per haver sigut la meva primera cordada a escalada (te'n recordes quins nervis?) i per haver-te convertit amb el temps en una gran companya. A la Rosana, per la gran hard-worker que ets, pel teu interès en la recerca del grup i pels moments on compartíem vitrina. Al David, per les converses tan interessants que hem tingut i per ser el creador del Daily Lab. A la Irene, per rebre'm a Mechelen i per les rialles tan divertides que hem tingut des de la carrera. A Javi, por haber introducido palabras desconocidas por entonces en nuestro vocabulario, y que ahora son tan útiles. Ahora que eres mi relevo en el piso, cuida de mi habitación ;). A Ornella, por sus risas incontroladas y por compartir habitación en Valencia (qué tiempos aquellos!). A la Marta B., per descobrir-me grups de música que desconeixia. A l'Arnau, per tot el que hem après amb tu quan estaves amb nosaltres.

A la gent que ha estat de pas pel laboratori, però que ha deixat empremta. Al Toni, per compartir gustos musicals i per la teva perseverança en les curses. A l'Albert, per recolzar-me en discussions polítiques i ser tan eixerit. A l'Enric, per ensenyar-me a ensenyar i pels teus riures i converses. A la Marta F., per acollir-nos a Stevenage i per les teves classes de ball. A M<sup>a</sup> Eugenia, por ser como sos, tan divertida y alegre, y por enseñarnos parte de Córdoba que desconocía. Al Raül, pel bon rotllo que desprens. A Juanlo y Lorena, por los consejos de química y por el buen ambiente que hacíais en el lab. Encara que són molts més els que han passat per les nostres vitrines i que han fet que els dies fossin més amens: Marta M., Maria, Deborah, Salva, Jordi B., Agnès, Ester, Natalia, Mattia, Alèxia, Daniela, Alicja, i molts que segur em deixo. A les noves incorporacions, Sandra, Andreaa, Eugènia i Katia, molta sort i paciència en aquesta nova etapa.

A mis compañeros del laboratorio de Farmacología, que aunque mi visita “abajo” ha sido fugaz, he podido conocer a gente que merece mucho la pena. En especial, a Emma B., mi maestra y una gran persona. Gracias por haberme enseñado tan bien y con tanta paciencia, pero sobre todo por las conversaciones y risas compartidas. Sé que me llevo una amiga del laboratorio 6 ;). A Gaia, por tus clases de cultivos y tus regalitos de USA. A Mohammad y Xevi, por haberme ayudado cuando me hacía falta. Al resto de compañeros del laboratorio, por las conversaciones espontaneas que alegraban el día. A Silvia y a Mar, por los apoyos técnicos y logísticos.

A la gente del laboratorio de Química Orgánica, por el intercambio de reactivos y de material, y por las birras y salidas en grupo. En particular, a Sònia (gràcies per l'ajuda amb l'HPLC), a Guillaume (merci pour ta compagnie à des conférences), a Elena, a Francesco, a Alex, a Juan Andrés, a Claudio, a Celeste, a Guilhem y a Caroline.

A los compañeros de master, sobre todo con los que compartimos casa en Valencia y horas fatídicas de estudio. Gracias a Manu, Alberto y Fabrizio.

I would like to thank the people I did my placement with in GSK, especially to Dr. Simon MacDonald and John Pritchard for welcoming me in their team. Also, to Dr. Niall Anderson, who was really helpful and kind to me, I really appreciate what you taught me. Thanks also to Anaïs, without you that year would have been really different, to Katharina for our exchange trips, and to Richard, for your Afrikaans and Khoisan's classes. I would also like to thank Dr. Allan Watson, my supervisor in Glasgow and lab mate in GSK. I am really happy for how your group is expanding, and to have been part of it even it was for a short period of time. I am also thankful to my lab mates in Scotland, for welcoming me and showing me the Scottish lifestyle, and in particular to Carolina for the climbing evenings and for your visit to Barcelona.

A mis compañeros de piso Irene, Sonia, David y Ana por alegrarme las tardes-noches después de un duro día de trabajo. Y en especial a Héctor, por las risas, las imitaciones y el diseño de la portada!

Als meus companys de viatges filipins, la Maria, la Lucía, el Pedro, el Jon, l'Anna i l'Anahí, pels moments d'evasió que he tingut amb vosaltres, per les històries tan divertides que hem viscut junts, i que segur no oblidarem! A en Macedo, n'Elisa, en Marc i n'Aina per acollir-nos de luxe al vostre santuari menorquí.

A mis amigas de siempre Sara, Melania y Clara, como decimos nosotras, por las historias acumuladas, por estar dispuestas a escuchar mis aventuras, y por intentar entender qué hago realmente. A l'Emma E., pels últims anys de carrera juntes i per la teva visita a Escòcia (i també al nostre bebè ;)).

A mi familia argentina-andorrana, por ser tan buen anfitriones cuando os he visitado, y por haberme aceptado como miembro de vuestra familia.

A los animales de la familia, y con esto me refiero a Bolo, a Miel y a Joy, por su compañía y su amor devoto.

A mis padres José y Ángela, por ser tan luchadores, por vuestros sabios consejos y por preocuparos por mí en todo momento. A mi tata Lidia, por ser tan divertida, por cuidarme tanto desde pequeña y por sacrificarse como lo hace. A mis tíos Lidia, Antonio y Milagros, y mis primas Irene y Ángela, por vuestro apoyo incondicional. Gracias también a mi familia de Barcelona. A todos vosotros por quererme tal como soy, por aceptar sin rechistar mis locas decisiones y por estar dispuestos a ayudarme siempre. Yo también lo estoy, os quiero!

I finalment, al Matías, per dedicar-te tant a mi, a cuidar-me i a treure'm un somriure de la cara sempre que pots i vols. Moltes gràcies per haver llegit i corregit la tesi, que no ha sigut tasca fàcil. I com diu aquella cançó, meu riso é tão feliz contigo, o meu melhor amigo é o meu amor.





## RESULTS

The present thesis has led to the following scientific publications, symposium communications and awards:

### Scientific publications:

1. Valverde, E.; Barroso, E.; Vázquez-Carrera, M.; Vázquez, S. *Scaffold-hopping for new soluble epoxide hydrolase with improved lipophilic ligand efficiency*. Scientific paper, writing in progress.
2. Vázquez, S.; Leiva, R.; Valverde, E. *New inhibitors of the 11 $\beta$ -HSD1 with potential use in therapeutics*. European patent application, writing in progress.
3. Valverde, E.; Seira, C.; Bidon-Chanal, A.; McBride, A.; Luque, F. J.; Webster, S. P.; Vázquez, S. *Searching for novel applications of the benzohomoadamantane scaffold in medicinal chemistry: synthesis of new 11 $\beta$ -HSD1 inhibitors*. *Bioorganic and Medicinal Chemistry* **2015**, accepted.
4. Vázquez, S.; Valverde, E.; Vázquez-Carrera, M. *Analogues of adamantyl ureas as soluble epoxide hydrolase inhibitors*. European patent application, EP15178618.3.
5. Barniol-Xicota, M.; Escandell, A.; Valverde, E.; Julián, E.; Torrents, E.; Vázquez, S. *Antibacterial activity of novel benzopolycyclic amines*. *Bioorganic and Medicinal Chemistry* **2015**, *23*, 290-293.
6. Valverde, E.; Sureda, F. X.; Vázquez, S. *Novel benzopolycyclic amines with NMDA receptor antagonist activity*. *Bioorganic and Medicinal Chemistry* **2014**, *22*, 2678-2683.

### Symposium communications:

1. Valverde, E.; Barroso, E.; Vázquez-Carrera, M.; Vázquez, S. *Novel soluble epoxide hydrolase inhibitors with enhanced lipophilic ligand efficiency via scaffold-hopping approaches*. XXXV Reunión Bienal de la Real Sociedad Española de Química (RSEQ), A Coruña (Spain), Flash communication, **2015**.
2. Valverde, E.; Seira, C.; Bidon-Chanal, A.; McBride, A.; Luque, F. J.; Webster, S. P.; Vázquez, S. *A quest for further uses of adamantane-like scaffolds in medicinal chemistry: discovery of new 11 $\beta$ -HSD1 inhibitors*. 14<sup>th</sup> Belgian Organic Synthesis Symposium, Louvain-la-Neuve (Belgium), Poster, **2014**.
3. Valverde, E.; Seira, C.; Bidon-Chanal, A.; McBride, A.; Luque, F. J.; Webster, S. P.; Vázquez, S. *Further applications of a novel scaffold as an adamantane surrogate: synthesis of new 11 $\beta$ -HSD1 inhibitors*. I Simposio de Jóvenes Investigadores de la Sociedad Española de Química Terapéutica, Madrid (Spain), Poster, **2014**.
4. Vázquez, S.; Valverde, E.; Torres, E.; Sureda, F. X. *Novel analogues of memantine with potent activity as glutamate N-methyl-D-aspartate receptor antagonists*. XVII<sup>th</sup> National Meeting on "Advances in Drug Discovery: Successes, Trends, and Future Challenges, Madrid (Spain), Poster, **2013**.

5. Valverde, E.; Lafuente, M.; Sureda, F. X.; Vázquez, S. *New benzopolycyclic cage amines with NMDA receptor antagonist activity*. XXXIV Reunión Bienal de la Real Sociedad Española de Química, Santander (Spain), Flash communication, 2013.
6. Vázquez, S.; Duque, M. D.; Torres, E.; Valverde, E.; Lafuente, M.; Sureda, F. X. *New benzopolycyclic cage amines with NMDA receptor antagonist activity*. VI Mediterranean Organic Chemistry Meeting, Granada (Spain), Poster, 2013.

#### Awards:

1. Valverde, E.; Vázquez-Carrera, M.; Vázquez, S. *Exploring adamantane-like scaffolds for a wide range of therapeutic targets*. Finalist of the Eli Lilly's awards for the excellence in the research of Ph.D. students, Lilly, Alcobendas (Spain), Poster, 2015.

#### Research stays:

1. *Development of new methods for organic synthesis based on control of boron solution speciation*. Dr. Allan J. B. Watson's group, Department of Pure and Applied Chemistry, University of Strathclyde, Glasgow (United Kingdom), September-December 2014.

#### Other scientific publications:

1. Fyfe, J. W. B.; Valverde, E.; Seath, C. P.; Kennedy, A. R.; Redmond, J. M.; Anderson, N. A.; Watson, A. J. B. *Speciation control during Suzuki-Miyaura cross-coupling of haloaryl and haloalkenyl MIDA boronic esters*. *Chemistry, a European Journal* 2015, 21, 8951-8964.
2. Anderson, N. A.; Fallon, B. J.; Valverde, E.; MacDonald, S. J. F.; Pritchard, J. M.; Suckling, C. J.; Watson, A. J. B. *Asymmetric rhodium-catalysed addition of arylboronic acids to acyclic unsaturated esters containing a basic  $\gamma$ -amino group*. *Synlett* 2012, 23, 2817-2821.
3. Valverde, E.; Torres, E.; Guardiola, S.; Naesens, L.; Vázquez, S. *Synthesis and antiviral evaluation of bisnoradamantane sulfites and related compounds*. *Medicinal Chemistry* 2011, 7, 135-140.
4. Duque, M. D.; Torres, E.; Valverde, E.; Barniol, M.; Guardiola, S.; Rey, M.; Vázquez, S. *Inhibitors of the M2 channel of influenza A virus*. *Recent Advances in Pharmaceutical Sciences* 2011, 35-64 ISBN: 978-81-7895-528-5, book chapter.
5. Duque, M. D.; Camps, P.; Torres, E.; Valverde, E.; Sureda, F. X.; López-Querol, M.; Camins, A.; Radhika Prathalingam, S.; Kelly, J. M.; Vázquez, S. *New oxapolycyclic cage amines with NMDA receptor antagonist and trypanocidal activities*. *Bioorganic and Medicinal Chemistry* 2010, 18, 46-57.



## Abbreviation list

ACU: *N*-adamantyl-*N'*-cyclohexylurea

AD: Alzheimer's disease

ADME: Absorption, Distribution, Metabolism and Excretion process

ADMET: Absorption, Distribution, Metabolism, Excretion and Toxicology

AEPU: *N*-adamantanyl-*N'*-(5-(2-(2-ethoxyethoxy)ethoxy)pentyl)urea

AIBN: azobisisobutyronitrile

AMCU: 1-adamantan-1-yl-3-(4-(3-morpholinopropoxy)cyclohexyl)urea

AMPA:  $\alpha$ -amino-3-hydroxy-5-methyl-4-isoxazolepropionic acid

APAU: *N*-(1-acetylpiperidin-4-yl)-*N'*-adamantylurea

API: active pharmaceutical ingredient

ARA: arachidonic acid

ATF3: activating transcription factor 3

ATF4: activating transcription factor 4

ATF6: activating transcription factor 6

AUDA: *N*-adamantanyl-*N'*-dodecanoic acid urea

AUSM: 4-(3-adamantan-1-yl-ureido)-2-hydroxyl-benzoic acid methyl ester

BBB: blood-brain barrier

BiP (or GRP78): immunoglobulin-heavy-chain-binding protein

BSA: bovine serum albumin

cAMP: cyclic adenosine monophosphate

CDI: *N,N'*-carbonyldiimidazole

CGC: cerebellar granule cells

CHOP (or GADD153): CCAAT enhancer-binding protein (C/EBP) homologous protein

CNS: central nervous system

COX: cyclooxygenase

CT: control

CV: cardiovascular

CYP450: cytochrome P-450

DAST: (diethylamino)sulfur trifluoride

DCE: 1,2-dichloroethane

DCM: dichloromethane

DCU: *N,N'*-dicyclohexylurea

DHET: dihydroeicosatrienoic acid

DIPEA: *N,N'*-diisopropylethylamine

DMAP: 4-dimethylaminopyridine

DMF: dimethylformamide

DMSO: dimethylsulfoxide

DNA: deoxyribonucleic acid

DPPA: diphenylphosphoryl azide

DPP-IV: dipeptidyl peptidase IV

DTBP: di-*tert*-butyl peroxide

EDC: 1-ethyl-3-(3'-dimethylaminopropyl)carbodiimide

EDG: electron-donating group

EET: epoxyeicosatrienoid acid

eIF2: eukaryotic translation initiation factor 2

EMA: European Medicines Agency

ER: endoplasmic reticulum

ERAD: ER-associated degradation

EWG: electron-withdrawing group  
FDA: Food & Drugs Administration  
Fura-2 AM: Fura-2-acetoxymethyl ester  
GABA:  $\gamma$ -aminobutyric acid  
GAPDH: glyceraldehyde 3-phosphate dehydrogenase  
GC: glucocorticoid  
GPCR: G protein-coupled receptor  
GR: glucocorticoid receptor  
GSK: GlaxoSmithKline  
HATU: 1-[bis(dimethylamino)methylene]-1H-1,2,3-triazolo[4,5-b]pyridinium 3-oxid hexafluorophosphate  
HDL: high-density lipoprotein  
hERG: human Ether-à-go-go-Related Gene  
HMPA: hexamethylphosphoramide  
HOAt: 7-aza-1-hydroxybenzotriazole  
HOBT: hydroxybenzotriazole  
HPA: hypothalamic-pituitary-adrenal  
HPLC: high performance liquid chromatography  
HRMS: high resolution-mass spectrometry  
11 $\beta$ -HSD1: 11 $\beta$ -hydroxysteroid dehydrogenase type 1  
11 $\beta$ -HSD2: 11 $\beta$ -hydroxysteroid dehydrogenase type 2  
17 $\beta$ -HSD: 17 $\beta$ -hydroxysteroid dehydrogenase  
HTS: high-throughput screening  
IC<sub>50</sub>: half-maximal inhibitory concentration  
IKK: inhibitor of  $\kappa$ B kinase  
IR: infrared  
IRE1: inositol-requiring enzyme 1  
JNK: c-Jun amino-terminal kinase  
LC-MS: liquid chromatography-mass spectrometry  
LDA: lithim diisopropylamide  
LE: ligand efficiency  
LHS: left-hand side  
LipE: lipophilic ligand efficiency  
LKT: leukotriene  
LOX: lipoxygenase  
MD: molecular dynamics  
mEH: microsomal epoxide hydrolase  
MetS: metabolic syndrome  
mp: melting point  
MR: mineralocorticoid receptor  
mRNA: messenger ribonucleic acid  
MS: mass spectrometry  
MW: molecular weight  
NADPH: nicotinamide adenine dinucleotide phosphate  
ND: not determined  
NEPC: 4-nitrophenyl-*trans*-2,3-epoxy-3-phenylpropyl carbonate  
NF- $\kappa$ B: nuclear factor- $\kappa$ B  
NMDA: *N*-methyl-D-aspartic acid  
NMDAR: *N*-methyl-D-aspartic acid receptor

NMR: nuclear magnetic resonance

NSAID: nonsteroidal anti-inflammatory drug

PAL: palmitate

PBA: 4-phenyl butyric acid

PCR: polymerase chain reaction

PD: pharmacodynamics

PDB: Protein Data Bank

PERK: PKR-like ER-regulated kinase

PG: prostaglandin

PHOME: (3-phenyl-oxiranyl)-acetic acid cyano-(6-methoxy-naphthalen-2-yl)-methyl ester

PK: pharmacokinetic

PP: primary pharmacophore

PPAR: peroxisome proliferator-activated receptor

PSA: polar surface area

PVT: polyvinyl toluene

RHS: right-hand side

ROS: reactive oxygen species

RT: room temperature

S: solubility

SAR: structure-activity relationship

SD: Standard deviation

SEM: Standard error of the mean

SET: single electron transfer

sEH: soluble epoxide hydrolase

SP: secondary pharmacophore

SPA: scintillation proximity assay

*t*-AUCB: *trans*-4-[4-(3-adamantan-1-ylureido)cyclohexyloxy]benzoic acid

T2DM: type 2 Diabetes Mellitus

*t*-DPPO: *trans*-diphenyl-propene oxide

TEA: triethylamine

TFA: trifluoroacetic acid

TFAA: trifluoroacetic anhydride

THF: tetrahydrofuran

TNF- $\alpha$ : tumor necrosis factor- $\alpha$

TP: tertiary pharmacophore

*t*-SO: *trans*-stilbene oxide

UPR: unfolded protein response

UV: ultraviolet

*vs*: *versus*

WHO: World Health Organization

XBPI: X-box-binding protein 1

$\mu$ W: microwave apparatus

# **INDEX**





**INTRODUCTION**

1. Adamantane: the precious nucleus	3
1.1 Origin of adamantane and first synthesis	3
1.2 Adamantane's physicochemical properties and its multidimensional value	6
1.2.1 Physicochemical properties	6
1.2.2 Adamantane ring as a pharmacophore	8
1.2.3 ADME properties of adamantane-containing compounds	8
1.3 Medicinal chemistry of adamantane: the promiscuous lipophilic pellet	10
1.3.1 Clinically approved adamantane-based drugs	10
1.3.2 Adamantane-containing candidates in development	13
1.4 Not all that glitters is gold: a moot point of perfection	16
1.4.1 High lipophilicity compromises PK properties	16
1.4.2 Ready access to intermediates that prevent scaffold optimization	19
1.4.3 Adamantane group as an imperfect space-filling pharmacophore	20
1.5 Adamantane alternatives: previous work of the group	20

**CHAPTER 1: NMDA receptor antagonism****INTRODUCTION**

1. NMDA receptor antagonism by adamantane-like scaffolds	29
1.1 The glutamatergic neurotransmitter system	29
1.1.1 NMDA receptor and its physiological function	29
1.1.2 Glutamate and related pathological states	31
1.2 NMDA as a therapeutic target	33
1.2.1 Competitive NMDAR antagonists	33

1.2.2 Uncompetitive NMDAR antagonists	34
1.2.3 Non-competitive NMDAR antagonists	36
1.3 The neuroprotector memantine	37
1.4 Previous work of the group: new antagonists of the NMDAR	40
OBJECTIVES	45
RESULTS & DISCUSSION	
1. Effect of the C-9 substitution in new benzopolycyclic compounds	49
1.1 Synthesis of the C9-demethylated compound, <b>23</b>	49
1.2 Exploration of the C-9 substitution of the benzo-homoadamantane scaffold	67
2. Pharmacological evaluation of new benzo-homoadamantane derivatives	73
2.1 Assessment of the NMDAR antagonistic activity	73
2.2 Electrophysiological measurements	77
CONCLUSIONS	83
<b>CHAPTER 2: 11<math>\beta</math>-HSD1 inhibition</b>	
INTRODUCTION	
1. 11 $\beta$ -HSD1 inhibition by adamantane-based derivatives	89
1.1 The glucocorticoid system and its physiological actions	89
1.1.1 GC regulation by 11 $\beta$ -HSD enzymes	89
1.2 11 $\beta$ -HSD1 as a pleiotropic therapeutical target	91
1.2.1 11 $\beta$ -HSD1 inhibition and type 2 diabetes mellitus, obesity and metabolic syndrome	93
1.2.2 11 $\beta$ -HSD1 inhibition and inflammation	96
1.2.2 11 $\beta$ -HSD1 inhibition and cognitive dysfunction with aging	97
1.2.3 11 $\beta$ -HSD1 inhibition for other diseases	99
1.3 Crystal structure of 11 $\beta$ -HSD1 and its binding site	100
1.4 11 $\beta$ -HSD1 inhibitors in development	102

1.4.1 Non-selective 11 $\beta$ -HSD1 inhibitors as tools	103
1.4.2 Studies with selective 11 $\beta$ -HSD1 inhibitors	104
1.4.3 Adamantane-based inhibitors of 11 $\beta$ -HSD1	107
OBJECTIVES	113
RESULTS & DISCUSSION	
1. Application of the benzopolycyclic scaffold as an adamantane analogue for 11 $\beta$ -HSD1 inhibition	117
1.1 Synthesis of the C-9 substituted 6,7,8,9,10,11-hexahydro-5,7:9,11-dimethano-5 <i>H</i> -benzocyclononen-7-yl derivatives	117
1.1.1 Preparation of amide compounds	120
1.1.2 Synthesis of the thiazolone scaffold	128
1.1.3 Urea group formation	129
1.2 Pharmacological evaluation of the C-9 substituted 6,7,8,9,10,11-hexahydro-5,7:9,11-dimethano-5 <i>H</i> -benzocyclononen-7-yl derivatives	130
1.3 Synthesis of the fluoro-benzohomoadamantane derivative of PF-877423	134
1.4 Pharmacological evaluation of the fluoro-benzohomoadamantane derivative of PF-877423	135
1.5 Computational studies of the first family of 11 $\beta$ -HSD1 inhibitors	136
2. Application of the scaffold as an adamantane analogue in 11 $\beta$ -HSD1 inhibitors	138
2.1 Synthesis of the derivatives	138
2.2 Pharmacological evaluation and computational studies of the derivatives	146
CONCLUSIONS	153
<b>CHAPTER 3: sEH inhibition</b>	
INTRODUCTION	

1. sEH inhibition by adamantane-based derivatives	159
1.1 Epoxyeicosatrienoic acids and their biological role	159
1.1.1 Oxidative pathways of arachidonic acid metabolism	159
1.1.2 Biological relevance of EETs and importance of the sEH management	160
1.2 Targeting sEH: an overview of its pharmacology	162
1.2.1 Regulation of inflammation by sEH inhibitors	162
1.2.2 Effects of sEH inhibitors on pain	164
1.2.3 sEH and cardiovascular disease	164
1.2.4 Role of sEH in the development of diabetes and metabolic syndrome. Involvement of ER stress	165
1.2.5 sEH inhibition for other clinical applications	166
1.3 sEH: crystal structure, catalytic mechanism, tissue expression and regulation	167
1.4 Discovery of sEH inhibitors	169
OBJECTIVES	179
RESULTS & DISCUSSION	
1. Scaffold-hopping approach for the development of new sEH inhibitors	183
1.1 Synthesis of <i>N</i> -adamantane-like- <i>N'</i> -(2,3,4-trifluorophenyl)ureas	186
1.1.1 Preparation of intermediate scaffolds	187
1.1.2 Preparation of urea <b>157</b>	197
1.1.3 Synthesis of final ureas <b>170-183</b>	201
1.2 Pharmacological evaluation of final ureas. IC <sub>50</sub> determination	202
1.2.1 A little of background	202
1.2.2 Tune-up of the screening assay	205
1.2.3 IC <sub>50</sub> determination of ureas <b>157</b> and <b>170-183</b>	208
1.3 Water solubility determination	211

1.4 Lipophilic ligand efficiency: a new metric for drug discovery	216
2. New ureas with selected scaffolds	220
2.1 Synthesis of new ureas with selected scaffolds	221
2.2 Pharmacological evaluation of new ureas with selected scaffolds	226
2.3 Water solubility, melting points and LipE	229
3. ER stress amelioration with selected sEH inhibitors. In vitro studies	231
CONCLUSIONS	241
MATERIALS & METHODS	
General methods	245
CHAPTER 1: NMDA receptor antagonism	
○ Preparation of 5,6,8,9-tetrahydro-5,9-propanebenzocycloheptane-7,11-dione, <b>27</b> and 7,11-epoxy-6,7,8,9-tetrahydro-5,9-propane-5 <i>H</i> -benzocycloheptane-7,11-diol, <b>28</b>	249
○ Preparation of 5,6,8,9-tetrahydro-5,9-propanebenzocycloheptane-11-ene-7-one, <b>25</b>	249
○ Preparation of 2-chloro- <i>N</i> -(9-hydroxy-5,6,8,9,10,11-hexahydro-7 <i>H</i> -5,9:7,11-dimethanobenzo[9]annulen-7-yl)acetamide, <b>34</b>	250
○ Preparation of 9-amino-5,6,8,9,10,11-hexahydro-7 <i>H</i> -5,9:7,11-dimethanobenzo[9]annulen-7-ol hydrochloride, <b>46·HCl</b>	251
○ Preparation of 9-(dimethylamino)-5,6,8,9,10,11-hexahydro-7 <i>H</i> -5,9:7,11-dimethanobenzo[9]annulen-7-ol hydrochloride, <b>50·HCl</b>	252
○ Preparation of 9-bromo-5,6,8,9,10,11-hexahydro-7 <i>H</i> -5,9:7,11-dimethanobenzo[9]annulen-7-amine, <b>47</b>	253
○ Preparation of 5,6,8,9,10,11-hexahydro-7 <i>H</i> -5,9:7,11-dimethanobenzo[9]annulen-7-amine hydrochloride, <b>23·HCl</b>	254
○ Preparation of <i>N,N</i> -dimethyl-5,6,8,9,10,11-hexahydro-7 <i>H</i> -5,9:7,11-dimethanobenzo[9]annulen-7-amine hydrochloride, <b>24·HCl</b>	255
○ Preparation of 2-chloro- <i>N</i> -(9-chloro-5,6,8,9,10,11-hexahydro-7 <i>H</i> -5,9:7,11-dimethanobenzo[9]annulen-7-yl)acetamide, <b>40</b>	256
○ Preparation of 9-chloro-5,6,8,9,10,11-hexahydro-7 <i>H</i> -5,9:7,11-dimethanobenzo[9]annulen-7-amine hydrochloride, <b>42·HCl</b>	257
○ Preparation of <i>N,N</i> -dimethyl-9-chloro-5,6,8,9,10,11-hexahydro-7 <i>H</i> -5,9:7,11-dimethanobenzo[9]annulen-7-amine hydrochloride, <b>49·HCl</b>	258
○ Preparation of 9-fluoro-5,6,8,9,10,11-hexahydro-7 <i>H</i> -5,9:7,11-dimethanobenzo[9]annulen-7-amine hydrochloride, <b>48·HCl</b>	259

- Preparation of 9-fluoro-*N,N*-dimethyl-5,6,8,9,10,11-hexahydro-7*H*-5,9:7,11-dimethanobenzo[9]annulen-7-amine hydrochloride, **51•HCl** 260
- Preparation of 9-methoxy-5,6,8,9,10,11-hexahydro-7*H*-5,9:7,11-dimethanobenzo[9]annulen-7-ol, **53** 261
- Preparation of 2-chloro-*N*-(9-methoxy-5,6,8,9,10,11-hexahydro-7*H*-5,9:7,11-dimethanobenzo[9]annulen-7-yl)acetamide, **54** 262
- Preparation of 9-methoxy-5,6,8,9,10,11-hexahydro-7*H*-5,9:7,11-dimethanobenzo[9]annulen-7-amine, **52** 263

## CHAPTER 2: 11 $\beta$ -HSD1 inhibition

1. Benzo-homoadamantane scaffolds
  - Preparation of 5,6,8,9-tetrahydro-5,9-propanebenzocycloheptane-7,11-diene, **29** 269
  - Preparation of *N*-(6,7,8,9,10,11-hexahydro-9-methyl-5,7:9,11-dimethano-5*H*-benzocyclononen-7-yl)chloroacetamide, **55** 269
  - Preparation of 6,7,8,9,10,11-hexahydro-9-methyl-5,7:9,11-dimethano-5*H*-benzocyclononen-7-amine, **19** 270
  - Preparation of (2*R*)-*tert*-butyl 2-[(9-hydroxy-6,7,8,9,10,11-hexahydro-5*H*-5,9:7,11-dimethanobenzo[9]annulen-7-yl)carbamoyl]pyrrolidine-1-carboxylate, **71** 270
  - Preparation of (2*R*)-*N*-(9-hydroxy-6,7,8,9,10,11-hexahydro-5*H*-5,9:7,11-dimethanobenzo[9]annulen-7-yl)pyrrolidine-2-carboxamide, **72** 271
  - Preparation of (2*R*)-1-ethyl-*N*-(9-hydroxy-6,7,8,9,10,11-hexahydro-5*H*-5,9:7,11-dimethanobenzo[9]annulen-7-yl)pyrrolidine-2-carboxamide, **56** 272
  - Preparation of (2*R*)-*tert*-butyl-2-[(9-methyl-6,7,8,9,10,11-hexahydro-5*H*-5,9:7,11-dimethanobenzo[9]annulen-7-yl)carbamoyl]pyrrolidine-1-carboxylate, **73** 273
  - Preparation of (2*R*)-*N*-(9-methyl-6,7,8,9,10,11-hexahydro-5*H*-5,9:7,11-dimethanobenzo[9]annulen-7-yl)pyrrolidine-2-carboxamide, **74** 274
  - Preparation of (2*R*)-1-ethyl-*N*-(9-methyl-6,7,8,9,10,11-hexahydro-5*H*-5,9:7,11-dimethanobenzo[9]annulen-7-yl)pyrrolidine-2-carboxamide, **57•tartrate** 275
  - Preparation of 4-amino-3,5-dichloro-*N*-(9-hydroxy-6,7,8,9,10,11-hexahydro-5*H*-5,9:7,11-dimethanobenzo[9]annulen-7-yl)benzamide, **58** 277
  - Preparation of 4-amino-3,5-dichloro-*N*-(9-methyl-6,7,8,9,10,11-hexahydro-5*H*-5,9:7,11-dimethanobenzo[9]annulen-7-yl)benzamide, **59** 278
  - Preparation of *N*-(9-methyl-6,7,8,9,10,11-hexahydro-

5 <i>H</i> -5,9:7,11-dimethanobenzo[9]annulen-7-yl)cyclohexanecarboxamide, <b>60</b>	279
○ Preparation of <i>N</i> -(9-methyl-6,7,8,9,10,11-hexahydro-5 <i>H</i> -5,9:7,11-dimethanobenzo[9]annulen-7-yl)thiourea, <b>76</b>	280
○ Preparation of 5,5-dimethyl-2-(9-methyl-6,7,8,9,10,11-hexahydro-5 <i>H</i> -5,9:7,11-dimethanobenzo[9]annulen-7-yl)amino]thiazol-4(5 <i>H</i> )-one, <b>61</b>	281
○ Preparation of <i>N</i> -(9-hydroxy-6,7,8,9,10,11-hexahydro-5 <i>H</i> -5,9:7,11-dimethanobenzo[9]annulen-7-yl)piperidine-1-carboxamide, <b>62</b>	282
○ Preparation of <i>N</i> -(9-methyl-6,7,8,9,10,11-hexahydro-5 <i>H</i> -5,9:7,11-dimethanobenzo[9]annulen-7-yl)piperidine-1-carboxamide, <b>63</b>	283
○ Preparation of <i>N</i> -(9-fluoro-5,6,8,9,10,11-hexahydro-7 <i>H</i> -5,9:7,11-dimethanobenzo[9]annulen-7-yl)piperidine-1-carboxamide, <b>64</b>	284
○ Preparation of <i>N</i> -(9-methoxy-5,6,8,9,10,11-hexahydro-7 <i>H</i> -5,9:7,11-dimethanobenzo[9]annulen-7-yl)piperidine-1-carboxamide, <b>65</b>	285
○ Preparation of (2 <i>R</i> )- <i>tert</i> -butyl-2-[(9-fluoro-6,7,8,9,10,11-hexahydro-5 <i>H</i> -5,9:7,11-dimethanobenzo[9]annulen-7-yl)carbamoyle]pyrrolidine-1-carboxylate, <b>78</b>	286
○ Preparation of (2 <i>R</i> )- <i>N</i> -(9-fluoro-6,7,8,9,10,11-hexahydro-5 <i>H</i> -5,9:7,11-dimethanobenzo[9]annulen-7-yl)pyrrolidine-2-carboxamide, <b>79</b>	287
○ Preparation of (2 <i>R</i> )-1-ethyl- <i>N</i> -(9-fluoro-6,7,8,9,10,11-hexahydro-5 <i>H</i> -5,9:7,11-dimethanobenzo[9]annulen-7-yl)pyrrolidine-2-carboxamide, <b>77•tartrate</b>	287
2. scaffolds	
Preparation of	
, <b>82</b>	291
Preparation of	
, <b>88</b>	292
Preparation of	
, <b>89</b>	293
Preparation of	
, <b>90</b>	293
Preparation of	
, <b>95•HCl</b>	294
Preparation of	
, <b>96</b>	294

Index

Preparation of	, 97	295
Preparation of	, 98-tartrate	295
Preparation of	, 99	296
Preparation of	, 100	297
Preparation of	, 101	298
Preparation of	, 102	299
Preparation of	, 103	300
Preparation of	, 104	301

CHAPTER 3: sEH inhibition

1. Chemistry

○ Preparation of	,	307
○ Preparation of	, 120-HCl	307
Preparation of	, 129	308
Preparation of	, 121-HCl	308
Preparation of	, 135	309
○ Preparation of	, 133	309
Preparation of the stereoisomeric mixture of	, 136	310
Preparation of the mixture of	, 137, and	310
	, 138	310
Preparation of the stereoisomeric mixture of	, 139	311
Preparation of the stereoisomeric mixture of	, 141	311
○ Preparation of	, 131	312



○ Preparation of	, 141	313
○ Preparation of	, 144	313
Preparation of		
	, 146	314
○ Preparation of	, 155	314
○ Preparation of	,	
122·HCl		315
Preparation of		
	, 143	316
Preparation of		
	, 145	316
Preparation of		
	, 147	317
Preparation of		
	, 149	317
Preparation of		
	, 156	318
Preparation of		
	, 123·HCl	318
○ Preparation of	, 164	319
○ Preparation of	, 166	320
Preparation of		
	, 160	321
Preparation of		
	, 161	321
Preparation of		
	, 162	322
Preparation of		
	, 159	322
Preparation of		
	, 169	323
Preparation of		
	, 157	324
○ General method for the synthesis of urea compounds 108-109 and 170-183		325
○ Preparation of	, 108	326
○ Preparation of	, 109	326
Preparation of		
	, 170	326
Preparation of		
	, 171	327
○ Preparation of		

Index

	, 172		328
Preparation of			
		, 173	329
Preparation of			
	, 174		330
Preparation of			
	, 175		331
Preparation of			
		, 176	332
Preparation of			
	, 177		333
Preparation of			
		, 178	334
Preparation of			
		, 179	335
Preparation of			
	, 180		336
Preparation of			
		, 181	337
Preparation of			
	, 182		338
Preparation of			
		, 183	339
o Preparation of		, 185	340
Preparation of			
	, 184		341
Preparation of			
	, 187		342
Preparation of			
	, 184		342
Preparation of			
	, 189		343
Preparation of			
		, 188	343
o Preparation of		, 191	344
o Preparation of		, 190·HCl	345
Preparation of			
	, 192		345
Preparation of			
		, 193	346
o Preparation of			

	, 195	348
2.	IC <sub>50</sub> assay determination	353
3.	Apparent or semi-equilibrium solubility measurements	357
4.	<i>In vitro</i> cell cultures	361
REFERENCES		365

# **INTRODUCTION**



## 1. ADAMANTANE: THE PRECIOUS NUCLEUS

For over eighty years, the adamantane nucleus has interested organic chemists for its simplicity and symmetry.<sup>1,2</sup> The rigid tricyclo[3.3.1.1<sup>3,7</sup>]decane skeleton has provided a unique structural template for evaluating important theoretical concepts in chemistry (Fig. 1).<sup>3,4,5,6,7</sup> From its discovery, adamantanes have been particularly useful for proving through-bond and through-space electronic effects of different substituents in saturated systems and have significantly contributed to our understanding of hyperconjugation and degenerate isomerization. Furthermore they have provided molecular scaffolds for investigating the chemical reactivity and the diastereoselectivity of addition/elimination reactions in saturated polycyclic cages.



**Fig. 1.** Structural representations of tricyclo[3.3.1.1<sup>3,7</sup>]decane, widely referred as *adamantane* ring. Hydrogen atoms are shown in blue. Representations done by ChemBio3D Ultra. Energy minimized through MM2.

The physical and chemical properties of the adamantane nucleus have largely overshadowed the structure's contribution to the discovery of human therapeutics. Nevertheless in the last decades its application has become more and more significant in medicinal chemistry, where the adamantane ring is identified as a key structural subunit in several synthetic drugs for multiple targets.<sup>8,9,10</sup> But *prior* to an in-depth analysis of adamantane's role in drug discovery, it is worth to introduce it from its onset.

### 1.1 Origin of adamantane and first synthesis

Adamantane belongs to the lower diamondoids, which are a group of saturated cage-like hydrocarbon compounds with a diamond structure present in crude oil in highly variable concentrations (Fig. 2).<sup>11</sup> Adamantane owes its name to its structural relation with

<sup>1</sup> Landa, S. *Chem. Listy* **1933**, *27*, 415-418 and **1933**, *27*, 443-448.

<sup>2</sup> Fort, R. C., Jr.; Schleyer, P. von R. *Chem. Rev.* **1964**, 277-300.

<sup>3</sup> Adcock, W.; Kok, G. B. *J. Org. Chem.* **1987**, *52*, 356-364.

<sup>4</sup> Duddeck, H. *Tetrahedron* **1978**, *34*, 247-251.

<sup>5</sup> Kaselji, M.; Adcock, J. L.; Luo, H.; Zhang, H.; Li, H.; William, J. le N. *J. Am. Chem. Soc.* **1995**, *117*, 7088-7091.

<sup>6</sup> Adcock, W.; Trout, N. A. *Chem. Rev.* **1999**, *99*, 1415-1435.

<sup>7</sup> Gleicher, G. J.; Schleyer, P. von R. *J. Am. Chem. Soc.* **1967**, *89*, 582-593.

<sup>8</sup> Wishnok, J. J. *Chem. Educ.* **1973**, *50*, 780-781.

<sup>9</sup> Wanka, L.; Iqbal, K.; Schreiner, P. R. *Chem. Rev.* **2013**, *113*, 3516-3604.

<sup>10</sup> Lamoureux, G.; Artavia, G. *Curr. Med. Chem.* **2010**, *17*, 2967-2978.

<sup>11</sup> Dahl, J. E.; Liu, S. G.; Carlson, R. M. K. *Science* **2003**, *299*, 96-99.

the diamond, as it is derived from the Greek *adamantinos* (of steel, of diamond).<sup>12</sup> The smallest diamondoid, adamantane ( $C_{10}H_{16}$ ), was the first isolated from petroleum oil in the early 1930s and its amount was estimated to be 0.0004% by volume.<sup>13</sup>

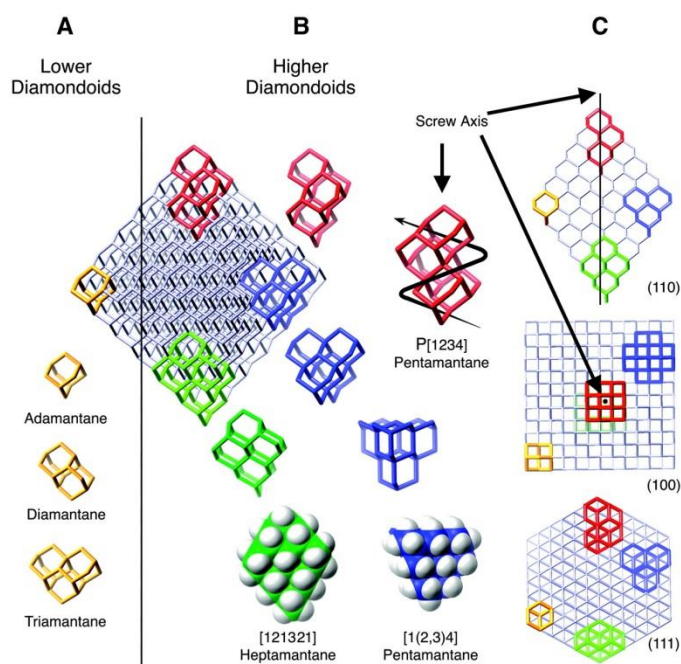


Fig. 2. The relation between the face-centered cubic diamond lattice and diamondoid structures.<sup>11</sup>

Nowadays diamondoids are of current interest because of their ready accessibility and the ease of selective functionalizations, yielding building blocks highly employed in nanotechnology and electronics.<sup>14</sup>

Nature is the oldest contributor to adamantane ring-containing substances and several natural products with biological activity incorporate an adamantane motif. Tetrodotoxin, the potent toxic principle from puffer fish (*Tora fugu*), contains an oxygenated adamantane framework in its structure,<sup>15</sup> and Nature-inspired heteroadamantane antiviral ansabaninin incorporates an azaadamantane moiety plus a “trioxadamantane” ring (Fig. 3).<sup>16</sup> Besides, other natural compounds enclose the adamantane hydrocarbon system itself, such as sampsonione I and hyperibone K, both of them showing moderate cytotoxicity against

<sup>12</sup> Senning, A. Elsevier's Dictionary of Chemoetymology; Elsevier: Oxford, **2007**.

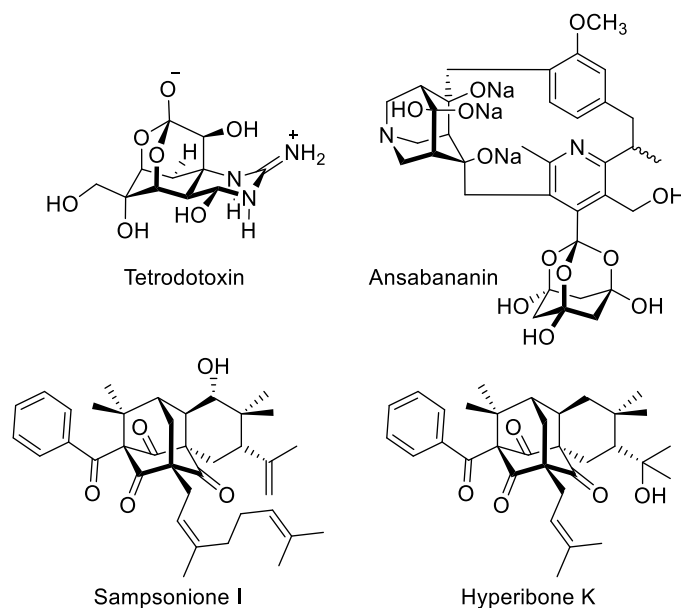
<sup>13</sup> Mair, B. J.; Shamaingar, M.; Krouskop, N. C.; Rossini, F. D. *Anal. Chem.* **1959**, *31*, 2082-2083.

<sup>14</sup> Schreiner, P. R.; Fokina, N. A.; Tkachenko, B. A.; Hausmann, H.; Serafin, M.; Dahl, J. E. P.; Liu, S.; Carlson, R. M. K.; Fokin, A. A. *J. Org. Chem.* **2006**, *71*, 6709-6720.

<sup>15</sup> Woodward, R. B.; Gougoutas, J. Z. *J. Am. Chem. Soc.* **1964**, *86*, 5030-5030.

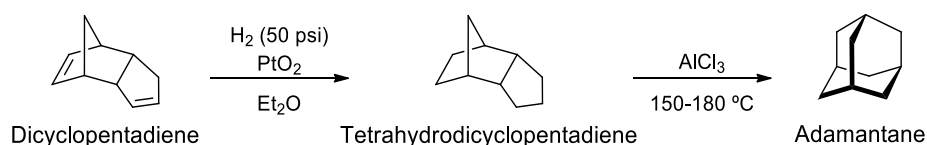
<sup>16</sup> Tanner, J. A.; Zheng, B.-J.; Zhou, J.; Watt, R. M.; Jiang, J.-Q.; Wong, K.-L.; Lin, Y.-P.; Lu, L.-Y.; He, M.-L.; Kung, H.-F.; Kesel, A. J.; Huang, J.-D. *Chem. Biol.* **2005**, *12*, 303-311.

different tumoral cell lines.<sup>17,18</sup> Even though adamantane is present in Nature, it is not considered as a “natural product” nor a “native biological substrate” but it is classified as a “mineral”.



**Fig. 3.** Nature-occurring and Nature-inspired adamantane-containing products.

Albeit adamantane was isolated from petroleum oil and synthesized chemically in earliest approaches,<sup>19</sup> its availability was limited until the Schleyer’s synthesis which allowed the wide study of adamantane and its functionalization.<sup>20,21</sup> The synthetic route entailed a Lewis-acid induced rearrangement of the C<sub>10</sub>H<sub>16</sub> precursor tetrahydrodicyclopentadiene (Scheme 1).



**Scheme 1.** Schleyer’s synthesis.

This ready access to the adamantane scaffold constituted its birth as a precursor in pharmaceutical sciences, while its derivatives expanded the application in medicinal chemistry thereof, and they are still doing so to date.

<sup>17</sup> Hu, L. H.; Sim, K. Y. *Org. Lett.* **1999**, *1*, 879-882.

<sup>18</sup> Tanaka, N.; Takaishi, Y.; Shikishima, Y.; Nakanishi, Y.; Bastow, K.; Lee, K.-H.; Honda, G.; Ito, M.; Takeda, Y.; Kodzhimatov, O. K.; Ashurmetov, O. *J. Nat. Prod.* **2004**, *67*, 1870-1875.

<sup>19</sup> Prelog, V.; Seiwerth, R. *Ber. Dtsch. Chem. Ges.* **1941**, *74*, 1644-1648.

<sup>20</sup> Schleyer, P. v. R. *J. Am. Chem. Soc.* **1957**, *79*, 3292-3292.

<sup>21</sup> Schleyer, P. v. R.; Donaldson, M. M.; Nicholas, R. D.; Cupas, C. *Org. Synth. Coll. Vol. V* **1973**, 16-19.

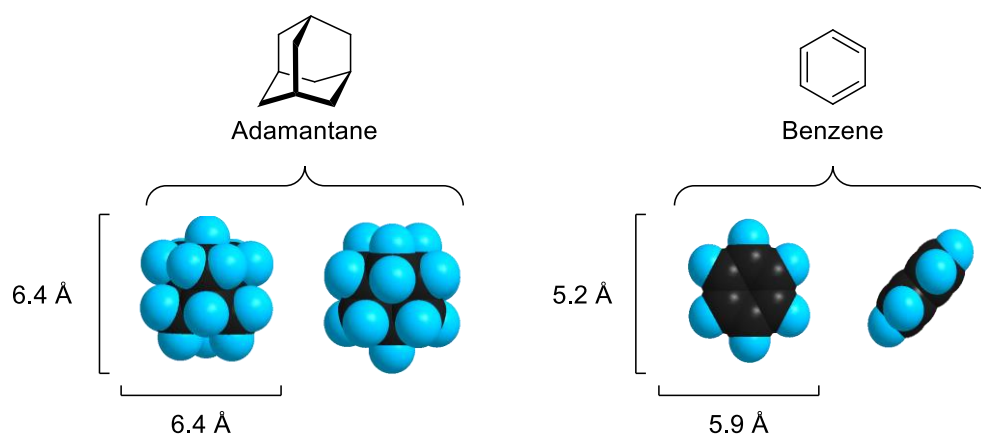


## 1.2 Adamantane's physicochemical properties and its multidimensional value

The closing section will provide the physicochemical profile of the adamantane moiety, the structural relationships between adamantane-bearing compounds and protein targets as well as the general aspects in the pharmacokinetics of the adamantane group, with the aim of supplying an overview of the role of this valuable ring.

### 1.2.1 Physicochemical properties

The four cyclohexanes in chair conformation contained within the adamantane ring are the source of its uniqueness in that it is both rigid and virtually stress-free. If we bear in mind the three-dimensional structure in figure 1, adamantane possesses a *spherical shape* with a diameter of about 6.4 Å.<sup>22</sup> Compared to a benzene molecule, the adamantane ring displays a larger volume not depending on its orientation, whereas the benzene ring is planar (Fig. 4).<sup>10</sup>



**Fig. 4.** Structural representations of adamantane and benzene in space-filling mode and their dimensions. Hydrogen bonds are shown in blue. Representations done by ChemBio3D Ultra. Energy minimized through MM2.

*Polarizability* is another property that affects the binding between the ligand or drug and its target, not only influencing the hydrophobicity but also the biological activity. Polarization is the phenomenon whereby the charge distribution in a molecule is modified due to the presence of an external field.<sup>23</sup> Whereas benzene shows a quadrupole, which forms  $\pi$ -type interactions, adamantane presents an octapole, with a higher polarizability value than benzene, which indicates that the electrostatic forces between adamantane and its target could have a greater effect on the binding than previously thought. It is worth to

<sup>22</sup> Morel-Desrosiers, N.; Morel, J.-P. *J. Solution Chem.* **1979**, *8*, 579-592.

<sup>23</sup> Leach, A. R. *Compr. Med. Chem. II* **2007**, *4*, 87-118.

highlight that the interest in the polarizable force fields for small molecules in organic and biochemical systems is currently increasing, drawing the attention of many scientists.<sup>24,25</sup>

Nevertheless, the most significant property that characterizes the adamantane group is its high *lipophilicity*. Considered the most important drug-like physical property, lipophilicity is one of the main criteria relevant for oral bioavailability, included in the well-known Lipinski's rules.<sup>26</sup> The lipophilic value is commonly estimated by the logarithm of the octanol/water partition coefficient (log P), which is defined as the ratio of non-ionized drug distributed between octanol and water phases at equilibrium. Higher values imply greater lipophilicity and often a log P value of 5 or higher is considered as an upper limit of desired lipophilicity in drug discovery.<sup>27</sup> Generally, an adamantane-bearing compound will be more lipophilic than the des-adamantyl analogue. Calculation of the hydrophobic substituent constant determined by non-empirical methods for the adamantane group, the clog P (calculated log P) measures of the known adamantane-containing compounds and the des-adamantyl derivatives, revealed a  $\pi_{\text{adamantyl}}$  value of 3.1.<sup>28</sup> That is, the incorporation of an adamantane motif will increase by about 3.1 log units the log P value of any given drug. As a consequence, adamantane is considered as a "lipophilic carrier" that allows poorly absorbed drugs to slipping across cell membranes, such as the Blood-Brain Barrier (BBB) enhancing Central Nervous System (CNS) access.<sup>29,30</sup>

Inasmuch as clog P is a composite property dependent on molecular size, polarity and hydrogen bonding,<sup>31</sup> it is related to *solubility*. In almost all cases the adamantane group lowers the clog P compared to the linear constitutional isomer (Fig. 5). This effect is partly due to the fact that the adamantane-based compounds feature a close lateral packing, with the interstitial space present in solution increasing the propensity towards solvation. Hence molecules hosting an adamantane moiety will have solubility properties more tractable in medicinal chemistry setting compared to other C10-based frameworks.<sup>28</sup>

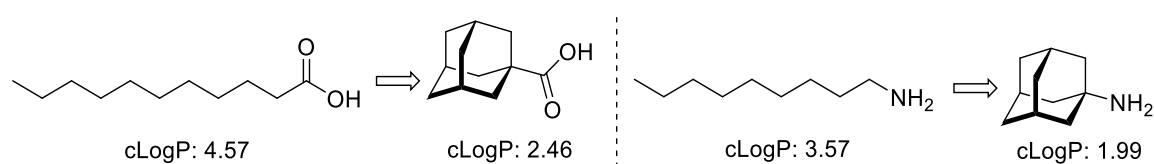


Fig. 5. clog P values of adamantane derivatives and their linear analogues, calculated using Bio-Loom<sup>®</sup>.

<sup>24</sup> Kaminski, G. A.; Stern, H. A.; Berne, B. J.; Friesner, R. A. *J. Phys. Chem. A* **2004**, *108*, 621-627.

<sup>25</sup> Maple, J. R.; Cao, Y.; Damm, W.; Halgren, T. A.; Kaminski, G. A.; Zhang, L. Y.; Friesner, R. A. *J. Chem. Theory Comput.* **2005**, *1*, 694-715.

<sup>26</sup> Lipinski, C. A.; Lombardo, F.; Dominy, B. W.; Feeney, P. J. *Adv. Drug Deliv. Rev.* **1997**, *23*, 3-25.

<sup>27</sup> Leeson, P. D.; Springthorpe, B. *Nat. Rev. Drug Discov.* **2007**, *6*, 881-890.

<sup>28</sup> Liu, J.; Obando, D.; Liao, V.; Lifa, T.; Codd, R. *Eur. J. Med. Chem.* **2011**, *46*, 1949-1963.

<sup>29</sup> Terasaki, T.; Pardridge, W. M. *J. Drug Targets* **2000**, *8*, 353-355.

<sup>30</sup> Tsuzuki, N.; Hama, T.; Kawada, M.; Hasui, A.; Konishi, R.; Shiwa, S.; Ochi, Y.; Futaki, S.; Kitagawa, K. *J. Pharm. Sci.* **1994**, *83*, 481-484.

<sup>31</sup> Abraham, M. H.; Chadha, H. S.; Whiting, G. S.; Mitchell, R. C. *J. Pharm. Sci.* **1994**, *83*, 1085-1100.

Worth to bear in mind, is the fact that, notwithstanding the increase in the solubility of the adamantane-containing compounds with respect to their linear structural isomers as a result of the above mentioned, incorporation of an adamantane ring in any given structure will compromise the water solubility of the molecule since the log P is enlarged by about 3.1 log units, which represents a considerable increment in drug design.

### 1.2.2 Adamantane ring as a pharmacophore

The three-dimensional structure is essential for the sheer activity of a drug, exerted by the fit into the receptor's binding site. The target-ligand interaction was generally described as the "key-lock" model, but currently the "induced fit" principle has been more accepted, which expresses a more dynamic understanding of the receptor–ligand interactions.<sup>32</sup> Accordingly, the adamantane core has been used to organize the spatial position of the functional groups that form the pharmacophore of a lead molecule, providing an ideal skeleton for this purpose. That is, to fix the molecular features that are essential for molecular recognition.<sup>10</sup> Thus adamantane scaffold plays a decisive role in the three-dimensional adjustment of the pharmacophores to its protein target. The favourable chemical and geometric properties of adamantane make it possible to introduce several functional groups, consisting drug, targeting part, linker, or similar, without undesirable interactions between such groups.<sup>33</sup>

Adamantane's physicochemical properties and structural uniqueness are in consequence directly related to its binding mode with specific therapeutic targets. Firstly, adamantane moiety can bind to hydrophobic pockets of *enzymes*, and secondly it can affect *ion channels* by disrupting the transmembrane flow. Worth to highlight is the difference between the term "blocker" and the term "antagonist". The first locution concerns the alteration of the permeability of the ion channels by the interaction of the ligand with these. The second term refers to these drugs binding to an enzyme or receptor, which can control an ion channel, preventing the binding of the natural mediator and thus eliminating the physiological response related to the enzyme/ion channel. A deeper but brief look into adamantane's role in medicinal chemistry will be discussed later on.

### 1.2.3 ADME properties of adamantane-containing compounds

As most part of the drugs that are administered, compounds incorporating adamantane as a building block suffer from metabolism once they are inside the organism. With regard to *Absorption* and *Distribution*, incorporation of the cage-shaped adamantane nucleus into medicinal agents has provided a viable approach for designing molecules that can access lipophilic cell membranes, as aforementioned. Therefore, targets of the CNS are being addressed today with, remarkably structurally simple adamantane derivatives, such as

---

<sup>32</sup> Spyrakis, F.; Bidon-Chanal, A.; Barril, X.; Luque, F. J. *Curr. Top. Med. Chem.* **2011**, *11*, 192-210.

<sup>33</sup> Mansoori, G. A.; George, T. F.; Assoufid, L.; Zhang, G. *Molecular building blocks for nanotechnology. From diamondoids to nanoscale materials and applications.* Springer: New York, **2007**.

amantadine and memantine, with anti-Parkinson and anti-Alzheimer activities respectively (Fig. 6).

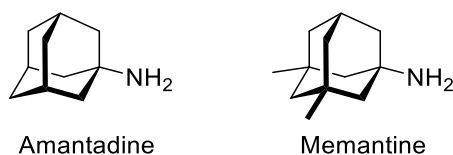


Fig. 6. Structures of amantadine and memantine.

In terms of *Metabolism* and *Excretion*, the cytochrome P-450 is believed to control the oxidative metabolism for a rapid excretion of the adamantane derivatives,<sup>34</sup> mainly through hydroxylation with mono- and dihydroxylated derivatives as common metabolites. As it can be deduced from the crystal structure of CYP450<sub>CAM</sub> (bacterial camphor hydroxylase P-450) complexed with adamantane, this process is generally not selective and, in the absence of further functional groups in the drug that could orientate the cage hydrocarbon, several sites are being hydroxylated, as can be seen with, for example, amantadine,<sup>35</sup> memantine,<sup>36</sup> rimantadine,<sup>37,38</sup> and saxagliptin<sup>39</sup> (Fig. 7).

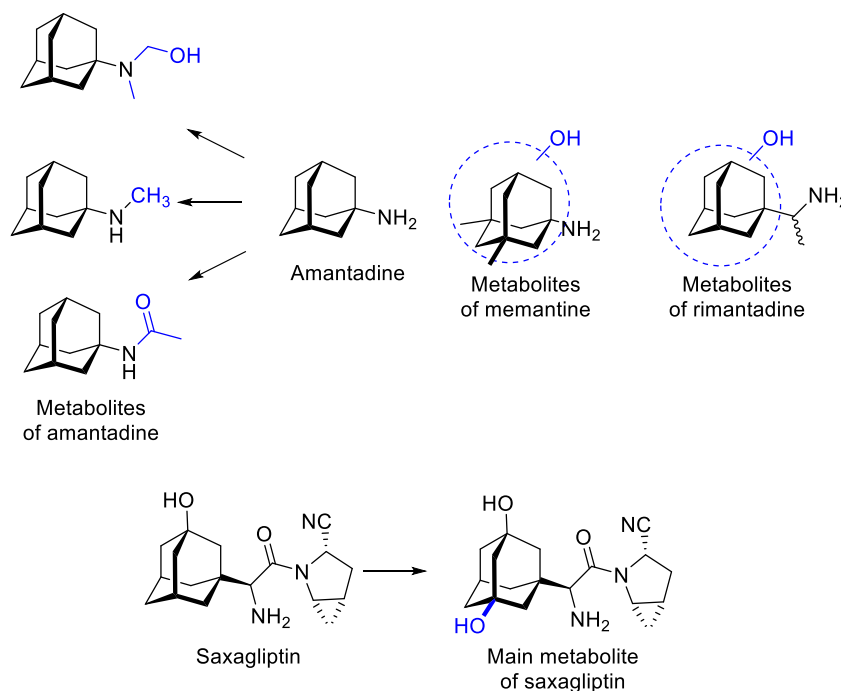


Fig. 7. Main metabolites of amantadine, memantine, rimantadine, and saxagliptin.

<sup>34</sup> Raags, R.; Poulos, T. L. *Biochemistry* **1991**, *30*, 2674-2684.

<sup>35</sup> Suckow, R. F. J. *Chromatogr. B Biomed. Sci. Appl.* **2001**, *764*, 313-325.

<sup>36</sup> Sturm, G.; Schollmeyer, J. D.; Wesemann, W. *IRCS Medical Science: Library Compendium*, **1976**, *4*, 55.

<sup>37</sup> Hayden, F. G.; Minocha, A.; Spyker, D. A.; Hoffman, H. E. *Antimicrob. Agents Chemother.* **1985**, *28*, 216-221.

<sup>38</sup> Rubio, F. A.; Choma, N.; Fukuda, E. K. J. *Chromatogr.* **1989**, *497*, 147-157.

<sup>39</sup> Su, H.; Boulton, D. W.; Barros, A. Jr.; Wang, L.; Cao, K.; Bonacorsi, S. J. Jr.; Iyer, R. A.; Humphreys, W. G.; Christopher, L. J. *Drug Metab. Dispos.* **2012**, *40*, 1345-1356.

Metabolism studies have shown that the bridgehead hydroxylation (tertiary carbon) is favoured over the secondary carbon positions, producing water-soluble hydroxyadamantane derivatives in the liver, which are then easily excreted. This hydroxylation mechanism is prevalent for electron-rich adamantane cores.<sup>40</sup> As an example, while amantadine is not metabolized by hydroxylation of the adamantane nucleus, cage hydroxylation is the main metabolic degradation for its dimethyl derivative memantine.

In addition, the steric bulk of the adamantane motif can reduce the amidase or esterase enzyme activity in the regions proximal to the scaffold, especially where the adamantyl group has been appended to the parent drug *via* an amide or an ester bond. So the rigid hydrocarbon skeleton protects functional groups in its proximity from metabolic cleavage, enhancing the duration of action of peptide-derived drugs, among others, that feature an adamantane ring.<sup>41</sup>

### 1.3 Medicinal chemistry of adamantane: the promiscuous lipophilic pellet

#### 1.3.1 Clinically approved adamantane-based drugs

At the time of writing this thesis, eight drugs are marketed featuring the adamantane motif. A brief introduction of each one will be commented below.

- *Amantadine*: considered the birth of the adamantane derivatives in medicinal chemistry, amantadine constituted the structurally simplest monofunctionalized adamantane drug with application in medicinal chemistry. Discovered in the early 1960s,<sup>42</sup> 1-aminoadamantane was found to be a selective antiviral, especially against *influenza A* and rubella virus. Related to *influenza A* virus, the mechanism of action consists in the blockade of the M2 ion channel. This protein is essential for viral replication and is involved in the endosomal uptake of protons, thus acidifying the interior of the virus that leads to the uncoating of the viral genetic material.<sup>43,44</sup> The inhibitory activity of amantadine is by different mechanisms; the adamantane hydrophobic sphere physically occludes the transmembrane flux of protons, locks the protein conformation in a single state hampering its plasticity, and perturbs the pK<sub>a</sub> of the His37 tetrad by H-bonding through the entry of water cluster.<sup>45</sup>

Furthermore, amantadine was found to be useful for the treatment of Parkinson's disease when in 1968 a patient who was taking amantadine to prevent the flu, experienced a remarkably remission in her symptoms of rigidity, tremor and akinesia.<sup>46</sup> This fortuitous

<sup>40</sup> Fokin, A. A.; Schreiner, P. R. *Chem. Rev.* **2002**, *102*, 1551-1593.

<sup>41</sup> Nagasawa, H. T.; Elberling, J. A.; Shirota, F. N. *J. Med. Chem.* **1975**, *18*, 826-830.

<sup>42</sup> Davies, W. L.; Grunert, R. R.; Haff, R. F.; McGahen, J. W.; Neumayer, E. M.; Paulshock, N.; Watts, J. C.; Wood, T. R.; Hermann, E. C.; Hoffman, C. E. *Science* **1964**, *144*, 862-863.

<sup>43</sup> De Clercq, E. *Nat. Rev. Drug Discov.* **2006**, *5*, 1015-1025.

<sup>44</sup> Cady, S. D.; Luo, W.; Hu, F.; Hong, M. *Biochemistry* **2009**, *48*, 7356-7364.

<sup>45</sup> Cady, S. D.; Wang, J.; Wu, Y.; DeGrado, W. F.; Hong, M. *J. Am. Chem. Soc.* **2011**, *133*, 4274-4284.

<sup>46</sup> Schwab, R. S.; England, A. C. Jr.; Poskanzer, D. C.; Young, R. R. *J. Am. Med. Assoc.* **1969**, *208*, 1168-1170.

finding marked the beginning of medicinal chemistry of adamantane derivatives in the context of diseases affecting the CNS, accounting for its lipophilicity and BBB-penetration, enhancing properties of the adamantane motif. In Parkinson's disease, the Food and Drugs Administration (FDA) approved amantadine has been demonstrated to act directly on the D2 dopamine receptors, resulting in enhanced dopamine release, while inhibiting post-synaptic uptake.

Besides, amantadine has antiglutamatergic properties *via* the non-competitive antagonism of *N*-methyl-D-aspartic acid (NMDA) receptors,<sup>47,48</sup> and displays trypanocidal activity along with rimantadine and memantine.<sup>49,50</sup> However, amantadine is not clinically used exploiting these properties.

- *Memantine*: the 3,5-dimethyl-1-aminoadamantane was approved in 2002 by the European Medicines Agency (EMA) and in 2003 by the FDA for use in treatment of patients with moderate-to-severe Alzheimer's disease (AD). Memantine is a non-competitive, low- to moderate-affinity NMDA receptor (NMDAR) antagonist, with strong voltage dependency and rapid blocking and unblocking kinetics.<sup>51,52</sup> Memantine is efficient in neurological diseases that are mediated, at least in part, by overactivation of NMDARs, producing excessive Ca<sup>2+</sup> influx through the receptor's associated ion channel and consequent free-radical formation, leading to cellular damage and death.<sup>53</sup> The NMDA receptor antagonism is a topic of the present thesis, hence it will be discussed further on.

- *Rimantadine*: soon after amantadine introduction in clinic, several compounds were developed with the insertion of a bridge of one or more carbon atoms between the 1-adamantyl and the amino group, which led to compounds with generally high antiviral activity, with rimantadine outperforming amantadine in terms of activity (Fig. 8).<sup>54</sup> The  $\alpha$ -methyl adamantanemethanamine have been found to be active among a wider range of viruses, although its main use is for the treatment and prophylaxis of *influenza A* infection.<sup>43</sup> Compared to amantadine, rimantadine has a comparable or higher oral availability, produces fewer side effects and is absorbed well from the gastrointestinal tract.<sup>55</sup> As well as amantadine, rimantadine is also a trypanocidal agent, whose activity is generally associated with a blockade of a membrane ion channel. *Trypanosoma brucei* is carried by the Tse-tse fly

---

<sup>47</sup> Kornhuber, J.; Bormann, J.; Hubers, M.; Rusche, K.; Riederer, P. *J Pharmacol.* **1991**, *206*, 297-300.

<sup>48</sup> Blanpied, T. A.; Clarke, R. J.; Johnson, J. W. *J. Neurosci.* **2005**, *25*, 3312-3322.

<sup>49</sup> Kelly, J. M.; Miles, M. A.; Skinner, A. C. *Antimicrob. Agents Chemother.* **1999**, *43*, 985-987.

<sup>50</sup> Kelly, J. M.; Quack, G.; Miles, M. A. *Antimicrob. Agents Chemother.* **2001**, *45*, 1360-1366.

<sup>51</sup> Rammes, G.; Danysz, W.; Parsons, C. G. *Curr. Neuropharmacol.* **2008**, *6*, 55-78.

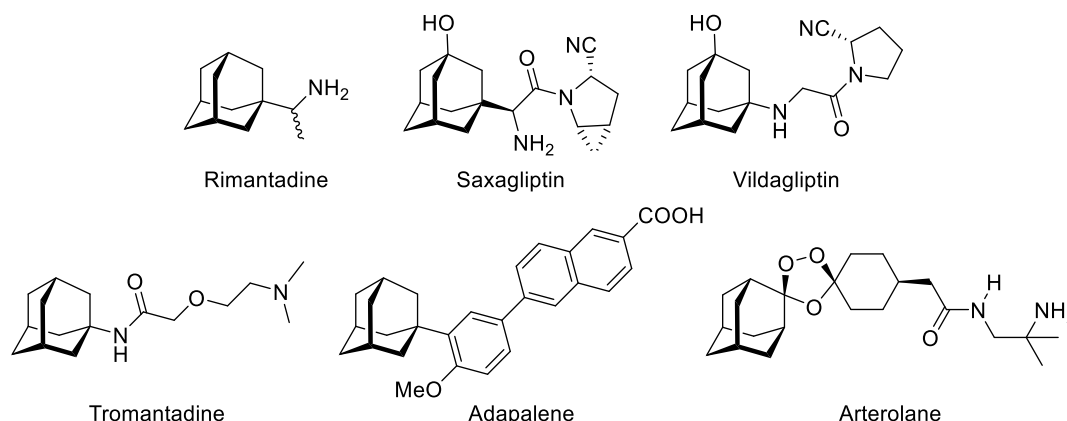
<sup>52</sup> Herrmann, N.; Li, A.; Lanctôt, K. *Expert Opin. Pharmacother.* **2011**, *12*, 787-800.

<sup>53</sup> Lipton, S. A. *Nat. Rev. Drug Discov.* **2006**, *5*, 160-170.

<sup>54</sup> Tsunoda, A.; Maassab, H. F.; Cochran, K. W.; Eveland, W. C. *Antimicrob. Agents Chemother.* **1965**, *5*, 553-560.

<sup>55</sup> Hayden, F. G.; Minocha, A.; Spyker, D. A.; Hoffman, H. E. *Antimicrob. Agents Chemother.* **1985**, *28*, 216-221.

and causes the so-called sleeping sickness, which is a serious health issue in many areas of the sub-Saharan Africa, considered as a “neglected disease”.<sup>56</sup>



**Fig. 8.** Structures of the adamantane-based drugs rimantadine, saxagliptin, vildagliptin, tromantadine, adapalene and arterolane.

• *Saxagliptin and vildagliptin*: in the multibillion dollar market of type 2 Diabetes Mellitus (T2DM), big pharmaceutical companies have initiated drug development programs around dipeptidyl peptidase IV (DPP-IV) inhibitors.<sup>57</sup> The activity of DPP-IV negatively affects glucose homeostasis, and its inhibition increases the levels of incretin hormones, such as glucagon-like peptide-1. This target is successfully hit by adamantane compounds; saxagliptin and vildagliptin, which have been approved in recent years.<sup>58,59</sup> The adamantyl group in saxagliptin and vildagliptin serves a dual role in terms of directing inter- and intramolecular interactions in the DPP-IV binding site and in reducing the propensity towards intramolecular cyclisation reactions, by means of the encumbrance supplied by the adamantane moiety (Fig. 9).<sup>60</sup> The production of the inactive cyclic amidine form of saxagliptin has been observed during process-scale production.

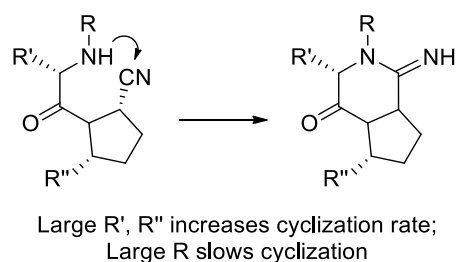
<sup>56</sup> Barret, M. P.; Burchmore, R. J. S.; Stich, A.; Lazzari, J. O.; Frasc, A. C.; Cazzulo, J. J.; Krishna, S. *Lancet* **2003**, *362*, 1469-1480.

<sup>57</sup> von Geldern, T. W.; Trevillyan, J. M. *Drug Dev. Res.* **2006**, *67*, 627-642.

<sup>58</sup> Villhauer, E. B.; Brinkman, J. A.; Naderi, G. B.; Burkey, B. F.; Dunning, B. E.; Prasad, K.; Mangold, B. L.; Russell, M. E.; Hughes, T. E. *J. Med. Chem.* **2003**, *46*, 2774-2789.

<sup>59</sup> Augeri, D. J.; Robl, J. A.; Betebenner, D. A.; Magnin, D. R.; Khanna, A.; Robertson, J. G.; Wang, A.; Simpkins, L. M.; Taunk, P.; Huang, Q.; Han, S.-P.; Abboa-Offei, B.; Cap, M.; Xin, L.; Tao, L.; Tozzo, E.; Welzel, G. E.; Egan, D. M.; Marcinkeviciene, J.; Chang, S. Y.; Biller, S. A.; Kirby, M. S.; Parker, R. A.; Hamann, L. G. *J. Med. Chem.* **2005**, *48*, 5025-5037.

<sup>60</sup> Metzler, W. J.; Yanchunas, J.; Weigelt, C.; Kish, K.; Klei, H. E.; Xie, D.; Zhang, Y.; Corbett, M.; Tamura, J. K.; He, B.; Hamann, L. G.; Kirby, M. S.; Marcinkeviciene, J. *Protein Sci.* **2008**, *17*, 240-250.



**Fig. 9.** Internal cyclization can play a decisive role in inactivating cyanopyrrolidine-based DPP-IV inhibitors.

• *Tromantadine*: this aminoadamantane marks the third adamantane derivative that was successfully introduced to the market, even though its identification as an anti-*Herpes simplex* agent was not so much the result of research specifically addressing this issue. Tromantadine is a derivative of amantadine that is used topically for the treatment of the herpes virus, being inactive against *influenza A*.<sup>61</sup> Its precise mechanism of action is still unknown, despite numerous studies taking aim at it. However, tromantadine apparently exerts, at least in part, its activity through influencing the fusion of lipid membranes.<sup>62</sup> Tromantadine is particularly interesting for the treatment of aciclovir-resistant strains since it does not require a viral kinase to become activated, unlike aciclovir.

• *Adapalene*: this adamantyl retinoid is used for the topical treatment of *Acne vulgaris* sold as hydrogel in combination with the antimicrobial benzoyl peroxide.<sup>63</sup> Its pharmacological and chemical properties include photochemical stability, local activity, high stability, and as expected, low local side-effect profile. The lipophilicity of the adamantyl group contributes to the low percutaneous flux of adapalene and an improved penetration into the pilosebaceous follicles.<sup>64</sup>

• *Arterolane*: this adamantyl ozonide has been recently approved for the treatment of *Plasmodium falciparum* infection. It constitutes the first Indian new molecular entity that has reached the market. Since 2014, this anti-malaria drug is available combined with piperazine phosphate in African and Asian countries.<sup>65</sup>

### 1.3.2 Adamantane-containing candidates in development

The quest for new applications of the adamantane ring is an issue on the rise in medicinal chemistry. Thanks to the great efforts from the academy and industry, many

<sup>61</sup> Rosenthal, K. S.; Sokol, M. S.; Ingram, R. L.; Subramanian, R.; Fort, R. C. *Antimicrob. Agents Chemother.* **1982**, *22*, 1031-1036.

<sup>62</sup> Ickes, D. E.; Venetta, T. M.; Phonphok, Y.; Rosenthal, K. S. *Antiviral Res.* **1990**, *14*, 75-85.

<sup>63</sup> Shroot, B.; Michel, S. *J. Am. Acad. Dermatol.* **1997**, *36* (Suppl.), S96-S103.

<sup>64</sup> Piérard, G. E.; Piérard-Franchimont, C.; Paquet, P.; Quatresooz, P. *Expert Opin. Drug Metab. Toxicol.* **2009**, *5*, 1565-1575.

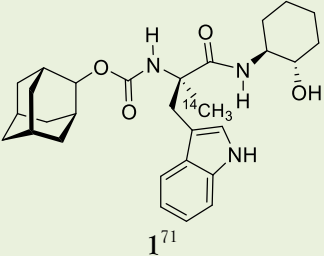
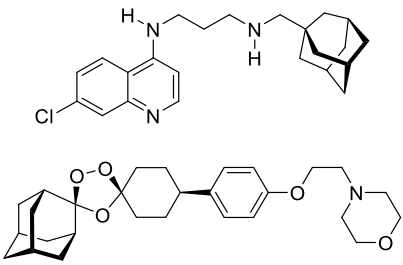
<sup>65</sup> Wells, T. N.; Alonso, P. L.; Gutteridge, W. E. *Nat. Rev. Drug Discovery* **2009**, *8*, 879-891.



adamantyl-based compounds have been studied as potential therapeutics for conditions including cancer,<sup>66</sup> neurological conditions, hypertension,<sup>67</sup> malaria,<sup>68,69</sup> and tuberculosis.<sup>70</sup>

For the sake of brevity, table 1 encloses some of the main targets that are hit by adamantane-bearing compounds that are still under development, as well as the pharmacodynamic (PD) and pharmacokinetic (PK) modulation exerted by adamantane. For a deeper study on the subject, the reading of the reviews by Wanka, Iqbal and Schreiner,<sup>9</sup> Lamoureux and Artavia,<sup>10</sup> and Codd and coworkers, is recommended.<sup>28</sup>

**Table 1.** Representative adamantane-based biologically active compounds. CCK-B: cholecystokinins B; ROS: reactive oxygen species.

Compound	Target	Condition	Main features
 <p>1<sup>71</sup></p>	CCK-B receptor	Anxiety	Neuropeptide with better penetration of the BBB
 <p>2 (top) and 3 (bottom)<sup>72,73</sup></p>	<i>Plasmodium falciparum</i>	Malaria	Improved pharmacological profile, whether displaying greater oral bioavailability or higher activity against resistant strains

<sup>66</sup> Glennon, R. A. *Drug Dev. Res.* **1992**, *26*, 251-274.

<sup>67</sup> Imig, J. D.; Zhao, X.; Zaharis, C. Z.; Olearczyk, J. J.; Pollock, D. M.; Newman, J. W.; Kim, I. H.; Watanabe, T.; Hammock, B. D. *Hypertension* **2005**, *46*, 975-981.

<sup>68</sup> Fieser, L. F.; Nazer, M. Z.; Archer, S.; Berberian, D. A.; Slighter, R. G. *J. Med. Chem.* **1967**, *10*, 517-521.

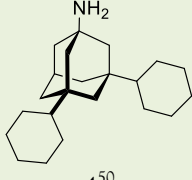
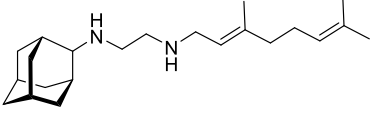
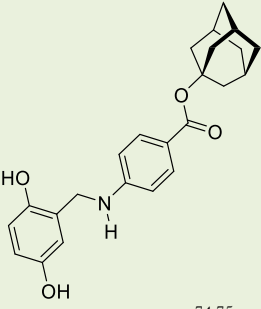
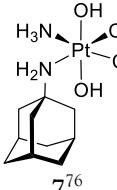
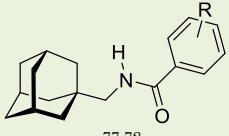
<sup>69</sup> Wang, X.; Dong, Y.; Wittlin, S.; Creek, D.; Chollet, J.; Charman, S. A.; SantoTomas, J.; Scheurer, C.; Snyder, C.; Vennerstrom, J. L. *J. Med. Chem.* **2007**, *50*, 5840-5847.

<sup>70</sup> Protopopova, M.; Hanrahan, C.; Nikonenko, B.; Samala, R.; Chen, P.; Gearhart, J.; Einck, L.; Nacy, C. A. *J. Antimicrob. Chemother.* **2005**, *56*, 968-974.

<sup>71</sup> Trivedi, B. K.; Padia, J. K.; Holmes, A.; Rose, S.; Wright, D. S.; Hinton, J. P.; Pritchard, M. C.; Eden, J. M.; Kneen, C.; Webdale, L.; Suman-Chauhan, N.; Boden, P.; Singh, L.; Field, M. J.; Hill, D. *J. Med. Chem.* **1998**, *41*, 38-45.

<sup>72</sup> Solaja, B. A.; Opsenica, D.; Smith, K. S.; Milhous, W. K.; Terzic, N.; Opsenica, I.; Burnett, J. C.; Nuss, J.; Gussio, R.; Bavari, S. *J. Med. Chem.* **2008**, *51*, 4388-4391.

<sup>73</sup> Moehrle, J. J.; Duparc, S.; Siethoff, C.; van Giersbergen, P. L.; Craft, J. C.; Arbe-Barnes, S.; Charman, S. A.; Gutierrez, M.; Wittlin, S.; Vennertrom, J. L. *Br. J. Clin. Pharmacol.* **2012**, *75*, 524-537.

 <p>4<sup>50</sup></p>	<i>Trypanosoma brucei</i>	Sleeping sickness	Improvement in the anti-parasitic activity
 <p>5<sup>70</sup></p>	<i>Mycobacterium tuberculosis</i>	Tuberculosis	Improved <i>in vivo</i> potency and limited <i>in vitro</i> and <i>in vivo</i> toxicity
 <p>6 (adaphostin)<sup>74,75</sup></p>	Tyrosine kinase and /or ROS	Cancer	Less susceptible of hydrolysis by means of a superior lipophilicity and encumbrance
 <p>7<sup>76</sup></p>	DNA	Cancer	Cisplatin-analogue with improved therapeutic index and oral bioavailability
 <p>8<sup>77,78</sup></p>	P2X <sub>7</sub> receptor	Inflammation	Good balance between potency, molecular weight and lipophilicity

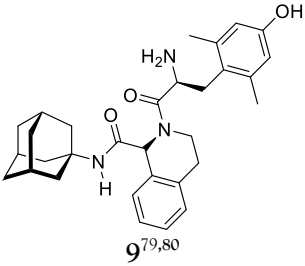
<sup>74</sup> Le, S. B.; Hailer, M. K.; Buhrow, S.; Wang, Q.; Flatten, K.; Pediaditakis, P.; Bible, K. C.; Lewis, L. D.; Sausville, E. A.; Pang, Y. P.; Ames, M. M.; Lemasters, J. J.; Holmuhamedov, E. L.; Kaufmann, S. H. *J. Biol. Chem.* **2007**, *282*, 8860-8872.

<sup>75</sup> Kaur, G.; Narayanan, V. L.; Risbood, P. A.; Hollingshead, M. G.; Stinson, S. F.; Varma, R. K.; Sausville, E. A. *Bioorg. Med. Chem.* **2005**, *13*, 1749-1761.

<sup>76</sup> Kelland, L. R.; Barnard, F. J.; Evans, I. G.; Murrer, B. A.; Theobald, B. R. C.; Wyer, S. B.; Goddard, P. M.; Jones, M.; Valenti, M.; Bryant, A.; Rogers, P. M.; Harrap, K. R. *J. Med. Chem.* **1995**, *38*, 3016-3024.

<sup>77</sup> Guile, S. D.; Alcaraz, L.; Birkinshaw, T. N.; Bowers, K. C.; Ebdon, M. R.; Furber, M.; Stocks, M. J. *J. Med. Chem.* **2009**, *52*, 3123-3141.

<sup>78</sup> Mehta, N.; Kaur, M.; Singh, M.; Chand, S.; Vyas, B.; Silakari, P.; Bahia, M. S.; Silakari, O. *Bioorg. Med. Chem.* **2014**, *22*, 54-88.

	$\delta/\mu$ -opioid receptors	Analgesia	Modification of the selectivity pattern, and better in crossing the BBB
---	--------------------------------	-----------	---

Other protein targets than the already introduced are hit by adamantane-based compounds. An emerging field is the inhibition of enzymes with therapeutically interesting profiles, such as the  $11\beta$ -hydroxysteroid dehydrogenase type 1 ( $11\beta$ -HSD1) and the soluble epoxide hydrolase (sEH). These targets will be two independent topics of this manuscript, hence they will be discussed in the next chapters.

All these examples prove that the value of the adamantyl group in drug design is multifunctional, and that its study is of major importance to understand the influence of this simple, yet potent, structural element.

#### 1.4 Not all that glitters is gold: a moot point of perfection

In the previous sections we have gone through the value of the adamantane nucleus in medicinal chemistry, and the early examples of adamantane-based compounds have shown that this precious ring modulates different properties essential for drug behaviour within the organism. Despite all the advantages the adamantane offers, a few drawbacks are identified, which render the adamantane group not as a magic bullet but as a ring whose introduction should be given careful considerations. The following section encloses these disadvantages and the way they affect to the drug discovery process.

##### 1.4.1 High lipophilicity compromises PK properties

Lipophilicity is the most critical property from the famous Lipinski's rule or 'rule of five',<sup>26</sup> which states that drug permeability and absorption are threatened if:

- i.  $\text{clog } P$  is  $> 5$ ;
- ii. molecular weight is  $> 500$  Da;
- iii. number of hydrogen-bond donors is  $> 5$ ;
- iv. number of hydrogen-bond acceptors is  $> 10$ .

Since its appearance, several studies have highlighted the polar surface area (PSA) and the number of rotatable bonds as other key parameters that control permeability and

<sup>79</sup> Horvat, S.; Varga-Defterdarovic, L.; Horvat, J.; Jukic, R.; Kantoci, D.; Chung, N. N.; Schiller, P. W.; Biesert, L.; Pfutzner, A.; Suhartono, H.; Rubsamen-Waigmann, H. *J. Pept. Sci.* **1995**, *1*, 303-310.

<sup>80</sup> Lovekamp, T.; Cooper, P. S.; Hardison, J.; Bryant, S. D.; Guerrini, R.; Balboni, G.; Salvadori, S.; Lazarus, L. H. *Brain Res.* **2001**, *902*, 131-134.

absorption.<sup>81</sup> Thus, overall oral bioavailability can be simply predicted by number of rule-of-five violations, PSA and number of rotatable bonds. Although these physical properties play an important role in the assessment of the drug bioavailability, lipophilicity stands out among them since it is decisive to avoid later attrition during the discovery of drug candidates, as numerous studies have confirmed it.<sup>82</sup>

During the last two decades, clog P has barely changed for approved oral drugs. However, there is a noted trend that lipophilicity increases as candidate molecules progress through clinical trials. A recent study published in 2007 compared the physicochemical properties of more than 500 marketed drugs and compounds in development from big pharmaceutical companies such as GlaxoSmithKline (GSK), Merck, AstraZeneca and Pfizer.<sup>27</sup> The authors observed that the average clog P value was higher than 4.1 in the patent literature, whereas the more recent drugs have a median clog P of 3.1 (Fig. 10).

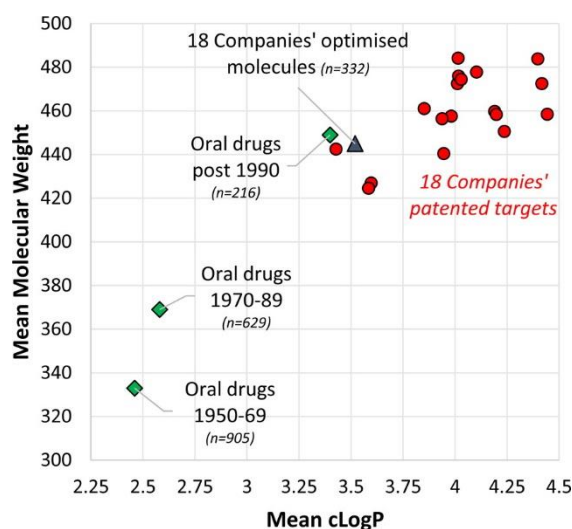


Fig. 10. Mean molecular weight and clog P values of oral drugs according to time of publication.<sup>83</sup>

On the other hand, a comparison of marketed oral drugs with compounds in early stages of the drug discovery shows that high lipophilicity (clog P > 4) leads to compounds with:

- i. poor solubility;
- ii. rapid metabolic turnover;
- iii. low bioavailability;
- iv. off-target promiscuity.

<sup>81</sup> Lu, J. J.; Crimin, K.; Goodwin, J. T.; Crivori, P.; Orrenius, C.; Xing, L.; Tandler, P. J.; Vidmar, T. J.; Amore, B. M.; Wilson, A. G. E.; Stouten, P. F. W.; Burton, P. S. *J. Med. Chem.* **2004**, *47*, 6104-6107.

<sup>82</sup> Arnott, J. A.; Planey, S. L. *Expert Opin. Drug Discov.* **2012**, *7*, 863-875.

<sup>83</sup> (a) Leeson, P. D.; Young, R. J. *ACS Med. Chem. Lett.* **2015**, *6*, 722-725. (b) Waring, M. J.; Arrowsmith, J.; Leach, A. R.; Leeson, P. D.; Mandrell, S.; Owen, R. M.; Pairaudeau, G.; Pennie, W. D.; Pickett, S. D.; Wang, J.; Wallace, O.; Weir, A. *Nat. Rev. Drug Discov.* **2015**, *14*, 475-486.

The later refers to the increase in the likelihood of binding to multiple targets, such as the human Ether-à-go-go-Related Gene (hERG) ion channel, that can result in the appearance of side effects and toxicology.

A deeper study performed by GSK from the ADMET profile and physicochemical data of ~ 30,000 molecules revealed that compounds that display a  $\text{clog } P < 4$  appear to be optimal for achieving appropriate physicochemical characteristics to ensure downstream drug success.<sup>84</sup> Table 2 summarizes the effects of the molecular weight and the  $\text{clog } P$  in the main set of PK assays applied in industry. Because of approximately two-thirds of all existing drug entities are classified as basic or acidic molecules,<sup>85</sup> these two types are the ones disclosed below.

**Table 2.** Influence of the key molecular properties on the ADMET parameters.<sup>84</sup>

Basic molecules	MW < 400 and $\text{clog } P < 4$	MW > 400 and $\text{clog } P > 4$
Solubility	high/average	low/average
Permeability	high/average	average
Bioavailability	average	low
Volume of distribution	high/average	high
Plasma protein binding	low	average
CNS penetration	high/average	average/low
Brain tissue binding	low	high
P-gp efflux	average	high/average
<i>in vivo</i> clearance	average	high/average
hERG inhibition	average/high	high
CYP450 inhibition	low 1A2, 2C9 & 2C19 inhibition	low 1A2 inhibition
CYP450 inhibition	average 2D6 & 3A4 inhibition	average 2C9 & 2C19 inhibition
P-450 inhibition		high 2D6 & 3A4 inhibition

<sup>84</sup> Gleeson, M. P. *J. Med. Chem.* **2008**, *51*, 817-834.

<sup>85</sup> Charifson, P. S.; Walters, W. P. *J. Med. Chem.* **2014**, *57*, 9701-9717.

Acidic molecules	MW < 400 and clog P < 4	MW > 400 and clog P > 4
Solubility	high	average/high
Permeability	low	average/low
Bioavailability	average	average
Volume of distribution	low	low
Plasma protein binding	average/higher	high
CNS penetration	low	low
Brain tissue binding	low	high
P-gp efflux	low	low
<i>in vivo</i> clearance	low/average	average
hERG inhibition	low	low
CYP450 inhibition	low 1A2, 2C9, 2C19, 2D6 & 3A4 inhibition	low 1A2, 2C19, 2D6 & 3A4 inhibition
CYP450 inhibition		high 2C9 inhibition

As mentioned in section 1.2.1, having an adamantane present in a test drug gives a molecule of significantly higher lipophilicity compared to a molecule with just a proton or a methyl group instead. Specifically, the log P increases 3.1 log units when an adamantane is incorporated into a molecule. An increase in lipophilicity can be beneficial, but there is obviously a “size limit” of the lipophilic add-on.

Considering the above mentioned, it seems evident that the adamantane ring does not always possess the optimal properties as a scaffold in medicinal chemistry. A decrease in the overall lipophilicity will lead to compounds with an improved PK profile, which will therefore be more “drug-like”.<sup>86</sup> In this sense, there is an urgent need for the development of new scaffolds that could provide compounds with more optimal physicochemical properties to avoid attrition in later stages of the drug discovery process.

#### 1.4.2 Ready access to intermediates that prevent scaffold optimization

Taking into account what it has been stated so far, it is logical to wonder why the adamantane ring is widely used in medicinal chemistry. And the answer is simple. Apart from the fact that in some cases the adamantane ring is the more suitable structure for any taken target, the easy access to adamantyl intermediates restrains the use of similar, yet disparate, analogues.

The adamantane-based pharmaceuticals are derived from a small library of adamantane derivatives, mostly bearing simple functional groups, like amines or carboxylic

<sup>86</sup> Zhang, M.-Q. *Methods Mol. Biol.* **2012**, *803*, 297-307.

acids. These intermediates are commercially available from common suppliers, such as Sigma-Aldrich, Fluorochem or TCI. In particular, from 100 to 150 derivatives can be easily purchased from their webpage in a timely and cost effective way, at least for the developed countries. For this reason, the adamantane ring is considered as a standard lipophilic building block in test drug library syntheses.

Frequently, the industry, with its desire to make more and more compounds for testing in a fast turnaround time, makes no efforts in the optimization of this kind of polycycles, since medicinal chemistry strategies around other functionalities and structures of parent molecules are more straightforward. However, the employment of similar polycycles as adamantane-like analogues can overcome the related issues to the use of the adamantane itself. Although some of the alternative cores entail tedious and long synthetic routes, others can be prepared in a synthetically feasible way.

#### 1.4.3 Adamantane group as an imperfect space-filling pharmacophore

The lipophilic cage structure of adamantane has been used to rigidify the pharmacophore. True is the fact that in some cases the adamantane ring possesses the optimum molecular dimensions to functionally hit its target. Notwithstanding that, the adamantane does not always fill perfectly the active site of the desired target. Its dimensions are limited and the adamantane moiety can exceed or lose in filling the space of the target cavity. The binding constant for the ligand-receptor interaction can be optimized by varying the shape, orientation and flexibility of the scaffold. Since adamantane is a rigid structure with a well-defined geometry, the manipulation of this structure can give rise to several different scaffolds with diverse effects on its interaction to the target.

Several research groups have worked, and still are, in the development of different polycycles for their use in diverse targets as surrogates of the adamantane ring with promising results. These adamantane-like scaffolds have been applied in targets such as *influenza A* and *vaccinia* viruses,<sup>87</sup> or against CNS disorders, targeting the  $\gamma$ -aminobutyric acid (GABA) or 5-HT<sub>2</sub> receptors of serotonin, among others.<sup>88,89</sup> This issue will be examined in detail in the section that follows.

### 1.5 Adamantane alternatives: previous work of the group

Over the last few years, the research group headed by Dr. Santiago Vázquez Cruz has gained a wide expertise in the synthesis of adamantane-like polycyclic scaffolds and their application to different therapeutical targets. In this regard, ring-expanded, ring-contracted, oxa-derivatives and related cage compounds have been explored by the group as analogues

---

<sup>87</sup> Jordan, R.; Bailey, T. R.; Rippin, S. R.; Dai, D. WO 2008130348, **2008**.

<sup>88</sup> Zoidis, G.; Papanastasiou, I.; Dotsikas, I.; Sandoval, A.; Dos Santos, R. G.; Papadopoulou-Daifoti, Z.; Vamvakides, A.; Kolocouris, N.; Felix, R. *Bioorg. Med. Chem.* **2005**, *13*, 2791-2798.

<sup>89</sup> Becker, D. P.; Flynn, D. L.; Shone, R. L.; Gullikson, G. *Bioorg. Med. Chem. Lett.* **2004**, *14*, 5509-5512.

to the drugs amantadine, memantine and rimantadine. Figure 11 summarizes the mentioned polycycles.

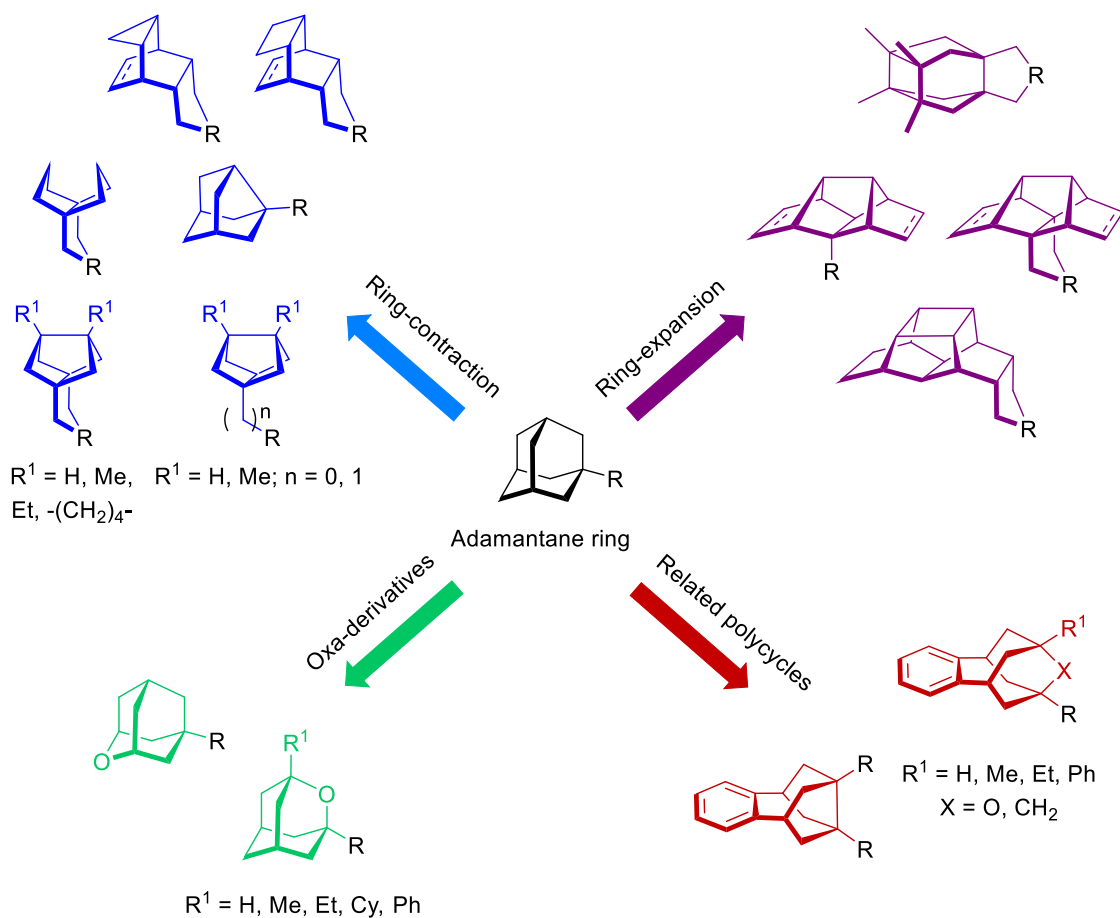


Fig. 11. Polycyclic scaffolds applied in different therapeutic targets by the group.

The potential of these polycycles to substitute the adamantane ring in known bioactive compounds has been proven in multiple cases for a few targets. At the beginning of this thesis, three main targets had been hit with these cage structures:

- the M2 channel of *influenza A virus*<sup>90,91,92,93,94</sup>

<sup>90</sup> Duque, M. D.; Ma, C.; Torres, E.; Wang, J.; Naesens, L.; Juárez-Jiménez, J.; Camps, P.; Luque, F. J.; DeGrado, W. F.; Lamb, R. A.; Pinto, L. H.; Vázquez, S. *J. Med. Chem.* **2011**, *54*, 2646-2657.

<sup>91</sup> Rey-Carrizo, M.; Torres, E.; Ma, C.; Barniol-Xicotá, M.; Wang, J.; Wu, Y.; Naesens, L.; Degrado, W. F.; Lamb, R. A.; Pinto, L. H.; Vázquez, S. *J. Med. Chem.* **2013**, *56*, 9265-9274.

<sup>92</sup> Torres, E.; Leiva, R.; Gazzarrini, S.; Rey-Carrizo, M.; Frigolé-Vivas, M.; Moroni, A.; Naesens, L.; Vázquez, S. *ACS Med. Chem. Lett.* **2014**, *5*, 831-836.

<sup>93</sup> Rey-Carrizo, M.; Barniol-Xicotá, M.; Ma, C.; Frigolé-Vivas, M.; Torres, E.; Naesens, L.; Llabrés, S.; Juárez-Jiménez, J.; Luque, F. J.; Degrado, W. F.; Lamb, R. A.; Pinto, L. H.; Vázquez, S. *J. Med. Chem.* **2014**, *57*, 5738-5747.

<sup>94</sup> Rey-Carrizo, M.; Gazzarrini, S.; Llabrés, S.; Frigolé-Vivas, M.; Juárez-Jiménez, J.; Font-Bardia, M.; Naesens, L.; Moroni, A.; Luque, F. J.; Vázquez, S. *Eur. J. Med. Chem.* **2015**, *96*, 318-329.



- and the NMDA receptor of glutamate and the parasite *Trypanosoma brucei*.<sup>95,96,97,98</sup>

The particular and unique shape and size of each scaffold has given new insights into the binding mode of the different targets, as well as a better understanding of how to rationally design compounds with improved activities and physicochemical properties. The chief idiosyncrasy of the new polycycles is the different space-filling that they provide within their target. The results that the group has obtained have evidenced the unsuitable fit of the adamantane ring into the different active sites of the considered targets.

Probably, the research around the inhibition of the M2 channel is the most clear and obvious example of this inappropriate space-filling of the adamantane. Briefly, inhibition of M2 channel by amantadine became futile with the appearance of mutant strains, namely L26F, V27A and S31N.<sup>99</sup> These amantadine-insensitive M2 channels display a different pore size, rendering the aminoadamantane ineffective. The design and synthesis of a wide array of adamantane-like scaffolds have provided molecules with greater activities against the wild-type than amantadine, establishing that the latter was not fully optimized inside the M2 channel lumen. Furthermore, enlarged derivatives have displayed interesting inhibitory activities against both wild-type and the V27A M2 mutant protein (Fig. 12).

---

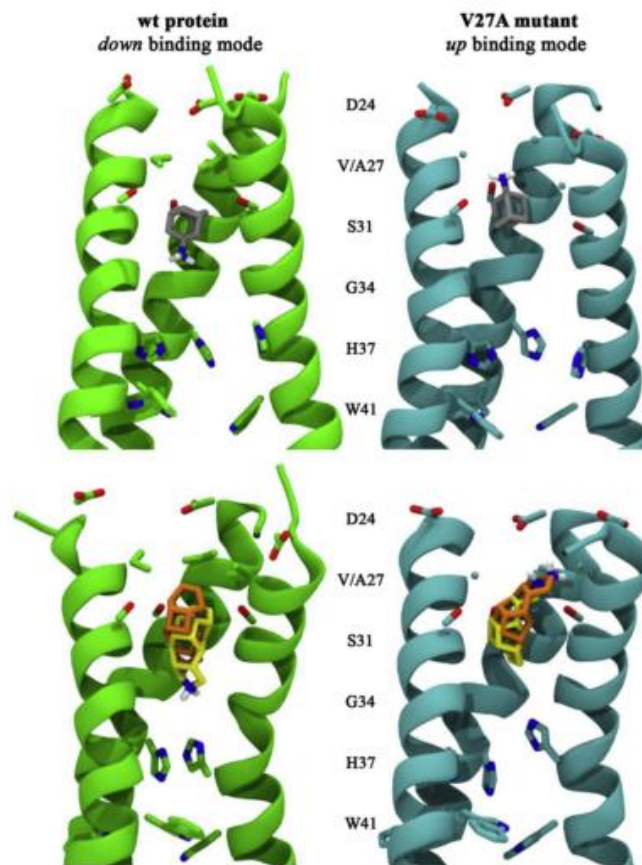
<sup>95</sup> Camps, P.; Duque, M. D.; Vázquez, S.; Naesens, L.; De Clercq, E.; Sureda, F. X.; López-Querol, M.; Camins, A.; Pallàs, M.; Prathalingam, S. R.; Kelly, J. M.; Romero, V.; Ivorra, D.; Cortés, D. *Bioorg. Med. Chem.* **2008**, *16*, 9925-9936.

<sup>96</sup> Duque, M. D.; Camps, P.; Profire, L.; Montaner, S.; Vázquez, S.; Sureda, F. X.; Mallol, J.; López-Querol, M.; Naesens, L.; De Clercq, E.; Prathalingam, S. R.; Kelly, J. M. *Bioorg. Med. Chem.* **2009**, *17*, 3198-3206.

<sup>97</sup> Duque, M. D.; Camps, P.; Torres, E.; Valverde, E.; Sureda, F. X.; López-Querol, M.; Camins, A.; Prathalingam, S. R.; Kelly, J. M.; Vázquez, S. *Bioorg. Med. Chem.* **2010**, *18*, 46-57.

<sup>98</sup> Torres, E.; Duque, M. D.; López-Querol, M.; Taylor, M. C.; Naesens, L.; Ma, C.; Pinto, L. H.; Sureda, F. X.; Kelly, J. M.; Vázquez, S. *Bioorg. Med. Chem.* **2012**, *20*, 942-948.

<sup>99</sup> Gu, R.-X.; Liu, L. A.; Wang, Y.-H.; Xu, Q.; Wei, D.-Q. *J. Phys. Chem. B* **2013**, *117*, 6042-6051.



**Fig. 12.** Representation of the predicted binding mode (down, up) of amantadine (shown as gray sticks) and two different polycyclic scaffolds (shown as orange and yellow sticks) in the interior of the wild type M2 channel and its V27A variant.<sup>94</sup>

With these encouraging results in hand, much is to be expected for adamantane-like scaffolds as modifiers or enhancers of active pharmacophores. This uncharted territory certainly holds great promise for the pharmaceutical industry.



# **CHAPTER 1: NMDA receptor antagonism**



# **Introduction**

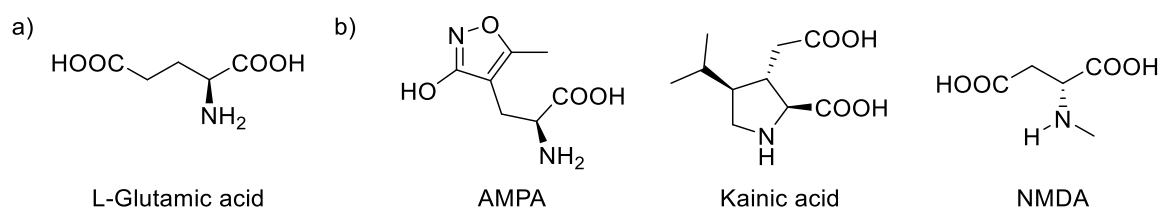


## 1. NMDA receptor antagonism by adamantane-like scaffolds

The following section will introduce the glutamatergic system and the NMDA receptor (NMDAR), as well as their role in the development of neurodegenerative disorders. More in detail, the adamantane-based compound memantine will be discussed as NMDAR antagonist, along with its application in the Alzheimer's disease (AD). Finally, a review of the previous work of the group related to the discovery of new NMDAR antagonists will be covered.

### 1.1 The glutamatergic neurotransmitter system

The amino acid glutamate is the main excitatory neurotransmitter and is involved in almost all CNS functions, especially in cortical and hippocampal regions, hence being crucial for the normal functioning of the brain (Fig. 14a).<sup>100</sup> It is released upon depolarization of the nerve terminals, which accumulate the glutamate in its inactive form glutamine.<sup>101</sup> Once in the extracellular fluid, the glutamate exerts its signalling function by binding to three different ionotropic receptors, which are classified according to their selective, synthetic agonists (Fig. 14b):  $\alpha$ -amino-3-hydroxy-5-methyl-4-isoxazolepropionic acid (AMPA), kainate, and NMDA receptors. These glutamate-gated ion channels are permeable to  $\text{Ca}^{2+}$ ,  $\text{Na}^+$  and/or  $\text{K}^+$  ions.<sup>102</sup>



**Fig. 14.** Glutamic acid (a) and its analogues (b). The compounds are represented in their neutral form, and named accordingly.

Worth to mention is that apart from the ionotropic receptors, glutamate binds also to metabotropic receptors, which are coupled to G-proteins and are divided into three major groups, I-III.<sup>103</sup>

#### 1.1.1 NMDA receptor and its physiological function

The tetrameric assembly of the NMDA receptor confers a three-dimensional channel that allows the influx of  $\text{Ca}^{2+}$  and  $\text{Na}^+$  ions and the efflux of  $\text{K}^+$  ions when opened. The NMDA receptor is unique among the ionotropic receptors since it needs the presence of two agonists for its activation; glutamate and glycine.<sup>104</sup> Albeit these are the two essential

<sup>100</sup> Watkins, J. C.; Evans, R. H. *Annu. Rev. Pharmacol. Toxicol.* **1981**, *21*, 165-204.

<sup>101</sup> Danbolt, N. C. *Prog. Neurobiol.* **2001**, *65*, 1-105.

<sup>102</sup> Traynelis, S. F.; Wollmuth, L. P.; McBain, C. J.; Menniti, F. S.; Vance, K. M.; Ogden, K. K.; Hansen, K. B.; Yuan, H.; Myers, S. J.; Dingledine, R. *Pharmacol. Rev.* **2010**, *62*, 405-496.

<sup>103</sup> Niswender, C. M.; Conn, P. J. *Annu. Rev. Pharmacol. Toxicol.* **2010**, *50*, 295-322.

<sup>104</sup> Kleckner, N. W.; Dingledine, R. *Science* **1988**, *241*, 835-837.



ligands, the NMDA receptor features several modulating binding sites for, for instance, polyamines.<sup>105</sup> The endogenous channel blocker is the  $Mg^{2+}$  ion, whose binding site is within the pore (Fig. 15).<sup>106</sup> The activation of the receptor is voltage-dependent, whereupon the  $Mg^{2+}$  ion is displaced. Thus, for the permeation of  $Ca^{2+}$  ions the two following conditions need to be fulfilled: activation by endogenous ligands, and depolarization of the neuron, for example prior activation of AMPA or kainate receptors.

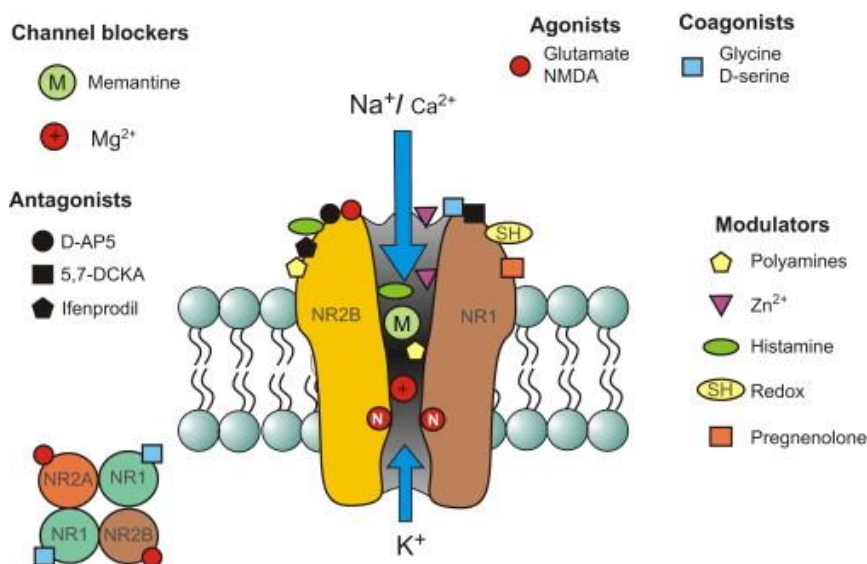


Fig. 15. Schematic representation of the NMDA receptor, including the topology and pharmacological recognition sites.<sup>107</sup>

The X-ray crystal structures of the intact heterodimeric and heterotetrameric NMDA receptor have been published recently almost simultaneously in two of the most distinguished journals; Science and Nature.<sup>108,109</sup> The NMDA receptor can be formed by combination of three different subunits designated as GluN1, GluN2A-D, and GluN3 (also referred as NR1, NR2 and NR3 in former literature). However, the heterotetramers are chiefly composed of two copies each of GluN1 and GluN2, where glycine binds to GluN1 and glutamate to GluN2.<sup>110</sup> The overall structure of the NMDA receptor possesses a modular domain architecture, with extracellular amino-terminal domains (ATDs) and ligand-binding domains (LBDs), a transmembrane domain (TMD) and an intracellular carboxy-terminal domain (CTD) (Fig. 16). The discovery of the crystal structure of the NMDA receptor offers new insights into the ion channel function and the allosteric binding of modulators and antagonists.

<sup>105</sup> Chris Parsons web page. Projects: NMDA receptors. <http://www.chrisparsons.de/Chris/nmda.htm> (accessed on 11<sup>th</sup> September 2015). Dr. Christopher Parsons is the head of the *In vitro* Pharmacology at Merz, the pharmaceutical company that developed memantine.

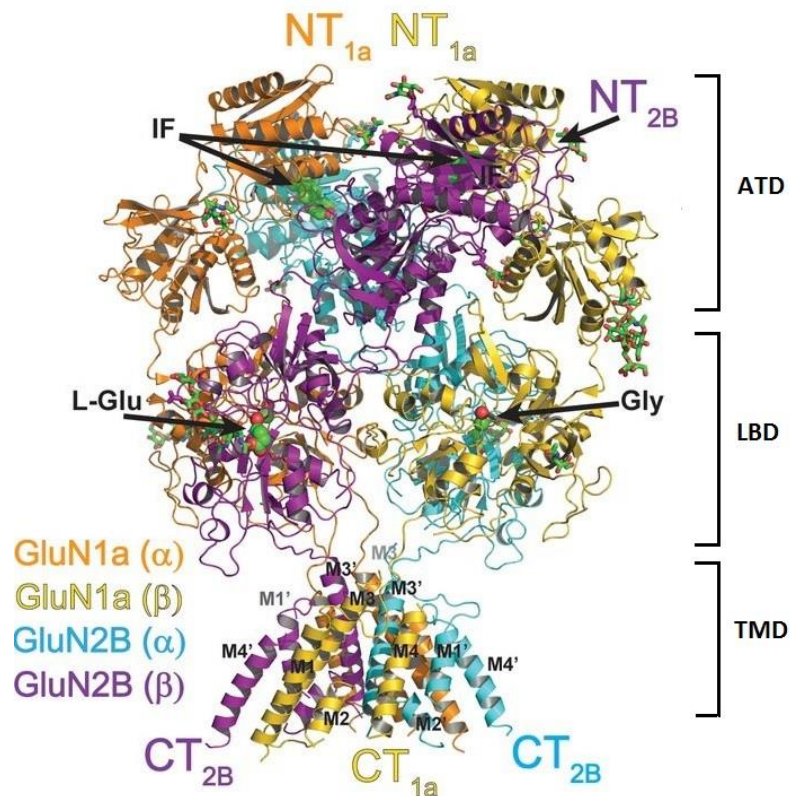
<sup>106</sup> Bleich, S.; Romer, K.; Wiltfang, J.; Kornhuber, J. *Int. J. Geriatr. Psychiatry* **2003**, *18*, S33-S40.

<sup>107</sup> Parsons, C. G.; Stöffler, A.; Danysz, W. *Neuropharmacology* **2007**, *53*, 699-723.

<sup>108</sup> Karakas, E.; Furukawa, H. *Science* **2014**, *344*, 992-997.

<sup>109</sup> Lee, C.-H.; Lü, W.; Michel, J. C.; Goehring, A.; Du, J.; Song, X.; Gouaux, E. *Nature* **2014**, *511*, 191-197.

<sup>110</sup> Karakas, E.; Regan, M. C.; Furukawa, H. *Trends Biochem. Sci.* **2015**, *40*, 328-337.



**Fig. 16.** Overall structure of the heterotetrameric GluN1a-GluN2B NMDA receptor. Protein Data Bank (PDB) code: 4PE5.<sup>108</sup>

A further significant characteristic of the NMDA receptor is its slow gating kinetics, which control the postsynaptic  $\text{Ca}^{2+}$  levels in physiological conditions. The influx of calcium ions triggers signal transduction cascades that control the strength of neural connectivity and neuroplasticity.<sup>111</sup> The specific attributes of the activation of the NMDA receptors by glutamate are accepted to be an intrinsic synaptic mechanism for cognition, learning and memory processes.<sup>112</sup>

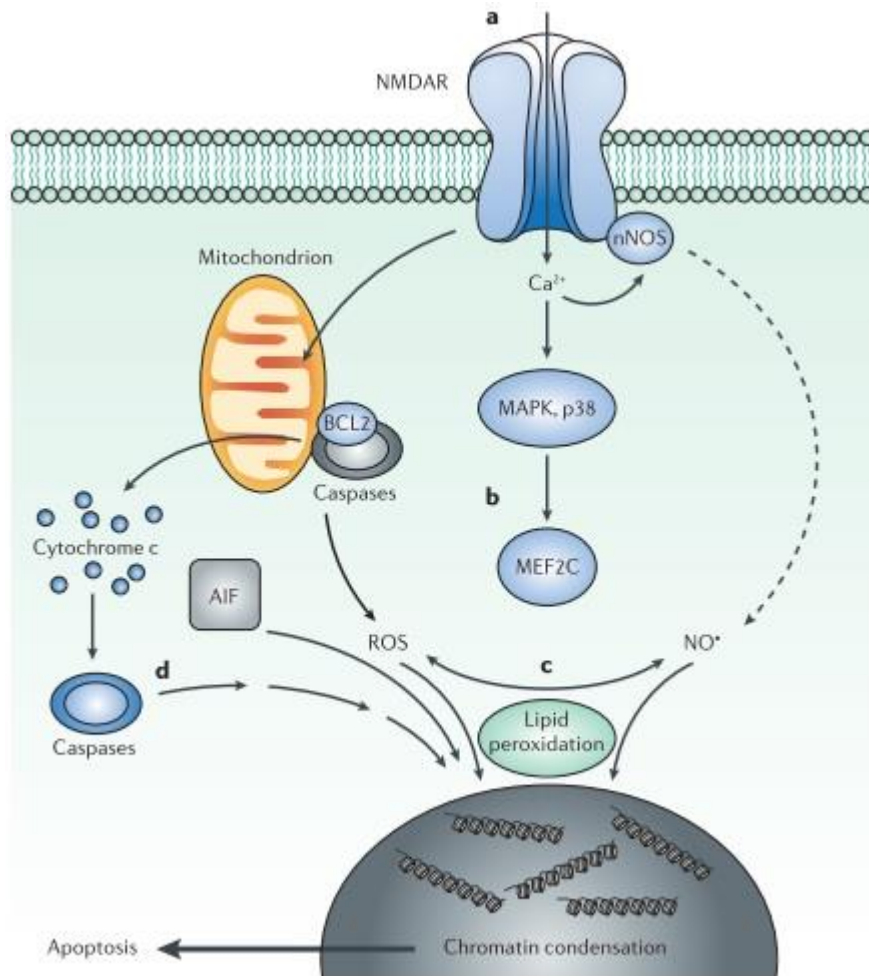
### 1.1.2 Glutamate and related pathological states

Normal glutamate receptor activity mediates, in large measure, physiological excitatory synaptic transmission in the brain, as just mentioned. The maintenance of low extracellular levels of glutamate is essential for controlling the CNS functions.<sup>101</sup> However, in a variety of pathological conditions, including various neurodegenerative disorders, there is an excessive activation of the NMDA receptor by the glutamate that leads to an increase in the intracellular calcium concentration. This contributes to the subsequent formation of

<sup>111</sup> Danysz, W.; Parsons, C. G. *Br. J. Pharmacol.* **2012**, *167*, 324-352.

<sup>112</sup> Butterfield, D. A.; Pocernich, C. B. *CNS Drugs* **2003**, *17*, 641-652.

harmful free radicals and activation of proteolytic cascades which eventually cause cell damage or death (Fig. 17).<sup>113,114</sup>



**Fig. 17.** Cellular apoptotic pathways triggered by excessive NMDAR activation. a) NMDAR hyperactivation; b) activation of the p38 mitogen-activated kinase (MAPK)-MEF2C pathway; c) toxic effects of free radicals such as ROS; and d) activation of apoptosis-inducing enzymes.<sup>115</sup>

This overactivation of the NMDAR is attributable to a combination of different occurrences. Firstly, glutamate is not cleared properly and/or can even be inappropriately released during acute and chronic neurodegenerative disorders.<sup>115</sup> Secondly, under these conditions, neurons become depolarized in a sustained manner and the cells cannot maintain their ionic homeostasis. This contributes to the permanent liberation of the Mg<sup>2+</sup> by NMDAR.<sup>116</sup> The combination of some or all of these events leads to the so-called *excitotoxicity*, which is defined as cell death from the toxicity of an excessive action of excitatory amino acids, such as glutamate.<sup>117</sup>

<sup>113</sup> Lipton, S. A.; Rosenberg, P. A. *N. Engl. J. Med.* **1994**, *330*, 613-622.

<sup>114</sup> Lipton, S. A.; Nicoretta, P. *Cell Calcium* **1998**, *23*, 165-171.

<sup>115</sup> Lipton, S. A. *Nat. Rev. Drug Discov.* **2006**, *5*, 160-170.

<sup>116</sup> Zeevalk, G. D.; Nicklas, W. J. *J. Neurochem.* **1992**, *59*, 1211-1220.

<sup>117</sup> Herrmann, N.; Li, A.; Lanctôt, K. *Expert Opin. Pharmacother.* **2011**, *12*, 787-800.

According to the aforementioned, disorders including Alzheimer's, Parkinson's and Huntington's diseases, depression, schizophrenia, ischemic injuries associated with stroke, HIV-associated dementia, multiple sclerosis, amyotrophic lateral sclerosis, neuropathic pain and glaucoma share a final common pathway to neuronal damage and death, i.e. overstimulation of the NMDAR and excitotoxicity.<sup>112,118,119,120</sup> NMDAR antagonism could therefore potentially be of therapeutic interest in a number of neurological disorders.

## 1.2 NMDA as a therapeutic target

The pursuit of strategies for the development of neuroprotective agents that are both effective and well tolerated has been burgeoning in the last decades.<sup>121</sup> Theoretically, any disorder of the CNS characterized by glutamate excitotoxicity-induced neuronal death, should be relieved by a treatment with NMDA receptor antagonists. In this sense, several NMDAR antagonists have been developed disclosing different binding modes and clinical tolerations.<sup>122,123,124</sup>

### 1.2.1 Competitive NMDAR antagonists

NMDAR antagonists that compete directly with glutamate at its binding site block the natural neuronal communication. Since the desired therapy must re-establish the normal function of this excitatory neurotransmitter, the development of competitive NMDAR blockers was dismissed due to the appearance of intolerable side effects. A few compounds have been identified as competitive NMDAR antagonist, although their use has been reduced only to comparative studies and target validation (Fig. 18).<sup>125,126,127,128,129</sup>

<sup>118</sup> Lange, K. W.; Kornhuber, J.; Riederer, P. *Neurosci. Biobehav. Rev.* **1997**, *21*, 393-400.

<sup>119</sup> Cioffi, C. L. *Bioorg. Med. Chem. Lett.* **2013**, *23*, 5034-5044.

<sup>120</sup> Rammes, G.; Danysz, W.; Parsons, C. G. *Curr. Neuropharmacol.* **2008**, *6*, 55-78.

<sup>121</sup> Lipton, S. A. *Nat. Rev. Neurosci.* **2007**, *8*, 803-808.

<sup>122</sup> Kemp, J. A.; McKernan, R. M. *Nat. Neurosci.* **2002**, *5* (Suppl.), 1039-1042.

<sup>123</sup> Koller, M.; Urwyler, S. *Expert Opin. Ther. Pat.* **2010**, *20*, 1683-1702.

<sup>124</sup> Strong, K. L.; Jing, Y.; Prosser, A. R.; Traynelis, S. F.; Liotta, D. C. *Expert Opin. Ther. Pat.* **2014**, *24*, 1349-1366.

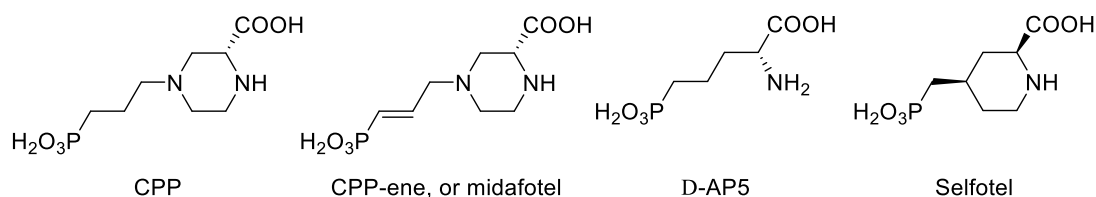
<sup>125</sup> Abraham, W. C.; Mason, S. E. *Brain Res.* **1988**, *462*, 40-46.

<sup>126</sup> Lehmann, J.; Schneider, J.; McPherson, S.; Murphy, D. E.; Bernard, P.; Tsai, C.; Bennett, D. A.; Pastor, G.; Steel, D. J.; Boehm, C. *J. Pharmacol. Exp. Ther.* **1987**, *240*, 737-746.

<sup>127</sup> Sveinbjornsdottir, S.; Sander, J. W.; Upton, D.; Thompson, P. J.; Patsalos, P. N.; Hirt, D.; Emre, M.; Lowe, D.; Duncan, J. S. *Epilepsy Res.* **1993**, *16*, 165-174.

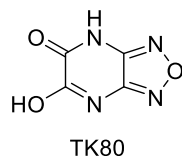
<sup>128</sup> Davis, S.; Butcher, S. P.; Morris, G. M. *J. Neurosci.* **1992**, *12*, 21-34.

<sup>129</sup> Yenari, M. A.; Bell, T. E.; Kotake, A. N.; Powell, M.; Steinberg, G. K. *Clin. Neuropharmacol.* **1998**, *21*, 28-34.



**Fig. 18.** Structures of competitive NMDAR antagonists. CPP: 3-(2-carboxypiperazin-4-yl)propyl-1-phosphonic acid; D-AP5: D-2-amino-5-phosphonopentanoate.

Recently, novel competitive antagonists with preference for the glycine-binding site in the GluN3B subunit have appeared, such as TK80 (Fig. 19).<sup>130</sup> Their discovery have clarified the structural differences between the orthosteric binding site of GluN1 and GluN3.



**Fig. 19.** Structure of a GluN3B subunit antagonist.

### 1.2.2 Uncompetitive NMDAR antagonists

Before explaining this type of antagonism, it is worth distinguishing it from the non-competitive one. The latter refers to the allosteric binding of the antagonist whose availability is not affected by the concentration of agonist – in this case glutamate – whereas in the uncompetitive antagonism the inhibitory effect depends on *prior* activation of the receptor by the agonist.<sup>121,122</sup>

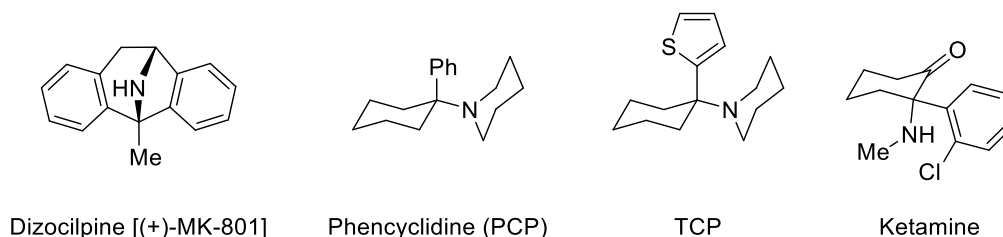
The majority of the uncompetitive NMDAR antagonists block the ion channel by occluding the pore, in a similar way to the  $Mg^{2+}$  ion. Among them, two classes of antagonists are differentiated depending on their off-rate constant:

- *High-affinity blockers*: these antagonists show slow ‘off’ constants and low voltage dependency. These features render the NMDA receptor virtually almost fully occupied by the blocker, which cannot be stimulated under physiological conditions. The inability of the receptor to recover from the inhibition is reflected in the appearance of side effects on the CNS, such as hallucination, agitation, catatonia, centrally-mediated increase in the blood pressure and anaesthesia. Indeed, some of these antagonists have been developed as anaesthetics only, like ketamine and phencyclidine (Fig. 20).<sup>131,132</sup>

<sup>130</sup> Kvist, T.; Greenwood, J. R.; Hansen, K. B.; Traynelis, S. F.; Bräuner-Osborne, H. *Neuropharmacology* **2013**, *75*, 324-336.

<sup>131</sup> Sonkusare, S. K.; Kaul, C. L.; Ramarao, P. *Pharmacol. Res.* **2005**, *51*, 1-17.

<sup>132</sup> Michaud, M.; Warren, H.; Drian, M. J.; Rambaud, J.; Cerruti, P.; Nicolas, J. P.; Vignon, J.; Privat, A.; Kamenka, J. M. *Eur. J. Med. Chem.* **1994**, *29*, 869-876.



**Fig. 20.** High-affinity uncompetitive NMDAR antagonists. PCP: *N*-(1-phenylcyclohexyl)piperidine; TCP: *N*-[1-(2-thienyl)cyclohexyl]piperidine. Ketamine is represented as racemate.

Besides, ketamine, dizocilpine and analogues of phencyclidine were studied as anticonvulsants, albeit their high neurobehavioural toxicity.<sup>133,134</sup>

- *Low- and moderate-affinity blockers*: offset kinetics are inversely related to affinity, and low- and moderate-affinity compounds show faster relief of blockade upon removal of the antagonist or upon physiological glutamatergic activation than high-affinity inhibitors.<sup>135</sup> This critical characteristic allows the inhibition only in pathological conditions, leaving physiological functions unaltered. Moreover, low- and moderate-affinity blockers have a better therapeutic window than high-affinity blockers.<sup>122</sup> For these reasons, low- and moderate-affinity antagonists have been more successful in clinical studies than the ones displaying high affinity. A few number of compounds have been identified as low- and moderate-affinity NMDAR antagonists in the last decades (Fig. 21).<sup>136,137,138,139,140</sup> Recently, propellamines have appeared with an affinity similar to amantadine and memantine to the PCP binding site.<sup>141</sup>

<sup>133</sup> White, J. M.; Ryan, C. F. *Drug Alcohol Rev.* **1996**, *15*, 145-155.

<sup>134</sup> Dorandeu, F.; Dhote, F.; Barbier, L.; Baccus, B.; Testylier, G. *CNS Neurosci. Ther.* **2013**, *19*, 411-427.

<sup>135</sup> Parsons, C. G.; Danysz, W.; Quack, G. *Amino Acids* **2000**, *19*, 157-166.

<sup>136</sup> Blanpied, T. A.; Clarke, R. J.; Johnson, J. W. *J. Neurosci.* **2005**, *25*, 3312-3322.

<sup>137</sup> Rammes, G. *Expert Rev. Clin. Pharmacol.* **2009**, *2*, 231-238.

<sup>138</sup> Mattia, C.; Coluzzi, F. *Drugs* **2007**, *10*, 636-644.

<sup>139</sup> Kiewert, C.; Hartmann, J.; Stoll, J.; Thekkumkara, T. J.; Van der Schyf, C. J.; Klein, J. *Neurochem. Res.* **2006**, *31*, 395-399.

<sup>140</sup> Rogawski, M. A. *Amino Acids* **2000**, *19*, 133-149.

<sup>141</sup> Torres-Gómez, H.; Lehmkühl, K.; Frehland, B.; Daniliuc, C.; Schepmann, D.; Ehrhardt, C.; Wünsch, B. *Bioorg. Med. Chem.* **2015**, *23*, 4277-4285.

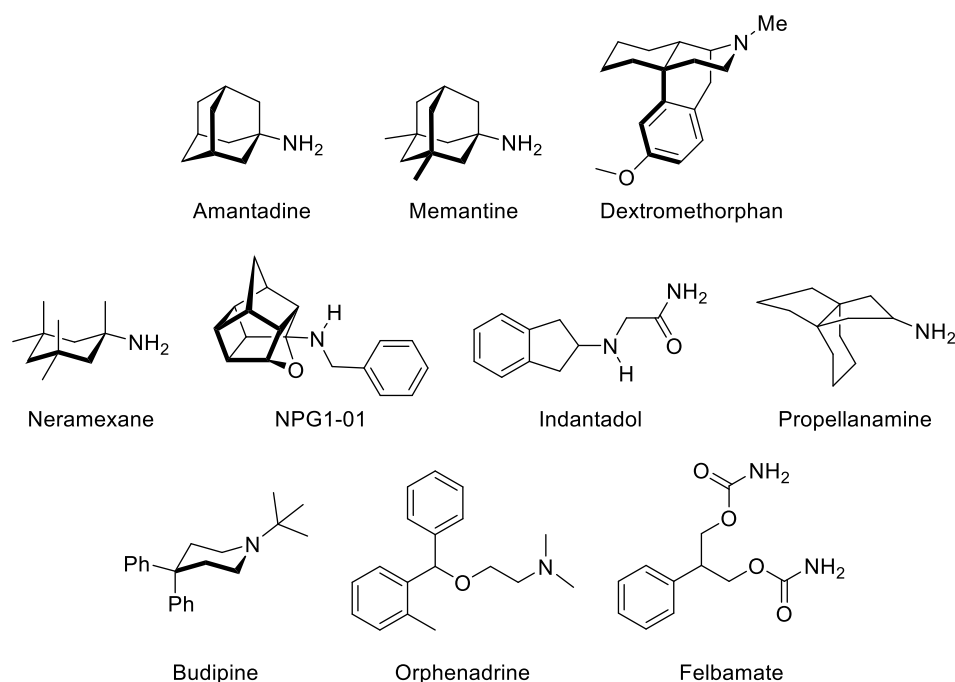


Fig. 21. Structures of low- and moderate-affinity uncompetitive NMDAR antagonists.

### 1.2.3 Non-competitive NMDAR antagonists

Whilst competitive antagonists bind to the same binding site as glutamate or glycine, and the uncompetitive antagonists we have seen so far exert their interactions within the ion channel, other types of blockers owe their activity by binding to allosteric sites. This is the case for the compounds ifenprodil and eliprodil, whose binding site is located in the GluN2B subunit (Fig. 22).<sup>142,143</sup> Ifenprodil has shown considerable attenuation of the neurotoxicity in animal models.<sup>144</sup> Ifenprodil and ifenprodil-like inhibitors have a reduced affinity and unbind from inactivated receptors leaving transiently activated receptors relatively unaffected.<sup>145</sup> Other high-affinity GluN2B ligands that modulate NMDAR activity have appeared recently, such as benzo[7]annulen-7-amines.<sup>146</sup> Similar to ifenprodil, TCN-201 binds also to allosteric sites, but in this case to GluN2A.<sup>147</sup> Many other allosteric modulators have emerged with distinct binding regions all along the ion channel.<sup>148</sup>

<sup>142</sup> Williams, K. *Curr. Drug Targets* **2001**, *2*, 285-298.

<sup>143</sup> Parsons, C. G.; Danysz, W.; Quack, G. *Neuropharmacology* **1999**, *38*, 735-767.

<sup>144</sup> Gotti, B.; Duverger, D.; Bertin, J.; Carter, C.; Dupont, R.; Frost, J.; Gaudilliere, B.; MacKenzie, E. T.; Rousseau, J.; Scatton, B.; Wick, A. *J. Pharmacol. Exp. Ther.* **1988**, *247*, 1211-1221.

<sup>145</sup> Kew, J. N. C.; Trube, G.; Kemp, J. A. *J. Physiol.* **1996**, *497*, 761-772.

<sup>146</sup> Gawaskar, S.; Schepmann, D.; Bonifazi, A.; Wünsch, B. *Bioorg. Med. Chem.* **2014**, *22*, 6638-6646.

<sup>147</sup> Bettini, E.; Sava, A.; Griffante, C.; Carignani, C.; Buson, A.; Capelli, A. M.; Negri, M.; Andretta, F.; Senar-Sancho, S. A.; Guiral, L.; Cardullo, F. *J. Pharmacol. Exp. Ther.* **2010**, *335*, 636-644.

<sup>148</sup> Regan, M. C.; Romero-Hernandez, A.; Furukawa, H. *Curr. Opin. Struct. Biol.* **2015**, *33*, 68-75.

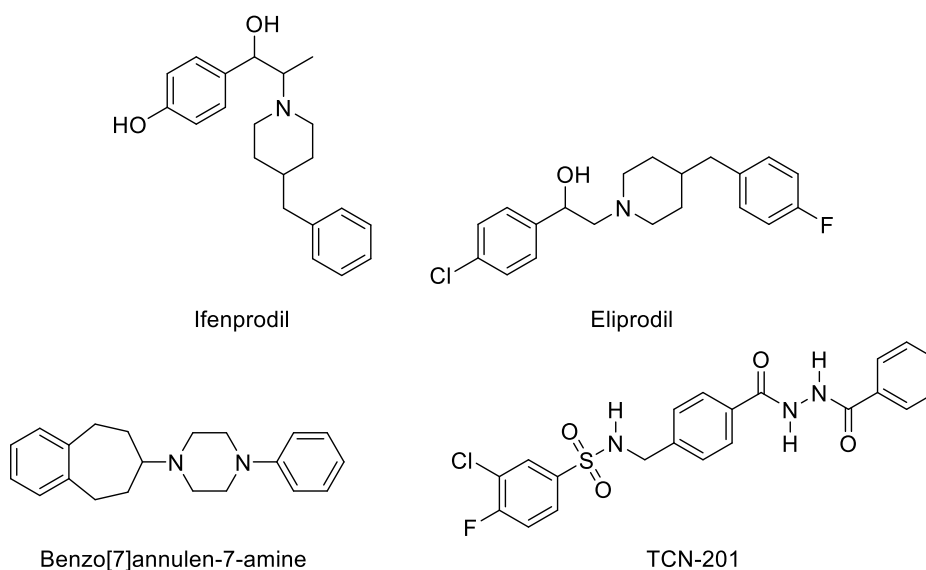


Fig. 22. NMDAR antagonists with allosteric binding mode.

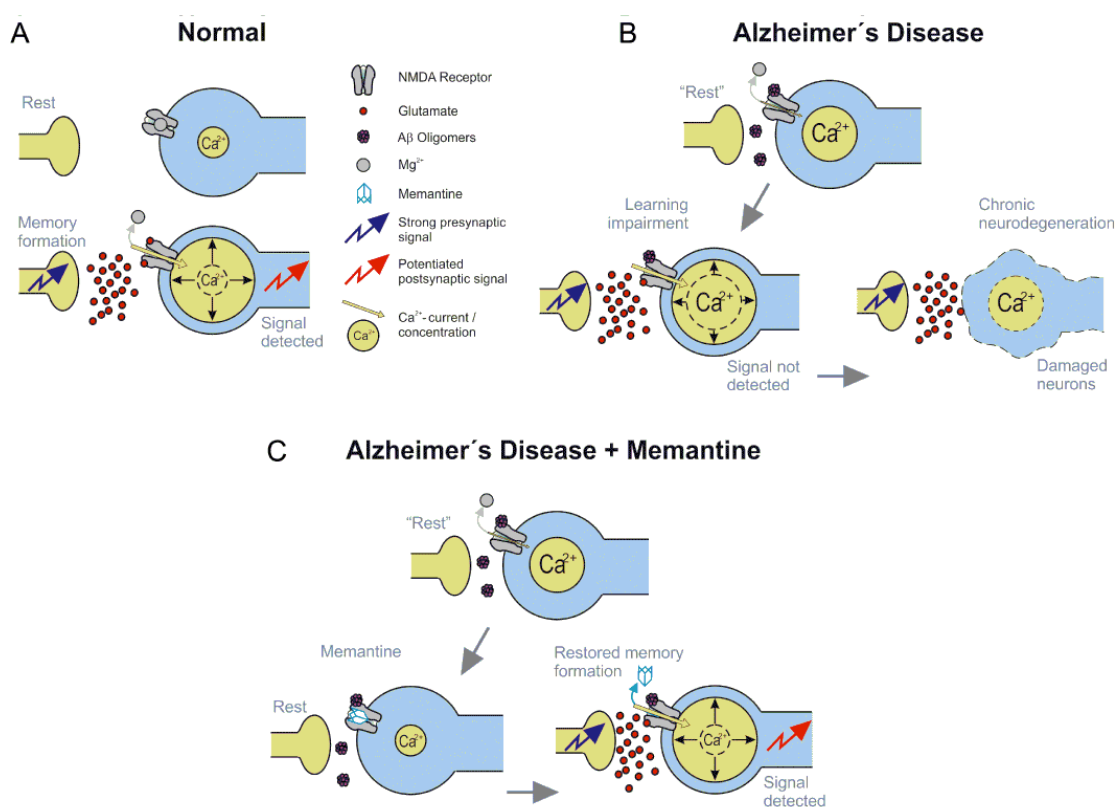
Inasmuch as the sole compound that has reached the market as NMDAR antagonist is memantine, a broader analysis will be performed thereof.

### 1.3 The neuroprotector memantine

Memantine is a low- to moderate-affinity uncompetitive NMDAR antagonist, with strong voltage dependency and rapid blocking and unblocking kinetics.<sup>120</sup> Thanks to these particular qualities, memantine shows the effect known as *partial trapping*, where around one sixth of the ion channels remain free of the antagonist under resting conditions and are directly available for physiological transmission, unlike in the presence of high-affinity antagonists.<sup>149</sup> Thus, memantine blocks the neurotoxicity of glutamate in pathological conditions without interfering with its physiological actions required for learning and memory (Fig. 23).<sup>111</sup>

<sup>149</sup> Blanpied, T. A.; Boeckman, F. A.; Aizenman, E.; Johnson, J. W. *J. Neurophysiology* **1997**, *77*, 309-323.





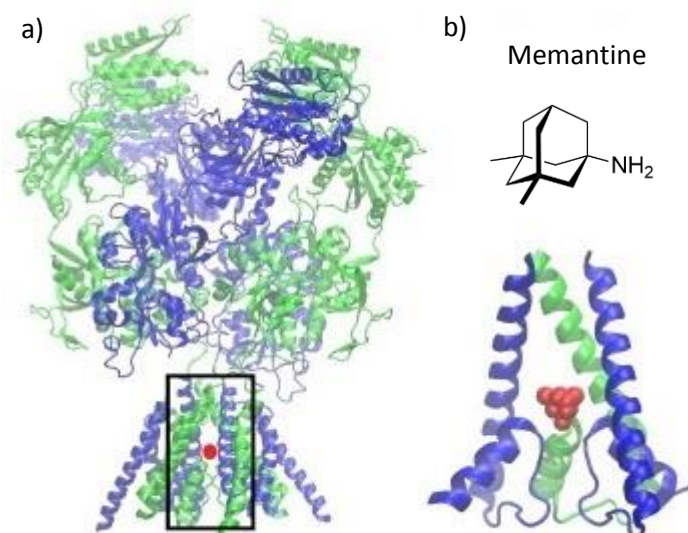
**Fig. 23.** Schematic illustration of the glutamatergic system involving the NMDA receptor based on the signal-noise hypothesis. A) Normal physiological transmission of glutamate resulting in a sufficient signal-to-noise ratio. B) In neurodegenerative disorders, like in AD, there is a sustained activation of the NMDARs, which leads to the rise of the synaptic noise. The impaired detection of the relevant synaptic signal hampers the learning and plasticity processes. C) Synaptic plasticity recovery by antagonism with memantine.<sup>111</sup>

Further studies indicate that memantine exerts its effect by binding at or near the Mg $^{2+}$  site within the ion channel (Fig. 24).<sup>150,151</sup> More precisely, it is believed that memantine is placed with the charged nitrogen close to the critical NMDAR channel asparagines. At the time of writing this thesis, there is any resolved structure of the NMDAR with a channel blocker. However, a recent computational study has revealed that the excellent affinity of memantine is due to the presence of hydrophobic binding pockets in the binding site for the two methyl groups of memantine. The removal of these two groups, leading to amantadine, or the addition of a third methyl group diminished affinity.<sup>152</sup>

<sup>150</sup> Chen, H. S. V.; Lipton, S. A. *J. Pharmacol. Exp. Ther.* **2005**, *314*, 961-971.

<sup>151</sup> Johnson, J. W.; Glasgow, N. G.; Povysheva, N. V. *Curr. Opin. Pharmacol.* **2015**, *20*, 54-63.

<sup>152</sup> Limapichat, W.; Yu, W. Y.; Branigan, E.; Lester, H. A.; Dougherty, D. A. *ACS Chem. Neurosci.* **2013**, *4*, 255-260.



**Fig. 24.** Images of NMDAR channel blocked by memantine, representing the likely location of memantine binding site. PDB code: 4TLM.<sup>109</sup>

Memantine was approved by the EMA in 2002 and by the FDA in 2003 for the treatment of moderate to severe AD.<sup>153,154</sup> AD is the most common type of dementia, and there is no effective cure. The American Alzheimer's association estimated current cost to the healthcare system of \$250 billion, and the number of patients to rise by three times by 2050.<sup>155</sup> In consequence, there is an urgent need to discover new therapeutics for the treatment of AD. Memantine has shown modest efficacy in randomized controlled trials in improving cognition, function, and global status, either as monotherapy or in combination with acetylcholinesterase inhibitors.<sup>117,156,157</sup> Memantine has also been shown to improve behavioural disturbances such as agitation and aggression.<sup>158</sup> In other dementias, memantine has not yet been shown to be beneficial, although an intense research is being conducted around that matter.<sup>159</sup> Besides, memantine has been studied for different conditions, such as Huntington's disease,<sup>160</sup> depression,<sup>161</sup> Down's syndrome,<sup>162</sup> and drug addiction.<sup>163</sup>

<sup>153</sup> European Medicines Agency, Ebixa (memantine).

[http://www.ema.europa.eu/ema/index.jsp?curl=pages/medicines/human/medicines/000463/human\\_med\\_000750.jsp&mid=WC0b01ac058001d124](http://www.ema.europa.eu/ema/index.jsp?curl=pages/medicines/human/medicines/000463/human_med_000750.jsp&mid=WC0b01ac058001d124) (accessed on 21<sup>st</sup> May 2015).

<sup>154</sup> FDA approves memantine drug for treating AD. *Am. J. Alzheimers Dis. Other Demen.* **2003**, *18*, 329-330.

<sup>155</sup> Alzheimer's association. <http://www.alz.org/> (accessed on 31<sup>st</sup> August 2015).

<sup>156</sup> Anand, R.; Gill, K. D.; Mahdi, A. A. *Neuropharmacology* **2014**, *76*, 27-50.

<sup>157</sup> Parsons, C. G.; Danysz, W.; Dekundy, A.; Pulte, I. *Neurotox. Res.* **2013**, *24*, 358-369.

<sup>158</sup> Herrmann, N.; Cappell, J.; Eryavec, G. M.; Lanctôt, K. L. *CNS Drugs* **2011**, *25*, 425-433.

<sup>159</sup> Peng, D.; Yuan, X.; Zhu, R. *J. Clin. Neurosci.* **2013**, *20*, 1482-1485.

<sup>160</sup> Brocardo, P. S.; Gil-Mohapel, J. M. *Curr. Physicopharmacol.* **2012**, *1*, 137-154.

<sup>161</sup> Dang, Y.-H.; Ma, X.-C.; Zhang, J.-C.; Ren, Q.; Wu, J.; Gao, C.-G.; Hashimoto, K. *Curr. Pharm. Des.* **2014**, *20*, 5151-5159.

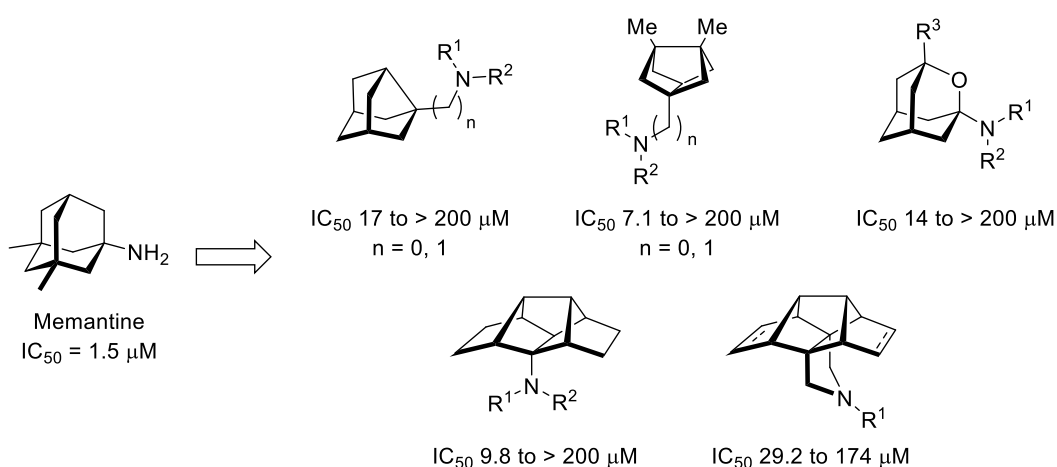
<sup>162</sup> Costa, A. C. S. *CNS Neurol. Disord. Drug Targets* **2014**, *13*, 16-25.

<sup>163</sup> Tomek, S. E.; LaCrosse, L. A.; Nemirovsky, N. E.; Foster Olive, M. *Pharmaceuticals* **2013**, *6*, 251-268.

On account to the outstanding mechanism of action of memantine and its success in the treatment of moderate to severe AD, numerous research groups from industry and academia have developed new NMDAR antagonist that are currently in distinct stages of the drug discovery process.<sup>124</sup> Related to this, the group of Dr. Santiago Vázquez Cruz has discovered several compounds with activity as NMDAR antagonists. The following section will cover them.

#### 1.4 Previous work of the group: new antagonists of the NMDAR

As stated in the previous introduction, the group has a wide expertise in the synthesis of cage compounds and their application as bioactive molecules. In 2008, a new research line targeting the NMDA receptor emerged with the initial results of the polycyclic amines shown in Figure 25.<sup>95,96,164</sup>

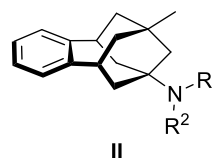
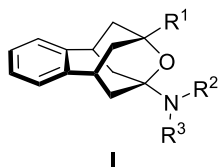


**Fig. 25.** Memantine analogues with moderate to good activity as NMDAR antagonists prepared by the group. R<sup>1</sup> and R<sup>2</sup> are H, alkyl, methylene-spaced aryl, guanidine or acetamidine. R<sup>3</sup> is H, alkyl or phenyl. Functional data were obtained from primary cultures of cerebellar granule neurons by measuring the intracellular calcium concentration. Cells were challenged with glutamate NMDA (100 μM). Data shown are means of at least three separate experiments carried out on three different batches of cultured cells.

Thereafter, several (1,2,3,5,6,7-hexahydro-1,5:3,7-dimethano-4-benzoxonin-3-yl)amines with general structure **I**, and 6,7,8,9,10,11-hexahydro-9-methyl-5,7:9,11-dimethano-5*H*-benzocyclononen-7-amines with general structure **II**, were synthesized by Dr. M. D. Duque and Dr. E. Torres and their activity against NMDAR was evaluated.<sup>97,98</sup> Table 3 includes the more potent polycyclic compounds of the two series.

<sup>164</sup> Duque, M. D. Ph.D. Dissertation, University of Barcelona, 2010.

**Table 3.** Benzo-homoxadamantane, **I**, and benzo-homoadamantane, **II**, derivatives active as NMDAR antagonists. Functional data were obtained from primary cultures of cerebellar granule neurons by measuring the intracellular calcium concentration. Cells were challenged with glutamate NMDA (100  $\mu\text{M}$ ). Data shown are means  $\pm$  SEM of at least three separate experiments carried out on three different batches of cultured cells.

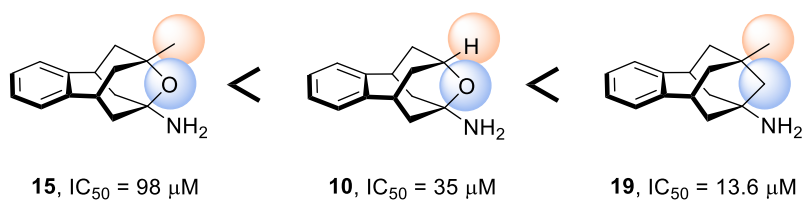


Comp.	R <sup>1</sup>	R <sup>2</sup>	R <sup>3</sup>	IC <sub>50</sub> ( $\mu\text{M}$ )
10	H	H	H	35 $\pm$ 6.8
11	H	Me	H	6.0 $\pm$ 1.3
12	H	Me	Me	3.8 $\pm$ 0.3
13	H	Et	Et	14 $\pm$ 1.1
14	H	-(CH <sub>2</sub> ) <sub>5</sub> -		30 $\pm$ 1.0
15	Me	H	H	98 $\pm$ 26
16	Me	Me	Me	3.9 $\pm$ 0.4
17	Me	Et	Et	7.7 $\pm$ 1.0
18	Et	H	H	> 200

Comp.	R <sup>1</sup>	R <sup>2</sup>	IC <sub>50</sub> ( $\mu\text{M}$ )
19	H	H	13.6 $\pm$ 3.4
20	H	Me	19.4 $\pm$ 3.3
21	Me	Me	11.8 $\pm$ 3.1
22		-(CH <sub>2</sub> ) <sub>5</sub> -	101 $\pm$ 25

Overall, a few trends were noted:

- Generally, tertiary amines were slightly more potent than their parent secondary amines, and the latter were more potent than the primary ones. For instance, compare **12** vs **11**, and **11** vs **10**. Also, small groups, such as methyl group, were more tolerated than large groups; see compound **12** vs **13**, and compound **16** vs **17**.
- Furthermore, 8-oxapolycyclic primary amines were less potent than their corresponding 8-carba analogues. For example, compound **19** showed a 7-fold increase in potency compared to its oxapolycyclic analogue **15**.
- Of note, while memantine (IC<sub>50</sub> = 1.5  $\pm$  0.1  $\mu\text{M}$ ), which features two methyl groups in its structure, is much more potent than amantadine (IC<sub>50</sub> = 92  $\pm$  29  $\mu\text{M}$ ), compound **10** was more active than its methyl analogue, **15**.
- The introduction of an oxygen atom was deleterious for the activity, as well as bearing an alkyl group at the bridgehead position (Fig. 26).



**Fig. 26.** Observed trend in the benzopolycyclic scaffolds. The increase in potency goes from left to right.

# Objetives



Bearing in mind what has been mentioned, it seems logical that derivative **23** which combines the best findings of our previously studies on benzo-adamantanolic amines, that is a hydrogen atom at C-9 position and a methylene group in C-8 position (Fig. 27), may display a better inhibitory activity against the NMDA receptor than its predecessors.

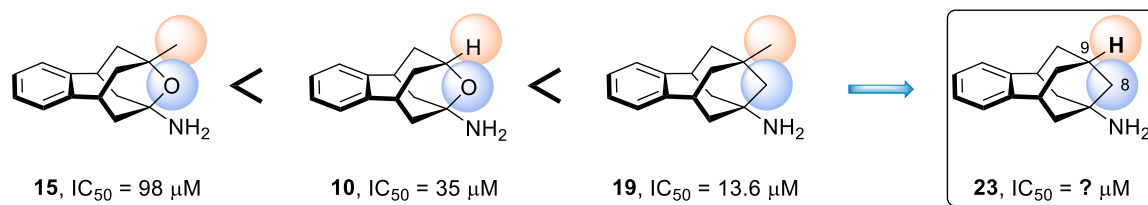


Fig. 27. Previous results suggest compound **23** as a potential NMDAR antagonist.

Considering this fact, we established the following goals of this chapter:

1. Synthesis and pharmacological evaluation of compound **23** and its corresponding methylated tertiary amine **24** (Fig. 28). The preparation of the secondary amine was discarded due to the preceding results, where tertiary amines proved to be the most potent derivatives. With this objective in mind, we aimed to confirm our hypothesis that both compounds would show higher potencies compared to previous derivatives.

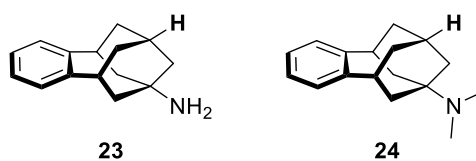
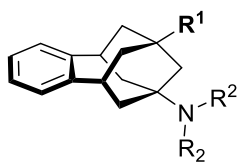


Fig. 28. Amines to synthesize as potential NMDAR antagonists.

2. Exploration of a structure-activity relationship (SAR) around the C-9 position, with the introduction of different groups such as halogens or a hydroxyl group (Fig. 29). This study would include the preparation of 5,6,8,9,10,11-hexahydro-7*H*-5,9:7,11-dimethanobenzo[9]annulen-7-amines with general structure **III**, as well as their corresponding tertiary amines. We aimed to find the effect of the different substituents at the C-9 position on the inhibitory activity.





III

R<sup>1</sup> = F, Cl, OH, OMe

R<sup>2</sup> = H or Me

Fig. 29. Amines with general structure III.

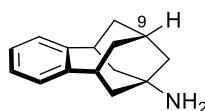
## **Results & Discussion**



## 1. Effect of the C-9 substitution in new benzopolycyclic compounds

### 1.1 Synthesis of the C9-demethylated compound, 23

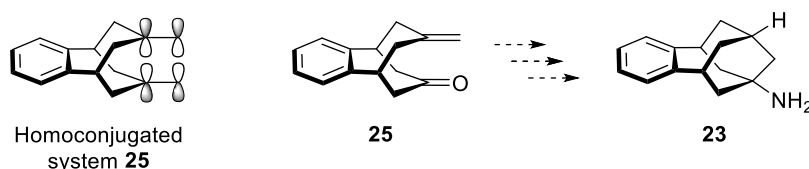
According to the previous work of the group related to the synthesis of benzopolycyclic cage amines, a benzo-homoadamantane with a hydrogen atom at the C-9 position would fulfil the gap existing between the former families. Hence, following the SAR studies we envisaged compound **23** as a potential antagonist of the NMDAR with hypothetical improved potency (Fig. 30).



**23**

Fig. 30. Compound to prepare from rational design.

The synthesis was designed based on prior synthetic routes described by our group. We conceived enone **25** as the starting point for the preparation of compound **23** (Scheme 2). This enone is a homoconjugated system that allows the 1,4-like addition of nucleophiles to the alkene, whereupon a transannular cyclization occurs with the attack to the carbonyl. This intramolecular through-space interaction between the two  $\pi$ -orbitals of **25** has been exploited in many transformations, such as in the intramolecular cyclization through a Ritter transformation, as it will be discussed later on.<sup>165,166</sup>



Scheme 2. Enone **25** as a precursor of amine **23**.

In this way, we decided to prepare enone **25** following the procedure firstly reported by Föhlisch *et al.*<sup>167,168</sup> and widely employed by our group. Starting from commercially available *o*-phthaldialdehyde and dimethyl-1,3-acetonedicarboxylate, a Weiss-Cook condensation took place affording tetraester intermediate **26**. Taking advantage of the keto-enol tautomerism of dimethyl-1,3-acetonedicarboxylate, the reaction proceeded through a double aldol condensation and subsequent dehydration, under basic catalysis.

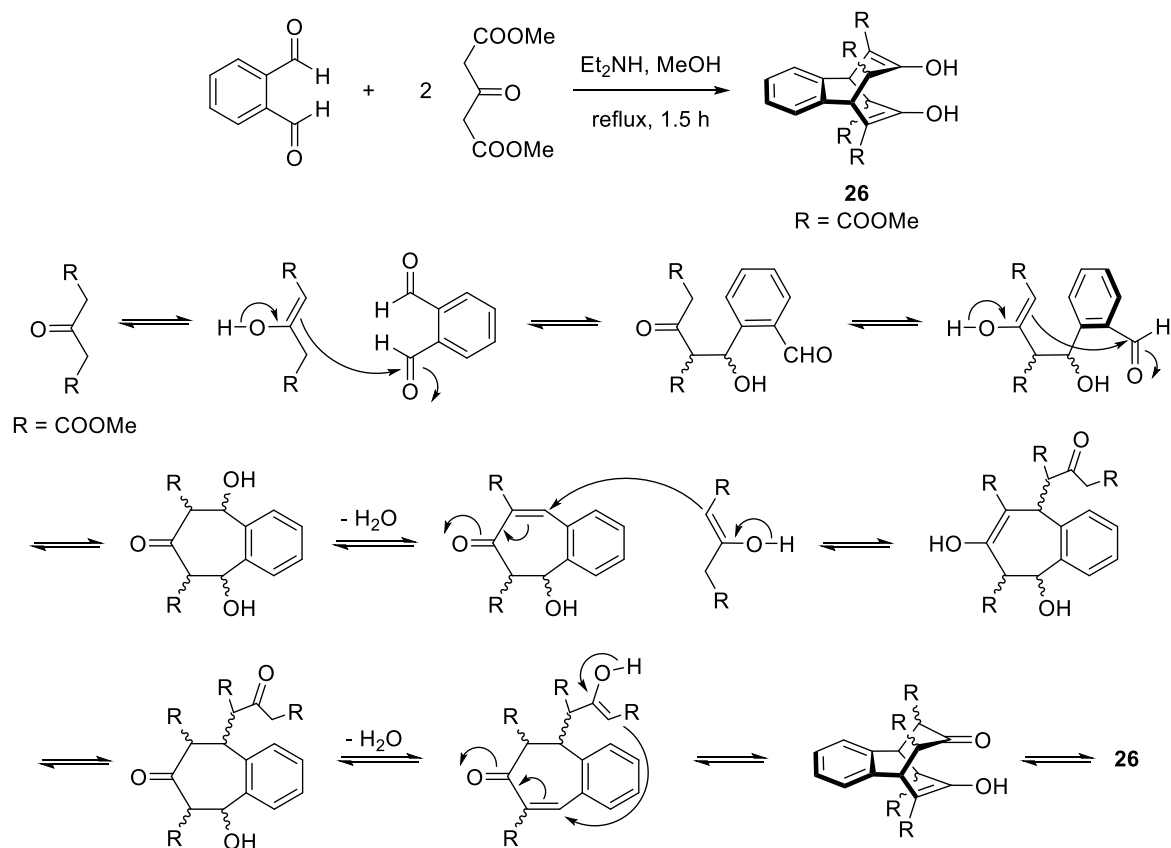
<sup>165</sup> Amini; Bishop, R. *Aust. J. Chem.* **1983**, *36*, 2465-2472.

<sup>166</sup> Amini; Bishop, R.; Burgess, G.; Craig, D. C.; Dance, I. G.; Scudder, M. L. *Aust. J. Chem.* **1989**, *42*, 1919-1928.

<sup>167</sup> Föhlisch, B.; Widmann, E.; Schupp, E. *Tetrahedron Lett.* **1969**, *28*, 2355-2358.

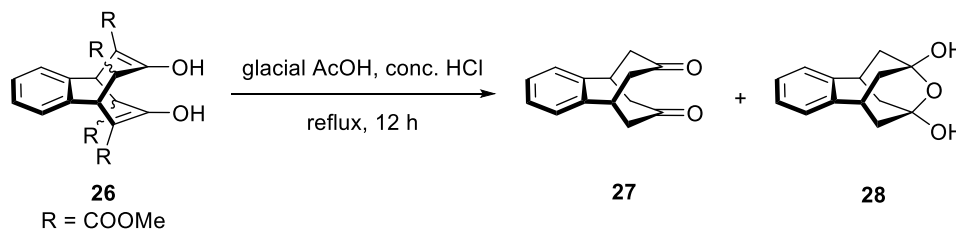
<sup>168</sup> Föhlisch, B.; Dukek, U.; Graessle, I.; Novotny, B.; Schupp, E.; Schwaiger, G.; Widmann, E. *Justus Liebigs Ann. Chem.* **1973**, 1839-1850.

The second equivalent of the  $\beta$ -keto ester underwent a double Michael addition to the  $\alpha,\beta$ -unsaturated ketone leading to the dienol-tetraester (Scheme 3).



**Scheme 3.** Weiss-Cook condensation of *o*-phthalaldehyde and two equivalents of dimethyl-1,3-acetonedicarboxylate.

Acid hydrolysis of the ester groups rendered  $\beta$ -keto acids which decarboxylated spontaneously to furnish a mixture of diketone **27** and its hydrate **28** in a 1:3 ratio (Scheme 4). Of note, the amount of the hydrate increased over time because of the atmospheric moisture, and even in a short period of time the equilibrium was utterly shifted to the hydrate. In order to procure the pure ketone, the mixture was refluxed in toluene using a Dean-Stark apparatus to finally provide pure diketone **27** in 64% overall yield.<sup>169</sup>

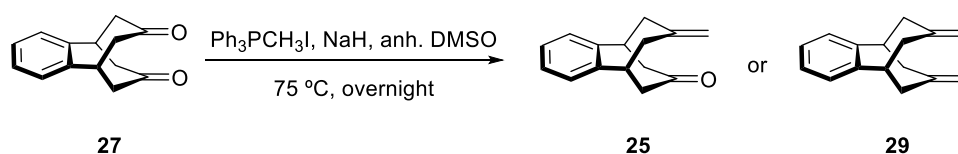


**Scheme 4.** Acid hydrolysis and decarboxylation of tetraester **26**.

<sup>169</sup> The previous method used for dehydration of the hydrate was to sublime the mixture at 160 °C and 0.5 Torr.

The next step was a Wittig reaction of a single ketone to form enone **25**. This conversion was inspired from the Corey procedure for the Wittig reaction,<sup>170,171</sup> and needed sodium hydride in anhydrous DMSO and methyltriphenylphosphonium iodide as the ylide counterpart. The double Wittig transformation of diketone **27** to form the corresponding diene **29** was earlier optimized by Dr. E. Torres, although using a large excess (8 equivalents) of NaH and of the Wittig reagent.<sup>172</sup> We believed that the reaction was poorly efficient due to the water content of the self-prepared anhydrous DMSO. Based on that, we aimed to optimize the mono-Wittig reaction adjusting the equivalents of both reagents and using a fresh bottle of anhydrous DMSO purchased from a chemical supplier. A short optimization process was performed (Table 4). Worth to note is the formation of diene **29** with only 2.1 equivalents of each reagent (entry 3), compared with the 8 equivalents needed in the previous procedure.

**Table 4.** Optimization process for the preparation of enone **25**. Yields are of isolated products.



Entry	Ph <sub>3</sub> PCH <sub>3</sub> I (eq.)	NaH (eq.)	<b>25</b> (% yield)	<b>29</b> (% yield)
1	1.1	1.1	63	-
2	1.25	1.25	84	-
3	2.1	2.1	-	80

In this transformation, a mixture of NaH in anhydrous DMSO was heated to 75 °C for 45 minutes so as to form the conjugate base of DMSO, which is the actual species that deprotonated the phosphonium salt upon its addition in order to obtain the ylide. Twenty minutes after, a solution of diketone **27** in anhydrous DMSO was added to the mixture and heated to 75 °C overnight. The best conditions were the ones from entry 2 in table 4, with 1.25 equivalents of the base and of the ylide that furnished desired enone **25** in 84% yield.

Apart from the reaction optimization, an easy and efficient purification process was required in order to remove the phosphine oxide, which in many cases can be tedious. With the aim of avoiding the purification by column chromatography, we came up with a handy method by means of packing the impure mixture with silica gel followed by extraction with an appropriate mixture of petroleum ether and diethyl ether.

<sup>170</sup> Greenwald, R.; Chaykovsky, M.; Corey, E. J. *J. Org. Chem.* **1963**, *28*, 1128-1129.

<sup>171</sup> Coxon, J. M.; MacLagan, R. G. A. R.; McDonald, D. Q.; Steel, P. J. *J. Org. Chem.* **1991**, *56*, 2542-2549.

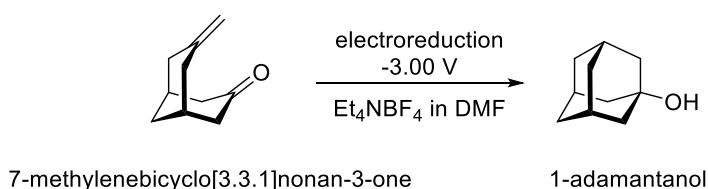
<sup>172</sup> Torres, E. Ph.D. Dissertation, University of Barcelona, 2013.

Noteworthy, all the reactions so far were carried out in a multigram scale.

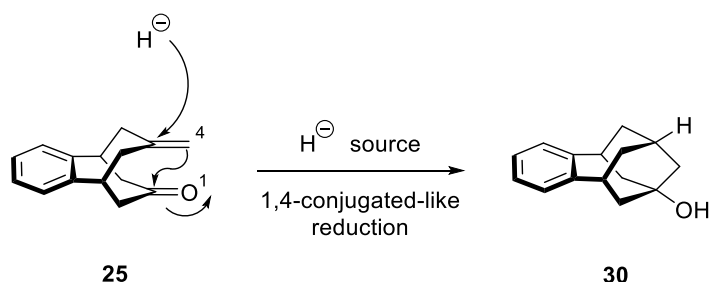
With pure enone **25** in hand, we envisaged the preparation of amine **23** from alcohol **30** (Scheme 5). A bridgehead alcohol can be replaced by an amino group *via* different procedures, such as the already mentioned Ritter reaction,<sup>173</sup> the metal-catalysed addition of ammonia to alcohols,<sup>174,175</sup> or the nucleophilic substitution *prior* functional group interconversion to a better leaving group, like a halide or a mesylate group.

Inspired by the work of Itoh *et al.*,<sup>176</sup> where 1-adamantanol was obtained from 7-methylenebicyclo[3.3.1]nonan-3-one through an electroreductive transannular reaction, and by the boron chemistry for the 1,4-enone reduction,<sup>177</sup> a 1,4-conjugated-like reduction of enone **25** would afford desired alcohol **30**.

Published work:



Intended work:



**Scheme 5.** Plausible formation of alcohol **30** from enone **25** by a 1,4-conjugated-like reduction.

Many hydrides have been applied as reductive agents in the 1,4-reduction of  $\alpha,\beta$ -unsaturated ketones. Especially, alkali metal trialkylborohydride reagents are excellent choices for enone reduction that have been proved to give very high regio- and stereoselectivities.<sup>178</sup> Organoboranes such as lithium tri-*sec*-butylborohydride (L-selectride<sup>®</sup>) or lithium *n*-butylborohydride have been largely employed in multiple reductions, although

<sup>173</sup> Fokin, A. A.; Merz, A.; Fokina, N. A.; Schwertfeger, H.; Liu, S. L.; Dahl, J. E. P.; Carlson, R. K. M.; Schreiner, P. R. *Synthesis* **2009**, 6, 909-912.

<sup>174</sup> Shimizu, K.-I.; Kanno, S.; Kon, K.; Hakim Siddiki, S. M. A.; Tanaka, H.; Sakata, Y. *Catal. Today* **2014**, 232, 134-138.

<sup>175</sup> Sigl, M.; Heidemann, T. Process for preparing a primary amine with a tertiary alpha carbon atom by reacting a tertiary alcohol with ammonia. WO 2009/053275 A1.

<sup>176</sup> Itoh, H.; Kato, I.; Unoura, K.; Senda, Y. *Bull. Chem. Soc. Jpn.* **2001**, 74, 339-345.

<sup>177</sup> Burkhardt, E. R.; Matos, K. *Chem. Rev.* **2006**, 106, 2617-2650.

<sup>178</sup> Fortunato, J. M.; Ganem, B. *J. Org. Chem.* **1976**, 41, 2194-2200.

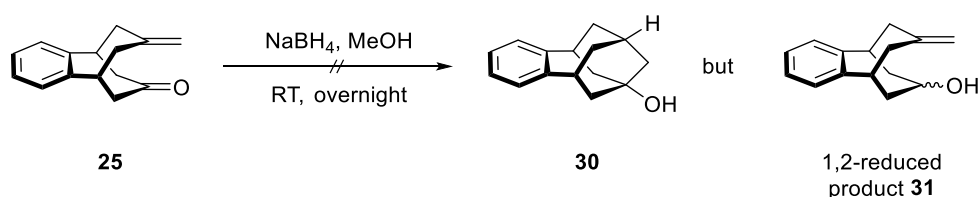
1,2- or 1,4-hydride additions are mainly controlled by substrate structure.<sup>179,180,181</sup> Hence, we treated enone **25** with L-selectride<sup>®</sup> in anhydrous THF with or without triethylamine (TEA), and under short or longer reaction times, without success under any condition (Table 5).

**Table 5.** Attempt to prepare alcohol **30** through reduction with lithium tri-*sec*-butylborohydride.

Entry	TEA	Temp. (°C)	Time (h)	<b>30</b> (% yield)
1	<del>✓</del>	-78	0.5	-
2	✓	25	18	-

On the other hand, sodium hydrogen telluride (NaHTe) was successfully employed in the selective 1,4-reduction of  $\alpha,\beta$ -unsaturated carbonyl compounds.<sup>182,183,184</sup> However, the requirement of its *in situ* formation from telluride powder and sodium borohydride was reason enough to preclude its use.

Then, we explored the 1,4-conjugated-like reduction of enone **25** with other hydride sources such as sodium borohydride, which has been proved as an efficient reducing agent in several conjugated systems.<sup>185,186</sup> Even though in most cases the 1,2-reduction prevails, we wondered if in our homoconjugated system the 1,4-reduction would overcome the 1,2-reduction (Scheme 6). Unfortunately, no expected compound was recovered but the 1,2-reduced product **31**.



**Scheme 6.** Reduction of the ketone after treatment of enone **25** with NaBH<sub>4</sub>.

<sup>179</sup> Martin, H. J.; Drescher, M.; Mulzer, J. *Angew. Chem. Int. Ed.* **2000**, *39*, 581-583.

<sup>180</sup> White, D. R. 6'-Alkylspectinomycins. US 4532336 A.

<sup>181</sup> Kim, S.; Choon Moon, Y.; Han Ahn, K. *J. Org. Chem.* **1982**, *47*, 3311-3315.

<sup>182</sup> Yamashita, M.; Kato, Y.; Suemitsu, R. *Chem. Lett.* **1980**, 847-848.

<sup>183</sup> Barton, D. H. R.; Bohé, L.; Lusinchi, X. *Tetrahedron* **1990**, *46*, 5273-5284.

<sup>184</sup> Yamashita, M.; Tanaka, Y.; Arita, A.; Nishida, M. *J. Org. Chem.* **1994**, *59*, 3500-3502.

<sup>185</sup> Marchand, A. P.; LaRoe, W. D.; Sharma, G. V. M.; Suri, S. C.; Reddy, D. S. *J. Org. Chem.* **1986**, *51*, 1622-1625.

<sup>186</sup> Jackson, W. R.; Zurqiyar, A. *J. Chem. Soc.* **1965**, 5280-5287.



Searching for an alternative approach for the preparation of alcohol **30**, different publications reached our hands reporting the catalytic hydrogenation at atmospheric pressure of 7-methylenebicyclo[3.3.1]nonan-3-one to afford 1-adamantanol in good yields.<sup>187,188</sup> To our disappointment, when this conditions were undertaken with enone **25**, we observed the double bond migration of enone **25** to furnish ketone **32**, as well as the dihydroxylated compound **33** (Table 6). The formation of the latter can be reasoned *via* the addition of a water molecule, coming from the moisture in the Pd/C, to the conjugated-like enone. The ratio of the resulting mixture depended on the reaction time and on the equivalents of the palladium catalyst.

**Table 6.** Catalytic hydrogenation of enone **25** to provide different mixtures of **32** and **33**.

Entry	Pd/C	Time (h)	Solvent	25 (% yield)	32 (% yield)	33 (% yield)
1	0.1	64	DCM	43	-	21
2	0.1	64	Toluene	60	-	30
3	0.2	72	Toluene	-	71	-
4	0.1	120	Toluene	50	-	50
5	0.4	64	Toluene	22	-	58
6	1	64	Toluene	-	24	15

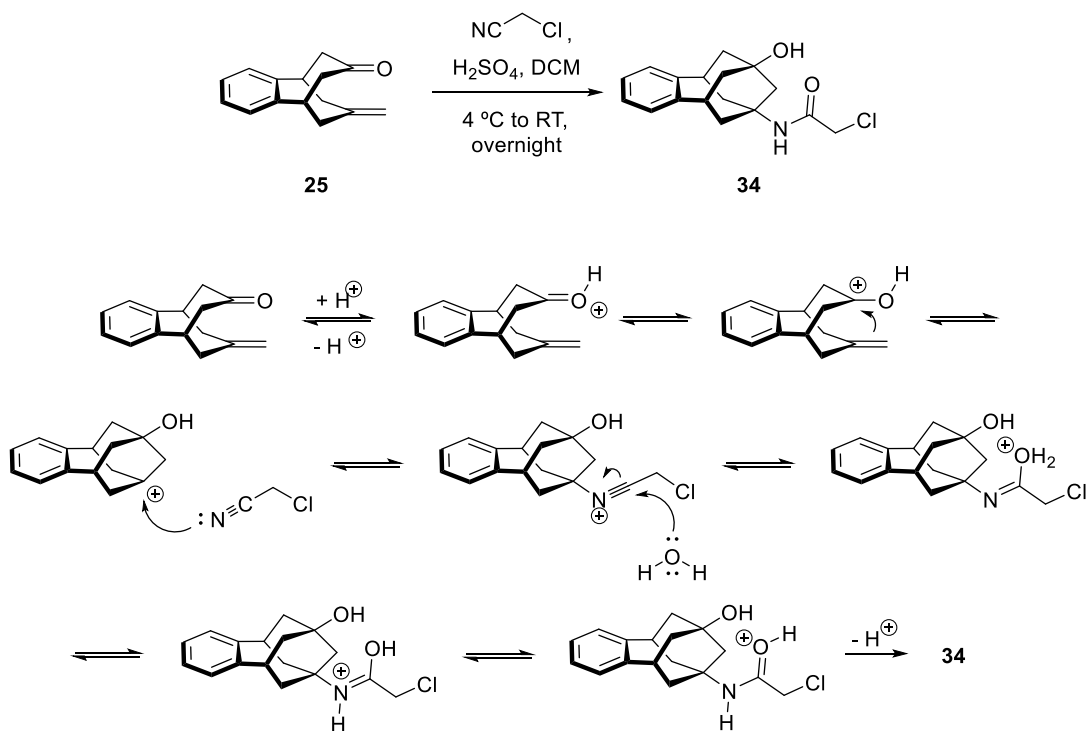
All these failures did not discourage us to persist in the quest for amine **23**, so we pursued its synthesis through a different approach. Instead of a conjugated-like addition to the well-known enone, we aimed to proceed by means of functional group replacement.

To do so, the synthesis continued with a Prins-Ritter transannular cyclization with chloroacetonitrile in the presence of sulphuric acid from the same enone **25**.<sup>165,166,189</sup> The reaction mechanism for the formation of chloroacetamide **34** is displayed in scheme 7. The reaction involves the protonation of the carbonyl group followed by the attack of the  $\pi$  electrons of the alkene (Prins reaction) to generate a stable carbenium ion. The nitrile's nitrogen then adds to the carbocation to give a nitrilium ion intermediate, which undergoes hydrolysis upon addition of water during the work-up affording the desired chloroacetamide (Ritter reaction).

<sup>187</sup> Ishiyama, J.; Senda, Y.; Imaizumi, S. *Chem. Lett.* **1983**, 771-774.

<sup>188</sup> Ishiyama, J.; Senda, Y.; Imaizumi, S. *Chem. Lett.* **1983**, 1243-1244.

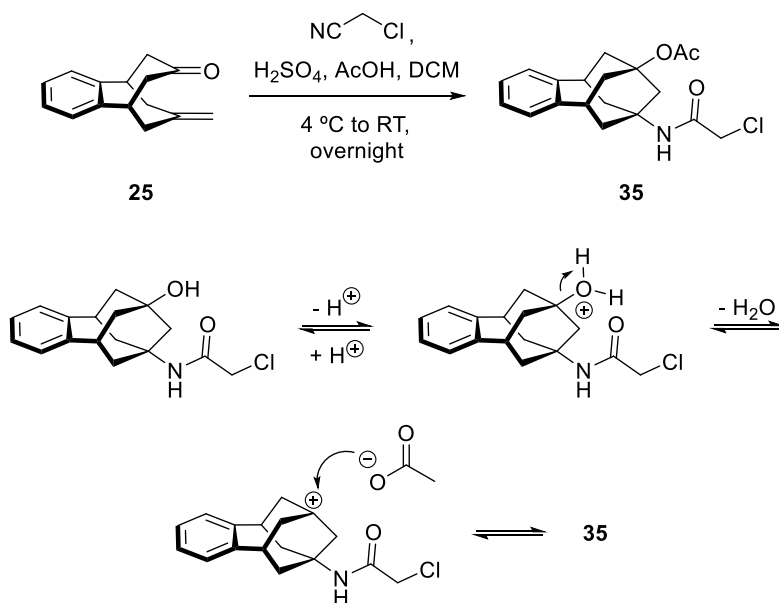
<sup>189</sup> Bishop, R. *Ritter-Type Reactions, Comprehensive Organic Synthesis II*; Elsevier Ltd., 2014.



**Scheme 7.** Mechanism of the Prins-Ritter transannulation.

Other preparations of similar chloroacetamides entailed the combination of glacial acetic acid and sulphuric acid.<sup>98,190</sup> The first attempts of the procedure led to the formation of the corresponding acetate **35**, whose formation can be explained by the protonation of the hydroxyl group of **34**, the formation of a stable carbenium ion with the loss of a molecule of water, and finally the nucleophilic addition of the acetate (Scheme 8). In the absence of acetic acid, the conjugate base of sulphuric acid is not nucleophilic enough to add to the carbocation. Hence, the hydroxyl group remains unaltered.

<sup>190</sup> Schwertfeger, H.; Würtele, C.; Sefarin, M.; Hausmann, H.; Carlson, R. M. K.; Dahl, J. E. P.; Schreiner, P. *R. J. Org. Chem.* **2008**, *73*, 7789-7792.



**Scheme 8.** Addition of an acetate to the carbocation generated during the course of the Prins-Ritter transformation.

Once chloroacetamide **34** was prepared in reasonable yield (49 %), we sought the known Barton-McCombie deoxygenation for the preparation of the chloroacetamide **36**. This type of transformation consists in the radical deoxygenation of previously-modified alcohols.<sup>191,192,193</sup> First, the alcohol needs to be temporally converted to an O-alkylthiocarbonyl derivative, whose sulphur atom reacts with a radical M<sup>•</sup> capable of forming a stable bond with it. The new bond fragments into a carbonyl compound and an alkyl radical, followed by a hydrogen atom abstraction to afford the reduced product (Scheme 9). The driving force of the reaction is the energy gained by the transition from the C=S to a C=O bond (C=S bond: 138 kcal mol<sup>-1</sup>, C=O bond: 178 kcal mol<sup>-1</sup>).<sup>194</sup> On the basis of thermochemical data, trialkyltin hydrides seemed to be particularly suitable because of their exceptional behaviour as hydrogen-donors and the high stability of the Sn-S bond (Sn-S bond: 110 kcal mol<sup>-1</sup>). Hence, the reaction mechanism normally implies a radical initiator, like azobisisobutyronitrile (AIBN), to initiate the radical process. However, due to the inherent toxicity of tin hydrides, the development of tin-free Barton-McCombie deoxygenations has been rising since its discovery.<sup>195,196,197</sup> Regarding O-alkylthiocarbonyl compounds, secondary and in a lesser extent primary and tertiary alcohols, are usually

<sup>191</sup> Barton, D. H. R.; McCombie, S. W. *J. Chem. Soc., Perkin Trans.* **1975**, *1*, 1574-1585.

<sup>192</sup> McCombie, S. W.; Motherwell, W. B.; Tozer, M. J. *Org. React.* **2012**, *77*, 161-591.

<sup>193</sup> Zard, S. Z. *Xanthates and Related Derivatives as Radical Precursors*, in *Encyclopedia of Radicals in Chemistry, Biology and Materials*; John Wiley & Sons, Ltd., Chichester, UK, 2012.

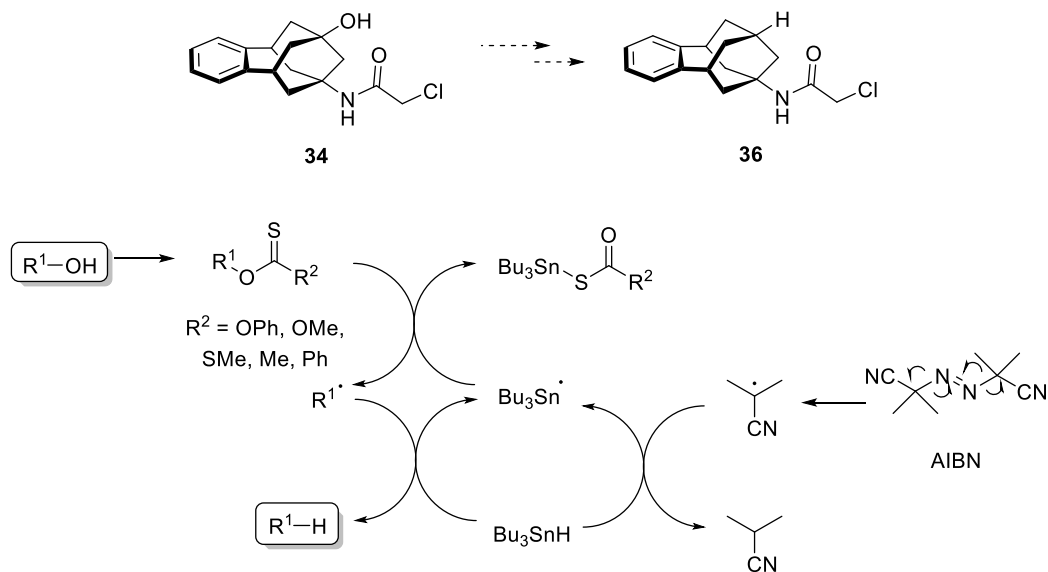
<sup>194</sup> Kerr, J. A. *Chem. Rev.* **1966**, *66*, 465-500.

<sup>195</sup> Chenneberg, L.; Baralle, A.; Daniel, M.; Fensterbank, L.; Goddard, J.-P.; Ollivier, C. *Adv. Synth. Catal.* **2014**, *356*, 2756-2762.

<sup>196</sup> Chatgijaloglu, C.; Ferreri, C. *Res. Chem. Intermed.* **1993**, *19*, 755-775.

<sup>197</sup> Schummer, D.; Hoefle, G. *Synlett* **1990**, *11*, 705-706.

transformed to thiocarbonates, xanthates and thioesters, whose reactivity in Barton-McCombie deoxygenations has been attested several times.



**Scheme 9.** Mechanism of the radical Barton-McCombie deoxygenation.

Encouraged by the literature precedents, we decided to convert **34** into phenylthiocarbonate **37** by applying the conditions reported in the literature (Table 7). Treatment of **34** with O-phenyl chlorothionoformate with no base added did not yield the expected product.<sup>198</sup> Neither did the reaction with addition of a base such as NaH, pyridine or 4-dimethylaminopyridine (DMAP).<sup>199,200,201,202,203</sup> In all the cases the starting material was recovered.

<sup>198</sup> Xu, J.; Yadan, J. C. *Tetrahedron Lett.* **1996**, *37*, 2421-2424.

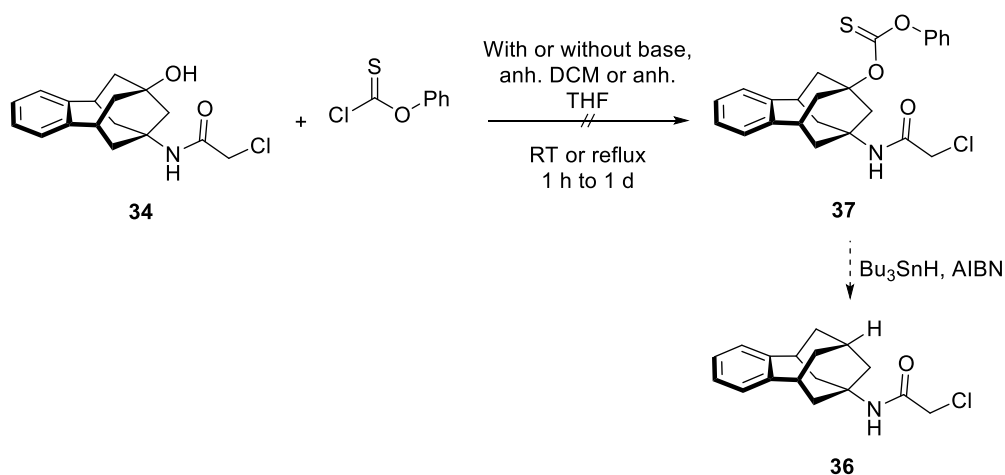
<sup>199</sup> Padwa, A.; Harring, S. R.; Semones, M. A. *J. Org. Chem.* **1998**, *63*, 44-54.

<sup>200</sup> Marino, J. P.; Osterhout, M. H.; Padwa, A. *J. Org. Chem.* **1995**, *60*, 2704-2713.

<sup>201</sup> Boussagnet, P.; Delmond, B.; Dumartin, G.; Pereyre, M. *Tetrahedron Lett.* **2000**, *41*, 3377-3380.

<sup>202</sup> Kaneko, S.; Watanabe, T.; Oda, K.; Mohan, R.; Schweiger, E. J.; Martin, R. Fused-ring pyrimidin-4(3H)-one derivatives, processes for the preparation and uses thereof. WO 03/106435 A1.

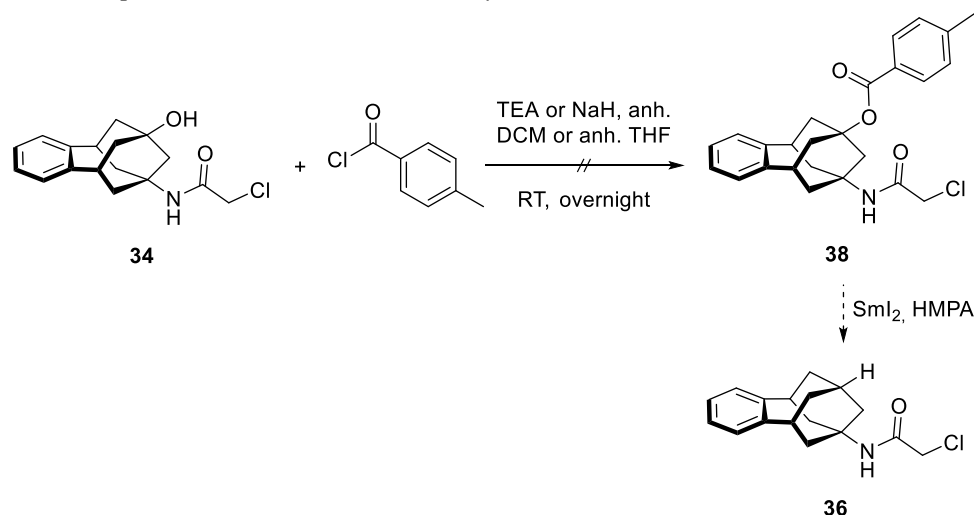
<sup>203</sup> Luzzio, F. A.; Fitch, R. W. *J. Org. Chem.* **1999**, *64*, 5485-5493.

**Table 7.** No reaction observed with the treatment of **34** with O-phenyl chlorothionoformate.

Entry	O-phenyl chlorothionoformate (eq.)	Base	Solvent	Temp. (°C)	Time (h)	37 (% yield)
1	1.2	DMAP (1.5 eq.)	DCM	25	21	-
2	1.1	NaH (3 eq.)	THF	25	3	-
3	2	NaH (4.4 eq.)	THF	reflux	21	-
4	1.5	Pyridine (excess)	DCM	25	24	-
5	2	-	THF	From -70 to 25	20	-

In accordance with radical deoxygenations, Markó and co-workers published a procedure using toluates as simple and versatile radical precursors for the reduction of alcohols to alkanes.<sup>204</sup> We contemplated hence the preparation of the corresponding toluate of **34** for its subsequent treatment with samarium(II) iodide and hexamethylphosphoramide (HMPA) (Table 8). The two different attempts for the formation of **38** did not afford the toluate and the starting material was again recovered. Thus, this approximation was abandoned.

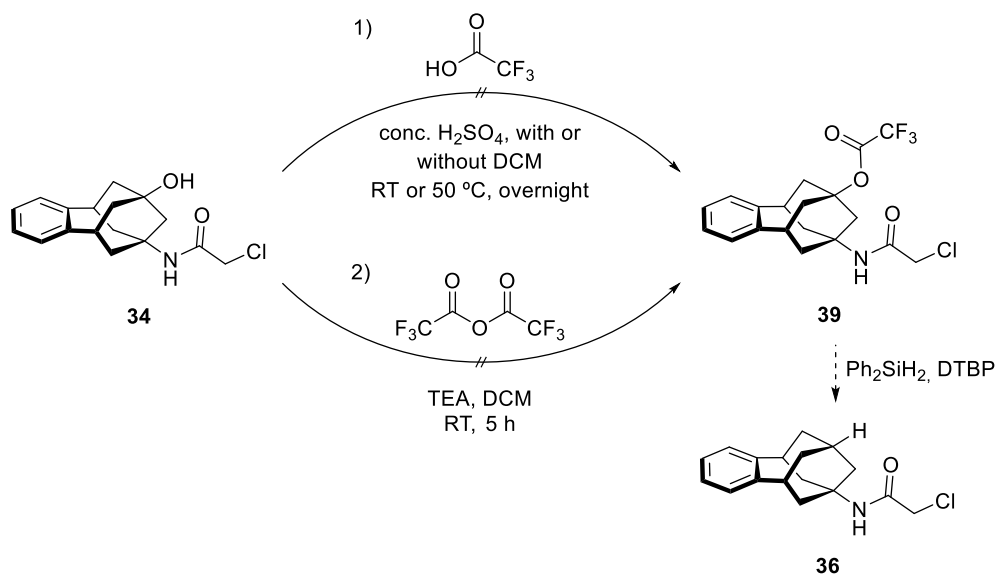
<sup>204</sup> Lam, K.; Markó, I. E. *Org. Lett.* **2008**, *10*, 2773-2776.

Table 8. Attempted reactions of **34** with toluoyl chloride and a base.

Entry	Base	Solvent	38 (% yield)
1	TEA (2 eq.)	DCM	-
2	NaH (2 eq.)	THF	-

A similar procedure appeared in 2001 dealing with the radical deoxygenation of alcohols *via* their trifluoroacetate derivatives with diphenylsilane and di-*tert*-butyl peroxide (DTBP).<sup>205</sup> In this case, the hydroxyl group of **34** needed to be turned into a trifluoroacetate group (Scheme 10). Two different pathways were essayed: 1) formation of a carbocation with conc. H<sub>2</sub>SO<sub>4</sub> and ensuing addition of trifluoroacetate; or 2) deprotonation of the alcohol and nucleophilic attack to trifluoroacetic anhydride (TFAA). Unfortunately, none of the tested conditions yielded the desired product **39** nor the starting material but only a mixture of unknown compounds. Specifically, we observed by <sup>1</sup>H-NMR the lack of proton signals for the methylene in C-8 position. This fact can be explained through a putative retro-Ritter reaction, although a mechanism cannot be postulated without having identified the product.

<sup>205</sup> Jang, D. O.; Kim, J.; Cho, D. H.; Chung, C.-M. *Tetrahedron Lett.* **2001**, 42, 1073-1075.



**Scheme 10.** Attempt to prepare compound **36** through a radical deoxygenation from a trifluoroacetate group.

This large list of negative results did not dishearten us in our pursuit of deoxygenated compound **36**. Further bibliographic search led us to the widely applied ionic deoxygenation triggered by organosilicon hydrides, which are used as a source of ionic hydride thanks to the presence of at least one Si-H bond.<sup>206</sup> For alcohols that can form a sufficiently stabilized carbenium ion, treatment with a Brønsted or Lewis acid in the presence of triethylsilane or similar leads to their reduction. Tertiary alcohols are more effective in the transformation into the corresponding alkanes than secondary and primary alcohols. The mechanism of reaction entails the coordination of the oxygen atom to the acid, formation of a carbenium ion *prior* addition of the hydride. Taking this into account, compound **36** could be prepared from hydroxylated compound **34** in just one step by addition of  $\text{Et}_3\text{SiH}$  and an acid.<sup>207,208,209,210</sup> Different conditions were tested, using trifluoroacetic acid (TFA) or boron trifluoride etherate as Brønsted or Lewis acids respectively, and changing the equivalents of both partners as well as the reaction time (Table 9). Regrettably, even the best conditions, i.e. a large excess of  $\text{Et}_3\text{SiH}$  and of  $\text{BF}_3 \cdot \text{Et}_2\text{O}$ , in anhydrous DCM at 75 °C for 3 days, only gave a mixture of the intended product, unreacted starting material and unidentified products.

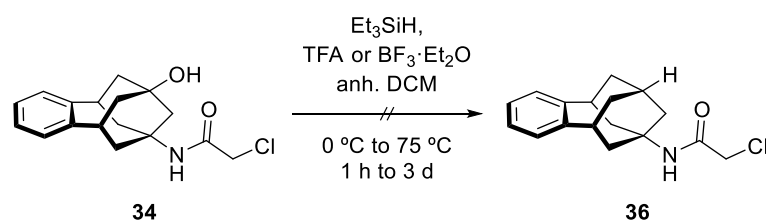
<sup>206</sup> Larson, G. L.; Fry, J. L. *Ionic and organometallic-catalyzed organosilane reductions*, in *Organic Reactions*; John Wiley & Sons, Ltd., Chichester, UK, 2008.

<sup>207</sup> Gevorgyan, V.; Rubin, M.; Benson, S.; Liu, J.-X.; Yamamoto, Y. *J. Org. Chem.* **2000**, *65*, 6179-6186.

<sup>208</sup> Duddeck, H.; Rosenbaum, D. *J. Org. Chem.* **1991**, *56*, 1707-1713.

<sup>209</sup> Banide, E. V.; Molloy, B. C.; Ortin, Y.; Müller-Bunz, H.; McGlinchey, M. J. *Eur. J. Org. Chem.* **2007**, 2611-2622.

<sup>210</sup> Ito, M.; Konno, F.; Kunamoto, T.; Suzuki, N.; Kawahata, M.; Yamaguchi, K.; Ishikawa, T. *Tetrahedron* **2011**, *67*, 8041-8049.

**Table 9.** Failed ionic hydrogenation of alcohol **34**.

Entry	Et <sub>3</sub> SiH (eq.)	Acid	Temp. (°C)	Time (h)	34 (% yield)	36 (% yield)
1	excess	TFA (excess)	25	1	Quant.	-
2	4	BF <sub>3</sub> ·Et <sub>2</sub> O (1 eq.)	25	1	86	-
3	excess	BF <sub>3</sub> ·Et <sub>2</sub> O (excess)	25	18	Quant.	-
4	4	BF <sub>3</sub> ·Et <sub>2</sub> O (1 eq.)	reflux	18	Quant.	-
5	excess	BF <sub>3</sub> ·Et <sub>2</sub> O (excess)	reflux	6	Quant.	-
6	excess	TFA (excess)	reflux	15	Quant.	-
7	excess	TFA (excess)	reflux	24	40	-
8	excess	BF <sub>3</sub> ·Et <sub>2</sub> O (excess)	reflux	24	32	25
9	excess	BF <sub>3</sub> ·Et <sub>2</sub> O (excess)	reflux	48	26	45
10	excess	BF <sub>3</sub> ·Et <sub>2</sub> O (excess)	reflux	72	16	50

Considering the high reactivity of bridgehead hydroxyl groups in traditional reductions, the difficulty of transforming alcohol **34** can be reasoned by the presence of the chloroacetamide in the molecule, which may facilitate the retro-Ritter reaction on one side, and possesses a high reactive chlorine atom on the other.

In spite of all the efforts in performing Barton-McCombie and ionic deoxygenation reactions, we decided to tackle the synthesis of amine **23** by applying a different approach. Exploring alternative methodologies, dehalogenation seemed at first glance a feasible way to remove a tertiary alcohol through its *prior* interconversion to a halide. Different publications have appeared reporting the dechlorination of adamantane groups through diverse procedures, such as the use of a hydride source (e.g. lithium aluminium hydride),<sup>211,212</sup> the radical dehalogenation with phenylsilane,<sup>213</sup> or the photoinduced reduction of organic halides with samarium(II) iodide.<sup>214</sup>

On that account, we needed to transform the hydroxyl group to a chloride. Alkyl chlorides are most easily prepared by reaction with thionyl chloride or phosphorous

<sup>211</sup> Ashby, E. C.; Deshpande, A. K. *J. Org. Chem.* **1994**, *59*, 3798-3805.

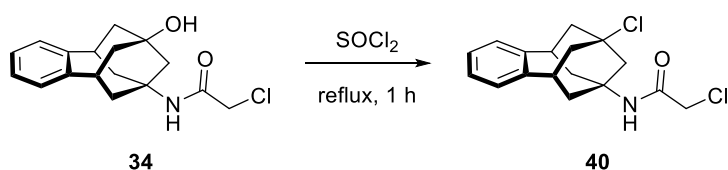
<sup>212</sup> Banister, S. D.; Yoo, D. T.; Chua, S. W.; Cui, J.; Mach, R. H.; Kassiou, M. *Bioorg. Med. Chem. Lett.* **2011**, *21*, 5289-5292.

<sup>213</sup> Jang, D. O. *Synth. Commun.* **1997**, *27*, 1023-1027.

<sup>214</sup> Sumino, Y.; Harato, N.; Tomisaka, Y.; Ogawa, A. *Tetrahedron* **2003**, *59*, 10499-10508.

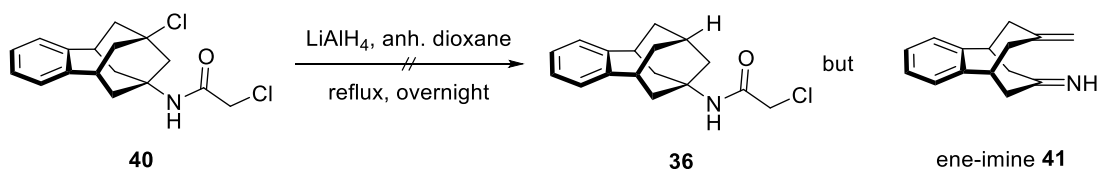


trichloride, among other reagents. Hence, we treated chloroacetamide **34** with neat thionyl chloride for one hour under reflux, giving desired chloride **40** in 56% yield after purification by column chromatography (Scheme 11).



**Scheme 11.** Replacement of the hydroxyl group by a chloride.

Afterwards, reaction of chloro compound **40** with  $\text{LiAlH}_4$  in anhydrous dioxane for 18 hours at reflux afforded a complex mixture of products. By gas chromatography-mass spectroscopy, the corresponding ene-imine product **41** was observed, whose formation can be explained by the attack of the hydride to the carbonyl group, which expelled the nitrogen atom generating an electron cascade movement with the final release of the chloride (Scheme 12).



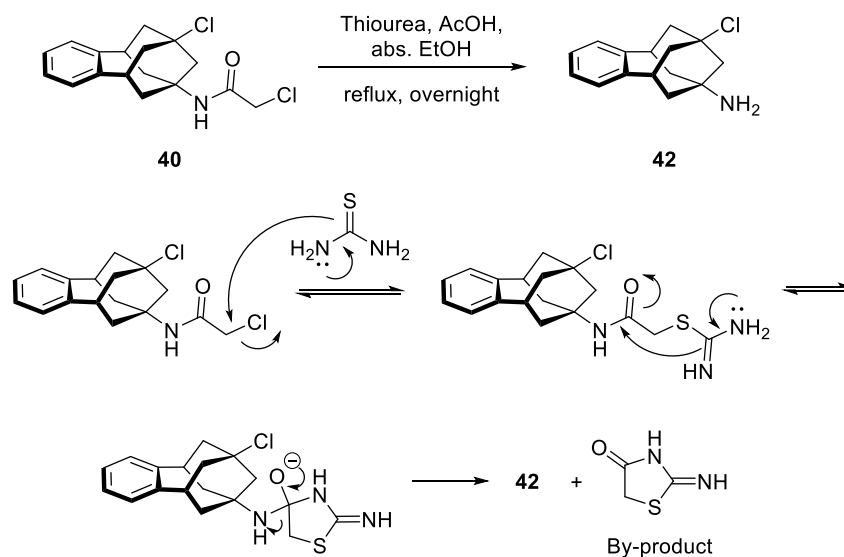
**Scheme 12.** Formation of ene-imine **41** after treatment of **40** with  $\text{LiAlH}_4$ .

Regardless of the unfortunate result of the aforementioned reaction, we wanted to further explore the potential of chloro derivative **40** as a precursor of unsubstituted scaffold in amine **23**. Among all the reagents for the formation of radicals from halides, samarium(II) iodide is possible the most versatile and widely used after tributyltin hydride.<sup>215</sup> In 2003, a publication came out describing the radical dechlorination of 1-chloroadamantane using  $\text{SmI}_2$  in anhydrous THF under irradiation with a tungsten lamp to afford the adamantane ring in 86% yield.<sup>214</sup> But because there is a potential coordination of samarium with the carboxyl group in a Lewis acid manner, we determined to hydrolyse the amide group *prior* to the radical dehalogenation in order to avoid side reactions. A previous exploration of the aqueous hydrolysis of related compounds gave either low yields in acid media, or high yields at the expense of drastic basic conditions.<sup>98</sup> Searching for a substitutive method, it was found that the chloroacetyl group could be cleaved by thiourea in an efficient way for the synthesis of *tert*-alkylamines.<sup>216</sup> Applying these conditions to our scaffold, chloroacetamide **40** was transformed into chloro-amine **42** in 73% yield (Scheme 13). The deprotection mechanism entails the nucleophilic substitution of the chloride by the attack of the sulphur atom, followed by the formation of a thiazolidine ring as a by-

<sup>215</sup> Rowlands, G. J. *Tetrahedron* **2009**, *65*, 8603-8655.

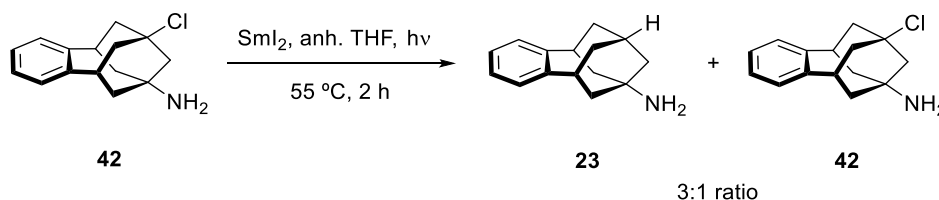
<sup>216</sup> Jirgensons, A.; Kauss, V.; Kalvinsh, I.; Gold, M. R. *Synthesis* **2000**, *12*, 1709-1712.

product. Subsequent elimination of the amine provided compound **42** and pseudothiohydantoin as a by-product. The reaction is also amenable in DCM.



**Scheme 13.** Deprotection of chloroacetamide with thiourea. The proton migrations have been obviated for the sake of clarity.

Once deprotected, chloro-amine **42** was reacted with  $\text{SmI}_2$  and irradiated with a 100 W lamp until the mixture shifted from dark blue to yellow.<sup>217</sup> To our surprise, desired amine **23** was recovered along with the starting material **42** in an optimized 3:1 ratio (Scheme 14). Regrettably, the mixture was inseparable through column chromatography.



**Scheme 14.** Partial dehalogenation of chloro-amine **42** with samarium(II) iodide.

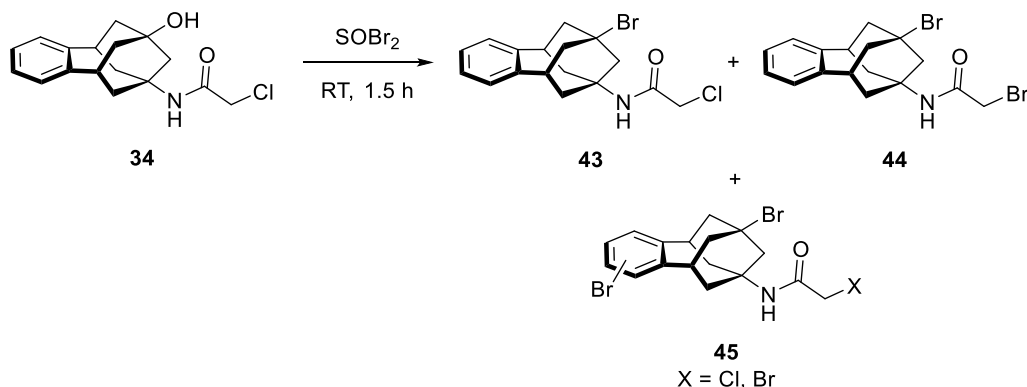
Based on the partial success of the previous reaction, we believed that the use of organotin reagents would facilitate the radical dehalogenation of our scaffold because of their proven reactivity and versatility.<sup>192,215,218,219</sup> In addition, it is well-known that the bond dissociation enthalpy of the halogen strongly determines the dehalogenation rate. Accordingly, bond enthalpies decrease as we move down the periodic table, i.e.  $\text{Cl} > \text{Br} > \text{I}$ . So, instead of working with the chloro derivative, we decided to replace the hydroxyl group of **34** by a bromide following the aforementioned procedure but in this case with thionyl bromide (Scheme 15). Albeit the excellent conversion of the alcohol, we observed

<sup>217</sup> The blue colour is distinctive of samarium(II), whereas the yellow colour of samarium(III).

<sup>218</sup> Jasch, H. Heinrich, M. R. *Tin hydrides and functional group transformations, in Encyclopedia of Radicals in Chemistry, Biology and Materials*; John Wiley & Sons, Ltd., Chichester, UK, 2012.

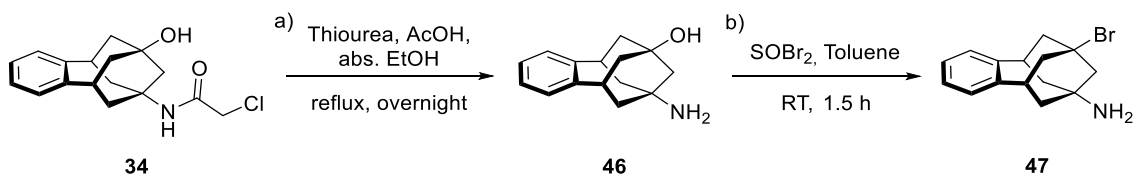
<sup>219</sup> Renaud, P.; Sibi, M. P. *Radicals in Organic Synthesis Vol. 1*; Wiley-VCH, Weinheim, Germany, 2001.

by gas chromatography-mass spectroscopy and  $^1\text{H-NMR}$ , the concomitant formation of bromoacetamide **44** by nucleophilic substitution of the chloro atom, as well as, to a lesser degree, the bromination of the aromatic ring as either chloro- or bromoacetamide, **45**, whose rate of formation varied from one reaction to another.



**Scheme 15.** Functional group interconversion of a hydroxyl group to a bromide.

In order to avoid the chloro-bromo exchange of the acetamide, we ended up moving one-step forward and deprotecting chloroacetamide **34** to obtain the corresponding aminoalcohol **46**. In this way, applying the previous conditions with thiourea and glacial acetic acid in absolute ethanol, primary amine **46** was prepared in quantitative yield (Scheme 16a). Afterwards, transformation of **46** to the bromo derivative with thionyl bromide in toluene afforded the desired halide **47** in 79% yield (Scheme 16b).

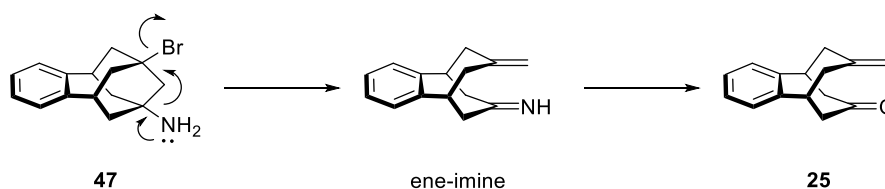


**Scheme 16.** Thiourea-mediated deprotection of chloroacetamide **34**, followed by bromination with thionyl bromide.

Surprisingly, purification of bromo-amine **47** either by column chromatography or by an acid-base extraction led to the formation of enone **25**. This fact can be explained through the elimination of the bromide pushed by the amino group. Final hydrolysis of the intermediate imine provides the former enone (Scheme 17). The formation of an enone from a cage-annulated fragmentation has been described, using in these cases different bases as the promoter of the ring-opening.<sup>220,221</sup> Regardless of the vain efforts put on the purification of compound **47**, we continued with the synthetic route without any purification. On the other hand, amine **47** was found to be bench-top unstable in a short period of time, so it had to be used right after its preparation in the next step.

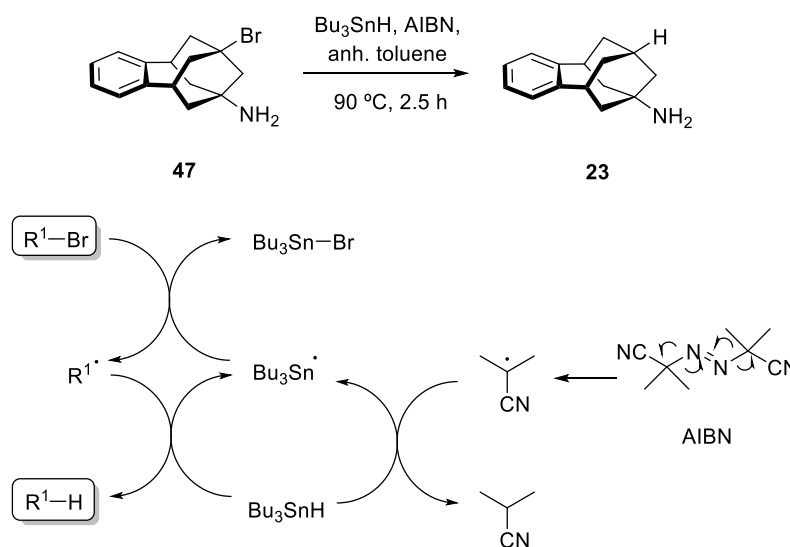
<sup>220</sup> Kumar, K.; Tepper, R. J.; Zeng, Y.; Zimmt, M. B. *J. Org. Chem.* **1995**, *60*, 4051-4066.

<sup>221</sup> Marchand, A. P.; Namboothiri, I. N. *Heterocycles* **2000**, *52*, 451-457.



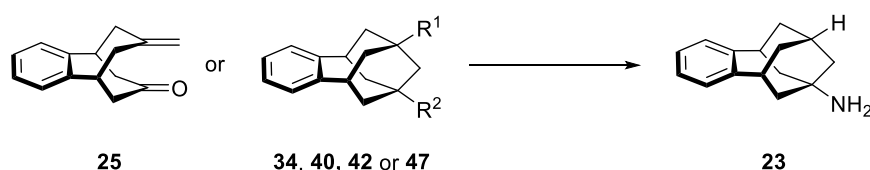
**Scheme 17.** Formation of enone **25** from bromo-amine **47**.

The impure and unstable amine **47** was subjected to radical debromination conditions with tri-*n*-butyltin hydride and AIBN as the radical initiator (Scheme 18). To our delight, amine **23** was finally secured as the hydrochloride salt after its purification by column chromatography, despite of the low overall yield (12%). The mechanism of the reaction entails similar pathways to those shown in scheme 9, although the driving force in this case is provided by the formation of a C-H bond at the expense of a Sn-H (C-H bond: 80 kcal mol<sup>-1</sup>, Sn-H bond: 64 kcal mol<sup>-1</sup>), and then a Sn-Br at the expense of a C-Br (Sn-Br bond: 81 kcal mol<sup>-1</sup>, C-Br bond: 67 kcal mol<sup>-1</sup>).



**Scheme 18.** Synthesis of amine **23** *via* radical dehalogenation.

Table 10 recapitulates the attempts for the synthesis of unsubstituted amine **23**.

**Table 10.** Summary of the different routes applied for the preparation of amine **23**.

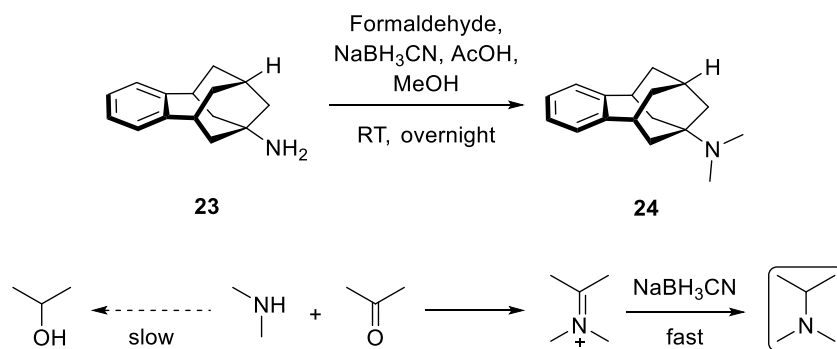
Entry	Starting material	R <sup>1</sup>	R <sup>2</sup>	Reagents	Product (% yield)
1	25	-	-	L-Selectride	-
2	25	-	-	NaBH <sub>4</sub>	1,2-addition product
3	25	-	-	H <sub>2</sub> , Pd/C	Isomerization + diol
4	34	OH	Chloroacetamide	O-phenyl chlorothionoformate	34
5	34	OH	Chloroacetamide	Toluoyl chloride	34
6	34	OH	Chloroacetamide	TFA, conc. H <sub>2</sub> SO <sub>4</sub>	Unknown products
7	34	OH	Chloroacetamide	TFAA, TEA	Unknown products
8	34	OH	Chloroacetamide	Et <sub>3</sub> SiH, TFA or BF <sub>3</sub> ·Et <sub>2</sub> O	Complex mixture
9	40	Cl	Chloroacetamide	LiAlH <sub>4</sub>	Ene-imine
10	42	Cl	NH <sub>2</sub>	SmI <sub>2</sub> , hv	23 : 42 (3:1 ratio)
11	47	Br	NH <sub>2</sub>	Bu <sub>3</sub> SnH, AIBN	23 (12%)

Once the desired amine **23** was prepared in reasonable amounts, we wished to appraise the effect on the alkylation on the amine group. As already mentioned in the introduction, the antagonist activity increased as the amine went from primary to secondary, and therefrom to tertiary. Moreover, it was observed that it was preferably to incorporate small alkyl groups, such as the methyl group. Taking into account the aforementioned, we settled the synthesis of dimethylated amine **24** following the described procedures.<sup>98</sup> We proceeded through a reductive alkylation of amine **23** with formaldehyde and sodium cyanoborohydride (Scheme 19). The latter was chosen as hydride donor because its noted selectivity for the reduction of the formed iminium ion over the ketone or aldehyde, which remains unaltered and free to react with the amine.<sup>222,223</sup> This phenomenon is due to the electron-withdrawing effect of the cyano moiety that stabilizes the negative charge on the boron, thus rendering it less reactive and more inclined to reduce the more unstable iminium ion than the carbonyl. Hence, this transformation can be performed in a one-pot

<sup>222</sup> Borch, R. F.; Bernstein, M. D.; Durst, H. D. *J. Am. Chem. Soc.* **1971**, *93*, 2897-2904.

<sup>223</sup> Lane, C. F. *Synthesis* **1975**, *1975*, 135-146.

fashion, where the amine is mixed with the desired ketone or aldehyde in the presence of  $\text{NaBH}_3\text{CN}$  in mild acidic conditions.



**Scheme 19.** Reductive alkylation of amine **23** and schematic representation of the kinetics of sodium cyanoborohydride-mediated reduction of imines *versus* ketones or aldehydes.

With compound **24** we expected an increase in the potency compared with primary amine **23**, in agreement with the observed trend in former families of compounds.

## 1.2 Exploration of the C-9 substitution of the benzo-homoadamantane scaffold

As discussed earlier, in relation with the metabolism of the adamantane group, a bridgehead hydroxylation is favoured over the secondary carbon positions, producing water-soluble 1-hydroxyadamantane derivatives in the liver, which are then readily excreted. Hence, one of the most applied strategies to avoid this issue is to prolong the pharmacokinetic stability by blocking the potential sites of metabolic activity with a fluorine or a hydroxyl group.<sup>224,225</sup>

In order to expand the SAR studies, we were encouraged to investigate the effect of the different substitution around the C-9 position of the benzo-homoadamantane polycycle that may lead to more metabolically stable compounds. Similar to the adamantane group, the benzo-homoadamantane scaffold is easily functionalized at the tertiary positions, allowing subsequent substitutions with other functionalities.

Hitherto, we have synthesized a few C-9-substituted derivatives thanks to the large exploration carried out during the preparation of amine **23**. Specifically, the different synthetic routes have led us to obtain in sufficient amounts the chloro **42**, hydroxyl **46**, and bromo **47** derivatives (Fig. 31).

<sup>224</sup> Rohde, J. J.; Pliushchev, M. A.; Sorensen, B. K.; Wodka, D.; Shuai, Q.; Wang, J.; Fung, S.; Monzon, K. M.; Chiou, W. J.; Pan, L.; Deng, X.; Chovan, L. E.; Ramaiya, A.; Mullally, M.; Henry, R. F.; Stolarik, D. F.; Imade, H. M.; Marsh, K. C.; Beno, D. W. A.; Fey, T. A.; Droz, B. A.; Brune, M. E.; Camp, H. S.; Sham, H. L.; Frevert, E. U.; Jacobson, P. B.; Link, J. T. *J. Med. Chem.* **2007**, *50*, 149-164.

<sup>225</sup> Jasys, V. J.; Lombardo, F.; Appleton, T. A.; Bordner, J.; Ziliox, M.; Volkmann, R. A. *J. Am. Chem. Soc.* **2000**, *122*, 466-473.

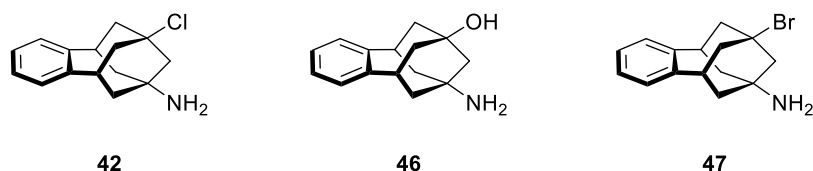


Fig. 31. Amines prepared from the previous synthetic routes.

The high instability observed in amine **47** prompted its exclusion for the screening as potential antagonist of the NMDA receptor.

In accordance to the most common strategy for the blockade of potential sites of metabolic activity, i.e. the introduction of a fluorine atom, we contemplated the formation of fluorinated compound **48** (Fig. 32).

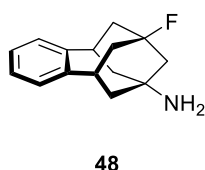


Fig. 32. New fluorinated derivative to prepare.

Incorporation of a fluorine atom has become in the last years a key designer component in the structure of modern biologically active compounds, agrochemicals and functional materials.<sup>226,227,228,229</sup> As fluorine is the most electronegative and the second-smallest atom in the periodic table, fluorine-containing molecules display different chemical, physical and biological properties from their parent compounds. Hence, the high carbon-fluorine bond strength (C-F bond: 105.4 kcal mol<sup>-1</sup>; C-H bond: 98.8 kcal mol<sup>-1</sup>)<sup>230</sup> provides the molecule high thermal and oxidative stability. Moreover, some fluorine effects are of special interest in pharmaceutical sciences: the increased lipophilicity enhances bioavailability, fluorine can block key metabolic positions and it can mimic enzyme substrates.<sup>231</sup> Because of its characteristics, fluorine is considered as a bioisostere of hydrogen.<sup>232</sup>

Taking into account the intrinsic characteristics of fluorine, it is plain to recognize that its introduction is in need of sophisticated synthetic procedures far from the conventional organic synthetic methods. During the last decade, organic chemists have developed new strategies to create carbon-fluorine (C-F) bonds on aromatic and aliphatic molecules.<sup>233</sup> In most cases, a single fluorine is successfully introduced using either nucleophilic agents, such

<sup>226</sup> Hagmann, W. K. *J. Med. Chem.* **2008**, *51*, 4359-4369.

<sup>227</sup> Müller, K.; Faeh, C.; Diederich, F. *Science* **2007**, *317*, 1881-1886.

<sup>228</sup> Furuya, T.; Kamlet, A. S.; Ritter, T. *Nature* **2011**, *473*, 470-477.

<sup>229</sup> Jeschke, P. *ChemBioChem* **2004**, *5*, 570-589.

<sup>230</sup> O'Hagan, D. *Chem. Soc. Rev.* **2008**, *37*, 308-319.

<sup>231</sup> *ChemBioChem* **2004**, *5*, 557-726 (special issue: Fluorine in Life Sciences).

<sup>232</sup> Meanwell, N. A. *J. Med. Chem.* **2011**, *54*, 2529-2591.

<sup>233</sup> Shimizu, M.; Hiyama, T. *Angew. Chem. Int. Ed. Engl.* **2004**, *44*, 214-231.

as (diethylamino)sulfur trifluoride (DAST)<sup>234</sup> or bis(2-methoxyethyl) aminosulfur trifluoride (Deoxofluor),<sup>235</sup> or electrophilic agents, such as 1-chloromethyl-4-fluorodiazoniabicyclo[2.2.2]octane bis(tetrafluoroborate) (Selectfluor)<sup>236,237</sup> (Fig. 33).

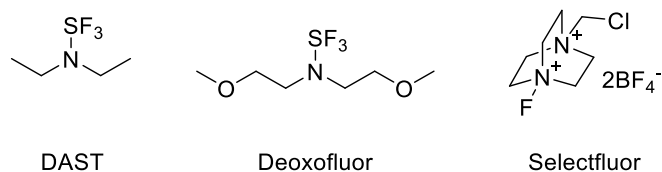


Fig. 33. Efficient nucleophilic and electrophilic fluorinating agents.

Following the procedure described by Johnson,<sup>238</sup> we first tested our chances in the preparation of amine **48** via nucleophilic substitution of the hydroxyl group of **46** using DAST as fluorinating agent. DAST is an aminosulfurane reagent that selectively exchanges hydroxyl groups for fluorine, and has proven highly applicable since its discovery in 1970.<sup>239</sup> The main advantage of DAST over previous fluorinating agents is that it is easily handled and versatile, unlike the more classical gaseous sulphur tetrafluoride. Luckily enough, we managed to obtain the desired fluorinated amine **48** in 44% yield under these conditions. The reaction goes through a deoxyfluorination mechanism where the oxygen atom of the substrate reacts with the sulfur, with elimination of a hydrogen fluoride molecule. The alkoxyaminosulfur difluoride intermediate eliminates a fluoride ion that attacks the sulfanylidene intermediate either by an  $S_N1$  or  $S_N2$  pathway, affording the desired product (Scheme 20). If the  $S_N2$  mechanism prevails over the  $S_N1$ , chiral alcohols predominantly suffer from the Walden inversion of configuration. Obviously, due to steric issues, in our case only a  $S_N1$  pathway can operate.

<sup>234</sup> Middleton, W. J. *J. Org. Chem.* **1975**, *40*, 574-578.

<sup>235</sup> Lal, G. S.; Pez, G. P.; Pesaresi, R. J.; Prozonc, F. M.; Cheng, H. *J. Org. Chem.* **1999**, *64*, 7048-7054.

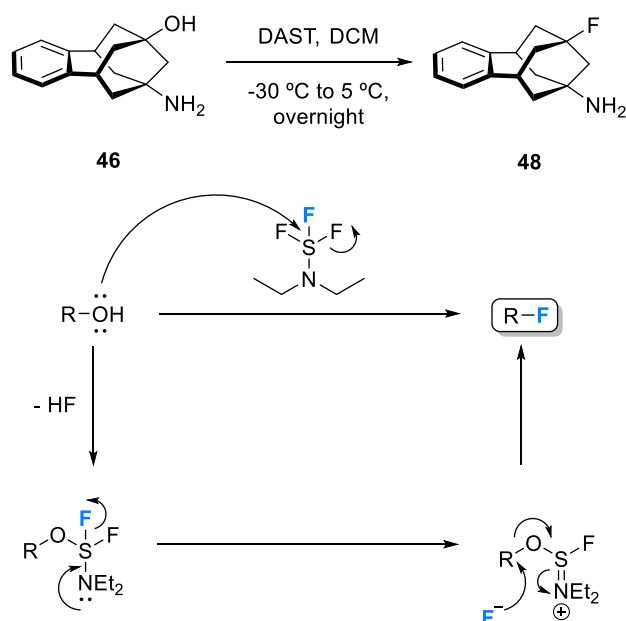
<sup>236</sup> Lal, G. S.; Pez, G. P.; Syvret, R. G. *Chem. Rev.* **1996**, *96*, 1737-1756.

<sup>237</sup> Sodeoka, M. *Science* **2011**, *334*, 1651-1652.

<sup>238</sup> Johnson, A. L. *J. Org. Chem.* **1982**, *47*, 5220-5222.

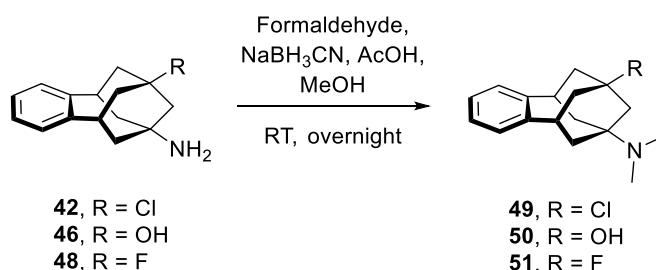
<sup>239</sup> Singh, R. P.; Shreeve, J. M. *Synthesis* **2002**, 2561-2578.





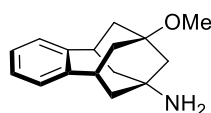
**Scheme 20.** Deoxyfluorination of alkanolamine **46** with DAST.

As in the case of unsubstituted amine **23** and its dimethylated analogue **24**, the chloro **42**, hydroxy **46**, and fluoro **48** derivatives were subjected to reductive alkylation conditions to obtain their corresponding dimethylated tertiary amines **49**, **50** and **51**, respectively (Scheme 21).



**Scheme 21.** Dimethylation of earlier amines by reductive alkylation.

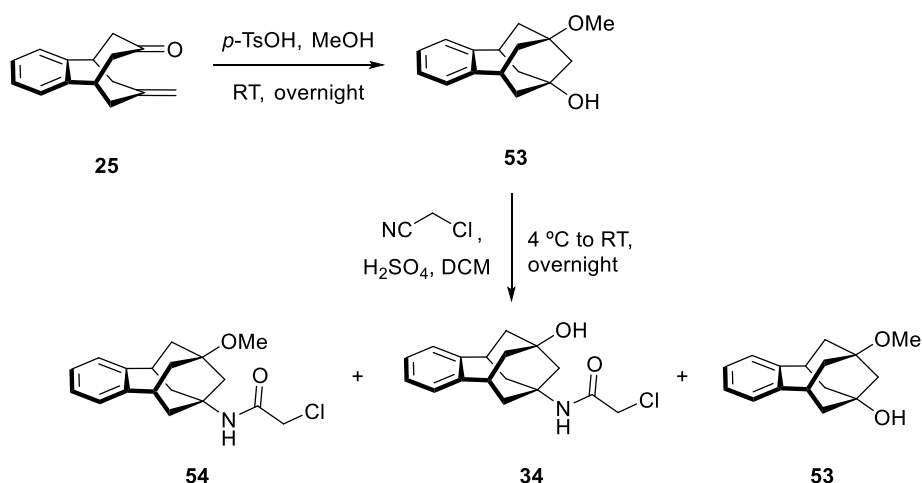
For the purpose of further inspecting the effect of the substitution on the C-9 position, and bearing in mind the intrinsic characteristic of enone **25** in relation to the 1,4-conjugated-like addition, our next goal was the synthesis of methoxy derivative **52**, which would add one extra group in our array of compounds (Fig. 34).



**52**

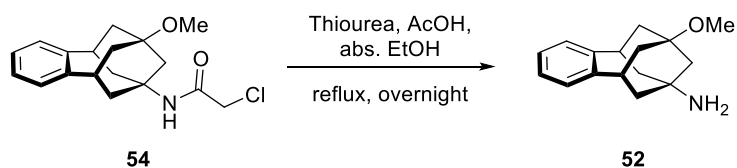
**Fig. 34.** The methoxy derivative closes this family of compounds.

Thus, enone **25** was submitted to the 1,4-conjugated-like addition of methanol with *p*-toulenesulfonic acid, as reported by Bishop *et al.*<sup>165</sup> The reaction provided alcohol **53** which was transformed to the corresponding chloroacetamide **54** in 31% yield *via* the already mentioned Ritter reaction (Scheme 22). In this case, the procedure entails the protonation of the bridgehead hydroxyl group, formation of a tertiary carbocation and later addition of the nitrile nitrogen. The mechanism continues as indicated in scheme 7. Likewise, the methoxy group was prone to elimination and chloroacetamide **34** was recovered in 37% yield. Furthermore, with the purification by column chromatography the starting material was recovered in 16% yield.



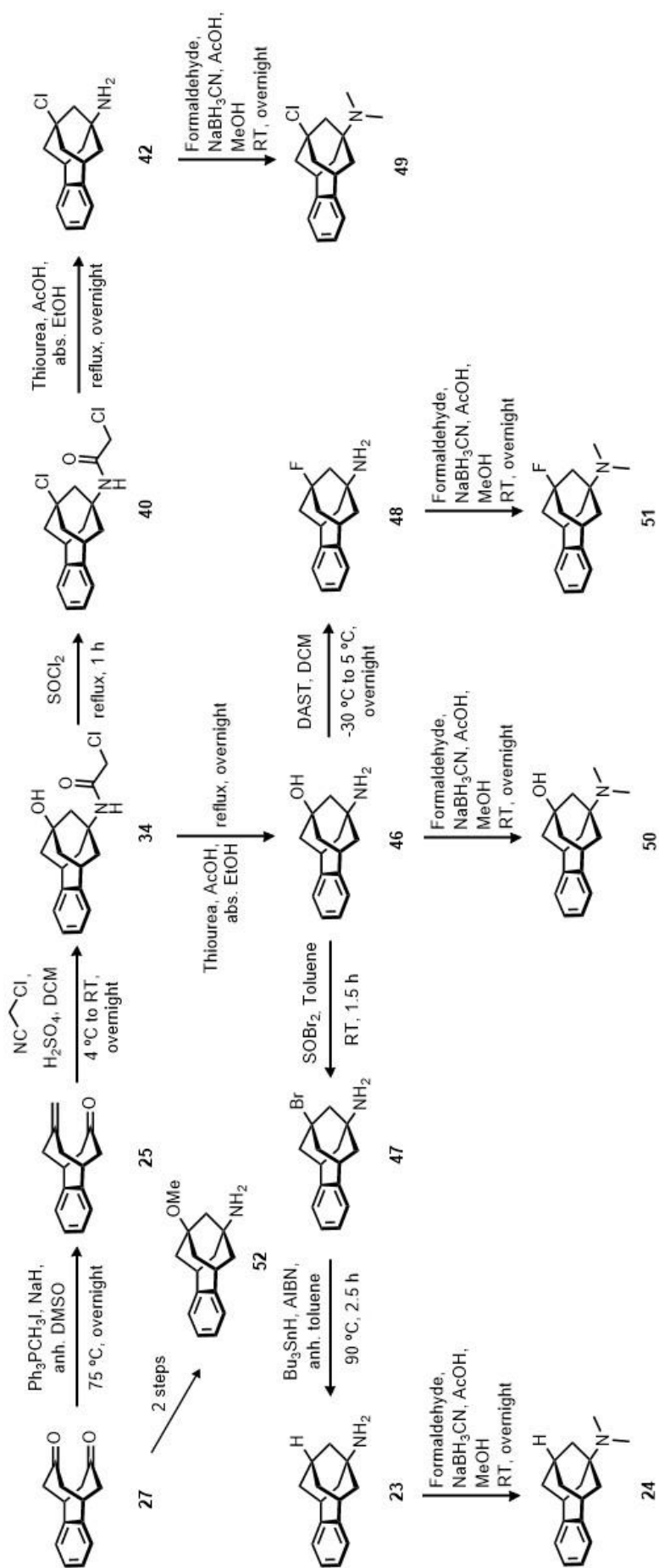
**Scheme 22.** Formation of alcohol **53** followed by the Ritter reaction, affording a mixture of **54**, **34** and the starting material.

The pure methoxy derivative **54** was deprotected under the previous conditions with thiourea and glacial acetic acid in absolute ethanol, to get final amine **52** in 59% yield (Scheme 23).



**Scheme 23.** Synthesis of amine **52** with thiourea under acid conditions.

To sum up, scheme 24 discloses the synthetic routes followed for the new derivatives. Globally, we have prepared unsubstituted amines **23** and **24**, along with C-9 substituted benzo-homoadamantanes bearing different substituents (hydroxyl and methoxy groups, and chloro and fluoro atoms).



**Scheme 24.** Synthetic route applied for the preparation of the new benzohomoadamantanes derivatives.

## 2. Pharmacological evaluation of new benzo-homoadamantane derivatives

### 2.1 Assessment of the NMDAR antagonistic activity

The synthesized compounds were first evaluated as NMDAR antagonists by the determination of their respective half-maximal inhibitory concentration or IC<sub>50</sub>. The IC<sub>50</sub> represents the concentration of a drug that is required to produce 50% inhibition of an enzymatic reaction at a specific substrate concentration.<sup>240</sup> This work was carried out by the research group of Dr. Francesc Xavier Sureda (University Rovira i Virgili, Reus, Spain).

The group of Dr. Sureda is highly specialized in testing the ability of a given ligand to prevent neurodegenerative changes in several animal models of AD, both *in vivo* and *in vitro*. Specifically, to demonstrate the interactions of the new analogues with glutamate physiological actions, Dr. Sureda evaluated the competence of the compounds to block the increase of intracellular calcium evoked by NMDA in cultured rat cerebellar granule cells (CGC). Since the 1990s, different protocols for the determination of the intracellular calcium concentration have been established. Most part of the glutamatergic receptors are coupled to signal transduction processes that are dependent on the levels of this secondary messenger. In consequence, the study of its modulation is a valuable tool for the assessment of new molecules as NMDAR agonists or antagonists.

The assay involves the addition of Fura-2-acetoxymethyl ester (Fura-2 AM) to the cultured CGCs, as previously reported.<sup>241</sup> Fura-2 AM is a membrane-permeable analogue of the ratiometric fluorescent probe calcium indicator Fura-2.<sup>242</sup> Once Fura-2 AM enters the cell, it is hydrolysed by nonspecific cytoplasmic esterases to Fura-2, which binds to free intracellular calcium and whose fluorescence depends on the concentration levels of the latter (Fig. 35). Both calcium-bound and calcium-free species fluoresce quite strongly, at 340 and 380 nm respectively, and the ratio of emissions at those wavelengths is directly related to the amount of intracellular calcium. Regardless of the levels of Ca<sup>2+</sup>, Fura-2 emits fluorescence at 510 nm.<sup>243</sup>

---

<sup>240</sup> Yung-Chi, C.; Prusoff, W. H. *Biochem. Pharmacol.* **1973**, *22*, 3099-3108.

<sup>241</sup> Verdaguer, E.; García-Jordà, E.; Jiménez, A.; Stranges, A.; Sureda, F. X.; Canudas, A. M.; Escubedo, E.; Camarasa, J.; Pallàs, M.; Camins, A. *Br. J. Pharmacol.* **2002**, *135*, 1297-1307.

<sup>242</sup> Grynkiewicz, G.; Poenie, M.; Tsien, R. Y. *J. Biol. Chem.* **1985**, *260*, 3440-3450.

<sup>243</sup> Life technologies web page. Ion indicators & ionophores: Fura-2.

<https://www.lifetechnologies.com/order/catalog/product/F1200> (accessed on 14<sup>th</sup> June 2015).

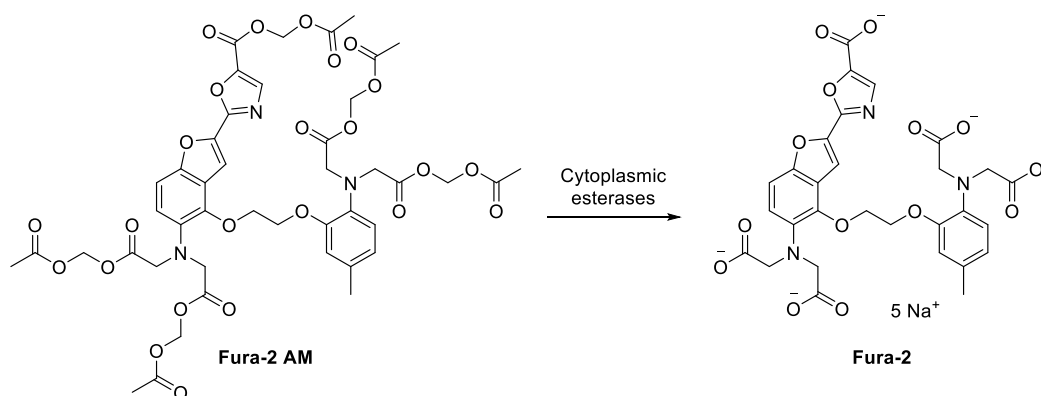


Fig. 35. Hydrolysis of Fura-2 AM to Fura-2.

Therefore, the determination of the calcium levels is based on the measurement of the fluorescence at 510 nm when excited at 340 (F<sub>340</sub>) and 380 (F<sub>380</sub>) nm, followed by the calculation of the ratio F<sub>340</sub>/F<sub>380</sub> (R).

For the assessment of the effect of the newly synthesized compounds against glutamate-induced Ca<sup>2+</sup> mobilization, the procedure is as follows. A single administration of the agonists glutamate (100 μM) and glycine (10 μM) leads to a significant increase in R value. After this stimulation, increasing cumulative concentrations of the compound to be tested are added, represented in blue arrows in figure 36.

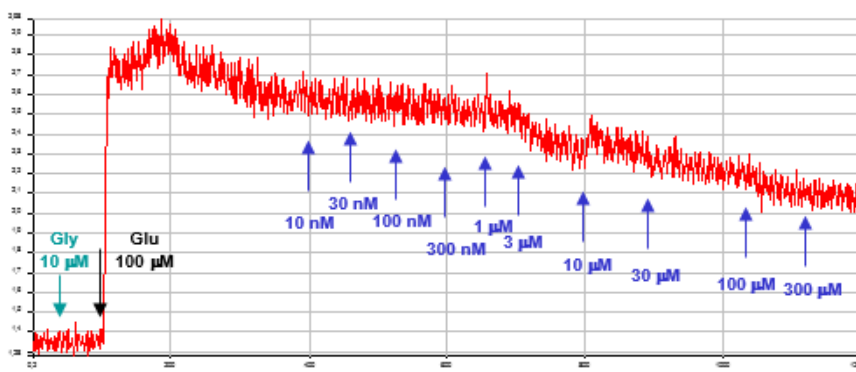


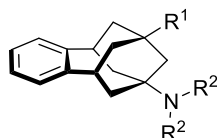
Fig. 36. Fluorescence detection after addition of the agonists glutamate and glycine *prior* administration of increasing concentrations of a given antagonist.

Final adjustment of the data to a concentration-response sigmoidal curve using a non-linear regression curve fitting (variable slope) gives the percentage of inhibition at every tested concentration of each compound, which in turn can be used for the calculation of the IC<sub>50</sub> values.

It is worth to highlight that the use of glutamate as agonist in the assay may lead to a calcium mobilization originated from the activation of other receptors different from the NMDAR, such as kainate. Therefore, for a better estimation of the effect of a plausible NMDAR antagonist, in most assays NMDA is used as the stimulator, allowing a 100% inhibition to be possible.

Evaluation of the ability of the new compounds to block the NMDAR by this technique revealed some interesting results. The data shown in table 11 are means of  $IC_{50}$  values  $\pm$  SEM of at least three separate experiments carried out on three different batches of cultured cells. Amantadine and memantine were used as standard controls.

**Table 11.**  $IC_{50}$  values ( $\mu$ M) for 5,6,8,9,10,11-hexahydro-7H-5,9:7,11-dimethanobenzo[9]annulen-7-amines as NMDAR antagonists.



Comp.	R <sup>1</sup>	R <sup>2</sup>	$IC_{50}$ (NMDA 100 $\mu$ M)
23	H	H	0.70 $\pm$ 0.12
24	H	Me	2.30 $\pm$ 0.10
42	Cl	H	4.99 $\pm$ 1.53
49	Cl	Me	17.0 $\pm$ 9.3
46	OH	H	16.2 $\pm$ 3.3
50	OH	Me	71.1 $\pm$ 9.9
48	F	H	1.93 $\pm$ 0.21
51	F	Me	16.5 $\pm$ 2.4
52	OMe	H	24.3 $\pm$ 2.0
19	Me	H	13.6 $\pm$ 3.4
Amantadine	-	-	92 $\pm$ 29
Memantine	-	-	1.5 $\pm$ 0.1

As aforementioned, the  $IC_{50}$  values were obtained by the measure of the antagonistic activity at varied concentrations of each compound, providing a concentration-response semi-logarithmic curve with the familiar sigmoidal shape. The plot in figure 37 includes the most potent compounds.

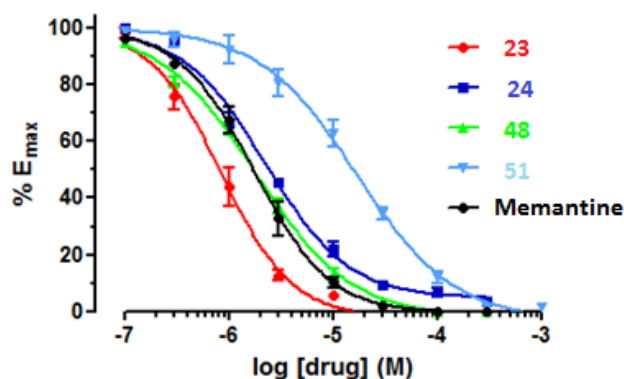


Fig. 37. IC<sub>50</sub> curves of compounds 23 and 48 and their dimethylated analogues 24 and 51 respectively, compared with memantine as a standard.

Gratifyingly, rationalisation of the results shown in table 11 led to some attractive outcomes and a SAR could be established around the C-9 substitution:

- All the new compounds have IC<sub>50</sub> values lower than that of amantadine, with amines **23**, **42**, **24** and **48** in the low micromolar range.
- Confirming our first hypothesis, compound **23** was the most potent compound with an IC<sub>50</sub> lower than that of memantine (0.70 and 1.5 μM, respectively). Pleasingly, primary amine **23** and its bioisostere **48** (1.93 μM) were clearly more potent than our previous synthesized families I and II (Fig. 38). Of note, the observed trend of going from **23** to its methylated analogue **19** (13.6 μM) is the opposite of the one observed in going from amantadine to its dimethylated derivative memantine.
- Considering solely primary amines, smaller substituents such as a hydrogen (**23**) or a fluorine (**48**) are better tolerated than larger groups, like hydroxyl (**46**), methoxy (**52**) or methyl (**19**). Particularly, either polar (**46** or **52**), or lipophilic electron-donating groups (EDG) as in the previously reported methylated compound **19** led to a significant reduction of the activity. Introduction of the electron-withdrawing chlorine (**42**) and fluorine (**48**) resulted in an increase on the potency compared with compounds bearing an EDG.
- Interestingly, within this novel series of benzo-homoadamantanes, all the tertiary amines were clearly less potent than the corresponding primary amines (**23** vs **24**, **42** vs **49**, **46** vs **50**, **48** vs **51**), in contrast to the behaviour observed in former families I and II.

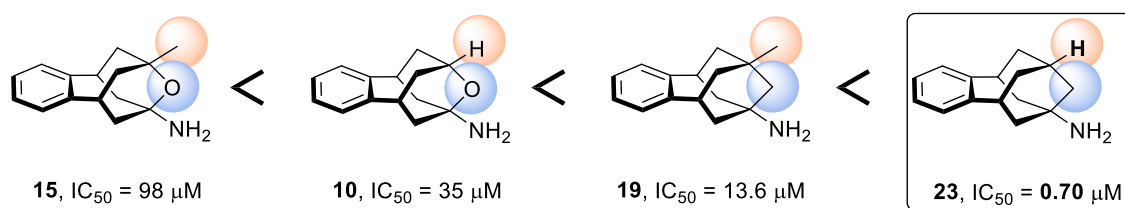


Fig. 38. Confirmation of our first hypothesis from the former families.

These results suggest that the combination of the size, the ability to form specific interactions, such as hydrophobic interactions or hydrogen bonds, and the inductive effects of the substituted group, alters greatly the activity as NMDAR antagonist of the molecule. The lack of a crystal structure of the ion channel resolved with an antagonist renders difficult the reasoning of the observed trends.

## 2.2 Electrophysiological measurements

In order to appraise if the new NMDA antagonists displayed a similar blocking mode to that of memantine, i.e. characterized by rapid and strongly voltage-dependent kinetics, Dr. David Soto from IBIDELL, performed a patch-clamp experiment with the more promising compounds, 23 and 48.

Briefly, the patch-clamp technique permits the study of membrane current contributions of individual ionic channels from cells of any size and particularly the study of small cells in culture.<sup>244</sup> It consists of the insertion of a micro-pipette into the cell membrane in a way that the connection is sealed. This tight seal isolates the membrane patch electrically, which means that all ions passing through the ion channels flow into the pipette. An electrode connected to a highly sensitive differential amplifier can record currents flowing through the membrane patch (Fig. 39). This technique has been widely used for NMDAR blockers.<sup>245,246,247,248,249</sup>

<sup>244</sup> Sakmann, B.; Neher, E. *Ann. Rev. Physiol.* **1984**, *46*, 455-472.

<sup>245</sup> Chen, H. S.; Pellegrini, J. W.; Aggarwal, S. K.; Lei, S. Z.; Warach, S.; Jensen, F. E.; Lipton, S. A. *J. Neurosci.* **1992**, *12*, 4427-4436.

<sup>246</sup> Parsons, G. R.; Gruner, R.; Rozental, J.; Millar, J.; Lodge, D. *Neuropharmacol.* **1993**, *32*, 1337-1350.

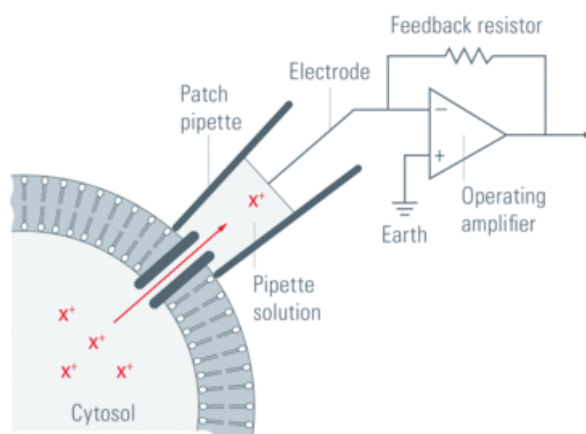
<sup>247</sup> Blanpied, T. A.; Clarke, R. J.; Johnson, J. W. *J. Neurosci.* **2005**, *25*, 3312-3322.

<sup>248</sup> Gilling, K.; Jatzke, C.; Wollenburg, C.; Vanejevs, M.; Kauss, V.; Jirgensons, A.; Parsons, C. G. *J. Neural Transm.* **2007**, *114*, 1529-1537.

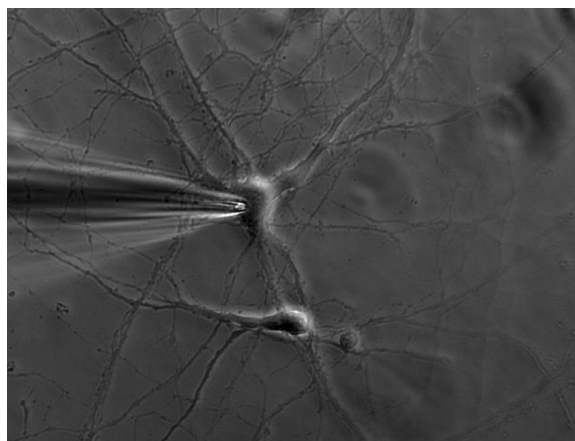
<sup>249</sup> Koller, M.; Urwyler, S. *Expert Opin. Ther. Pat.* **2010**, *20*, 1683-1702.



A



B



**Fig. 39.** (A) Schematic representation of the patch-clamp principle and (B) image of a patch pipette attached to the membrane of a neuron.<sup>250</sup>

During the experiment, the ion channels undergo different stages, which affect the current that flows through the membrane patch:

1. Baseline conditions: voltage of  $-60$  mV with the ion channels closed.
2. Addition to the media of agonists (glutamate and glycine): ion channels are now open with the entrance of cations until normalization. Reduction on the intensity.
3. Addition of antagonist to the former media: some ion channels are now blocked. Increase on the intensity.
4. Application of a positive pulse of  $+60$  mV: release of the blockers.
5. Stop of the positive pulse and addition of agonists + antagonist: recovery of the state in step 3.

<sup>250</sup> Science Lab website. The patch-clamp technique. <http://www.leica-microsystems.com/science-lab/the-patch-clamp-technique/> (accessed on 18<sup>th</sup> September 2015).

6. Withdrawal of the antagonist, but with agonists: recovery of the state in step 2.
7. Application of a positive pulse of +60 mV: to check if the antagonist is an open-channel blocker or, in other words, voltage-dependent blocker. If the intensity of the second positive pulse is higher than the first one, it means that the antagonist is a non-voltage-dependent blocker.

Following thus this protocol, amine **23** and **48** were assayed along with memantine for comparison (Fig. 40).

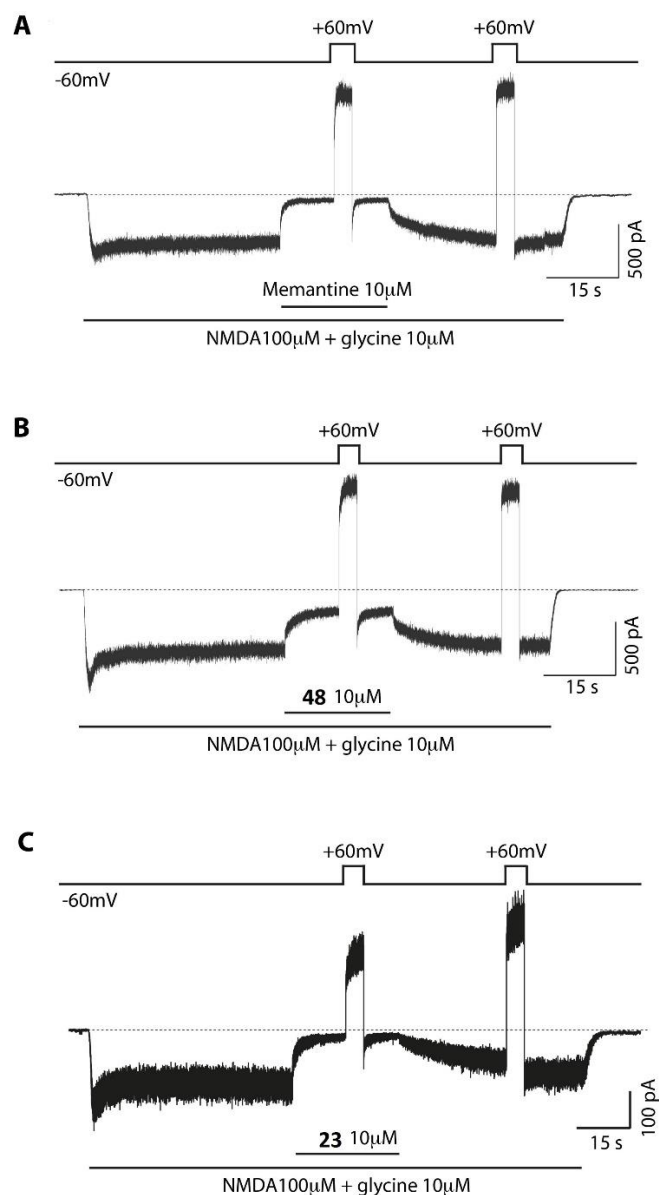


Fig. 40. Results from electrophysiological studies with (A) memantine, (B) amine **48** and (C) amine **23**.

As shown in figure 40, amine **48**, which bears a fluorine atom in its structure, compares well with memantine, with a similar kinetic profile after running the experiment. However, this is not the case for amine **23**, which presents a low-binding kinetic profile. Specifically, when **23** enters in the media, there is a rapid blockade of the NMDARs, and this blockade is slightly more intense than for the other two antagonists. In contrast, the recovery of the baseline levels is slower than memantine and amine **48**. Altogether, the data suggests that amine **23** shows a similar association rate constant ( $k_{on}$ ) but a smaller dissociation rate constant ( $k_{off}$ ) than memantine. On the other hand, when applying the second positive pulse, the intensity in this case is higher than the one from the first pulse. This fact indicates that actually amine **23** is a non-voltage-dependent and non-open channel blocker.

Therefore, amine **23** and **48**, despite containing two bioisostere groups, bind to the channel in a distinct way. One hypothesis is that amine **23** behaves as a high-affinity NMDA receptor antagonist. At the time of writing this thesis, work is still ongoing in order to further study the electrophysiological behaviour of our NMDAR antagonists.

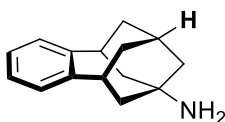
# **Conclusions**



In this first part of the thesis, 12 new compounds, revolving around the benzo-homoadamantane structure, have been synthesized and fully characterized by their spectroscopic and analytical data. Among them, 10 were pharmacologically evaluated as NMDA receptor antagonists.

From the data of the first chapter of this dissertation, we can conclude the following:

1. Amine **23** was prepared following a radical dehalogenation in low yield, after several synthetic attempts.
2. A SAR study has been developed around the substitution pattern at the C-9 position, with polar and non-polar substituents, partly thanks to the synthetic exploration performed for the synthesis of amine **23**.
3. The activity displayed by compound **23** confirmed our first hypothesis that an unsubstituted benzo-homoadamantane would exhibit a higher activity than the previous series of compounds. Indeed, amine **23** displayed the lowest  $IC_{50}$  value ever described to date for the benzo-homoadamantane scaffold as surrogate of the adamantane group of memantine ( $IC_{50}$  of  $0.70 \mu\text{M}$  for **23** vs  $1.5 \mu\text{M}$  for memantine, Fig. 41).



**23**,  $IC_{50} = 0.70 \mu\text{M}$

**Fig. 41.** Best compound identified from this family of benzo-homoadamantanes.

4. The second most active structure discovered with this series of compounds was the fluoro derivative **48**, bioisostere of **23** and with an equipotent activity compared with memantine ( $IC_{50}$  of  $1.93 \mu\text{M}$ ).
5. Halides were better tolerated than hydroxyl and methoxy groups. Thus, compounds bearing a fluorine (**48**,  $IC_{50}$  of  $1.93 \mu\text{M}$ ) or a chlorine (**42**,  $IC_{50}$  of  $4.99 \mu\text{M}$ ) were more potent as NMDA receptor antagonists than compounds with a hydroxyl (**46**,  $IC_{50}$  of  $16.2 \mu\text{M}$ ) or a methoxy (**52**,  $IC_{50}$  of  $24.3 \mu\text{M}$ ).
6. All the tertiary amines were less active than their corresponding primary amines.
7. Electrophysiological studies revealed that amine **48** possessed a similar kinetic profile than memantine in a patch-clamp assay, with a voltage-dependent binding mode, whereas amine **23** tended to stay longer time within the channel, in a non-voltage-dependent mode. Hence, amine **23** could not be considered as an open-channel blocker but, probably, as a high-affinity antagonist.



**CHAPTER 2:**  
**11 $\beta$ -HSD1 inhibition**





# **Introduction**



## 1. 11 $\beta$ -HSD1 inhibition by adamantane-based derivatives

The following section will discuss the glucocorticoid effects in the organism and the regulation of these stress hormones by the 11 $\beta$ -HSD1 enzyme, which has been found to be relevant in the development of multiple diseases, such as the metabolic syndrome (MetS), inflammation and cognitive dysfunction. A brief disclosure of the developed 11 $\beta$ -HSD1 inhibitors will be covered. Particularly, the adamantane-based compounds will be studied in order to understand their binding mode in the active site of the enzyme as well as their progress throughout the drug discovery process.

### 1.1 The glucocorticoid system and its physiological actions

Glucocorticoids (GCs) are well-known ubiquitous hormones playing a key role in modulating immune and inflammatory responses, regulating energy metabolism and cardiovascular homeostasis and the body's responses to stress. Opposing the action of insulin, GCs promote gluconeogenesis, inhibit  $\beta$ -cell insulin secretion and peripheral glucose uptake. Moreover, GCs contribute to lipolysis, with subsequent fatty acid mobilization, and proteolysis. Thus, overall, GCs prompt catabolic states.<sup>251,252</sup>

The active human GC cortisol, is synthesized by the adrenal cortex with a strong circadian rhythm. Its secretion is controlled by the hypothalamic-pituitary-adrenal (HPA) axis and induced in stressful conditions. Serum cortisol readily passes cell membranes and exerts its intracellular functions by binding to GC receptors (GRs), which are ligand-activated nuclear receptors. GRs regulate, directly or indirectly, the expression of a plethora of genes involved in various physiological processes, including peroxisome proliferator-activated receptor  $\gamma$  (PPAR- $\gamma$ ), CCAAT enhancer-binding protein and nuclear factor- $\kappa$ B (NF- $\kappa$ B), *inter alia*.<sup>253,254</sup> Furthermore, GCs bind to mineralocorticoid receptors (MRs), which regulate blood pressure and sodium balance in the kidney.<sup>255</sup>

#### 1.1.1 GC regulation by 11 $\beta$ -HSD enzymes

Along with the HPA axis, GC's homeostasis is controlled by the 11 $\beta$ -HSD enzyme. Two isoforms of this enzyme, 11 $\beta$ -HSD type 1 (11 $\beta$ -HSD1) and type 2 (11 $\beta$ -HSD2), catalyse the interconversion between active 11-hydroxy forms (cortisol in humans, and corticosterone in rodents) and inert 11-ketosteroids (cortisone in humans, and 11-dehydrocorticosterone in rodents), with the concomitant conversion of NADPH cofactor to NAD<sup>+</sup> (Fig. 42). 11 $\beta$ -HSD1 is anchored to the membrane of the endoplasmic reticulum (ER) by the N-terminus, with the catalytic domain located within the lumen of the ER.

<sup>251</sup> Dallman, M. F.; Strack, A. M.; Akana, S. F.; Bradbury, M. J.; Hanson, E. S.; Scribner, K. A.; Smith, M. *Front. Neuroendocrinol.* **1993**, *14*, 303-347.

<sup>252</sup> Sapolsky, R. M.; Romero, L. M.; Munck, A. U. *Endocr. Rev.* **2000**, *21*, 55-89.

<sup>253</sup> Rosen, E. D.; MacDougald, O. A. *Nat. Rev. Mol. Cell Bio.* **2006**, *7*, 885-896.

<sup>254</sup> Smoak, K. A.; Cidlowski, J. A. *Mech. Ageing Dev.* **2004**, *125*, 697-706.

<sup>255</sup> Arriza, J. L.; Weinberger, C.; Cerelli, G.; Glase, T. M.; Handelin, B. L.; Housman, D. E.; Evans, R. M. *Science* **1987**, *237*, 268-275.

Hexose-6-phosphate dehydrogenase, also located in the ER, is thought to supply adequate concentrations of NADPH cofactor, which favour the behaviour of the 11 $\beta$ -HSD1 as a reductase *in vivo*.<sup>256,257</sup> Besides, the higher affinity of 11 $\beta$ -HSD1 for cortisone than cortisol enhances this oxoreductive activity. In *in vitro* conditions, though, 11 $\beta$ -HSD1 is bidirectional and can also act as a dehydrogenase.

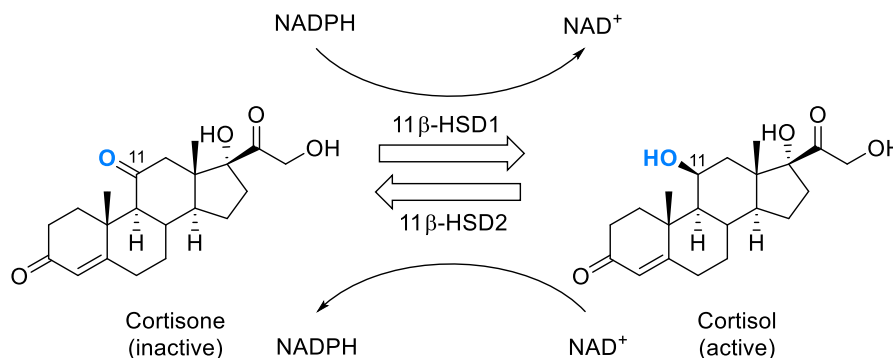


Fig. 42. Interconversion of cortisone to cortisol in humans catalyzed by 11 $\beta$ -HSD enzyme.

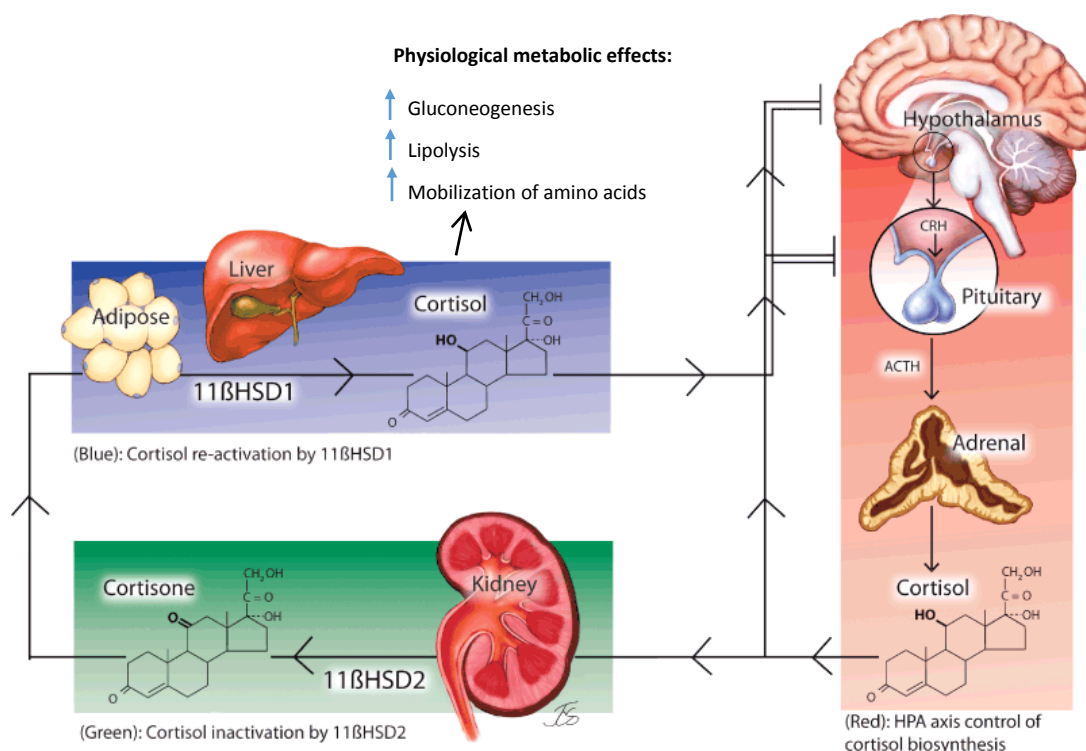
11 $\beta$ -HSD1 is mainly expressed in liver, adipose tissue, bone, pancreas, vasculature and brain, whilst 11 $\beta$ -HSD2 is found chiefly in mineralocorticoid target tissues such as the kidney, colon, pancreas and the salivary gland.<sup>258</sup> In mineralocorticoid tissues, the MR have the same binding affinity for cortisol as aldosterone; 11 $\beta$ -HSD2 protects the MR from inappropriate activation by cortisol and allows aldosterone to act as the ligand, by inactivating cortisol to cortisone.<sup>259</sup> Figure 43 summarizes what has been commented hitherto.

<sup>256</sup> Dzyakanchuk, A. A.; Balázs, Z.; Nashev, L. G.; Amrein, K. E.; Odermatt, A. *Mol. Cell. Endocrinol.* **2009**, *301*, 137-141.

<sup>257</sup> Atanasov, A. G.; Nashev, L. G.; Gelman, L.; Legeza, B.; Sack, R.; Portmann, R.; Odermatt, A. *Biochim. Biophys. Acta* **2008**, *1783*, 1536-1543.

<sup>258</sup> Hardy, R. S.; Seibel, M. J.; Cooper, M. S. *Curr. Opin. Pharmacol.* **2013**, *13*, 440-444.

<sup>259</sup> Edwards, C. R.; Stewart, P. M.; Burt, D.; Brett, L.; McIntyre, M. A.; Sutanto, W. S. de Kloet, E. R.; Monder, C. *Lancet* **1988**, *2*, 986-989.



**Fig. 43.** Biosynthesis of cortisol by adrenal gland under HPA axis control, and tissue-specific metabolism of GC by 11β-HSD enzymes. CRH: corticotropin-releasing hormone; ACTH: adrenocorticotropic hormone.<sup>260,261</sup>

It is worth to highlight that cortisone is not the only substrate of 11β-HSD1, but several additional substrates have been identified such as 7-oxygenated steroids, 7-ketocholesterol and non-steroidal unspecific carbonyl compounds, thus endowing the enzyme with an important role in the detoxification of exogenous substances.<sup>262,263,264</sup>

### 1.2 11β-HSD1 as a pleiotropic therapeutical target

The rationale for the inhibition of 11β-HSD1 came from the striking resemblances between the phenotype of hypercortisolism, also known as Cushing's syndrome, and the symptoms of the MetS. The Cushing's syndrome reveals a set of phenotypical characteristics such as insulin resistance, hypertension, dyslipidaemia, and osteoporosis (Fig. 44).<sup>265</sup> While the Cushing's syndrome is rare, it does exemplify the pathological effects associated with imbalances in circulating cortisol levels.

<sup>260</sup> Hollis, G.; Huber, R. *Diabetes Obes. Metab.* **2011**, *13*, 1-6.

<sup>261</sup> Staab, C. A.; Maser, E. J. *Steroid Biochem. Mol. Biol.* **2010**, *119*, 56-72.

<sup>262</sup> Odermatt, A.; Nashev, L. G. J. *Steroid Biochem. Mol. Biol.* **2010**, *119*, 1-13.

<sup>263</sup> Mitić, T.; Andrew, R.; Walker, B. R.; Hadoke, P. W. F. *Biochimie* **2013**, *95*, 548-555.

<sup>264</sup> Odermatt, A.; Klusonova, P. J. *Steroid Biochem. Mol. Biol.* **2015**, *151*, 85-92.

<sup>265</sup> Gathercole, L. L.; Lavery, G. G.; Morgan, S. A.; Cooper, M. S.; Sinclair, A. J.; Tomlinson, J. W.; Stewart, P. M. *Endocr. Rev.* **2013**, *34*, 525-555.

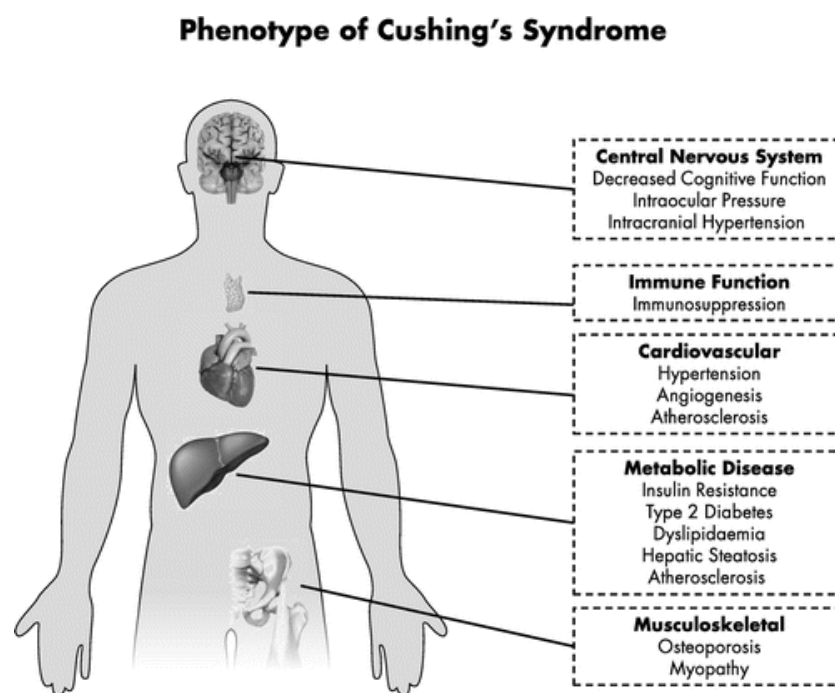


Fig. 44. The pleiotropic effects of GC excess in Cushing's syndrome.

Endogenous GC production and metabolism have been highlighted as having a pivotal role in the aetiology of several disorders. While this production underlies the attractiveness of pharmacological inhibition of 11 $\beta$ -HSD1 to modulate local GC action, it requires to inhibit selectively this specific isoform to avoid undesired effects associated with the binding to 11 $\beta$ -HSD2, or other hydroxysteroid dehydrogenase enzymes, such as 17 $\beta$ -HSD.<sup>266</sup> It has been demonstrated that a deficient 11 $\beta$ -HSD2 activity (as a result of gene mutation, or by inhibition of this isoform) results in an impaired cortisol inactivation and apparent mineralocorticoid excess, leading to hypokalemia and hypernatremia, eventually inducing hypertension and related cardiovascular problems.<sup>265,267</sup> On the other hand, inhibition of 17 $\beta$ -HSD affects local estrogen metabolism. Worth to note is that 11 $\beta$ -HSD1 is also expressed in areas of the brain relevant to metabolic control.<sup>268</sup> Although it has been demonstrated that 11 $\beta$ -HSD1 activity in brain does not contribute to systemic cortisol/cortisone turnover,<sup>269</sup> inhibition of 11 $\beta$ -HSD1 must be considered with caution since it may result in the risk of compensatory cortisol production *via* up-regulation of the

<sup>266</sup> Klein, T.; Henn, C.; Negri, M.; Frotscher, M. *PLoS One* **2011**, *6*, 1-13.

<sup>267</sup> Kotelevtsev, Y.; Brown, R. W.; Fleming, S.; Kenyon, C.; Edwards, C. R.; Seckl, J. R.; Mullins, J. J. *J. Clin. Invest.* **1999**, *103*, 683-689.

<sup>268</sup> Bisschop, P. H.; Dekker, M. J. H. J.; Osterthun, W.; Kwakkel, J.; Anink, J. J.; Boelen, A.; Unmehopa, U. A.; Koper, J. W.; Lamberts, S. W. J.; Stewart, P. M.; Swaab, D. F.; Fliers, E. *J. Neuroendocrinol.* **2013**, *25*, 425-432.

<sup>269</sup> Kilgour, A. H. M.; Semple, S.; Marshall, I.; Andrews, P.; Andrew, R.; Walker, B. R. *J. Clin. Endocrinol. Metab.* **2015**, *100*, 483-489.

HPA axis.<sup>270</sup> 11 $\beta$ -HSD1 is considered as a pre-receptor target since it controls the binding of active cortisol to GR by modulating its metabolism.

In recent years, there has been a rapid growth in publications concerning 11 $\beta$ -HSD1 as a promising target.<sup>271</sup> Many research groups in academia and in the pharmaceutical industry have put forth great efforts to determine the role of 11 $\beta$ -HSD1 in the development of multiple diseases, and hence to discover suitable inhibitors to overcome these disorders. As just seen, selectivity and tissue-targeting specificity are the ultimate criteria in the discovery of potent 11 $\beta$ -HSD1 inhibitors.

### 1.2.1 11 $\beta$ -HSD1 inhibition and type 2 diabetes mellitus, obesity and metabolic syndrome

Type 2 diabetes mellitus (T2DM) is characterized by increased cellular insulin resistance with an initial phase of enhanced insulin secretion followed by pancreatic  $\beta$ -cell failure. Regarding obesity, a person with a body mass index of 30 or more is considered obese, entailing health risks. T2DM and obesity are considered as first-world epidemics and are nowadays great healthcare challenges in the developed countries. According to the World Health Organization (WHO), in 2014, 9% of the worldwide adult population had diabetes.<sup>272</sup> That same year, the percentage of total health expenditure in T2DM reached US \$ 612 billion. The expected increase on the diabetic population by 2035 is about 205 million, which will elevate the total health cost still higher.<sup>273</sup> Concerning obesity, in 2014 more than 1.9 billion adults were overweight, and of these, 600 million were obese.<sup>274</sup>

From another standpoint, the MetS is a cluster of metabolic disorders and it is diagnosed in a given patient if visceral obesity and two or more risk factors are present, including elevated fasting plasma glucose, elevated triglycerides, elevated blood pressure and reduced high-density lipoprotein (HDL), as it has been recently redefined by the International Diabetes Foundation (Fig. 45). Conversely, the WHO was the first to tie together the key components of insulin resistance, obesity, dyslipidaemia and hypertension.<sup>275,276</sup>

<sup>270</sup> Robb, G. R.; Boyd, S.; Davies, C. D.; Dossetter, A. G.; Goldberg, F. W.; Kemmitt, P. D.; Scott, J. S.; Swales, J. G. *Med. Chem. Commun.* **2015**, *6*, 926-934.

<sup>271</sup> Wamil, M.; Seckl, J. R. *Drug Discov. Today* **2007**, *12*, 504-520.

<sup>272</sup> WHO web page. Diabetes Fact Sheet. <http://www.who.int/mediacentre/factsheets/fs312/en/> (accessed on 26<sup>th</sup> June 2015).

<sup>273</sup> European Commission web page. Major and chronic diseases: Diabetes. [http://ec.europa.eu/health/major\\_chronic\\_diseases/diseases/diabetes/index\\_en.htm#fragment7](http://ec.europa.eu/health/major_chronic_diseases/diseases/diabetes/index_en.htm#fragment7) (accessed on 2<sup>nd</sup> July 2015).

<sup>274</sup> WHO web page. Obesity and overweight Fact Sheet. <http://www.who.int/mediacentre/factsheets/fs311/en/> (accessed on 26<sup>th</sup> June 2015).

<sup>275</sup> Grundy, S. M.; Brewer, H. B.; Cleeman, J. I.; Smith, S. C.; Lenfant, C. *Circulation* **2004**, *109*, 433-438.

<sup>276</sup> Huang, P. L. *Dis. Model Mech.* **2009**, *2*, 231-237.





Fig. 45. Combination of the above risk factors leads to the MetS.

Currently, the predominant therapeutic strategy for preventing or managing T2DM and MetS is the individual treatment of the set of risk factors instead of treating the disorder as a whole. The increase in the prevalence of T2DM and MetS over the last few decades in the developed countries has propelled a growing need for the development of novel therapies to treat MetS and its associated disorders.

Unlike the Cushing's syndrome, where elevated circulating cortisol levels cause the phenotypic changes, in MetS circulating GC levels are not usually elevated, despite the fact that, until recently, the extended belief was that the major contributor to the symptomatology was the level of free cortisol in plasma and the densities of GR and MR in target tissues. Therefore, it has been speculated that inter- and intracellular local levels of GC regulated by the 11 $\beta$ -HSD enzyme are responsible for metabolic abnormalities.

The impact of tissue-specific GC activation by 11 $\beta$ -HSD1 in metabolic homeostasis has been examined using several transgenic mouse models. Experiments in mice with adipose tissue-targeted 11 $\beta$ -HSD1 overexpression developed a phenotype similar to the one of Cushing's syndrome, including insulin resistance, visceral obesity, dyslipidaemia and hypertension, without an increase in the GC plasmatic levels.<sup>277,278</sup> On the other hand, overexpression of 11 $\beta$ -HSD1 in liver tissue led to the appearance of MetS but without impaired glucose tolerance and obesity.<sup>279</sup> In contrast, 11 $\beta$ -HSD1 knock-out [11 $\beta$ -HSD1(<sup>-/-</sup>)] mice had reduced triglyceride and non-esterified fatty acids, improved glucose tolerance

<sup>277</sup> Masuzaki, H.; Paterson, J.; Shinyama, H.; Morton, N. M.; Mullins, J. J.; Seckl, J. R.; Flier, J. S. *Science* **2001**, *294*, 2166-2170.

<sup>278</sup> Masuzaki, H.; Yamamoto, H.; Kenyon, C. J.; Elmquist, J. K.; Morton, N. M.; Paterson, J. M.; Shinyama, H.; Sharp, M. G. F.; Fleming, S.; Mullins, J. J.; Seckl, J. R.; Flier, J. S. *J. Clin. Invest.* **2003**, *1125*, 83-90.

<sup>279</sup> Paterson, J.; Morton, N.; Fievet, C.; Kenyon, C.; Holmes, M.; Staels, B.; Seckl, J. R.; Mullins, J. J. *Proc. Natl. Acad. Sci. USA* **2004**, *101*, 7088-7093.

and higher HDLs on a high-fat diet.<sup>280,281,282</sup> Parallely, overexpression of adipose-specific 11 $\beta$ -HSD2 resulted in reduced fat mass, and increased glucose tolerance and insulin sensitivity.<sup>283</sup>

Several studies have appeared over the recent years proving the relationship between tissue-specific alterations in 11 $\beta$ -HSD1 expression in human T2DM, obesity and MetS.<sup>284</sup> For instance, the expression of 11 $\beta$ -HSD1 in human adipose tissue is positively correlated with the degree of obesity.<sup>285,286,287</sup> In view of all these studies, it is likely that an aberrant 11 $\beta$ -HSD1 expression/activity in several key metabolic tissues underlies the pathogenesis of these diseases (Fig. 46).<sup>288</sup>

---

<sup>280</sup> Kotelevtsev, Y.; Holmes, M. C.; Burchell, A.; Houston, P. M.; Schmall, D.; Jamieson, P.; Best, R.; Brown, R.; Edwards, C. R.; Seckl, J. R.; Mullins, J. J. *Proc. Natl. Acad. Sci. USA* **1997**, *94*, 14924-14929.

<sup>281</sup> Morton, N. M.; Paterson, J. M.; Masuzaki, H.; Holmes, M. C.; Staels, B.; Fievet, C.; Walker, B. R.; Flier, J. S.; Mullins, J. J.; Seckl, J. R. *Diabetes* **2004**, *53*, 931-938.

<sup>282</sup> Morton, N. M.; Holmes, M. C.; Fievet, C.; Staels, B.; Tailleux, A.; Mullins, J. J.; Seckl, J. R. *J. Biol. Chem.* **2001**, *276*, 41293-41300.

<sup>283</sup> Kershaw, E. E.; Morton, N. M.; Dhillon, H.; Ramage, L.; Seckl, J. R.; Flier, J. S. *Diabetes* **2005**, *54*, 1023-1031.

<sup>284</sup> Morgan, S. A.; Tomlinson, J. W. *Expert Opin. Investig. Drugs* **2010**, *19*, 1067-1076.

<sup>285</sup> Wake, D. J.; Rask, E.; Livingstone, D. E.; Soderberg, S.; Olsson, T.; Walker, B. R. *J. Clin. Endocrinol. Metab.* **2003**, *88*, 3983-3988.

<sup>286</sup> Valsamakis, G.; Anwar, A.; Tomlinson, J. W.; Shackleton, C. H. L.; McTernan, P. G.; Chetty, R.; Wood, P. J.; Banerjee, A. K.; Holder, G.; Barnett, A. H.; Stewart, P. M.; Kumar, S. *J. Clin. Endocrinol. Metab.* **2004**, *89*, 4755-4761.

<sup>287</sup> Wang, M. *Drug Dev. Res.* **2006**, *67*, 567-569.

<sup>288</sup> Cooper, M. S.; Stewart, P. M. *J. Clin. Endocrinol. Metab.* **2009**, *94*, 4645-4654.

<b>LIVER TISSUE</b>	
Expressed at high level Promotes gluconeogenesis, steatosis and hypertriglyceridemia Inhibition improves insulin sensitivity ↓ activity with weight gain and/or insulin resistance	
<b>ADIPOSE TISSUE</b>	
<b>VISCERAL:</b> Promotes adipocyte differentiation and ↑ size No net production of glucocorticoids in human studies ↑ expression with TNF $\alpha$ ↓ expression with IGF-1/GH	<b>SUBCUTANEOUS:</b> ↑ expression with differentiation ↑ expression with obesity ↑ expression with acute weight loss
<b>VASCULATURE</b>	
Inhibition reduces progression of atherosclerosis in mice ↑ expression in vascular smooth muscle <i>in vitro</i> but not <i>in vivo</i> Capable of oxysterol metabolism and this may compete with glucocorticoids	
<b>MUSCLE</b>	
↓ expression proposed to protect against insulin resistance ↑ expression in rodent models of diabetes	
<b>PANCREATIC ISLETS</b>	
Expression in $\beta$ -and/or $\alpha$ -cells Inhibits insulin and glucagon secretion	

Fig. 46. Role of 11 $\beta$ -HSD1 in the pathogenesis of the MetS and related disorders.

Hence, modulation of 11 $\beta$ -HSD enzyme, and in particular inhibition of 11 $\beta$ -HSD1 in adipose tissue and liver, are of special interest as pharmacotherapeutic strategies in the medical treatment of the MetS and associated disorders.<sup>289,290,291</sup>

### 1.2.2 11 $\beta$ -HSD1 inhibition and inflammation

The anti-inflammatory effects of pharmacological levels of GCs are well known and widely exploited.<sup>292</sup> Short-term therapy with GCs, chiefly cortisone, is broadly described to treat acute inflammation. However, endogenous GCs are immunomodulatory rather than simply anti-inflammatory agents.<sup>293,294</sup> GCs both enhance or suppress immune responses depending on concentration and timing, by affecting the migration of immune cells, their differentiated states, and the production of a range of inflammatory cytokines.<sup>288</sup> Ultimately, GCs shape an ongoing inflammatory response as it progresses, depending on the local environment. With respect to 11 $\beta$ -HSD1, it is expressed in certain immune cells,

<sup>289</sup> Morton, N. M. *Mol. Cell. Endocrinol.* **2010**, *316*, 154-164.

<sup>290</sup> Joharapurkar, A.; Dhanesha, N.; Shah, G.; Kharul, R.; Jain, M. *Pharmacol. reports* **2012**, *64*, 1055-1065.

<sup>291</sup> Anderson, A.; Walker, B. R. *Drugs* **2013**, *73*, 1385-1393.

<sup>292</sup> McEwen, B. S.; Biron, C. A.; Brunson, K. W.; Bulloch, K.; Chambers, W. H.; Dhabhar, F. S.; Goldfarb, R. H.; Kitson, R. P.; Miller, A. H.; Spencer, R. L.; Weiss, J. M. *Brain Res. Rev.* **1997**, *23*, 79-133.

<sup>293</sup> Sapolsky, R. M.; Romero, L. M.; Munck, A. U. *Endocr. Rev.* **2000**, *21*, 55-89.

<sup>294</sup> Yeager, M. P.; Guyre, P. M.; Munck, A. U. *Acta Anaesthesiol. Scand.* **2004**, *48*, 799-813.

such as the differentiated monocytes and in most lymphocyte populations.<sup>295</sup> Regulation of 11 $\beta$ -HSD1 at this cellular level provides a further mechanism to fine-tune cellular immune responses.

In chronic inflammatory processes, such as rheumatoid arthritis, atherosclerosis and rhinitis, there is an imbalance on the expression/activity of the two isoforms of the 11 $\beta$ -HSD.<sup>296,297,298</sup> It has been suggested that dysregulation of the normal reciprocal control of 11 $\beta$ -HSD1 and 11 $\beta$ -HSD2 may contribute to the failure of resolution during chronic inflammatory states. Therefore, the control of GC's bioavailability within immune cells by 11 $\beta$ -HSD1 provides a checkpoint for the attenuation of unwanted immune responses.<sup>299,300</sup> Hence, modulation of 11 $\beta$ -HSD1 expressed in immune cells may offer an alternative approach for the treatment of rheumatoid arthritis, rhinitis and atherosclerosis, diseases highly linked to MetS. Of note, metabolic disorders such as obesity and T2DM are associated with a dysregulated immune response,<sup>301</sup> thereby underpinning the potential of the inhibition of 11 $\beta$ -HSD1 as a new therapeutic strategy for such conditions.

### 1.2.2 11 $\beta$ -HSD1 inhibition and cognitive dysfunction with aging

The hippocampus region of the brain is an area that plays an important role in the formation of long-lasting memories and wields an executive level of control over the HPA axis.<sup>300,302</sup> In this particular region, 11 $\beta$ -HSD1 but not 11 $\beta$ -HSD2 is greatly expressed, together with GRs and MRs. As already discussed, GCs are known to deeply influence metabolism, immune system and neuronal function.<sup>292</sup> Bearing in mind the phenotype of Cushing's syndrome depicted in figure 3, deficient regulation of the HPA axis with resultant chronically elevated levels of GCs exerts deleterious effects on specific areas of the brain, eventually resulting in cognitive dysfunction. Specifically, excessive GC concentrations in the brain enhance neuronal death due to a series of conditions such as increase of the levels of amyloid precursor protein, hypoxia and excitotoxic concentrations of glutamate (therefore connected with the previous chapter).<sup>303,304</sup> There is mounting evidence from human and rodent studies that this GC-related cognitive decline is apparent

<sup>295</sup> Chapman, K. E.; Coutinho, A. E.; Gray, M.; Gilmour, J. S.; Savill, J. S.; Seckl, J. R. *Mol. Cell. Endocrinol.* **2009**, *301*, 123-131.

<sup>296</sup> Hardy, R. S.; Seibel, M. J.; Cooper, M. S. *Curr. Opin. Pharmacol.* **2013**, *13*, 440-444.

<sup>297</sup> Hadoke, P. W. F.; Kipari, T.; Seckl, J. R.; Chapman, K. E. *Curr. Atheroscler. Rep.* **2013**, *15*, 320-330.

<sup>298</sup> Jun, Y. J.; Park, S. J.; Hwang, J. W.; Kim, T. H.; Jung, K. J.; Jung, J. Y.; Hwang, G. H.; Lee, S. H.; Lee, S. H. *Clin. Exp. Allergy* **2014**, *44*, 197-211.

<sup>299</sup> Chapman, K. E.; Gilmour, J. S.; Coutinho, A. E.; Savill, J. S.; Seckl, J. R. *Mol. Cell. Endocrinol.* **2006**, *248*, 3-8.

<sup>300</sup> Chapman, K. E.; Seckl, J. R. *Neurochem. Res.* **2008**, *33*, 624-636.

<sup>301</sup> Hotamisligil, G. S. *Nature* **2006**, *444*, 860-867.

<sup>302</sup> Squire, L. R. *Psychol. Rev.* **1992**, *99*, 195-231.

<sup>303</sup> Sapolsky, R. M.; Pulsinelli, W. A. *Science* **1985**, *229*, 1397-1400.

<sup>304</sup> Beraki, S.; Litrus, L.; Soriano, L.; Monbureau, M.; To, L. K.; Braithwaite, S. P.; Nikolich, K.; Urfer, R.; Oksenberg, D.; Shamloo, M. *PLoS One* **2013**, *8*, 1-13.

with aging.<sup>305,306,307</sup> Indeed, GCs are strongly implicated in the pathogenesis of age-related cognitive impairment and AD.<sup>308,309,310</sup> It is believed that low intracellular concentration of GCs in hippocampus activates MRs, whose stimulation lead to increased memory, whilst high concentration of GCs saturates MRs and over-activates GRs, thus affecting memory processes.<sup>311</sup> Moreover, inhibition of 11 $\beta$ -HSD1 reduces A $\beta$  plaque burden and plasma A $\beta$  in AD animal models.<sup>312,313</sup>

In a similar way as for the previous disorders, influence on the metabolism of GCs within target tissues may offer a route for tissue-selective control of GC exposure. In this sense, 11 $\beta$ -HSD1 inhibition may assist in keeping the GC levels low throughout life, which may prevent the appearance of cognitive deficits with aging. This fact has been confirmed in aged [11 $\beta$ -HSD1(<sup>-/-</sup>)] mice, which are protected from GC-associated hippocampal dysfunction with aging.<sup>314</sup> In contrast to aged wild type mice, [11 $\beta$ -HSD1(<sup>-/-</sup>)] counterparts learn as young mice, avoiding the normal cognitive decline seen with aging. On the other hand, it has been demonstrated that inhibition of 11 $\beta$ -HSD1 ameliorates age-related cognitive impairments in mice, suggesting that 11 $\beta$ -HSD1 is a potential target for the treatment of cognitive dysfunction.<sup>315,316</sup> A study carried out by Seckl and co-workers proved that the use of a non-selective 11 $\beta$ -HSD inhibitor for 4-6 weeks improved the cognitive functions in healthy and diabetic elderly.<sup>305</sup> T2DM is a risk factor of dementia, whose pathogenesis is triggered by an overactivation of the HPA axis.<sup>317</sup>

<sup>305</sup> Sandeep, T. C.; Yau, J. L. W.; Maclullich, A. M. J.; Noble, J.; Deary, I. J.; Walker, B. R.; Seckl, J. R. *Proc. Natl. Acad. Sci. USA* **2004**, *101*, 6734-6739.

<sup>306</sup> Meaney, M. J.; O'Donnell, D.; Rowe, W.; Tannenbaum, B.; Steverman, A.; Walker, M.; Nair, N. P.; Lupien, S. *Exp. Gerontol.* **1995**, *30*, 229-251.

<sup>307</sup> Yau, J. L. W.; Wheelan, N.; Noble, J.; Walker, B. R.; Webster, S. P.; Kenyon, C. J.; Ludwig, M.; Seckl, J. R. *Neurobiol. Aging* **2015**, *36*, 334-343.

<sup>308</sup> de Quervain, D. J.-F.; Poirier, R.; Wollmer, M. A.; Grimaldi, L. M. E.; Tsolaki, M.; Streffer, J. R.; Hock, C.; Nitsch, R. M.; Mohajeri, M. H.; Papassotiropoulos, A. *Hum. Mol. Genet.* **2004**, *13*, 47-52.

<sup>309</sup> Martocchia, A.; Stefanelli, M.; Falaschi, G. M.; Toussan, L.; Ferri, C.; Falaschi, P. *Aging Clin. Exp. Res.* **2015**, *ahead of print*. DOI: 10.1007/s40520-015-0353-0.

<sup>310</sup> Katz, D. A.; Liu, W.; Locke, C.; Jacobson, P.; Barnes, D. M.; Basu, R.; An, G.; Rieser, M. J.; Daszkowski, D.; Groves, F.; Heneghan, G.; Shah, A.; Gevorkyan, H.; Jhee, S. S.; Ereshefsky, L.; Marek, G. J. *Transl. Psychiatry* **2013**, *3*, e295.

<sup>311</sup> Yau, J. L. W.; Noble, J.; Seckl, J. R. *J. Neurosci.* **2011**, *31*, 4188-4193.

<sup>312</sup> Green, K. N.; Billings, L. M.; Roozendaal, B.; McGaugh, J. L.; LaFerla, F. M. *J. Neurosci.* **2006**, *26*, 9047-9056.

<sup>313</sup> Sooy, K.; Noble, J.; McBride, A.; Binnie, M.; Yau, J. L. W.; Seckl, J. R.; Walker, B. R.; Webster, S. P. *Endocrinology* **2015**, *ahead of print*. DOI: 10.1210/en.2015-1395.

<sup>314</sup> Yau, J. L. W.; Noble, J.; Kenyon, C. J.; Hibberd, C.; Kotelevtsev, Y.; Mullins, J. J.; Seckl, J. R. *Proc. Natl. Acad. Sci. USA* **2001**, *98*, 4716-4721.

<sup>315</sup> Sooy, K.; Webster, S. P.; Noble, J.; Binnie, M.; Walker, B. R.; Seckl, J. R.; Yau, J. L. W. *J. Neurosci.* **2010**, *30*, 13867-13872.

<sup>316</sup> Mohler, E. G.; Browman, K. E.; Roderwald, V. A.; Cronin, E. A.; Markosyan, S.; Bitner, R. S.; Strakhova, M. I.; Drescher, K. U.; Hornberger, W.; Rohde, J. J.; Brune, M. E.; Jacobson, P. B.; Rueter, L. E. *J. Neurosci.* **2011**, *31*, 5406-5413.

<sup>317</sup> Strachan, M. W. J.; Reynolds, R. M.; Frier, B. M.; Mitchell, R. J.; Price, J. F. *Diabetes Obes. Metab.* **2009**, *11*, 407-414.

### 1.2.3 $11\beta$ -HSD1 inhibition for other diseases

$11\beta$ -HSD1 inhibition has been investigated also for other indications, such as glaucoma,<sup>318</sup> osteoporosis,<sup>319</sup> wound healing and age-associated skin damage.<sup>320,321</sup> For the sake of brevity, these disorders are not discussed any further, the reader is referred to the titled references if desired.

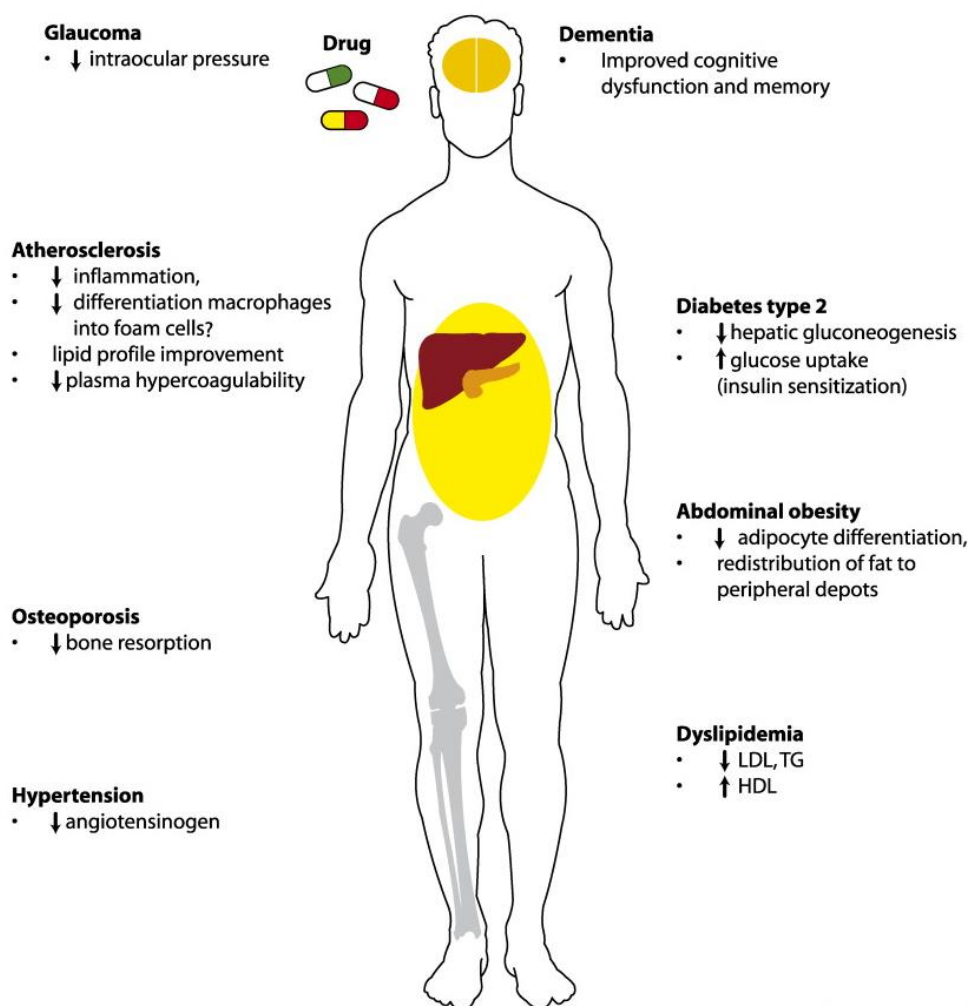


Fig. 47. Plausible therapeutic indications arising from  $11\beta$ -HSD1 inhibition.<sup>271</sup>

<sup>318</sup> Anderson, S.; Carreiro, S.; Quenzer, T.; Gale, D.; Xiang, C.; Gukasyan, H.; Lafontaine, J.; Cheng, H.; Krauss, A.; Prasanna, G. *J. Ocul. Pharmacol. Ther.* **2009**, *25*, 215-222.

<sup>319</sup> Park, J. S.; Bae, S. J.; Choi, S.-W.; Son, Y. H.; Park, S. B.; Rhee, S. D.; Kim, H. Y.; Jung, W. H.; Kang, S. K.; Ahn, J. H.; Kim, S. H.; Kim, K. Y. *J. Mol. Endocrinol.* **2014**, *52*, 191-202.

<sup>320</sup> Tiganescu, A.; Tahrani, A. A.; Morgan, S. A.; Otranto, M.; Desmoulière, A.; Abrahams, L.; Hassan-Smith, Z.; Walker, E. A.; Rabbitt, E. H.; Cooper, M. S.; Amrein, K.; Lavery, G. G.; Stewart, P. M. *J. Clin. Invest.* **2013**, *123*, 3051-3060.

<sup>321</sup> Terao, M.; Murota, H.; Kimura, A.; Kato, A.; Ishikawa, A.; Igawa, K.; Miyoshi, E.; Katayama, I. *PLoS One* **2011**, *6*, 1-11.

With the data provided so far, it would be logical to consider 11 $\beta$ -HSD1 inhibition as a potential panacea for the most prevalent diseases of the developed countries originated by HPA axis overactivation and subsequent chronically elevated GCs. In the light of the current insights of the role of 11 $\beta$ -HSD1 in tissue-specific reactivation of cortisone to cortisol and the pathological effects of an excess of GCs, perhaps we are in a position to re-evaluate the use of cortisone as anti-inflammatory agent for the treatment of arthritis and other inflammatory conditions, which was the subject of the Noble Prize in Physiology and Medicine in 1950.<sup>322</sup>

### 1.3 Crystal structure of 11 $\beta$ -HSD1 and its binding site

11 $\beta$ -HSD1 is a 34 kD protein of 292 amino acids that forms homodimers and tetramers in solution, which are believed to be the functional unit *in vivo*.<sup>323,324</sup> The enzyme is comprised of 4 main regions, i.e. (i) a transmembrane domain at the N-terminus linked to the ER membrane; (ii) a cofactor binding domain, characterized by a Rossman fold; (iii) a cluster of key residues that constitute the catalytic site; and (iv) a region essential for enzyme dimerization at the C-terminus.

The Rossman fold is highly conserved in the so-called short-chain dehydrogenase/reductase family of enzymes, whereof 11 $\beta$ -HSD1 is member. This particular three-dimensional structure consists of seven-stranded parallel  $\beta$ -sheets flanked by three  $\alpha$ -helices on the left and right sides each.<sup>325</sup> In 11 $\beta$ -HSD1, the cofactor-binding site is placed in between the Rossman fold, and close to the location of the catalytic site of the substrate (Fig. 48).

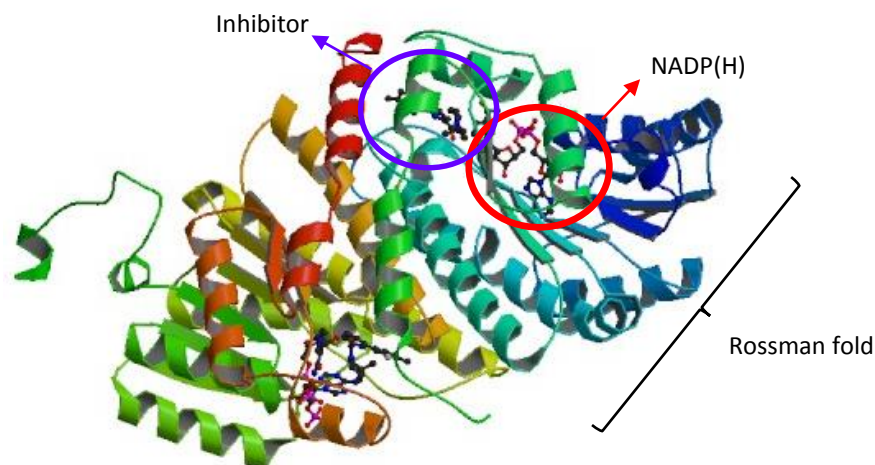
---

<sup>322</sup> Hench, P. S.; Kendall, E. C.; Slocumb, C. H.; Polley, H. F. *Ann. Rheum. Dis.* **1949**, *8*, 97-104.

<sup>323</sup> Sandeep, T. C.; Walker, B. R. *Trends Endocrinol. Metab.* **2001**, *12*, 446-453.

<sup>324</sup> Zhang, J.; Osslund, T. D.; Plant, M. H.; Clogston, C. L.; Nybo, R. E.; Xiong, F.; Delaney, J. M.; Jordan, S. R. *Biochemistry* **2005**, *44*, 6948-6957.

<sup>325</sup> Schuster, D.; Maurer, E. M.; Laggner, C.; Nashev, L. G.; Wilckens, T.; Langer, T.; Odermatt, A. *J. Med. Chem.* **2006**, *49*, 3454-3466.



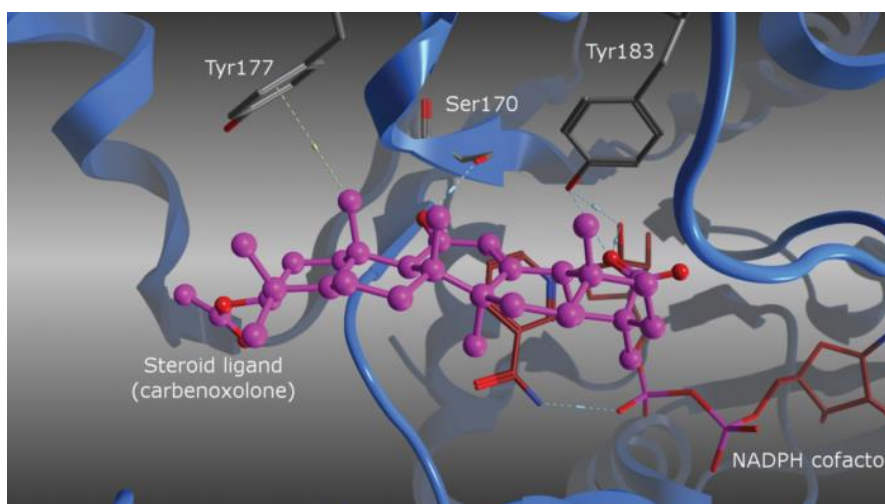
**Fig. 48.** X-ray crystal structure of 11 $\beta$ -HSD1 bound to cofactor NADPH and a novel inhibitor. PDB code: 3CH6.<sup>326</sup>

The substrate catalytic site shows the amino acid sequence Tyr-X-X-X-Lys (specifically Tyr183 and Lys187, wherein X-X-X is a certain combination of amino acids). The X-X-X motif often includes a conserved serine residue (Ser170), that participates in ligand binding, stabilizes the orientation of the substrate within the catalytic site, and catalyses the proton transfer to and from reduced and oxidized intermediates.<sup>327</sup> In contrast, Lys187 forms hydrogen bonds with the nicotinamide ribose of NADP(H) and lowers the  $pK_a$  of the hydroxyl group of the neighbouring Tyr183, which also binds to the substrate and cofactor. The also known as catalytic triad Tyr183 - Ser170 - Lys187, interacts thus with the substrate and promotes the proton transfer to the reactive keto-oxygen of cortisone to furnish the active GC cortisol (Fig. 49).

<sup>326</sup> Wang, H.; Ruan, Z.; Li, J. J.; Simpkins, L. M.; Smirk, R. A; Wu, S. C.; Hutchins, R. D.; Nirschl, D. S.; Van Kirk, K.; Cooper, C. B.; Sutton, J. C.; Ma, Z.; Golla, R.; Seethala, R.; Salyan, M. E. K.; Nayeem, A.; Krystek, S. R.; Sheriff, S.; Camac, D. M.; Morin, P. E.; Carpenter, B.; Robl, J. A; Zahler, R.; Gordon, D. A; Hamann, L. G. *Bioorg. Med. Chem. Lett.* **2008**, *18*, 3168-3172.

<sup>327</sup> Hosfield, D. J.; Wu, Y.; Skene, R. J.; Hilgers, M.; Jennings, A.; Snell, G. P.; Aertgeerts, K. *J. Biol. Chem.* **2005**, *280*, 4639-4648.





**Fig. 49.** Binding mode of a steroid ligand (carbenoxolone) and cofactor NADPH with key residues highlighted similar to the endogenous substrate. PDB code: 2BEL.<sup>328</sup>

Despite the residues that establish key hydrogen bond interactions, the catalytic pocket is largely hydrophobic.<sup>329</sup> Furthermore, both ends of the catalytic site are open to the solvent, thus ligands that are too long to fit within the pocket can extend out of it and contact with surface residues.

The distinctive binding site of the steroid substrate and the conformational flexibility in crystal structures assert 11 $\beta$ -HSD1 as an ideal target for rational drug design. It has been suggested that the murine structure can provide a reliable model for the design of inhibitors for the human enzyme.<sup>330</sup> Notwithstanding that, the preferred structure for the computer-aided drug design is the human protein, as it can be seen in most resolved crystal structures so far.

#### 1.4 11 $\beta$ -HSD1 inhibitors in development

Since the discovery of 11 $\beta$ -HSD1, there has been a rapid growth in small molecules that inhibit this enzyme as potential therapeutics for the treatment of multiple conditions. Many pharmaceutical companies have pursued development programmes targeting 11 $\beta$ -HSD1, which still represent an important area. The patent literature surrounding the development of novel 11 $\beta$ -HSD1 inhibitors has been extremely rich in the last decade, with

<sup>328</sup> Scott, J. S.; Chooramun, J. *11 $\beta$ -hydroxysteroid dehydrogenase Type 1 (11 $\beta$ -HSD1) inhibitors in development*, in *RSC Drug Discovery Series No. 27*, The Royal Society of Chemistry, 2012.

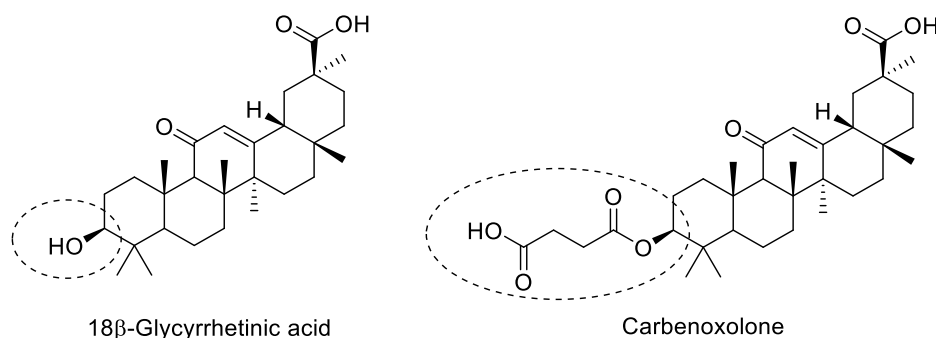
<sup>329</sup> Thomas, M. P.; Potter, B. V. L. *Future Med. Chem.* **2011**, *3*, 367-390.

<sup>330</sup> Zhang, J.; Osslund, T. D.; Plant, M. H.; Clogston, C. L.; Nybo, R. E.; Xiong, F.; Delaney, J. M.; Jordan, S. R. *Biochemistry* **2005**, *44*, 6948-6957.

more than 250 patent applications published, as well as several publications from academia and industry covering biologically active inhibitors.<sup>331,332,333,334,335</sup>

#### 1.4.1 Non-selective 11 $\beta$ -HSD1 inhibitors as tools

The Tibetan remedy liquorice root was used for the treatment of disorders in respiratory and digestive systems, biliary tracts and kidneys, paralysis with nervous origin, anaemia and as antidote in snake and wild dog bites.<sup>336</sup> More than 250 active molecules have been identified from the extracts of this ancient medicine, and among them, the 18 $\beta$ -glycyrrhetic acid was isolated. This naturally occurring steroid is a potent, non-selective inhibitor of 11 $\beta$ -HSDs with IC<sub>50</sub> values in the nano-molar range (Fig. 50).<sup>337</sup> Interestingly, structural modification of the 18 $\beta$ -glycyrrhetic acid led to inhibitors with a reverse selectivity towards 11 $\beta$ -HSD2.<sup>338,339</sup> Later on, its hemisuccinate ester derivative carbenoxolone, which also inhibits both 11 $\beta$ -HSD1 and 11 $\beta$ -HSD2, was approved in the 1960s in UK for the treatment of gastric ulcers and inflammation.<sup>340</sup>



**Fig. 50.** Structure of 18 $\beta$ -glycyrrhetic acid and its synthetically derived carbenoxolone, a clinically used inhibitor of 11 $\beta$ -HSDs.

Despite inhibiting both isoforms, carbenoxolone has been used in animal and human studies as a proof-of-concept during the target validation of 11 $\beta$ -HSD1. Several studies have confirmed the increase of hepatic insulin sensitivity in humans with carbenoxolone, and

<sup>331</sup> Webster, S. P.; Pallin, T. D. *Expert Opin. Ther. Pat.* **2007**, *17*, 1407-1422.

<sup>332</sup> Hughes, K. A.; Webster, S. P.; Walker, B. R. *Expert Opin. Investig. Drugs* **2008**, *17*, 481-496.

<sup>333</sup> St. Jean Jr., D. J.; Wang, M.; Fotsch, C. *Curr. Top. Med. Chem.* **2008**, *8*, 1508-1523.

<sup>334</sup> Boyle, C. D.; Kowalski, T. J. *Expert Opin. Ther. Pat.* **2009**, 801-826.

<sup>335</sup> Scott, J. S.; Goldberg, F. W.; Turnbull, A. V. *J. Med. Chem.* **2014**, *57*, 4466-4486.

<sup>336</sup> Pavlova, S. I.; Uteshev, B. S.; Sergeev, A. V. *Pharm. Chem. J.* **2003**, *37*, 314-317.

<sup>337</sup> Bühler, H.; Perschel, F. H.; Hierholzer, K. *Biochim. Biophys. Acta* **1991**, *1075*, 206-212.

<sup>338</sup> Su, X.; Lawrence, H.; Ganeshpillai, D.; Cruttenden, A.; Purohit, A.; Reed, M. J.; Vicker, N.; Potter, B. V. L. *Bioorg. Med. Chem.* **2004**, *12*, 4439-4457.

<sup>339</sup> Pandya, K.; Dietrich, D.; Seibert, J.; Vederas, J. C.; Odermatt, A. *Bioorg. Med. Chem.* **2013**, *21*, 6274-6281.

<sup>340</sup> Wang, M. *Inhibitors of 11 $\beta$ -hydroxysteroid dehydrogenase type 1 in antidiabetic therapy, in Diabetes – Perspectives in Drug Therapy, Handbook of Experimental Pharmacology*, 203, Springer-Verlag Berlin Heidelberg, 2011.

attenuation of the symptoms of MetS and atherogenesis in obese mice.<sup>341,342,343</sup> Moreover, carbenoxolone improved cognitive function in healthy elderly men and type 2 diabetics, as commented before.<sup>305</sup> However, the therapeutical potential of carbenoxolone is limited due to the hypokalemia and hypertension derived from 11 $\beta$ -HSD2 inhibition.

#### 1.4.2 Studies with selective 11 $\beta$ -HSD1 inhibitors

Since the discovery of the latter dual inhibitors of 11 $\beta$ -HSDs, the surge of research and clinical interest in this area has resulted in many companies and academic groups developing selective 11 $\beta$ -HSD1 inhibitors from a variety of structural classes. The large majority of 11 $\beta$ -HSD1 inhibitors feature a hydrogen bond acceptor functionality such as amides, lactams, ureas, carbamates, sulphones, sulphonamides or heterocycles flanked by bulky lipophilic radicals such as cyclohexanes, adamantanes or benzene rings. A great part of the candidates can be sorted in a few groups: arylsulphonamides, triazoles, piperazine sulphonamides, piperidine carboxamides, thiazolones, heterocyclic and adamantyl amides, ureas, etc. From the available X-ray crystal structures of different inhibitors resolved with the protein,<sup>344</sup> a few points can be drawn for the assistance when designing potential ligands:

- the H-bond acceptor unit mimics the reducible keto function of the endogenous substrate cortisone by interacting with the residues of the active site.
- The bulky lipophilic groups fit the buried hydrophobic pockets of the catalytic site, generally near the binding region of the nicotinamide unit of NADP(H) or the steroid substrate.
- The catalytic site is open to the solvent region, which allows the binding pocket to accommodate extended ligands. In this area, tyrosine 177 plays an important role in interacting with the hydrophobic regions of the molecules.

---

<sup>341</sup> Walker, B. R.; Connacher, A. A.; Lindsay, R. M.; Webb, D. J.; Edwards, C. R. *J. Clin. Endocrinol. Metab.* **1995**, *80*, 3155-3159.

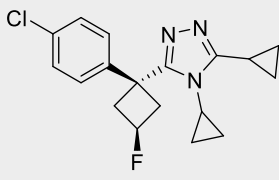
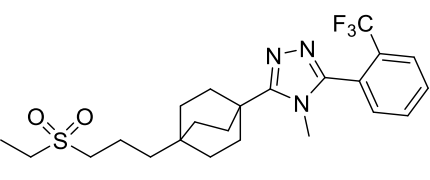
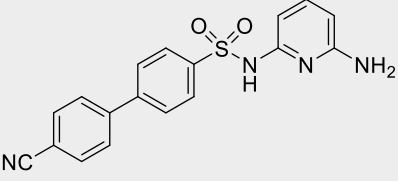
<sup>342</sup> Andrews, R. C.; Rooyackers, O.; Walker, B. R. *J. Clin. Endocrinol. Metab.* **2003**, *88*, 285-291.

<sup>343</sup> Nuotio-Antar, A. M.; Hachey, D. L.; Hasty, A. H. *Am. J. Physiol. Endocrinol. Metab.* **2007**, *293*, E1517-E1528.

<sup>344</sup> PDB codes: 2BEL, 3D4N, 3D3E, 2ILT, 3BYZ, 3CZR, 3CH6, among others. See also reference 329 for a detailed analyses of the crystal structures of 11 $\beta$ -HSD1.

Table 12 includes the most relevant candidates that have reached clinical trials in the last few years.<sup>345,346,347,348,349</sup> The positive data from human studies validate 11 $\beta$ -HSD1 as a target for the treatment of T2DM, MetS, related disorders and AD.

**Table 12.** List of drug candidates that have achieved clinical trials as inhibitors of the 11 $\beta$ -HSD1.

Compound	Company	Status
 <b>MK-0916</b>	Merck	No longer in company pipeline (achieved Phase II in 2004)
 <b>MK-0736</b>	Merck	No longer in company pipeline (achieved Phase II in 2005)
 <b>PF-915275</b>	Pfizer	Discontinued Phase II (2007)

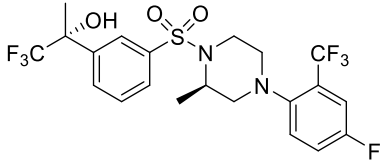
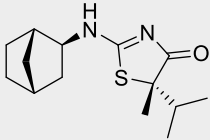
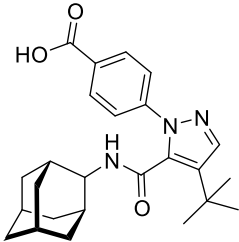
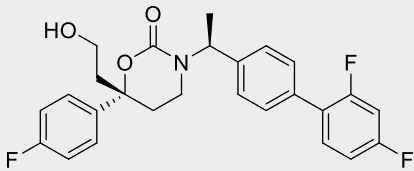
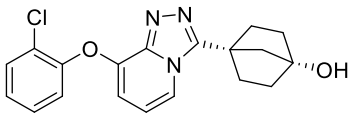
<sup>345</sup> Stefan, N.; Ramsauer, M.; Jordan, P.; Nowotny, B.; Kantartzis, K.; Machann, J.; Hwang, J.H.; Nowotny, P.; Kahl, S.; Harreiter, J.; Hornemann, S.; Sanyal, A. J.; Stewart, P. M.; Pfeiffer, A. F.; Kautzky-Willer, A.; Roden, M.; Häring, H. U.; Fürst-Recktenwald, S. *Lancet Diabetes Endocrinol.* **2014**, *2*, 406-416.

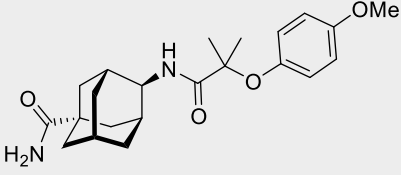
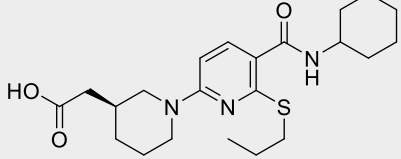
<sup>346</sup> Siu, M.; Johnson, T. O.; Wang, Y.; Nair, S. K.; Taylor, W. D.; Cripps, S. J.; Matthews, J. J.; Edwards, M. P.; Pauly, T. A.; Ermolieff, J.; Castro, A.; Hosea, N. A.; LaPaglia, A.; Fanjul, A. N.; Vogel, J. E. *Bioorg. Med. Chem. Lett.* **2009**, *19*, 3493-3497.

<sup>347</sup> Feig, P. U.; Shah, S.; Hermanowski-Vosatka, A.; Plotkin, D.; Springer, M. S.; Donahue, S.; Thach, C.; Klein, E. J.; Lai, E.; Kaufman, K. D. *Diabetes Obes. Metab.* **2011**, *13*, 498-504.

<sup>348</sup> Shah, S.; Hermanowski-Vosatka, A.; Gibson, K.; Ruck, R. A.; Jia, G.; Zhang, J.; Hwang, P. M. T.; Ryan, N. W.; Langdon, R. B.; Feig, P. U. *J. Am. Soc. Hypertens.* **2011**, *5*, 166-176.

<sup>349</sup> Clinical trials web site. 11 $\beta$ -HSD1. <https://www.clinicaltrials.gov/> (accessed on 28<sup>th</sup> July 2015).

 <p><b>HSD-016</b></p>	Wyeth	Discontinued Phase I (2008)
 <p><b>AMG-221/BVT-83370</b></p>	Amgen/Biovitrum	Discontinued Phase I (2011)
 <p><b>AZD-8329</b></p>	AstraZeneca	Discontinued Phase I (2011)
<p><b>INCB13739</b> Structure not released yet</p>	Incyte	Phase I completed
<p><b>RO5093151</b> Structure not released yet</p>	Hoffman-La Roche	Phase I completed
 <p><b>BI 135585</b></p>	Boehringer Ingelheim	Phase I completed
 <p><b>BMS-770767</b></p>	Bristol-Myers Squibb	Phase II completed

 <b>ABT-384</b>	Abbott	Phase II completed
<b>P2202</b> Structure not released yet	Eli Lilly & Piramal	Phase II completed
 <b>AZD-4017</b>	AstraZeneca	Phase II (recruiting)
<b>UE2343</b> Structure not released yet	University of Edinburgh - Actinogen	Phase II (recruiting)
<b>ASP3662</b> Structure not released yet	Astellas Pharma	Phase II (recruiting)

In the interest of this project,  $11\beta$ -HSD1 inhibitors that are adamantane-based compounds will be discussed in more detail.

#### 1.4.3 Adamantane-based inhibitors of $11\beta$ -HSD1

The adamantyl group appears to be a privileged scaffold present in many  $11\beta$ -HSD1 inhibitors disclosed in the patent and scientific literature, and a few of them have reached clinical trials (see Table 12). As in the previous examples, the inhibitors bearing an adamantane moiety feature an H-bond acceptor functionality attached at one end to an adamantane group, which fits one of the hydrophobic pockets of the catalytic site. Despite of these general binding characteristics, different subclasses of adamantane-based compounds have been revealed, from amides and ureas to triazoles and thiazolones. A brief

compilation of the most significant adamantanyl 11 $\beta$ -HSD1 inhibitors is contained in figure 51.<sup>350,351,352,353,354,355,356,357,358,359,360</sup>

<sup>350</sup> Cheng, H.; Hoffman, J.; Le, P.; Nair, S. K.; Cripps, S.; Matthews, J.; Smith, C.; Yang, M.; Kupchinsky, S.; Dress, K.; Edwards, M.; Cole, B.; Walters, E.; Loh, C.; Ermolieff, J.; Fanjul, A.; Bhat, G. B.; Herrera, J.; Pauly, T.; Hosea, N.; Paderes, G.; Rejto, P. *Bioorg. Med. Chem. Lett.* **2010**, *20*, 2897-2902.

<sup>351</sup> Johansson, L.; Fotsch, C.; Bartberger, M. D.; Castro, V. M.; Chen, M.; Emery, M.; Gustafsson, S.; Hale, C.; Hickman, D.; Homan, E.; Jordan, S. R.; Komorowski, R.; Li, A.; McRae, K.; Moniz, G.; Matsumoto, G.; Orihuela, C.; Palm, G.; Veniant, M.; Wang, M.; Williams, M.; Zhang, J. *J. Med. Chem.* **2008**, *51*, 2933-2943.

<sup>352</sup> Tice, C. M.; Zhao, W.; Xu, Z.; Cacatian, S. T.; Simpson, R. D.; Ye, Y. J.; Singh, S. B.; McKeever, B. M.; Lindblom, P.; Guo, J.; Krosky, P. M.; Kruk, B. A.; Berbaum, J.; Harrison, R. K.; Johnson, J. J.; Bukhtiyarov, Y.; Panemangalore, R.; Scott, B. B.; Zhao, Y.; Bruno, J. G.; Zhuang, L.; McGeehan, G. M.; He, W.; Claremon, D. A. *Bioorg. Med. Chem. Lett.* **2010**, *20*, 881-886.

<sup>353</sup> Olson, S.; Aster, S. D.; Brown, K.; Carbin, L.; Graham, D. W.; Hermanowski-Vosatka, A.; LeGrand, C. B.; Mundt, S. S.; Robbins, M. A.; Schaeffer, J. M.; Slossberg, L. H.; Szymonifka, M. J.; Thieringer, R.; Wright, S. D.; Balkovec, J. M. *Bioorg. Med. Chem. Lett.* **2005**, *15*, 4359-4362.

<sup>354</sup> Rohde, J. J.; Pliushchev, M. A.; Sorensen, B. K.; Wodka, D.; Shuai, Q.; Wang, J.; Fung, S.; Monzon, K. M.; Chiou, W. J.; Pan, L.; Deng, X.; Chovan, L. E.; Ramaiya, A.; Mullally, M.; Henry, R. F.; Stolarik, D. F.; Imade, H. M.; Marsh, K. C.; Beno, D. W. A.; Fey, T. A.; Droz, B. A.; Brune, M. E.; Camp, H. S.; Sham, H. L.; Frevert, E. U.; Jacobson, P. B.; Link, J. T. *J. Med. Chem.* **2007**, *50*, 149-164.

<sup>355</sup> Richards, S.; Sorensen, B.; Jae, H.-S.; Winn, M.; Chen, Y.; Wang, J.; Fung, S.; Monzon, K.; Frevert, E. U.; Jacobson, P.; Sham, H.; Link, J. T. *Bioorg. Med. Chem. Lett.* **2006**, *16*, 6241-6245.

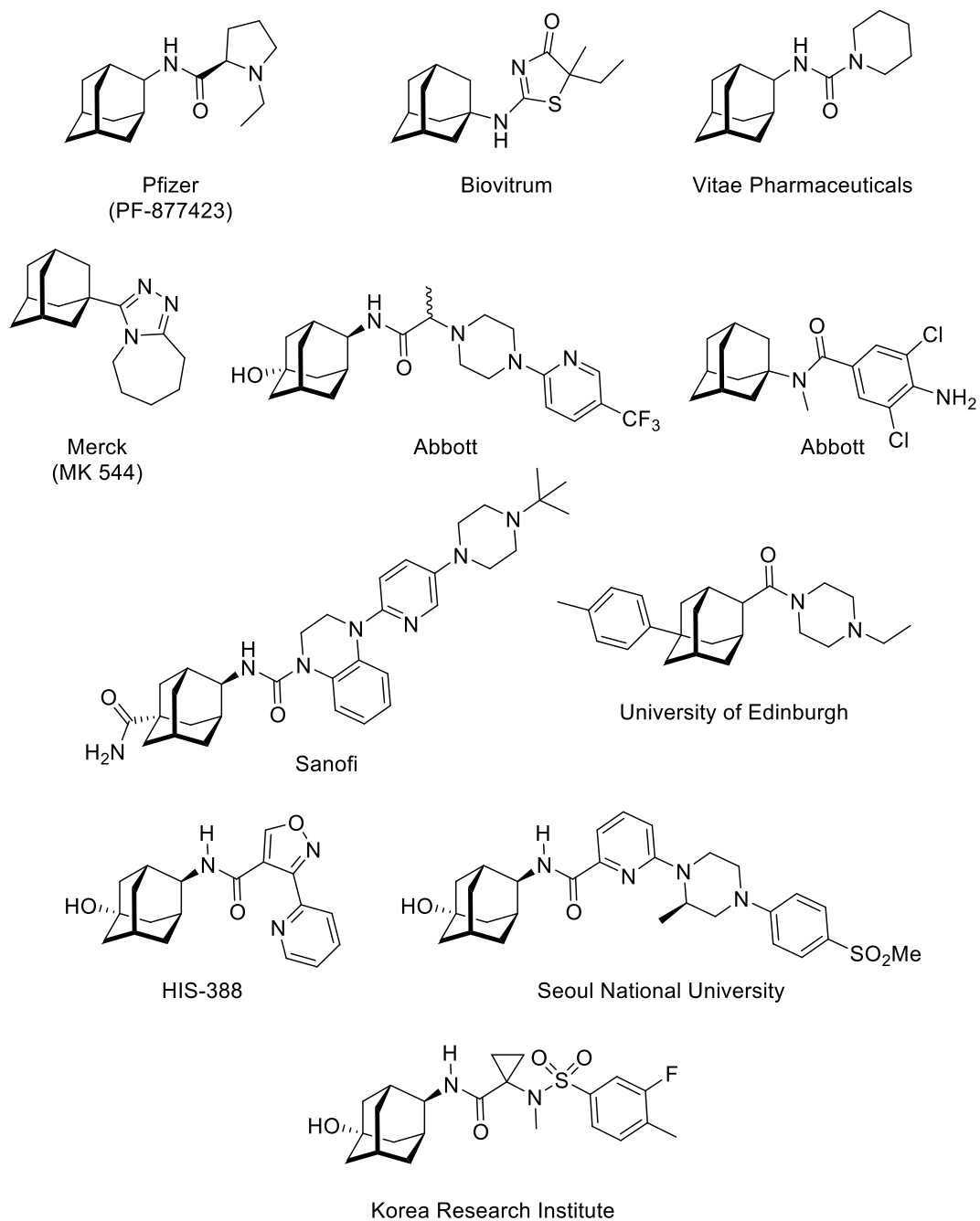
<sup>356</sup> Venier, O.; Pascal, C.; Braun, A.; Namane, C.; Mougnot, P.; Crespin, O.; Pacquet, F.; Mougnot, C.; Monseau, C.; Onofri, B.; Dadji-Faihun, R.; Leger, C.; Ben-Hassine, M.; Van-Pham, T.; Ragot, J. L.; Philippo, C.; Farjot, G.; Noah, L.; Maniani, K.; Boutarfa, A.; Nicolai, E.; Guillot, E.; Pruniaux, M. P.; Güssregen, S.; Engel, C.; Coutant, A. L.; de Miguel, B.; Castro, A. *Bioorg. Med. Chem. Lett.* **2013**, *23*, 2414-2421.

<sup>357</sup> Webster, S. P.; Ward, P.; Binnie, M.; Craigie, E.; McConnell, K. M. M.; Sooy, K.; Vinter, A.; Seckl, J. R.; Walker, B. R. *Bioorg. Med. Chem. Lett.* **2007**, *17*, 2838-2843.

<sup>358</sup> Okazaki, S.; Takahashi, T.; Iwamura, T.; Nakaki, J.; Sekiya, Y.; Yagi, M.; Kumagai, H.; Sato, M.; Sakami, S.; Nitta, A.; Kawai, K. *J. Pharmacol. Exp. Ther.* **2014**, *351*, 181-189.

<sup>359</sup> Ryu, J. H.; Kim, S.; Lee, J. A.; Han, H. Y.; Son, H. J.; Lee, H. J.; Kim, Y. H.; Kim, J.-S.; Park, H. *Bioorg. Med. Chem. Lett.* **2015**, *15*, 1679-1683.

<sup>360</sup> Kim, Y. H.; Kang, S. K.; Lee, G. Bin; Lee, K. M.; Kumar, J. A.; Kim, K. Y.; Rhee, S. D.; Joo, J.; Bae, M. A.; Lee, W. K.; Ahn, J. H. *Med. Chem. Commun.* **2015**, *6*, 1360-1369.



**Fig. 51.** Selection of adamantane-based inhibitors of 11β-HSD1 in development.

The preponderance of the adamantane ring in many 11β-HSD1 inhibitors suggests that this precious polycycle forms tight-binding interactions within the hydrophobic binding pockets. Regardless of the good match that the adamantane moiety exerts in the binding site of the enzyme, the high lipophilicity furnished by the adamantane leads to potential solubility and metabolic stability problems, as seen in the introductory part of the present thesis. The initial pharmacological results imply that increasing the hydrophobicity of the inhibitors generally entails an improvement of 11β-HSD1 inhibitory potency, but this progression is often counterbalanced by a poor performance in the PD assay. With the goal of improving PK and PD profiles, academic and industrial research groups have carried



out different approaches. On one hand, the introduction of polar groups at key positions, such as amides, sulphonamides and hydroxyl groups, with diverse orientations on the ring stabilize the hydrophobic ring from metabolism and increase water solubility. On the other hand, replacement of the adamantane group by other scaffolds, such as bicyclo[2.2.2]octane, provides candidates that possess excellent PK and PD profiles in target tissues. Merck followed this strategy in a development programme with success, leading to MK-0736 (see table 12).<sup>361,362,363</sup> These findings suggest that it is possible to optimize the lipophilic adamantane moiety effectively for clinical administration targeting the promising 11 $\beta$ -HSD1 enzyme.

---

<sup>361</sup> Waddell, S. T.; Balkovec, J. M.; Kevin, N. J.; Gu, X. Preparation of triazoles derivatives as inhibitors of 11 $\beta$ -hydroxysteroid dehydrogenase-1. WO 2007047625.

<sup>362</sup> Wang, H.; Robl, J. A.; Hamann, L. G.; Simpkins, L. M.; Golla, R.; Li, X.; Seethala, R.; Zvyaga, T.; Gordon, D. A.; Robl, J. A.; Li, J. L. *Bioorg. Med. Chem. Lett.* **2011**, *21*, 4146-4149.

<sup>363</sup> Bauman, D. R.; Whitehead, A.; Contino, L. C.; Cui, J.; Garcia-Calvo, M.; Gu, X.; Kevin, N.; Ma, X.; Pai, L.; Shah, K.; Shen, X.; Stribling, S.; Zokian, H. J.; Metzger, J.; Shevell, D. E.; Waddell, S. T. *Bioorg. Med. Chem. Lett.* **2013**, *23*, 3650-3653.

# Objetives

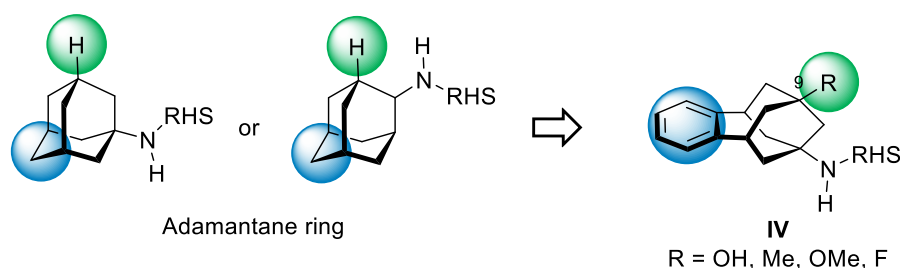


At the time of the present dissertation, no  $11\beta$ -HSD1 inhibitor had reached the market, what illustrates the difficultness of developing drug candidates with optimal PK and PD profiles and the need for discovering new active pharmaceutical ingredients (API) that may overcome these issues.

From the available data drawn from the X-ray crystal structures of different inhibitors bound to the  $11\beta$ -HSD1 catalytic site, a general trend can be deduced. For the most part, two hydrophobic moieties are linked by an H-bond acceptor, which fill the buried hydrophobic pockets and interact with the key residues of the catalytic site, respectively. These crucial pieces constitute the pharmacophore of the  $11\beta$ -HSD1 inhibitors. From this observation, we hypothesized that different scaffolds can be placed as hydrophobic moieties instead of the adamantane group in order to achieve structures with more appropriate profiles.

Taking advantage of the extended expertise of our research group in the synthesis of polycyclic scaffolds, we started a new project related to the discovery of novel  $11\beta$ -HSD1 inhibitors bearing adamantane-like scaffolds as hydrophobic counterparts. We hypothesized that the substitution of the adamantane moiety for other polycyclic cage structures may offer compounds with improved PK and PD profiles whilst keeping good binding affinity to the target. Under these premises, we determined the following goals of this chapter:

1. Synthesis and pharmacological evaluation of a family of compounds with the general structure of the benzo-homoadamantane **IV** (Fig. 52). This scaffold, already seen in the previous chapter of the present thesis, embodies a phenyl ring in its structure and lets the introduction of different substituents at the C-9 position, which may alter the binding mode along with PK properties.



**Fig. 52.** Replacement of the adamantane group by a scaffold with general structure **IV**. RHS: right-hand side.

2. Synthesis and pharmacological evaluation of a family of compounds with general structure **V** (Fig. 53). This structure provides a larger lipophilic scaffold than the adamantane group. Derived from the synthetic route, both dienes and alkanes can be prepared. We aimed to determine the effect of an expanded adamantane analogue in the binding affinity of the new compounds.

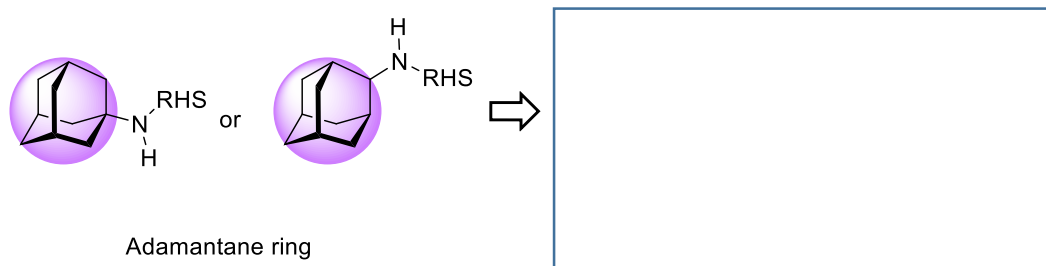


Fig. 53. Incorporation of  $V$  as surrogates of the adamantane moiety.

In order to test our polycycles we designed the compounds based on the literature. In this manner, we chose as the right-hand side of the molecules a diversity of already proven subunits stemming from the work of a few pharmaceutical companies (Fig. 54).<sup>350,351,352,355</sup>

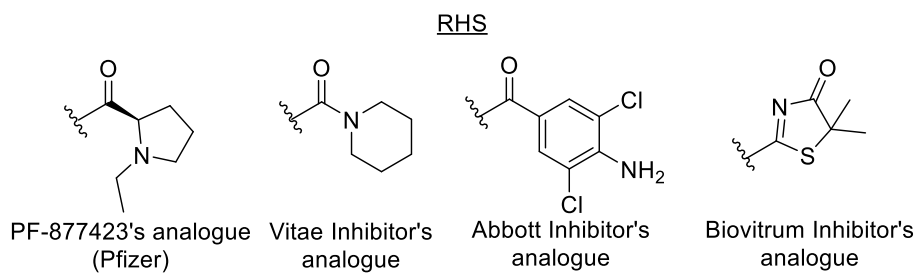


Fig. 54. Right-hand sides (RHS) applied in the synthesis of the new compounds.

## **Results & Discussion**



## 1. Application of the benzopolycyclic scaffold as an adamantane analogue for 11 $\beta$ -HSD1 inhibition

### 1.1 Synthesis of the C-9 substituted 6,7,8,9,10,11-hexahydro-5,7:9,11-dimethano-5H-benzocyclononen-7-yl derivatives

For the design of the new compounds, we have adopted a hybrid strategy whereby the inhibitor is partitioned into a hydrophobic adamantane-like unit (left-hand side of the molecule) and a cyclic structure (right-hand side), linked by an amido- or urea-like unit (Fig. 55). The adamantane moiety has been replaced by the benzo-homoadamantane polycycle **IV**. This strategy obeys a twofold purpose. First, the introduction of the phenyl ring, together with polar and non-polar groups attached to the polycycle (OH, OMe, F, Me) is intended to modify the PK properties of the compounds, and particularly the metabolism at specific ring positions. Second, the incorporation of the phenyl moiety is expected to establish new binding interactions in the hydrophobic cage. In addition, this insertion involves a size expansion of the carbocyclic structure. At this point, it is worth noting that the active site of the enzyme seems to be wide enough as to accommodate this polycycle, as suggested upon inspection of the available X-ray structures. On the other hand, a series of carbocyclic and heterocyclic subunits previously tested as 11 $\beta$ -HSD1 inhibitors are integrated into the final polar moiety as the RHS. Finally, the amido- or urea-like unit present in the linker should enable the formation of key hydrogen bonds at the binding site.

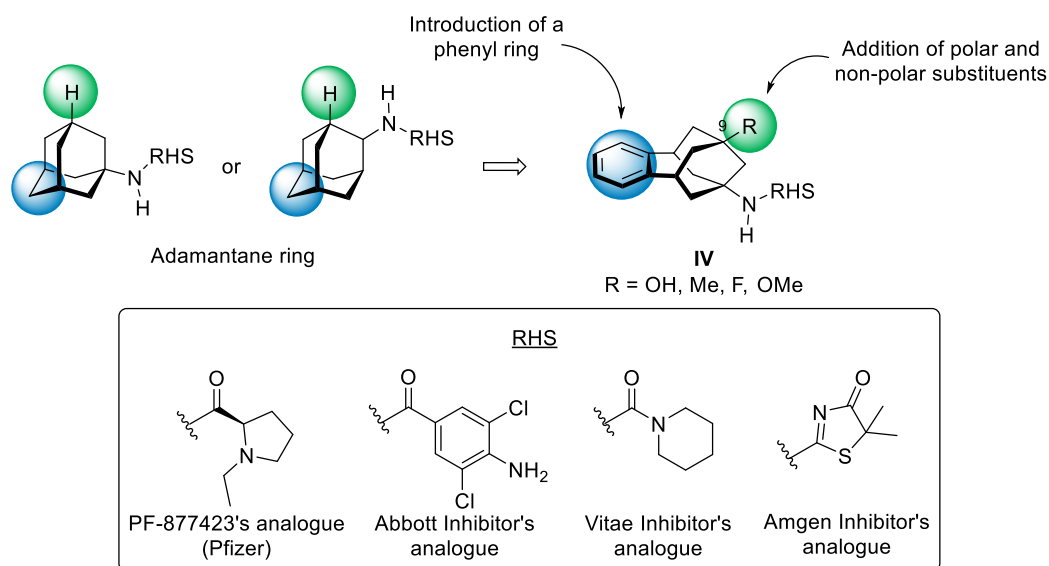


Fig. 55. Design of the new 11 $\beta$ -HSD1 inhibitors with general structure **IV**.

The selection of the different moieties as the RHS was in accordance to a balance between the ease on their synthesis and the reasonable inhibitory activity.<sup>350,351,352,355</sup> Figure 56 includes the IC<sub>50</sub> values of the parent inhibitors. Worth to consider is the fact that the IC<sub>50</sub> of Vitae's inhibitor was determined in an enzymatic assay, which may differ from the value obtained by a cellular assay (not available). Thus, a direct comparison cannot be made



with the rest of the IC<sub>50</sub> values, but it provides some indications of how potent is the compound.

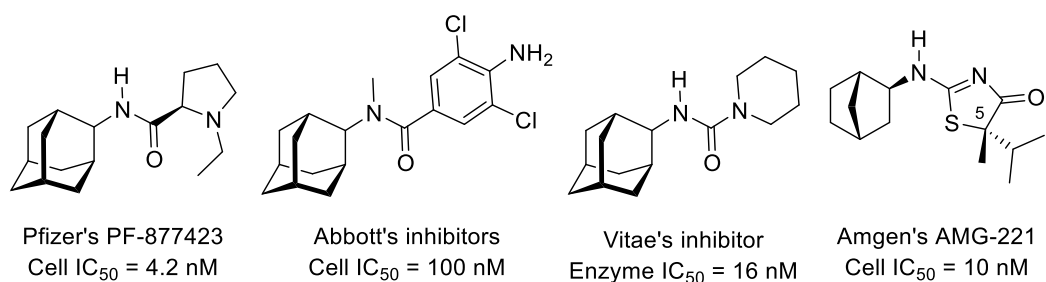


Fig. 56. Biological activity of the 11 $\beta$ -HSD1 inhibitors taken as templates.

Moreover, we decided to reduce the complexity of the Amgen's analogue by placing two identical substituents in C-5 position, i.e. two methyl groups as shown in figure 55. In this manner, any stereochemistry derived from the substitution pattern is avoided.

Taking advantage of the C-9-substitution patterns obtained from the previous chapter of the thesis, we sought to explore the different combinations derived from the substitution at the C-9 position of the adamantane-like polycycle and each one of the selected polar units as RHS. First, we decided to use four of our amines as starting points (Fig. 57). Amine **23** was not included due to its low-yielding synthetic procedure.

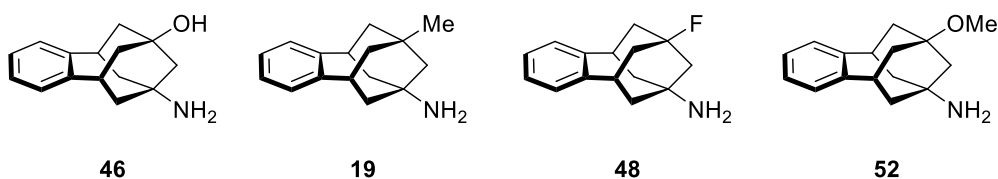
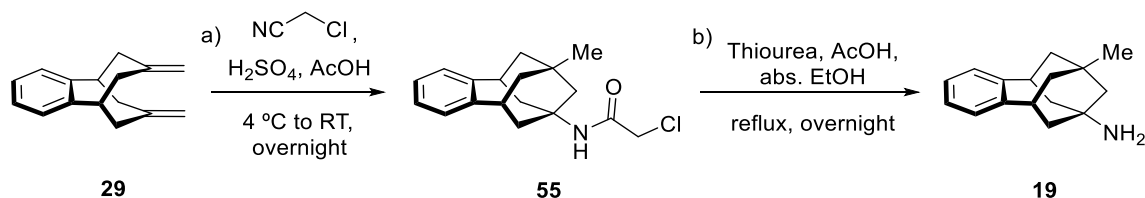


Fig. 57. Amines **46**, **19**, **48** and **52** used as left-hand side of the putative new 11 $\beta$ -HSD1 inhibitors.

Amine **19** preparation was similar to the synthesis of hydroxyl derivative **46**. Likewise, Prins-Ritter transannular cyclization of diene **29** with chloroacetonitrile and sulphuric acid in neat glacial acetic acid, followed by thiourea-mediated deprotection of the chloroacetamide group gave the desired intermediate, amine **19**, in 56% yield (two steps) (Scheme 25).

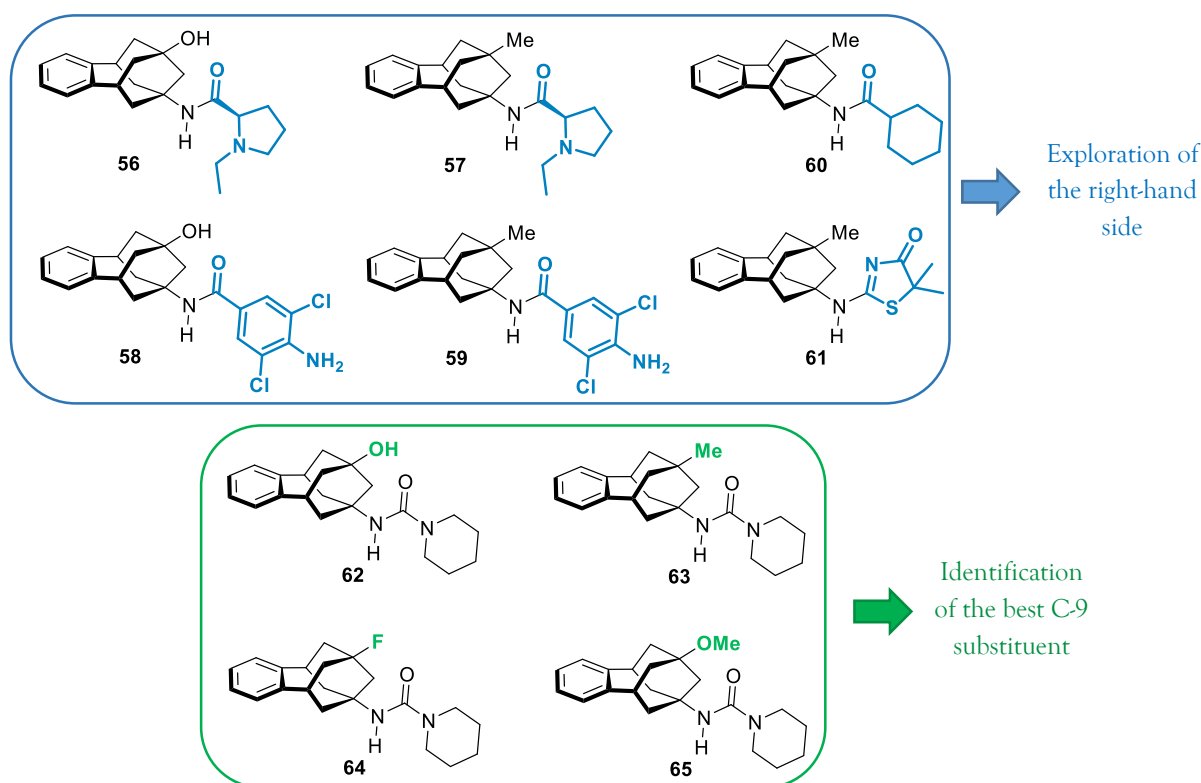


Scheme 25. Prins-Ritter transannular cyclization of **29**, followed by thiourea-mediated deprotection of chloroacetamide.

To optimize the synthesis, we applied the following strategy to detect the perfect match between the C-9 substituent and the polar unit:

- Explore the effects on the C-9 substitution, essentially with polar and non-polar groups. We chose piperidine-1-carboxamide as the right-hand side of the molecule due to the ease of preparation of the final compounds.
- Identify the polar unit from figure 55 that performs best with the scaffold at issue. To do so, we used amines **46** and **19** featuring a hydroxyl and a methyl group, respectively, so as to have one polar and one non-polar substituent to compare.

With this in mind, the compounds that needed to be synthesized are depicted in figure 58.



**Fig. 58.** Compounds to be made to assess the effect of the different substitutions in benzo-homoadamantane as a scaffold for 11 $\beta$ -HSD1 inhibitors.

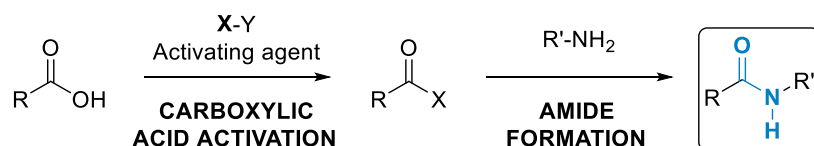
Compound **60**, which contains a cyclohexyl amide attached to the polycyclic structure, was also included in the list of polar units. We intended to analyse whether the replacement of a urea by an amide, a common functional group in most 11 $\beta$ -HSD1 inhibitors, might affect the inhibitory activity. This structure was previously tested by our group in a different series of compounds.<sup>364</sup>

The syntheses will be organized according to the different functionalities of the core moiety.

<sup>364</sup> Leiva, R.; Seira, C.; McBride, A.; Binnie, M.; Luque, F. J.; Bidon-Chanal, A.; Webster, S. P.; Vázquez, S. *Bioorg. Med. Chem. Lett.* **2015**, *25*, 4250-4253.

## 1.1.1 Preparation of amide compounds

Chemical reactions for the formation of amide bonds are among the most executed transformations in organic and medicinal chemistry.<sup>365</sup> The current methods for amide formation are remarkably general but at the same time widely regarded as expensive and inelegant.<sup>366</sup> Acylation of amines with activated carboxylic acids is the most frequent reaction performed in the synthesis of pharmaceuticals and in peptide chemistry, representing more than 70% of all acylations and related processes executed in medicinal chemistry (Scheme 26).<sup>367,368</sup>



**Scheme 26.** Carboxylic acid activation for subsequent amine attack and final amide bond formation.

Based on the success and broad use of the activating or coupling agents, the titled amides were prepared following two different procedures. In these cases, the acylating agent is generated *in situ* from the acid in presence of the amine, by the addition of a coupling agent. The first approach implied the use of carbodiimides as coupling agents, which were the first activating reagents to be used in synthesis.<sup>369</sup> Different carbodiimides are currently employed, such as dicyclohexyl carbodiimide (DCC), diisopropyl carbodiimide (DIC) and 1-ethyl-3-(3'-dimethylaminopropyl)carbodiimide (EDC), each of one showing its own pros and cons. As for the reaction mechanism, the first step of the process involves the attack of the carboxylic acid to the carbodiimide to form O-acylisourea **66**. This intermediate can yield a number of different products, depending on which species reacts with it: i) formation of the desired amide **67** *via* coupling with the amine; ii) formation of anhydride **68**, which can lead to amide **67** after attack of the amine (it requires two equivalent of the carboxylic acid); and iii) generation of *N*-acylurea **69** by rearrangement of the common intermediate. To exemplify the mechanism of this coupling it is represented in scheme 27 using EDC. This carbodiimide was selected as the coupling agent due to its high water solubility, facilitating its removal by aqueous washes.

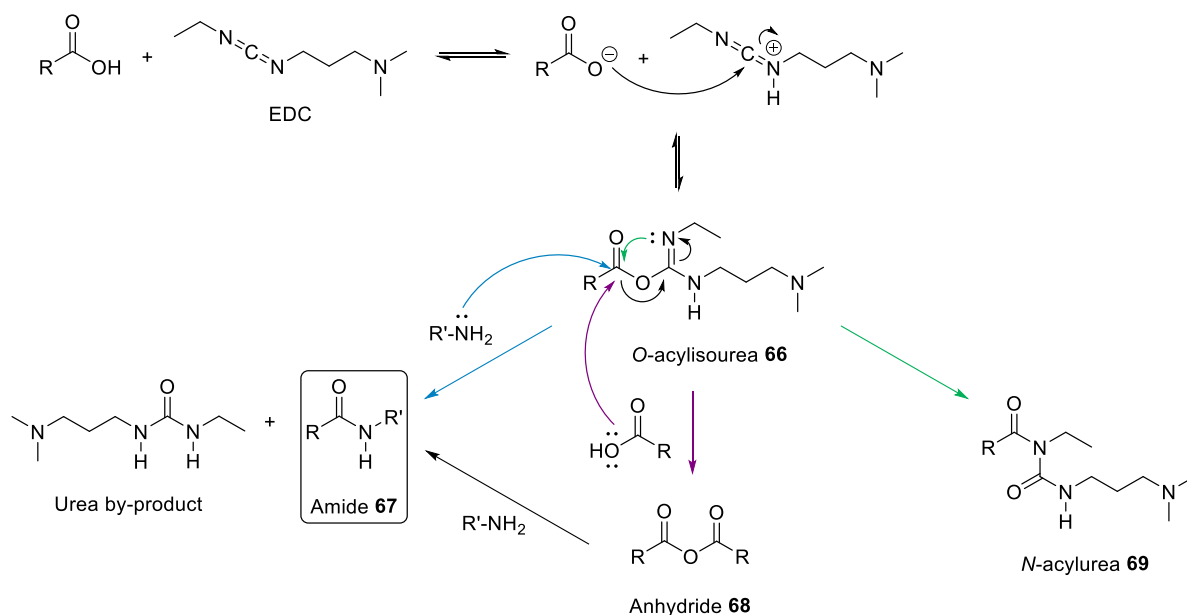
<sup>365</sup> Roughley, S. D.; Jordan, A. M. *J. Med. Chem.* **2011**, *54*, 3451-3479.

<sup>366</sup> Pattabiraman, V. R.; Bode, J. W. *Nature* **2011**, *480*, 471-479.

<sup>367</sup> Montalbetti, C. A. G. N.; Falque, V. *Tetrahedron* **2005**, *61*, 10827-10852.

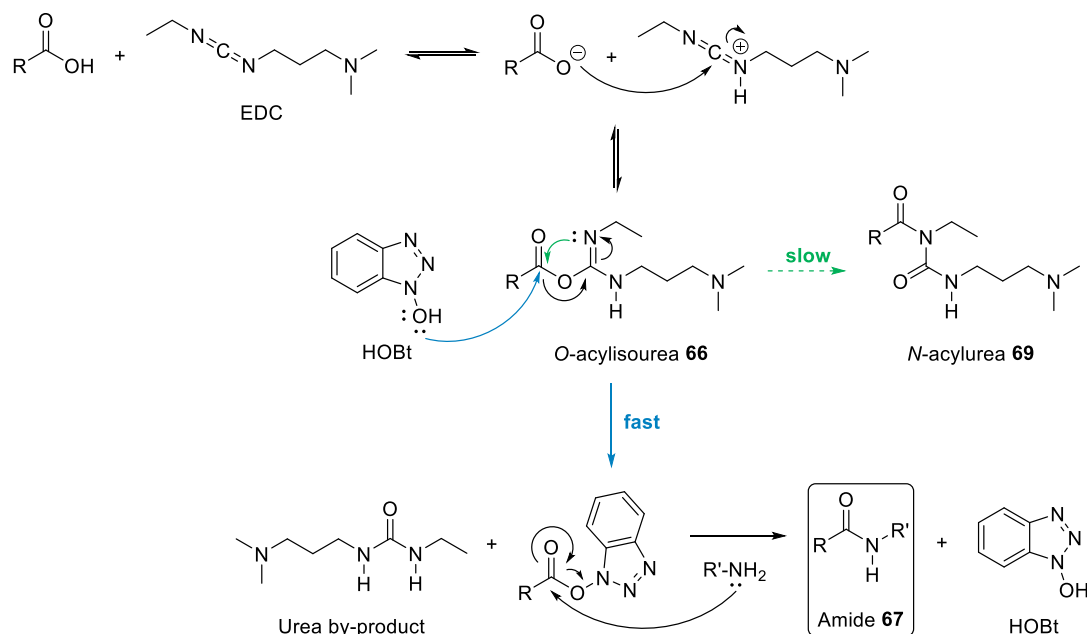
<sup>368</sup> Valeur, E.; Bradley, M. *Chem. Soc. Rev.* **2009**, *38*, 606-631.

<sup>369</sup> Sheehan, J. C.; Hess, G. P. *J. Am. Chem. Soc.* **1955**, *77*, 1067-1068.



**Scheme 27.** One-pot coupling of carboxylic acids with amines using EDC.

Inasmuch as part of the acid partner is lost with the formation of the *N*-acylurea **69**, it was reasoned that the addition of a selected nucleophile that reacted faster than the competing acyl transfer, generating an intermediate still active enough to couple with the amine might avoid this side reaction. Hydroxybenzotriazole or HOBT is one of those nucleophiles.<sup>370</sup> Hence, the established procedures consist in the addition of EDC as coupling agent, HOBT as additive, as shown in scheme 28.



**Scheme 28.** Avoidance of the formation of *N*-acylurea **69** by addition of HOBT.

<sup>370</sup> Chan, L. C.; Cox, B. G. *J. Org. Chem.* **2007**, *72*, 8863-8869.

As the evolution in the coupling agents progressed, novel activators appeared with the purpose of preventing the use of two reagent species and increasing the reactivity. Onium salts based upon 7-aza-1-hydroxybenzotriazole (HOAt) have replaced the predominant carbodiimide and HOBT technique.<sup>371,372</sup> Among them, 1-[bis(dimethylamino)methylene]-1*H*-1,2,3-triazolo[4,5-*b*]pyridinium 3-oxid hexafluorophosphate (HATU) has become one of the most popular coupling agents. When first reported, HATU was described as an uronium salt (*O*-isomer), but X-ray crystal structure revealed that the preferred state is as guanidinium salt (*N*-isomer) (Fig. 59).<sup>373</sup> However, there is an equilibrium between the two forms in solution.

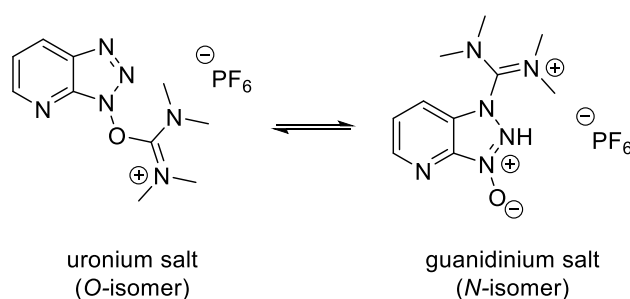


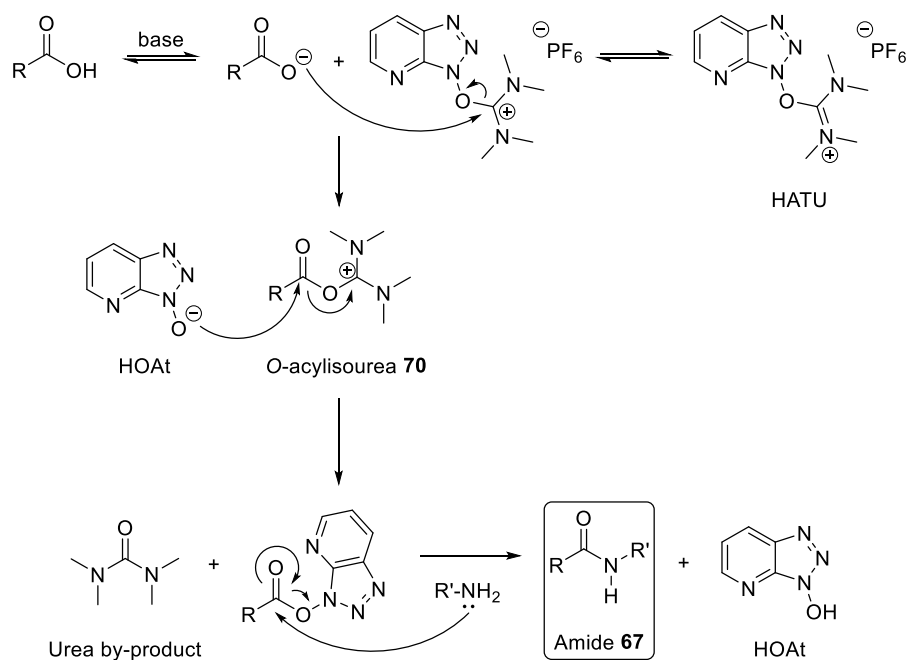
Fig. 59. Different isomers of HATU, the *N*-isomer being the predominant form in the crystal structure.

The coupling mechanism entails first the generation of both an activated *O*-acylisourea **70** and a HOAt unit. The negatively charged oxygen atom of this same benzotriazole reacts with the activated acid in a similar manner to the previous mechanism. Elimination of tetramethylurea, *prior* to the coupling of the amine to the highly reactive ester-like species, affords the desired amide compound (Scheme 29). The generation of the urea by-product is the driving force of the reaction.

<sup>371</sup> Carpino, L. A. *J. Am. Chem. Soc.* **1993**, *115*, 4397-4398.

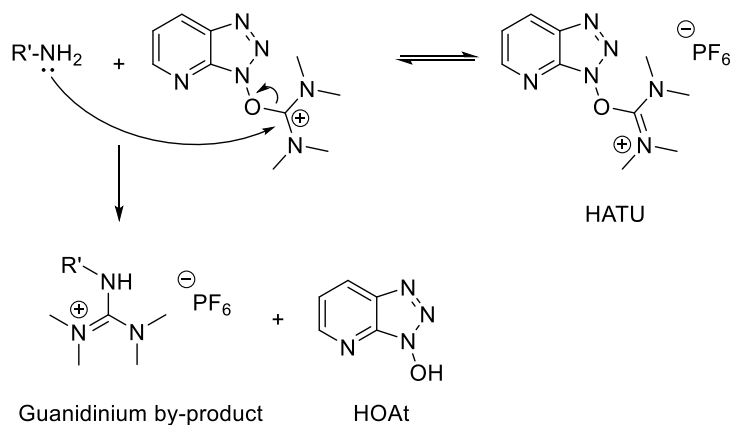
<sup>372</sup> Albericio, F.; Bofill, J. M. El-Faham, A.; Kates, S. A. *J. Org. Chem.* **1998**, *63*, 9678-9683.

<sup>373</sup> Carpino, L. A.; Imazumi, H.; El-Faham, A.; Ferrer, F. J.; Zhang, C.; Lee, Y.; Foxman, B. M.; Henklein, P.; Hanay, C.; Mügge, C.; Wenschuh, H.; Klose, J.; Beyermann, M.; Bienert, M. *Angew. Chem. Int. Ed.* **2002**, *41*, 441-445.



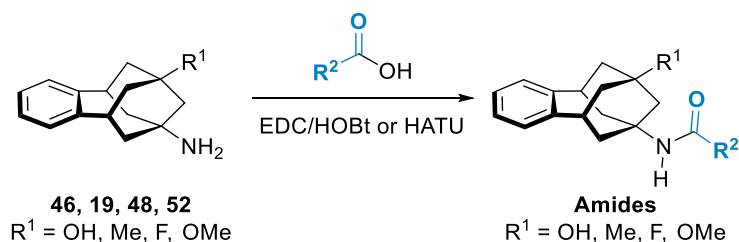
**Scheme 29.** Activation process of carboxylic acids using uronium/guanidinium type coupling agents.

Despite the high efficiency of HATU, especially in difficult sterically hindered couplings, the amine can react with the coupling agent to give a guanidinium by-product as a side reaction (Scheme 30).



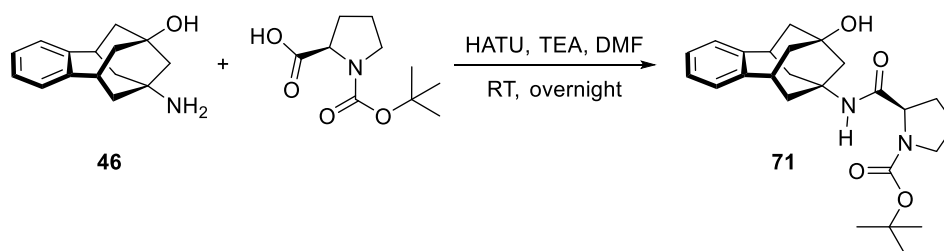
**Scheme 30.** Possible guanidinium side-product when using HATU.

Having introduced these two approaches, i.e. the use of EDC/HOBt or HATU as coupling agents, starting from amines **46**, **19**, **48** and **52**, the synthetic procedure towards the obtaining of final amides is outlined in scheme 31.



**Scheme 31.** Amide coupling of amines **46**, **19**, **48** and **52** and selected carboxylic acids applied in this thesis.

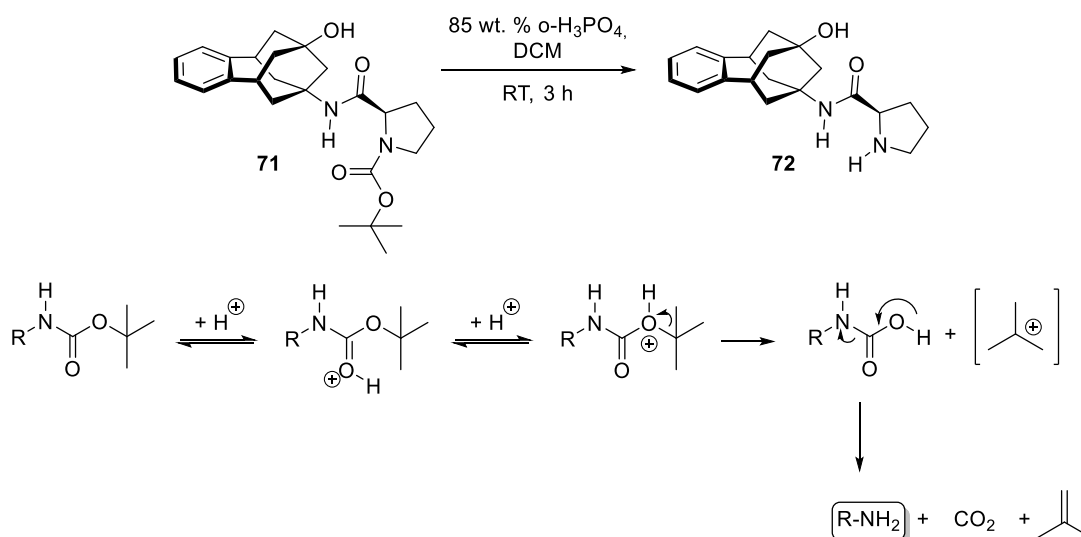
The first attempt was using HATU as the activating reagent, because of the known high efficiency of this agent in difficult sterically hindered couplings. Beginning with the preparation of proline derivative **56**, the synthetic route started with the amide coupling between amine **46** and the commercially available *N*-Boc-D-proline (Scheme 32). A slightly excess of the amine was used over the non-natural amino acid, in order to prevent the guanidinium side reaction, as well as for HATU and the base. The reaction afforded the desired Boc-protected pyrrolidine **71** in 50% yield after purification by column chromatography.



**Scheme 32.** Coupling of amine **46** with *N*-Boc-D-proline gave amide **71**.

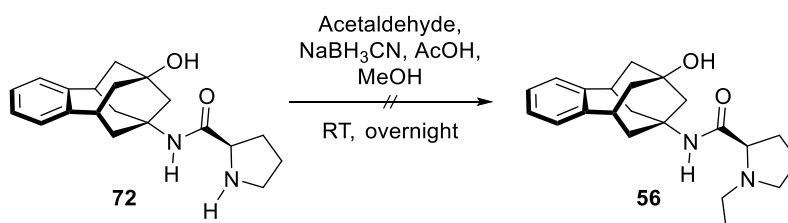
The synthetic sequence towards amide **56** continued with the deprotection of the *t*-butyl carbamate group following the procedure reported by Li *et al.*<sup>374</sup> The method consisted in the use of aqueous phosphoric acid, which is an acid whose conjugate base is non-nucleophilic. This hampers the dehydration of the hydroxyl group at the tertiary position and subsequent introduction of the conjugate base. After neutralization of the media, deprotected pyrrolidine **72** was secured in 87% yield as a free base (Scheme 33). These two simple steps furnished the first compound for pharmacological testing that was also central to access the next final compound.

<sup>374</sup> Li, B.; Bemish, R.; Buzon, R. A.; Chiu, C. K. F.; Colgan, S. T.; Kissel, W.; Le, T.; Leeman, K. R.; Newell, L.; Roth, J. *Tetrahedron Lett.* **2003**, *44*, 8113-8115.



**Scheme 33.** Deprotection of boc-protected pyrrolidine **71** to afford free amine **72**. The reaction entails the formation of isobutene and carbon dioxide.

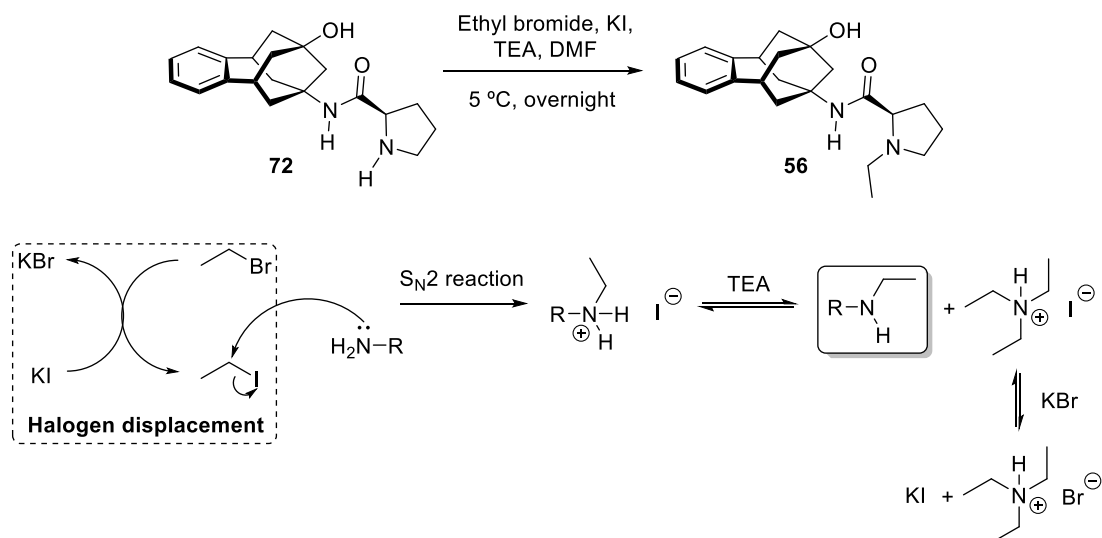
With amine **72** in hand, we proceeded to the reductive alkylation following our previously mentioned methodology. We treated the free amine with acetaldehyde and sodium cyanoborohydride under the same conditions as scheme 19 (NMDA chapter), but regrettably no alkylated amine was observed (Scheme 34), and the starting material was fully recovered.



**Scheme 34.** Attempt of reductive alkylation of amine **72** with acetaldehyde and  $\text{NaBH}_3\text{CN}$ .

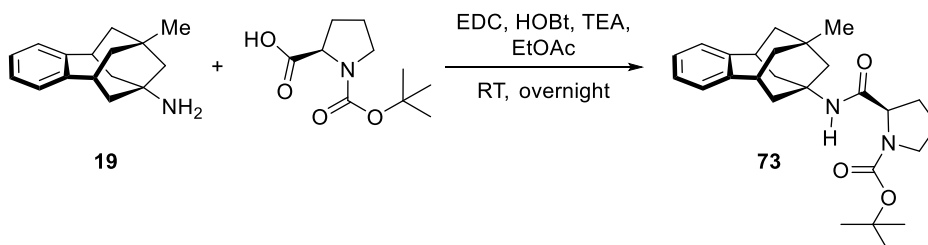
Unhappy with the result, we applied the procedure described in the literature for the preparation of PF-877423 derivative, which involved the *N*-alkylation with ethyl bromide in the presence of a base and potassium iodide. The latter was used in catalytic amounts in order to displace the bromide in an  $\text{S}_{\text{N}}2$  fashion and promote the attack of the amine to the alkylating agent, transformation known as Finkelstein reaction (Scheme 35). Pleasingly, amide **56** was obtained in 72% yield without need of column chromatography.





**Scheme 35.** N-alkylation of amine **72** with ethyl iodide after halogen displacement.

Once hydroxyl derivative **56** was prepared, we next moved to the synthesis of its C-9 methylated analogue **57**. Despite the avoidance of extra additives when using HATU as coupling agent, the moderate yield obtained in the preparation of **71** (50% yield) showed a partial success of the reaction. In consequence, we essayed the peptide-like coupling using EDC and HOBT as activating agents. Based on standard protocols,<sup>375,376,377</sup> we subjected amine **19** to a coupling process with 1.5 equivalents of both agents, along with TEA as a base in ethyl acetate (Scheme 36). After several aqueous washes, pure amide **73** was obtained in 84% yield without any purification needed.



**Scheme 36.** Formation of an amide bond with EDC and HOBT.

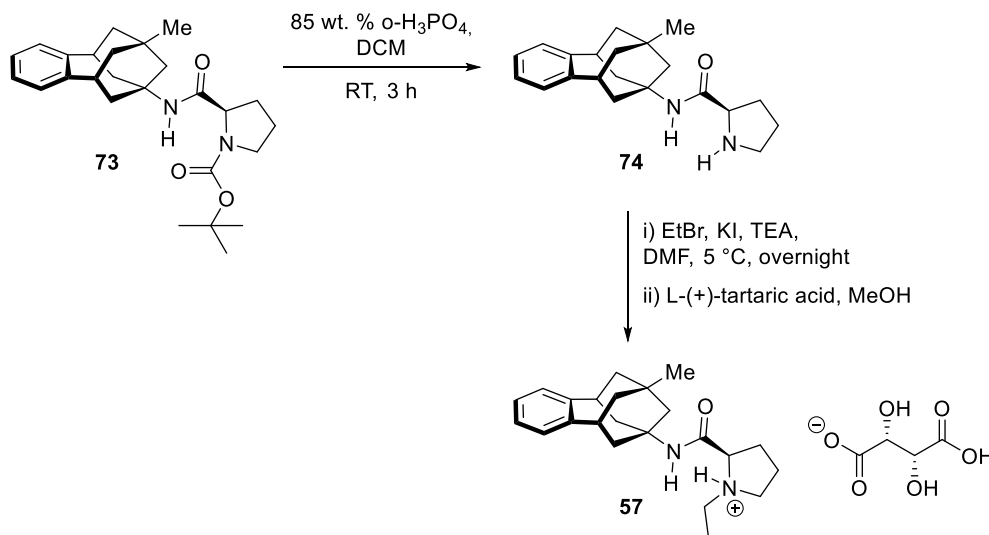
Amide **73** was in turn submitted to Boc-deprotection with 85% aqueous ortho-phosphoric acid to provide free amine **74** in quantitative yield. Primary amine **74** was purified and fully characterized for pharmacological evaluation. Last, N-alkylation with

<sup>375</sup> Dragovich, P. S.; Prins, T. J.; Zhou, R.; Johnson, T. O.; Hua, Y.; Luu, H. T.; Sakata, S. K.; Brown, E. L.; Maldonado, F. C.; Tuntland, T.; Lee, C. A.; Fuhrman, S. A.; Zalman, L. S.; Patick, A. K.; Matthews, D. A.; Wu, E. Y.; Guo, M.; Borer, B. C.; Nayyar, N. K.; Moran, T.; Chen, L.; Rejto, P. A.; Rose, P. W.; Guzman, M. C.; Doval Santos, E. Z.; Lee, S.; McGee, K.; Mohajeri, M.; Liese, A.; Tao, J.; Kosa, M. B.; Liu, B.; Batugo, M. R.; Gleeson, J. P. R.; Wu, Z. P.; Liu, J.; Meador, J. W.; Ferre, R. A. *J. Med. Chem.* **2003**, *46*, 4572-4585.

<sup>376</sup> Nikitenko, A.; Alimardanov, A.; Afragola, J.; Schmid, J.; Kristofova, L.; Evrard, D.; Hatzenbuehler, N. T.; Marathias, V.; Stack, G.; Lenicek, S.; Potski, J. *Org. Process Res. Dev.* **2009**, *13*, 91-97.

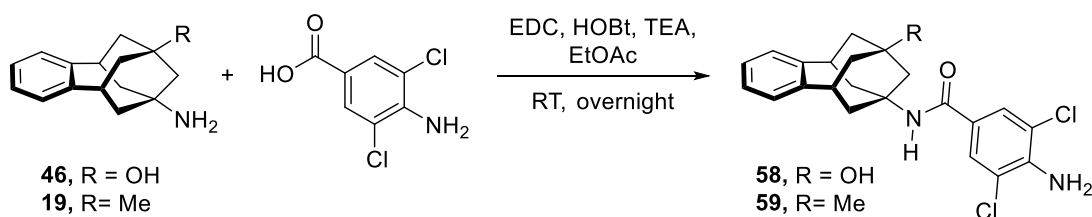
<sup>377</sup> Sasaki, N. A.; Garcia-Álvarez, M. C.; Wang, Q.; Ermolenko, L.; Franck, G.; Nhiri, N.; Martin, M. T.; Audic, N.; Potier, P. *Bioorg. Med. Chem.* **2009**, *17*, 2310-2320.

ethyl bromide, KI and TEA afforded final compound **57** in moderate yield (44%), which was isolated as the L-(+)-tartrate salt after column chromatography (Scheme 37). Previous attempts to precipitate the resulting amine as its hydrochloride salt yielded a hygroscopic solid, which did not meet the required physical properties for pharmacological evaluation.



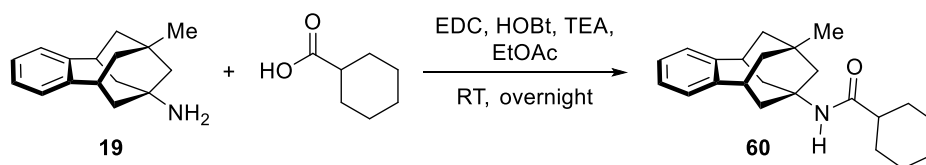
**Scheme 37.** Boc-deprotection and N-alkylation reaction to provide **57•tartrate**.

In line with our objectives, aryl amides **58** and **59** were synthesized according to the best conditions obtained for the amide coupling, that is the combination of EDC and HOBT (84% *vs* 50% yield with HATU). Therefore, a slightly excess of amines **46** and **19** were added to a mixture of commercially available 4-amino-3,5-dichlorobenzoic acid, EDC, HOBT and TEA in ethyl acetate to produce the corresponding final amides **58** and **59** in 95% and 53% yield, respectively (Scheme 38). The significant differences in the yields indicate that the substitution on the C-9 position may affect directly the reactivity of the amine group, or indirectly by changes in solubility.



**Scheme 38.** Amide coupling between amines **46** and **19** with 4-amino-3,5-dichlorobenzoic acid.

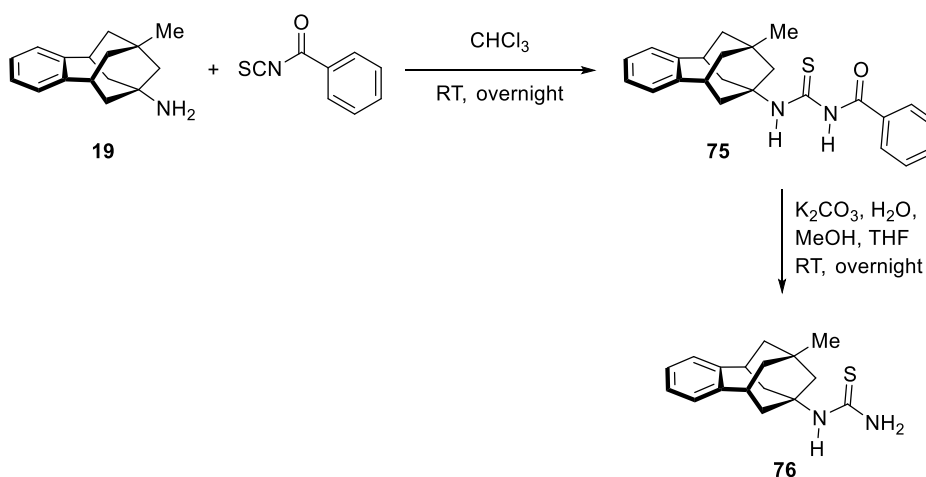
The synthesis of the last amide **60** was performed by the same protocol, in this case with cyclohexanecarboxylic acid. Satisfyingly, reaction with amine **19** furnished the corresponding final amide **60** in excellent yield (Scheme 39).



**Scheme 39.** Reaction of amine **19** with cyclohexanecarboxylic acid under amide coupling conditions provided **60** in 96% yield.

### 1.1.2 Synthesis of the thiazolone scaffold

The 2-amino-1,3-thiazol-4(5H)-one skeleton was built following the described procedures.<sup>378,379</sup> Starting from amine **19**, the intermediate thiourea **76** was prepared *via* a two-step protocol. First, treatment with benzoyl isothiocyanate provided benzamide **75** that was subsequently hydrolysed under basic conditions to give **76** in 52% overall yield (Scheme 40).

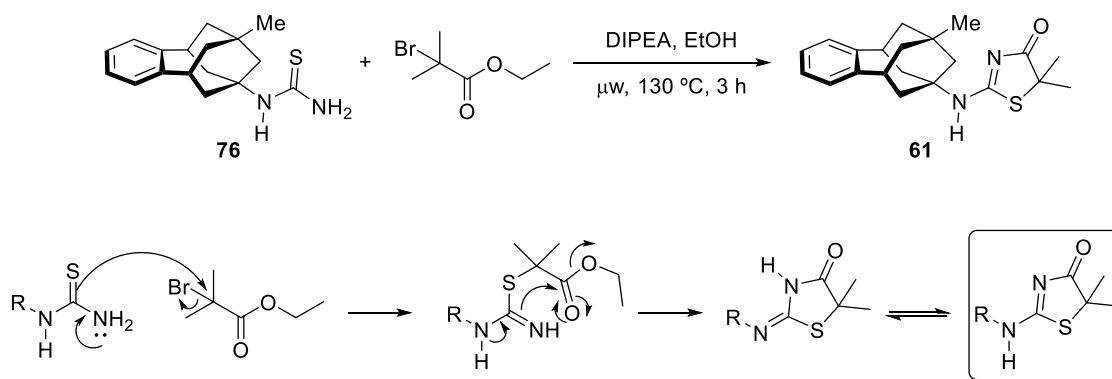


**Scheme 40.** Transformation of amine **19** to thiourea **76** after reaction with benzoyl isothiocyanate and later basic hydrolysis.

The construction of the thiazolone ring system was accomplished by a substitution/cyclization reaction between thiourea **76** and ethyl 2-bromoisobutyrate in the presence of *N,N*-diisopropylethylamine (DIPEA) under microwave irradiation (Scheme 41). Researchers from Biovitrum found that this process required long reaction times (3-8 days) heating to 90-105 °C by conventional methods. Nevertheless, the reaction time was substantially reduced by microwave-assisted heating to 130 °C, but at the expense of lowering the yield (13%).

<sup>378</sup> Jean, D. J. S.; Yuan, C.; Bercot, E. A.; Cupples, R.; Chen, M.; Fretland, J.; Hale, C.; Hungate, R. W.; Komorowski, R.; Veniant, M.; Wang, M.; Zhang, X.; Fotsch, C. *J. Med. Chem.* **2007**, *50*, 429-432.

<sup>379</sup> Johansson, L.; Fotsch, C.; Bartberger, M. D.; Castro, V. M.; Chen, M.; Emery, M.; Gustafsson, S.; Hale, C.; Hickman, D.; Homan, E.; Jordan, S. R.; Komorowski, R.; Li, A.; McRae, K.; Moniz, G.; Matsumoto, G.; Orihuela, C.; Palm, G.; Veniant, M.; Wang, M.; Williams, M.; Zhang, J. *J. Med. Chem.* **2008**, *51*, 2933-2943.



**Scheme 41.** Substitution/cyclization sequence to assemble the thiazolone ring with a thiourea and an  $\alpha$ -bromoester. For the sake of clarity, the proton exchanges have been omitted.

### 1.1.3 Urea group formation

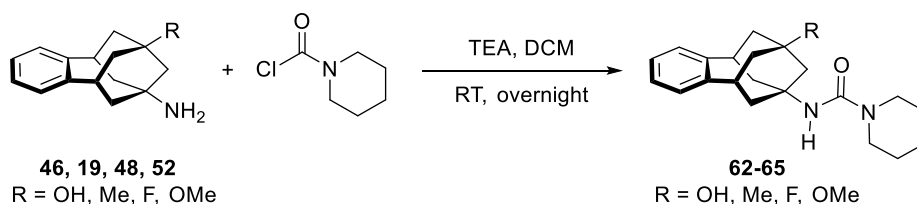
Different approaches have been described for the synthesis of the urea moiety of many 11 $\beta$ -HSD1 inhibitors, from direct coupling of amines with isocyanates to the use of amine-activating agents such as triphosgene or carbonyldiimidazole (CDI).<sup>380,381</sup> Some of them will be reviewed in the last chapter of the thesis.

Alternatively, another method to install a urea functionality concerns the reaction of an amine with a carbamoyl chloride in the presence of a base, in a similar way than with an isocyanate.<sup>382</sup> Since we aimed to prepare a urea embodied in a piperidine ring, we pursued its synthesis following this last approach, where amines **46**, **19**, **48** and **52** were reacted with 1-piperidinecarbonyl chloride in TEA to afford the corresponding final ureas **62-65** in low to medium yields (Scheme 42). In all cases, the final compounds were purified by column chromatography and/or crystallization in order to eliminate the excess of the starting material. The reaction mechanism is simple, and entails the addition of the amine to the carbonyl, with the subsequent elimination of the chloride, which is trapped by the base as the hydrochloride salt.

<sup>380</sup> Tice, C. M.; Zhao, W.; Xu, Z.; Cacatian, S. T.; Simpson, R. D.; Ye, Y.J.; Singh, S. B.; McKeever, B. M.; Lindblom, P.; Guo, J.; Krosky, P. M.; Kruk, B. A.; Berbaum, J.; Harrison, R. K.; Johnson, J. J.; Bukhtiyarov, Y.; Panemangalore, R.; Scott, B. B.; Zhao, Y.; Bruno, J. G.; Zhuang, L.; McGeehan, G. M.; He, W.; Claremon, D. A. *Bioorg. Med. Chem. Lett.* **2010**, *20*, 881-886.

<sup>381</sup> Claremont, D. A.; Zhuang, L.; Ye, Y.; Singh, S. B.; Tice, C. M. Carbamate and urea inhibitors of 11beta-hydroxysteroid dehydrogenase 1. US 2011/0112062 A1.

<sup>382</sup> Jimenez, H. N.; Ma, G.; Li, G.; Grenon, M.; Doller, D. Adamantyl amide derivatives and uses of same. WO 2011/087758 A1.



**Scheme 42.** Formation of ureas **62-65** *via* reaction of amine **46, 19, 48** and **52** with a carbamoyl chloride.

## 1.2 Pharmacological evaluation of the C-9 substituted 6,7,8,9,10,11-hexahydro-5,7:9,11-dimethano-5*H*benzocyclononen-7-yl derivatives

A preliminary *in vitro* screening was performed to evaluate if the synthesized compounds were able to inhibit human 11 $\beta$ -HSD1. The research group of Dr. Scott Webster at the University of Edinburgh (United Kingdom) carried out these assays. Screening for 11 $\beta$ -HSD1 potency was accomplished using a functional scintillation proximity assay or SPA employing microsomes isolated from human embryonic kidney cells (HEK 293) overexpressing human 11 $\beta$ -HSD1. We should clarify at this point that this procedure measures the blockade of 11 $\beta$ -HSD1 isoform exclusively.

The SPA is a well-established high throughput screening assay for the evaluation of the ligand binding affinity to 11 $\beta$ -HSD1.<sup>383,384</sup> The principle of this technique consists of microscopic beads that contain scintillant compounds. There are two types of beads: i) plastic beads such as polyvinyl toluene (PVT) beads; ii) crystalline beads such as yttrium silicate beads. In the PVT beads, the more common ones, the scintillator is diphenylanthracene.<sup>385</sup> This molecule emits light when radiolabelled cortisol (<sup>3</sup>H-cortisol) binds to specific anti-cortisol antibodies that are exposed in the surface of the bead. The generation of light comes from the activation of the scintillator through energy transfer derived from the emitted radiation after binding. The amount of light is proportional to the amount of [<sup>3</sup>H]-cortisol molecules that binds to the beads. The emitted light is quantified by a scintillation detector and converted into concentration of cortisol present in the media. Thus, the assay measures the production of [<sup>3</sup>H]-cortisol from [<sup>3</sup>H]-cortisone by the action of 11 $\beta$ -HSD1 contained in the microsomes. Figure 60 illustrates the SPA principle.

<sup>383</sup> Mundt, S.; Solly, K.; Thieringer, R.; Hermanowski-Vosatka, A. *Assay Drug Dev. Technol.* **2005**, *3*, 367-375.

<sup>384</sup> Solly, K.; Mundt, S. S.; Zokian, H. J.; Ding, G. J.; Hermanowski-vosatka, A.; Strulovici, B.; Zheng, W. *Assay Drug Dev. Technol.* **2005**, *3*, 377-384.

<sup>385</sup> PerkinElmer website. Radiometric assays and detection, SPA bead Technology.

[http://www.perkinelmer.com/Resources/TechnicalResources/ApplicationSupportKnowledgebase/radiometric/spa\\_bead.xhtml#top](http://www.perkinelmer.com/Resources/TechnicalResources/ApplicationSupportKnowledgebase/radiometric/spa_bead.xhtml#top) (accessed on 11<sup>th</sup> August 2015).

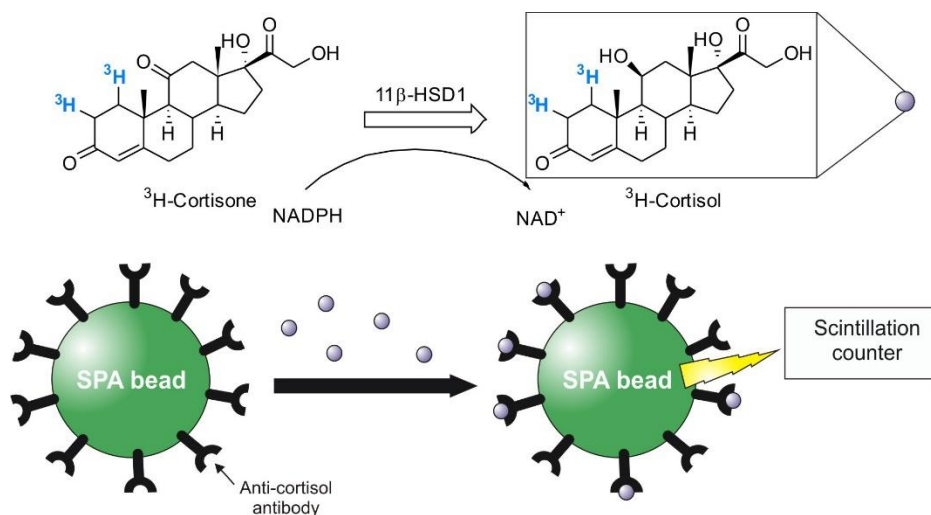
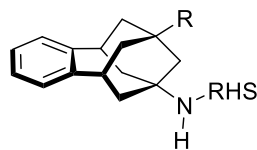


Fig. 60. Schematic representation of the SPA procedure.

When an inhibitor is added in the media in high concentrations, the production of [ $^3\text{H}$ ]-cortisol is reduced with a resultant decrease on the amount of emitted light from the SPA beads.

In order to assess the binding affinity of each inhibitor, a first screening was carried out with a fixed concentration of every inhibitor (10  $\mu\text{M}$ ). Compounds with 70% or higher of inhibition were then further evaluated by determination of their  $\text{IC}_{50}$  values. The enzyme activity was measured with increasing concentrations of each compound, providing a dose-response plot obeying a Langmuir isotherm. Normalization to the signal from the activity with no inhibitor added and further mathematical calculations furnished the  $\text{IC}_{50}$  values, which are included in table 13.

**Table 13.** Percentage of inhibition of the tested compounds at 10  $\mu$ M and the IC<sub>50</sub> value of amide 57. ND: not determined. PF-877423 was used as a standard.

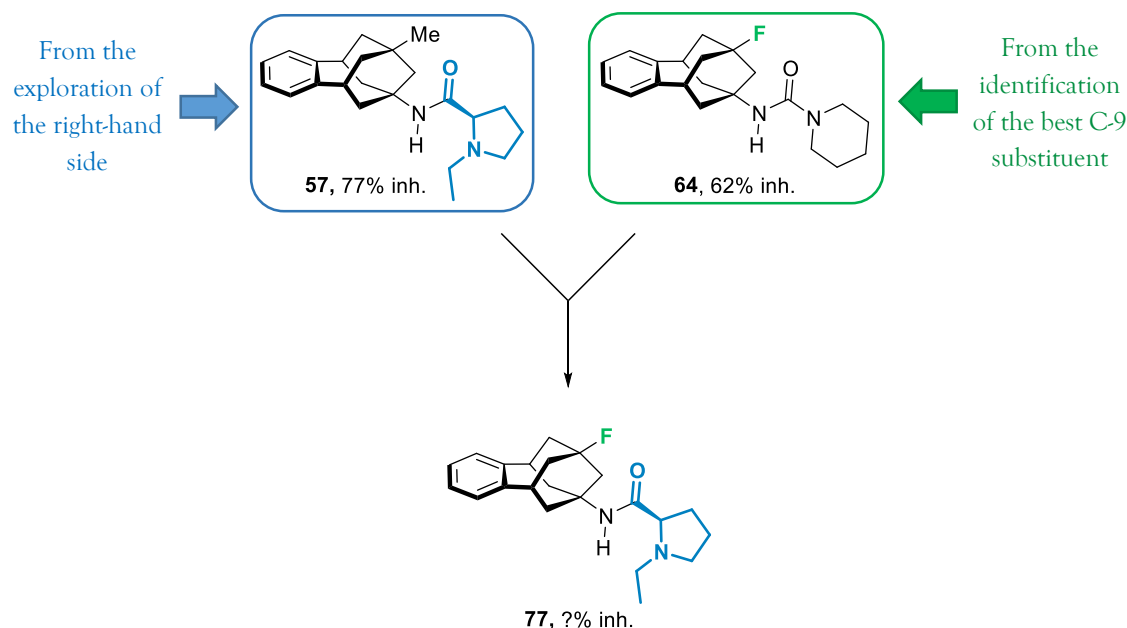
Comp.	R	RHS	% inhibition at 10 $\mu$ M	IC <sub>50</sub> ( $\mu$ M)
72	OH		15	ND
56	OH		24	ND
74	Me		57	ND
57	Me		77	1.0 $\pm$ 0.3
58	OH		31	ND
59	Me		36	ND
60	Me		52	ND
61	Me		35	ND
62	OH		30	ND
63	Me		36	ND
64	F		62	ND
65	OMe		41	ND
PF-877423	-	-	93	0.004

From the above results, some conclusions can be tentatively drawn for this first series of compounds:

- Four compounds (**74**, **57**, **60** and **64**) were found to have an inhibitory effect larger than 50% at a single dose of 10  $\mu$ M.
- Comparing the C-9-methylated derivatives, the *N*-ethyl-D-proline subunit behaved better than the other tested right-hand sides. Within this family of compounds, the alkylation of the proline ring led to an increase in the inhibitory activity (compare **72** vs **56**; **74** vs **57**).
- The replacement of the nitrogen atom in **63** by a methine group in **60** caused an enhancement of the potency against 11 $\beta$ -HSD1.
- The introduction of a polar group at the C-9 position (hydroxyl in **72**, **56**, **58** and **62**; or methoxide in **65**) was deleterious for the inhibitory activity, whereas lipophilic groups (methyl in **74**, **57**, **59**, **60**, **61**, and **63**; or fluorine in **64**) were generally better tolerated. Thus, the inhibitory activity improved as the lipophilicity increased. For a better understanding of this fact, compare **56** vs **57**, and **62** vs **65**.
- Considering the urea compounds **62-65**, the fluorinated derivative **64** displayed the higher percentage of inhibition compared to the rest of substituents.
- The substitution of the adamantane ring in PF-877423 by the benzo-homoadamantane scaffold in **56** and **57** was detrimental to the inhibitory activity, with a 250-fold lower affinity.

Taking into account the aforementioned, we identified the *N*-ethyl-D-proline subunit as the best right-hand side for the new scaffold (compound **57**) when considering only the C-9-methylated derivatives. On the other hand, the introduction of a fluorine atom at the C-9 position performed better in the assay than the other substitution patterns. According to that, we hypothesized that the compound featuring both substituents would afford an inhibitor with improved potency (Fig. 61). This highlights the relevant role played by the polar moiety at the right-hand side as well as by the C-9 substituent.

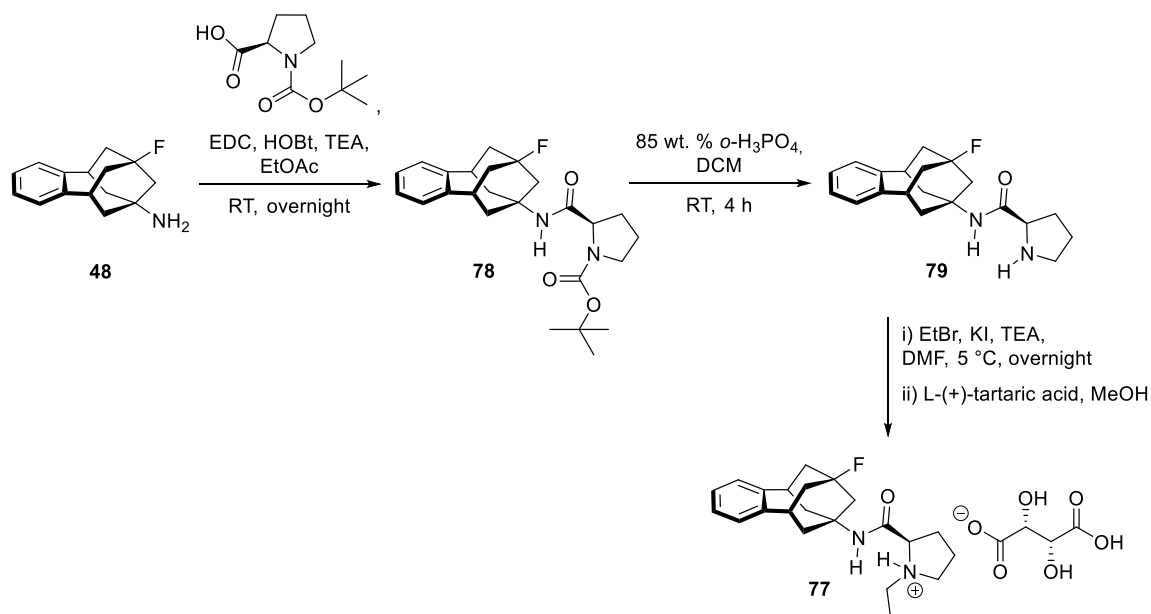




**Fig. 61.** Compound **77** combines the best findings from the previous series of analogues.

### 1.3 Synthesis of the fluoro-benzohomadamantane analogue of PF-877423

For the preparation of the fluorinated analogue **77** the same synthetic route as for the compounds **56** and **57** was applied. The amide coupling reaction of amine **48** with (*R*)-pyrrolidine-2-carboxylic acid under EDC and HOBt conditions afforded the desired Boc-protected pyrrolidine **78** in 92% yield (Scheme 43). Next, the product was subjected to deprotection with aqueous phosphoric acid to provide proline **79** in quantitative yield. Final *N*-alkylation of the free amine with ethyl bromide under the already described conditions produced the final amide **77** in moderate yield. Similar to compound **57**, the hydrochloride salt produced a hygroscopic solid. In order to have a compound suitable for characterization and pharmacological evaluation, PF-877423's analogue **77** was prepared as its L-(+)-tartrate salt.

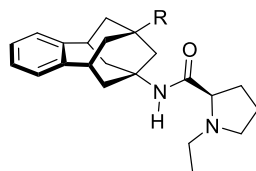


**Scheme 43.** Full synthetic route for the preparation of amide **77** from intermediate **48**.

#### 1.4 Pharmacological evaluation of the fluoro-benzohomoadamantane derivative of PF-877423

The research group of Dr. Scott Webster (University of Edinburgh) tested the (*R*)-proline **77** as an 11 $\beta$ -HSD1 inhibitor in the SPA. At a concentration of 10  $\mu$ M, the compound inhibited 76% of the total enzyme, not far away from the percentage of inhibition of its methylated analogue **57** (Table 14). Pleasingly, in the IC<sub>50</sub> determination, the threefold reduction on its value confirmed our first assumption, that the compound bearing a fluorine atom at the C-9 position and the *N*-ethyl-D-proline as the polar unit would result in an 11 $\beta$ -HSD1 inhibitor with enhanced potency, compared to the previous series of compounds.

**Table 14.** Results of the pharmacological evaluation of amide **77** and its comparison with the methylated analogue **57** and the standard PF-877423.



Comp.	R	% inhibition at 10 $\mu$ M	IC <sub>50</sub> ( $\mu$ M)
<b>57</b>	Me	77	1.0 $\pm$ 0.3
<b>77</b>	F	76	0.35 $\pm$ 0.20
PF-877423	-	93	0.004

However, compound **77** is around ~100-fold less potent than the adamantyl analogue PF-877423. Therefore, it can be argued that the substitution of the adamantane moiety by the size-expanded benzopolycycle might be detrimental for the binding to the enzyme. To check this hypothesis, molecular modelling studies were performed.

### 1.5 Computational studies of the first family of 11 $\beta$ -HSD1 inhibitors

To gain insight on the mode of inhibition of the most potent compounds **57** and **77**, the research group of Prof. Dr. F. Javier Luque of the University of Barcelona examined the binding of both prolines **57** and **77** on the 11 $\beta$ -HSD1 enzyme through docking and molecular dynamics simulations.

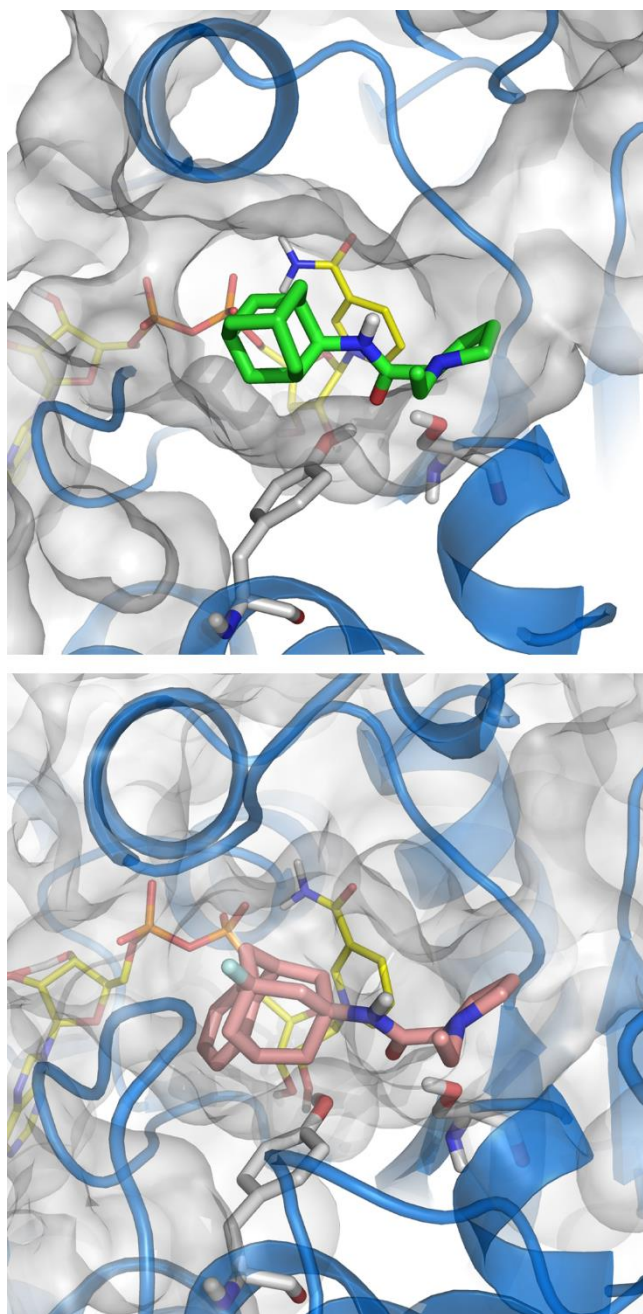
Preliminary docking calculations performed with Glide supported the ability of the ring-expanded benzopolycycle to fill the binding cavity of human 11 $\beta$ -HSD1.<sup>386</sup> The docking scores of **57** (-8.1 kcal/mol) and **77** (-8.2 kcal/mol) compared well with PF-877423 (-7.8 kcal/mol). Moreover, the best scored poses of both inhibitors indicated that, on one hand, the polar units mimicked the binding mode of PF-877423, retaining the hydrogen bond formed between the amide carbonyl oxygen and the hydroxyl group of Ser170. On the other hand, the hydrophobic cage filled the site occupied by the adamantane unit in PF-877423.

Despite the tolerable binding of new compounds **57** and **77** observed in the docking studies, we aimed to investigate further the reason for that difference on the inhibitory activity. With this in mind, the structural integrity of the best poses of compounds **57** and **77** was explored by means of molecular dynamics (MD) simulations. Three independent 50 ns MD simulations were run for each ligand-receptor complex, yielding the following characteristics:

- All the simulations were stable, as noted in the root-mean square deviation profiles ranging from 1.5 to 2.4 Å for the protein backbone, and from 2.5 to 3.5 Å for the residues in the binding site. This fact reflected the enhanced flexibility of the loops that enclose the binding pocket.
- The ligand pose was preserved along the simulations. Particularly, the hydrogen bond formed between the inhibitor and Ser170 residue was maintained in all cases, with an average distance of  $2.8 \pm 0.2$  Å (Fig. 62).
- The relative binding affinities were estimated from solvent interaction energy calculations, which revealed that compounds **57** and **77** should be stronger binders, by 0.5 and 1.1 kcal/mol, respectively, than PF-877423.

---

<sup>386</sup> Friesner, R. A.; Murphy, R. B.; Repasky, M. P.; Frye, L. L.; Greenwood, J. R.; Halgren, T. A.; Sanschagrin, P. C.; Mainz, D. T. *J. Med. Chem.* **2006**, *49*, 6177-6196.



**Fig. 62.** Representative snapshots taken from the MD simulations of the complexes between human 11 $\beta$ -HSD1 and compounds PF-877423 (top; green sticks) and 77 (bottom; pink sticks). Residues Tyr183 and Ser170 are shown as gray sticks, the NADP cofactor as yellow-based sticks and the protein backbone as blue cartoon. For the sake of clarity only polar hydrogens are shown. The shape of the binding cavity is shown as a white contour.

While the preceding results support the assumption that the insertion of a phenyl ring should lead to an enhanced binding affinity, the reduction of inhibitory potency may alternatively be ascribed to a lower effective concentration due to the increase in the hydrophobicity of the polycycle. In order to confirm this hypothesis, the log P was determined using quantum mechanical IEF/MST calculations for the most favourable

conformations of compounds **57**, **77** and PF-877423.<sup>387</sup> The study indicated that the introduction of a phenyl ring in the polycyclic structure increases the log P value by 1.5 units for amide **57** and 0.9 units for amide **77** relative to the adamantyl parent compound PF-877423.

Taken together, the *in silico* results suggest that the ring-expansion strategy performed with the benzopolycyclic scaffold might lead to effective inhibitors of human 11 $\beta$ -HSD1 enzyme. Nevertheless, the data from log P calculations along with the pharmacological results have demonstrated that a proper balance of hydrophobicity, furnished chiefly by the adamantane-like scaffold, is necessary to attain an optimum pharmacological profile.

## 2. Application of the adamantane scaffold as an adamantane analogue in 11 $\beta$ -HSD1 inhibitors

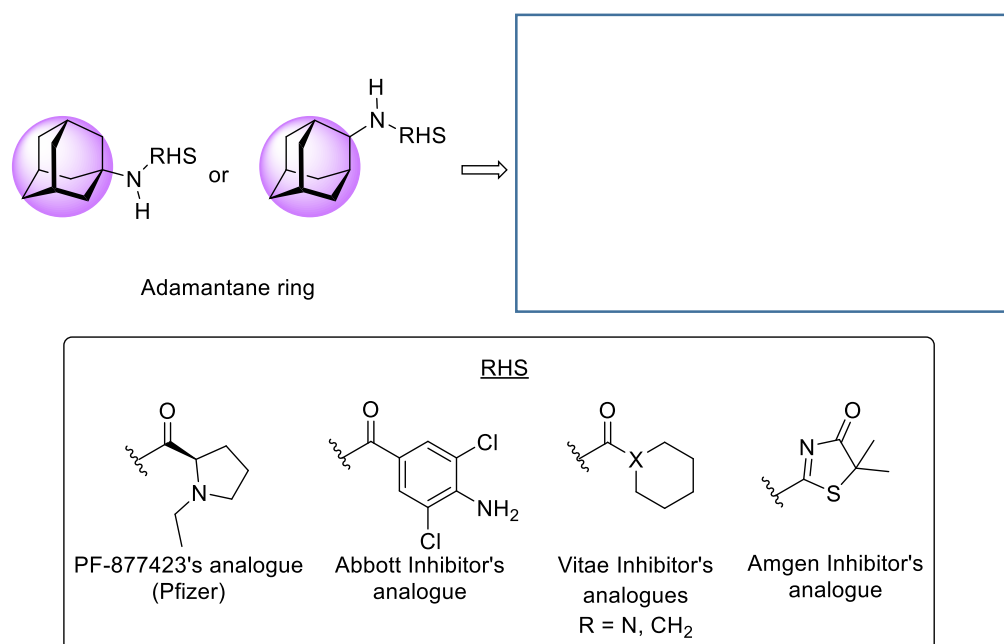
Before starting with this section, it is worth to mention that the work presented henceforth was developed simultaneously with the previous family of compounds. Consequently, an iterative process could not be achieved to reshape the design of the new family of compounds.

### 2.1 Synthesis of the adamantane derivatives

Following the analogy-based approach applied in the former section, and bearing in mind the flexibility of the binding pocket of the 11 $\beta$ -HSD1 protein arisen from the available X-ray data, we pursued the preparation of a new family of compounds featuring a size-expanded ring in lieu of the adamantane group. Specifically, we decided to assemble the adamantane scaffold **V** and amido- or urea-like units so as to assess the effect of this hydrophobic adamantane-like structure in the inhibition of 11 $\beta$ -HSD1 (Fig. 63). The polar groups attached to this polycycle consisted of the already tested moieties, again referred as right-hand sides (RHS). These functionalities should enable the formation of key hydrogen bonds at the binding site, whilst the polycyclic structure should fill one of the hydrophobic pockets of the catalytic site.

---

<sup>387</sup> Curutchet, C.; Orozco, M.; Luque, F. J. *J. Comput. Chem.* **2001**, *22*, 1180-1193.



**Fig. 63.** Design of the new 11 $\beta$ -HSD1 inhibitors with general structure V.

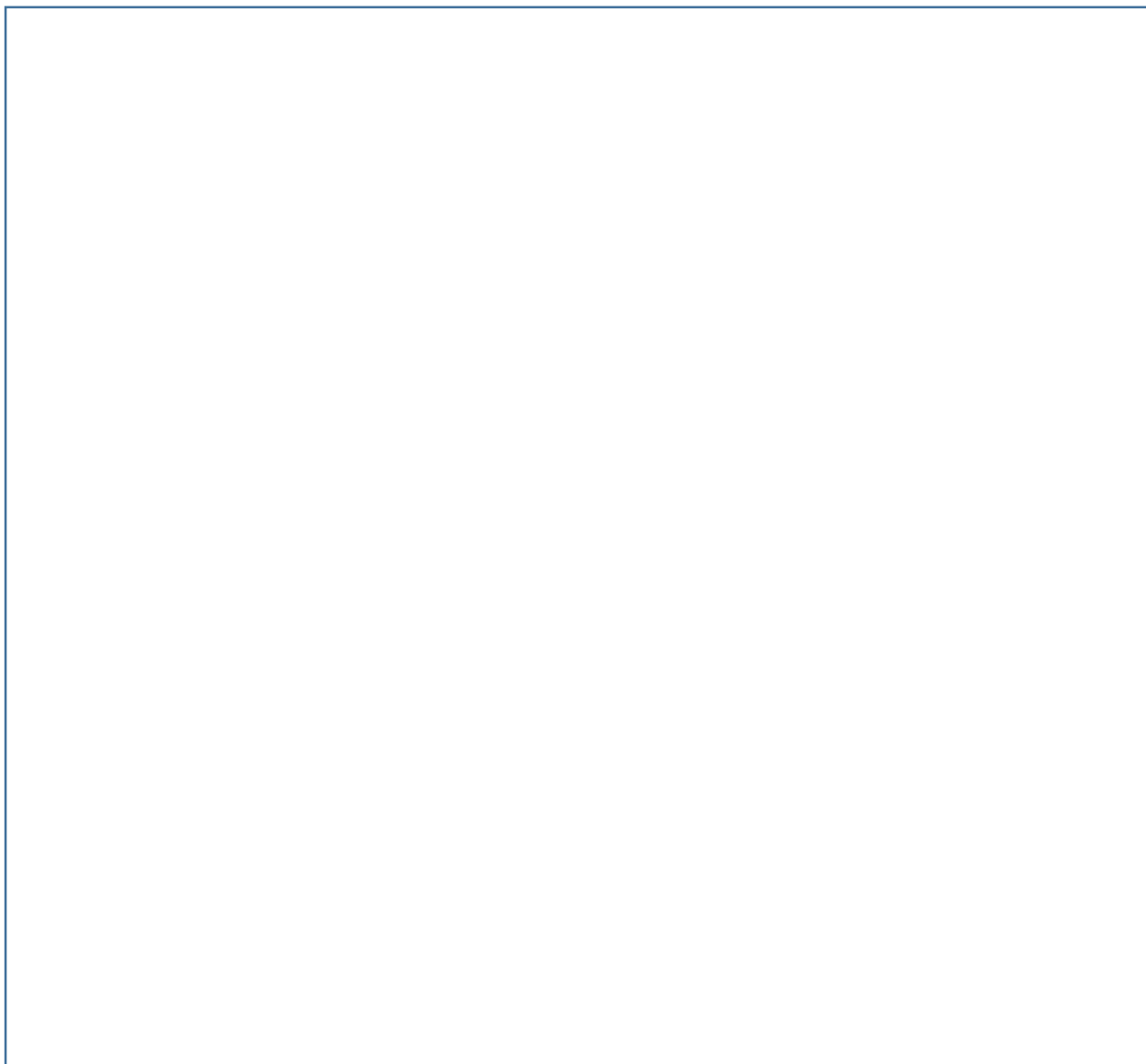
The preparation of the **V** has been described and applied multiple times by our research group.<sup>90,164,172</sup> The synthetic pathway started with an

originally published by two independent groups;<sup>388,389</sup> In the first step, (prior to distillation from commercially available ) was deprotonated with sodium hydride, whose anion **80** self-coupled through low-temperature iodine-promoted oxidation, to generate *in situ* **81** (Scheme 44). The latter underwent a after the addition of one equivalent of , yielding a mixture of **82** and **83**, which are referred , respectively.<sup>390</sup> Along with them, **84** and **85** were formed as side-products.

388

389

390

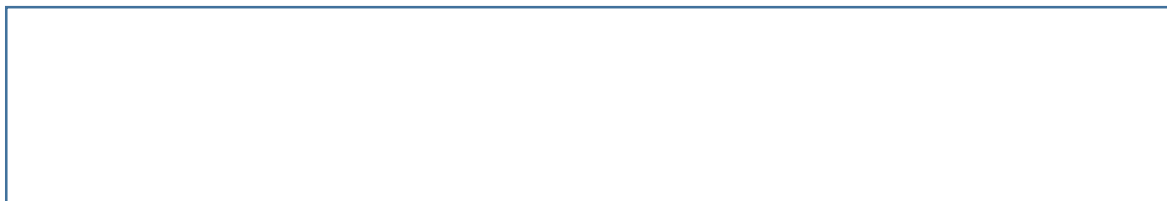


**Scheme 44.** Domino Diels-Alder reaction of **81** and **82**

The earlier procedures applied a tedious purification that implied difficult distillations. Fortunately, a few years later a more straightforward purification method appeared, allowing the separation of the pair of **82** and **83**.<sup>391</sup> Taking advantage of the solubility properties of the products, **82** and **83** were isolated by precipitation of the side-products **84** and **85** with diethyl ether and subsequent filtration. This experimental-related improvement permitted to scale-up the reaction up to 40 g of final mixture.

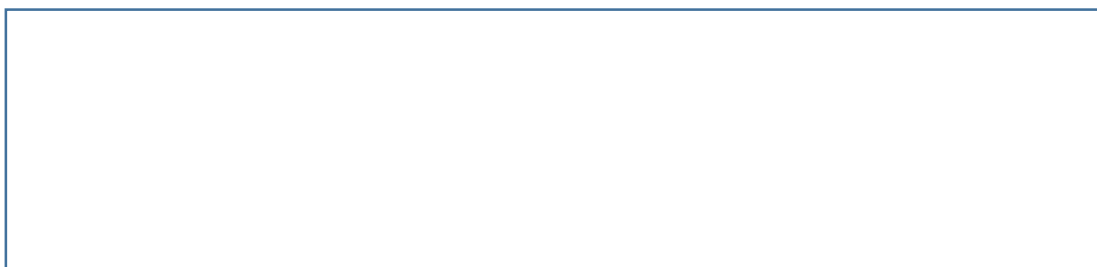
Separation of **82** and **83** was achieved by selective hydrolysis of the less sterically hindered **83**. Treatment with aqueous potassium hydroxide solution in methanol at room temperature for a short period of time afforded **87**, which was

isolated from the intact **82** in the aqueous work-up (Scheme 45). In this way, we prepared 20 g of the desired **82** in 7% overall yield.

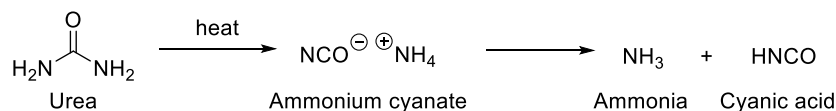


**Scheme 45.** Selective hydrolysis of **83** vs **82** due to steric hindrance.

Employing harsher conditions, **82** could be hydrolysed providing its corresponding **88** in 81% yield (Scheme 46). Next, **88** was subjected to formation with neat urea at 220 °C to afford **89** in 86% yield. At this temperature, the already melt urea undergoes thermal decomposition to supply cyanic acid and ammonia, which is the actual nucleophile that adds to each one of the carboxylic acids.<sup>392</sup>



Urea decomposition:



**Scheme 46.** Basic hydrolysis of **82** and later formation.

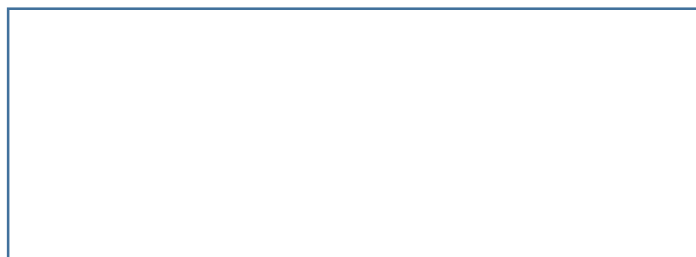
Afterwards, the was transformed to the corresponding **90** based on the protocol formerly described by our research group.<sup>393</sup> Unlike the more common reductive agents, such as lithium aluminium hydride, sodium bis(2-methoxyethoxy)aluminium hydride (Vitride<sup>®</sup> or Red-Al<sup>®</sup>) is soluble in most of the common organic solvents, which facilitates the handling of the substance, and reacts less strongly with water than LiAlH<sub>4</sub>, although it is still moisture sensitive.<sup>394</sup> Besides, Red-Al<sup>®</sup> is highly efficient in the reduction of multiple functional groups, such as nitriles, isocyanates and sulfonamides, *inter alia*. Thus, **89** was reduced with Red-Al<sup>®</sup> to produce **90** in 92% yield (Scheme 47).

<sup>392</sup> For further study on the pyrolysis of urea: Schaber, P. M.; Colson, J.; Higgins, S.; Thielen, D.; Anspach, B.; Brauer, J. *Thermochim. Acta* **2004**, *424*, 131-142.

<sup>393</sup> Rey-Carrizo, M. Ph.D. Dissertation, University of Barcelona, 2014.

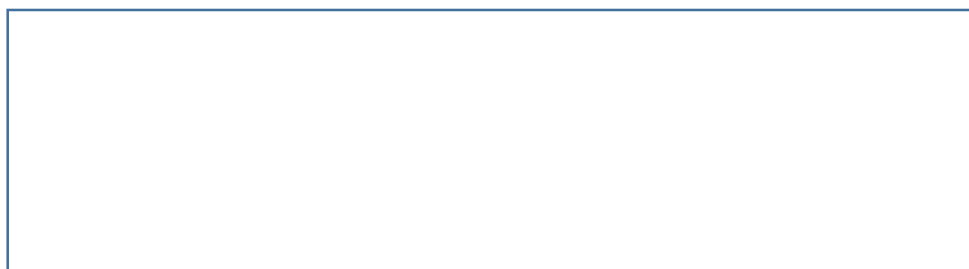
<sup>394</sup> Gugelchuk, M.; Silva, L. F. Jr.; Vasconcelos, R. S.; Quintiliano, S. A. P. *e-EROS* **2007**, 1-8.





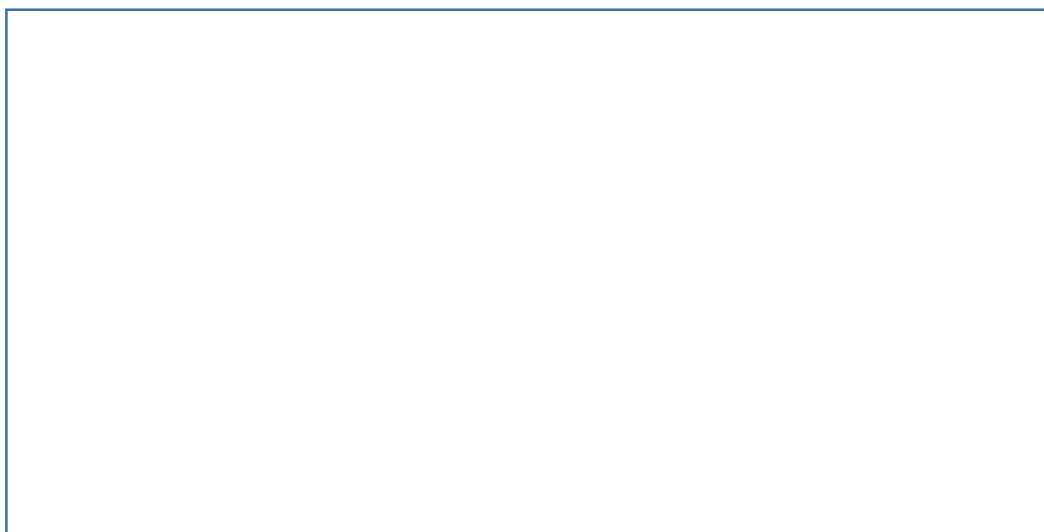
**Scheme 47.** reduction with Red-Al<sup>®</sup>.

With key intermediate **90** in hand, we proceeded to the coupling of this to the different polar units showed in figure 63. Applying the same procedures as in section 1, we started with the amide coupling with *N*-Boc-D-proline using EDC and HOBT as activating agents to provide hexacyclic amide **91** in 90% yield (Scheme 48).



**Scheme 48.** Amide bond formation with (*R*)-*N*-boc-pyrrolidine-2-carboxylic acid.

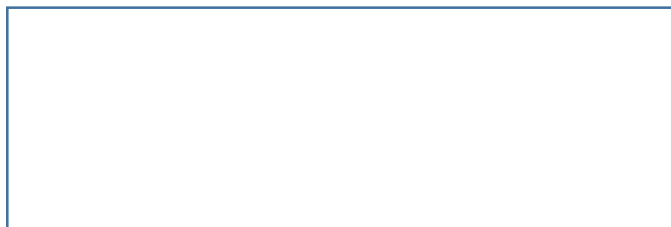
Regrettably, when the Boc-protected pyrrolidine **91** was subjected to acid conditions for its deprotection, only a complex was obtained, from which the desired amine **92** was could not be isolated. Illustrative computational studies revealed the feasibility that one part of the product might have been lost in the intramolecular attack of the amine to one of the , giving compound **94** as a plausible side-product (Scheme 49).<sup>395</sup>



**Scheme 49.** Possible explanation for the absence of desired amine **92**.

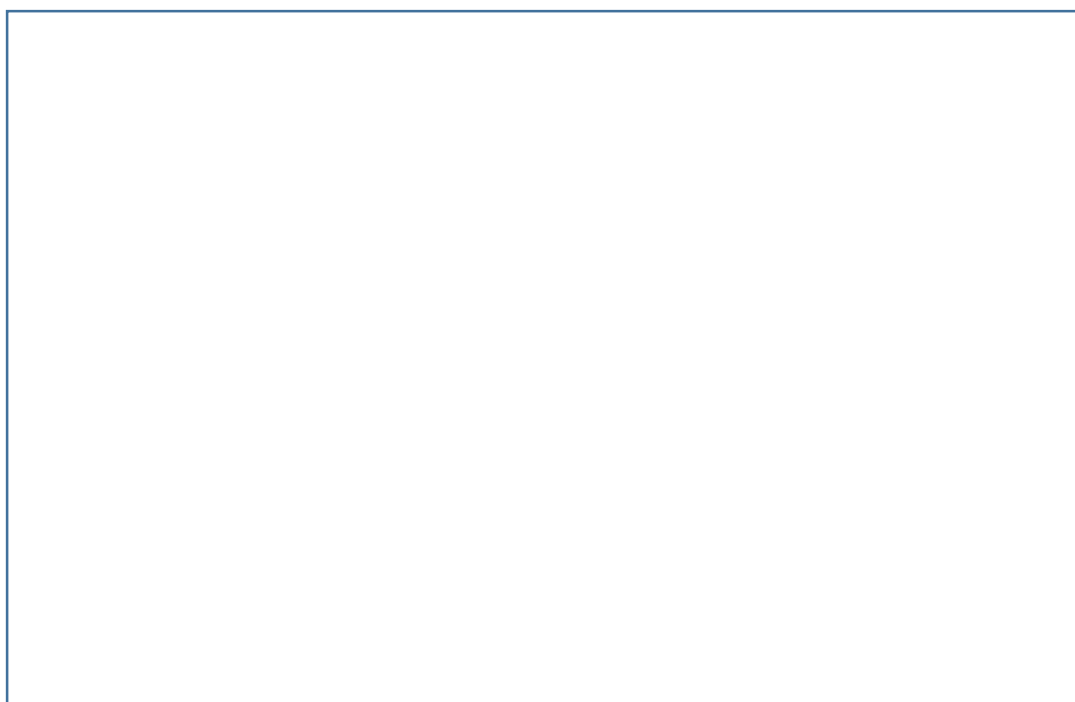
<sup>395</sup> Data from computational studies is not shown.

To avoid this issue, we decided to reduce the *prior* to the amide coupling, even though it meant to skip the no preparation of the final compound **93**. For the provision of **95** for further uses, **90** was hydrogenated under atmospheric pressure and at room temperature for 4 hours, whereupon **95** was recovered after filtration of the catalyst in 86% yield (Scheme 50).



**Scheme 50.** Catalytic hydrogenation of **90** at atmospheric pressure.

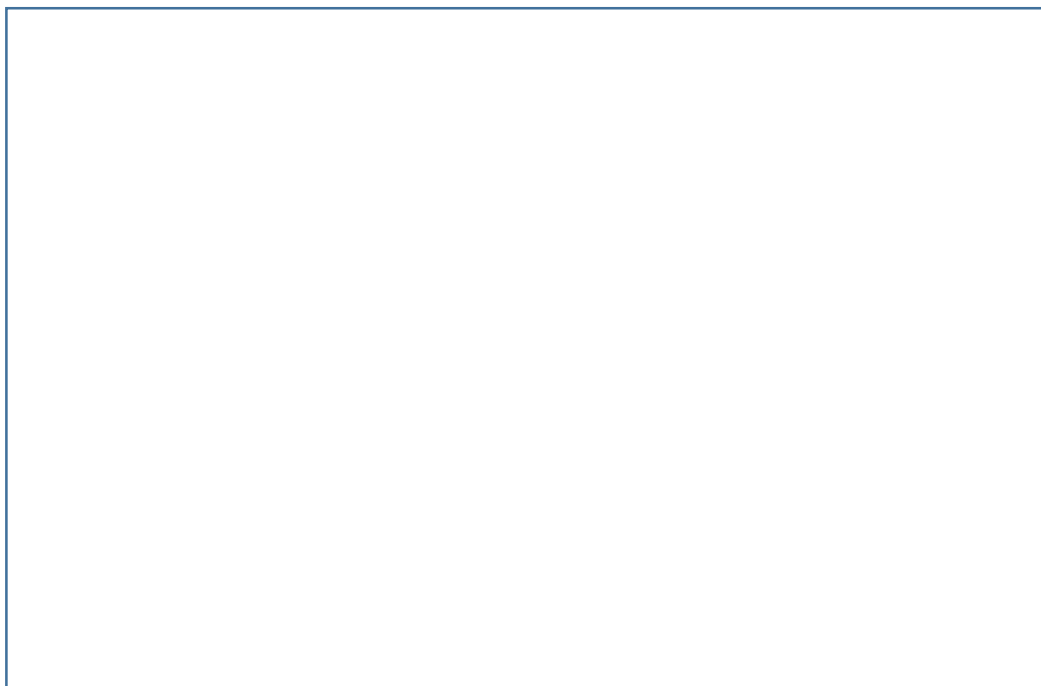
Starting now from **95**, final ethylated proline **98** was synthesized after amide bond formation with *N*-Boc-D-proline, followed by deprotection of the carbamate group with aqueous phosphoric acid and subsequent *N*-alkylation with ethyl bromide and catalytic amounts of potassium iodide, as shown in the scheme below. Of note were the requirement of column chromatography after the acid deprotection affording compound **97** in 36% yield, and the isolation of the final **98** as tartrate salt for its full characterization and pharmacological evaluation.



**Scheme 51.** Synthetic pathway for the preparation of **98** from **95**.

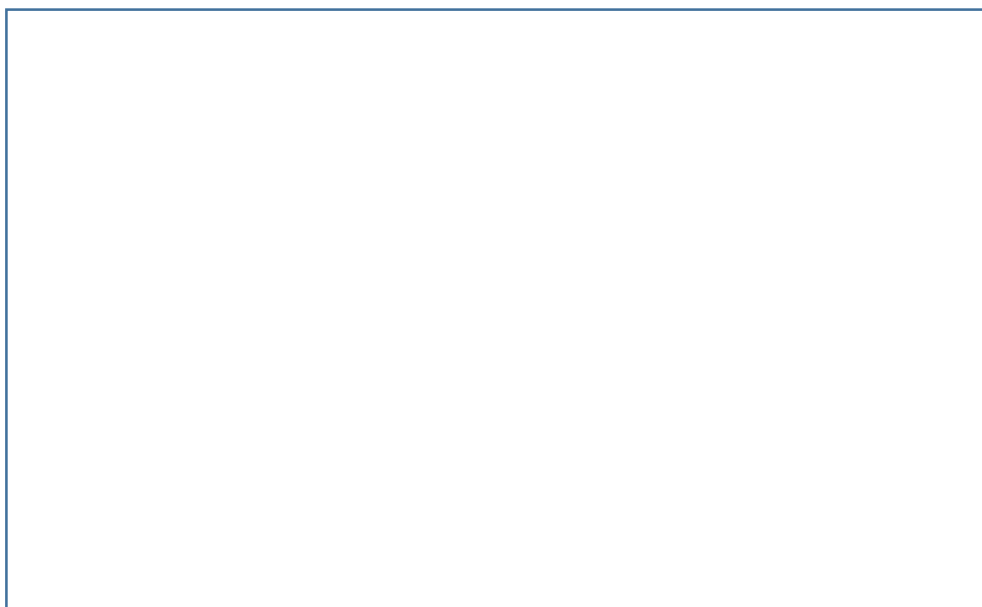
The substituted phenyl analogue **99** and its saturated derivative **100** were prepared applying the same conditions as before, i.e. amide coupling with EDC and HOBT, and

catalytic hydrogenation with palladium on carbon, affording the corresponding products in 47% and 89% yield, respectively (Scheme 52).



**Scheme 52.** Amide coupling between **90** with 4-amino-3,5-dichlorobenzoic acid, then hydrogenation at 1 atm.

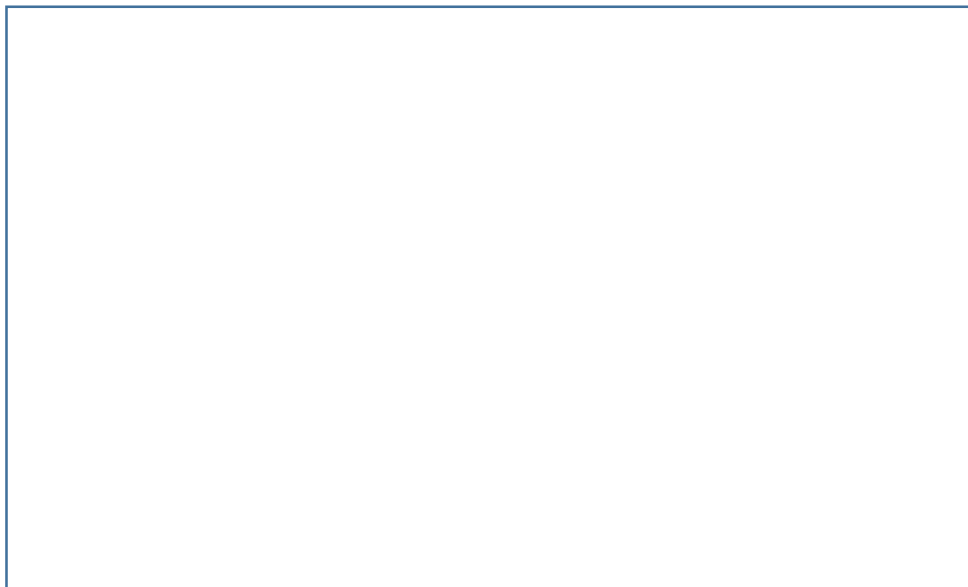
Similarly, the pair of cyclohexyl amides **101** and **102** were obtained under the same procedures in moderate and excellent yields, respectively (Scheme 53).



**Scheme 53.** Synthesis of saturated and unsaturated cyclohexyl amides **101** and **102**.

Next, we moved to the derivatives bearing a urea unit as the polar core of the molecule. In analogy with the previous benzopolycyclic scaffold, secondary amine **90** was reacted with 1-piperidinecarbonyl chloride in the presence of a base to provide

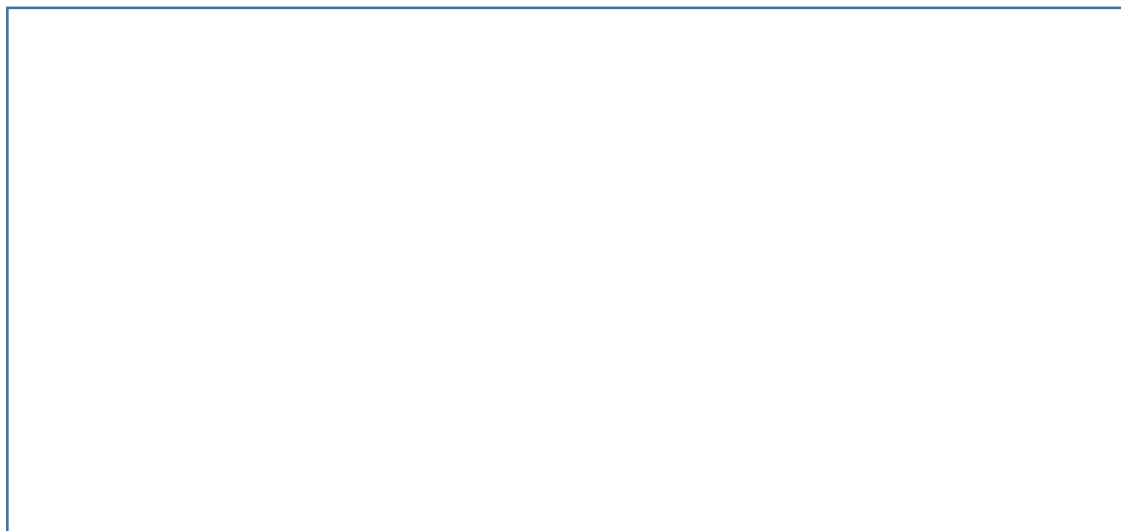
unsaturated urea **103** in 71% yield (Scheme 54). Albeit multiple attempts to purify the product, from different gradient elution systems in column chromatography to several solvent mixtures in crystallization techniques, urea **103** did not achieve the adequate purity for pharmacological testing. Because of that, **103** was subjected to catalytic hydrogenation, furnishing **104** in 72% yield and pure enough for its biological evaluation.



**Scheme 54.** Urea formation with a carbamoyl chloride *prior* to reduction of .

For the synthesis of the last analogue of this family, which featured a thiazolone ring in the right-hand side of the molecule, pyrrolidine **90** was reacted with benzoyl isothiocyanate in chloroform to give carbonyl thiourea derivative **105** in quantitative yield (Scheme 55). Basic hydrolysis with potassium carbonate and water did not afford the desired thiourea **106**, and the starting material was fully recovered. An alternative for the formation of thiourea **106** was adapted from the literature and consisted in the hydrazine-promoted debenzoylation under solvent-free conditions at room temperature.<sup>396</sup> Worth the mention is the fact that if the reaction was carried out in chloroform at reflux, triazole-ring formation takes place instead of the debenzoylation. Nevertheless, neither thiourea **106** nor the corresponding triazole ring were formed, but again the starting material was recovered. We reasoned the lack of reactivity was coming from the steric hindrance furnished by the ring-expanded scaffold.

<sup>396</sup> Kodomari, M.; Suzuki, M.; Tanigawa, K.; Aoyama, T. *Tetrahedron Lett.* **2005**, *46*, 5841-5843.



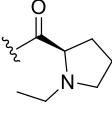
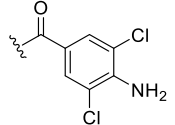

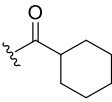
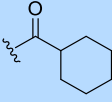
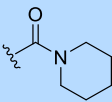
**Scheme 55.** Conversion of **90** to benzoylthiourea **105**, and failed attempts of hydrolysis.

In the end, this family of derivatives comprehended 6 new compounds that were tested as 11 $\beta$ -HSD1 inhibitors.

## 2.2 Pharmacological evaluation and computational studies of the derivatives

Compounds **98-102** and **104** were tested, using the SPA technique, by Dr. Scott Webster in the University of Edinburgh. As for the previous family, compounds with a percentage of inhibition of 70% or higher at 10  $\mu$ M were further evaluated with their IC<sub>50</sub> determination (Table 15).

**Table 15.** Inhibition of the 11 $\beta$ -HSD1 by the new compounds. ND: not determined. PF-877423 was used as a standard.

Comp.	RHS	% inhibition at 10 $\mu$ M	IC <sub>50</sub> ( $\mu$ M)
98		56	ND
99		98	2.77
100		98	0.414
101		95	1.076
102		103	0.289
104		101	0.320
PF-877423	-	93	0.004

These data allowed us to deduce the following:

- Five compounds (**98-102** and **104**) inhibited almost totally the 11 $\beta$ -HSD1 enzyme in the SPA at 10  $\mu$ M concentration.
- Generally, aliphatic amides **101-102** and urea **104** were slightly more potent than aromatic amides **99-100**.
- In contrast with the previous benzopolycyclic family, the PF-877423's analogue **98** showed the lowest activity for this series of compounds.
- As a common trend, **100** and **102** were more potent than their parent **99** analogues (compare **100** vs **99** and **102** vs **101**).
- The replacement of the methine group in **102** by a nitrogen atom in **104** did not greatly improve the activity, unlike the previous family.

- The substitution of the adamantane ring in PF-877423 for the scaffold led to a significant reduction in the inhibitory activity.

The fact that proline derivative **98** was the least potent compound of this series, but the most potent analogue for the benzo-homoadamantane series, reflected that the lipophilic scaffold oriented the polar units in a way that could alter their binding mode within the catalytic site. Thus, a specific right-hand side should not necessarily behave similarly for any given scaffold. Consequently, for each scaffold a screening of polar subunits should be performed in order to identify the best combination of fragments. In order to shed light on the reasoning of the binding mode of the new structures, Prof. Luque performed preliminary MD studies of the most active compounds **102** and **104**, and simultaneously, the adamantane derivative **107**, synthesized by our group, was evaluated (Fig. 64).<sup>364</sup>

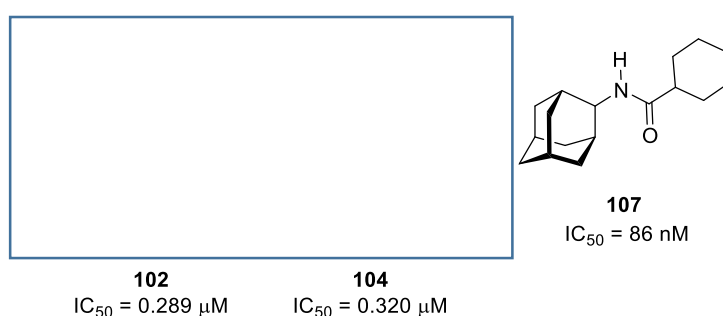
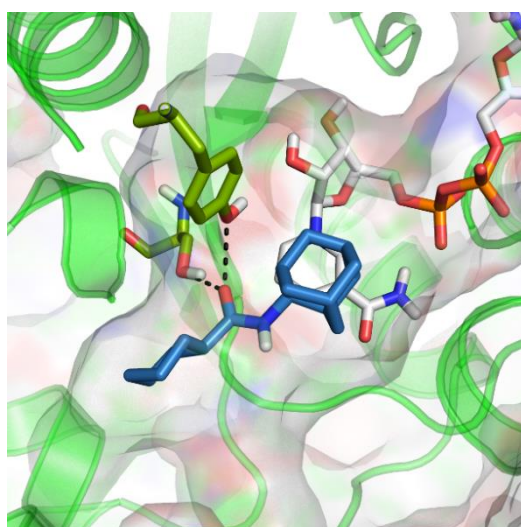
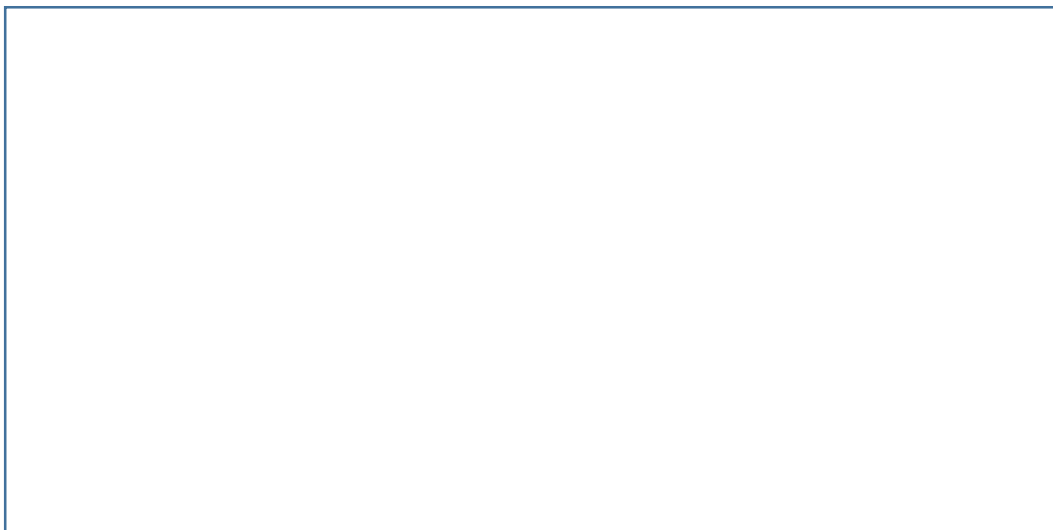


Fig. 64. Three selected compounds for MD simulations.

From the preliminary results, two main conclusions are depicted:

- The scaffold occupies a larger space than the adamantane, being practically the upper-limit the size the lipophilic scaffold can reach. In other words, the scaffold is too big to properly fit within the hydrophobic pocket (Fig. 65).
- There is no significant difference between **102** and **104** in their binding mode. Thus, the nitrogen does not seem to affect the potency, as reflected by their very similar  $IC_{50}$  values.



**Fig. 65.** Representative snapshots taken from the MD simulations of the complexes between human 11 $\beta$ -HSD1 and compounds **102** (top left; purple sticks), **104** (top right, yellow sticks) and **107** (bottom; blue sticks). Residues Tyr183 and Ser170 are shown as green sticks, the NADP cofactor as orange-based sticks and the protein backbone as green cartoon. For the sake of clarity only polar hydrogens are shown. The shape of the binding cavity is shown as a white contour.

As a final remark, the larger inhibitory potency of compounds **100** and **102** (also **104**, although it was not possible to test its parent compound **103**) could also reflect the increase in hydrophobicity resulting from in **99** and **101**, respectively, as expected from

The decreased activity of the benzopolycyclic and hexacyclic compounds compared to the adamantyl analogue underlined the requirement of both a perfect match and the reduction of the overall lipophilicity of a bulky group in this pocket to achieve high potency. Hence, the incorporation of nuclei with enhanced polarity and reduced size appears to be a suitable strategy for developing novel inhibitors.



It is worth to mention that taking advantage of the conclusions drawn from the two sets of compounds reported in this manuscript, the Ph.D. student Rosana Leiva, in her thesis, has synthesized novel 11 $\beta$ -HSD1 inhibitors with low nanomolar IC<sub>50</sub> values.

# **Conclusions**



In the second chapter of the thesis, 19 new final compounds were prepared and thoroughly characterized by means of spectroscopic and analytical techniques. Concretely, the families prepared in this work and the conclusion derived from them are:

- **6,7,8,9,10,11-hexahydro-5,7:9,11-dimethano-5*H*benzocyclononen-7-yl derivatives:**

1. From the synthetic point of view: since the intermediate scaffolds were already prepared in the previous chapter, only procedures described in the literature were followed for the final reactions.
2. From a pharmacological activity point of view: only two derivatives, **57** and **77**, displayed enough percentage of inhibition at 10  $\mu\text{M}$  (77 and 76%, respectively) for their  $\text{IC}_{50}$  determination (Fig. 66). The methylated compound **57** showed low inhibitory activity in the SPA ( $\text{IC}_{50}$  of 1.0  $\mu\text{M}$ ), and this activity was slightly improved with the fluorinated analogue **77** ( $\text{IC}_{50}$  of 0.35  $\mu\text{M}$ ). None of the others benzo-homoadamantane compounds were active as  $11\beta\text{-HSD1}$  inhibitors. The substitution of the adamantane group for the benzo-homoadamantane nucleus is unfavourable.

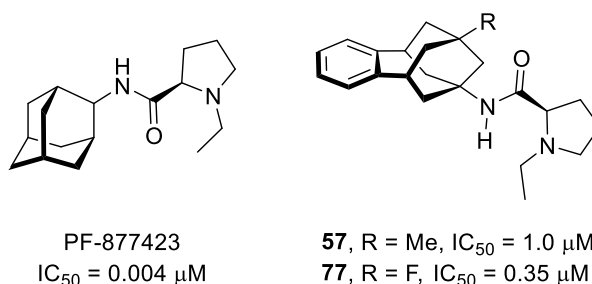


Fig. 66. Active compounds from the first family.

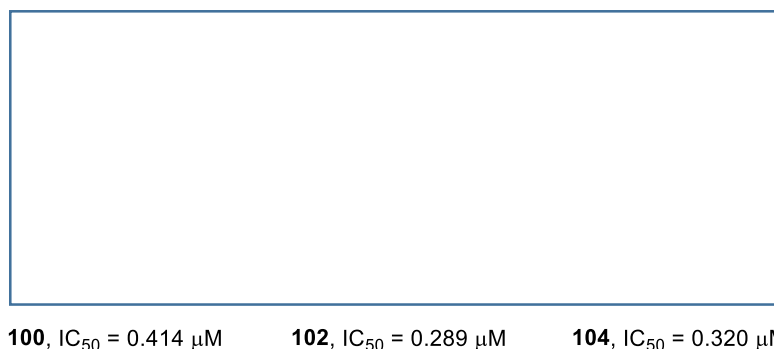
3. From a computational point of view: docking and MD simulations revealed that the insertion of a phenyl ring in the bulky group should not be detrimental for the activity, compared with the standard PF-877423. However, the lack of inhibitory activity of the benzo-homoadamantane derivatives may be due to an improper balance of lipophilicity.

- **derivatives:**

1. From the synthetic point of view: their preparation entailed the synthesis first of the scaffold, through a 5-step sequence, implying an . The subsequent reaction conditions were taken from the previous family of compounds.

However, not all the reactions were efficient, and a few of the targeted products were abandoned.

- From a pharmacological activity point of view: except for compound **98**, all the tested compounds were active as inhibitors of the 11 $\beta$ -HSD1, showing moderate potency. Of note is the increase on the potency with the  $\text{C}_{10}$  scaffold, resulting in the most potent compounds of the series **100**, **102** and **104** ( $\text{IC}_{50}$  of 0.414, 0.289 and 0.320  $\mu\text{M}$ , respectively) (Fig. 67). The different RHSs do not alter significantly the activity between them. The substitution of the adamantane ring for the  $\text{C}_{10}$  nucleus is unfavourable.



**Fig. 67.** Active compounds from the second family.

- From a computational point of view: preliminary MD simulations of **102** and **104** revealed that the  $\text{C}_{10}$  scaffold fills the hydrophobic cavity to a larger extent than the adamantane standard **107**, diminishing the activity. No significant difference was observed between the binding mode of **102** and **104**. Finally, the increase on the activity with saturated compounds **100**, **102** and **104** can be due to changes on the lipophilicity from their parent compounds.

## **CHAPTER 3: sEH inhibition**



# **Introduction**





## 1. sEH inhibition by adamantane-based derivatives

The last chapter of the present thesis will deal with the discovery of sEH as a pleiotropic target for drug development, as well as the manifold therapeutic benefits that its inhibition may lead. A summary of the sEH inhibitors that are currently in development will be included, most of which integrate an adamantane ring as the bulky moiety. Finally, the issues that have arisen over the drug discovery process will be discussed in order to comprehend the current needs for the development of future drug candidates.

### 1.1 Epoxyeicosatrienoic acids and their biological role

#### 1.1.1 Oxidative pathways of arachidonic acid metabolism

One of the principal metabolic pathways in the organism is the arachidonate cascade, which revolves around the arachidonic acid (ARA), an  $\omega$ -6, 20-carbon polyunsaturated fatty acid that is produced from membrane phospholipids of activated cells upon various stimuli.<sup>398</sup> ARA is transformed to lipid chemical mediators with pro-inflammatory properties, such as prostaglandins (PGs) and leukotrienes (LKTs), by the action of cyclooxygenase (COX) and lipoxygenase (LOX) enzymes respectively, which are well-known drug targets against inflammation (Fig. 68).<sup>399</sup> The most recently discovered cytochrome P450 (CYP450) branch of the cascade, which has not been exploited as a pharmaceutical target yet, also generates physiologically important eicosanoids.<sup>400</sup> Among them, epoxyeicosatrienoic acids (EETs) are formed after epoxidation of ARA by mainly CYP2C and CYP2J, and possess an opposite effect than their counterpart products from COX and LOX metabolism.<sup>401</sup> Detailed discussions on each of these three pathways are beyond the scope of this thesis.

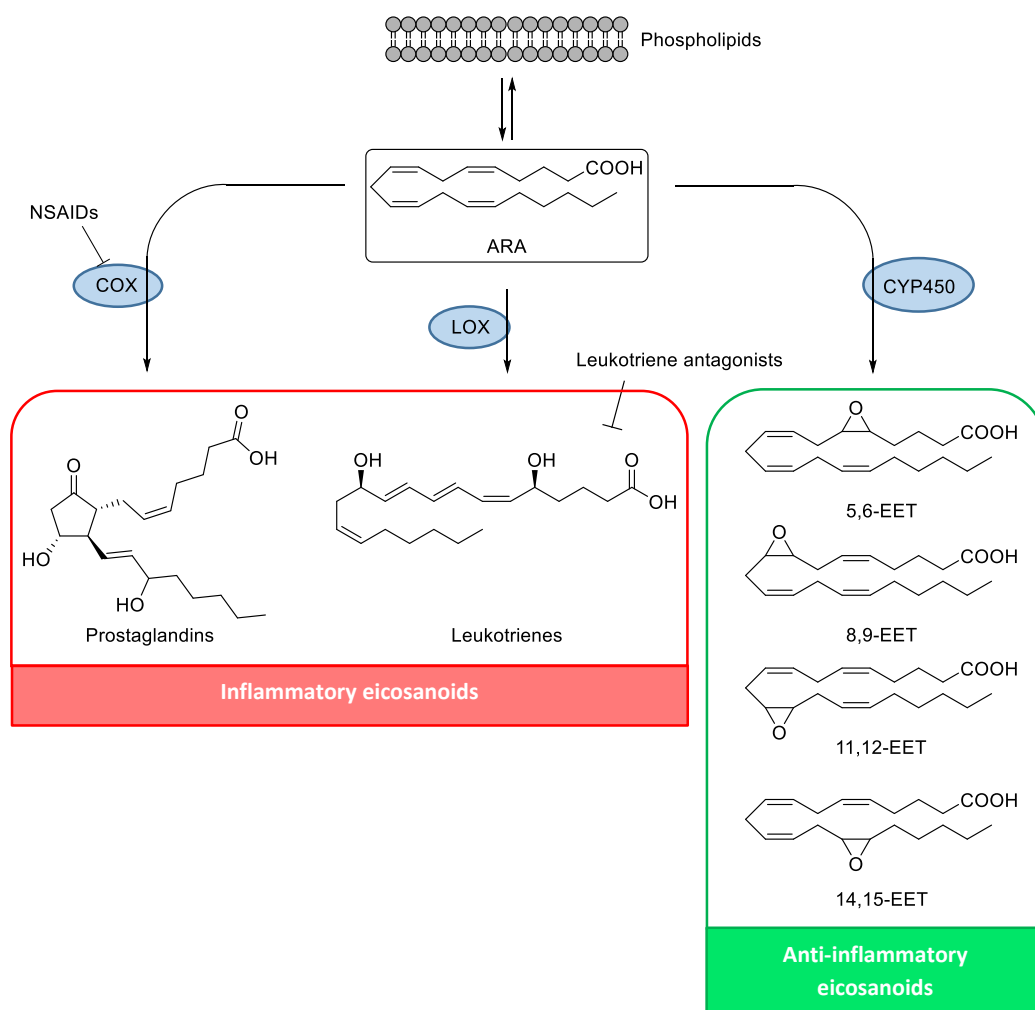
---

<sup>398</sup> Harizi, H.; Corcuff, J. B.; Gualde, N. *Trends Mol. Med.* **2008**, *14*, 461-469.

<sup>399</sup> Funk, C. D. *Science* **2001**, *294*, 1871-1875.

<sup>400</sup> Zeldin, D. C. *J. Biol. Chem.* **2001**, *276*, 36059-36062.

<sup>401</sup> Node, K.; Huo, Y.; Ruan, X.; Yang, B.; Spiecker, M.; Ley, K.; Zeldin, D. C.; Liao, J. K. *Science* **1999**, *285*, 1276-1279.



**Fig. 68.** Three metabolic pathways of ARA: the COX, LOX and CYP450 enzymatic routes, resulting in an array of chemical mediators involved in inflammatory processes. Inhibitors of COX (COX-1 and COX-2) (NSAIDs) are used for the treatment of pain and inflammation. Leukotriene antagonists are indicated in asthmatic and allergic states. NSAIDs: nonsteroidal anti-inflammatory drugs.

### 1.1.2 Biological relevance of EETs and importance of the sEH management

Generally, EETs are lipid mediators that move biological processes towards a homeostatic or *status quo* condition. EETs are autocrine and paracrine endothelium-derived factors that display attractive effects particularly in vascular and renal systems. To begin with, EETs are potent vasodilatory and anti-inflammatory agents.<sup>402</sup> The vasodilatory properties of EETs are associated with an increased open-state probability of calcium-activated potassium channels, which lead to hyperpolarization of the vascular smooth muscle.<sup>403</sup> Of note, EETs seem to encourage the resolution of inflammation rather than prevent it *via* inhibition of the nuclear factor  $\kappa$ B (NF- $\kappa$ B), activation of subfamilies of nuclear peroxisome proliferator-activated receptors (PPARs), and decreasing the expression

<sup>402</sup> Morisseau, C.; Hammock, B. D. *Annu. Rev. Pharmacol. Toxicol.* **2013**, *53*, 37-58.

<sup>403</sup> Fleming, I. *Circ. Res.* **2001**, *89*, 753-762.

of inducible COX-2. Besides, EETs exhibit other beneficial effects on biological systems, such as analgesic, anti-hypertensive, anti-platelet aggregation, fibrinolytic, pro-angiogenic and anti-apoptotic effects.<sup>404,405</sup> In addition, some metabolic events are mediated by EETs, such as control of insulin release and modulation of insulin sensitivity.<sup>406,407</sup> Taken together, EETs are considered important chemical mediators that interact with a plethora of proteins to generate a set of wholesome effects. Experimental studies have revealed that EETs act through an intracellular mechanism by binding to fatty-acid-binding proteins and PPARs, *inter alia*.<sup>408</sup> However, the cascade processes derived from the action of EETs are still unknown for some of the abovementioned effects. For the moment, an EET receptor has yet to be identified. Figure 69 includes a schematic representation of the potential mechanism for the anti-inflammatory, cardiovascular and analgesic effects of EETs.<sup>409</sup>

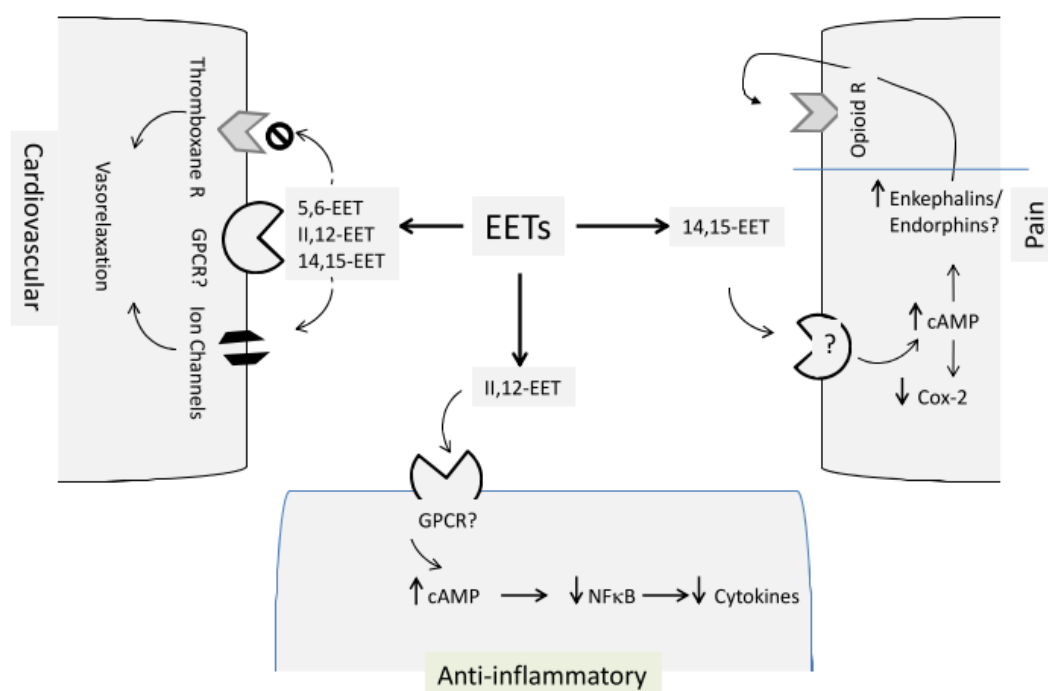


Fig. 69. Plausible mode of action of EETs in cardiovascular system, inflammation and pain.

GPCR: G protein-coupled receptor; cAMP: cyclic adenosine monophosphate.

The metabolic fate of the EETs is under control of the sEH, an enzyme that belongs to the  $\alpha/\beta$  hydrolase family and facilitates the addition of water to an epoxide, leading to the formation of a vicinal diol.<sup>410</sup> Thus, EETs are subjected to epoxide-ring opening to

<sup>404</sup> El-Sherbeni, A. A.; El-Kadi, A. O. S. *Arch. Toxicol.* **2014**, *88*, 2013-2032.

<sup>405</sup> Dufлот, T.; Roche, C.; Lamoureux, F.; Guerrot, D.; Bellien, J. *Expert Opin. Drug Discov.* **2014**, *9*, 1-15.

<sup>406</sup> Falck, J. R.; Manna, S.; Moltz, J.; Chacos, N.; Capdevila, J. *Biochem. Biophys. Res. Commun.* **1983**, *114*, 743-749.

<sup>407</sup> Skepner, J. E.; Shelly, L. D.; Ji, C.; Reidich, B.; Luo, Y. *Prostaglandins Other Lipid Mediat.* **2011**, *94*, 3-8.

<sup>408</sup> Imig, J. D.; Hammock, B. D. *Nat. Rev. Drug Discov.* **2009**, *8*, 794-805.

<sup>409</sup> Pillarisetti, S. *Inflamm. Allergy - Drug Targets* **2012**, *11*, 143-158.

<sup>410</sup> Harris, T. R.; Hammock, B. D. *Gene* **2013**, *526*, 61-74.

afford dihydroeicosatrienoic acids (DHETs), whereby the biological effects of EETs are diminished, eliminated or altered (Fig. 70).<sup>411</sup>

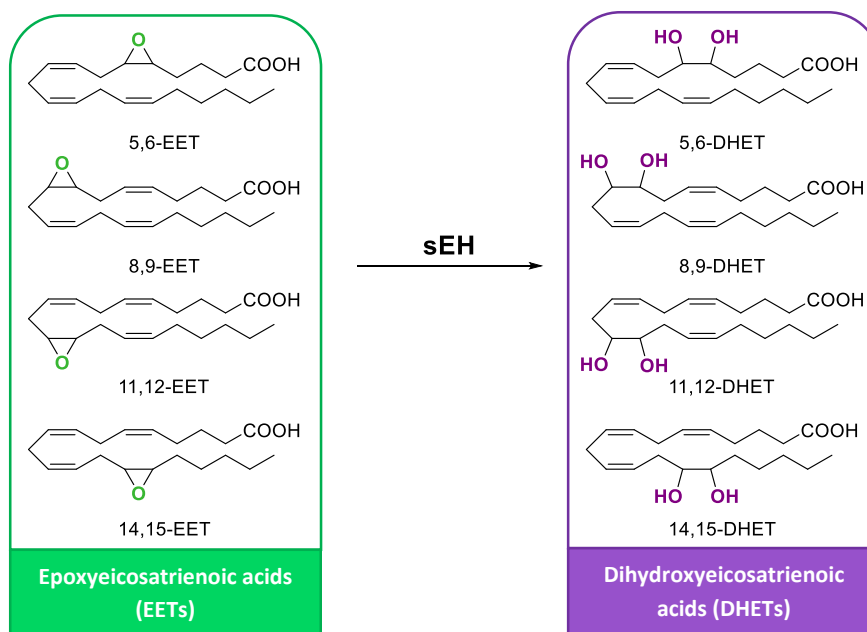


Fig. 70. Transformation of active EETs to inactive DHETs through the sEH enzyme.

Consequently, since the discovery of the biological role of EETs and their metabolism, sEH has emerged as a promising therapeutic strategy for the treatment of multiple conditions. Inhibition of sEH stabilizes the levels of EETs for the maintenance of the cellular homeostasis. Because other metabolic routes different from the sEH have been described that ensure the control of EETs' concentration in plasma and tissues even in the absence of sEH activity, EETs levels can only increase moderately with the inhibition of sEH.<sup>412</sup> Hence, limited target-related side effects are predicted with the administration of potent sEH inhibitors.

## 1.2 Targeting sEH: an overview of its pharmacology

Over the past decade, the appreciation of the importance of EETs and their regulation by sEH has greatly accelerated due to the huge therapeutic potential derived from the inhibition of sEH. Since the first studies performed 30 years ago, the value of the sEH inhibition in various animal models of diseases has been demonstrated. The contribution of these studies will be covered in order to understand the beneficial outcomes from sEH inhibition.

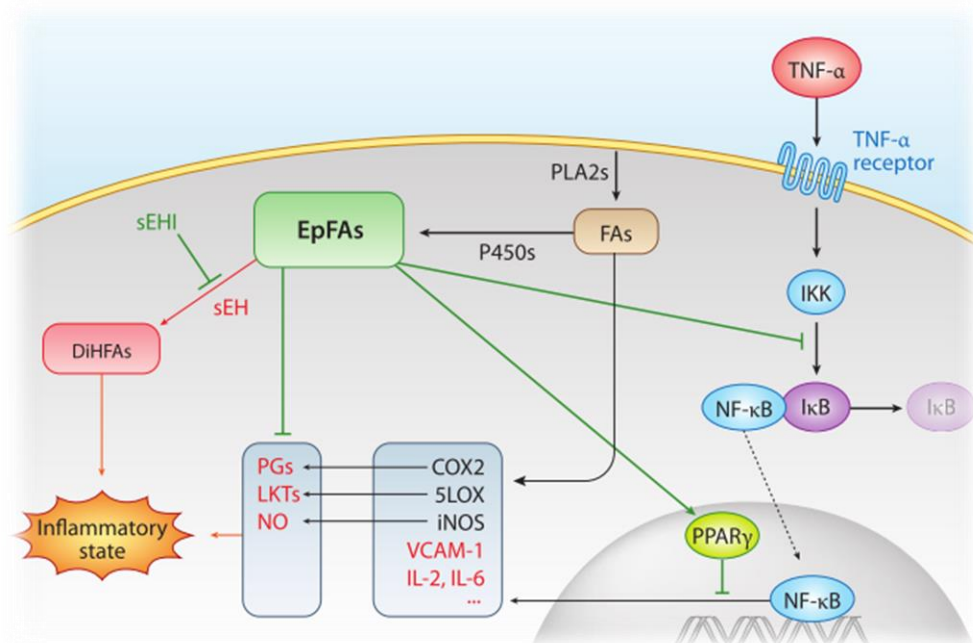
### 1.2.1 Regulation of inflammation by sEH inhibitors

The *anti-inflammatory* role of EETs has been demonstrated using multiple strategies including overexpression of CYP450, deletion of sEH in animal models or use of sEH

<sup>411</sup> Morisseau, C.; Hammock, B. D. *Annu. Rev. Pharmacol. Toxicol.* **2005**, *45*, 311-333.

<sup>412</sup> Imig, J. D. *Physiol. Rev.* **2012**, *92*, 101-130.

inhibitors and directly monitoring EET effects.<sup>413,414,415</sup> Reduced activation of the NF- $\kappa$ B is a key event in the anti-inflammatory activity of EETs, specially of 11,12-EET and 14,15-EET, as previously indicated. This reduction seems to follow three complementary cellular mechanisms (Fig. 71): i) decrease of the activation of NF- $\kappa$ B induced by tumor necrosis factor- $\alpha$  (TNF- $\alpha$ ); ii) activation of PPAR- $\gamma$  activity; iii) reduction of the prostaglandin E<sub>2</sub> (PGE<sub>2</sub>).<sup>402,416</sup>



**Fig. 71.** Action of epoxy-fatty acids (EpFAs) in the inflammatory process. PLA2: phospholipase A2. FAs: fatty acids. DiHFAs: dihydroxy-fatty acids. IKK: inhibitor of  $\kappa$ B kinase. iNOS: inducible nitric oxide synthase. VCAM-1: vascular cell adhesion molecule 1. IL: interleukin. NO: nitric oxide.

Furthermore, the agents that elevate cAMP are known to be anti-inflammatory, also by inhibiting NF- $\kappa$ B transcription.<sup>417</sup> Thus, it is likely that the elevation of cAMP, *prior* activation of GPCR, is another major mechanism behind the anti-inflammatory effects of EETs.

All in all, these data indicate that sEH is an emerging therapeutic target in a number of diseases that have inflammation as a common underlying cause.

<sup>413</sup> Node, K.; Huo, Y.; Ruan, X.; Yang, B.; Spiecker, M.; Ley, K.; Zeldin, D. C.; Liao, J. K. *Science* **1999**, *285*, 1276-1279.

<sup>414</sup> Schmelzer, K. R.; Kubala, L.; Newman, J. W.; Kim, I.; Eiserich, J. P.; Hammock, B. D. *Proc. Natl. Acad. Sci. USA* **2005**, *102*, 9772-9777.

<sup>415</sup> Deng, Y.; Edin, M. L.; Theken, K. N.; Schuck, R. N.; Flake, G. P.; Kannon, M. A.; DeGraff, L. M.; Lih, F. B.; Foley, J.; Bradbury, J. A.; Graves, J. P.; Tomer, K. B.; Falck, J. R.; Zeldin, D. C.; Lee, C. R. *FASEB J.* **2011**, *25*, 703-713.

<sup>416</sup> Liu, Y.; Zhang, Y.; Schmelzer, K.; Lee, T. S.; Fang, X.; Zhu, Y.; Spector, A. A.; Gill, S.; Morrisseau, C.; Hammock, B. D.; Shyy, J. Y. J. *Proc. Natl. Acad. Sci. USA* **2005**, *102*, 16747-16752.

<sup>417</sup> Ollivier, V.; Parry, G. C. N.; Cobb, R. R.; de Prost, D.; Mackman, N. *J. Biol. Chem.* **1996**, *271*, 20828-20835.

### 1.2.2 Effects of sEH inhibitors on pain

Neuropathic pain is a component of many disease states, such as T2DM, and there is no current treatment to suppress it. Despite the intensive efforts and resulting gains in understanding the mechanisms underlying neuropathic pain, limited success in therapeutic approaches has been attained. A recently identified, non-channel, non-neurotransmitter therapeutic target for pain is the enzyme sEH.<sup>418</sup> Given the effectiveness in reducing inflammation in some rodent models, it was not surprising that the inhibition of sEH also reduced *inflammatory and neuropathic pain*. This effect has been subsequently detected in multiple animal models of pain in which sEH inhibitors and EETs reduced pain perception.<sup>419,420</sup> The mechanism by which the sEH intervenes in the nociception process has been confirmed to imply opioid and GABAergic pathways, as well as PPARs.<sup>421</sup> As it will be discussed later on, the sEH has also been associated with the endoplasmic reticulum (ER) stress, a causative agent of neuropathic pain.<sup>422,423</sup>

Interestingly, the sEH inhibitors are more effective than the opioid morphine in relieving some pain conditions, with no change in behaviour or sedation, unlike many opiates. Some studies have demonstrated that the co-administration of sEH inhibitors and NSAIDs produced a valuable analgesic and anti-inflammatory effect with a reduction of cardiovascular toxicity derived from the NSAID treatment.<sup>424</sup> The efficacy of sEH inhibitors against diabetic neuropathic pain is noteworthy because of its potential to address the unmet therapeutic need of relieving this chronic pain condition.

### 1.2.3 sEH and cardiovascular disease

Another therapeutic area of interest for sEH inhibitors is cardiovascular diseases. EETs are putative endothelium-derived hyperpolarizing factors (EDHP) that increase open-state frequency of calcium ion channels leading to vasodilatation of vascular smooth muscle by activation of potassium channels, through a cAMP/protein kinase A-dependent mechanism that involves the intracellular translocation of transient receptor potential channels.<sup>425</sup> The identification of their vasodilatory properties suggested a role of the sEH in *blood pressure regulation*. EETs also promote natriuresis, regulating indirectly the blood

<sup>418</sup> Hammock, B. D.; Wagner, K.; Inceoglu, B. *Pain Manag.* **2011**, *1*, 383-386.

<sup>419</sup> Wagner, K.; Inceoglu, B.; Dong, H.; Yang, J.; Hwang, S. H.; Jones, P.; Morisseau, C.; Hammock, B. D. *Eur. J. Pharmacol.* **2013**, *700*, 93-101.

<sup>420</sup> Sing, K.; Lee, S.; Liu, J.; Wagner, K. M.; Pakhomova, S.; Dong, H.; Morisseau, C.; Fu, S. H.; Yang, J.; Wang, P.; Ulu, A.; Mate, C. A.; Nguyen, L. V.; Hwang, S. H.; Edin, M. L.; Mara, A. A.; Wul, H.; Newcomer, M. E.; Zeldin, D. C.; Hammock, B. D. *J. Med. Chem.* **2014**, *57*, 7016-7030.

<sup>421</sup> Pillarisetti, S.; Khanna, I. *Drug Discov. Today* **2015**, *In press*. DOI: 10.1016/j.drudis.2015.07.017.

<sup>422</sup> Bettaieb, A.; Nagata, N.; Aboubechara, D.; Chahed, S.; Morisseau, C.; Hammock, B. D.; Haj, F. G. *J. Biol. Chem.* **2013**, *288*, 14189-14199.

<sup>423</sup> Inceoglu, B.; Bettaieb, A.; Trindade da Silva, C. A.; Lee, K. S. S.; Haj, F. G.; Hammock, B. D. *Proc. Natl. Acad. Sci. USA* **2015**, *112*, 9082-9087.

<sup>424</sup> Schmelzer, K. R.; Inceoglu, B.; Kubala, L.; Kim, I.; Jinks, S. L.; Eiserich, J. P.; Hammock, B. D. *Proc. Natl. Acad. Sci. USA* **2006**, *103*, 13646-13651.

<sup>425</sup> Fleming, I.; Rueben, A.; Popp, R.; Fisslthaler, B.; Schrodt, S.; Sander, A.; Haendeler, J.; Falck, J. R.; Morisseau, C.; Hammock, B. D.; Busse, R. *Arterioscler. Thromb. Vasc. Biol.* **2007**, *27*, 2612-2618.

pressure.<sup>426</sup> This hypothesis has been confirmed in several studies using inhibitors of sEH, which led to an increase in the EETs' levels, resulting in a reduction of blood pressure in angiotensin-driven hypertensive rodent models.<sup>427</sup>

Ulu *et al.* showed that inhibition of sEH in a mammalian model of *atherosclerosis* by an orally administered agent reduced the formation of aortic plaques.<sup>428</sup> A recent study performed with mice treated with a sEH inhibitor revealed a reduction in the size of atherosclerotic plaques, along with an improvement in the cholesterol levels.<sup>429</sup> Numerous studies with sEH inhibitors have also shown cardiovascular-protective effects in cerebral and cardiac ischaemia, arrhythmia, hypertrophy and blood clotting,<sup>430,431,432,433</sup> proving once more the great potential of the sEH as a *cardiovascular regulator*.

The data regarding the cardiovascular effects of sEH inhibition has been compiled in several reviews.<sup>408,412,434,435</sup> These findings encourage the use of sEH inhibitors in patients who have cardiovascular problems.

#### 1.2.4 Role of sEH in the development of diabetes and metabolic syndrome. Involvement of ER stress

Metabolic processes are coordinately regulated by lipids, where EETs display a significant role in the pathophysiology of the endocrine system in relation to glucose homeostasis.<sup>406</sup> Whilst EETs and sEH inhibitors do not alter the levels of glucose and insulin in healthy patients, they have proven efficient in the regulation of glycemic states in some models of diabetes and MetS. Luo *et al.* demonstrated that sEH inhibitors or sEH knockout [*EHPX2*(<sup>-/-</sup>)] control glucose homeostasis in streptozotocin-treated mice. Specifically, they observed reduction of the glycemic levels, increase of insulin secretion and islet apoptosis reduction.<sup>436</sup> These alterations of the pancreatic islets and the improvement of the glucose homeostasis have been also confirmed in an animal model of insulin resistance.<sup>437</sup>

<sup>426</sup> Imig, J. D. *Am. J. Physiol. Regul. Integr. Comp. Physiol.* **2004**, *287*, R3-5

<sup>427</sup> Loch, D.; Hoey, A.; Morisseau, C.; Hammock, B. O.; Brown, L. *Cell Biochem. Biophys.* **2007**, *47*, 87-98.

<sup>428</sup> Ulu, A.; Davis, B. B.; Tsai, H.; Kim, I.; Morisseau, C.; Inceoglu, B.; Fiehn, O.; Hammock, B. D.; Weiss, R. H. *J. Cardiovasc. Pharmacol.* **2008**, *52*, 314-323.

<sup>429</sup> Shen, L.; Peng, H.; Peng, R.; Fan, Q.; Zhao, S.; Xu, D.; Morisseau, C.; Chiamvimonvat, N.; Hammock, B. D. *Atherosclerosis* **2015**, *239*, 557-565.

<sup>430</sup> Shrestha, A.; Krishnamurthy, P. T.; Thomas, P.; Hammock, B. D.; Hwang, S. H. *J. Pharm. Pharmacol.* **2014**, *66*, 1251-1258.

<sup>431</sup> Xu, D.; Davis, B. B.; Wang, Z.; Zhao, S.; Wasti, B.; Liu, Z.; Li, N.; Morisseau, C.; Chiamvimonvat, N.; Hammock, B. D. *Int. J. Cardiol.* **2013**, *167*, 1298-1304.

<sup>432</sup> Zhang, W.; Otsuka, T.; Sugo, N.; Ardeshiri, A.; Alhadid, Y. K.; Iliff, J. J.; DeBarber, A. E.; Koop, D. R.; Alkayed, N. J. *Stroke* **2008**, *39*, 2073-2078.

<sup>433</sup> Xu, D.; Li, N.; He, Y.; Timofeyev, V.; Lu, L.; Tsai, H.; Kim, I.; Tuteja, D.; Mateo, R. K. P.; Singapur, A.; Davis, B. B.; Low, R.; Hammock, B. D.; Chiamvimonvat, N. *Proc. Natl. Acad. Sci. USA* **2006**, *103*, 18733-18738.

<sup>434</sup> Duflo, T.; Roche, C.; Lamoureux, F.; Guerrot, D.; Bellien, J. *Expert Opin. Drug Discov.* **2014**, *9*, 1-15.

<sup>435</sup> Deng, Y.; Thenken, K. N.; Lee, C. R. *J. Mol. Cell. Cardiol.* **2010**, *48*, 331-353.

<sup>436</sup> Luo, P.; Chang, H. H.; Zhou, Y.; Zhang, S.; Hwang, S. H.; Morisseau, C.; Wang, C.-Y.; Inscho, E. W.; Hammock, B. D.; Wang, M. H. *J. Pharmacol. Exp. Ther.* **2010**, *334*, 430-438.

<sup>437</sup> Luria, A.; Beltaieb, A.; Xi, Y.; Shieh, G.-J.; Liu, H.-C.; Inoue, H.; Tsai, H.-J.; Imig, J. D.; Haj, F. G.; Hammock, B. D. *Proc. Natl. Acad. Sci. USA* **2011**, *108*, 9038-9043.



EETs also regulate the levels of lipids and adipogenesis by activation of PPARs.<sup>438</sup> In addition, the diet-induced MetS in rats was ameliorated with the administration of sEH inhibitors, with a notable reduction of the blood pressure and the body weight gain, an increase of the insulin sensitivity and an improvement of the inflammation markers.<sup>439</sup> Moreover, sEH has been related to the ER stress in liver and adipose tissue, whose dysfunction is a contributor to metabolic diseases.<sup>422</sup> Perturbation of the ER function and chronic ER stress are also associated with many other pathologies ranging from neurodegenerative diseases to cancer and inflammation.<sup>440</sup> ER stress will be covered in more depth later on in the present chapter.

The (patho)physiological importance of the sEH in the glucose and lipid homeostasis indicates that treatment with sEH inhibitors may address major comorbidities of diabetes, obesity and MetS.

### 1.2.5 sEH inhibition for other potential clinical applications

The inhibition of the sEH has been studied for other conditions with positive results. In brief, inhibitors of the sEH display a protective effect on renal damage induced by hypertension or inflammation.<sup>441,442</sup> Furthermore, the inhibition of sEH has resulted effective in the treatment of chronic obstructive pulmonary disease, especially when cigarette smoke is a risk factor, and pulmonary fibrosis.<sup>443,444,445</sup> On the other hand, because of the structural similarity of some inhibitors of sEH with sorafenib, the only FDA-approved small molecule used for the treatment of advanced hepatocellular carcinoma, their cytotoxicities were also similar to sorafenib in various human cancer cell lines.<sup>446,447</sup>

---

<sup>438</sup> De Taeye, B. M.; Morisseau, C.; Coyle, J.; Covington, J. W.; Luria, A.; Yang, J.; Murphy, S. B.; Friedman, D. B.; Hammock, B. B.; Vaughan, D. E. *Obesity* **2010**, *18*, 489-498.

<sup>439</sup> Iyer, A.; Kauter, K.; Alam, M. A.; Hwang, S. H.; Morisseau, C.; Hammock, B. D.; Brown, L. *Exp. Diabetes Res.* **2012**, *2012*, 14-16.

<sup>440</sup> Wang, S.; Kaufman, R. J. *J. Cell Biol.* **2012**, *197*, 857-867.

<sup>441</sup> Zhao, X.; Yamamoto, T.; Newman, J. W.; Kim, I. H.; Watanabe, T.; Hammock, B. D.; Stewart, J.; Pollock, J. S.; Pollock, D. M.; Imig, J. D. *J. Am. Soc. Nephrol.* **2004**, *15*, 1244-1253.

<sup>442</sup> Olearczyk, J. J.; Quigley, J. E.; Mitchell, B. C.; Yamamoto, T.; Kim, I.-H.; Newman, J. W.; Luria, A.; Hammock, B. D.; Imig, J. D. *Clin. Sci.* **2009**, *116*, 61-70.

<sup>443</sup> Wang, L.; Yang, J.; Guo, L.; Uyeminami, D.; Dong, H.; Hammock, B. D.; Pinkerton, K. E. *Am. J. Respir. Cell Mol. Biol.* **2012**, *46*, 614-622.

<sup>444</sup> Podolin, P. L.; Bolognese, B. J.; Foley, J. F.; Long, E.; Peck, B.; Umbrecht, S.; Zhang, X.; Zhu, P.; Schwartz, B.; Xie, W.; Quinn, C.; Qi, H.; Sweitzer, S.; Chen, S.; Galop, M.; Ding, Y.; Belyanskaya, S. L.; Israel, D. I.; Morgan, B. A.; Behm, D. J.; Marino, J. P.; Kurali, E.; Barnette, M. S.; Mayer, R. J.; Booth-Genthe, C. L.; Callahan, J. F. *Prostaglandins Other Lipid Mediators* **2013**, *104-105*, 25-31.

<sup>445</sup> Zhou, Y.; Sun, G. Y.; Liu, T.; Duan, J. X.; Zhou, H. F.; Lee, K. S.; Hammock, B. D.; Fang, X.; Jiang, J. X.; Guan, C. X. *Cell Tissue Res.* **2015**, *Ahead of print*. DOI: 10.1007/s00441-015-2262-0.

<sup>446</sup> Weckslar, A. T.; Hwang, S. H.; Wettersten, H. I.; Gilda, J. E.; Patton, A.; Leon, L. J.; Carraway, K. L.; Gomes, A. V.; Baar, K.; Weiss, R. H.; Hammock, B. D. *Anticancer. Drugs* **2014**, *25*, 433-446.

<sup>447</sup> Weckslar, A. T.; Hwang, S. H.; Liu, J. Y.; Wettersten, H. I.; Morisseau, C.; Wu, J.; Weiss, R. H.; Hammock, B. D. *Cancer Chemother. Pharmacol.* **2014**, *75*, 161-171.

Besides, schizophrenia, seizures and hepatic fibrosis has been recently related to sEH.<sup>448,449,450</sup> The potential clinical indications of sEH inhibitors are shown in Figure 72.

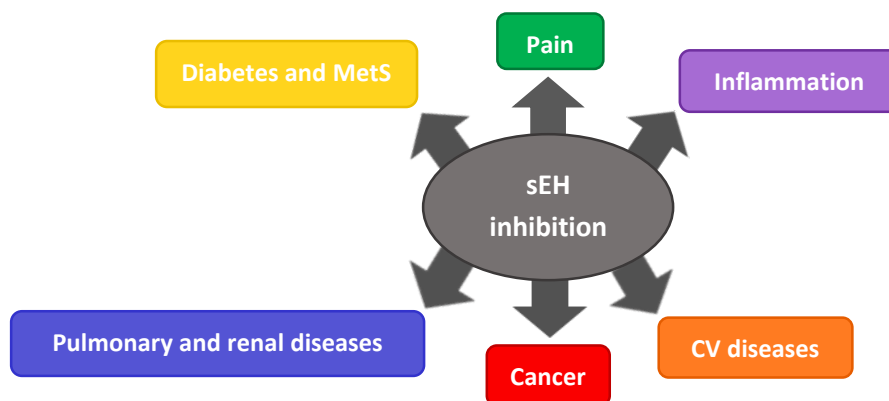


Fig. 72. Potential clinical indications for the use of sEH inhibitors.

### 1.3 sEH: crystal structure, catalytic mechanism, tissue expression and regulation

There are several mammalian epoxide hydrolases, including microsomal EH (mEH) and sEH, which are named according to their subcellular location. They can be also differentiated by their substrate specificity. Whereas mEH activity is focused on the metabolism of xenobiotics, where it degrades preferentially epoxides on cyclic systems, such as arenes, sEH is prone to hydrolyze endogenous epoxide-fatty acids, such as the oxidation products of linoleic acid, linolenic acid or the EETs themselves.<sup>451</sup> 14,15-EET is the preferred substrate of sEH with the highest  $V_{max}$  and lowest  $K_m$ , followed by 11,12-EET, 8,9-EET and 5,6-EET.<sup>405</sup> Other epoxide hydrolases have been identified and studied, such as cholesterol and hepoxilin epoxide hydrolases, but they are beyond the purpose of the present thesis.<sup>452</sup>

The *EPHX-2* gene, located on the short arm of chromosome 8, with nearly 45 kb and 19 exons, encodes the sEH.<sup>410</sup> Human sEH is a homodimer formed by two ~ 62 kDa monomeric subunits arranged in an anti-parallel fashion and separated by a short proline-rich linker (Fig. 73).<sup>453</sup> The epoxide hydrolase activity resides in the C-terminal domain, whereas the N-terminal domain exhibits a phosphatase activity that apparently acts on lysophosphatidic acids.<sup>454</sup>

<sup>448</sup> Ma, M.; Ren, Q.; Fujita, Y.; Ishima, T.; Zhang, J. C.; Hashimoto, K. *Pharmacol. Biochem. Behav.* **2013**, *110*, 98-103.

<sup>449</sup> Inceoglu, B.; Zolkowska, D.; Yoo, H. J.; Wagner, K. M.; Yang, J.; Hackett, E.; Hwang, S. H.; Lee, K. S. S.; Rogawski, M. A.; Morisseau, C.; Hammock, B. D. *PLoS One* **2013**, *8*, 8-17.

<sup>450</sup> Harris, T. R.; Bettaieb, A.; Kodani, S.; Dong, H.; Myers, R.; Chiamvimonvat, N.; Haj, F. G.; Hammock, B. D. *Toxicol. Appl. Pharmacol.* **2015**, *286*, 102-111.

<sup>451</sup> Newman, J. W.; Morisseau, C.; Hammock, B. D. *Prog. Lipid Res.* **2005**, *44*, 1-51.

<sup>452</sup> Fretland, A. J.; Omiecinski, C. J. *Chem. Biol. Interact.* **2000**, *129*, 41-59.

<sup>453</sup> Gomez, G. A.; Morisseau, C.; Hammock, B. D.; Christianson, D. W. *Biochemistry* **2004**, *43*, 4716-4723.

<sup>454</sup> Morisseau, C.; Schebb, N. H.; Dong, H.; Ulu, A.; Aronov, P. A.; Hammock, B. D. *Biochem. Biophys. Res. Commun.* **2012**, *419*, 796-800.

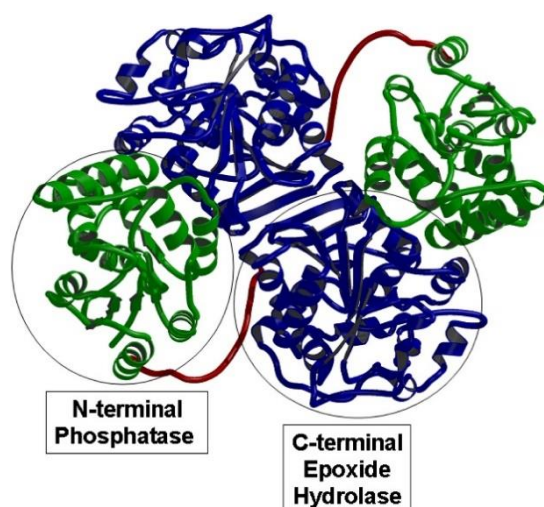


Fig. 73. X-ray crystal structure of the sEH homodimer. PDB code: 1S80.<sup>455</sup>

A prerequisite for the development of potent and selective inhibitors is the understanding of the sEH mechanism of action. The catalytic mechanism of the sEH has been elucidated in the last few years with the aim of defining the key residues involved in the hydrolysis. As a result, X-ray crystallographic data has revealed that the hydrolase catalytic pocket consists of two tyrosine residues (Tyr382 and Tyr465) which act as hydrogen bond donors to promote epoxide-ring opening by the backside attack *via* an  $S_N2$ -type reaction of an aspartic acid residue (Asp334) to form a hydroxyl alkyl-enzyme intermediate (Fig. 74).<sup>411</sup> In this step, the nucleophilic Asp334 is oriented and activated by a histidine residue (His523). Then, different proton shifts, which have yet to be proven, occur and a water molecule attacks the intermediate releasing the diol product and the original enzyme.

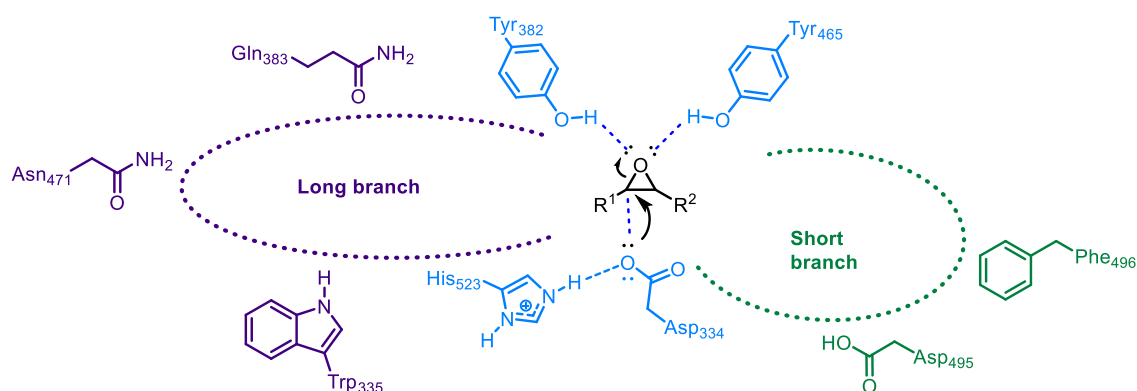
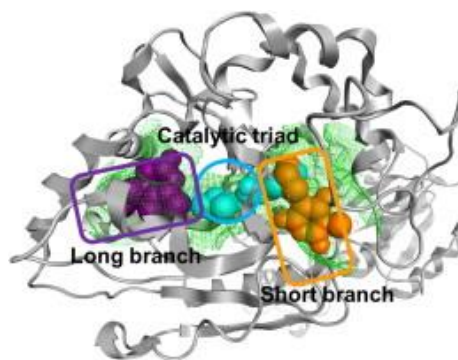


Fig. 74. Schematic representation of the polarization of the epoxide by the two tyrosine residues and subsequent attack of the aspartic acid residue. Catalytic triad (blue), long branch (purple) and short branch (green).

<sup>455</sup> Gorman, J.; Shapiro, L. *Acta Crystallogr. Sect. D* **2004**, *60*, 1600-1605.

Extensive enzymological and structural studies revealed an “L”-shaped hydrophobic tunnel of the binding site, whose branches measure 10 and 15 Å, respectively, and with the catalytic triad placed between them (Fig. 75). Albeit being largely hydrophobic, each branch of the pocket features residues that are involved in specific interactions, such as hydrogen bonds, Van der Waals and  $\pi$ -stacking interactions, and are open to the solvent.



**Fig. 75.** Overview of the catalytic pocket, with representative fragments bound to each site (catalytic triad: cyan; long branch: purple; short branch: orange).<sup>456</sup>

Although at different levels, sEH is expressed in all organs and tissues and differs from the expression of mEH. The specific activity of sEH is highest in the liver, followed by kidney, heart, lung and brain.<sup>457,458</sup> In a lesser extent, sEH activity has been detected in spleen, adrenals, intestine, urinary bladder, vascular endothelium and smooth muscle, placenta, skin, mammary gland, testicles and leucocytes.<sup>451</sup> Concerning the regulation of the sEH, both PPAR- $\alpha$  and PPAR- $\gamma$  agonists, e.g. fibrates and glitazones, have proven to alter sEH expression, underlying the close relationship between PPARs and sEH.<sup>416,459,460</sup> Angiotensin II and homocysteine, which appears to depend on activating transcription factor 6 (ATF6), are inducers of sEH.<sup>461,462</sup>

#### 1.4 Discovery of sEH inhibitors

In an effort to explore sEH inhibition as an avenue for the development of therapeutic agents, many academic and industrial groups have entered the arena of the discovery of potent sEH inhibitors. The research group of Prof. Dr. Hammock has been the major contributor to sEH inhibitors.<sup>463,464</sup> A detailed understanding of the catalytic mechanism of the enzyme and later multiple crystal structures helped in the identification of a diversity of functional groups that can be considered for the ligand design. The structural types of

<sup>456</sup> Amano, Y.; Yamaguchi, T.; Tanabe, E. *Bioorg. Med. Chem.* **2014**, *22*, 2427-2434.

<sup>457</sup> Gill, S. S.; Hammock, B. D. *Biochem. Pharmacol.* **1980**, *29*, 389-395.

<sup>458</sup> Enayetallah, A. E.; French, R. A.; Thibodeau, M. S.; Grant, D. F. *J. Histochem. Cytochem.* **2004**, *52*, 447-454.

<sup>459</sup> Fang, X.; Hu, S.; Watanabe, T.; Weintraub, N. L.; Snyder, G. D.; Yao, J.; Liu, Y.; Shyy, J. J. Y.; Hammock, B. D.; Spector, A. A. *J. Pharmacol. Exp. Ther.* **2005**, *314*, 260-270.

<sup>460</sup> Wong, S. L.; Huang, Y. *Clin. Exp. Pharmacol. Physiol.* **2011**, *38*, 356-357.

<sup>461</sup> Ai, D.; Fu, Y.; Guo, D.; Tanaka, H.; Wang, N.; Tang, C.; Hammock, B. D.; Shyy, J. J. Y.; Zhu, Y. *Proc. Natl. Acad. Sci. USA* **2007**, *104*, 9018-9023.

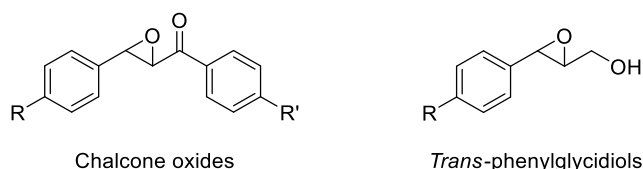
<sup>462</sup> Zhang, D.; Xie, X.; Chen, Y.; Hammock, B. D.; Kong, W.; Zhu, Y. *Circ. Res.* **2012**, *110*, 808-817.

<sup>463</sup> Shen, H. C. *Expert Opin. Ther. Pat.* **2010**, *20*, 941-956.

<sup>464</sup> Shen, H. C.; Hammock, B. D. *J. Med. Chem.* **2012**, *55*, 1789-1808.

sEH inhibitors are extremely broad, which is consistent with the wide binding pocket of the enzyme.

From a historical point of view, the first generation of sEH inhibitors were potent competitive epoxide molecules and included chalcone oxides and *trans*-3-phenylglycidols (Fig. 76).<sup>465,466</sup> These compounds were generally transient inhibitors with low turnover rates. Also, these substrates were rapidly inactivated by glutathione transferases, rendering them ineffective in *in vitro* and *in vivo* assays.



**Fig. 76.** Early inhibitors of sEH bearing an epoxide moiety. R and R' are various substituents.

Just to mention, heavy metals such as Zn, Hg, Cu and Cd have been reported also to inhibit sEH activity *via* interactions with the phosphatase domain.<sup>467</sup>

Since the early 2000s, several pharmacophores have emerged and major advances in the potency and pharmacokinetic properties of the inhibitors have been made. It was demonstrated that functional groups such as ureas, carbamates, amides, thioesters, carbonates, esters, thioureas, guanidines, *inter alia*, fit well into the active site and display a similar binding to that of endogenous epoxides.<sup>468,469,470,471</sup> Therefore, in recent years there has been a significant and rapid development of compounds featuring mainly a urea or amide group as reversible sEH inhibitors. The urea group, which is the most exploited functionality for the design of sEH inhibitors, mimics the endogenous epoxide substrate by binding to the key residues of the catalytic triad. Thus, the carbonyl oxygen is involved in a hydrogen bonding interaction with both tyrosines, Tyr382 and Tyr465, whereas the NH groups act as hydrogen bond donors to the aspartic acid residue Asp334 (Fig. 77).<sup>472</sup> These specific interactions are responsible for their consideration as tight-binding sEH inhibitors, referred as “transition state competitive inhibitors”.<sup>473</sup>

<sup>465</sup> Morisseau, C.; Du, G.; Newman, J. W.; Hammock, B. D. *Arch. Biochem. Biophys.* **1998**, *356*, 214-228.

<sup>466</sup> Dietze, E. C.; Kuwano, E.; Casas, J.; Hammock, B. D. *Biochem. Pharmacol.* **1991**, *42*, 1163-1175.

<sup>467</sup> Draper, A. J.; Hammock, B. D. *Toxicol. Sci.* **1999**, *52*, 23-32.

<sup>468</sup> Morisseau, C.; Goodrow, M. H.; Dowdy, D.; Zheng, J.; Greene, J. F.; Sanborn, J. R.; Hammock, B. D. *Proc. Natl. Acad. Sci. USA* **1999**, *96*, 8849-8854.

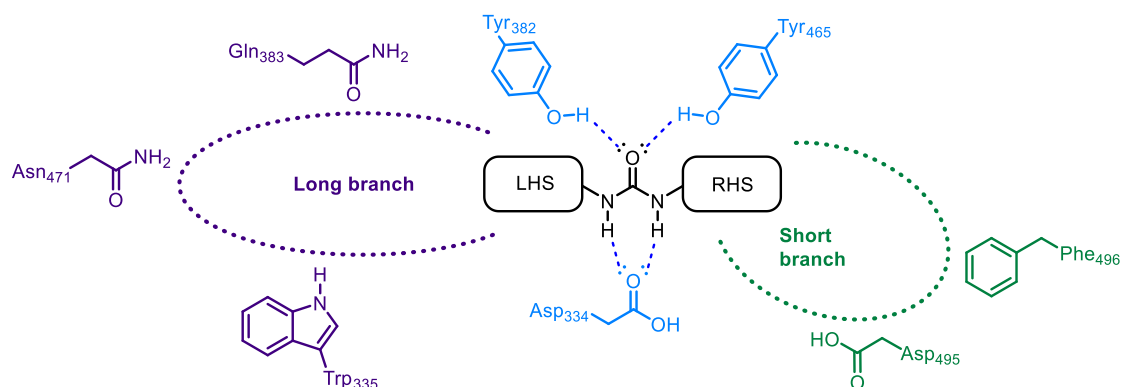
<sup>469</sup> Nakagawa, Y.; Wheelock, C. E.; Morisseau, C.; Goodrow, M. H.; Hammock, G.; Hammock, B. D. *Bioorg. Med. Chem.* **2000**, *8*, 2663-2675.

<sup>470</sup> McElroy, N. R.; Jurs, P. C.; Morisseau, C.; Hammock, B. D. *J. Med. Chem.* **2003**, *46*, 1066-1080.

<sup>471</sup> Anandan, S. K.; Do, Z. N.; Webb, H. K.; Patel, D. V.; Gless, R. D. *Bioorg. Med. Chem. Lett.* **2009**, *19*, 1066-1070.

<sup>472</sup> Gomez, G. A.; Morisseau, C.; Hammock, B. D.; Christianson, D. W. *Protein Sci.* **2006**, *15*, 58-64.

<sup>473</sup> Kodani, S. D.; Hammock, B. D. *Drug Metab. Dispos.* **2015**, *43*, 788-802.



**Figure 77.** General binding mode of urea-based sEH inhibitors and key residues of the binding pocket of sEH: catalytic triad (blue), long branch (purple) and short branch (green). LHS: left-hand side; RHS: right-hand side.

1,3-Disubstituted ureas have undergone a remarkable evolution since their discovery. The earliest symmetrical  $N,N'$ -disubstituted ureas displayed good inhibitory activities. Their design was based on the fact that the catalytic triad is in between two hydrophobic pockets, which could be filled with cycloalkyl groups for the establishment of Van der Waals-like interactions. Thus, the side chains of the urea were selected according to these premises and DCU ( $N,N'$ -dicyclohexylurea) appeared as a promising inhibitor with proven efficacy lowering blood pressure in hypertensive rats.<sup>474</sup> Other carbocyclic substituents were introduced, such as phenyl, cyclooctyl and adamantyl groups.<sup>475</sup> Despite the fact that this type of compounds showed potent inhibitory activities, they lacked optimal physicochemical properties for good oral absorption. These dialkylureas had high crystal lattice energies as indicated by their high melting points, and limited solubility in water.

From this first series of compounds, the adamantane nucleus afforded a superior enzyme inhibition. Taking into account the characteristics of the binding site of sEH and the overall high hydrophobicity of the tunnel, the introduction of an adamantane ring has proven a successful strategy for the space-filling of the cavity. Thus, several sEH inhibitors incorporate an adamantane moiety on the LHS exhibiting high affinity and potency. Since the bulky adamantane ring can occupy one of two sides of the active site tunnel, it is possible that 1-adamantyl-urea-based inhibitors bind in the active site of human sEH with different orientations.<sup>476</sup> Figure 78a highlights the binding mode of an adamantane-based inhibitor. In the present introduction, only the adamantane-based sEH inhibitors will be examined, despite the fact that further development has been done regarding other scaffolds, mainly substituted phenyl rings (Fig. 78b).<sup>477,478</sup>

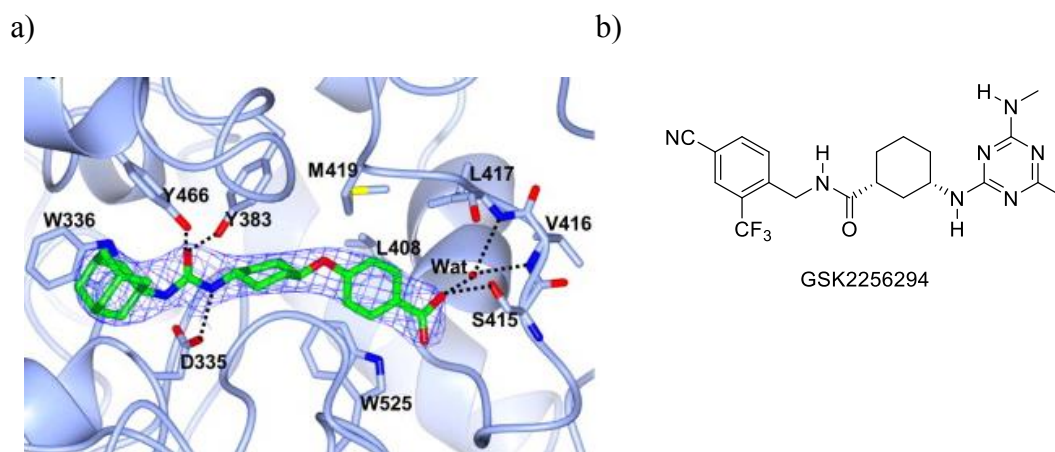
<sup>474</sup> Yu, Z.; Xu, F.; Huse, L. M.; Morisseau, C.; Draper, A. J.; Newman, J. W.; Parker, C.; Graham, L.; Engler, M. M.; Hammock, B. D.; Zeldin, D. C.; Kroetz, D. L. *Circ. Res.* **2000**, *87*, 992-998.

<sup>475</sup> Morisseau, C.; Goodrow, M. H.; Newman, J. W.; Wheelock, C. E.; Dowdy, D. L.; Hammock, B. D. *Biochem. Pharmacol.* **2002**, *63*, 1599-1608.

<sup>476</sup> Chen, H.; Zhang, Y.; Ye, C.; Feng, T. T.; Han, J. G. *J. Biomol. Struct. Dyn.* **2014**, *32*, 1231-1247.

<sup>477</sup> Anandan, S.-K.; Webb, H. K.; Do, Z. N.; Gless, R. D. *Bioorg. Med. Chem. Lett.* **2009**, *19*, 4259-4263.

<sup>478</sup> Rose, T. E.; Morisseau, C.; Liu, J.-Y.; Inceoglu, B.; Jones, P. D.; Sanborn, J. R.; Hammock, B. D. *J. Med. Chem.* **2010**, *53*, 7067-7075.



**Figure 78.** (a) Crystal structure of *t*-AUCB (*vide infra*) bound to sEH. PDB code: 3WKE;<sup>456</sup> (b) Structure of GlaxoSmithKline's candidate that entered phase I clinical trials in 2013.<sup>444,473</sup>

Structural refinement of the first generation of inhibitors led to the discovery of adamantyl ureas attached to long alkyl chains featuring a terminal polar functionality, so as to resemble the carboxylic acid in a putative endogenous substrate, in an attempt to render these compounds more druggable. In this manner, *N*-adamantanyl-*N'*-dodecanoic acid urea (AUDA) emerged as an improved inhibitor with excellent inhibition of murine and human sEH and enhanced water solubility.<sup>479</sup> AUDA has been extensively used as a tool molecule to validate efficacy in models of hypertension, cardio-protection and inflammation.<sup>431,480,481</sup> Addition of polar ethylene glycol linkers in the alkyl chain afforded new compounds with similar properties as AUDA, such as *N*-adamantanyl-*N'*-(5-(2-(2-ethoxyethoxy)ethoxy)pentyl)urea (AEPU).<sup>482</sup> Although improving water solubility, these compounds were rapidly metabolized through  $\beta$ -oxidation of the alkyl chain.<sup>483</sup>

To avoid this issue, the incorporation of a conformationally restricted unit on the RHS of the molecule, such as an heterocycle or a phenyl ring, led to sEH inhibitors with improved metabolic stability whilst maintaining the potency.<sup>484,478</sup> Here is where came into play the “pharmacophore model”, which may consist of three parts, the “primary pharmacophore or PP”, the “secondary pharmacophore or SP” and the “tertiary pharmacophore or TP” (Fig. 79).<sup>485,486</sup> PP refers to the urea, amide, carbamate, ... group

<sup>479</sup> Morisseau, C.; Goodrow, M. H.; Newman, J. W.; Wheelock, C. E.; Dowdy, D. L.; Hammock, B. D. *Biochem. Pharmacol.* **2002**, *63*, 1599-1608.

<sup>480</sup> Dorrance, A. M.; Rupp, N.; Pollock, D. M.; Newman, J. W.; Hammock, B. D.; Imig, J. D. *J. Cardio. Pharm.* **2005**, *46*, 842-848.

<sup>481</sup> Imig, J. D.; Zhao, Z.; Zaharis, C. Z.; Olearczyk, J. J.; Pollock, D. M.; Newman, J. W.; Kim, I. H.; Watanabe, T.; Hammock, B. D. *Hypertension* **2005**, *46*, 975-981.

<sup>482</sup> Hammock, B. D.; Kim, I. H.; Morisseau, C.; Watanabe, T.; Newman, J. W. Inhibitors of the soluble epoxide hydrolase. US 2005/0164951 A1.

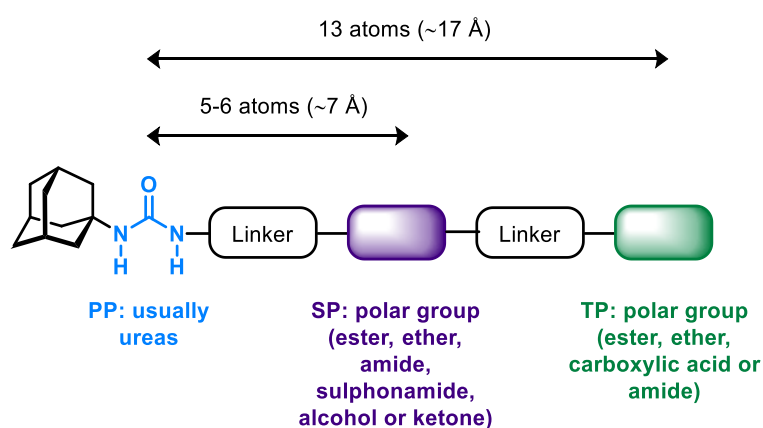
<sup>483</sup> Hwang, S. H.; Tsai, H.; Liu, J.; Morisseau, C.; Hammock, B. D. *J. Med. Chem.* **2007**, *50*, 3825-3840.

<sup>484</sup> Jones, P. D.; Tsai, H. J.; Do, Z. N.; Morisseau, C.; Hammock, B. D. *Bioorg. Med. Chem. Lett.* **2006**, *16*, 5212-5216.

<sup>485</sup> Kim, I.; Morisseau, C.; Watanabe, T.; Hammock, B. D. *J. Med. Chem.* **2004**, *47*, 2110-2122.

<sup>486</sup> Kim, I.; Tsai, H.; Nishi, K.; Kasagami, T.; Morisseau, C.; Hammock, B. D. *J. Med. Chem.* **2007**, *50*, 5217-5226.

bearing the bulky hydrophobic adamantane nucleus on one side. SP is a polar group, e.g. ester, ether, amide, sulphonamide, alcohol or ketone, normally positioned approximately 7 Å from the carbonyl group of the PP.<sup>479,487</sup> In addition, a polar TP such as ester, ether, carboxylic acid, or amide that is 13 atoms or ~ 17 Å away from the urea carbonyl has also been identified and applied. Hydrophobic linkers join the PP to the SP, and the SP to the TP, where the presence of cyclic groups seem to increase oral bioavailability compared to linear alkyl chains.<sup>488</sup> Apart from improving the metabolic stability of the RHS, the incorporation of the SP and TP enhanced the water solubility and lowered the melting points.



**Figure 79.** Representation of the “pharmacophore model”.

Table 16 summarizes the evolution of the adamantane-based sEH inhibition over the course of their development.

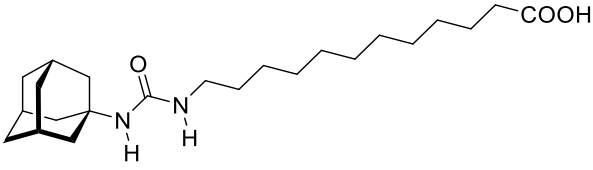
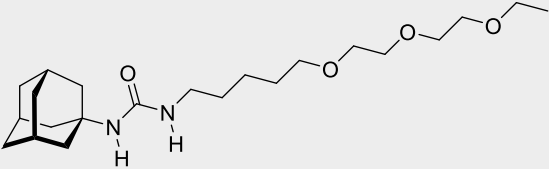
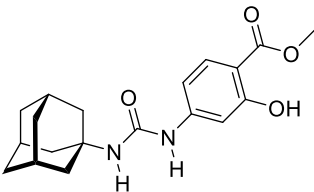
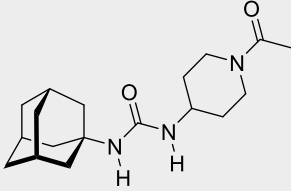
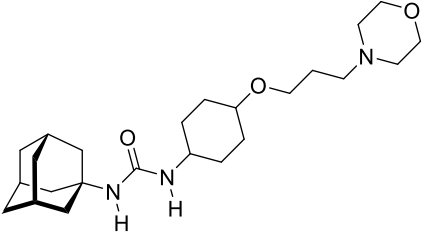
**Table 16.** Representative adamantane-based sEH inhibitors and their evolution in chronological order.

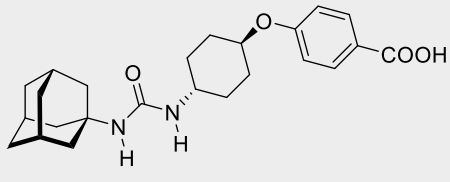
sEH inhibitor	Pharmacophore model & Structural features	Characteristics
<p><i>N</i>-adamantyl-<i>N'</i>-cyclohexylurea (ACU)</p>	PP; two hydrophobic side chains	High potency, low solubility, poor PK

<sup>487</sup> Kim, I. H.; Heirtzler, F. R.; Morisseau, C.; Nishi, K.; Tsai, H. J.; Hammock, B. D. *J. Med. Chem.* **2005**, *48*, 3621-3629.

<sup>488</sup> Kasagami, T.; Kim, I. H.; Tsai, H. J.; Nishi, K.; Hammock, B. D.; Morisseau, C. *Bioorg. Med. Chem. Lett.* **2009**, *19*, 1784-1789.



 <p style="text-align: center;"><b>AUDA</b></p>	<p>“PP”; long carbon chain with a terminal carboxylic acid</p>	<p>High potency, improved solubility, poor PK</p>
 <p style="text-align: center;"><b>AEPU</b></p>	<p>“PP”; long carbon chain with ethylene glycol units</p>	<p>High potency, improved solubility, poor PK</p>
 <p style="text-align: center;"><b>4-(3-adamantan-1-yl-ureido)-2-hydroxybenzoic acid methyl ester (AUSM)</b></p>	<p>SP; benzoic acid methyl ester</p>	<p>High potency, improved solubility, enhanced PK</p>
 <p style="text-align: center;"><b>N-(1-acetylpiperidin-4-yl)-N'-adamantylurea (APAU, AR9281)</b></p>	<p>SP; conformationally restricted amide</p>	<p>High potency, improved solubility, enhanced PK</p>
 <p style="text-align: center;"><b>1-adamantan-1-yl-3-(4-(3-morpholinopropoxy)cyclohexyl)urea (AMCU)</b></p>	<p>TP; ether and morpholine ring groups as pharmacophores</p>	<p>High potency, improved solubility, enhanced PK</p>

 <p><i>trans</i>-4-[4-(3-adamantan-1-ylureido)cyclohexyloxy]benzoic acid (<i>t</i>AUCB)</p>	<p>TP; ether and carboxylic acid groups as pharmacophores</p>	<p>High potency, improved solubility, enhanced PK</p>
--	---	---

Among these compounds, APAU or AR9281, developed by Arête Therapeutics, was the only adamantane-based sEH inhibitor that reached phase II clinical trials. It showed a high level of safety but failed to show efficacy in early-stage hypertension and impaired glucose tolerance. This failure was attributed to poor PK properties or variable effects of the inhibitor.<sup>405,489</sup>

Regardless of the efforts made to procure drug candidates, it still remains a significant challenge to develop sEH inhibitors with excellent inhibitory activities and optimum solubility and PK profiles. A vast number of sEH inhibitors in development enclose an adamantane moiety, which possess particular properties that determine the behaviour of the future drug candidates:

- Its pronounced lipophilicity compromises negatively the overall water solubility of the molecule, which is an important physicochemical parameter in the early stages of drug discovery.<sup>490,491</sup> In addition, the general stability of the adamantyl compounds' crystal structures, indicated by their high melting points, leads to a general lack of solubility even in organic solvents.
- Besides, the adamantane nucleus is prone to rapid metabolism *in vivo* giving rise to a variety of inactive, hydroxylated derivatives and leading to low drug concentrations in blood and short *in vivo* half-life.
- Again, the high lipophilicity of the inhibitors furnished chiefly by the adamantyl unit results in an increased likelihood of binding to multiple targets, leading to apparent toxicity.<sup>492</sup>

Considering the above mentioned, it seems evident that the adamantane ring does not possess the optimal properties as a scaffold for sEH inhibition. A decrease in the overall lipophilicity will lead to more soluble and metabolically stable compounds, which will therefore be more “drug-like”.<sup>29,30</sup> In this sense, there is an urgent need for the development

<sup>489</sup> Clinical trials web site. AR9281. <https://www.clinicaltrials.gov/> (accessed on 5<sup>th</sup> September 2015).

<sup>490</sup> Bhattachar, S. N.; Deschenes, L. A.; Wesley, J. A. *Drug Discov. Today* **2006**, *11*, 1012-1018.

<sup>491</sup> Di, L.; Fish, P. V.; Mano, T. *Drug Discov. Today* **2012**, *17*, 486-495.

<sup>492</sup> Leeson, P. D.; Springthorpe, B. *Nat. Rev. Drug Discov.* **2007**, *6*, 881-890.

of new scaffolds that provide compounds with more optimal physicochemical properties to avoid attrition in later stages of the drug discovery process.


# Objetives

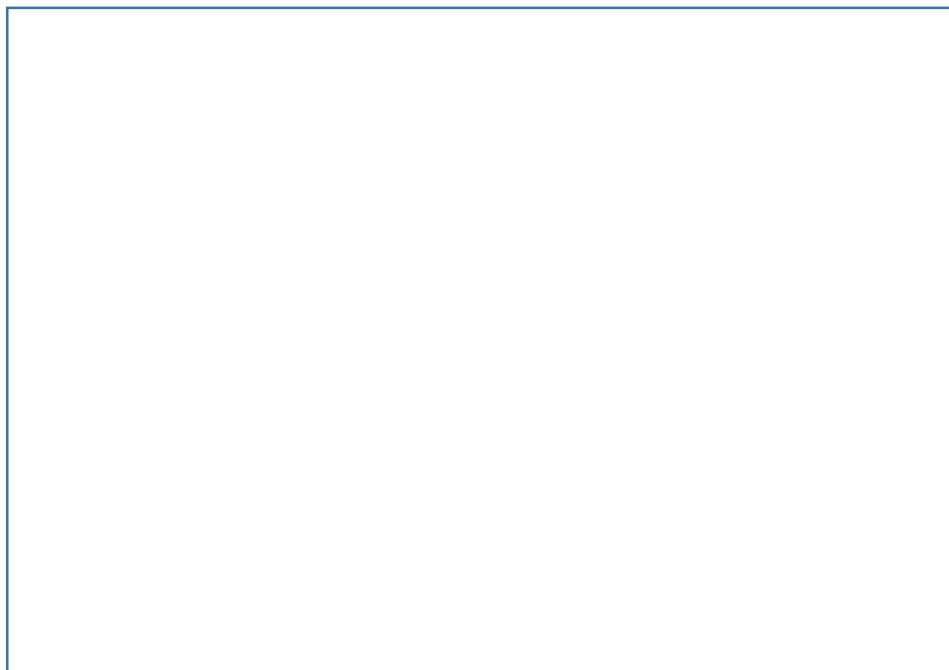


Regardless of the gigantic effort made from academic and industrial research groups in the development of drug candidates, only a few sEH inhibitors have entered into clinical trials. At the time of writing the present dissertation, no sEH inhibitor had got into the market, and only two compounds have reached human clinical trials, one of which contains an adamantane group, as mentioned previously. This points out that the drug discovery process of sEH inhibitors is complex and highly challenging. Some development limitations are: inappropriate physicochemical properties, especially high lipophilicity and low water solubility, and chemical and metabolic instability. Therefore, there is a demand for the development of new sEH inhibitors that, having an acceptable inhibitory activity, will overcome these issues.

The adamantane nucleus seems to be a privileged scaffold in sEH inhibitors since it is the most exploited bulky group when designing a new drug candidate. This precious ring, together with the urea group as primary pharmacophore, fits into one of the hydrophobic pockets of the catalytic site of the enzyme. However, considering that the adamantane does not possess the optimum properties (i.e. lipophilicity, water solubility, etc...) for a urea-based sEH inhibitor, we hypothesized that the replacement of the adamantane moiety by other polycyclic cage structures may afford compounds with improved PK and PD profiles by changes in the physicochemical properties, whilst maintaining a good binding affinity for the target.

In line with the previous chapter of the thesis, and taking advantage of the extended expertise of our research group in the synthesis of polycyclic scaffolds, we started a new project related to the discovery of novel sEH inhibitors bearing adamantane-like scaffolds as hydrophobic counterparts. Thus, these were the main goals of this chapter:

1. Synthesis of a variety of scaffolds, including , attached to an already reported substituted urea (Fig. 80).



**Fig. 80.** Replacement of the adamantane group by a variety of scaffolds.

2. Pharmacological evaluation of these scaffolds to provide useful information of the threshold of tolerance of the catalytic site to accept a diversity of structures. Determination of water solubility as well as calculation of  $\log P$  of each new compound to assess the changes in physicochemical properties.
3. Determination of the ability to ameliorate the ER stress in human hepatocytes of selected inhibitors, according to the results from 2. With the *in vitro* assays, the cell permeation and cytotoxicity will be also evaluated.

## **Results & Discussion**



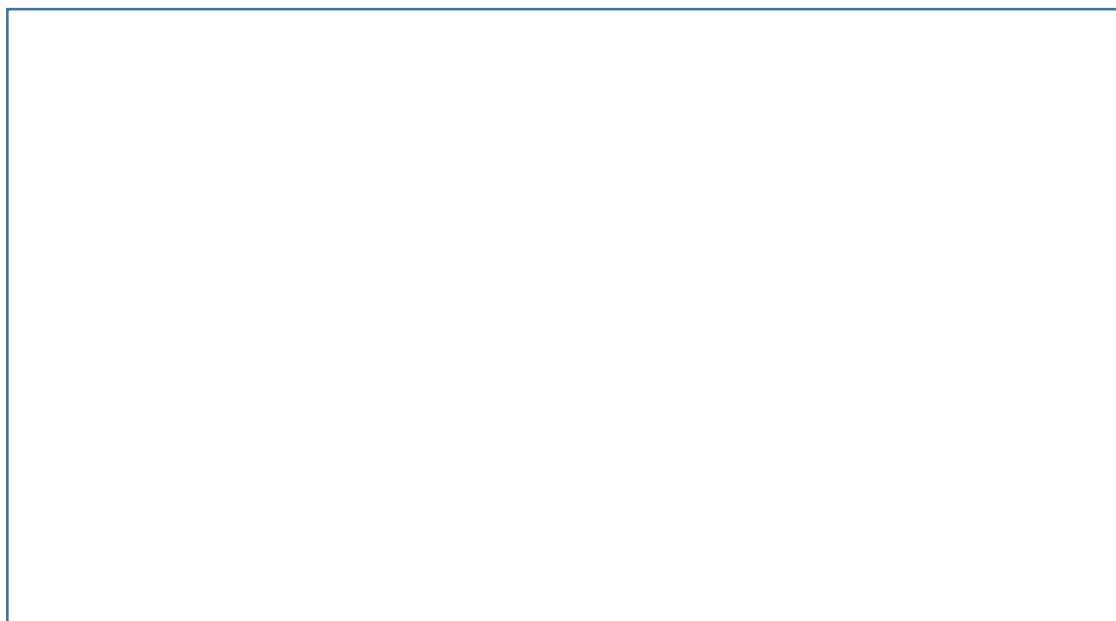


## 1. Scaffold-hopping approach for the development of new sEH inhibitors

From the available data regarding sEH and its inhibition by small molecules, we identified a few relevant issues:

- The adamantane ring is predominantly chosen as the bulky group for the space-filling of the hydrophobic pockets of the sEH catalytic site.
- On the other hand, the adamantane group provides a remarkable increase in the overall lipophilicity of the molecule, compromising the water solubility and the pharmacokinetic profile.
- From the crystal structure of sEH, it has been suggested that, while the catalytic tunnel is restricted around the catalytic residues, it enlarges as one moves away from the site of reaction to yield relatively large cavities. These structural features show that the enzyme can accommodate larger groups on both sides of the urea moiety.
- Additionally, polar groups can be incorporated into one of the alkyl substituents without loss of activity if they are placed at an appropriate distance from the urea function.

Considering the aforementioned, we aimed to pursue a small and medium-step scaffold-hopping approach *via* the replacement of the adamantane nucleus by diverse polycycles that possess different physicochemical properties and varied shapes and sizes (Fig. 81). *Scaffold-hopping* is a strategy widely applied in medicinal chemistry whose purpose is to identify novel structures that are active against a given target with acceptable pharmacological properties defined by marketed drugs.<sup>493</sup>



**Fig. 81.** Design of new sEH inhibitors by scaffold-hopping approach.

<sup>493</sup> Sun, H.; Tawa, G.; Wallqvist, A. *Drug Discov. Today* **2012**, *17*, 310-324.

The design of these compounds was carefully studied in order to fulfil most of the established criteria (potency, molecular weight and lipophilicity), wherein the adamantane-like ring plays a crucial role. Because of the shape and size of the active site tunnel as well as its hydrophobicity, varying the polycyclic cages may affect how the urea moiety of the molecule sits within the tunnel, thereby affecting inhibition. Bearing in mind the existence of residues capable of establishing hydrogen bonds and  $\pi$ -stacking interactions in the long branch of the binding site of sEH, we hypothesized that the

may be tolerated. In addition, the size and shape of that branch may assist the adjustment of the dimensions of the lipophilic group. Table 17 outlines the selected scaffolds, including their structural contributions and antecedent applications in medicinal chemistry.

**Table 17.** Selected polycycles for the design of novel sEH inhibitors. CB: cannabinoid receptor.

Entry	Scaffold	Structural features	Previous uses in medicinal chemistry
1			
2			

3	
4	
5	
6	
7	

In order to assess the effect of each new scaffold in the sEH inhibition, we placed them as the left-hand side (LHS) of the urea group and a selected unit from the literature was chosen as the right-hand side (RHS) (Fig. 82). Particularly, 2,3,4-trifluorophenyl group was selected due to its facile synthesis and high inhibitory activity against sEH. In fact, both 1-(1-adamantyl)-3-(2,3,4-trifluorophenyl)urea **108** and 1-(2-adamantyl)-3-(2,3,4-trifluorophenyl)urea **109** were firstly reported as anti-tuberculosis agents whose mechanism

of action consists in the inhibition of the epoxide hydrolase family of enzymes (*Mycobacterium tuberculosis* epoxide hydrolases B and E, but also human sEH).<sup>497,498</sup>

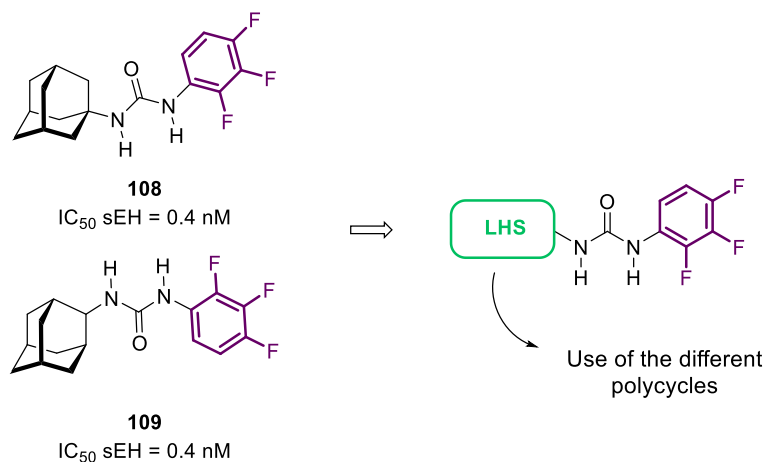


Fig. 82. 2,3,4-Trifluorophenyl unit as RHS.

### 1.1 Synthesis of *N*-adamantane-like-*N'*-(2,3,4-trifluorophenyl)ureas

The synthetic plan of the final ureas was simple and straightforward, and consisted in the coupling of an amine with an isocyanate. Because of the handy experience of our research group in the preparation of polycyclic cage amines, and that 2,3,4-trifluorophenyl isocyanate was commercially available, we prepared the adamantyl-based ureas as showed in scheme 56.

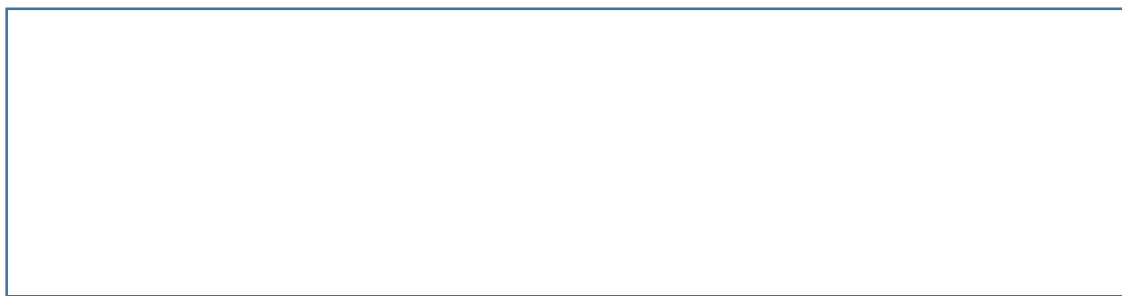


Scheme 56. General procedure for the preparation of adamantyl-like ureas.

In order to save time and resources, in certain cases we started the synthesis from intermediate amines already prepared by former group members or myself in earlier time (Fig. 83).

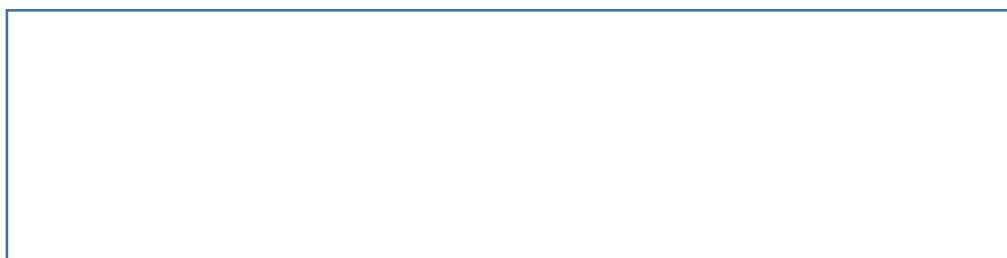
<sup>497</sup> Brown, J. R.; North, E. J.; Hurdle, J. G.; Morisseau, C.; Scarborough, J. S.; Sun, D.; Korduláková, J.; Scherman, M. S.; Jones, V.; Grzegorzewicz, A.; Crew, R. M.; Jackson, M.; McNeil, M. R.; Lee, R. E. *Bioorg. Med. Chem.* **2011**, *19*, 5585-5595.

<sup>498</sup> Scherman, M. S.; North, E. J.; Jones, V.; Hess, T. N.; Grzegorzewicz, A. E.; Kasagami, T.; Kim, I. H.; Merzlikin, O.; Lenaerts, A. J.; Lee, R. E.; Jackson, M.; Morisseau, C.; McNeil, M. R. *Bioorg. Med. Chem.* **2012**, *20*, 3255-3562.



**Fig. 83.** Intermediate amines formerly synthesized by the group.

The rest of the amines were prepared from different intermediates, and some of them starting from scratch (Fig. 84).



**Fig. 84.** Intermediate amines to prepare.

### 1.1.1 Preparation of intermediate scaffolds

#### 1.1.1.1 Synthesis of \_\_\_\_\_, **120**:

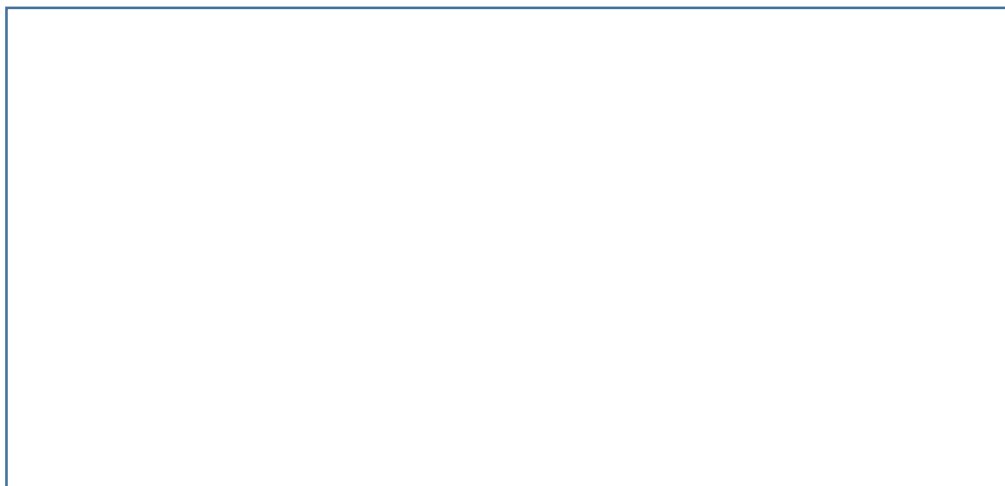
The \_\_\_\_\_ **120** was prepared following the procedure firstly described by Gagneux and Meier in 1969 and broadly applied by our research group.<sup>499,500,501</sup> Starting from known \_\_\_\_\_ **125**, a \_\_\_\_\_ took place affording compound **126** in 57% yield (Scheme 57). In this step, reaction with \_\_\_\_\_ yielded an \_\_\_\_\_ intermediate, which was reduced following a \_\_\_\_\_ mechanism upon the addition of a hydride source in a one-pot fashion. This intramolecular attack is possible due to the presence of a \_\_\_\_\_

---

499

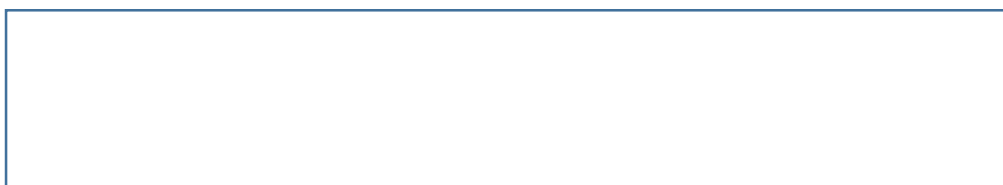
500

501



**Scheme 57.** Formation of **126** from **125** and subsequent precipitation as the hydrochloride salt. The proton shifts have been avoided for the sake of clarity.

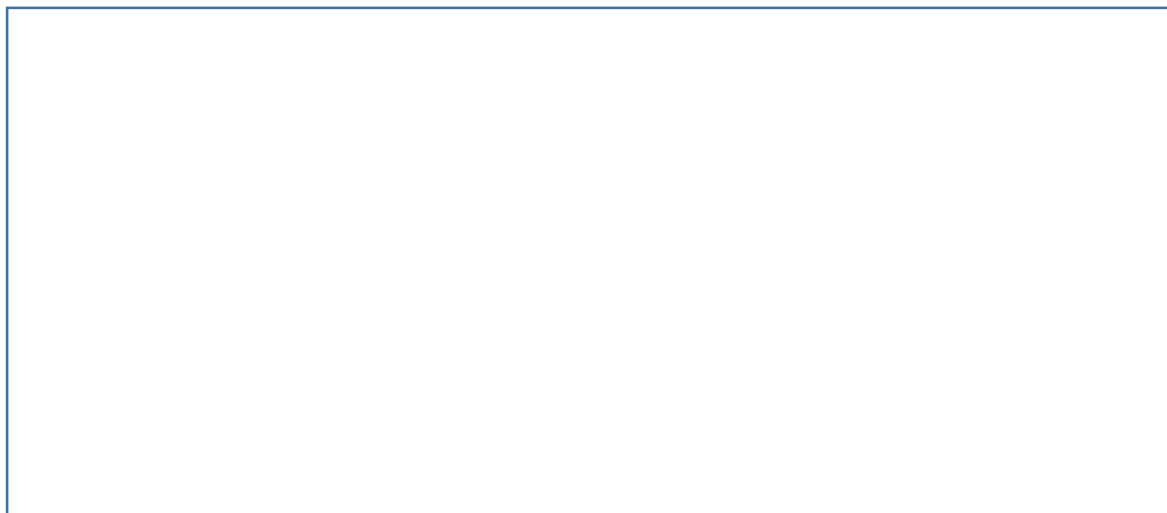
With **126** in hand, hydrogenolysis of the **120** in quantitative yield, isolated as its hydrochloride salt (Scheme 58).



**Scheme 58.** Deprotection of **120** by catalytic hydrogenation at atmospheric pressure.

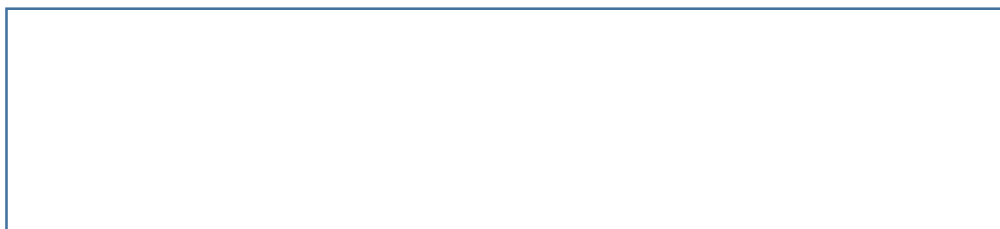
#### 1.1.1.2 Preparation of **121**:

The synthesis of **121** was based on the work of **127** and co-workers, and started by using the **127**.<sup>502</sup> Analogously to the latter intermediate, **127** was subjected to a **128**. In this procedure, azeotropic distillation with toluene led the dehydration of the reaction intermediate to afford **128**, which was then reduced with sodium borohydride. Subsequent catalytic hydrogenation provided deprotected amine **121** in 30% overall yield (Scheme 59).



**Scheme 59.** Preparation of **121** starting from commercially available **127**.

In accordance to what was described in chapter 1 (see page 66), the formation of compound **130** was reported by [redacted] and co-workers from the selective reduction of the imine with sodium cyanoborohydride instead of the [redacted] in compound **128**.<sup>503</sup> The resulting [redacted] attacked the carbonyl group providing a compound (Scheme 60). To avoid this, sodium borohydride is needed. Thus, the [redacted] is first reduced, releasing a [redacted] ready to add to the [redacted] moiety, and finally affording the desired [redacted] compound **129**.



**Scheme 60.** Selective reduction of **128**.

### 1.1.1.3 Synthesis of **122** and **123**:

**122** and **123** were prepared following a long and tedious synthetic pathway inspired from the previous work of the group. The key step of the route revolves around an [redacted] **131** and **132**, which can lead to the desired [redacted] after classical synthetic transformations (Fig. 85). **132** was taken from previously prepared samples by former group members.



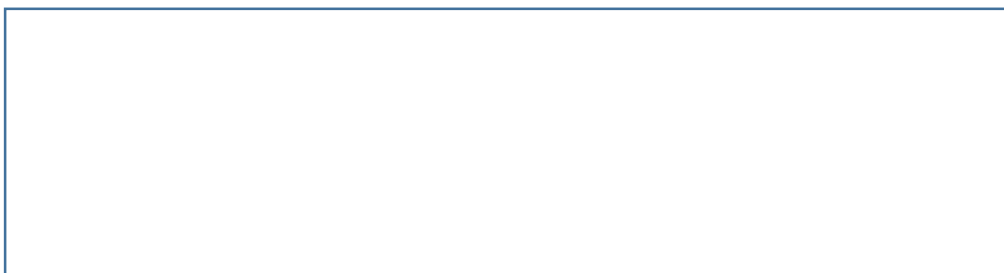
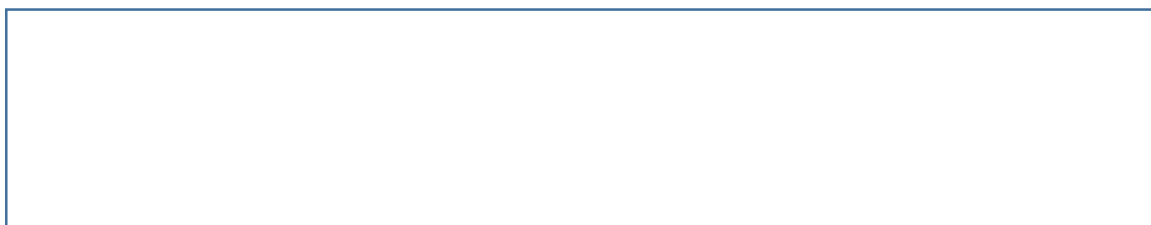


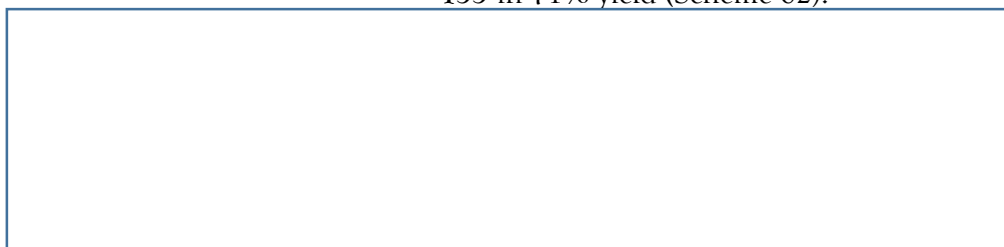
Fig. 85. Planned synthesis of 122 and 123 from 131 and 132, respectively.

For the preparation of 131, the first step was the synthesis of 133 through a reaction in a multigram scale. Following the procedure reported in *Organic Syntheses*,<sup>504</sup> two equivalents of 1,3-dimethyl-acetondicarboxylate were condensed with 132 in the presence of sodium hydroxide as a base (Scheme 61). After neutralization of 134, 135 was obtained in 55% yield. The reaction mechanism is analogous to that from scheme 3 in chapter 1, and consisted in a double aldol condensation *prior* to a double Michael addition.



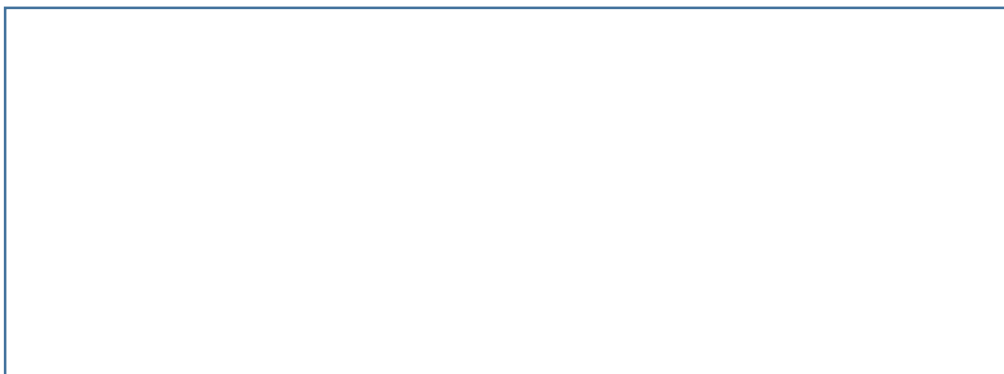
Scheme 61. Weiss-Cook condensation of 132 and 133.

Without further purification, 135 was treated with acidic aqueous solution for the hydrolysis of the ester groups and concomitant decarboxylation to yield 133 in 71% yield (Scheme 62).



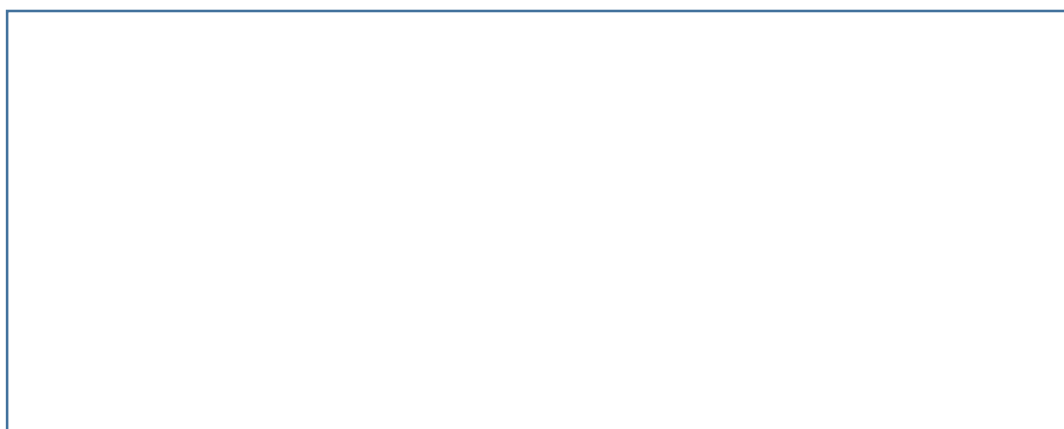
Scheme 62. Acid hydrolysis of 135 to yield 133 after acid hydrolysis.

The synthesis continued with the reaction of 133 with sodium cyanide and sulphuric acid.<sup>505</sup> In this step, the slow addition of 40% H<sub>2</sub>SO<sub>4</sub> solution to sodium cyanide in aqueous media supplied *in situ*-formed cyanide ions that added to the carbonyl carbon of 133, giving a stereoisomeric mixture of 136 (Scheme 63).



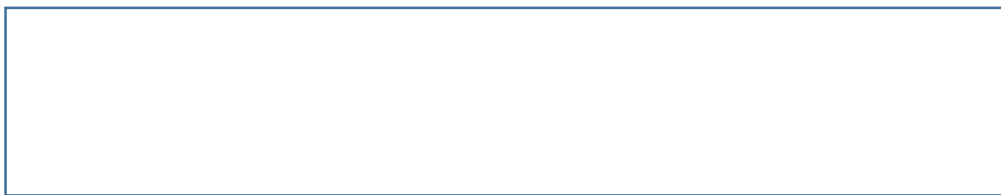
**Scheme 63.** Double addition of cyanide to **133** for obtaining a mixture of **136**.

**136** were transformed into **137** and **138** in the presence of thionyl chloride and pyridine under reflux. Under these conditions, dehydration of **136** led to a regioisomeric mixture of **137** and **138** in 44% yield (Scheme 64). The reaction begins with the addition of the oxygen atom of the hydroxyl group to  $\text{SOCl}_2$  and later elimination of a chloride ion. The base subtracts the  $\alpha$ -proton to form the vinyl system, eliminating sulphur dioxide and eventually hydrochloric acid, which is trapped by the base.



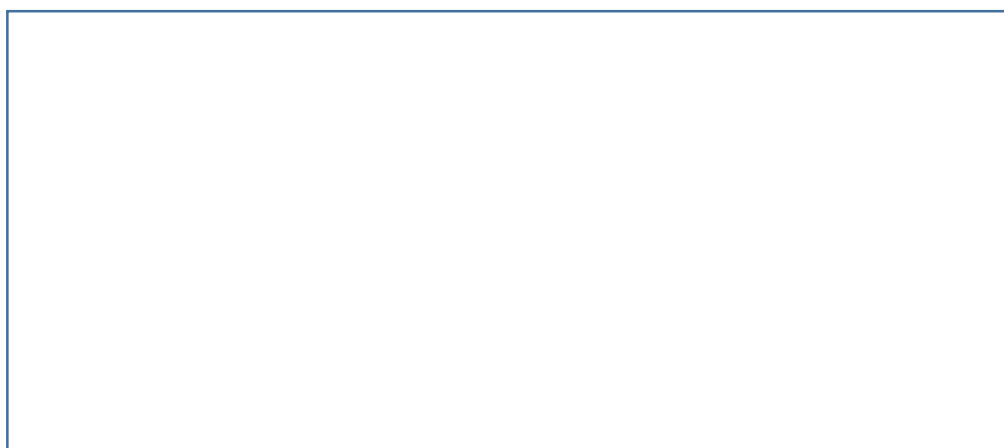
**Scheme 64.** Dehydration of **136** with thionyl chloride in the presence of pyridine.

Following the procedure, the mixture of **137** and **138** was submitted to a very slow catalytic hydrogenation due to the steric encumbrance around the double bonds. After 3 days at 27 atm of hydrogen, a complex stereoisomeric mixture of **139** was obtained in a ratio of 2:1.3:1; respectively, in 87% yield (Scheme 65).



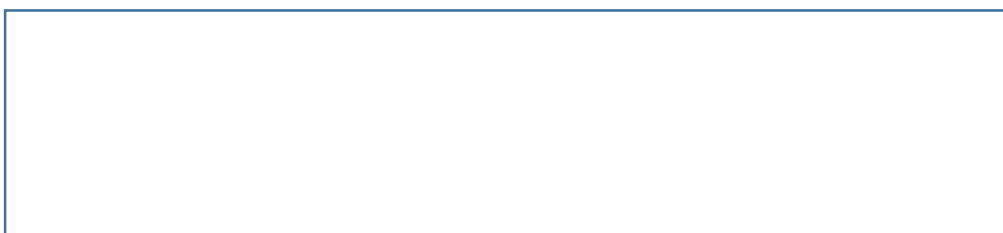
**Scheme 65.** Formation of the stereoisomeric mixture **139** after hydrogenation of **137** and **138**.

The next step was the hydrolysis of the \_\_\_\_\_ with potassium hydroxide and water, followed by a Fischer esterification with anhydrous methanol and conc. H<sub>2</sub>SO<sub>4</sub>, providing a mixture of \_\_\_\_\_ **141** in 62% yield (2 steps) (Scheme 66).<sup>506</sup>



**Scheme 66.** Hydrolysis of \_\_\_\_\_ **139** and \_\_\_\_\_ of **140** to **141**.

The next step can be consider as the most important transformation of the whole synthetic route, consisting of the \_\_\_\_\_ to build the system (Fig. 86).



**Fig. 86.** Intramolecular cyclization of **141**.

Many different procedures have been reported since the first dimerization of enolates was described in 1935, where Ivanoff *et al.* published the generation of the enolate of a carboxylic acid with a Grignard reagent for the posterior treatment with bromine to give the desired dimer.<sup>507</sup> Later on, similar methods for the homo- and heterocoupling of enolates appeared, all of them with common features: use of a strong base for the  $\alpha$ -deprotonation, such as lithium *N*-(*tert*-butyl)cyclohexanamide or lithim diisopropylamide

<sup>506</sup>

<sup>507</sup> Ivanoff, D.; Spassoff, A. *Bull. Soc. Chim. Fr.* **1935**, 2, 76-78.

(LDA), and an oxidant agent, such as copper(II) bromide or chloride, iron(III) chloride, titanium(IV) chloride or iodine.<sup>508,509,510,511,512,513,514</sup>

Despite these alternatives, we decided to apply the method already employed by the group.<sup>515,506</sup> The system of **131** was thus formed starting from the stereoisomeric mixture of **141** by an oxidative homocoupling with iodine as oxidant and LDA as base (formed *in situ* from diisopropylamine and *n*-butyllithium) in 36% yield (Scheme 67). The actual mechanism of this reaction is still unclear, albeit different studies have been performed to understand it.<sup>516</sup> It is believed that the treatment of **141** with LDA generates **A** that can undergo two different reaction pathways: i) reaction with iodine by a single electron transfer (SET) to give diradical **B** (path a), which can collapse to directly provide the ring-closed diester **131**; ii) formation of iodide **C** by an ionic mechanism (path b), which can be displaced in an intramolecular S<sub>N</sub>2-type reaction. The steric hindrance of the dianions plays an important role in determining the reaction pathway.

---

<sup>508</sup> Rathke, M. W.; Lindert, A. *J. Am. Chem. Soc.* **1971**, *93*, 4605-4606.

<sup>509</sup> Ito, Y.; Konoike, T.; Saegusa, T. *J. Am. Chem. Soc.* **1975**, *97*, 2912-2914.

<sup>510</sup> Frazier, R. H. Jr.; Harlow, R. L. *J. Org. Chem.* **1980**, *45*, 5408-5411.

<sup>511</sup> Kise, N.; Tokioka, K.; Aoyama, Y.; Matsumura, Y. *J. Org. Chem.* **1995**, *60*, 1100-1101.

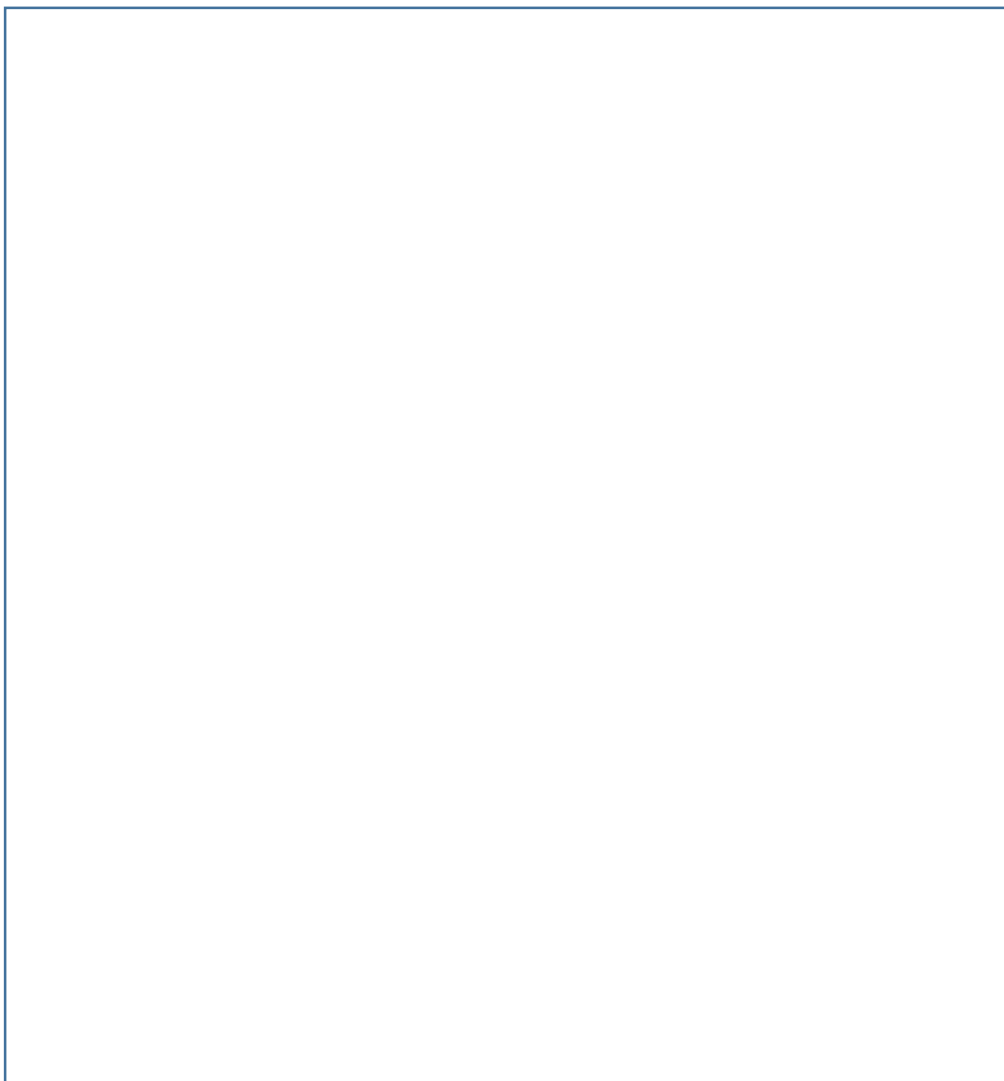
<sup>512</sup> Paquette, L. A.; Bzowej, E. I.; Branan, B. M.; Stanton, K. J. *J. Org. Chem.* **1995**, *60*, 7277-7283.

<sup>513</sup> Baran, P. S.; DeMartino, M. P. *Angew. Chem. Int. Ed. Engl.* **2006**, *45*, 7083-7086.

<sup>514</sup> DeMartino, M. P.; Chen, K.; Baran, P. S. *J. Am. Chem. Soc.* **2008**, *130*, 11546-11560.

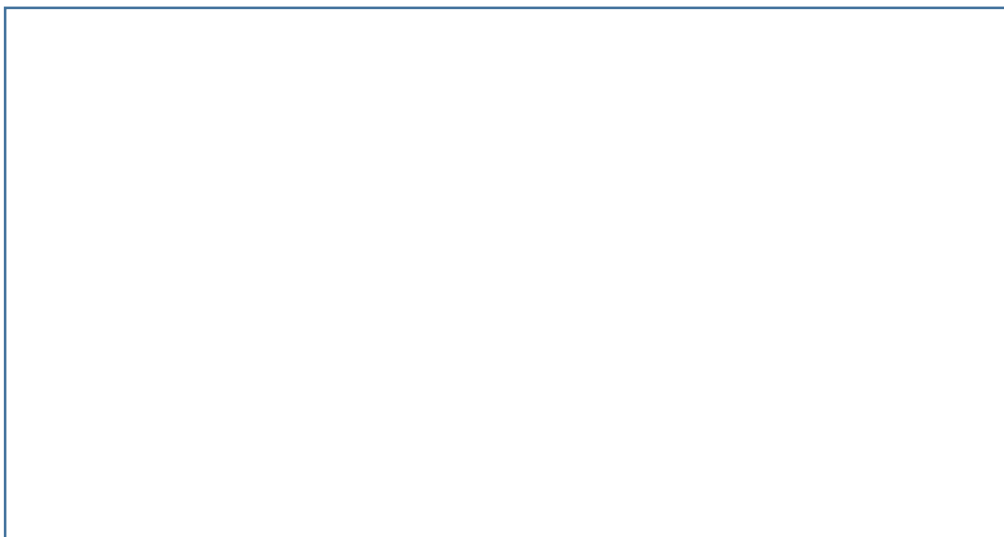
<sup>515</sup>

<sup>516</sup> Renaud, P.; Fox, M. A. *J. Org. Chem.* **1988**, *53*, 3745-3752.



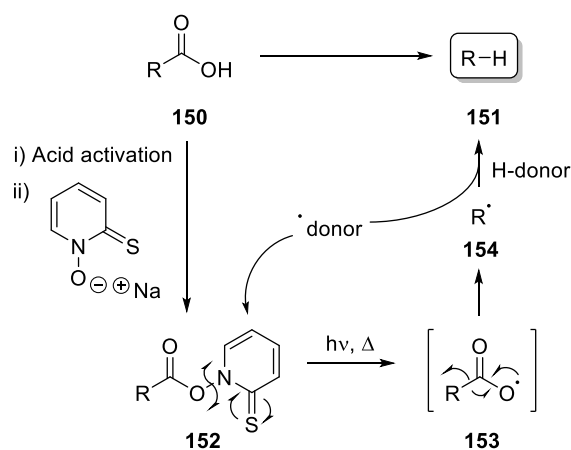
**Scheme 67.** Intramolecular oxidative cyclization of **141**.

At this point, the syntheses of **122** and **123** were concurrently run. With the goal of achieving these **131** and **132**, we needed to differentiate the **131** in order to selectively eliminate one of them (Scheme 68). For this purpose, **131** and **132** were hydrolysed under basic conditions to furnish the corresponding **142** and **143** in quantitative yields. Afterwards, the treatment of the aforementioned with neat acetic anhydride produced **144** and **145** in 72% and quantitative yield, respectively. Then, the **144** was opened in the presence of sodium methoxide and methanol to **146** and **147** in low yields due to the presence of adventitious water from the solvent. In both cases, diacids **142** and **143** were recovered.



**Scheme 68.** Functional group differentiation of **131** and **132**.

Next, **146** and **147** were converted to the corresponding **148** and **149** through a Barton radical decarboxylation.<sup>517,518</sup> The procedure consists in the protodecarboxylation of a carboxylic acid **150** in the presence of a suitable hydrogen bond donor (H-donor) to furnish the corresponding hydrocarbon **151**. Fundamental to the Barton decarboxylation protocol is the alkyl thiohydroxamic ester **152**, also known as Barton ester, which is readily prepared from the reaction of an activated carboxylic acid and the sodium salt of 1-hydroxypyridine-2(1*H*)-thione.<sup>519,520</sup> By means of applying light and heat, the Barton ester undergoes rapid homolytic decomposition yielding the corresponding alkyl acyloxy radical **153**, which is subjected to decarboxylation. The remaining alkyl radical **154** intercepts a proton from the H-donor, whereupon **151** is recovered (Scheme 69).



**Scheme 69.** Mechanism of reaction of the Barton decarboxylation.

<sup>517</sup> Barton, D. H. R.; Crich, D.; Motherwell, W. B. *J. Chem. Soc. Chem. Commun.* **1983**, 939-941.

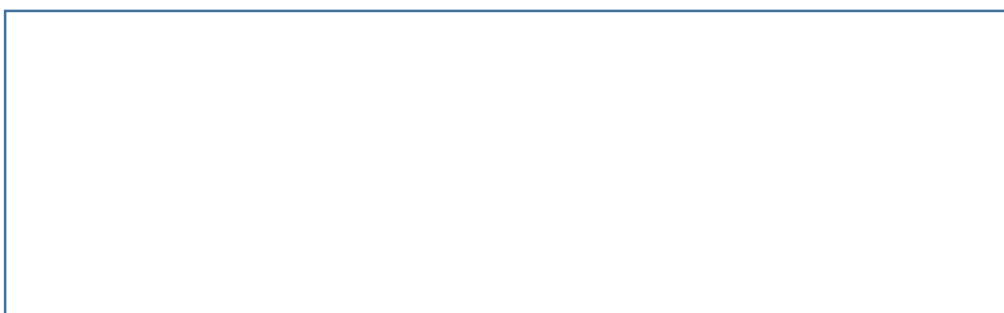
<sup>518</sup> Barton, D. H. R.; Hervé, Y.; Potier, P.; Thierry, J. *J. Chem. Soc. Chem. Commun.* **1984**, 1298-1299.

<sup>519</sup> Barton, D. H. R.; Crich, D.; Motherwell, W. B. *Tetrahedron* **1985**, *41*, 3901-3924.

<sup>520</sup> Barton, D. H. R.; Samadi, M. *Tetrahedron* **1992**, *48*, 7083-7090.

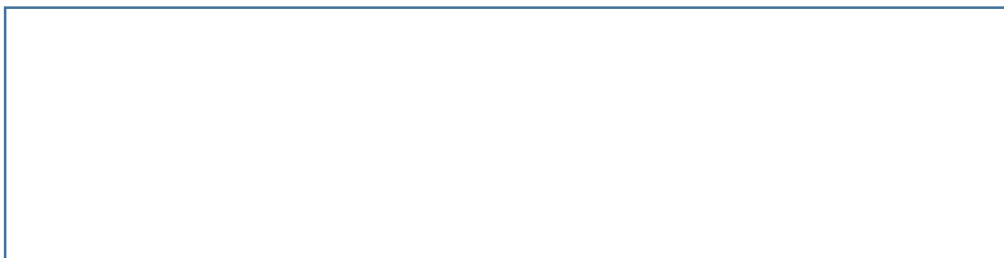
Former protocols of the Barton decarboxylation applied by our group entailed the use of 2,2'-dithiobis(pyridine-*N*-oxide) as precursor of the Barton ester and *n*-tributylphosphine for its pre-activation.<sup>172</sup> As H-donor, *t*-butylthiol was the preferred proton source, despite the fact that its use implied that the reaction should be set up in a special laboratory for highly smelly and toxic reactions.

On the other hand, the utility of chloroform as both solvent and H-donor in Barton decarboxylation has been recently demonstrated.<sup>521,522</sup> Taking advantage of this finding, we performed the reaction under *t*-butylthiol-free conditions within chloroform (Scheme 70). Pleasingly, **146** and **147** were easily transformed to their corresponding **148** and **149** (86% yield for **149**). Because of the high volatility of **148**, the solvents were distilled off after the work up to give the monoester along with reaction by-products. The crude was used in next step without any purification.



**Scheme 70.** Barton decarboxylation of **39** and **40** with chloroform as H-donor.

The **148** and **149** was followed by a basic hydrolysis of **148** and **149** to **155** and **156** in 73% and 61% yield (2 steps), respectively (Scheme 71).



**Scheme 71.** Basic hydrolysis of **148** and **149**.

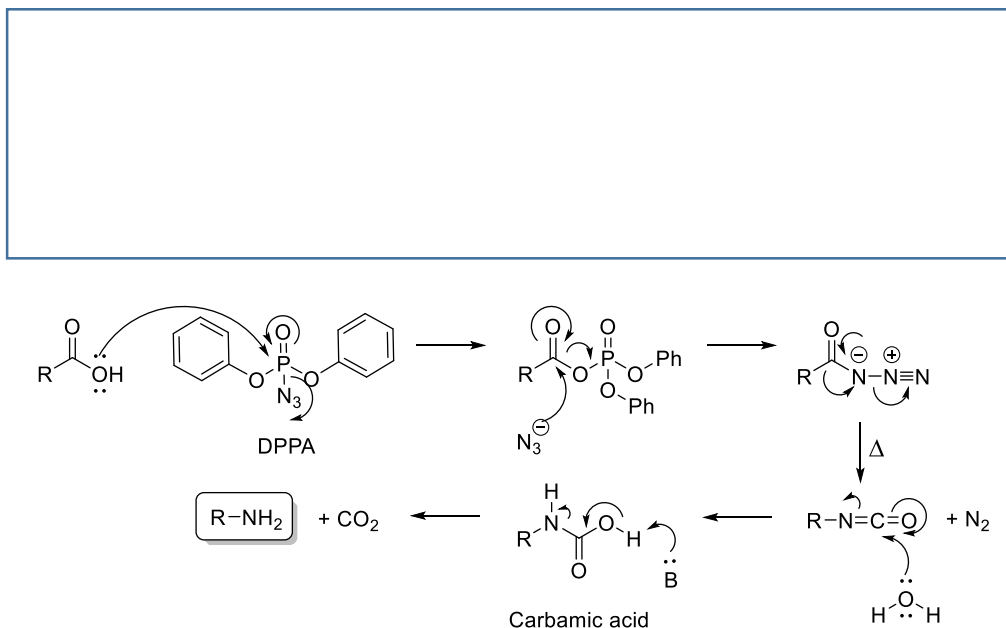
The last step for the preparation of **122** and **123** involved a Curtius rearrangement, which led to the one-step functional interconversion of a carboxylic acid to a primary amine with concomitant loss of one carbon atom through an acyl azide intermediate. In this transformation, the thermal decomposition of carboxylic azides produces an isocyanate, which can be hydrolysed to yield the corresponding amine. In our case, we applied the Yamada's modification of the Curtius reaction, which employs diphenylphosphoryl azide (DPPA) as the azide source.<sup>523,95</sup> Thus, addition of DPPA to a

<sup>521</sup> Ko, E. J.; Savage, G. P.; Williams, C. M.; Tsanaktsidis, J. *Org. Lett.* **2011**, *13*, 1944-1947.

<sup>522</sup> Ho, J.; Zheng, J.; Meana-Pañeda, R.; Truhlar, D. G.; Ko, E. J.; Savage, G. P.; Williams, C. M.; Coote, M. L.; Tsanaktsidis, J. *J. Org. Chem.* **2013**, *78*, 6677-6687.

<sup>523</sup> Ninomiya, K.; Shioiri, T.; Yamada, S. *Tetrahedron* **1974**, *30*, 2151-2157.

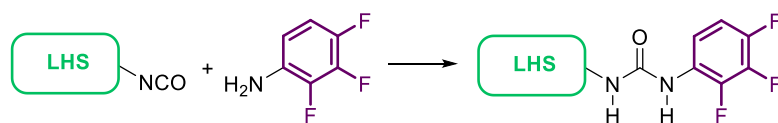
solution of both **155** and **156** supplied finally **122** and **123** in 31% and quantitative yield, respectively (Scheme 72).



**Scheme 72.** Curtius rearrangement with DPPA.

### 1.1.2 Preparation of urea **157**

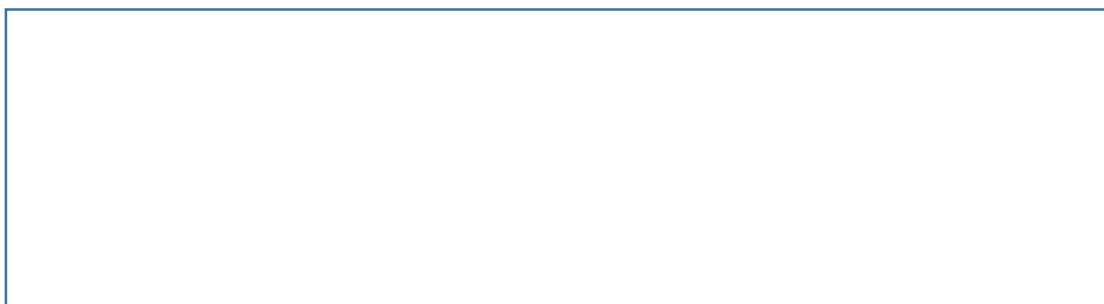
M. D. Duque in her doctoral thesis observed that **124** was unstable under her reaction conditions.<sup>164</sup> Several attempts to isolate desired **124** were fruitless, probably due to a high reactivity of the **124** in the acidic media. Lest the same quandary, for the preparation of the final ring-expanded urea **157** we decided to swap functionalities so as to react the 2,3,4-trifluoroaniline with the corresponding isocyanate as the LHS (Scheme 73).



**Scheme 73.** Inverted procedure for the preparation of urea **157**.

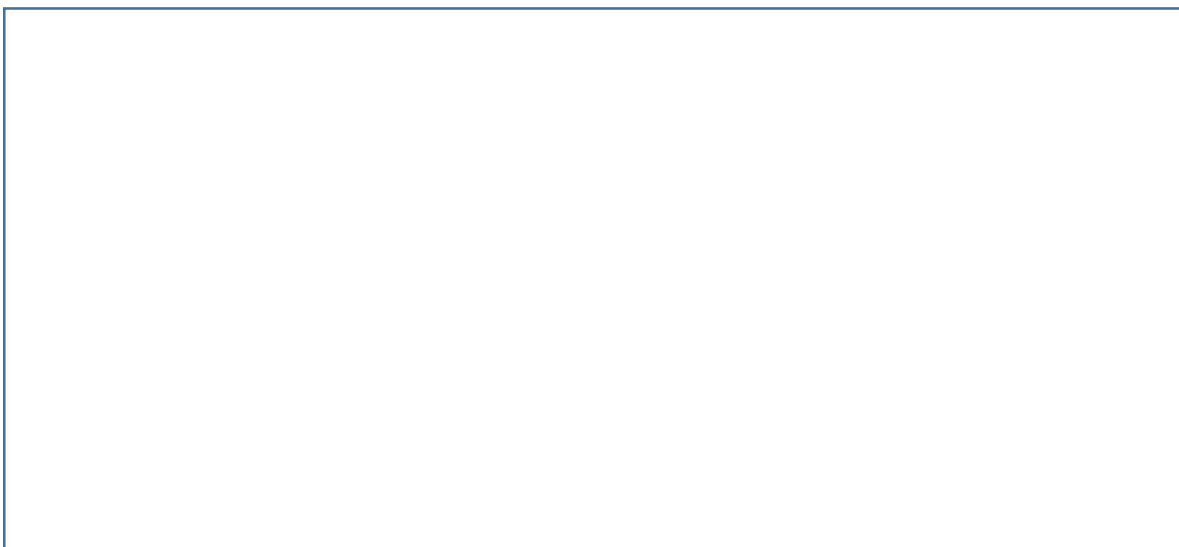
Consequently, we envisioned the preparation of **158** from unsaturated **159** through a Curtius rearrangement, which in turn can be prepared from the already seen **88** (Scheme 74).





**Scheme 74.** Retrosynthetic scheme for urea **157**.

Starting from the **88**, we produced **159** using a synthetic sequence previously described by our group, analogous to the synthetic route for **122** and **123** (Scheme 75).<sup>524,90</sup> Accordingly, **88** was subjected to anhydride formation with neat acetic anhydride to give compound **160** in 88% yield, which was treated with sodium methoxide in anhydrous methanol for the functional group differentiation. Thus, **161** was obtained in 60% yield, recovering part of **88** after purification by column chromatography. Barton reductive decarboxylation with 2,2'-dithiobis(pyridine-*N*-oxide) in chloroform, the latter acting as a solvent and H-donor, afforded **162** in 59% yield, which is lower than the reported value of 91%. This reduction in the yield can be attributed to a lower reactivity of the chloroform as H-donor than *t*-BuSH for this specific alkyl radical. Finally, basic hydrolysis **162** furnished **159** in 31% yield.

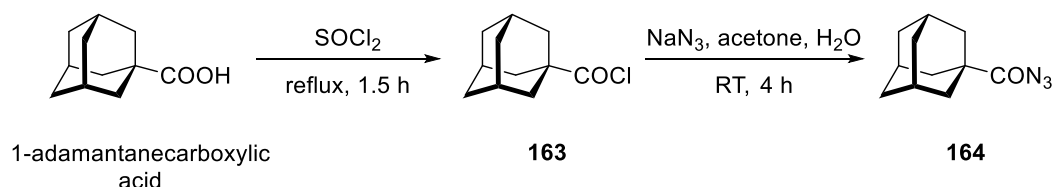


**Scheme 75.** Synthetic route for the preparation of **159** from **88**.

Our wide experience with these kind of polycycles warned us that isocyanate **158** might be highly volatile, a property that makes it difficult to isolate. This volatility is attributed to the low molecular weight of the scaffold (12 carbon atoms) and to the planarity around the  $sp^2$  atoms of the isocyanate group, whereupon no stable intermolecular interaction can be formed. With this in mind, we first explored the proposed synthetic route in scheme 76

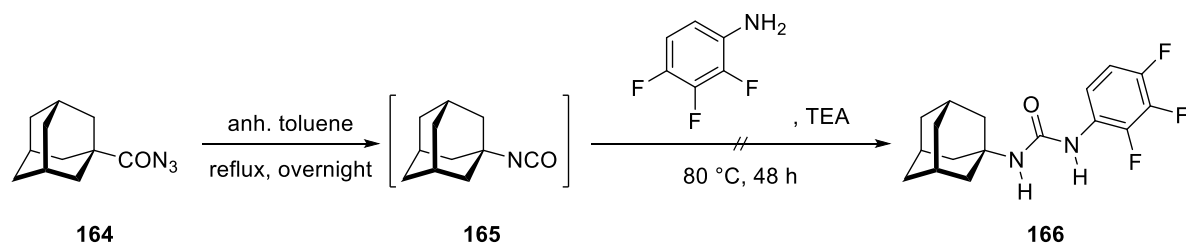
<sup>524</sup> Camps, P.; Lukach, A. E.; Rossi, R. A. *J. Org. Chem.* **2001**, *66*, 5366-5373.

using the adamantane derivative as template, since the scaffold is more valuable in terms of synthetic effort than adamantane, which is commercially available. Thus, we applied classical chemical transformations to produce acyl azide **164** from 1-adamantanecarboxylic acid. Treatment of the latter with thionyl chloride afforded acyl chloride **163** in quantitative yield, which was then subjected to an addition-elimination reaction with sodium azide to give **164** in quantitative yield. Both interconversions were controlled by infrared (IR) spectroscopy.



**Scheme 76.** Functional group interconversion of 1-adamantanecarboxylic acid.

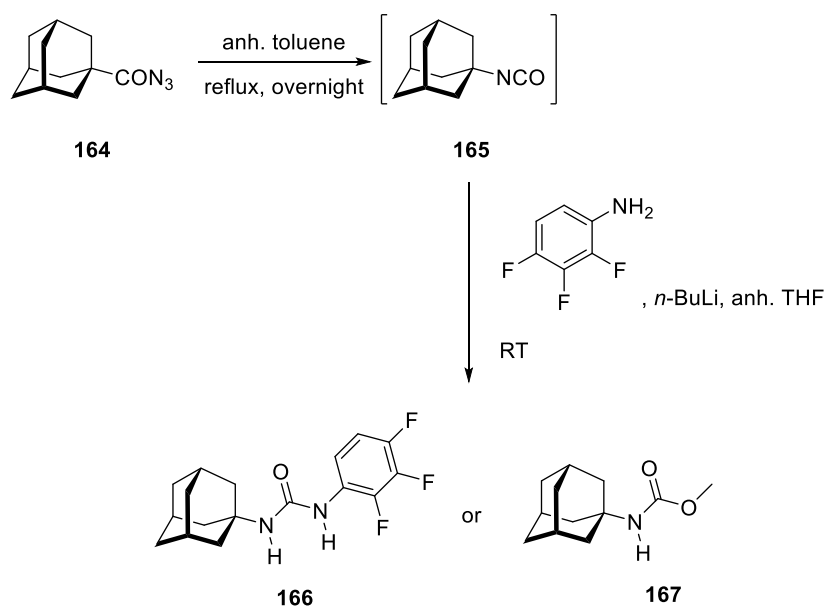
In order to avoid any type of isolation of isocyanate **165**, we aimed to form it *in situ* through a Curtius rearrangement upon heating **164**, for the subsequent addition to the media of 2,3,4-trifluoroaniline and final formation of desired urea **166** (Scheme 77). Following the conditions reported by Lee and co-workers,<sup>525</sup> we *in situ*-formed isocyanate **165**, whose formation was monitored by IR spectroscopy, for later adding the aniline and triethylamine as base. Unfortunately, no product was recovered but the starting materials, despite of the long reaction time.



**Scheme 77.** Intended formation of urea **166** with TEA as base.

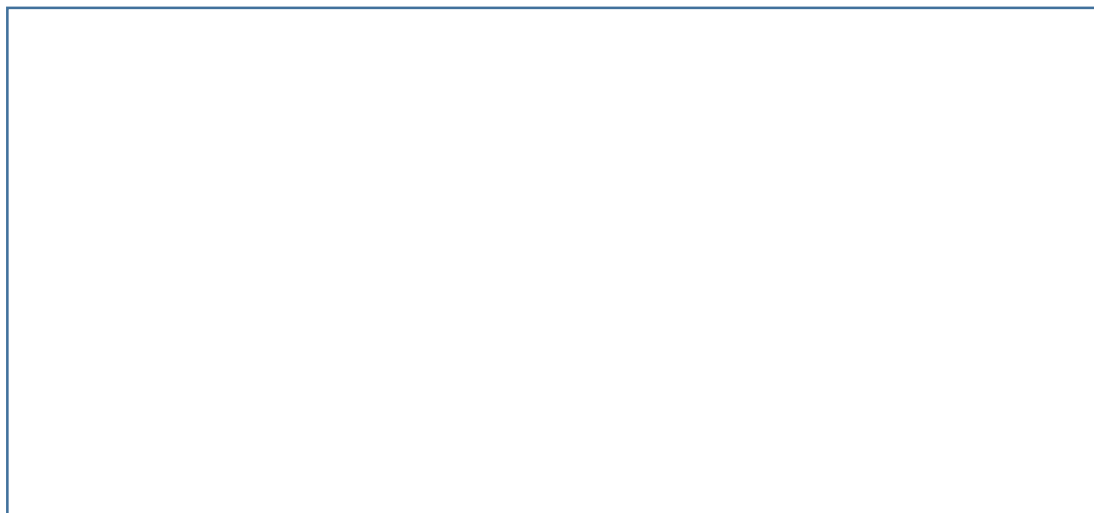
In the hope of optimizing the reaction and assuming that the base was the variable to adjust, we next explored the effectiveness of *n*-butyllithium as base. As the published procedure indicated,<sup>525</sup> the reaction mixture was stirred for 1 hour at room temperature and quenched with methanol. Alas, no product was again recovered but, in this case, methyl carbamate **167**. The formation of this side-product came from the attack of methanol to isocyanate **165**. This fact illustrated that longer reaction times were needed. Therefore, when the reaction was performed overnight, desired urea **166** was obtained with no further purification (Table 18).

<sup>525</sup> North, E. J.; Scherman, M. S.; Bruhn, D. F.; Scarborough, J. S.; Maddox, M. M.; Jones, V.; Grzegorzewicz, A.; Yang, L.; Hess, T.; Morisseau, C.; Jackson, M.; McNeil, M. R.; Lee, R. E. *Bioorg. Med. Chem.* **2013**, *21*, 2587-2599.

Table 18. Preparation of urea **166** with *n*-BuLi as base.

Entry	Time (h)	<b>166</b>	<b>167</b>
<b>1</b>	1	<del>✓</del>	✓
<b>2</b>	18	✓	<del>✓</del>

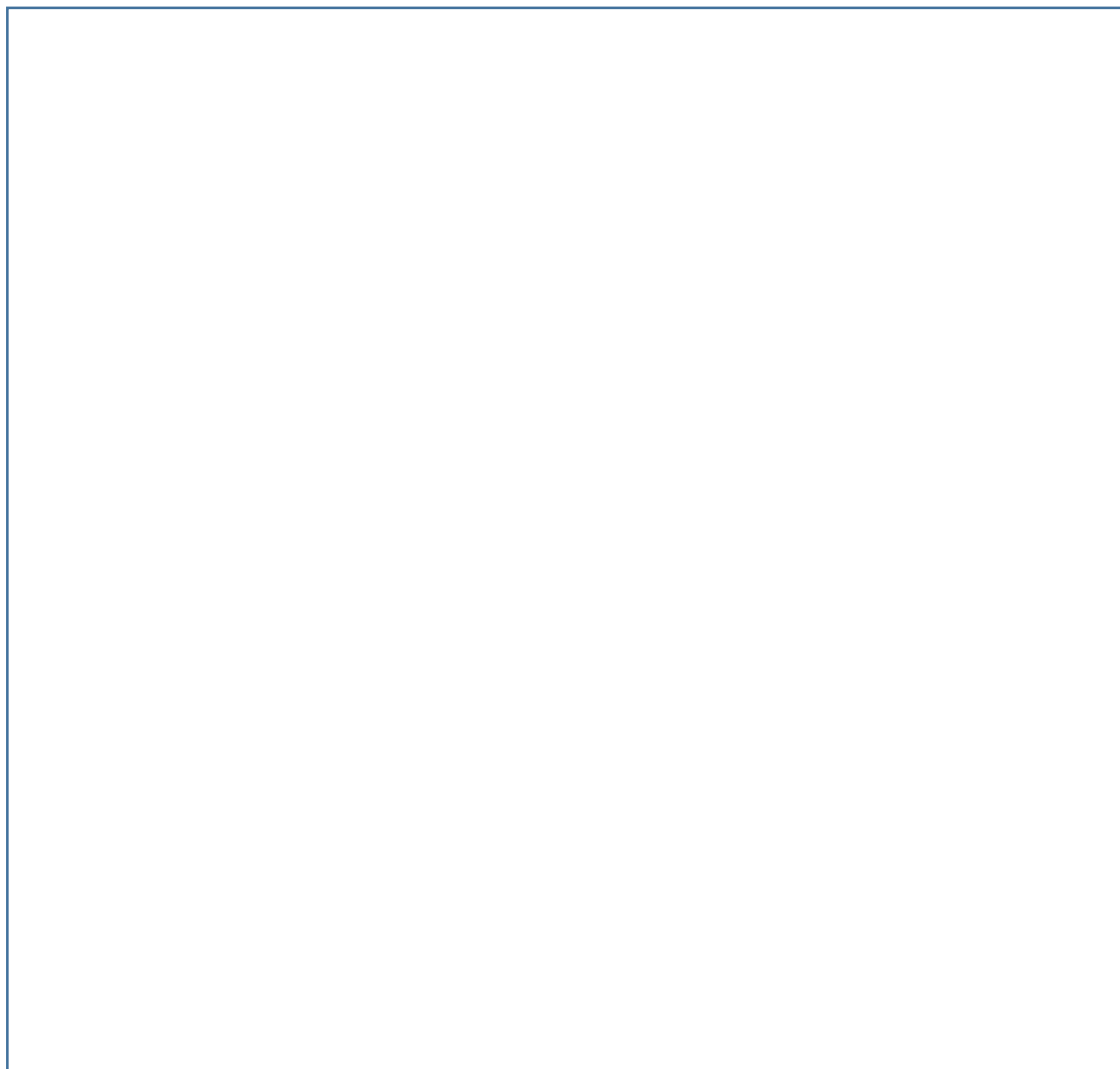
Once the optimum conditions identified, we proceeded to the preparation of pentacyclic derivative **157** (Scheme 78). Hence, monoacid **159** was converted to acyl chloride **168** with thionyl chloride in quantitative yield, followed by the reaction with an excess of sodium azide to furnish acyl azide **169** in 88% yield. Their structures were confirmed also by IR spectroscopy. Then, Curtius reaction took place upon heating **169**, providing isocyanate **158** that was trapped by 2,3,4-trifluoroaniline, and finally achieving desired **157** in 25% overall yield after purification by column chromatography.



**Scheme 78.** Synthetic pathway for the preparation of urea **157**. Transformation from **169** to **157** was in one-pot.

### 1.1.3 Synthesis of final ureas **170-183**

After the quest and preparation of intermediate amines **110-123**, we progressed in our goal to synthesize the 2,3,4-trifluorophenyl ureas for their testing as sEH inhibitors. As described earlier, our synthetic strategy consisted in the coupling between intermediate amines **110-123** with 2,3,4-trifluorophenyl isocyanate, using triethylamine as base and anhydrous dichloromethane as solvent. Satisfyingly, ureas **170-183** were produced in variable yields (Scheme 79). Apart from them, 1-adamantanyl, **108**, and 2-adamantanyl, **109**, ureas were synthesized as standard compounds for comparison.



**Scheme 79.** Final ureas and their yields.

Just to mention that the low yield achieved for compound **182** was attributed to the low purity of the sample used as the starting amine.

## 1.2 Pharmacological evaluation of final ureas. IC<sub>50</sub> determination

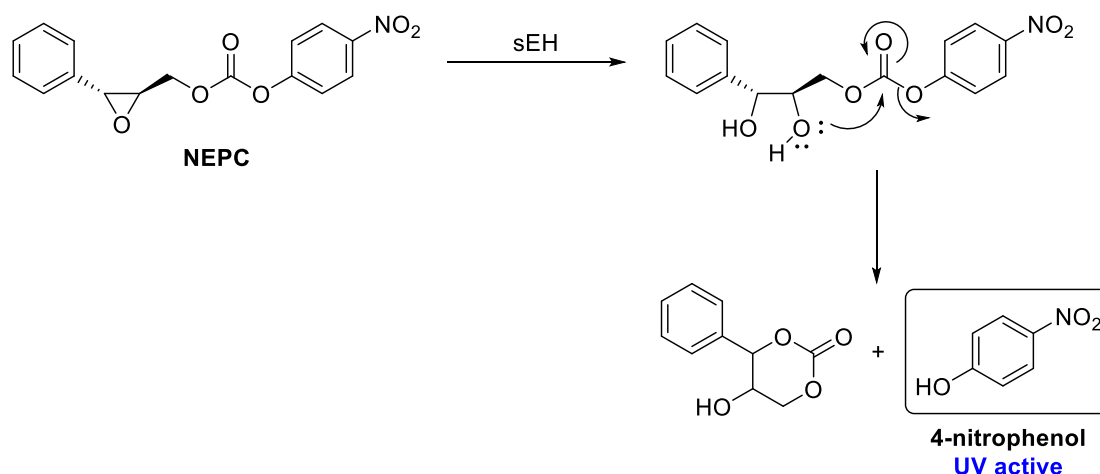
As part of the research project, we pursued the measurement of the inhibitory activity of new ureas **157** and **170-183** by means of determining their IC<sub>50</sub> values. *Prior* to entering into details of the IC<sub>50</sub> evaluation, a brief introduction of the enzymatic assays will be disclosed.

### 1.2.1 A little of background

The appearance of the sEH as potential therapeutic target, and the discovery of large libraries of small molecules as inhibitors of this enzyme, urged the finding of an enzymatic assay that needed to fulfil critical requirements, such as robustness and sensitivity. The availability of homogenous, recombinant sEH from human and model species have been crucial for the development of the screening assays.

The screening assays have evolved in the last years as the demand of assays that could distinguished among the most potent inhibitors increased over time:

1. Earlier rapid kinetic spectrophotometric assays employed recombinant sEH and epoxy esters or carbonates as substrates. The most used substrates were *trans*-stilbene oxide (*t*-SO), *trans*-diphenyl-propene oxide (*t*-DPPO) and 4-nitrophenyl-*trans*-2,3-epoxy-3-phenylpropyl carbonate (NEPC).<sup>526</sup> These substrates cyclize spontaneously upon or during hydrolysis of the epoxide functionality by sEH, releasing an alcohol that can be directly detected by UV-vis spectrophotometry, or after a second reaction with them (Scheme 80).



**Scheme 80.** Hydrolysis of NEPC by sEH and detection of 4-nitrophenol by UV spectrophotometry.

However, these assays became ineffective because they were not sensitive enough to differentiate among the best compounds based on their  $IC_{50}$  values. Moreover, the aqueous instability of these photometric substrates required short incubation times. Thus, they could not be employed in long-term assay systems as it is often the case in the screening of large compound libraries.

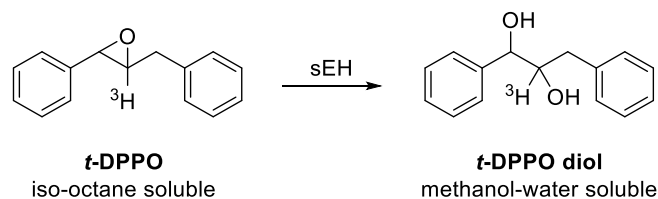
2. Several radiochemical and chromatographic assays were developed to overcome the limitations of the previous procedures.<sup>527</sup> The most used radiolabelled substrates are [ $^3H$ ]-*t*-SO and [ $^3H$ ]-*t*-DPPO, which represent the first-rate surrogates that are employed in radiometric assays. These assays are based on differential partitioning between the epoxide substrate, the 1,2-diol product, and (if necessary) glutathione conjugates, and thus need two different solvent systems for the selective extraction (Scheme 81).<sup>528</sup> Despite of the improvement with respect to former techniques, they are too slow, costly and labour intensive to screen larger amounts of compounds.

<sup>526</sup> Dietze, E. C.; Kuwano, E.; Hammock, B. D. *Anal. Biochem.* **1974**, *216*, 176-187.

<sup>527</sup> Borhan, B.; Mebrahtu, T.; Nazarian, S.; Kurth, M. J.; Hammock, B. D. *Anal. Biochem.* **1995**, *231*, 188-200.

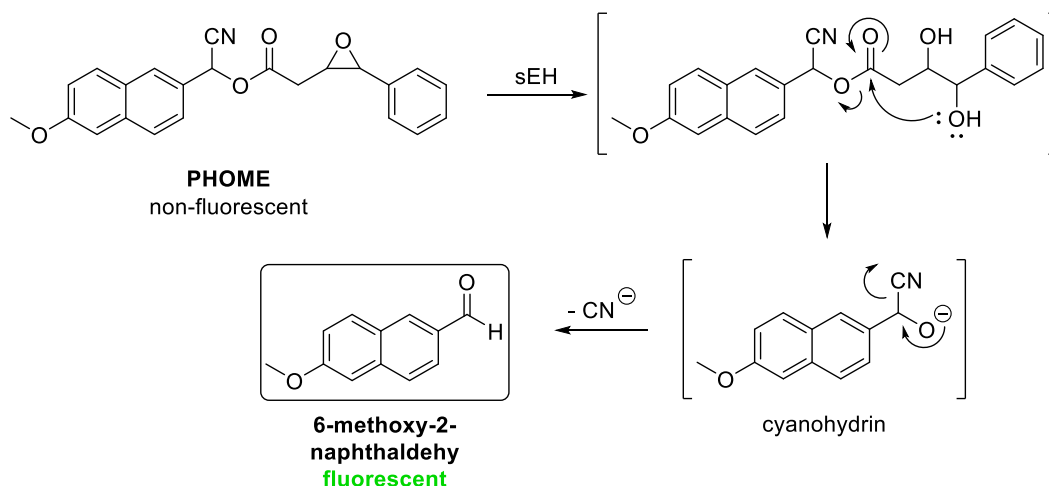
<sup>528</sup> Morisseau, C.; Hammock, B. D. *Curr. Protoc. Toxicol.* **2007**, *Suppl. 33*, 4.23.1-4.23.18.

Moreover, unlike [ $^3\text{H}$ ]-*t*-SO, [ $^3\text{H}$ ]-*t*-DPPO is not commercially available and needs to be prepared *prior* to assaying.



**Scheme 81.** Different polarity of [ $^3\text{H}$ ]-*t*-DPPO and its hydrolyzed product.

3. Fluorescent substrates appeared as an alternative with higher sensitivities and rapid responses.<sup>529</sup> These substrates combine the decomposition mechanism of NEPC with the latent fluorophore of  $\alpha$ -cyanoesters and  $\alpha$ -cyanocarbonates. After hydrolysis of the epoxide by sEH, O-deacylation liberates a cyanohydrin intermediate that rapidly decomposes to the highly fluorescent 6-methoxy-2-naphthaldehyde, which is characterized by a large Stoke's shift (Scheme 82). Among all the known fluorescent substrates, CMNPC (cyano(2-methoxynaphthalen-6-yl)methyl (3-phenyloxiran-2-yl)methyl carbonate) and PHOME ((3-phenyl-oxiranyl)-acetic acid cyano-(6-methoxy-naphthalen-2-yl)-methyl ester) are the most employed due to their high sensitivity and improved aqueous stability and solubility. Thus, this type of substrates have been widely applied in high-throughput screening (HTS) assays with long incubation times. They required, however, the use of purified enzyme or at least a preparation free of competing enzymes activities (e.g. esterases and glutathione-S-transferase).



**Scheme 82.** Hydrolysis of the epoxide moiety of PHOME by sEH, followed by an intramolecular cyclization, resulting in the release of a cyanohydrin, which decomposes into a cyanide ion as well as the highly fluorescent 6-methoxy-2-naphthaldehyde.

<sup>529</sup> Jones, P. D.; Wolf, N. M.; Morisseau, C.; Whetstone, P.; Hock, B.; Hammock, B. D. *Anal. Biochem.* **2005**, *343*, 66-75.

4. The last developed assays consist in the use of natural epoxides, which are neither UV-absorbent nor fluorescent, and are not available in a radioactive form. For their detection, an LC-MS/MS method was developed by Newman *et al.*<sup>530</sup> Although providing an alternative, this technique is less sensitive than the previous ones and a challenge remains to distinguish among inhibitors with picomolar IC<sub>50</sub> values. However, they are recommended to verify the activity of lead inhibitors.<sup>464</sup>

### 1.2.2 Tune-up of the screening assay

Since it was the first time that our research group dealt with the pharmacological evaluation of small molecules, in particular of sEH inhibitors, we first explored the different available alternatives for the determination of the IC<sub>50</sub> values. To our delight, a sEH inhibitor screening assay using fluorescent substrates was commercially available from Cayman Chemical Company (from now on referred as Cayman).<sup>531</sup> This ready-to-use assay kit utilizes PHOME as substrate, and provides the necessary items to run the assay, i.e. 96-wells black plate, 25 mM 2{bis[2-hydroxyethyl(imino)-2-(hydroxymethyl)]-1,3-propanediol (bis-Tris) assay buffer (pH 7.0), human recombinant sEH and the assay protocol.

Thus, we decided first to test the ability to run the assay with both standards **108** and **109** at their reported IC<sub>50</sub> (0.4 nM for both).<sup>497</sup> For the fluorescence reading, we used a BMG FLUOstar optima microplate reader at an excitation wavelength of 337 nm and an emission wavelength of 460 nm. Following the established procedure, we managed to obtain a few times around 50% of inhibition for both standards at 0.4 nM. Unfortunately, several attempts to repeat these positive results were unsuccessful, and we were not able to reproduce our first data set.

Thanks to the personal advises from the research group of Prof. Hammock and Dr. Morisseau in University of California Davis (United States of America), we identified the key elements that were altering our results. From the available data, we considered different causes:

- Cayman includes in the kit the substrate already dissolved in DMSO in an adequate amount for running more than one plate. That means that the PHOME solution was frozen and thawed several times in between assays, compromising its stability. This fact was reflected in the signal-to-noise ratio, where the fluorescence of 100% activity (wells with sEH enzyme and substrate but without inhibitor) was too close to that of the background activity (wells with PHOME but without sEH enzyme and inhibitor). Calculation of the Z' value, which is a statistical parameter that evaluates and validates HTS assays,

---

<sup>530</sup> Newman, J. W.; Watanabe, T.; Hammock, B. D. *J. Lipid Res.* **2002**, *43*, 1563-1578.

<sup>531</sup> Cayman Chemical Company website. Soluble epoxide hydrolase inhibitor screening assay kit. <https://www.caymanchem.com/app/template/Product.vm/catalog/10011671> (accessed on 13<sup>th</sup> September 2015)



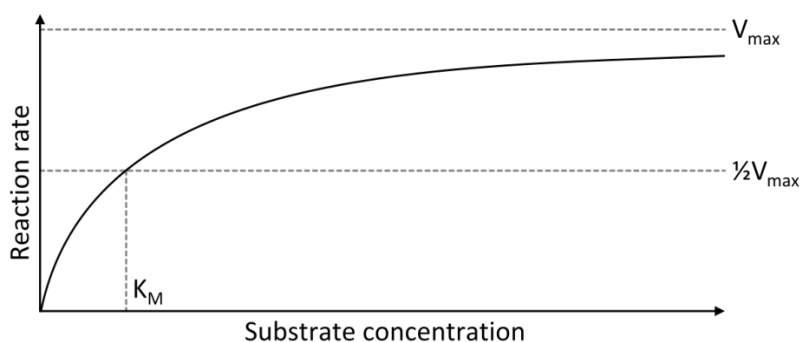
showed to be less than 0.5, indicating that it was not possible to discern inhibition potency because of the spontaneous hydrolysis of the substrate (data not shown).<sup>532</sup>

- The final concentration of the substrate [S] in each well was 0.25  $\mu\text{M}$ , which is below the estimated  $K_m$  value of 1.5  $\mu\text{M}$  by Cayman. Nevertheless, experts on the field have published a  $K_m$  much larger (272  $\mu\text{M}$ ) for this particular substrate.<sup>533</sup>

The Michaelis-Menten is a theory of enzyme kinetics that helped us to understand how the assay works. The Michaelis-Menten parameters  $K_m$  and  $V_{max}$  characterize enzyme-substrate interactions regarding substrate turnover.<sup>534</sup> The relation between these two parameters is expressed in the following equation 1, which relates the reaction rate ( $v$ ) to [S]:

$$v = \frac{V_{max} [S]}{K_m + [S]} \quad \text{Equation 1}$$

The graphic below represents this relationship (Fig. 87).



**Fig. 87.** Schematic plot of initial reaction rate  $v$  vs substrate concentration [S] following the theory of Michaelis-Menten.  $V_{max}$ : maximal velocity;  $K_m$ : Michaelis-Menten constant or the [S] at which the  $v$  is half the  $V_{max}$ .

At high substrate concentration, substrate turnover rates are more stable. Under such conditions, small variations in enzyme amount or other assay conditions such as temperature or pH should not influence the velocity significantly, resulting in a reproducible and stable assay. If the [S] is very low with respect to  $K_m$ , any variation in the assay will affect greatly the activity. With lower [S], one gains in sensitivity but loses in reproducibility and stability. For competitive inhibitors, the  $IC_{50}$  is dependent upon the [S], where the  $IC_{50}$  value will increase with the [S].

<sup>532</sup> Zhang, J. H.; Chung, T. D. Y.; Oldenburg, K. R. *J. Biomol. Screen.* **1999**, *4*, 67-73.

<sup>533</sup> Wolf, N. M.; Morisseau, C.; Jones, P. D.; Hock, B.; Hammock, B. D. *Anal. Biochem.* **2006**, *355*, 71-80.

<sup>534</sup> Reuveni, S.; Urbakh, M.; Klafter, J. *Proc. Natl. Acad. Sci. USA* **2014**, *111*, 4391-4396.

All the aforementioned indicated that we needed to increase the [S] in order to have a stable and robust assay, as well as to use a freshly prepared solution of PHOME lest its hydrolysis. In fact, Hammock studied the kinetics of PHOME and human sEH and found that the optimized concentrations of both were 50  $\mu\text{M}$  and 3 nM, respectively. Using these concentrations, they were able to ensure a linear substrate hydrolysis over a long period of time. However, our supplier of pure human recombinant sEH, Cayman, did not provide information on the final concentration of the enzyme which they considered confidential. Nevertheless, we performed a Bradford assay to quantify the amount of protein present in a sample, determining a concentration of 1.56 nM.

Knowing the approximate concentration of the sEH, we carried out a screening of substrate concentration in a checkboard experiment in which [PHOME] varied from 0.25 to 20  $\mu\text{M}$  (0.25, 2.5, 5, 10 and 20  $\mu\text{M}$ ). The solutions of PHOME in DMSO were freshly prepared from a solid stock. The best results were the ones using PHOME at 5  $\mu\text{M}$ , with the highest and most consistent inhibition.

Simultaneously, we decided to prepare ourselves the assay buffer. Cayman sells a pre-mixture of the assay buffer that needed to be diluted with HPLC-grade water to achieve a final concentration of 25 mM of *bis*-Tris, pH 7.0. So, we prepared the assay buffer according to the protocol from Cayman. Sadly, we could not reach the same levels of inhibition when testing ureas **108** and **109**. In these cases, once again, the signal-to-noise ratio was too small to differentiate any inhibition. Reviewing the literature, most part of the reported assays included bovine serum albumin (BSA) in the buffer.<sup>528,533</sup> The role of the BSA in the assay is double:

- i. The BSA helps the substrate to be more soluble. Thus, the [S] that the enzyme encounters is higher, improving the signal-to-noise ratio.
- ii. Inhibitors can bind lousily to BSA through hydrophobic interactions. Hence, adding BSA is a simple way to eliminate low-potency inhibitors.

Having considered the aforementioned, we finally achieved the optimum conditions as follows:

- *In situ* prepared PHOME solution at a final concentration of 5  $\mu\text{M}$ .
- Self-prepared assay buffer with 25 mM *bis*-Tris containing 0.1 mg/mL BSA.
- Human recombinant sEH from Cayman, with a likely concentration of 1.56 nM.
- Total volume was 200  $\mu\text{L}$  with a final DMSO concentration of 1% (v/v).
- Assay reaction time was less than 20 minutes.
- Assay performed at room temperature ( $23 \pm 2$  °C).
- 96-wells black plate from Greiner Bio-one (Fig. 88).

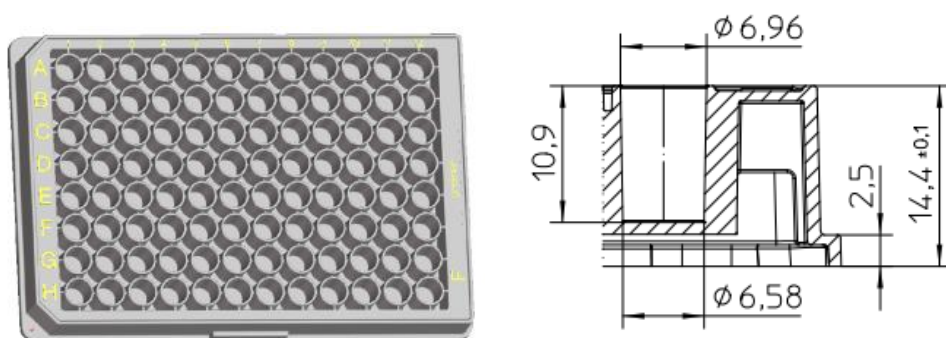


Fig. 88. Drawing of the used microplate and its dimensions in mm.

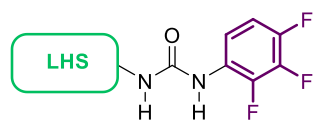
### 1.2.3 $IC_{50}$ determination of ureas 157 and 170-183

With the optimized conditions in hand, we proceeded to determine the  $IC_{50}$  of the new sEH inhibitors. For each measure, it was necessary to have at least two wells designated as background, three wells designated as 100% activity, and three wells for each one of the inhibitor concentrations to test. The assay was performed as indicated below:

1. Addition of assay buffer to each well.
2. Addition of DMSO to background and 100% activity wells.
3. Addition of inhibitors to the corresponding wells.
4. Addition of sEH to 100% activity and inhibitors wells.
5. Addition of PHOME to all the wells.
6. Incubation of 5 minutes at room temperature and fluorescence detection during the next 15 minutes.

The curve was generated from 5 different concentrations of inhibitor, ranging from 0.05 to 20 nM. The  $IC_{50}$  was calculated from at least three separate runs. The  $IC_{50}$  values of the new compounds are disclosed in table 19. The obtained values should be directly compared with our data for standard ureas 108 and 109, and not with the reported values, since assay conditions may violate Michaelis-Menten assumptions, and it is difficult to compare inhibitor potencies among laboratories.

**Table 19.** Inhibition of the sEH by the new compounds. Ureas 108 and 109 were used as standards. SE: standard error.



Comp.	LHS	IC <sub>50</sub> ± SE (nM)	Comp.	LHS	IC <sub>50</sub> ± SE (nM)
108		7.74 ± 0.06	177		14.1 ± 4.2
109		4.04 ± 0.45	178		0.86 ± 0.31
170		2.58 ± 0.28	179		4.16 ± 1.06
171		21.3 ± 5.4	180		10.3 ± 1.6
172		8.08 ± 3.16	157		37.1 ± 10.2
173		17.6 ± 3.6	181		25.5 ± 11.5
174		21.3 ± 4.3	182		0.80 ± 0.13
175		47.4 ± 11.4	183		25.7 ± 1.2

176		$31.4 \pm 3.2$	
-----	--	----------------	--

Satisfyingly, all the new adamantyl-like ureas were potent sEH inhibitors, with  $IC_{50}$  values ranging from 0.80 to 47.4 nM. Outstanding are compounds **170**, **178** and **182**, with  $IC_{50}$  values lower than the adamantyl standards. In general, some trends could be deduced from these data:

- Replacement of [redacted] led to an increase in the inhibitory activity (compare **108** ( $IC_{50}$  = 7.74 nM) vs **170** ( $IC_{50}$  = 2.58 nM)). These data indicated that the insertion of [redacted] is tolerated, far from what was observed by [redacted].
- Position of the [redacted] within the adamantane ring is significant for the activity, with the highest inhibition when the [redacted] is in C-2 position and not in C-5 (compare **170** ( $IC_{50}$  = 2.58 nM) vs **175** ( $IC_{50}$  = 47.4 nM)).
- Regarding the [redacted] **170-174**, it seemed that the [redacted], the worse the inhibitory activity. **171** ( $IC_{50}$  = 21.3 nM) escaped a little bit this trend, with a higher  $IC_{50}$  value than the next larger compound **172** ( $IC_{50}$  = 8.08 nM). This fact can be reasoned by a worse performance in the assay of **171**, probably underpinning a lower solubility. It is likely that [redacted] disrupt the binding of the inhibitor within the catalytic pocket of the enzyme.
- The use of the [redacted] scaffold in **176** was detrimental for the activity, with an  $IC_{50}$  of 31.4 nM. However, **176** was prepared and tested as a racemic mixture, and thus the data has to be taken with a pinch of salt.
- [redacted] scaffolds **177-179** also exhibited good inhibitory activities. Worth to highlight, the introduction of [redacted] in **178** ( $IC_{50}$  = 0.86 nM) and **179** ( $IC_{50}$  = 4.16 nM) significantly improved the activity compared with the [redacted] compound **177** ( $IC_{50}$  = 14.1 nM). This increase in the activity reflected the better space-filling of **178-179** than **177** thanks to the [redacted], which could provide a most favourable interaction within the catalytic site of sEH. Of note, it is compound **178** with a lower  $IC_{50}$  value than the adamantyl standards **108** ( $IC_{50}$  = 7.74 nM) and **109** ( $IC_{50}$  = 4.04 nM).

- On the other hand, analogue **180** showed good inhibitory potency, even though it was assayed also as a racemate.
- compounds **157** and **181** displayed lower activities compared with the standards, although showing good potency ( $IC_{50}$  of 37.1 and 25.5 nM, respectively). No significant difference was observed in the transition from **157** to **181**.
- Finally, scaffolds were also permitted. A first observation was that the replacement of the in **182** ( $IC_{50}$  = 0.80 nM) by and oxygen atom in **183** ( $IC_{50}$  = 25.7 nM) conduced to a decrease in the activity, a trend observed in the previous scaffolds (except for compound **170**). Nevertheless, the in the molecule gave the most potent compound of the series (**182** with an  $IC_{50}$  of 0.80 nM), being useful for enhancing inhibitory potency. This suggests that larger scaffolds than the adamantane nucleus are well tolerated. In addition, the may establish discrete interactions with specific residues in the catalytic site.

Thus, in terms of sEH inhibition, the most promising compounds were **170**, **178** and **182** (Fig. 89). The structural variety of the scaffolds below indicates that the catalytic pocket of sEH is largely flexible.

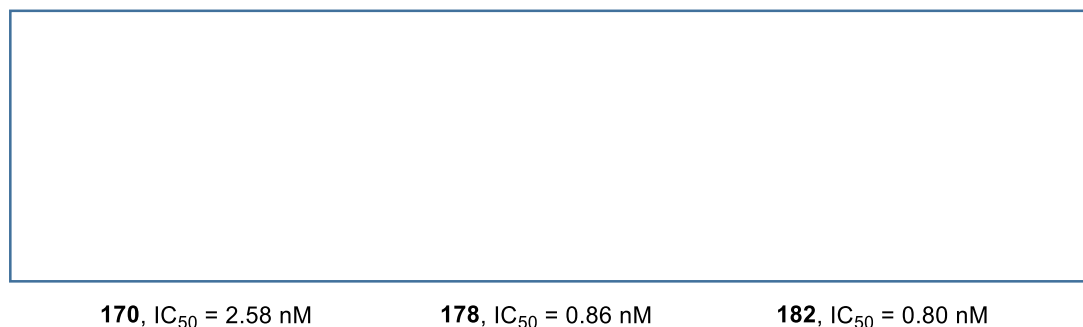


Fig. 89. Most potent compounds identified with a fluorescence screening assay.

### 1.3 Water solubility determination

It is well known that the solubility profile can be improved by salt/solid form selection and formulation, as well as through chemical structure modification, the latter being our approximation.<sup>536</sup> To further assess the ability of the new scaffolds to surrogate the adamantane group, we aimed to measure the water solubility of our new sEH inhibitors.

Solubility is a physical parameter that plays an important role in all phases of drug discovery and development. Solubility is central in *in vivo* assays (affecting the ADME process) and *in vitro* screenings (affecting reproducibility and reliability).<sup>537</sup> Among the five

<sup>536</sup> Sugano, K.; Okazaki, A.; Sugimoto, S.; Tavornvivas, S.; Omura, A.; Mano, T. *Drug Metab. Pharmacokinet.* **2007**, *22*, 225-254.

<sup>537</sup> Bhattachar, S. N.; Deschenes, L. A.; Wesley, J. A. *Drug Discov. Today* **2006**, *11*, 1012-1018.

key physicochemical properties in early compound screenings (pKa, solubility, permeability, stability and lipophilicity), poor solubility is on the top list of undesirable compound properties. Attrition in later stages of the drug discovery process are partly due to solubility issues.<sup>538</sup>

In a broad sense, solubility may be defined as the amount of a substance that dissolves in a given volume of solvent at a specified temperature. Various solubility assays are performed routinely in many pharmacological companies, and three major types of solubilities have been identified depending on the incubation time:

- Equilibrium or thermodynamic solubility: maximum amount of compound that can remain in solution in a given volume of the solvent under equilibrium conditions (days).
- Apparent or semi-equilibrium solubility: long incubation time with intention of reaching equilibrium (hours to one day).
- Kinetic solubility: solubility of a given compound measured regardless of the incubation time. Normally, after the addition of the sample into an aqueous media (minutes to a few hours).

Since the thermodynamic solubility is more time-consuming, and needs pure samples of the compounds, kinetic solubility is applied as HTS in early stages of drug discovery throughout the development process. Yet, both measurements are not interchangeable since they rely on fundamentally different physical properties.

Likewise, the solubility assays can be classified as:

- Solubility measurement using a DMSO stock solution of the compound (anti-solvent precipitation method).
- Solubility measurement using powder material (dissolution method).

After looking up the literature related to the discovery of sEH inhibitors, different procedures reached our hands describing how to measure water solubility. Since our research group was completely inexperienced with water solubility determinations, we turned once again to the group of Prof. Hammock in order to get some advises regarding these protocols. Kindly, they suggested following the method described by Tsai *et al.*, which consisted of an apparent or semi-equilibrium solubility measurement.<sup>539</sup> Starting off with a powdered sample of each compound, sodium phosphate buffer (pH 7.4) was added and the suspension was equilibrated during 24 h of shaking at room temperature ( $23 \pm 2$  °C). After extraction, the amount of each compound dissolved in buffer was determined by HPLC (fully protocol described in Material & Methods). Figure 90 includes an example of a solubility assay followed by Roche, and similar to our procedure.

---

<sup>538</sup> Di, L.; Fish, P. V.; Mano, T. *Drug Discov. Today* **2012**, *17*, 486-495.

<sup>539</sup> Tsai, H. J.; Hwang, S. H.; Morisseau, C.; Yang, J.; Jones, P. D.; Kasagami, T.; Kim, I. H.; Hammock, B. D. *Eur. J. Pharm. Sci.* **2010**, *40*, 222-238.

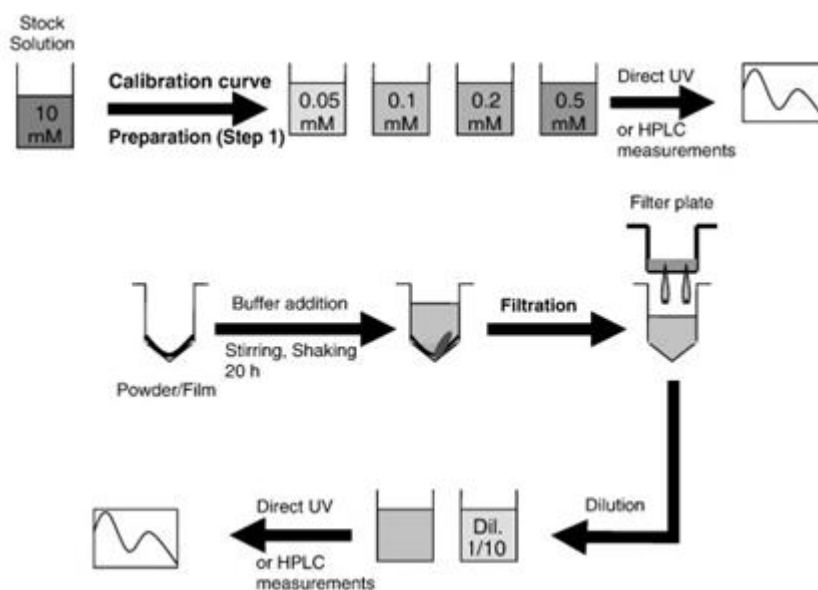
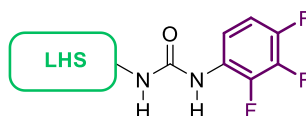


Fig. 90. Example of assay applied in a pharmaceutical company.<sup>540</sup>

Table 20 compiles the solubility data of compounds 157 and 170-183, and of the standard 109.

**Table 20.** Water solubility of the new compounds. Urea 109 was used as standard. S: solubility, SD: standard deviation.



Comp.	LHS	S ± SD (µg/mL)	Comp.	LHS	S ± SD (µg/mL)
109		1.66 ± 0.20	177		8.03 ± 1.46
170		16.1 ± 3.5	178		5.50 ± 0.40
171		3.01 ± 0.87	179		3.74 ± 2.14

<sup>540</sup> Alsenz, J.; Kansy, M. *Adv. Drug Deliv. Rev.* **2007**, *59*, 546-567.



172		$4.18 \pm 2.76$	180		$2.36 \pm 0.39$
173		$2.57 \pm 0.53$	157		$3.19 \pm 0.22$
174		$7.26 \pm 0.83$	181		$5.77 \pm 1.39$
175		$5.67 \pm 0.97$	182		$4.26 \pm 0.69$
176		$2.19 \pm 0.10$	183		$2.52 \pm 0.17$

Examination of the data included in table 20 allowed us to identify a few structure-solubility relationships:

- All the new scaffolds were slightly more soluble than the adamantyl standard **109** with small differences between them.
- With reference to the                    series,                    compound **170** was 10-times more soluble than **109** ( $16.1 \mu\text{g/mL}$  vs  $1.66 \mu\text{g/mL}$ ).
- Concerning the                    , an appealing trend was detected with a decrease in the water solubility as the number of carbon atoms increased. Thus, the                    **177** showed the largest solubility for this series ( $8.03 \mu\text{g/mL}$ ), followed by the                    **178** ( $5.50 \mu\text{g/mL}$ ) and the                    **179** ( $3.74 \mu\text{g/mL}$ ). However, this trend was not observed in the oxaadamantyl series.
- Surprisingly,                    **182** was more soluble than its corresponding                    **183** ( $4.26 \mu\text{g/mL}$  vs  $2.52 \mu\text{g/mL}$ ).

The disparity on the data points out that it should be carefully considered, because of two main reasons:

1. The crystal form affects the solubility of a compound, and amorphous material is usually more soluble than crystalline material. As indicated in Material &

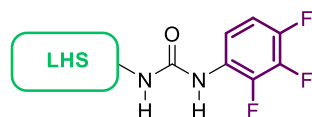
Methods, some of the new sEH inhibitors were crystallized for purity, whereas others came from column chromatography *prior* to evaporation of solvents using rotary-vacuum, which often generates amorphous material.

2. The establishment of intermolecular interactions determines the molecular packing, which directly affects solubility.

Although the increase in the water solubility is not remarkable, if we consider that our strategy has been the modulation of only one part of the molecule (LHS) so far, and that that modulation has been around the introduction of adamantane-like scaffolds, we can say that small changes on the molecule can affect substantially the solubility. For instance, just the replacement of a  means a 10-fold increase in water solubility, which is significant when it comes to developing drug candidates.

An indirect approach to test the solubility is by means of the melting point. The melting point provides a reasonable indication of the strength of intermolecular solute-solute interactions in the solid material. In general, high melting points are an indication of high crystal lattice energies, which lead to a lack of solubility both in organic solvents and in water, as just seen.<sup>541</sup> Taking into account this, we determined the melting points of the new ureas, with the values in table 21.

**Table 21.** Melting points of the new compounds. Ureas **108** and **109** were used as standards.<sup>497</sup>  
mp: melting point.



Comp.	LHS	mp (°C)	Comp.	LHS	mp (°C)
108		216-219	177		185-186
109		229-230	178		174-175
170		196-198	179		133-134

<sup>541</sup> Morisseau, C.; Newman, J. W.; Tsai, H. J.; Baecker, P. A.; Hammock, B. D. *Bioorg. Med. Chem. Lett.* **2006**, *16*, 5439-5444.

171		195-197	180		148-150
172		165-166	157		217-219
173		193-195	181		> 220 dec.
174		150-152	182		206-207
175		211-213	183		257-259
176		152-154			

Except for compounds **157**, **181** and **183** that did not alter or reduce somewhat the value with respect to the standards, the new scaffolds provided compounds with lower melting points. This observation is in accordance to the overall increase in the water solubility from table 20.

#### 1.4 Lipophilic ligand efficiency: a new metric for drug discovery

The strong relationship between solubility and lipophilicity is often discussed in the literature, and unsurprisingly as  $\text{clog } P$  increases, solubility on average decreases.<sup>84</sup> Compounds may be less water soluble if i) they are lipophilic and/or ii) they form cohesive, stable crystalline lattices. Indeed, Banerjee *et al.* suggested an empirical equation that relates solubility, melting point and  $\log P$  [ $\log P = 6.5 - 0.89(\log S) - 0.015\text{mp}$ ].<sup>542</sup> Hence, these three characteristics are interrelated. In consequence, fine-tuning of lipophilicity is one of the most applied strategies for improving water solubility, and eventually refining the “drug-

<sup>542</sup> Banerjee, S. *Environ. Sci. Technol.* **1980**, *14*, 1227-1229.

likeness".<sup>27,536</sup> In fact, this has been our approach with the modulation of adamantane's structure (scaffold-hopping), thus affecting log P, as it will be discussed later on.

In the last few years, novel metrics different from the traditional Lipinski's rule of five have appeared, and are employed to expedite the optimization process by combining several of these factors into guidelines for medicinal chemists.<sup>543,544,545</sup> All of them are designed to define the "drug-like" space. Among them, ligand efficiency (LE) is one of the most important and commonly employed metrics in drug discovery, first published by Kuntz in 1999 and redefined by Hopkins in 2004.<sup>546,547</sup> LE quantifies the average contribution of a heavy atom to the binding (Equation 2). As the name suggests, it measures the efficiency of the ligand in the potency.

$$\begin{aligned} \text{LE} &= \Delta G / \text{number of heavy atoms} \\ &\text{or} \\ \text{LE} &= \text{pIC}_{50} (\text{or pK}_i) / \text{number of heavy atoms} \end{aligned} \quad \text{Equation 2}$$

Another major metric is the lipophilic ligand efficiency (LLE or LipE), which is an estimate of the specificity of a molecule in binding to the target relative to lipophilicity. In other words, LipE normalizes potency relative to log P.<sup>548</sup> It is calculated by applying a relative simple equation 3.

$$\text{LipE} = -\log(K_i \text{ or } \text{IC}_{50}) - \log D \text{ (or clog P)} \quad \text{Equation 3}$$

It reasserts the principle of minimal hydrophobicity, which states that "without convincing evidence to the contrary, drugs should be made as hydrophilic as possible without loss of efficacy".<sup>549</sup> Increasing LipE is likely to be associated with better selectivity, efficient polar atom ligand-protein contacts, and specific hydrophobic binding.<sup>83</sup> Based on the properties of an average oral drug, with a clog P of ~2.5–3.0 and potency in the range of ~1–10 nM, an ideal LipE value for an optimized drug candidate is ~5–7 units or greater. Negative LipE values are clearly unfavourable. Many oral drugs occupy optimal combined ligand efficiency space for their specific targets, showing the importance of balancing biological activity, size, and lipophilicity in lead optimization.

In order to assess the changes on the clog P, and hence on the LipE, as a result of our scaffold-hopping strategy, we first calculated the clog P using Bio-Loom<sup>®</sup> software, and then we applied equation 3. The results are summarized in table 22.

<sup>543</sup> Meanwell, N. A. *Chem. Res. Toxicol.* **2011**, *24*, 1420-1456.

<sup>544</sup> Abad-Zapatero, C.; Champness, E. J.; Segall, M. D. *Future Med. Chem.* **2014**, *6*, 577-593.

<sup>545</sup> Hopkins, A. L.; Keserü, G. M.; Leeson, P. D.; Rees, D. C.; Reynolds, C. H. *Nat. Rev. Drug Discov.* **2014**, *13*, 105-121.

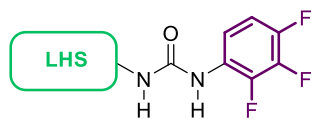
<sup>546</sup> Kuntz, I. D.; Chen, K.; Sharp, K. A.; Kollman, P. A. *Proc. Natl. Acad. Sci. USA* **1999**, *96*, 9997-10002.

<sup>547</sup> Hopkins, A. L.; Groom, C. R.; Alex, A. *Drug Discov. Today* **2004**, *9*, 430-431.

<sup>548</sup> Freeman-Cook, K. D.; Hoffman, R. L.; Johnson, T. W. *Future Med. Chem.* **2013**, *5*, 113-115.

<sup>549</sup> Hansch, C.; Björkroth, J. P.; Leo, A. J. *J. Pharm. Sci.* **1987**, *76*, 663-687.

**Table 22.** Values of clog P and LipE for the new sEH inhibitors. Ureas **108** and **109** were used as standards.



Comp.	LHS	clog P	LipE	Comp.	LHS	clog P	LipE
108		4.04	4.07	177		2.93	4.92
109		5.08	3.31	178		3.96	5.11
170		2.71	5.58	179		5.36	3.02
171		3.23	4.44	180		5.19	2.80
172		3.76	4.33	157		2.59	4.84
173		5.26	2.50	181		3.55	4.04
174		4.27	3.40	182		5.48	3.62
175		2.14	5.18	183		4.21	3.38

176		1.67	5.83	
-----	--	------	------	--

Some interesting aspects could be deduced from the evaluation of the clog P values:

- The clog P varied with every different scaffold, with values ranging from 1.67 to 5.48. Since adamantyl standards **108** and **109** showed clog P values of 4.04 and 5.08, respectively, most part of the new compounds lowered the lipophilicity, whilst others increased moderately the clog P.
- Compounds bearing an **170-176** displayed a significant reduction in the clog P, except for compounds **173** and **174** (clog P of 5.26 and 4.27, respectively), which contain substituents. Outstanding are ureas **170**, **175** and **176** (clog P of 2.71, 2.14 and 1.67, respectively) with a clog P value < 3 and 1 to 2 log units less than adamantyl ureas **108** and **109** (clog P of 4.04 and 5.08, respectively).
- For both families, the lipophilicity was enhanced as the number of atoms increased, as expected.
- Among the , compounds **177** and **178** (clog P of 2.93 and 3.96, respectively) lowered the clog P significantly compared with 1-adamantyl-urea **108**.
- Surprisingly, **157** and **181** (clog P of 2.59 and 3.55, respectively) reduced lipophilicity around 0.5-2.5 log units when compared to standards **108** and **109** (clog P of 4.04 and 5.08, respectively).
- Finally, scaffolds featuring a **182** and **183** (clog P of 5.48 and 4.21, respectively) displayed a larger clog P than the adamantyl ureas **108** and **109** because of their skeleton. Besides, the insertion of a in **183** reduced the lipophilicity compared with its analogue **182**.

Evaluation of the LipE values led us to the identification of three different situations:

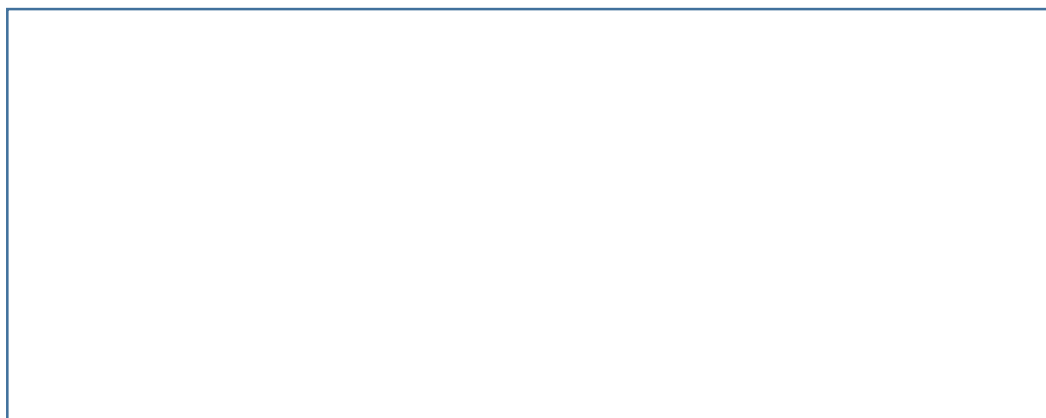
- Enhanced LipE with a reduction of both IC<sub>50</sub> and clog P values: this is case of compounds **170** and **178** (LipE of 5.58 and 5.11, respectively).
- Enhanced LipE because of a remarkable reduction in the lipophilicity: here are included compounds **171** (LipE of 4.44), **172** (LipE of 4.33), **175** (LipE of 5.18), **176** (LipE of 5.83), **177** (LipE of 4.92), **157** (LipE of 4.84) and **181** (LipE of 4.04).
- Reduced LipE due to loss in the inhibitory activity and to an increase in the lipophilicity: this behaviour is showed in compounds **173** (LipE of 2.50), **174** (LipE of 3.40), **179** (LipE of 3.02), **180** (LipE of 2.80) and **183** (LipE of 3.38).

A special case is urea **182** (LipE of 3.62), with a LipE in between both standards **108** and **109** (LipE of 4.07 and 3.31, respectively), which despite of the dramatic gain in the lipophilicity (clog P of 5.48), is more efficient than the adamantyl analogues in the binding, as it is reflected in its  $IC_{50}$  (0.80 nM).

This last observation, along with the former statements, showed that the adamantane ring is not the most efficient bulky hydrophobic group as LHS of sEH inhibitors, and that a variety of scaffolds may replace it with properties that are more appropriate.

## 2. New ureas with selected scaffolds

In order to confirm the ability of the new scaffolds to surrogate the adamantane in sEH inhibitors, we aimed to build a second batch of compounds with the more promising scaffolds. The selection of the polycycles were in accordance to the overall performance in the inhibition assay, solubility measurement and LipE calculation, but also to the ease on the synthesis of the scaffold. Figure 91 resumes the selected scaffolds.



**Fig. 91.** Selection of scaffolds from the previous series of compounds.

We applied the scaffolds from compounds **170**, **176** and **178** to the synthesis of further ureas with the aim of proving the efficiency of these structures as lipophilic groups in the design of sEH inhibitors. In this case, we selected the RHS of the known inhibitors *t*-AUCB and APAU. Both compounds display potent activities against sEH ( $IC_{50}$  values of 1.3 nM and 7 nM, respectively) and improved physicochemical properties (Fig. 92).<sup>484,483</sup>

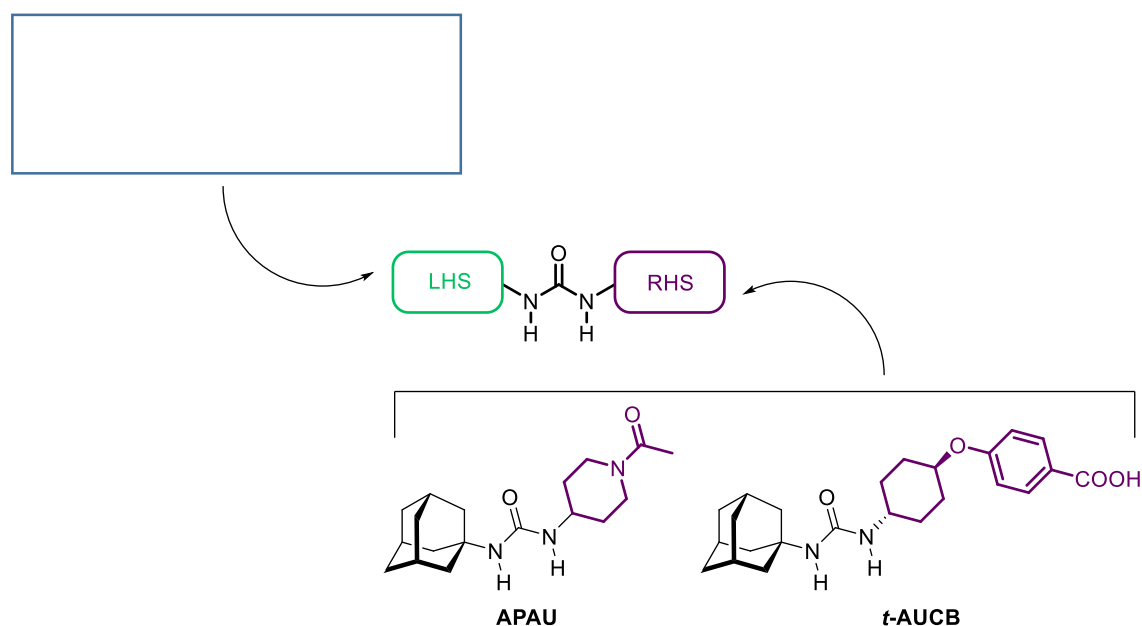
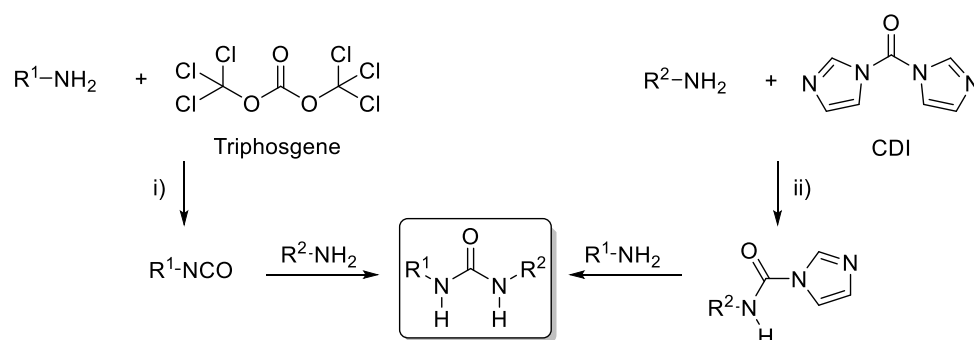


Fig. 92. New approach for the synthesis of new ureas.

## 2.1 Synthesis of new ureas with selected scaffolds

For the preparation of the next ureas, we could not apply the synthetic approach used for the previous batch, since no required isocyanate was commercially available. In the exploration of the different strategies to build ureas groups, two procedures stood out: i) formation of an intermediate isocyanate with triphosgene from the first amine, and subsequent attack of the second amine, or ii) use of the coupling agent carbonyldiimidazole (CDI) (Scheme 83). Both routes implied the use of a transfer reagent, which functionalized one of the amine counterparts in order to react with the other one.<sup>550</sup>



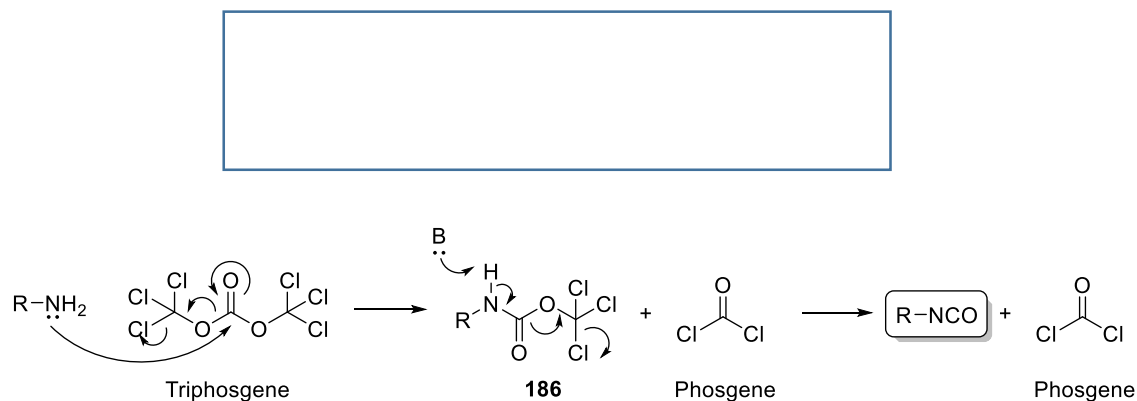
Scheme 83. Two alternatives to form a urea functionality.

To test the feasibility of both protocols in our scaffolds, we applied both conditions for the preparation of the *N*-(1-acylpyrrolidin-4-yl)-*N'*-( )urea **184**, analogue to APAU. We decided to make first the corresponding isocyanate **185** from the treatment of **120** with triphosgene, a source of the highly toxic

<sup>550</sup> Pdiya, K. J.; Gavade, S.; Kardile, B.; Tiwari, M.; Bajare, S.; Mane, M.; Gaware, V.; Varghese, S.; Harel, D.; Kurhade, S. *Org. Lett.* **2012**, *14*, 2814-2817.

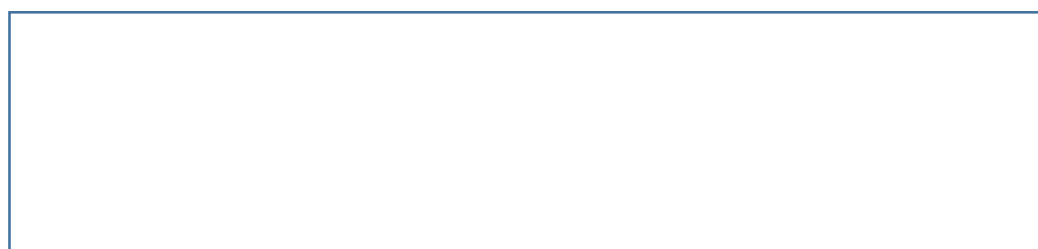


phosgene.<sup>551,552,553</sup> Triphosgene has the advantage of being safer than phosgene when working with the substance since it is a solid crystal, as opposed to phosgene that is a gas. Its name came from the idea that triphosgene contains three molecules of phosgene, which are released upon reaction. Thus, the reaction mechanism starts with the attack of the nucleophilic amine to the triphosgene carbonyl, liberating one molecule of phosgene and the carbamate intermediate **186**. This intermediate eliminates another molecule of phosgene to give the desired isocyanate **185** in 86% yield (Scheme 84). The two *in situ*-formed molecules of phosgene can react with the starting amine **120**. Hence, only a third of the equivalents of triphosgene is enough for the reaction to be efficient.



**Scheme 84.** Formation of an isocyanate *via* the reaction of an amine with triphosgene.

Next, isocyanate **185** was reacted with 1-acetyl-4-aminopiperidine under the same conditions used for the preparation of the former trifluorophenyl ureas. In this manner, urea **184** was produced in 52% yield after purification by column chromatography (Scheme 85).



**Scheme 85.** Reaction of isocyanate **185** with a commercially available amine.

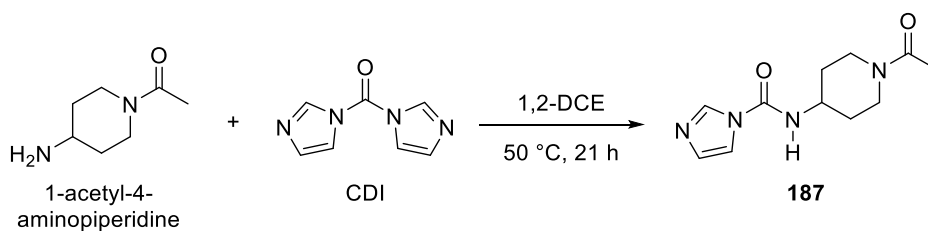
For the second alternative, we proceeded to the synthesis of the corresponding imidazole carboxamide **187** by reacting CDI with 1-acetyl-4-aminopiperidine in 1,2-dichloroethane (Scheme 86).<sup>554</sup> The titled compound **187** was obtained in 75% yield, and fully characterized.

<sup>551</sup> Sciuto, A. M.; Hurt, H. H. *Inhal. Toxicol.* **2004**, *16*, 565-580.

<sup>552</sup> Ichikawa, Y.; Matsukawa, Y.; Nishiyama, T.; Isobe, M. *Eur. J. Org. Chem.* **2004**, *2004*, 586-591.

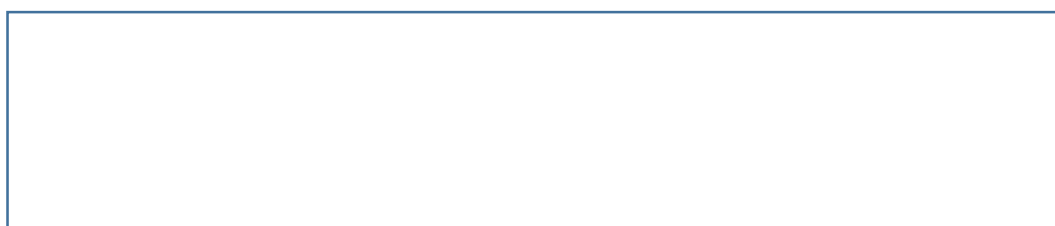
<sup>553</sup> Davis, M. C.; Dahl, J. E. P.; Carlson, R. M. K. *Synth. Commun.* **2008**, *38*, 1153-1158.

<sup>554</sup> Rawling, T.; McDonagh, A. M.; Tattam, B.; Murray, M. *Tetrahedron* **2012**, *68*, 6065-6070.



**Scheme 86.** Preparation of the intermediate **187** through an addition-elimination reaction mechanism.

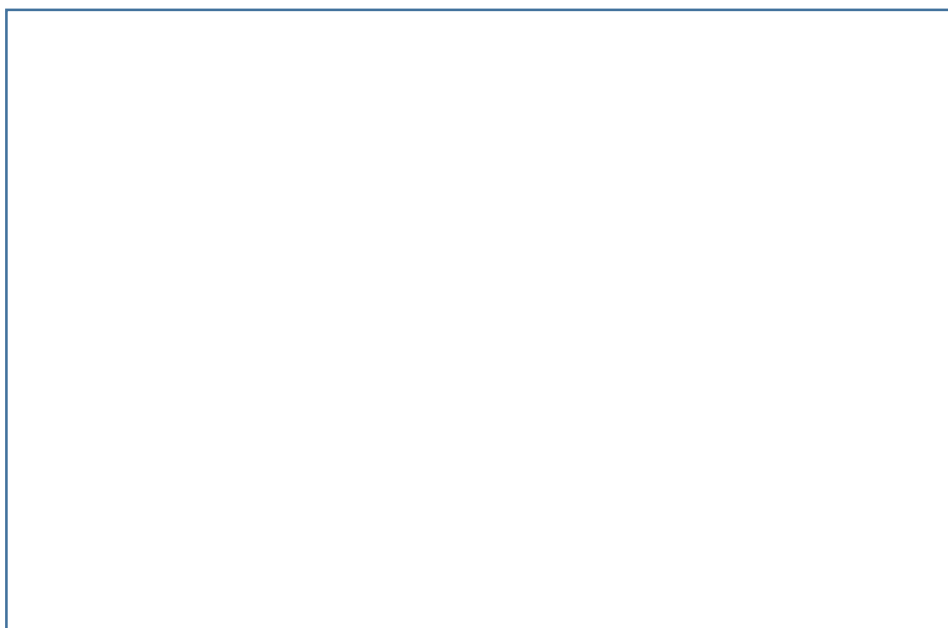
Then, imidazole carboxamide **187** was subjected to the attack of **120** to afford the desired urea **184** in 53% yield, comparable to the previous procedure with triphosgene (Scheme 87).



**Scheme 87.** Synthesis of final urea **184** following the protocol with CDI as the transfer reagent.

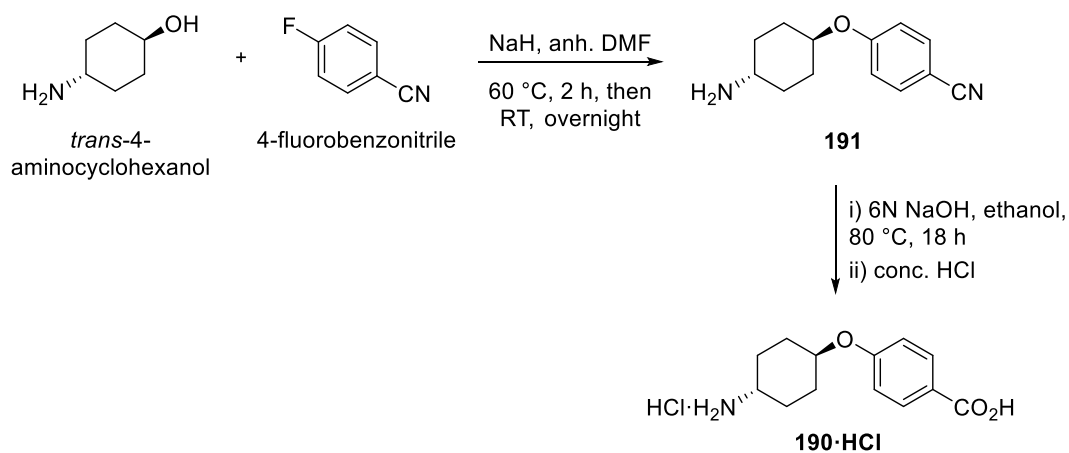
With these two syntheses, we concluded that both alternatives were comparable in terms of yield. Nevertheless, the procedure with CDI as transfer reagent needed harsher conditions (long reaction times while heating). Accordingly, we applied the triphosgene route, whenever possible, for the preparation of the following ureas.

Analogously, **188** was built by means of the preparation of its corresponding isocyanate **189** in quantitative yield from amine **121**, and subsequent transformation to urea **188** with the addition of 1-acetyl-4-aminopiperidine in 26% yield (Scheme 88).



**Scheme 88.** Synthetic sequence for the preparation of urea **188**.

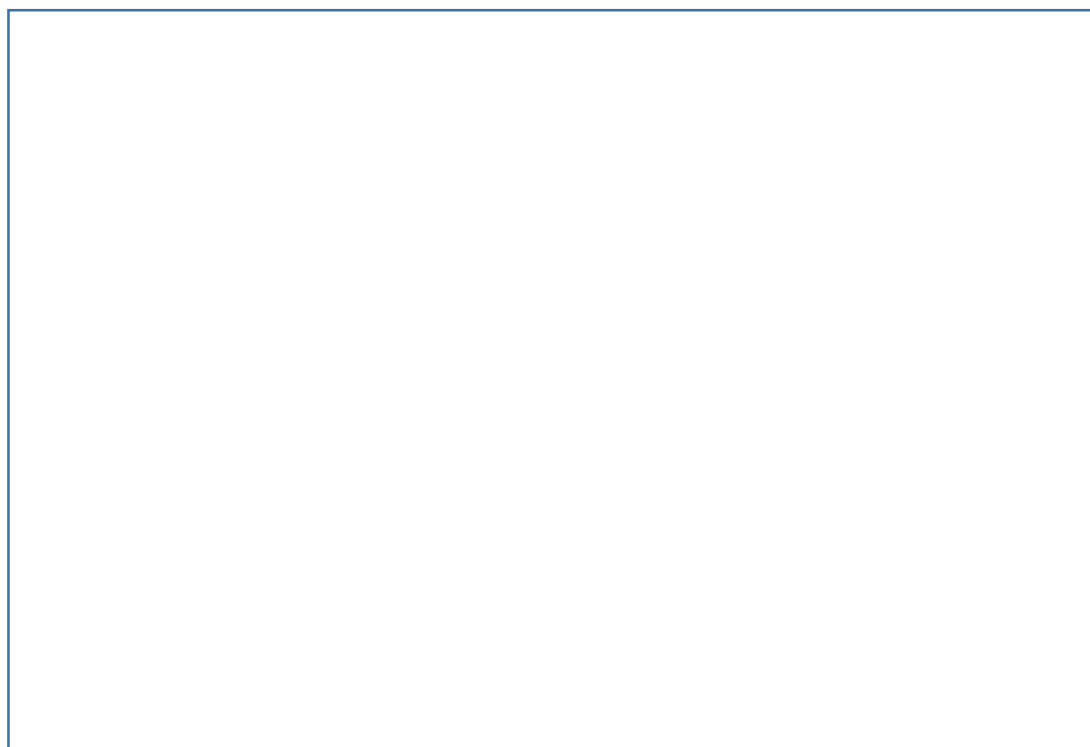
In the case of the analogues of the sEH inhibitor *t*-AUCB, the corresponding amine **190** was not commercially available. So, we followed the reported methodologies by Hwang *et al.* for the construction of the RHS of the molecule.<sup>483,555</sup> The synthetic pathway consisted in the nucleophilic aromatic substitution of fluorobenzonitrile by *trans*-4-aminocyclohexanol, and consecutive hydrolysis of nitrile **191** to carboxylic acid **190** under basic conditions in 44% overall yield (Scheme 89). The success of the nucleophilic aromatic substitution was due to the presence of an EWG in *para*-position (nitrile).



**Scheme 89.** Nucleophilic aromatic substitution and basic hydrolysis for the preparation of intermediate amine **190** as its hydrochloride salt.

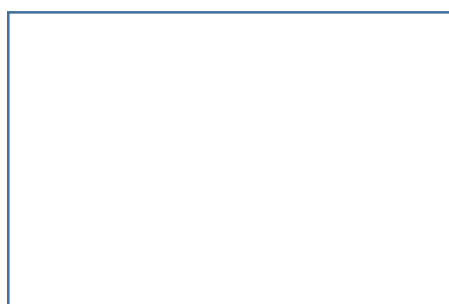
<sup>555</sup> Hwang, S. H.; Weckler, A. T.; Zhang, G.; Morisseau, C.; Nguyen, L. V; Fu, S. H.; Hammock, B. D. *Bioorg. Med. Chem. Lett.* **2013**, *23*, 3732-3737.

Once intermediate amine **190** was prepared in sufficient amounts, ureas **192** and **193** were obtained in 24 and 50% yield, respectively, from the corresponding isocyanates **185** and **189** (Scheme 90).



**Scheme 90.** Attack of the primary amine of **190** to each one of the isocyanates to provide final ureas **192** and **193**.

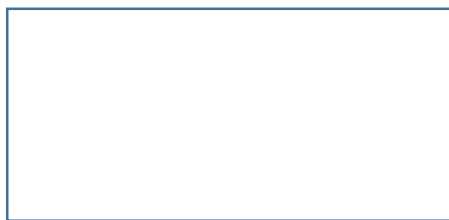
Special cases were the \_\_\_\_\_ analogues with general structure **VI**, the last scaffold to prepare (Fig. 93).



**Fig. 93.** \_\_\_\_\_ ureas to prepare.

For the synthesis of these particular ureas, we encountered two handicaps:

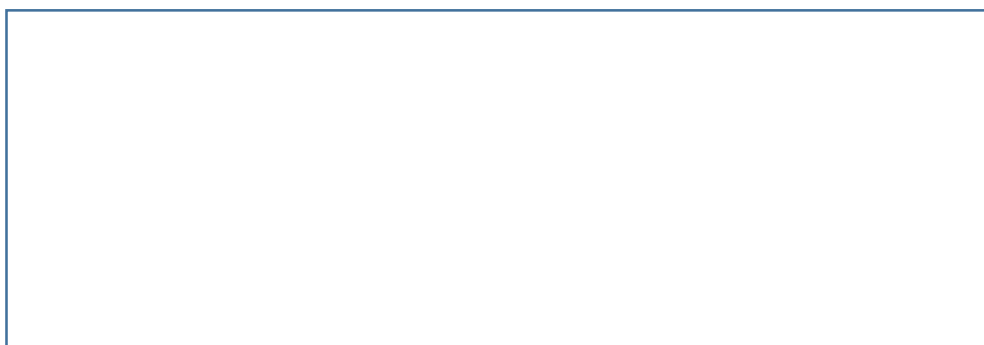
1. We envisioned that the corresponding isocyanate **194** should be volatile under the reaction conditions and posterior work-up procedure (Fig. 94). This volatility may be due to the small molecular weight ( \_\_\_\_\_ Da) and to the lack of strong intermolecular interactions.



**Fig. 94.** We hypothesized the volatility of isocyanate **194**.

2. Because of the low-yielding synthetic route to construct the scaffold, we had only enough amounts of starting amine **123** to prepare a single derivative.

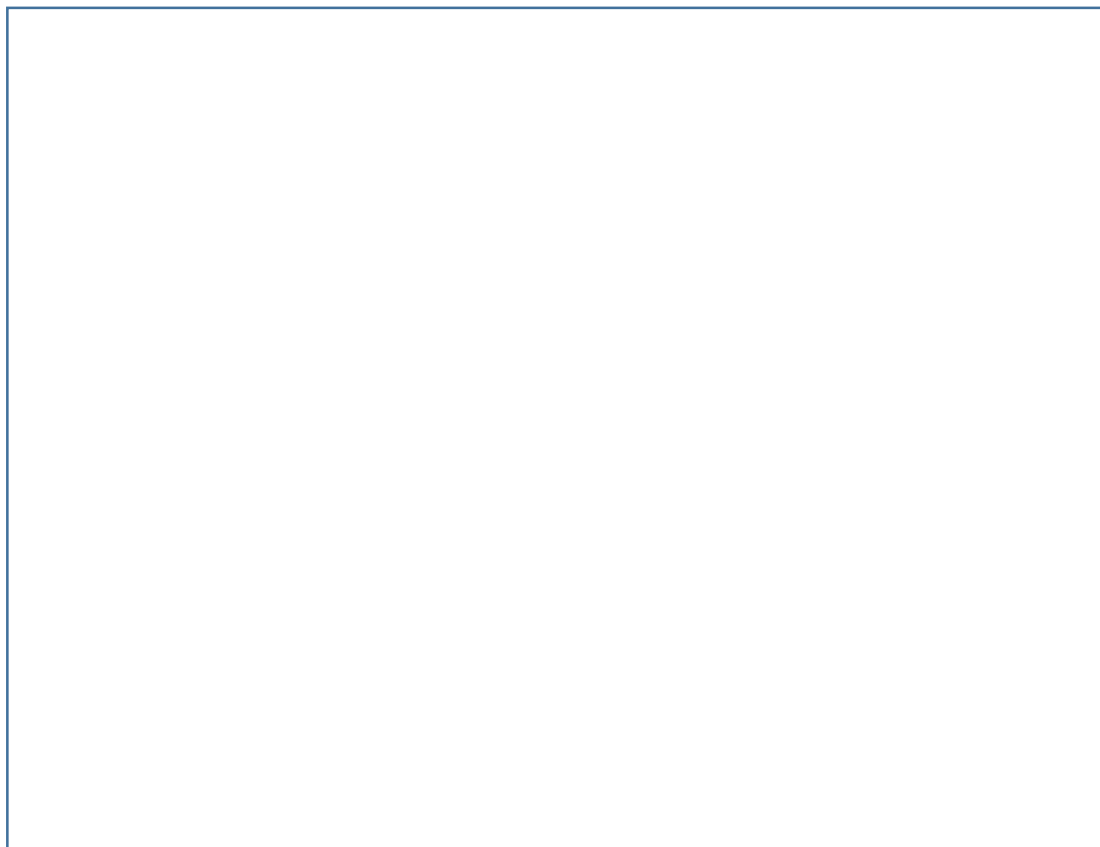
All in all, we pursued the synthesis of APAU's derivative **195** implementing the procedure that entailed CDI as transfer reagent. In this sense, amine **123** was reacted with the imidazole carboxamide **187** in the presence of triethylamine to furnish final urea **195** in 77% yield (Scheme 91).



**Scheme 91.** Synthesis of the last derivative of the series.

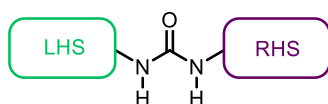
## 2.2 Pharmacological evaluation of new ureas with the selected scaffolds

The five new ureas were tested as sEH inhibitors under our optimized screening assay (Fig. 95).



**Fig. 95.** New ureas to test as sEH inhibitors.

We performed the inhibitory screening assay under the previous conditions for the determination of the  $IC_{50}$  values, using the commercially available *t*-AUCB as standard (Table 23).

**Table 23.** Inhibition of the sEH by the new ureas. *t*-AUCB was used as standard.<sup>483,484</sup>

Comp.	LHS	RHS	IC <sub>50</sub> ± SE (nM)
<i>t</i> -AUCB			1.87 ± 0.14 (reported 1.3 nM)
APAU			reported 7 nM
184			19.8 ± 6.2
188			50.8 ± 11.9
192			13.4 ± 4.0
193			40.6 ± 8.9
195			8.41 ± 0.59

According to the above data, the following conclusions may be drawn for this second batch of ureas:

- Any new scaffold improved the inhibitory activity of the standard *t*-AUCB under the assay conditions.

- Among the three different scaffolds tested, **195** (IC<sub>50</sub> of 8.41 nM) was the most potent inhibitor compared with other structures.
- Regarding the ureas **184** and **192** (IC<sub>50</sub> of 19.8 and 13.4 nM, respectively) displayed lower IC<sub>50</sub> values than ureas **188** and **193** (IC<sub>50</sub> of 50.8 and 40.6 nM, respectively).
- Between the two different RHSs assayed (when a direct comparison was possible), APAU derivatives showed lower inhibitory potency than *t*-AUCB derivatives; compare **184** with **192** (IC<sub>50</sub> of 19.8 and 13.4 nM, respectively) and **188** and **193** (IC<sub>50</sub> of 50.8 and 40.6 nM, respectively).

Although showing higher IC<sub>50</sub> values than the adamantyl standard, the potent activity of the selected scaffolds as sEH inhibitors underpinned their ability to surrogate the adamantane nucleus in this kind of bioactive molecules.

Taking into account the excellent potency of the ring-contracted APAU derivative **195** (IC<sub>50</sub> of 8.41 nM), and that the inhibitors bearing the RHS from *t*-AUCB displayed higher activities, it seems logical that the missing piece of this puzzle is the corresponding *t*-AUCB derivative **196** (Fig. 96). Unfortunately, there was not enough time during the present thesis to prepare this promising compound.

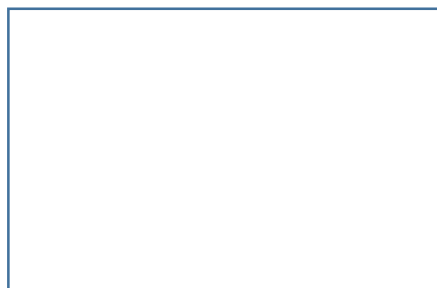


Fig. 96. Urea to prepare to combine the best findings from table 23.

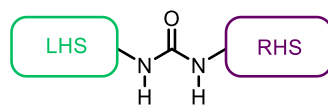
### 2.3 Water solubility, melting points and LipE

To further assess the new sEH inhibitors, we aimed to determine some physicochemical properties as in the case of the former series of compounds. Thus, we measured the water solubility, determined the melting points, and calculated the clog P and the LipE in order to compare these structures with the adamantyl standards (Table 24).

Worth to mention is that, in the case of compounds **184**, **188** and **195**, which lack a chromophore group and therefore showed lower absorbance in the HPLC measurement, a mathematical adjustment was required in order to extrapolate the values to the calibration curve (see Materials & Methods).



**Table 24.** Water solubility, melting points, clog P and LipE of the new ureas. *t*-AUCB was used as standard.<sup>483</sup> mp: melting point. ND: not determined.



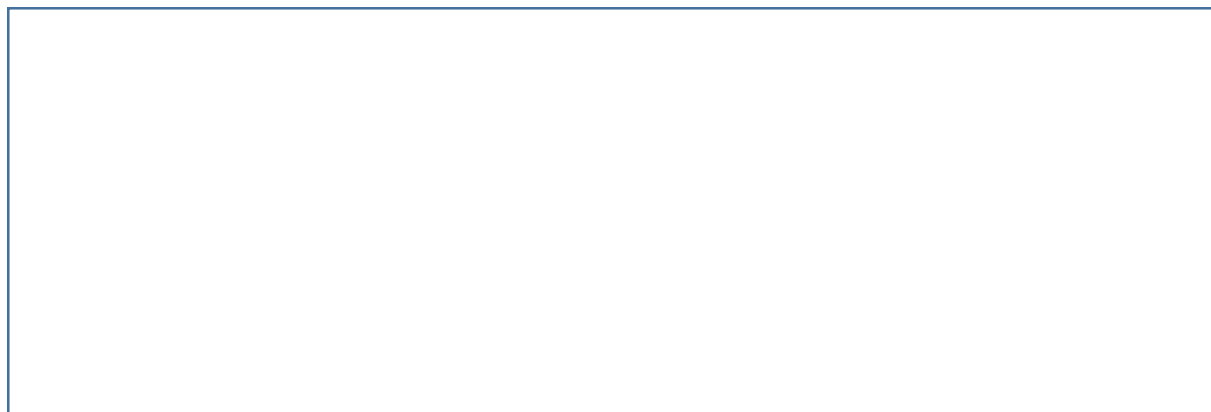
Comp.	LHS	RHS	S ± SD (µg/mL)	mp (°C)	clog P	LipE
<i>t</i> -AUCB			reported > 200	250-255	4.84	3.89
APAU			reported > 200	205-206	0.77	7.38
184			232.9 ± 12.1	172-173	-0.37	8.07
188			258.1 ± 17.4	164-166	-1.41	8.70
192			72.1 ± 2.9	255-257	3.70	4.17
193			138.6 ± 3.5	254-256	2.67	4.72
195			295.9 ± 26.6	165-167	0.69	7.39

The data shown in table 24 revealed interesting features:

- Although we could not afford to determine the water solubility of the standards under our procedure, all the prepared ureas displayed good solubility values, better suited than the previous ones for a possible pharmaceutical.

- Compound **195** showed the highest water solubility (295.9  $\mu\text{g/mL}$ ), whereas *t*AUCB derivatives **192** and **193** exhibited the worst results (72.1 and 138.6  $\mu\text{g/mL}$ , respectively). This is in accordance with the high melting points for these two ureas. Presumably, the extraordinary energy lattices of the crystal structure of these compounds affects significantly their water solubility.
- *clog P* values extremely decreased when 1-acetylpiperidine was placed as the RHS (compounds **184**, **188** and **195**), to a level that they were no longer considerable as drug candidates (-1.41 to 0.69). Because of this, LipE values were remarkably high for these type of structures.
- *t*AUCB derivatives **192** and **193** showed a more “drug-like” profile with acceptable water solubilities, optimum *clog P* values, and appropriate LipE.

Compiling the data obtained so far, we have identified some scaffolds as excellent surrogates of the adamantane nucleus in sEH inhibitors, a few of them with remarkable physicochemical properties. From this point, the next step was the evaluation of these new sEH inhibitors in *in vitro* studies, so as to assess their ability to inhibit the sEH enzyme in a cellular level. Because of the close relationship of the sEH in the development of the endoplasmic reticulum (ER) stress (*vide infra*), we aimed to test a few of our more promising compounds in ER stress studies. Consequently, we selected three compounds that displayed a perfect balance between inhibitory activity and *clog P* (expressed in the LipE) and that entailed easy synthetic routes for the preparation of the scaffolds. The latter point was envisioning that these structures would progress throughout the drug discovery process. The selected molecules are disclosed in figure 97.



**Fig. 97.** Selected compounds for *in vitro* studies.

### 3. ER stress amelioration with selected sEH inhibitors. *In vitro* studies

The ER is a membranous network that functions in the synthesis, folding and maturation of newly secretory and membrane proteins, and is highly responsive to nutrients and energy status of the cell. When certain pathological stress conditions disrupt ER homeostasis, such as nutrient excess or deficiency, stress, inflammation, hypoxia or infection, the folding capacity of the ER is exceeded and consequently misfolded proteins

accumulate and lead to the so-called ER stress.<sup>556</sup> For instance, obesity is a chronic stimulus for ER stress in peripheral tissues, and is a core mechanism involved in triggering insulin resistance and T2DM.<sup>557</sup> In addition, obese individuals exhibit increased expression of multiple markers of ER stress.<sup>558</sup> On the other hand, ER stress also provides several links with the emergence of inflammatory processes, mainly by activation of both c-Jun amino-terminal kinase (JNK) and inhibitor of  $\kappa$   $\beta$  kinase (IKK), both related to the development of insulin resistance.<sup>559,560</sup> Taken together, the effector arms of ER stress and the associated stress responses are tightly linked to inflammatory pathways at many levels that are crucial for insulin action and metabolic homeostasis. Thus, understanding the role of ER stress may be of therapeutic potential for the treatment of metabolic diseases, specially obesity and T2DM.<sup>301,561</sup> In addition, ER stress is a key piece to the pathogenesis of other diseases such as neurodegenerative disorders and cancer.<sup>440</sup>

In response to the accumulation of unfolded proteins in the ER, a sequential process takes place; the rate of general translation initiation is attenuated, the expression of ER resident protein chaperones and protein foldases is induced, the ER compartment proliferates, and ER-associated degradation (ERAD) is activated to eliminate irreparable misfolded proteins.<sup>556,562</sup> If these survival mechanisms fail to facilitate ER homeostasis, ER-stress triggers apoptotic processes.<sup>563,564</sup> The adaptive mechanisms to mitigate ER stress and to restore homeostasis are collectively termed as the unfolded protein response (UPR), which consists of a signal transduction system linking the ER lumen with the cytoplasm and nucleus.<sup>565</sup> UPR signalling consists of three branches initiated by the ER transmembrane proteins PKR-like ER-regulated kinase (PERK), inositol-requiring enzyme 1 (IRE1), and activating transcription factor 6 (ATF6).<sup>559,566,567</sup> These sensor proteins respond to changes in protein folding status in the ER and convey information to activate distinct and sometimes overlapping pathways, leading to diverse developmental and metabolic processes. PERK phosphorylates the  $\alpha$ -subunit of eukaryotic translation initiation factor 2 (eIF2) at Ser51, leading to rapid and transient attenuation of protein

<sup>556</sup> Schröder, M.; Kaufman, R. J. *Annu. Rev. Biochem.* **2005**, *74*, 739-789.

<sup>557</sup> Ozcan, U.; Cao, Q.; Yilmaz, E.; Lee, A. H.; Iwakoshi, N. N.; Ozdelen, E.; Tuncman, G.; Görgün, C.; Glimcher, L. H.; Hotamisligil, G. S. *Science* **2004**, *306*, 457-461.

<sup>558</sup> Sharma, N. K.; Das, S. K.; Mondal, A. K.; Hackney, O. G.; Chu, W. S.; Kern, P. A.; Rasouli, N.; Spencer, H. J.; Yao-Borengasser, A.; Elbein, S. C. *J. Clin. Endocrinol. Metab.* **2008**, *93*, 4532-4541.

<sup>559</sup> Hummasti, S.; Hotamisligil, G. S. *Circ. Res.* **2010**, *107*, 579-591.

<sup>560</sup> Hotamisligil, G. S. *Int. J. Obs.* **2008**, *32*, S52-S54.

<sup>561</sup> Eizirik, D. L.; Cardozo, A. K.; Cnop, M. *Endocr. Rev.* **2008**, *29*, 42-61.

<sup>562</sup> Wu, J.; Kaufman, R. J. *Cell Death Differ.* **2006**, *13*, 374-384.

<sup>563</sup> Zinszner, H.; Kuroda, M.; Wang, X.; Batchvarova, N.; Lightfoot, R. T.; Remotti, H.; Stevens, J. L.; Ron, D. *Genes Dev.* **1998**, *12*, 982-995.

<sup>564</sup> Nishitoh, H.; Matsuzawa, A.; Tobiume, K.; Saegusa, K.; Takeda, K.; Inoue, K.; Hori, S.; Kakizuka, A.; Ichijo, H. *Genes Dev.* **2002**, *16*, 1345-1355.

<sup>565</sup> Pluquet, O.; Pourtier, A.; Abbadie, C. *Am. J. Physiol. Cell Physiol.* **2015**, *308*, C415-C425.

<sup>566</sup> Ron, D.; Walter, P. *Nat. Rev. Mol. Cell Biol.* **2007**, *8*, 519-529.

<sup>567</sup> Hotamisligil, G. S. *Cell* **2010**, *140*, 900-917.

synthesis to decrease protein influx into the ER lumen.<sup>568,569</sup> eIF2 $\alpha$  promotes the activating transcription factor 4 (ATF4), which induces genes involved in ER function, ER-induced apoptosis, and an inhibitory feedback to prevent hyperactivation of the UPR, among other effects.<sup>570,571</sup> IRE1 activation leads to the unconventional splicing of X-box-binding protein 1 (XBP1) mRNA, leading to the synthesis of a nuclear XBP1 form that induces the transcription of genes encoding ER chaperones and ERAD.<sup>572,573,574</sup> The third canonical branch includes ATF6, which, upon ER stress, traffics to the Golgi apparatus, where it is cleaved to liberate a fragment that translocates to the nucleus to induce genes encoding ER chaperones and ERAD functions, independently or synergistically with XBP1 and ATF4.<sup>575,576</sup>

The master initiator of the UPR is the immunoglobulin-heavy-chain-binding protein or BiP, which is a negative effector of the UPR, known as well as 78 kDa glucose-regulated protein (GRP78). In physiological states, this chaperone is known to be expressed constitutively and binds to the luminal domains of PERK, IRE1, and ATF6 in their inactive forms.<sup>577</sup> Under conditions that promote accumulation of misfolded proteins, GRP78 is overexpressed and preferentially binds to hydrophobic regions of unfolded/misfolded proteins that accumulate in the ER lumen.<sup>578</sup> Consequently, BiP is sequestered and dissociates from the ER stress sensors to allow their signalling.<sup>579,580,581</sup>

As stated before, chronic or severe ER stress activates the UPR leading to apoptosis. Persistent activation of PERK-eIF2 $\alpha$ -ATF4 and ATF6 pathways culminates in the induction of the CCAAT enhancer-binding protein (C/EBP) homologous protein (CHOP or GADD153), which up-regulates apoptosis-related genes.<sup>563,582,583</sup>

---

<sup>568</sup> Shi, Y.; Vattem, K. M.; Sood, R.; An, J.; Liang, J.; Stramm, L.; Wek, R. C. *Mol. Cell. Biol.* **1998**, *18*, 7499-7509.

<sup>569</sup> Novoa, I.; Zhang, Y.; Zeng, H.; Jungreis, R.; Harding, H. P.; Ron, D. *EMBO J.* **2003**, *22*, 1180-1187.

<sup>570</sup> Harding, H. P.; Zhang, H.; Zeng, I.; Novoa, P. D.; Lu, M.; Calton, N.; Sadri, C.; Yun, B.; Popko, R.; Paules Stojdl, D. F.; Bell, J. C.; Hettmann, T.; Leiden, J. M.; Ron, D. *Mol. Cell.* **2003**, *11*, 619-633.

<sup>571</sup> Hiramatsu, N.; Messah, C.; Han, J.; LaVail, M. M.; Kaufman, R. J.; Lin, J. H. *Mol. Biol. Cell* **2014**, *25*, 1411-1420.

<sup>572</sup> Sidrauski, C.; Walter, P. *Cell* **1997**, *90*, 1031-1039.

<sup>573</sup> Yoshida, H.; Matsui, T.; Yamamoto, A.; Okada, T.; Mori, K. *Cell* **2001**, *107*, 881-891.

<sup>574</sup> Calton, M.; Zeng, H.; Urano, F.; Till, J. H.; Hubbard, S. R.; Harding, H. P.; Clark, S. G.; Ron, D. *Nature* **2002**, *415*, 92-96.

<sup>575</sup> Ye, J.; Rawson, R. B.; Komuro, R.; Chen, X.; Davé, U. P.; Prywes, R.; Brown, M. S.; Goldstein, J. L. *Mol. Cell* **2000**, *6*, 1355-1364.

<sup>576</sup> Okada, T.; Yoshida, H.; Akazawa, R.; Negishi, M.; Mori, K. *Biochem. J.* **2002**, *366*, 585-594.

<sup>577</sup> Bertolotti, A.; Zhang, Y.; Hendershot, L. M.; Harding, H. P.; Ron, D. *Nat. Cell Biol.* **2000**, *2*, 326-332.

<sup>578</sup> Sanderson, T.; Gallaway, M.; Kumar, R. *Int. J. Mol. Sci.* **2015**, *16*, 7133-7142.

<sup>579</sup> Shen, J.; Chen, X.; Hendershot, L.; Prywes, R. *Dev. Cell* **2002**, *3*, 99-111.

<sup>580</sup> Liu, C. Y.; Wong, H. N.; Schauerer, J. A.; Kaufman, R. J. *J. Biol. Chem.* **2002**, *277*, 18346-18356.

<sup>581</sup> Kimata, Y.; Kimata, Y. I.; Shimizu, Y.; Abe, H.; Farcasanu, I. C.; Takeuchi, M.; Rose, M. D.; Kohno, K. *Mol. Biol. Cell* **2003**, *14*, 2559-2569.

<sup>582</sup> Ma, Y.; Brewer, J. W.; Diehl, J. A.; Hendershot, L. M. *J. Mol. Biol.* **2002**, *318*, 1351-1365.

<sup>583</sup> Rutkowski, D. T.; Arnold, S. M.; Miller, C. N.; Wu, J.; Li, J.; Gunnison, K. M.; Mori, K.; Sadighi Akha, A. A.; Raden, D.; Kaufman, R. J. *PLoS Biol.* **2006**, *4*, e374.

Figure 98 summarizes what has been discussed so far.

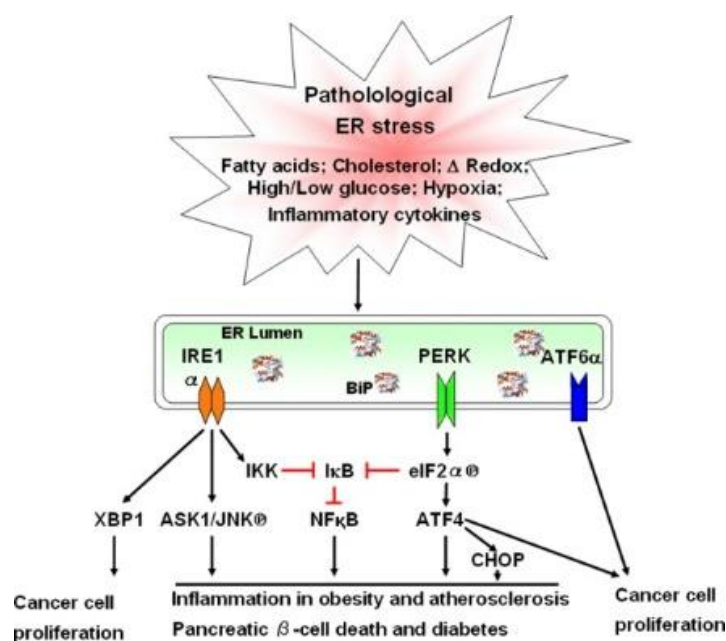


Fig. 98. UPR activation in response to the ER stress.

The machinery concerning ER stress is thus intricate and complex. Although still unknown to some extent, different proteins have been identified to play a trivial role in the development of the ER stress. Among them, activating transcription factor 3 (ATF3) is an ER stress marker whose expression is increased in such conditions. It is related to insulin signalling and lipogenesis.<sup>584</sup>

Over the multiple studies that have been performed in relation to the ER stress, different ER stress-inducers have been identified. Among them, the saturated fatty acid palmitate,<sup>585,586,587</sup> followed by thapsigargin (by depletion of  $\text{Ca}^{2+}$  from the ER), tunicamycin (by blockade of protein glycosylation in the ER)<sup>588</sup> and borrelidin.<sup>589</sup> On the other hand, several substances have emerged as restorers of ER stress, such as unsaturated fatty acids

<sup>584</sup> Koh, I.; Lim, J. H.; Joe, M. K.; Kim, W. H.; Jung, M. H.; Yoon, J. B.; Song, J. *FEBS J.* **2010**, *277*, 2304-2317.

<sup>585</sup> Guo, W.; Wong, S.; Xie, W.; Lei, T.; Luo, Z. *Am. J. Physiol. Endocrinol. Metab.* **2007**, *293*, E576-E586.

<sup>586</sup> Gwiazda, K. S.; Yang, T. L.; Lin, Y.; Johnson, J. D. *Am. J. Physiol. Endocrinol. Metab.* **2009**, *296*, E690-701.

<sup>587</sup> Wei, Y.; Wang, D.; Gentile, C. L.; Pagliassotti, M. J. *Mol. Cell. Biochem.* **2009**, *331*, 31-40.

<sup>588</sup> Srivastava, R. K.; Sollott, S. J.; Khan, L.; Hansford, R.; Lakatta, E. G.; Longo, D. L. *Mol. Cell Biol.* **1999**, *19*, 5659-5674.

<sup>589</sup> Sidhu, A.; Miller, J. R.; Tripathi, A.; Garshott, D. M.; Brownell, A. L.; Chiego, D. J.; Arevang, C.-J.; Zeng, Q.; Jackson, L. C.; Bechler, S. A.; Callaghan, M. U.; Yoo, G. H.; Sethi, S.; Lin, H.-S.; Callaghan, J. H.; Tamayo-Castillo, G.; Sherman, D. H.; Kaufman, R. J.; Fribley, A. M. *ACS Med. Chem. Lett.* **2015**, ASAP. DOI: 10.1021/acsmchemlett.5b00133.

(oleate and linolate),<sup>590,591</sup> the PPAR $\alpha$  agonist fenofibrate,<sup>592</sup> and the chemical chaperon 4-phenyl butyric acid (PBA),<sup>593</sup> and tauroursodeoxycholic acid (TUDCA).<sup>594</sup>

In 2013, sEH was identified as a key regulator of the ER stress.<sup>595</sup> Epoxy fatty acids have proven to be upstream modulators of ER stress pathways.<sup>596,597</sup> In consequence, attenuation or inhibition of sEH leads to an amelioration of the ER stress, therefore reasserting its potential as a therapeutic target for obesity-related comorbidities. Taken together these studies and due to the wide expertise of the research group of Dr. Manuel Vázquez Carrera in the study of the ER stress in skeletal muscle and in animal models of insulin resistance,<sup>590,598</sup> we envisioned that our sEH inhibitors would be able to attenuate the ER stress when produced by a stimuli.

For our studies, human hepatocytes, from the cell line Huh-7,<sup>599</sup> were chosen because of their availability and ease to maintain for cell cultures, coupled with the fact that sEH is widely expressed in liver, as seen in the introductory part of this chapter. Cells were treated with palmitate *prior* to conjugation of this fatty acid with BSA, as previously described by the group.<sup>590</sup> Based on our experience in ER stress and the reported studies, we proceeded to run the *in vitro* assays in a single final concentration of each inhibitor (170, 176 and 192) and palmitate (1  $\mu$ M/L and 0.5 mM/L, respectively) during 48 hours. After the treatment, samples were recovered for RNA and total protein extraction. We used again urea 109 as standard for comparison. Worth to note is the fact that adamantyl urea 109 has not been tested in human cell cultures *prior* to our studies.

To assess the resolution of ER stress with our sEH inhibitors, we examined their effects on the expression of the ER stress markers *Bip/Grp78*, *Chop* and *Atf3*. Levels of mRNA of the three genes were determined by Real Time-PCR with GAPDH as housekeeping gene. Human Huh-7 hepatocytes exposed to 0.5 mmol/L palmitate showed an increase in *Bip/Grp78*, *Chop* and *Atf3* mRNA levels compared with cells exposed only to BSA (Fig. 99). Interestingly, co-incubation of cells with palmitate (0.5 mmol/L) and each one of the inhibitors (1  $\mu$ mol/L) considerably blocked the effects of the saturated fatty acid, with a

<sup>590</sup> Salvadó, L.; Coll, T.; Gómez-Foix, A. M.; Salmerón, E.; Barroso, E.; Palomer, X.; Vázquez-Carrera, M. *Diabetologia* **2013**, *56*, 1372-1382.

<sup>591</sup> Maruyama, H.; Takahashi, M.; Sekimoto, T.; Shimada, T.; Yokosuka, O. *Lipids Health Dis.* **2014**, *13*, 1-8.

<sup>592</sup> Rahman, S. M.; Qadri, I.; Janssen, R. C.; Friedman, J. E. *J. Lipid Res.* **2009**, *50*, 2193-2202.

<sup>593</sup> Xiao, C.; Giacca, A. Lewis, L. F. *Diabetes* **2011**, *60*, 918-924.

<sup>594</sup> Ozcan, U.; Yilmaz, E.; Ozcan, L.; Furuhashi, M.; Vaillancourt, E.; Smith, R. O.; Görgün, C. Z.; Hotamisligil, G. S. *Science* **2006**, *313*, 1137-1140.

<sup>595</sup> Bettaieb, A.; Nagata, N.; Aboubechara, D.; Chahed, S.; Morisseau, C.; Hammock, B. D.; Haj, F. G. *J. Biol. Chem.* **2013**, *288*, 14189-14199.

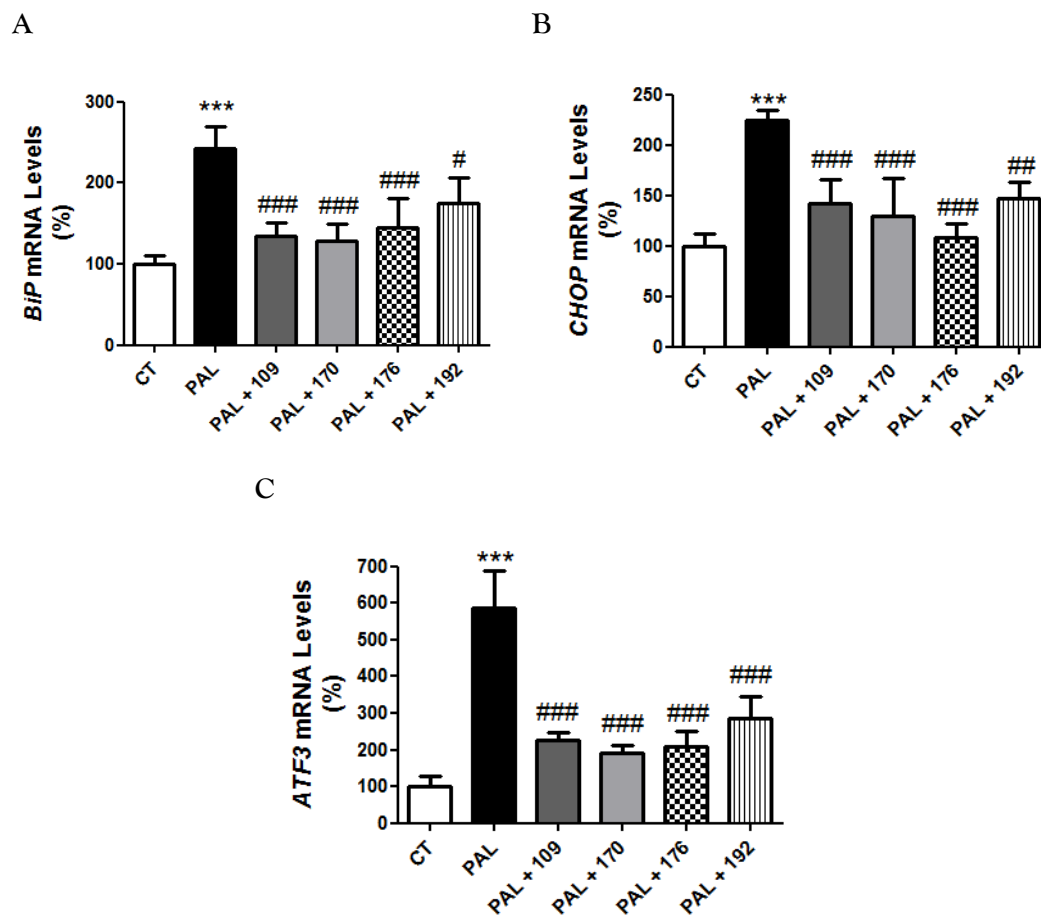
<sup>596</sup> López-Vicario, C.; Alcaraz-Quiles, J.; García-Alonso, V.; Rius, B.; Hwang, S. H.; Titos, E.; Lopategi, A.; Hammock, B. D.; Arroyo, V.; Clària, J. *Proc. Natl. Acad. Sci. USA* **2015**, *112*, 536-541.

<sup>597</sup> Inceoglu, B.; Bettaieb, A.; Trindade da Silva, C. A.; Lee, K. S. S.; Haj, F. G.; Hammock, B. D. *Proc. Natl. Acad. Sci. USA* **2015**, *112*, 9082-9087.

<sup>598</sup> Salvadó, L.; Palomer, X.; Barroso, E.; Vázquez-Carrera, M. *Trends Endocrinol. Metab.* **2015**, *26*, 438-448.

<sup>599</sup> Huh-7 cell line website. <http://huh7.com/> (accessed on 18<sup>th</sup> September 2015).

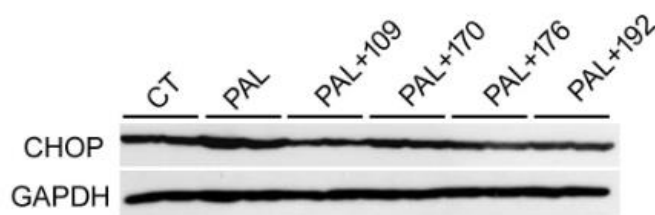
significant reduction of the mRNA levels for the three markers. This trend was more remarkable for *Atf3* (Fig. 99C).



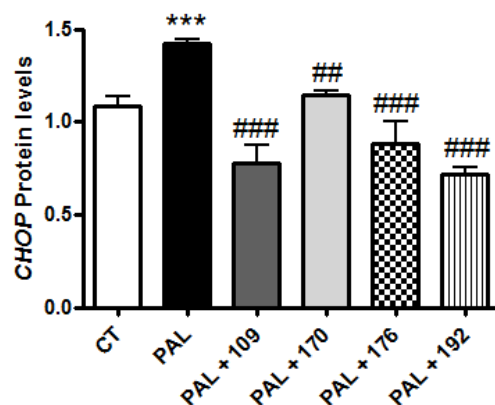
**Fig. 99.** Assessment by quantitative real-time RT-PCR of mRNA abundance of *BiP/Grp78* (A), *Chop* (B) and *Atf3* (C). Huh-7 hepatocytes were incubated for 48 h in the absence (Control, CT) or in the presence of 0.5 mmol/L palmitate (PAL) and the compounds tested. Data are presented as the mean  $\pm$  SD ( $n = 6$  per group). \*\*\*:  $P < 0.001$  vs control. #:  $P < 0.05$ , ##:  $P < 0.01$  and ###:  $P < 0.001$  vs palmitate-exposed cells.

In agreement with the changes in *Chop* mRNA levels, CHOP protein levels were only increased in cells exposed to palmitate (Fig. 100).

A



B



**Fig. 100.** Levels of protein of CHOP (A) and their quantification (B). Huh-7 hepatocytes were incubated for 48 h in the absence (Control, CT) or in the presence of 0.5 mmol/L palmitate (PAL) and the compounds tested. Data are presented as the mean  $\pm$  SD (n = 3 per group).

\*\*\*:  $P < 0.001$  vs control. ##:  $P < 0.01$  and ###:  $P < 0.001$  vs palmitate-exposed cells.

The reduction of the mRNA and protein levels of BiP, CHOP and ATF3 markers resulting from the sEH inhibition from our three tested compounds prompted the following conclusions:

- In general, sEH inhibition at a low concentration provided a remarkable protection against palmitate-induced ER stress and reduced the levels of these markers to those present in control cells.
- Except for compound **192**, new inhibitors **170** and **176** led to an extremely significant reduction of the ER stress comparable with the adamantyl standard **109**.
- Addition of compound **192**, although providing less benefit than the other tested compounds, resulted in a very significant recovery of the ER stress.
- Only in mRNA levels, compound **170** showed a better behaviour preventing palmitate-induced ER stress than the adamantane analogue **109**.
- The positive outcomes of these *in vitro* studies showed that the four sEH inhibitors are able to cross cell membrane and are not cytotoxic.

As a whole, the findings of this study show that sEH inhibition contributes to the prevention of palmitate-induced ER stress, and that our scaffolds compare well with the adamantane nucleus.



To our delight, these experiments with sEH inhibitors in Huh-7 cell line are, to date and to the best of our knowledge, the first *in vitro* studies concerning sEH and ER stress performed under this new protocol.

# **Conclusions**

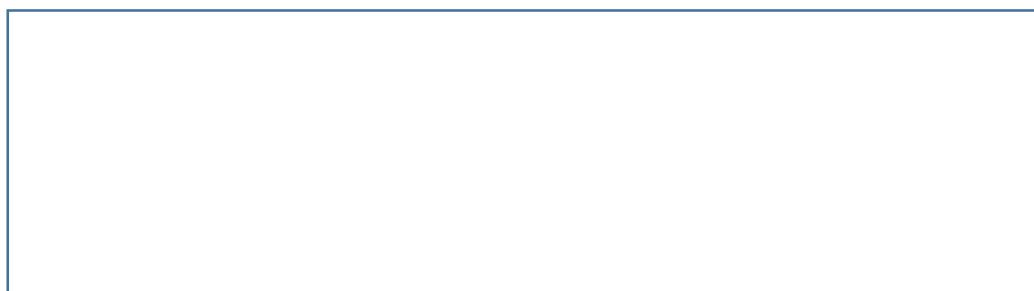


This chapter involves the synthesis of 20 new ureas with 15 different adamantane-like polycycles through a scaffold-hopping approach; none of them had been previously described in the literature. The new structures have been thoroughly characterized by spectroscopic and analytical means. None of the scaffolds had been previously applied in the design and synthesis of sEH inhibitors.

The pharmacological evaluation was carried out, and entailed the optimization of the assay conditions, followed by the determination of the  $IC_{50}$  values of each new compound. Furthermore, an unexplored method for the water solubility measurement was applied, and the values of solubility were used for the assessment of each scaffold. Finally, the lipophilic ligand efficiency of each new sEH inhibitor was calculated from the  $IC_{50}$  and clog P data.

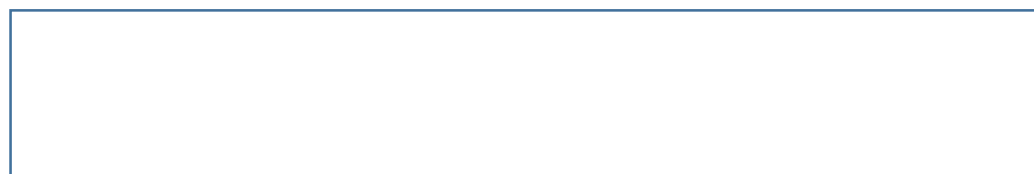
As the main conclusions of this chapter, in chronological order:

1. All the 15 polycyclic scaffolds were potent sEH inhibitors, with  $IC_{50}$  values ranging from 0.80 to 50.8 nM.
2. Three different structures were identified with higher inhibitory activities than the adamantanyl standards **108** and **109** ( $IC_{50}$  of 7.74 and 4.04 nM, respectively) (Fig. 101).



**Fig. 101.** Most potent compounds found in this chapter.

3. According to the results obtained from water solubility and LipE, and taking into account the ease in the synthesis of each structure, three scaffolds were selected for the preparation of optimized sEH inhibitors (Fig. 102).



**Fig. 102.** Selected scaffolds as adamantane surrogates for the second batch of compounds.

4. Five new ureas were prepared following described methods, in order to test their *in vitro* potency against human sEH. Albeit showing higher  $IC_{50}$  values than the standard *t*-AUCB, all of them were potent sEH inhibitors (from 8.41 to 50.8 nM).

5. After the determination of their water solubility and LipE, these scaffolds have proven to be efficient surrogates of the adamantane ring for this specific target, with more appropriate physicochemical properties than the adamantane group.
6. *In vitro* cellular studies have demonstrated their ability to cross cell membrane and to attenuate ER stress induced by palmitate, without promoting cell death. These experiments with the human Huh-7 cell line are, to date, the first ever reported that link sEH and ER stress under this protocol.

This work has been focused on investigating structure-activity relationships of adamantane-like derivatives as human sEH inhibitors, which provided an important base for developing valuable compounds that are not only highly potent inhibitors but show improved physicochemical properties.

As a general conclusion of this dissertation, we have demonstrated that the adamantane nucleus is not necessarily the perfect lipophilic bullet, and that a fine-tuning is required in order to optimize the binding mode of the molecule for each specific target as well as to adjust its physicochemical properties. Exploration around adamantane-like scaffolds for the discovery of improved drug candidates is still an underexploited research area.

# **MATERIALS & METHODS**



## General Methods

Melting points were determined in open capillary tubes with a MFB 59510M Gallenkamp or a Büchi B - 540 melting point apparatuses.

300 MHz  $^1\text{H}$  NMR spectra, 400 MHz  $^1\text{H}/100.6$  MHz  $^{13}\text{C}$  NMR spectra, and 500MHz  $^1\text{H}/125.7$  MHz  $^{13}\text{C}$  NMR spectra were recorded on Varian Gemini 300, Varian Mercury 400, and Varian Inova 500 spectrometers, respectively. The chemical shifts are reported in ppm ( $\delta$  scale) relative to internal tetramethylsilane, or to solvent peak, and coupling constants are reported in Hertz (Hz). The used abbreviations were: s, singlet; d, doublet; t, triplet; q, quadruplet; m, multiplet; or combinations thereof.

IR spectra were run on FTIR Perkin-Elmer Spectrum RX I spectrophotometer using potassium bromide (KBr) pellets or attenuated total reflectance (ATR) technique. Absorption values are expressed as wavenumbers ( $\text{cm}^{-1}$ ); only significant absorption bands are given.

The GC/MS analyses were carried out in an inert Agilent Technologies 5975 gas chromatograph equipped with a DB-5MS (30 m x 25 mm) capillary column with a stationary phase of phenylmethylsilicon (5% diphenyl-9% dimethylpolysiloxane), using the following conditions: initial temperature of 50 °C ( 1 min), with a gradient of 15 °C/min up to 300 °C, and a temperature in the source of 230 °C. solvent decay of 3 minutes and pressure of 7.5 psi. The electron impact (70 eV) or chemical ionization ( $\text{CH}_4$ ) techniques were used. Only significant ions are given, those with higher relative ratio, except for the ions with higher  $m/z$  values.

The accurate mass analyses were carried out at Unitat d'Espectrometria de Masses dels Centres Científics i Tecnològics de la Universitat de Barcelona (CCiTUB), Faculty of Chemistry, using a LC/MSD-TOF spectrophotometer.

The elemental analyses were carried out in a Flash 1112 series Thermofinnigan elemental microanalyzer (A5) to determine C, H, and N, and in a tiroprocessor Methrom 808 to determine Cl, at the Servei de Microanàlisi of IIQAB (CSIC) of Barcelona.

To concentrate solvents in *vacuo* a Büchi GKR-50 rotavapor was used.

Column chromatography was performed on either silica gel 60 Å (35-70 mesh, SDS), or on aluminium oxide, neutral, 60 Å (50-200  $\mu\text{m}$ , Brockmann I).

Thin-layer chromatography was performed with aluminium-backed sheets with either silica gel 60 F254 or aluminum oxide 60 Å, and spots were visualized with UV light, 1% aqueous solution of  $\text{KMnO}_4$  and/or iodine.

All new compounds that were subjected to a pharmacological evaluation, possessed a purity  $\geq 95\%$  as evidenced by their analytical data, if possible.



Solvent purification was carried out following the procedures described in: Perrin, D. D.; Armarego, W. L. F. *Purification of Laboratory Chemicals*, 4<sup>th</sup> Edition, Butterworth-Heinemann: Oxford, 1996.

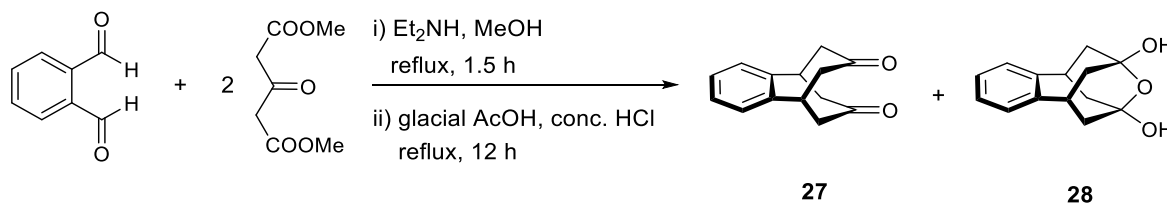
The NMR data and the synthetic procedure of all the compounds synthesized for the first time in our laboratory are included in the current manuscript. Regarding the compounds described previously in the literature, the synthetic procedure is described along with the reference corresponding with their preparation.

A complete characterization of all the new compounds synthesized in this thesis, was carried out including  $^1\text{H}$  and  $^{13}\text{C}$ , IR, elemental analysis or accurate mass and GC/MS. All  $^1\text{H}$  and  $^{13}\text{C}$  NMR signals were assigned by reason of homocorrelation  $^1\text{H}/^1\text{H}$  (COSY and NOESY) and heterocorrelation  $^1\text{H}/^{13}\text{C}$  (HSQC) experiments.

# **Chapter 1**



Preparation of 5,6,8,9-tetrahydro-5,9-propanebenzocycloheptane-7,11-dione, **27** and 7,11-epoxy-6,7,8,9-tetrahydro-5,9-propane-5*H*-benzocycloheptane-7,11-diol, **28**<sup>168</sup>



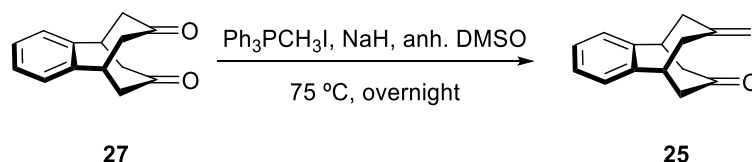
a) Tetraester's formation:

To a solution of *o*-phthalaldehyde (9.80 g, 73.1 mmol) and dimethyl 1,3-acetonedicarboxylate (25.9 g, 149 mmol) in methanol (200 mL) were added 15 drops of diethylamine, and the solution was heated at reflux for 1.5 hours. Then 12 drops more of diethylamine were added and the mixture was cooled to 4 °C overnight. The resulting precipitated was filtered in *vacuo* and washed with cold methanol (25 mL) to give the intermediate tetraester as white crystals (22.2 g, 68% yield).

b) Preparation of the diketone **27** and its hydrate **28**:

To a round bottom flask containing the intermediate tetraester prepared in the last step (22.2 g, 49.8 mmol), glacial acetic acid (125 mL) and conc. HCl (35 mL) were added and the mixture was heated at reflux for 12 hours. The acids were then removed under *vacuo* and the resulting solid was digested with diethyl ether (150 mL) for 15 minutes and cooled to 4 °C overnight. Filtration in *vacuo* gave a mixture of diketone **27** and hydrate **28** with a 1:3 ratio as a white solid (10.5 g). Dehydration of the mixture by a Dean-Stark system with toluene (250 mL) as the solvent gave the pure diketone **27** (9.8 g, 93% yield), whose spectroscopic data matched with those previously published.

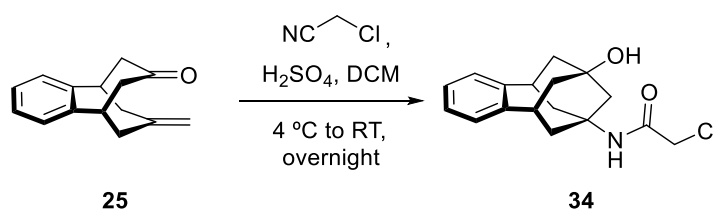
Preparation of 5,6,8,9-tetrahydro-5,9-propanebenzocycloheptane-11-ene-7-one, **25**<sup>165</sup>



A suspension of sodium hydride, 60% dispersion in mineral oil (1.00 g, 25.17 mmol) in anh. DMSO (50 mL) was heated to 75 °C for 45 minutes under N<sub>2</sub> atmosphere. After the reaction mixture was tempered, a solution of triphenylmethylphosphonium iodide (10.55 g, 25.17 mmol) in anh. DMSO (60 mL) was added and the resulting yellow solution was stirred at room temperature for 20 minutes. Then a suspension of diketone **27** (4.31 g, 20.14 mmol) in anh. DMSO (50 mL) was added and the obtained solution was heated to 75 °C overnight. The resulting black solution was allowed to cool to room temperature and

then poured into water (150 mL). Hexane (50 mL) was added and the phases were separated. The aqueous phase was extracted with further hexane (2 x 50 mL) and the combined organic phases were washed with brine (50 mL), dried over anhydrous  $\text{Na}_2\text{SO}_4$ , filtered and concentrated *in vacuo* to give a white solid (3.93 g). Purification by packing the solid with silica gel and extracting with 10% petroleum ether/diethyl ether mixture gave **25** (3.34 g, 84% yield) as a white solid. The spectroscopic data were identical to those previously published.

**Preparation of 2-chloro-*N*-(9-hydroxy-5,6,8,9,10,11-hexahydro-7*H*-5,9:7,11-dimethanobenzo[9]annulen-7-yl)acetamide, **34****



To a solution of enone **25** (2.09 g, 9.86 mmol) in DCM (15 mL) was added chloroacetonitrile (0.62 mL, 9.86 mmol) and the mixture was cooled to 0-5 °C with an ice bath. Then conc.  $\text{H}_2\text{SO}_4$  (0.79 mL, 14.82 mmol) was added dropwise without reaching a temperature greater than 10 °C. After the addition, the reaction mixture was allowed to reach room temperature and stirred overnight. Then to the resulting solution was added ice (25 g) and the mixture was stirred at room temperature for few minutes. DCM (30 mL) was added, the phases were separated and the aqueous phase was extracted with further DCM (2 x 30 mL). The combined organic phases were dried over anhydrous  $\text{Na}_2\text{SO}_4$ , filtered and evaporated *in vacuo* to give a white solid (2.68 g). Purification by column chromatography ( $\text{Al}_2\text{O}_3$ , 0-5% methanol/DCM) gave **34** (1.46 g, 49% yield) as a white solid.

Analytical and spectroscopic data of compound **34**:

Melting point: 184 - 185 °C.

IR (ATR)  $\nu$ : 3300 - 2800 (3315, 3247, 3217, 3065, 3021, 2925, 2851), 1911, 1664, 1560, 1494, 1441, 1413, 1361, 1300, 1224, 1202, 1151, 1107, 1037, 911, 757, 668, 571, 512, 471  $\text{cm}^{-1}$ .

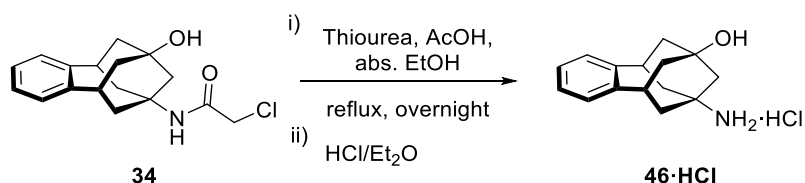
$^1\text{H-NMR}$  (400 MHz,  $\text{CDCl}_3$ )  $\delta$ : 1.78 [d,  $J = 12.8$  Hz, 2 H, 10(13)- $\text{H}_b$ ], 1.97 [m, 2 H, 10(13)- $\text{H}_a$ ], 2.04 [d,  $J = 12.8$  Hz, 2 H, 6(12)- $\text{H}_b$ ], 2.12 (s, 2 H, 8- $\text{H}_2$ ), 2.19 [m, 2 H, 6(12)- $\text{H}_a$ ], 3.21 [t,  $J = 6.4$  Hz, 2 H, 5(11)-H], 3.93 (s, 2 H,  $\text{CH}_2\text{Cl}$ ), 6.36 (s, 1 H, NH), 7.08 [m, 2 H, 1(4)-H], 7.13 [m, 2 H, 2(3)-H].

$^{13}\text{C-NMR}$  (100.6 MHz,  $\text{CDCl}_3$ )  $\delta$ : 38.2 [ $\text{CH}_2$ , C6(12)], 39.9 [CH, C5(11)], 42.4 [ $\text{CH}_2$ , C10(13)], 42.8 ( $\text{CH}_2$ ,  $\text{CH}_2\text{Cl}$ ), 47.9 ( $\text{CH}_2$ , C8), 57.3 (C, C7), 70.7 (C, C9), 126.8 [CH, C2(3)], 128.1 [CH, C1(4)], 144.9 [C, C4a(C11a)], 164.6 (C, CO).

MS (EI),  $m/z$  (%); significant ions: 307 (10), 305 ( $M^+$ , 30), 270 [ $(M-^{35}Cl)^+$ , 12], 212 (100), 197 (17), 194 (22), 179 (26), 169 (13), 155 (58), 142 (25), 129 (32), 115 (26), 91 (7), 77 (9), 65 (2), 55 (4), 49 (4).

HRMS-ESI+  $m/z$  [ $M+H$ ]<sup>+</sup> calcd for  $[C_{17}H_{20}ClNO_2+H]^+$ : 306.1255, found: 306.1249.

Preparation of 9-amino-5,6,8,9,10,11-hexahydro-7H-5,9:7,11-dimethanobenzo[9]annulen-7-ol hydrochloride, 46·HCl



To a solution of chloroacetamide **37** (710 mg, 2.32 mmol) in abs. ethanol (40 mL) were added thiourea (0.212 g, 2.79 mmol) and glacial acetic acid (1.4 mL) and the mixture was heated at reflux overnight. The resulting suspension was then tempered to room temperature, water (20 mL) was added and the pH adjusted to ~12 with 5 N NaOH solution. DCM (20 mL) was added, the phases were separated and the aqueous phase was extracted with further DCM (2 x 20 mL). The combined organic phases were dried over anh. Na<sub>2</sub>SO<sub>4</sub>, filtered and concentrated in *vacuo* to give **46** as a white solid. Its hydrochloride was obtained by adding an excess of Et<sub>2</sub>O·HCl to a solution of the amine in DCM, followed by filtration of the white precipitated (602 mg, quantitative yield). The analytical sample was obtained by crystallization with methanol/diethyl ether.

Analytical and spectroscopic data of compound **46·HCl**:

Melting point: > 315 °C (dec.).

IR (ATR)  $\nu$ : 3273, 2902, 2872, 2638, 2569, 2088, 1633, 1531, 1493, 1441, 1355, 1314, 1272, 1106, 1094, 1015, 972, 902, 764, 640, 580 cm<sup>-1</sup>.

<sup>1</sup>H-NMR (500 MHz, CD<sub>3</sub>OD)  $\delta$ : 1.75 [d,  $J = 12.5$  Hz, 2 H, 6(12)-H<sub>b</sub>], 1.81 [d,  $J = 13.0$  Hz, 2 H, 10(13)-H<sub>b</sub>], 1.89 (s, 2 H, 8-H<sub>2</sub>), 1.98 [m, 2 H, 6(12)-H<sub>a</sub>], 2.05 [m, 2 H, 10(13)-H<sub>a</sub>], 3.30 [tt,  $J = 6.5$  Hz,  $J' = 1.5$  Hz, 2 H, 5(11)-H], 7.13 (m, 4 H, Ar-H).

<sup>13</sup>C-NMR (125.7 MHz, CD<sub>3</sub>OD)  $\delta$ : 39.0 [CH<sub>2</sub>, C10(13)], 40.7 [CH, C5(11)], 42.8 [CH<sub>2</sub>, C6(12)], 47.9 (CH<sub>2</sub>, C8), 57.5 (C, C7), 70.9 (C, C9), 128.3 [CH, C2(3)], 129.3 [CH, C1(4)], 145.7 [C, C4a(C11a)].

MS (EI),  $m/z$  (%); significant ions: 229 ( $M^+$ , 100), 214 (10), 196 ( $C_{15}H_{16}^+$ , 10), 187 (37), 186 (16), 172 (14), 171 (11), 170 (23), 168 (18), 158 (11), 157 (20), 156 (29), 155 (12), 144 (49), 143 (47), 129 (28), 128 (32), 115 (26), 110 (33), 96 (29).

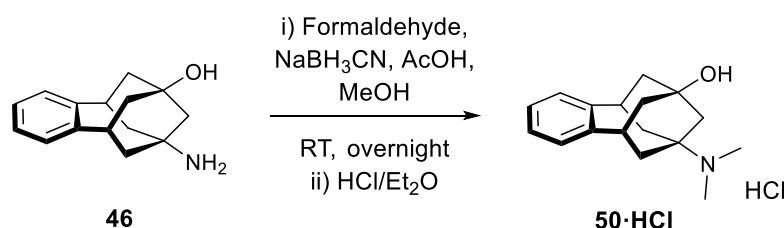
Elemental analysis:

Calculated for  $C_{15}H_{20}ClNO$ : C 67.79% H 7.58% Cl 13.34% N 5.27%

Calculated for  $C_{15}H_{20}ClNO \cdot 0.20H_2O$ : C 66.87% H 7.63% Cl 13.16% N 5.20%

Found: C 66.87% H 7.71% Cl 13.08% N 4.98%

**Preparation of 9-(dimethylamino)-5,6,8,9,10,11-hexahydro-7H-5,9:7,11-dimethanobenzo[9]annulen-7-ol hydrochloride, 50·HCl**



To a solution of amine **46** (250 mg, 1.09 mmol) in methanol (8 mL) were added formaldehyde (0.25 mL, 37% wt in aqueous solution, 3.32 mmol), glacial acetic acid (0.23 mL) and sodium cyanoborohydride (206.2 mg, 3.12 mmol) and the mixture was stirred at room temperature for 7 hours. Then further NaBH<sub>3</sub>CN (206.2 mg, 3.12 mmol) and formaldehyde (0.25 mL, 37% wt in aqueous solution, 3.32 mmol) were added and the solution was stirred at room temperature overnight. The reaction mixture was then evaporated to dryness in *vacuo* and the resulting residue partitioned between water (5 mL) and EtOAc (5 mL). The pH was adjusted to ~12 with 5 N NaOH solution and the phases were separated. The aqueous phase was extracted with further EtOAc (2 x 5 mL) and the combined organic layers were dried over anh. Na<sub>2</sub>SO<sub>4</sub>, filtered and concentrated in *vacuo*. The residue was taken in DCM and the amine **50** was precipitated as its hydrochloride (104.9 mg, 33% yield) by adding an excess of Et<sub>2</sub>O·HCl. The analytical sample was obtained by crystallization with methanol/diethyl ether.

Analytical and spectroscopic data of compound **50·HCl**:

Melting point: 241-242 °C.

IR (ATR)  $\nu$ : 3424, 3224, 2956, 2855, 2533, 2429, 1665, 1487, 1451, 1412, 1361, 1348, 1310, 1211, 1183, 1141, 1094, 1078, 990, 978, 969, 908, 769, 702, 621, 591 cm<sup>-1</sup>.

<sup>1</sup>H-NMR (500 MHz, CD<sub>3</sub>OD)  $\delta$ : 1.74 [d,  $J$  = 14.0 Hz, 2 H, 6(12)-H<sub>b</sub>], 1.96-2.02 [m, 6 H, 10(13)-H<sub>b</sub>, 8-H<sub>2</sub>, 6(12)-H<sub>a</sub>], 2.14 [m, 2 H, 10(13)-H<sub>a</sub>], 2.83 (s, 6 H, N-CH<sub>3</sub>), 3.38 [tt,  $J$  = 6.5 Hz,  $J'$  = 1.5 Hz, 2 H, 5(11)-H], 7.14 (s, 4 H, Ar-H).

<sup>13</sup>C-NMR (125.7 MHz, CD<sub>3</sub>OD)  $\delta$ : 34.1 [CH<sub>2</sub>, C10(13)], 37.5 (CH<sub>3</sub>, N-CH<sub>3</sub>), 40.5 [CH,

C5(11)], 42.6 [CH<sub>2</sub>, C6(12)], 45.5 (CH<sub>2</sub>, C8), 69.0 (C, C7), 71.6 (C, C9), 128.3 [CH, C2(3)], 129.3 [CH, C1(4)], 145.6 [C, C4a(C11a)].

MS (EI), *m/z* (%); significant ions: 257 (M<sup>+</sup>, 100), 242 (16), 240 (20), 215 (43), 214 (14), 198 (14), 187 (54), 184 (19), 172 (18), 155 (16), 138 (18), 129 (19), 128 (22), 127 (12), 124 (23), 115 (19), 85 (17).

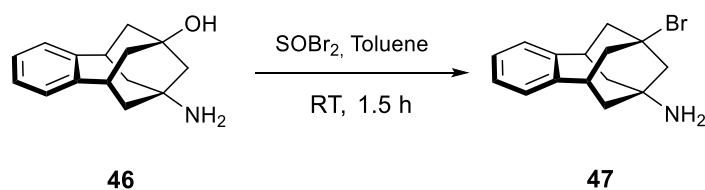
Elemental analysis:

Calculated for C<sub>17</sub>H<sub>24</sub>ClNO: C 69.49% H 8.23% Cl 12.07% N 4.77%

Calculated for C<sub>17</sub>H<sub>24</sub>ClNO·0.50H<sub>2</sub>O: C 67.42% H 8.32% Cl 11.71% N 4.63%

Found: C 67.70% H 8.51% Cl 11.80% N 4.44%

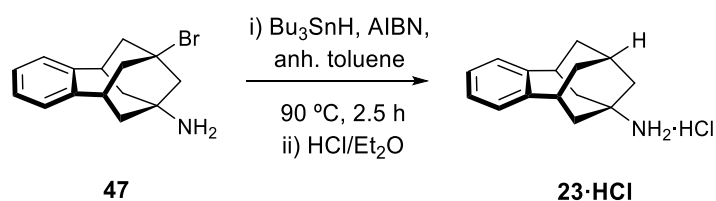
Preparation of 9-bromo-5,6,8,9,10,11-hexahydro-7*H*-5,9:7,11-dimethanobenzo[9]annulen-7-amine, **47**



To a solution of amine **46** (700 mg, 3.06 mmol) in toluene (23 mL) and few drops of DCM was added thionyl bromide (7 mL, 90.05 mmol). The resulting orange solution was stirred at room temperature for 1.5 hours. The reaction mixture was then concentrated to dryness in *vacuo*. Toluene (50 mL) was added and the resulting solution concentrated in *vacuo*. The procedure was repeated five times more until it was obtained an orange solid (1.33 g). The crude was partitioned between DCM (15 mL) and saturated aqueous NaHCO<sub>3</sub> solution (15 mL) and the phases were separated. The aqueous layer was extracted with further DCM (2 x 15 mL) and the combined organic layers were dried over anhydrous Na<sub>2</sub>SO<sub>4</sub>, filtered and concentrated in *vacuo* to give the amine **47** (709.5 mg, 79% yield) as a brown solid. The product was used in next steps without further purification or characterization.



Preparation of 5,6,8,9,10,11-hexahydro-7H5,9:7,11-dimethanobenzo[9]annulen-7-amine hydrochloride, 23·HCl



To a solution of amine **47** (700 mg, 2.54 mmol) in dry and deoxygenated toluene (14.2 mL) under N<sub>2</sub> atmosphere were added tri-*n*-butyltin hydride (1.2 mL, 4.56 mmol) and 2,2'-azobisisobutyronitrile (AIBN) (62.5 mg, 0.38 mmol). The resulting solution was heated to 95 °C for 1 hour. After addition of further AIBN (62.5 mg, 0.38 mmol) the solution was kept to 95 °C for 90 minutes. The reaction mixture was then cooled to room temperature and concentrated to dryness in *vacuo*. The residue was partitioned between DCM (15 mL) and 2 N HCl solution (15 mL). The phases were separated and the organic layer was extracted with further 2 N HCl solution (2 x 10 mL). The combined aqueous phases were basified to pH ~12 with 10 N NaOH solution and then extracted with DCM (3 x 15 mL). The combined organic layers were dried over anh. Na<sub>2</sub>SO<sub>4</sub>, filtered and concentrated in *vacuo* to give a yellow oil (236 mg). The residue was taken in DCM and the amine **23** was precipitated as its hydrochloride (72.9 mg, 12% yield) by adding an excess of Et<sub>2</sub>O·HCl.

Analytical and spectroscopic data of compound **23·HCl**:

Melting point: > 330 °C (dec.).

IR (ATR)  $\nu$ : 3426, 2987, 2903, 2856, 2633, 2545, 2159, 2050, 1604, 1506, 1493, 1446, 1371, 1312, 1273, 1220, 1119, 1092, 1059, 1006, 954, 752, 611 cm<sup>-1</sup>.

<sup>1</sup>H-NMR (500 MHz, CD<sub>3</sub>OD)  $\delta$ : 1.79 [dm, *J* = 14.0 Hz, 2 H, 10(13)-H<sub>b</sub>], 1.91 [d, *J* = 13.0 Hz, 2 H, 6(12)-H<sub>b</sub>], 1.97 (s, 2 H, 8-H<sub>2</sub>), 2.01 [m, 2 H, 10(13)-H<sub>a</sub>], 2.13 [m, 2 H, 6(12)-H<sub>a</sub>], 2.45 [m, 1 H, 9-H], 3.17 [tt, *J* = 6.0 Hz, *J'* = 2.0 Hz, 2 H, 5(11)-H], 7.09 (broad s, 4 H, Ar-H).

<sup>13</sup>C-NMR (125.7 MHz, CD<sub>3</sub>OD)  $\delta$ : 32.2 (CH, C9), 34.7 [CH<sub>2</sub>, C10(13)], 39.9 [CH<sub>2</sub>, C6(12)], 40.5 (CH<sub>2</sub>, C8), 41.8 [CH, C5(11)], 54.0 (C, C7), 127.9 [CH, C2(3)], 129.3 [CH, C1(4)], 146.8 [C, C4a(C11a)].

MS (EI), *m/z* (%); significant ions: 213 (M<sup>+</sup>, 90), 198 (20), 172 (15), 171 (91), 170 (30), 157 (21), 156 (100), 155 (15), 144 (28), 143 (21), 141 (31), 130 (19), 129 (27), 128 (34), 115 (34), 94 (26), 77 (11), 57 (12).

Elemental analysis:

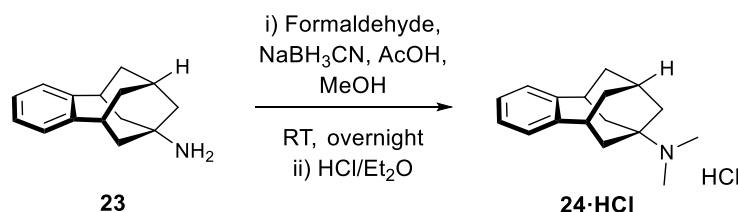
Calculated for C<sub>15</sub>H<sub>20</sub>ClN:

C 72.13% H 8.07% Cl 14.19% N 5.61%

Calculated for  $C_{15}H_{20}ClN \cdot 0.60H_2O$ : C 69.14% H 8.20% Cl 13.60% N 5.38%

Found: C 68.85% H 7.91% Cl 13.68% N 5.417%

Preparation of *N,N*-dimethyl-5,6,8,9,10,11-hexahydro-7*H*-5,9:7,11-dimethanobenzo[9]annulen-7-amine hydrochloride, 24·HCl



To a solution of amine **23** (140 mg, 0.55 mmol) in methanol (4 mL) were added formaldehyde (0.13 mL, 37% wt in aqueous solution, 1.71 mmol), glacial acetic acid (0.12 mL) and sodium cyanoborohydride (107 mg, 1.62 mmol) and the mixture was stirred at room temperature for 8 hours. Then further NaBH<sub>3</sub>CN (107 mg, 1.62 mmol) and formaldehyde (0.13 mL, 37% wt in aqueous solution, 1.71 mmol) were added and the solution was stirred at room temperature overnight. The reaction mixture was then evaporated to dryness in *vacuo* and the resulting residue partitioned between water (5 mL) and DCM (5 mL). The pH was adjusted to ~12 with 10 N NaOH solution and the phases were separated. The aqueous phase was extracted with further DCM (2 x 5 mL) and the combined organic phases were dried over anh. Na<sub>2</sub>SO<sub>4</sub>, filtered and concentrated in *vacuo*. An excess of Et<sub>2</sub>O·HCl was added to a solution of the amine **24** in DCM to form its hydrochloride, followed by evaporation to dryness in *vacuo* (101.4 mg, 69 yield).

Analytical and spectroscopic data of compound **24·HCl**:

Melting point: 253 - 255 °C.

IR (ATR)  $\nu$ : 3414, 3014, 2930, 2904, 2850, 2599, 2473, 2151, 1635, 1491, 1447, 1416, 1377, 1309, 1287, 1272, 1220, 1188, 1156, 1089, 1046, 1011, 957, 902, 756, 631, 608 cm<sup>-1</sup>.

<sup>1</sup>H-NMR (500 MHz, CD<sub>3</sub>OD)  $\delta$ : 1.78 [broad d,  $J = 14.0$  Hz, 2 H, 6(12)-H<sub>b</sub>], 2.00-2.09 [m, 6 H, 6(12)-H<sub>a</sub>, 8-H, 10(13)-H<sub>b</sub>], 2.19 [dm,  $J = 12.5$  Hz,  $J' = 6.5$  Hz, 2 H, 10(13)-H<sub>a</sub>], 2.53 [m, 1 H, 9-H], 2.80 [s, 6 H, N-CH<sub>3</sub>], 3.26 [broad t,  $J = 6.5$  Hz, 2 H, 5(11)-H], 7.10 (m, 4 H, Ar-H).

<sup>13</sup>C-NMR (125.7 MHz, CD<sub>3</sub>OD)  $\delta$ : 32.8 (CH, C9), 34.6 [CH<sub>2</sub>, C6(12)], 35.0 [CH<sub>2</sub>, C10(13)], 37.0 (CH<sub>3</sub>, N-CH<sub>3</sub>), 37.8 (CH<sub>2</sub>, C8), 41.8 [CH, C5(11)], 65.6 (C, C7), 128.0 [CH, C2(3)], 129.2 [CH, C1(4)], 146.7 [C, C4a(C11a)].

MS (EI),  $m/z$  (%); significant ions: 241 (M<sup>+</sup>, 84), 226 (21), 200 (18), 199 (100), 198 (33), 184 (39), 172 (21), 171 (16), 170 (15), 155 (30), 141 (43), 129 (30), 128 (35), 122 (20), 115

(33), 108 (21), 85 (43), 84 (14), 71 (16), 70 (21), 58 (18).

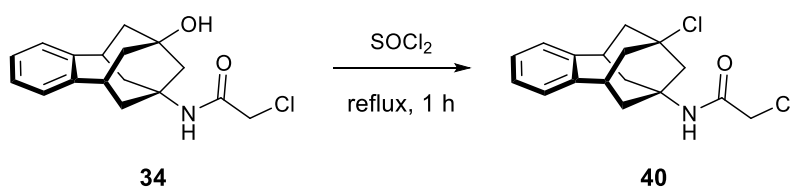
Elemental analysis:

Calculated for  $C_{17}H_{24}ClN$ : C 73.49% H 8.71% Cl 12.76% N 5.04%

Calculated for  $C_{17}H_{24}ClN \cdot 1.3H_2O \cdot 0.15HCl$ : C 66.57% H 8.79% Cl 13.29% N 4.57%

Found: C 66.51% H 8.52% Cl 13.08% N 4.60%

**Preparation of 2-chloro-*N*-(9-chloro-5,6,8,9,10,11-hexahydro-7*H*-5,9:7,11-dimethanobenzo[9]annulen-7-yl)acetamide, 40**



A solution of chloroacetamide **37** (500 mg, 1.64 mmol) in thionyl chloride (20.5 mL) was heated at reflux for 1 hour. The reaction mixture was then tempered to room temperature and evaporated to dryness in *vacuo*. Toluene (25 mL) was added and the resulting solution concentrated in *vacuo*. The procedure was repeated twice more to give a yellow oil (592mg). Purification by column chromatography ( $Al_2O_3$ , 0-10% methanol/DCM) gave **40** (297 g, 56% yield) as a white solid. The analytical sample was obtained by crystallization with methanol/diethyl ether.

Analytical and spectroscopic data of compound **40**:

Melting point: 195 - 197 °C.

IR (ATR)  $\nu$ : 3292, 3074, 2947, 2910, 2856, 1654, 1552, 1492, 1450, 1426, 1359, 1331, 1307, 1281, 1251, 1206, 1153, 1091, 1044, 998, 941, 892, 803, 756, 734, 692, 676  $cm^{-1}$ .

$^1H$ -NMR (400 MHz,  $CDCl_3$ )  $\delta$ : 2.05 [d,  $J = 13.2$  Hz, 2 H, 6(12)- $H_b$ ], 2.18 [d,  $J = 13.2$  Hz, 2 H, 10(13)- $H_b$ ], 2.27 [m, 2 H, 6(12)- $H_a$ ], 2.40 [m, 2 H, 10(13)- $H_a$ ], 2.55 [s, 2 H, 8-H], 3.28 [tt,  $J = 6.8$  Hz,  $J' = 1.6$  Hz, 2 H, 5(11)-H], 3.94 [s, 2 H, 14-H], 6.35(s, 1 H, NH), 7.07 [m, 2 H, 2(3)-H], 7.13 [m, 2 H, 1(4)-H].

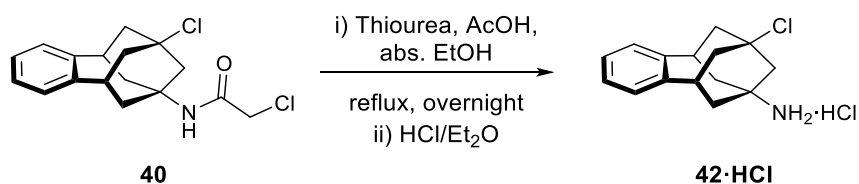
$^{13}C$ -NMR (100.6 MHz,  $CDCl_3$ )  $\delta$ : 37.8 [ $CH_2$ , C6(12)], 41.0 [CH, C5(11)], 42.8( $CH_2$ , C14), 44.3 [ $CH_2$ , C10(13)], 49.6 ( $CH_2$ , C8), 56.7 (C, C9), 68.7 (C, C7), 127.0 [CH, C2(3)], 128.2 [CH, C1(4)], 144.4 [C, C4a(C11a)], 164.6 (C, C14).

MS (EI),  $m/z$  (%); significant ions: 327 [ $M^+$  ( $^{37}Cl_2$ )], 5], 325 [ $M^+$  ( $^{35}Cl^{37}Cl$ )], 20], 323 [ $M^+$  ( $^{35}Cl_2$ )], 32], 290 [ $(C_{17}H_{19}^{37}ClNO)^+$ ], 13], 288 [ $(C_{17}H_{19}^{35}ClNO)^+$ ], 34], 233 (14), 232 (42), 231

(40), 230 [(C<sub>15</sub>H<sub>15</sub><sup>35</sup>Cl)<sup>+</sup>, 100], 207 (21), 196 (19), 195 [(C<sub>15</sub>H<sub>15</sub>)<sup>+</sup>, 88], 194 (23), 181 (28), 179 (24), 175 (23), 165 (24), 155 (36), 153 (24), 141 (41), 129 (24), 128 (31), 115 (33), 77 (15).

HRMS-ESI<sup>+</sup>  $m/z$  [M+H]<sup>+</sup> calcd for [C<sub>17</sub>H<sub>19</sub>Cl<sub>2</sub>NO+H]<sup>+</sup>: 324.0916, found: 324.0913.

**Preparation of 9-chloro-5,6,8,9,10,11-hexahydro-7H-5,9:7,11-dimethanobenzo[9]annulen-7-amine hydrochloride, 42·HCl**



To a solution of chloroacetamide **40** (350 mg, 1.08 mmol) in abs. ethanol (23 mL) were added thiourea (98mg, 1.29 mmol) and glacial acetic acid (0.75 mL) and the mixture was heated at reflux overnight. The resulting suspension was then tempered to room temperature, water (10 mL) was added and the pH adjusted to ~12 with 5 N NaOH solution. DCM (10 mL) was added, the phases were separated and the aqueous phase was extracted with further DCM (2 x 10 mL). The combined organic phases were dried over anh. Na<sub>2</sub>SO<sub>4</sub>, filtered and concentrated in *vacuo* to give **42** as a yellow solid. An excess of Et<sub>2</sub>O·HCl was added to a solution of the amine in DCM to form its hydrochloride, followed by filtration of the white precipitated (230.3 mg, 73 yield). The analytical sample was obtained by crystallization with methanol/diethyl ether.

Analytical and spectroscopic data of compound **42·HCl**:

Melting point: > 315 °C (dec.).

IR (ATR)  $\nu$ : 2906, 2850, 2673, 2559, 2176, 1601, 1509, 1494, 1452, 1361, 1309, 1297, 1213, 1170, 1090, 1070, 1036, 1007, 967, 945, 877, 804, 756 cm<sup>-1</sup>.

<sup>1</sup>H-RMN (500 MHz, CD<sub>3</sub>OD)  $\delta$ : 1.87 [d,  $J$  = 13 Hz, 2 H, 10(13)-H<sub>b</sub>], 2.10-2.17 [complex signal, 4 H, 10(13)-H<sub>a</sub>, 6(12)-H<sub>b</sub>], 2.35 (s, 2 H, 8-H<sub>2</sub>), 2.41 [m, 2 H, 6(12)-H<sub>a</sub>], 3.33 [tt,  $J$  = 6.5 Hz,  $J'$  = 1.5 Hz, 2 H, 5(11)-H], 7.12-7.17 (complex signal, 4 H, Ar-H).

<sup>13</sup>C-RMN (125.7 MHz, CD<sub>3</sub>OD)  $\delta$ : 38.3 [CH<sub>2</sub>, C10(13)], 41.8 [CH, C5(11)], 45.0 [CH<sub>2</sub>, C6(12)], 50.0 (CH<sub>2</sub>, C8), 56.9 (C, C7), 68.4 (C, C9), 128.5 (CH) and 129.4 (CH) [C1(4) and C2(3)], 145.1 [C, C4a(C11a)].

MS (EI),  $m/z$  (%); significant ions: 248 [(M+H)<sup>+</sup>, 12], 214 (52), 213 [(M-Cl+H)<sup>+</sup>, 100], 212 (62), 158 (16), 157 (27), 156 (21), 155 (19), 152 (10), 129 (12), 128 (14), 115 (15).

HRMS-ESI<sup>+</sup>  $m/z$  [M+H]<sup>+</sup> calcd for [C<sub>15</sub>H<sub>18</sub>ClNO+H]<sup>+</sup>: 248.1021, found: 248.1202.

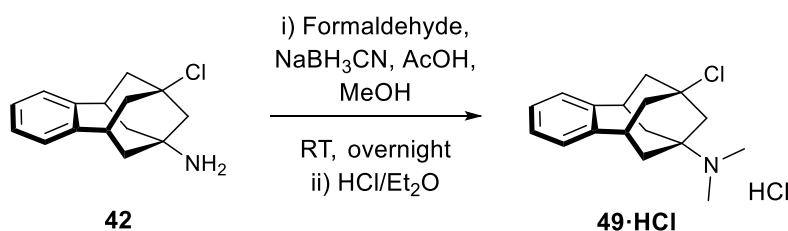
Elemental analysis:

Calculated for C<sub>15</sub>H<sub>19</sub>Cl<sub>2</sub>N: C 63.39% H 6.74% N 4.93%

Calculated for C<sub>15</sub>H<sub>19</sub>Cl<sub>2</sub>N·0.50H<sub>2</sub>O: C 61.44% H 6.87% N 4.78%

Found: C 61.37% H 6.61% N 4.78%

**Preparation of *N,N*-dimethyl-9-chloro-5,6,8,9,10,11-hexahydro-7*H*-5,9:7,11-dimethanobenzo[9]annulen-7-amine hydrochloride, 49·HCl**



To a solution of amine **42** (200 mg, 0.80 mmol) in methanol (6 mL) were added 37% formaldehyde solution (0.19 mL, 2.48 mmol), glacial acetic acid (0.17 mL) and sodium cyanoborohydride (155 mg, 2.35 mmol) and the mixture was stirred at room temperature for 6 hours. Then further NaBH<sub>3</sub>CN (155 mg, 2.35 mmol) and 37% formaldehyde solution (0.19 mL, 2.48 mmol) were added and the solution was stirred at room temperature overnight. The reaction mixture was then evaporated to dryness in *vacuo* and the resulting residue partitioned between water (5 mL) and EtOAc (5 mL). The pH was adjusted to ~12 with 5 N NaOH solution and the phases were separated. The aqueous phase was extracted with further EtOAc (2 x 5 mL) and the combined organic phases were dried over anhydrous Na<sub>2</sub>SO<sub>4</sub>, filtered and concentrated in *vacuo*. Purification by column chromatography (Al<sub>2</sub>O<sub>3</sub>, 0-2% methanol/DCM) gave **49** (75.2 g, 57% column yield) as a white solid. The purified product was taken in DCM and the amine **49** was precipitated as its hydrochloride (44.4 mg, 19.6% overall yield) by adding an excess of Et<sub>2</sub>O·HCl.

Analytical and spectroscopic data of compound **49·HCl**:

Melting point: 265 - 270 °C.

IR (ATR)  $\nu$ : 3484, 3415, 2937, 2867, 2553, 2441, 1481, 1467, 1449, 1367, 1316, 1252, 1218, 1177, 1158, 1143, 1091, 1048, 1012, 975, 936, 900, 822, 802, 783, 764, 737, 632 cm<sup>-1</sup>.

<sup>1</sup>H-NMR (500 MHz, CD<sub>3</sub>OD)  $\delta$ : 2.02 [d, *J* = 12.5 Hz, 2 H, 6(12)-H<sub>b</sub>], 2.13 [d, *J* = 13.5 Hz, 2 H, 10(13)-H<sub>b</sub>], 2.23 [m, 2 H, 6(12)-H<sub>a</sub>], 2.44 [m, 2 H, 8-H, 10(13)-H<sub>a</sub>], 2.47 (s, 2 H, 8-H<sub>2</sub>), 2.85 [s, 6 H, N(CH<sub>3</sub>)<sub>2</sub>], 3.41 [t, *J* = 7 Hz, 2 H, 5(11)-H], 7.16 (s, 4 H, Ar-H).

<sup>13</sup>C-NMR (125.7 MHz, CD<sub>3</sub>OD)  $\delta$ : 33.6 [CH<sub>2</sub>, C6(12)], 37.7 [CH<sub>3</sub>, N(CH<sub>3</sub>)<sub>2</sub>], 41.6 [CH, C5(11)], 44.9 [CH<sub>2</sub>, C10(13)], 47.2 (CH<sub>2</sub>, C8), 68.2 (C, C7), 69.2 (C, C9), 128.6 (CH) and

129.4 (CH) [C1(4) and C2(3)], 145.0 [C, C4a(C11a)].

MS (EI),  $m/z$  (%); significant ions: 275 ( $M^+$ , 18), 240 [( $M-Cl$ ) $^+$ , 100], 233 (11), 184 (17).

HRMS-ESI $^+$   $m/z$  [ $M+H$ ] $^+$  calcd for [ $C_{17}H_{23}ClN+H$ ] $^+$ : 276.1514, found: 276.1514.

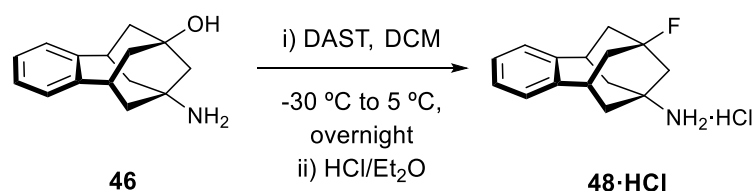
Elemental analysis:

Calculated for  $C_{17}H_{23}Cl_2N$ : C 65.39% H 7.42% Cl 22.70% N 4.49%

Calculated for  $C_{17}H_{23}Cl_2N \cdot 0.80MeOH$ : C 63.27% H 7.81% Cl 20.98% N 4.16%

Found: C 63.12% H 7.54% Cl 20.74% N 4.16%

**Preparation of 9-fluoro-5,6,8,9,10,11-hexahydro-7*H*-5,9:7,11-dimethanobenzo[9]annulen-7-amine hydrochloride, 48·HCl**



A solution of amine **46** (400 mg, 1.75 mmol) in DCM (6 mL) was cooled to  $-30\text{ }^{\circ}\text{C}$  with a dry ice in acetone bath. Then (diethylamino)sulfur trifluoride (DAST) (0.97 mL, 6.98 mmol) was added and the reaction mixture was stirred with the dry ice in acetone bath overnight. To the resulting solution was added water (10 mL) and the pH adjusted to  $\sim 12$  with a 1 N NaOH solution. The phases were separated and the aqueous phase was extracted with further DCM (2 x 8 mL), and the combined organic phases were dried over anhydrous  $\text{Na}_2\text{SO}_4$ , filtered and concentrated in *vacuo* to about 5 mL. An excess of  $\text{Et}_2\text{O} \cdot \text{HCl}$  was added and the amine **48·HCl** was recovered by filtration in *vacuo* (205.5 mg, 44% yield) as a white solid.

Analytical and spectroscopic data of compound **48·HCl**:

Melting point:  $280\text{ }^{\circ}\text{C}$  (dec.).

IR (ATR)  $\nu$ : 3280, 2934, 2854, 2701, 2649, 2580, 1626, 1542, 1493, 1453, 1367, 1326, 1259, 1218, 1094, 998, 900, 860, 757, 708, 594,  $577\text{ cm}^{-1}$ .

$^1\text{H-NMR}$  (500 MHz,  $\text{CD}_3\text{OD}$ )  $\delta$ : 1.85 [broad d,  $J = 15\text{ Hz}$ , 2 H, 6(12)- $\text{H}_b$ ], 1.89 [broad d,  $J = 10\text{ Hz}$ , 2 H, 10(13)- $\text{H}_b$ ], 2.10-2.15 [m, 4 H, 6(12)- $\text{H}_a$ , 8- $\text{H}_2$ ], 2.19 [m, 2 H, 10(13)- $\text{H}_a$ ], 3.39 [m, 2 H, 5(11)-H], 7.15 (s, 4 H, Ar-H).

$^{13}\text{C-NMR}$  (125.7 MHz,  $\text{CD}_3\text{OD}$ )  $\delta$ : 38.7 [ $\text{CH}_2$ , s, C6(12)], 40.2 [CH, d,  $^3J_{\text{CF}} = 12.8\text{ Hz}$ , C5(11)], 40.6 [ $\text{CH}_2$ , d,  $^2J_{\text{CF}} = 20.5\text{ Hz}$ , C10(13)], 45.9 ( $\text{CH}_2$ , d,  $^2J_{\text{CF}} = 20.5\text{ Hz}$ , C8), 58.2 (C,

d,  $^3J_{CF} = 10.7$  Hz, C7), 94.5 (C, d,  $^1J_{CF} = 179.1$  Hz, C9), 128.5 [CH, s, C2(3)], 129.4 [CH, s, C1(4)], 145.2 [C, s, C4a(C11a)].

MS (EI),  $m/z$  (%); significant ions: 231 ( $M^+$ , 100), 216 (17), 211 (11), 196 (20), 190 (12), 189 (73), 188 (12), 170 (34), 169 (18), 168 (56), 159 (13), 156 (44), 155 (13), 144 (18), 141 (14), 129 (17), 128 (24), 115 (26), 112 (25).

HRMS-ESI+  $m/z$  [ $M+H$ ] $^+$  calcd for  $[C_{15}H_{18}FN+H]^+$ : 232.1496, found: 232.1496.

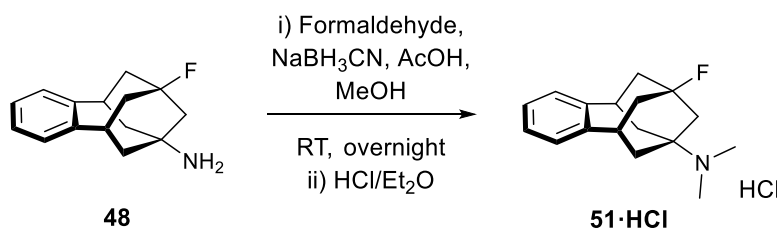
Elemental analysis:

Calculated for  $C_{15}H_{19}ClFN$ : C 67.28% H 7.15% Cl 13.24% N 5.23%

Calculated for  $C_{15}H_{19}ClFN \cdot 0.75H_2O$ : C 64.05% H 7.35% Cl 12.60% N 4.98%

Found: C 63.61% H 7.32% Cl 13.11% N 4.75%

#### Preparation of 9-fluoro-*N,N*-dimethyl-5,6,8,9,10,11-hexahydro-7*H*-5,9:7,11-dimethanobenzo[9]annulen-7-amine hydrochloride, 51·HCl



To a solution of amine **48** (228 mg, 0.99 mmol) in methanol (8 mL) were added formaldehyde (0.23 mL, 37% wt in aqueous solution, 3.01 mmol), glacial acetic acid (0.21 mL) and sodium cyanoborohydride (189.2 mg, 2.86 mmol) and the mixture was stirred at room temperature for 6 hours. Then further NaBH<sub>3</sub>CN (189.2 mg, 2.86 mmol) and formaldehyde (0.23 mL, 37% wt in aqueous solution, 3.01 mmol) were added and the solution was stirred at room temperature overnight. The reaction mixture was then evaporated to dryness in *vacuo* and the resulting residue partitioned between water (5 mL) and EtOAc (5 mL). The pH was adjusted to ~12 with 5 N NaOH solution and the phases were separated. The aqueous phase was extracted with further EtOAc (2 x 10 mL) and the combined organic phases were dried over anh. Na<sub>2</sub>SO<sub>4</sub>, filtered and concentrated in *vacuo* to about 5 mL. An excess of Et<sub>2</sub>O·HCl was added and the solvents were removed under *vacuo* to give the amine **51·HCl** (67 mg, 23% yield).

Analytical and spectroscopic data of compound **51·HCl**:

Melting point: 249 - 251 °C.

IR (ATR)  $\nu$ : 3398, 3034, 2936, 2860, 2511, 2415, 1470, 1368, 1341, 1322, 1220, 1186, 1136,

1088, 1057, 983, 968, 929, 903, 882, 757, 656, 582  $\text{cm}^{-1}$ .

$^1\text{H-NMR}$  (500 MHz,  $\text{CD}_3\text{OD}$ )  $\delta$ : 1.89 [d,  $J = 12.5$  Hz, 2 H, 6(12)- $\text{H}_b$ ], 1.99 [d,  $J = 12$  Hz, 2 H, 10(13)- $\text{H}_b$ ], 2.19-2.24 [m, 6 H, 6(12)- $\text{H}_a$ , 8- $\text{H}_2$ , 10(13)- $\text{H}_a$ ], 2.85 (s, 6 H, N- $\text{CH}_3$ ), 3.47 [m, 2 H, 5(11)-H], 7.17 (s, 4 H, Ar-H).

$^{13}\text{C-NMR}$  (125.7 MHz,  $\text{CD}_3\text{OD}$ )  $\delta$ : 33.9 [ $\text{CH}_2$ , s, C6(12)], 37.8 ( $\text{CH}_3$ , s, N- $\text{CH}_3$ ), 39.9 [ $\text{CH}$ , d,  $^3J_{\text{CF}} = 12.8$  Hz, C5(11)], 40.6 [ $\text{CH}_2$ , d,  $^2J_{\text{CF}} = 20.5$  Hz, C10(13)], 43.3 ( $\text{CH}_2$ , d,  $^2J_{\text{CF}} = 21.6$  Hz, C8), 69.5 (C, d,  $^3J_{\text{CF}} = 10.7$  Hz, C7), 94.8 (C, d,  $^1J_{\text{CF}} = 179.1$  Hz, C9), 128.3 [ $\text{CH}$ , s, C2(3)], 129.3 [ $\text{CH}$ , s, C1(4)], 145.1 [C, s, C4a(C11a)].

MS (EI),  $m/z$  (%); significant ions: 259 ( $\text{M}^+$ , 100), 258 (18), 244 (13), 217 (55), 216 (13), 184 (23), 173 (12), 159 (10), 141 (11), 140 (12), 128 (12), 115 (12), 85 (10).

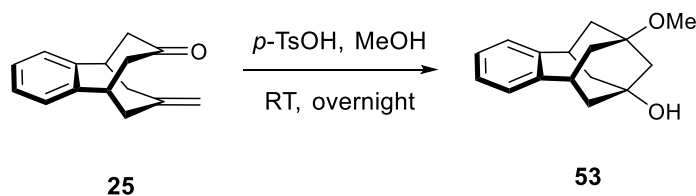
Elemental analysis:

Calculated for  $\text{C}_{17}\text{H}_{23}\text{ClFN}$ : C 69.02% H 7.84% Cl 11.98% N 4.73%

Calculated for  $\text{C}_{17}\text{H}_{23}\text{ClFN} \cdot 0.30\text{H}_2\text{O} \cdot 0.05\text{HCl}$ : C 67.38% H 7.87% Cl 12.28% N 4.62%

Found: C 67.32% H 7.91% Cl 12.20% N 4.67%

Preparation of 9-methoxy-5,6,8,9,10,11-hexahydro-7*H*-5,9:7,11-dimethanobenzo[9]annulen-7-ol, **53**<sup>165</sup>



To a solution of enone **25** (500 mg, 2.36 mmol) in methanol (10 mL) was added *p*-toluenesulfonic acid monohydrate (112 mg, 0.59 mmol) and the reaction mixture was stirred at room temperature overnight. To the resulting solution was then concentrated in *vacuo* and the obtained residue partitioned between DCM (10 mL) and saturated aqueous  $\text{NaHCO}_3$  solution (10 mL). The phases were separated and the aqueous one was extracted with further DCM (2 x 10 mL). The combined organic layers were dried over anhyd.  $\text{Na}_2\text{SO}_4$ , filtered and evaporated in *vacuo* to give a yellow gum (541.3 mg). Purification by column chromatography ( $\text{Al}_2\text{O}_3$ , DCM/methanol mixture) gave **53** (367.5 mg, 64% yield) as a white solid.

Analytical and spectroscopic data of compound **53**:

Melting point: 97 - 98  $^\circ\text{C}$ .



IR (ATR)  $\nu$ : 3359, 2930, 2851, 1723, 1495, 1444, 1356, 1296, 1239, 1193, 1094, 1061, 981, 900, 846, 758, 663  $\text{cm}^{-1}$ .

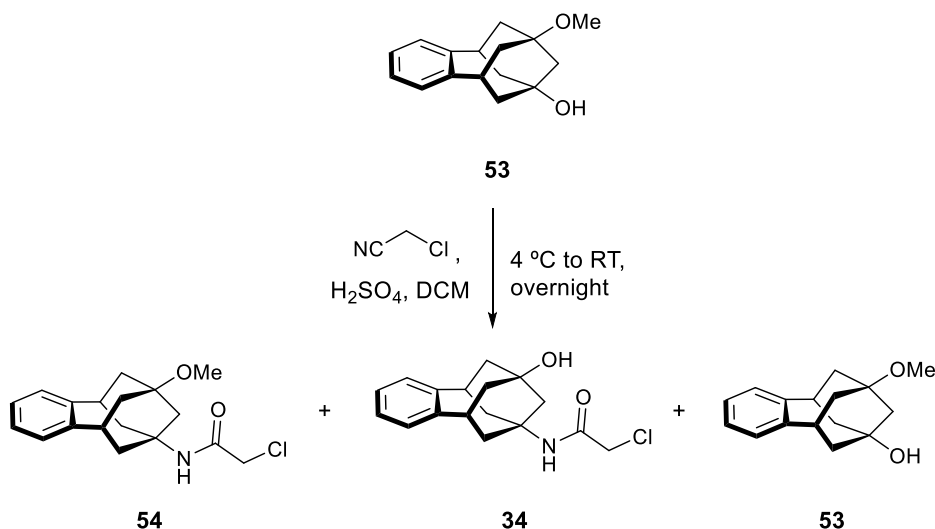
$^1\text{H-NMR}$  (400 MHz,  $\text{CDCl}_3$ )  $\delta$ : 1.74 [dm,  $J = 12.0$  Hz, 2 H, 10(13)- $\text{H}_b$ ], 1.78 [s, 2 H, 8- $\text{H}_2$ ], 1.81 [d,  $J = 13.0$  Hz, 2 H, 6(12)- $\text{H}_b$ ], 1.90 [m, 4 H, 6(12)- $\text{H}_a$ , 10(13)- $\text{H}_a$ ], 3.23 [tt,  $J = 6.4$  Hz,  $J' = 2.0$  Hz, 2 H, 5(11)-H], 3.24 (s, 3 H,  $\text{OCH}_3$ ), 7.07-7.15 (m, 4 H, Ar-H).

$^{13}\text{C-NMR}$  (100.6 MHz,  $\text{CDCl}_3$ )  $\delta$ : 37.8 [ $\text{CH}_2$ , C10(13)], 39.6 [ $\text{CH}$ , C5(11)], 42.7 [ $\text{CH}_2$ , C6(12)], 48.4 ( $\text{CH}_3$ ,  $\text{OCH}_3$ ), 48.9 ( $\text{CH}_2$ , C8), 72.5 (C, C9), 76.5 (C, C7), 126.7 [ $\text{CH}$ , C2(3)], 128.1 [ $\text{CH}$ , C1(4)], 145.1 [C, C4a(C11a)].

MS (EI),  $m/z$  (%); significant ions: 244 ( $\text{M}^+$ , 100), 213 (42), 201 (17), 172 (22), 171 (30), 159 (38), 158 (72), 157 (28), 155 (48), 154 (16), 153 (16), 144 (17), 143 (22), 141 (23), 132 (12), 130 (12), 129 (63), 128 (52), 127 (19), 125 (40), 115 (48), 111 (25), 107 (12), 91 (13).

HRMS-ESI+  $m/z$  [ $\text{M}+\text{H}]^+$  calcd for [ $\text{C}_{16}\text{H}_{19}\text{O}+\text{H}$ ; fragment] $^+$ : 227.1431, found: 227.1430.

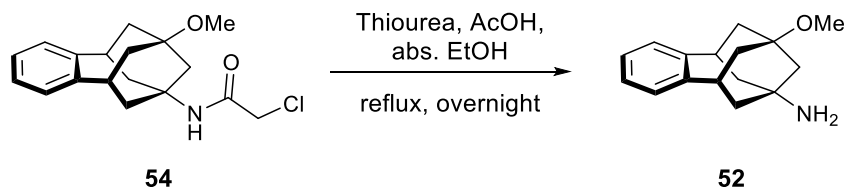
#### Preparation of 2-chloro-*N*-(9-methoxy-5,6,8,9,10,11-hexahydro-7*H*-5,9:7,11-dimethanobenzo[9]annulen-7-yl)acetamide, **54**



To a solution of alcohol **53** (545 mg, 2.23 mmol) in DCM (5 mL) was added chloroacetonitrile (0.140 mL, 2.23 mmol) and the mixture was cooled to 0-5 °C with an ice bath. Then conc.  $\text{H}_2\text{SO}_4$  (0.180 mL, 3.38 mmol) was added dropwise without reaching a temperature greater than 10 °C. After the addition, the reaction mixture was stirred at room temperature overnight. Then the resulting solution was poured into ice (10 g) and DCM (10 mL) was added. The phases were separated and the aqueous phase was extracted with further DCM (2 x 10 mL). The combined organic phases were dried over anh.  $\text{Na}_2\text{SO}_4$ , filtered and evaporated in *vacuo* to give a white gum (570 mg). Column chromatography ( $\text{Al}_2\text{O}_3$ , Hexane/EtOAc mixture) gave in order of elution **54** (222 mg, 31% yield), **34** (210

mg, 37% column yield) and **53** (91 mg, 16% column yield) as white solids. The product was used in next steps without further purification or characterization.

Preparation of 9-methoxy-5,6,8,9,10,11-hexahydro-7*H*-5,9:7,11-dimethanobenzo[9]annulen-7-amine, **52**



To a solution of chloroacetamide **54** (136.8 mg, 0.43 mmol) in abs. ethanol (9 mL) were added thiourea (39.2 mg, 0.52 mmol) and glacial acetic acid (0.3 mL) and the mixture was heated at reflux overnight. The reaction mixture was then tempered to room temperature and concentrated in *vacuo*. The crude was partitioned between water (10 mL) and DCM (10 mL) and the aqueous phase was acidified to pH ~2 with 2 N HCl solution. The phases were separated, the pH adjusted to ~12 with 2 N NaOH solution and the aqueous phase was then extracted with DCM (3 x 10 mL). The combined organic phases were dried over anh. Na<sub>2</sub>SO<sub>4</sub>, filtered and concentrated in *vacuo* to give **52** (62 mg, 59% yield) as a white solid.

Analytical and spectroscopic data of compound **52**:

Melting point: 71 – 73 °C.

IR (ATR)  $\nu$ : 3500–2850 (3507, 3389, 3329, 3307, 3263, 3126, 3019, 2936, 2852), 1651, 1605, 1490, 1441, 1360, 1210, 1113, 1059, 1047, 1010, 969, 947, 893, 847, 754, 666, 630, 584 cm<sup>-1</sup>.

<sup>1</sup>H-NMR (400 MHz, CDCl<sub>3</sub>)  $\delta$ : 1.61-1.66 [m, 4 H, 6(12)-H<sub>b</sub>, 8-H<sub>2</sub>], 1.77 [m, 2 H, 6(12)-H<sub>a</sub>], 1.83-1.90 [m, 4 H, 10(13)-H<sub>2</sub>], 3.19 [broad t,  $J = 6.0$  Hz, 2 H, 5(11)-H], 3.23 (s, 3 H, OCH<sub>3</sub>), 7.05-7.13 (m, 4 H, Ar-H).

<sup>13</sup>C-NMR (100.6 MHz, CDCl<sub>3</sub>)  $\delta$ : 37.8 [CH<sub>2</sub>, C10(13)], 40.2 [CH, C5(11)], 43.3 [CH<sub>2</sub>, C6(12)], 48.2 (CH<sub>3</sub>, OCH<sub>3</sub>), 49.5 (CH<sub>2</sub>, C8), 52.5 (C, C7), 75.4 (C, C9), 126.6 [CH, C2(3)], 128.0 [CH, C1(4)], 145.4 [C, C4a(C11a)].

MS (EI),  $m/z$  (%); significant ions: 243 (M<sup>+</sup>, 100), 228 (17), 212 (27), 201 (13), 200 (14), 171 (20), 170 (18), 156 (23), 155 (14), 144 (20), 129 (15), 128 (19), 124 (28), 115 (18), 110 (41).

HRMS-ESI<sup>+</sup>  $m/z$  [M+H]<sup>+</sup> calcd for [C<sub>16</sub>H<sub>21</sub>O+H]<sup>+</sup>: 244.1696, found: 244.1704.

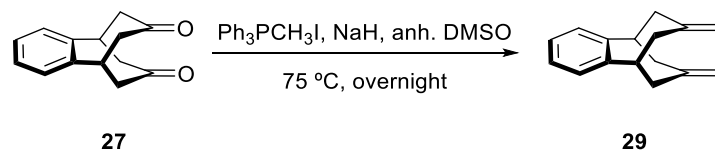


## **Chapter 2**

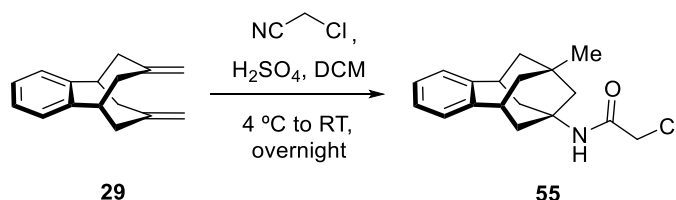


# **Benzohomoadamantane scaffolds**



Preparation of 5,6,8,9-tetrahydro-5,9-propanebenzocycloheptane-7,11-diene, **29**<sup>165</sup>

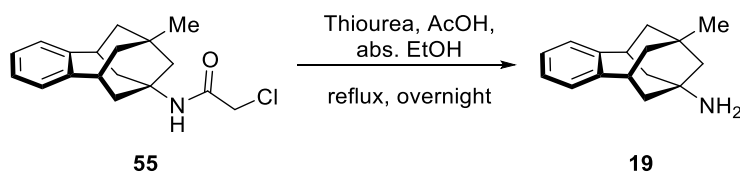
A suspension of sodium hydride, 60% dispersion in mineral oil (0.78 g, 19.64 mmol) in anh. DMSO (50 mL) was heated to 75 °C for 45 minutes. After the reaction mixture was tempered, a solution of triphenylmethylphosphonium iodide (8.2 g, 19.64 mmol) in anh. DMSO (70 mL) was added and the resulting yellow solution was stirred at room temperature for 20 minutes. Then a suspension of diketone **27** (2 g, 9.35 mmol) in anh. DMSO (20 mL) was added and the obtained solution was heated to 75 °C overnight. The resulting black solution was allowed to cool to room temperature and then poured into water (150 mL). Hexane (100 mL) was added and the phases were separated. The aqueous phase was extracted with further hexane (3 x 50 mL) and the combined organic phases were washed with brine (50 mL), dried over anh. Na<sub>2</sub>SO<sub>4</sub>, filtered and concentrated in *vacuo* to give an orange gum (2.32 g). Purification by packing the solid with silica gel and extracting with 100% petroleum ether gave **29** (1.56 g, 80% yield) as a white solid. The spectroscopic data were identical to those previously published.

Preparation of *N*-(6,7,8,9,10,11-hexahydro-9-methyl-5,7:9,11-dimethano-5*H*-benzocyclononen-7-yl)chloroacetamide, **55**<sup>98</sup>

A solution of diene **29** (5.02 g, 23.9 mmol) in chloroacetonitrile (6.05 mL, 95.6 mmol) and glacial acetic acid (15 mL) was cooled to 0-5 °C with an ice bath. Then conc. H<sub>2</sub>SO<sub>4</sub> (7.6 mL, 143.4 mmol) was added dropwise without reaching a temperature greater than 10 °C. After the addition, the reaction mixture was stirred at room temperature overnight. Then the resulting solution was poured into ice (100 g) and DCM (40 mL) was added. The phases were separated and the aqueous phase was extracted with further DCM (2 x 40 mL). The combined organic phases were dried over anh. Na<sub>2</sub>SO<sub>4</sub>, filtered and evaporated in *vacuo* to give **55** (5.86 g, 81% yield) as a white solid, whose spectroscopic data were those corresponding to the previously published.

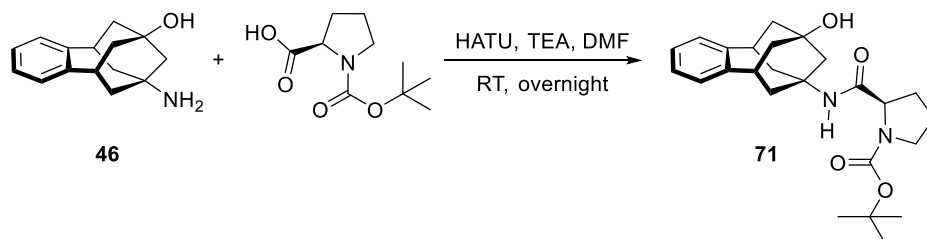


Preparation of 6,7,8,9,10,11-hexahydro-9-methyl-5,7:9,11-dimethano-5*H*-benzocyclononen-7-amine, **19**<sup>98</sup>



To a solution of chloroacetamide **55** (5.86 g, 19.4 mmol) in abs. ethanol (150 mL) were added thiourea (1.76 g, 23.2 mmol) and glacial acetic acid (14 mL) and the mixture was heated at reflux overnight. The reaction mixture was then tempered to room temperature and concentrated in *vacuo*. The crude was partitioned between water (200 mL) and EtOAc (100 mL) and the aqueous phase was acidified to pH ~2 with 1N HCl solution. The phases were separated, the pH adjusted to ~12 with 5N NaOH solution and the aqueous phase was then extracted with EtOAc (4 x 100 mL). The combined organic phases were dried over anh. Na<sub>2</sub>SO<sub>4</sub>, filtered and concentrated in *vacuo* to give **19** (3.03 g, 69% yield) as a white solid. The spectroscopic data were identical to those previously published.

Preparation of (2*R*)-tert-butyl 2-[(9-hydroxy-6,7,8,9,10,11-hexahydro-5*H*-9:7,11-dimethanobenzo[9]annulen-7-yl)carbamoyl]pyrrolidine-1-carboxylate, **71**



To a solution of amine **46** (500 mg, 2.18 mmol) in DMF (10 mL) were added Boc-D-proline (445.8 mg, 2.07 mmol), HATU (328.4 mg, 2.18 mmol) and triethylamine (0.6 mL, 4.36 mmol) and the resulting solution was stirred at room temperature overnight. The reaction mixture was then diluted with EtOAc/benzene (2:1, 25 mL) and washed with 0.5 N HCl aqueous solution (2 x 25 mL), brine (25 mL), saturated NaHCO<sub>3</sub> aqueous solution (2 x 25 mL) and brine (25 mL). The organic phase was separated, dried over anh. Na<sub>2</sub>SO<sub>4</sub>, filtered and concentrated in *vacuo* to give an orange oil (765 mg). Column chromatography (Al<sub>2</sub>O<sub>3</sub>, hexane/ethyl acetate mixture) gave **12** (438 mg, 50% yield) as a white solid. The analytical sample was obtained by crystallization from EtOAc/pentane.

Analytical and spectroscopic data of compound **71**:

Melting point: 98 – 103 °C.

IR (ATR)  $\nu$ : 3408, 3327, 2975, 2927, 1677, 1538, 1451, 1400, 1366, 1300, 1247, 1163, 1119,

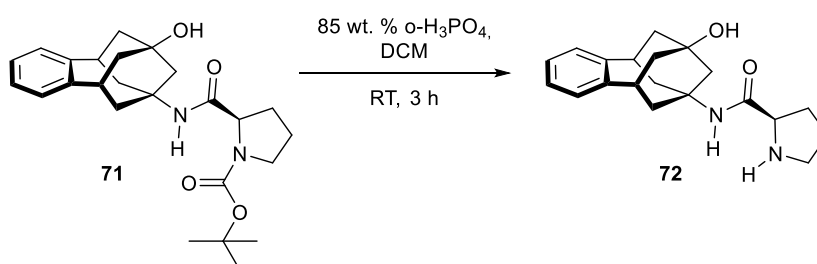
1088, 1045, 978, 922, 862, 758  $\text{cm}^{-1}$ .

$^1\text{H-NMR}$  (500 MHz,  $\text{CDCl}_3$ )  $\delta$ : 1.45 [s, 9 H,  $\text{OC}(\underline{\text{C}}\text{H}_3)_3$ ], 1.73 (m, 2 H, 17-H), 1.76 [d,  $J = 13.0$  Hz, 2 H, 10(13)- $\text{H}_b$ ], 1.83 (broad signal, 1 H, 16- $\text{H}_a$ ), 1.93-2.31 [complex signal, 9 H, 10(13)- $\text{H}_a$ , 6(12)- $\text{H}_2$ , 8-H, 16- $\text{H}_b$ ], 3.17 [t,  $J = 6.5$  Hz, 2 H, 5(11)-H], 3.37 (m, 2 H, 18-H), 4.21 (m, 1 H, 15-H), 5.81 (broad s, 1 H, OH), 6.94 (broad s, 1 H, NH), 7.06 [m, 4 H, 1(4)-H], 7.10 [m, 2 H, 2(3)-H].

$^{13}\text{C-NMR}$  (125.7 MHz,  $\text{CDCl}_3$ )  $\delta$  (mixture of two rotamers): 23.7 ( $\text{CH}_2$ ) and 24.1 ( $\text{CH}_2$ ) (two rotamers, C17), 28.4 [ $\text{CH}_3$ ,  $\text{OC}(\underline{\text{C}}\text{H}_3)_3$ ], 31.1 (broad  $\text{CH}_2$ , C16), 38.4 [ $\text{CH}_2$ , C6(12)], 40.0 [ $\text{CH}$ , C5(11)], 42.4 [ $\text{CH}_2$ , C10(13)], 47.1 ( $\text{CH}_2$ , C18), 48.2 ( $\text{CH}_2$ , C8), 56.6 (C, C7), 61.2 (CH) and 61.9 (CH) (C15, two rotamers), 70.8 (C, C9), 80.4 (C, C20), 126.6 [ $\text{CH}$ , C2(3)], 128.1 [ $\text{CH}$ , C1(4)], 145.2 [d, C, C4a(C11a)], 154.7 (C) and 156.1 (C) (NCO, two rotamers), 170.9 (C) and 171.6 (C) (CO, two rotamers).

HRMS-ESI+  $m/z$  [ $\text{M}+\text{H}$ ] $^+$  calcd for  $[\text{C}_{25}\text{H}_{34}\text{N}_2\text{O}_4+\text{H}]^+$ : 427.2591, found: 427.2593.

#### Preparation of (2*R*)-*N*-(9-hydroxy-6,7,8,9,10,11-hexahydro-5*H*-5,9:7,11-dimethanobenzo[9]annulen-7-yl)pyrrolidine-2-carboxamide, 72



A solution of Boc-protected pyrrolidine 71 (438.5 mg, 1.03 mmol) in DCM (5 mL) and 85% *o*-phosphoric acid (1.05 mL, 15.4 mmol) was stirred at room temperature for 3 hours. To the reaction mixture was then added water (8 mL) and the pH was adjusted to  $\sim 12$  with 5 N NaOH solution. The phases were separated, the aqueous phase was extracted with further DCM (2 x 8 mL) and the combined organic phases were dried over anhydrous  $\text{Na}_2\text{SO}_4$  and filtered. Evaporation in *vacuo* of the combined organic layers gave 72 (290.8 mg, 87% yield) as a white solid.

Analytical and spectroscopic data of compound 72:

Melting point: 175 – 180  $^\circ\text{C}$ .

IR (ATR)  $\nu$ : 3441, 3368, 3262, 2945, 2863, 1639, 1521, 1507, 1475, 1434, 1401, 1378, 1361, 1336, 1300, 1230, 1194, 1115, 1050, 887, 846, 799, 767, 731, 698, 552  $\text{cm}^{-1}$ .

$^1\text{H-NMR}$  (500 MHz,  $\text{CDCl}_3$ )  $\delta$ : 1.66 (complex signal, 2 H, 17- $\text{H}_2$ ), 1.78 [d,  $J = 13$  Hz, 2 H,

10(13)-H<sub>b</sub>], 1.85 (m, 1H, 16-H<sub>a</sub>), 1.90-1.99 [complex signal, 4 H, 6(12)-H<sub>b</sub>, 10(13)-H<sub>a</sub>], 2.04-2.11 (complex signal, 4 H, 8-H, 16-H<sub>b</sub>), 2.15-2.25 [complex signal, 2 H, 6(12)-H<sub>a</sub>], 2.83 (dt,  $J = 10.5$  Hz,  $J' = 6.5$  Hz, 1 H, 18-H<sub>a</sub>), 2.97 (dt,  $J = 10.5$  Hz,  $J' = 6.5$  Hz, 1 H, 18-H<sub>b</sub>), 3.17 [broad t,  $J = 6.5$  Hz, 2 H, 5(11)-H], 3.59 (dd,  $J = 9$  Hz,  $J' = 5.5$  Hz, 1 H, 15-H), 7.06 [m, 2 H, 1(4)-H], 7.08 [m, 2 H, 2(3)-H], 7.60 (broad s, 1 H, NH).

<sup>13</sup>C-NMR (125.7 MHz, CDCl<sub>3</sub>)  $\delta$ : 26.1 (CH<sub>2</sub>, C17), 30.8 (CH<sub>2</sub>, C16), 38.5 (CH<sub>2</sub>) and 38.6 (CH<sub>2</sub>) (C6 and C12), 40.1 [CH, C5(11)], 42.4 [CH<sub>2</sub>, C10(13)], 47.2 (CH<sub>2</sub>, C18), 48.1 (CH<sub>2</sub>, C8), 55.9 (C, C7), 61.0 (CH, C15), 70.7 (C, C9), 126.6 [CH, C2(3)], 128.1 [CH, C1(4)], 145.3 [C, C4a(C11a)], 174.1 (C, CO).

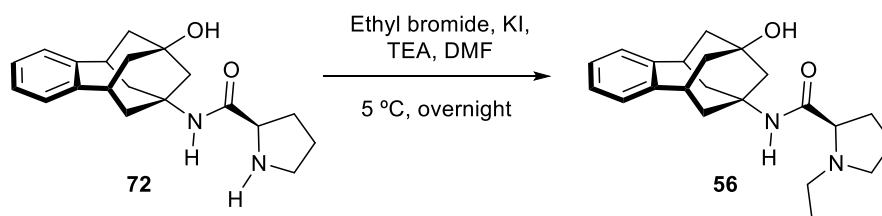
Elemental analysis:

Calculated for C<sub>20</sub>H<sub>26</sub>N<sub>2</sub>O<sub>2</sub>:                      C 73.59%    H 8.03%    N 8.58%

Calculated for C<sub>20</sub>H<sub>26</sub>N<sub>2</sub>O<sub>2</sub>·0.15DCM:        C 71.36%    H 7.82%    N 8.26%

Found:    C 71.48%    H 7.78%    N 8.07%

#### Preparation of (2*R*)-1-ethyl-*N*-(9-hydroxy-6,7,8,9,10,11-hexahydro-5*H*-9,7,11-dimethanobenzo[9]annulen-7-yl)pyrrolidine-2-carboxamide, 56



A solution of pyrrolidine 72 (170 mg, 0.52 mmol) in DMF (3 mL) was cooled to 5 °C with an ice bath. Then KI (8.64 mg, 0.052 mmol) and triethylamine (0.278 mL, 2.08 mmol) were added, followed by the dropwise addition of ethyl bromide (0.04 mL, 0.55 mmol). The reaction mixture was stirred at room temperature in an ice-water bath overnight. The resulting suspension was then filtered and the solids were washed with EtOAc (10 mL). The combined filtrates were washed with saturated aqueous NaHCO<sub>3</sub> solution (10 mL) and brine (10 mL). The organic phase was separated, dried over anh. Na<sub>2</sub>SO<sub>4</sub>, filtered and concentrated in *vacuo* to give 56 (133 mg, 72% yield) as a white solid. The analytical sample was obtained by crystallization from EtOAc/pentane.

Analytical and spectroscopic data of compound 56:

Melting point: 150 – 152 °C.

IR (ATR)  $\nu$ : 3388, 2931, 2871, 1647, 1511, 1440, 1384, 1358, 1335, 1304, 1234, 1194, 1117,

1088, 1060, 761, 647  $\text{cm}^{-1}$ .

$^1\text{H-NMR}$  (500 MHz,  $\text{CDCl}_3$ )  $\delta$ : 1.04 (t,  $J = 7.5$  Hz, 3 H,  $\text{NCH}_2\text{CH}_3$ ), 1.59-1.82 (complex signal, 3 H, 16- $\text{H}_a$ , 17-H), 1.77 [d,  $J = 12.5$  Hz, 2 H, 10(13)- $\text{H}_b$ ], 1.92 [d,  $J = 13$  Hz, 2 H, 6(12)- $\text{H}_b$ ], 1.97 [dd,  $J = 12.5$  Hz,  $J' = 6.5$  Hz, 2 H, 10(13)- $\text{H}_a$ ], 2.02 (broad s, 1 H, OH), 2.11 (m, 1 H, 16- $\text{H}_b$ ), 2.14 (s, 2 H, 8-H), 2.17-2.30 [complex signal, 3 H, 6(12)- $\text{H}_a$ , 19- $\text{H}_a$ ], 2.45 (m, 1 H, 18- $\text{H}_a$ ), 2.58 (m, 1 H, 18- $\text{H}_b$ ), 3.85 (dd,  $J = 10.0$  Hz,  $J' = 4.5$  Hz, 1 H, 15-H), 3.12 (m, 1 H, 19- $\text{H}_b$ ), 3.18 [dt,  $J = 6.5$  Hz,  $J' = 1.5$  Hz, 2 H, 5(11)-H], 7.07 [m, 2 H, 1(4)-H], 7.11 [m, 2 H, 2(3)-H], 7.45 (broad s, 1 H, NH).

$^{13}\text{C-NMR}$  (125.7 MHz,  $\text{CDCl}_3$ )  $\delta$ : 14.8 ( $\text{CH}_3$ ,  $\text{NCH}_2\text{CH}_3$ ), 24.1 ( $\text{CH}_2$ , C17), 30.7 ( $\text{CH}_2$ , C16), 38.6 ( $\text{CH}_2$ ) and 38.7 ( $\text{CH}_2$ ) (C6 and C12), 40.1 [ $\text{CH}$ , C5(11)], 42.4 [ $\text{CH}_2$ , C10(13)], 48.1 ( $\text{CH}_2$ , C8), 49.7 ( $\text{CH}_2$ , C18), 53.8 ( $\text{CH}_2$ ,  $\text{NCH}_2\text{CH}_3$ ), 55.8 (C, C7), 67.8 ( $\text{CH}$ , C15), 70.7 (C, C9), 126.6 [ $\text{CH}$ , C2(3)], 128.1 [ $\text{CH}$ , C1(4)], 145.3 [d, C, C4a(C11a)], 174.3 (C, CO).

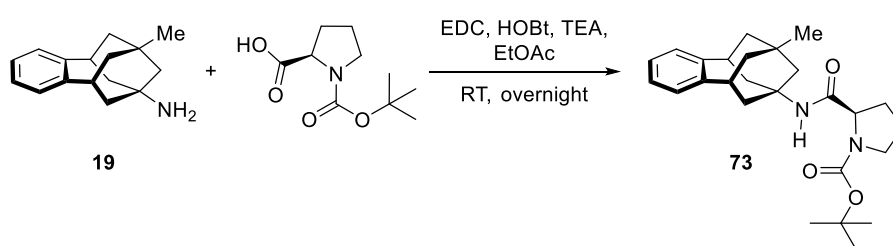
Elemental analysis:

Calculated for  $\text{C}_{22}\text{H}_{30}\text{N}_2\text{O}_2$ : C 74.54% H 8.53% N 7.90%

Calculated for  $\text{C}_{22}\text{H}_{30}\text{N}_2\text{O}_2 \cdot 0.1\text{EtOAc}$ : C 74.06% H 8.55% N 7.71%

Found: C 73.93% H 8.64% N 7.71%

#### Preparation of (2*R*)-tert-butyl-2-[(9-methyl-6,7,8,9,10,11-hexahydro-5*H*-9,7,11-dimethanobenzo[9]annulen-7-yl)carbamoyl]pyrrolidine-1-carboxylate, 73



Boc-D-proline (336 mg, 1.56 mmol), HOBT (316 mg, 2.34 mmol), EDC (363 mg, 2.34 mmol) and triethylamine (0.48 mL, 3.43 mmol) were added to a solution of amine **19** (388 mg, 1.71 mmol) in EtOAc (20 mL) and the mixture was stirred at room temperature overnight. To the resulting suspension was then added water (15 mL) and the phases were separated. The organic phase was washed with saturated aqueous  $\text{NaHCO}_3$  solution (15 mL) and brine (15 mL), dried over anhydrous  $\text{Na}_2\text{SO}_4$  and filtered. Evaporation in *vacuo* of the combined organic layers gave **73** (556 mg, 84% yield) as a white solid, that was washed with pentane for obtaining an analytical sample.

Analytical and spectroscopic data of compound **73**:

Melting point: 168 – 169 °C.

IR (ATR)  $\nu$ : 3296, 2917, 1706, 1684, 1657, 1560, 1450, 1385, 1363, 1287, 1238, 1179, 1161, 1123, 1089, 1048, 1009, 982, 920, 756, 673, 574  $\text{cm}^{-1}$ .

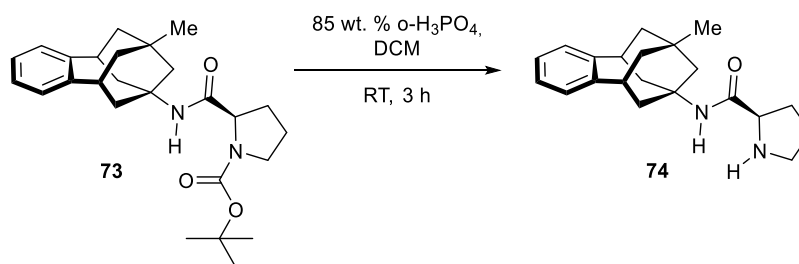
$^1\text{H-NMR}$  (400 MHz,  $\text{CDCl}_3$ )  $\delta$  (two rotamers): 0.91 (s, 3 H, C9- $\text{CH}_3$ ), 1.46 [s, 9 H,  $\text{OC}(\text{CH}_3)_3$ ], 1.53 [broad d,  $J = 13.5$  Hz, 2 H, 10(13)- $\text{H}_b$ ], 1.65 [broad dd,  $J = 13.5$  Hz,  $J' = 6.5$  Hz, 2 H, 10(13)- $\text{H}_a$ ], 1.75-1.88 (complex signal, 4 H, 8-H, 17-H), 2.01 [broad d,  $J = 13$  Hz, 2 H, 6(12)- $\text{H}_b$ ], 2.13 [m, 2 H, 6(12)- $\text{H}_a$ ], 2.3 (very broad signal, 1 H, 16- $\text{H}_b$ ), 3.06 [t,  $J = 6$  Hz, 2 H, 5(11)-H], 3.39 (broad m, 2 H, 18-H), 4.11 (very broad signal, 1 H, 15-H), 6.77 (broad s, 1 H, NH), 7.05 [m, 4 H, Ar-H].

$^{13}\text{C-NMR}$  (100.6 MHz,  $\text{CDCl}_3$ )  $\delta$  (two rotamers): 24.2 (broad  $\text{CH}_2$ , C17), 28.4 [ $\text{CH}_3$ ,  $\text{C}(\text{CH}_3)_3$ ], 31.1 (broad  $\text{CH}_2$ , C16), 32.2 ( $\text{CH}_3$ , C9- $\text{CH}_3$ ), 33.6 (C, C9), 38.9 and 39.0 [ $\text{CH}_2$ , C6(12)], 41.0 and 41.1 [CH, C5(11)], 41.11 and 41.15 [ $\text{CH}_2$ , C10(13)], 47.0 ( $\text{CH}_2$ , C8), 47.2 (broad signal,  $\text{CH}_2$ , C18), 54.1 (C, C7), 60.6 and 61.9 (CH, C15), 126.2 [CH, C2(3)], 127.9 [CH, C1(4)], 146.2 [broad C, C4a(C11a)], 170.8 (very broad C, CO).

MS-DIP (EI),  $m/z$  (%); significant ions: 424 ( $\text{M}^+$ , <1), 211 ( $\text{C}_{16}\text{H}_{19}^+$ , 14), 171 (22), 170 (14), 155 (19), 140 (8), 115 (22), 114 (100), 70 (60), 57 (22).

HRMS-ESI+  $m/z$  [ $\text{M}+\text{H}$ ] $^+$  calcd for  $[\text{C}_{26}\text{H}_{36}\text{N}_2\text{O}_3+\text{H}^+]$ : 425.2799, found: 425.2803.

### Preparation of (2*R*)-*N*-(9-methyl-6,7,8,9,10,11-hexahydro-5*H*-9,9:7,11-dimethanobenzo[9]annulen-7-yl)pyrrolidine-2-carboxamide, **74**



A solution of Boc-protected pyrrolidine **73** (556.1 mg, 1.31 mmol) in DCM (6 mL) and 85%  $\text{o}$ -phosphoric acid (1.33 mL, 19.6 mmol) was stirred at room temperature for 18 hours. To the reaction mixture was then added water (15 mL) and the aqueous phase was basified until pH  $\sim$ 12 with 5 N NaOH solution. The phases were separated and the aqueous phase was extracted with further DCM (2 x 10 mL). The combined organic layers were dried over anhydrous  $\text{Na}_2\text{SO}_4$ , filtered and evaporated in *vacuo* to give **74** (419.5 mg, quantitative).

yield) as a white solid. The analytical sample was obtained by crystallization from EtOAc/pentane.

Analytical and spectroscopic data of compound **74**:

Melting point: 116 - 119 °C.

IR (ATR)  $\nu$ : 3289, 3257, 3017, 2920, 2897, 2864, 2839, 1646, 1515, 1492, 1467, 1450, 1359, 1345, 1307, 1245, 1208, 1153, 1135, 1110, 1090, 1046, 1006, 948, 914, 877, 856, 800, 754, 700, 613, 644, 558, 488  $\text{cm}^{-1}$ .

$^1\text{H-NMR}$  (500 MHz,  $\text{CDCl}_3$ )  $\delta$ : 0.91 (s, 3 H, C9- $\text{CH}_3$ ), 1.53 [d,  $J = 13.0$  Hz, 2 H, 10(13)- $\text{H}_b$ ], 1.66 [complex signal, 4 H, 17-H, 10(13)- $\text{H}_a$ ], 1.86 (complex signal, 3 H, 8-H, 16- $\text{H}_a$ ), 1.99 [dq,  $J = 13.0$  Hz,  $J' = 1.5$  Hz, 2 H, 6(12)- $\text{H}_b$ ], 2.07 (m, 1 H, 16- $\text{H}_b$ ), 2.17 [m, 2 H, 6(12)- $\text{H}_a$ ], 2.84 (dt,  $J = 10.5$  Hz,  $J' = 6.5$  Hz, 1 H, 18- $\text{H}_a$ ), 2.97 (dt,  $J = 10.5$  Hz,  $J' = 6.5$  Hz, 1 H, 18- $\text{H}_b$ ), 3.06 [tq,  $J = 6.5$  Hz,  $J' = 1.5$  Hz, 2 H, 5(11)-H], 3.60 (dd,  $J = 9.0$  Hz,  $J' = 5.5$  Hz, 1 H, 15-H), 7.02-7.08 [complex signal, 4 H, Ar-H], 7.50 (broad s, 1 H, NH).

$^{13}\text{C-NMR}$  (125.7 MHz,  $\text{CDCl}_3$ )  $\delta$ : 26.1 ( $\text{CH}_2$ , C17), 30.8 ( $\text{CH}_2$ , C16), 32.2 ( $\text{CH}_3$ , C9- $\text{CH}_3$ ), 33.5 (C, C9), 38.9 ( $\text{CH}_2$ ) and 39.0 ( $\text{CH}_2$ ) (C6 and C12), 41.0 [CH, C5(11)], 41.1 ( $\text{CH}_2$ ) and 41.2 ( $\text{CH}_2$ ) (C10 and C13), 47.0 ( $\text{CH}_2$ , C8), 47.2 ( $\text{CH}_2$ , C18), 53.3 (C, C7), 61.1 (CH, C15), 126.2 [CH, C2(3)], 127.9 [CH, C1(4)], 146.3 [d, C, C4a(C11a)], 173.9 (C, CO).

MS (CI),  $m/z$  (%); significant ions: 324 ( $\text{M}^+$ , <1), 211 ( $\text{C}_{16}\text{H}_{19}^+$ , 1), 155 (4), 70 (100).

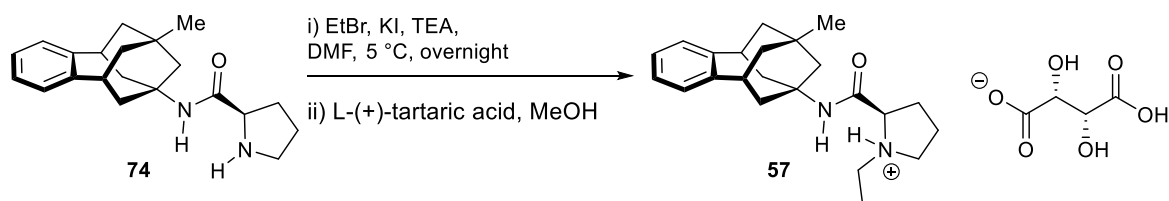
Elemental analysis:

Calculated for  $\text{C}_{21}\text{H}_{28}\text{N}_2\text{O}$ : C 77.74% H 8.70% N 8.63%

Calculated for  $\text{C}_{21}\text{H}_{28}\text{N}_2\text{O} \cdot 0.2\text{EtOAc} \cdot 0.15\text{Pentane}$ : C 76.75% H 8.97% N 7.94%

Found: C 76.78% H 8.95% N 7.89%

Preparation of (2*R*)-1-ethyl-*N*-(9-methyl-6,7,8,9,10,11-hexahydro-5*H*-5,9:7,11-dimethanobenzo[9]annulen-7-yl)pyrrolidine-2-carboxamide, **57**·tartrate



A solution of pyrrolidine **74** (504 mg, 1.55 mmol) in DMF (10 mL) was cooled to 5 °C with an ice bath. Then KI (26 mg, 0.16 mmol) and triethylamine (0.87 mL, 6.2 mmol) were

added, followed by the dropwise addition of ethyl bromide (0.12 mL, 1.63 mmol). The reaction mixture was stirred at room temperature in an ice-water bath overnight. To the resulting solution was added EtOAc (5 mL) and water (20 mL). The phases were separated and the aqueous layer was extracted with further EtOAc (2 x 15 mL). The combined organic phases were washed with saturated aqueous NaHCO<sub>3</sub> solution (15 mL) and brine (15 mL), dried over anh. Na<sub>2</sub>SO<sub>4</sub>, filtered and concentrated in *vacuo* to give a clear oil (446 mg). Column chromatography (Al<sub>2</sub>O<sub>3</sub>, hexane/EtOAc mixtures) gave **57** (255 mg, 44% yield) as a white solid. A solution of L-(+)-tartaric acid (108.8 mg, 0.72 mmol) in methanol (2 mL) was added to **57** directly. The solvents were removed under *vacuo* to give **57** as its tartrate salt. The analytical sample was obtained by crystallization from methanol/diethyl ether.

Analytical and spectroscopic data of compound **57**·tartrate:

Melting point: 177-179 °C.

IR (ATR)  $\nu$ : 3426, 3250, 3023, 2915, 1694, 1667, 1573, 1453, 1361, 1306, 1243, 1217, 1116, 1080, 948, 893, 800, 761, 666 cm<sup>-1</sup>.

<sup>1</sup>H-NMR (500 MHz, CD<sub>3</sub>OD)  $\delta$ : 0.94 (s, 3 H, C9-CH<sub>3</sub>), 1.27 (t,  $J$  = 7.5 Hz, 3 H, NCH<sub>2</sub>CH<sub>3</sub>), 1.50 [d,  $J$  = 13.5 Hz, 2 H, 10(13)-H<sub>b</sub>], 1.69 [dd,  $J$  = 13.0 Hz,  $J'$  = 6.0 Hz, 2 H, 10(13)-H<sub>a</sub>], 1.80 (s, 2 H, 8-H<sub>2</sub>), 1.93-1.99 (complex signal, 3 H, 16-H<sub>a</sub>, 17-H), 2.11 [m, 2 H, 6(12)-H<sub>a</sub>], 2.17 [d,  $J$  = 13 Hz, 2 H, 6(12)-H<sub>b</sub>], 2.46 (m, 1 H, 16-H<sub>b</sub>), 3.08 [tt,  $J$  = 6.5 Hz,  $J'$  = 2 Hz, 2 H, 5(11)-H], 3.13 (m, 1 H, 18-H<sub>a</sub>), 3.19 (q,  $J$  = 7.5 Hz, 2 H, NCH<sub>2</sub>CH<sub>3</sub>), 3.66 (m, 1 H, 18-H<sub>b</sub>), 3.96 (dd,  $J$  = 9 Hz,  $J'$  = 6.5 Hz, 1 H, 15-H), 4.41 (s, 2 H, tartrate-CH), 7.02-7.065 [complex signal, 4 H, Ar-H].

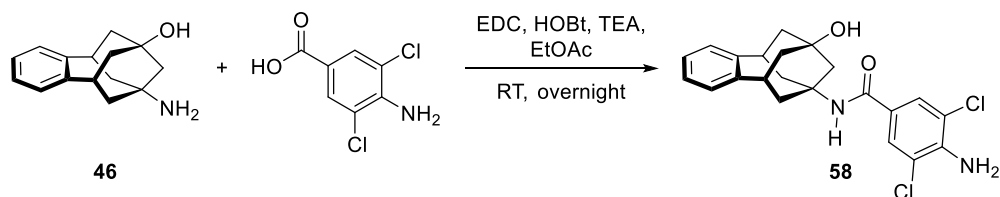
<sup>13</sup>C-NMR (125.7 MHz, CD<sub>3</sub>OD)  $\delta$ : 11.5 (CH<sub>3</sub>, NCH<sub>2</sub>CH<sub>3</sub>), 24.0 (CH<sub>2</sub>, C17), 31.2 (CH<sub>2</sub>, C16), 32.8 (CH<sub>3</sub>, C9-CH<sub>3</sub>), 34.5 (C, C9), 39.5 (CH<sub>2</sub>) and 39.6 (CH<sub>2</sub>) (C6 and C12), 42.4 [CH and CH<sub>2</sub>, C5(11), C10(13)], 48.0 (CH<sub>2</sub>, C8), 51.3 (CH<sub>2</sub>, NCH<sub>2</sub>CH<sub>3</sub>), 55.6 (CH<sub>2</sub>, C18), 56.1 (C, C7), 68.6 (CH, C15), 74.1 (CH, tartrate-CH), 127.5 [CH, C2(3)], 129.0 [CH, C1(4)], 147.4 [C, C4a(C11a)], 168.6 (C, CO), 176.6 (C, tartrate-CO).

MS (CI),  $m/z$  (%); significant ions: 393 (M+41, 7), 381 (M+29, 18), 354 (27), 353 (M+1, 100), 211 (12), 98 (26).

Elemental analysis:

Calculated for C <sub>27</sub> H <sub>38</sub> N <sub>2</sub> O <sub>7</sub> :	C 64.52%	H 7.62%	N 5.57%
Calculated for C <sub>27</sub> H <sub>38</sub> N <sub>2</sub> O <sub>7</sub> ·1H <sub>2</sub> O:	C 62.29%	H 7.74%	N 5.38%
Found:	C 62.50%	H 7.50%	N 5.13%

Preparation of 4-amino-3,5-dichloro-*N*-(9-hydroxy-6,7,8,9,10,11-hexahydro-5H-5,9:7,11-dimethanobenzo[9]annulen-7-yl)benzamide, **58**



4-Amino-3,5-dichlorobenzoic acid (220.9 mg, 1.07 mmol), 1-hydroxybenzotriazole (HOBt) (216.7 mg, 1.6 mmol), 1-ethyl-3-(3-dimethylaminopropyl)carbodiimide (EDC) (248.0 mg, 1.6 mmol) and triethylamine (0.327 mL, 2.2 mmol) were added to a solution of amine **46** (270 mg, 1.18 mmol) in EtOAc (15 mL) and DMF (1 mL) and the reaction mixture was stirred at room temperature for 21 hours. To the resulting suspension was then added water (20 mL) and the phases were separated. The organic phase was washed with 5% aqueous NaHCO<sub>3</sub> solution (15 mL) and brine (15 mL), dried over anhydrous Na<sub>2</sub>SO<sub>4</sub> and filtered. Evaporation *in vacuo* of the combined organic phases gave **58** (422 mg, 95% yield) as a white solid. The analytical sample was obtained by crystallization from DCM.

Analytical and spectroscopic data of compound **58**:

Melting point: 236 – 237 °C.

IR (ATR)  $\nu$ : 3362, 2923, 2853, 2160, 1976, 1643, 1606, 1547, 1519, 1492, 1452, 1321, 1299, 1269, 1230, 1201, 1101, 1020, 864, 748, 570 cm<sup>-1</sup>.

<sup>1</sup>H-NMR (500 MHz, CDCl<sub>3</sub>)  $\delta$ : 1.58 (broad s, 1 H, OH), 1.81 [d,  $J = 12.5$  Hz, 2 H, 10(13)-H<sub>b</sub>], 2.00 [m, 2 H, 10(13)-H<sub>a</sub>], 2.12 [d,  $J = 13$  Hz, 2 H, 6(12)-H<sub>b</sub>], 2.19 (s, 2 H, 8-H), 2.27 [ddd,  $J = 13.0$  Hz,  $J' = 6.5$  Hz,  $J'' = 1.0$  Hz, 2 H, 6(12)-H<sub>a</sub>], 3.23 [tt,  $J = 6.5$  Hz,  $J' = 1.5$  Hz, 2 H, 5(11)-H], 4.73 (broad s, 2 H, Ar-NH<sub>2</sub>), 5.72 (broad s, 1 H, CONH), 7.09 [m, 2 H, 1(4)-H], 7.13 [m, 2 H, 3(2)-H], 7.54 [s, 2 H, 16(20)].

<sup>13</sup>C-NMR (125.7 MHz, CDCl<sub>3</sub>)  $\delta$ : 38.6 [CH<sub>2</sub>, C6(12)], 40.0 [CH, C5(11)], 42.5 [CH<sub>2</sub>, C10(13)], 48.4 (CH<sub>2</sub>, C8), 57.4 (C, C7), 70.9 (C, C9), 118.9 [C, C17(19)], 125.4 (C, C15), 126.7 [C, C16(20)], 126.8 [CH, C2(3)], 128.1 [CH, C1(4)], 142.6 (C, C18), 145.1 [d, C, C4a(C11a)], 164.2 (C, CO).

MS (EI),  $m/z$  (%); significant ions: 418 (21), 416 (M<sup>+</sup>, 32), 212 (43), 207 (36), 205 (46), 194 (16), 190 (63), 188 (100), 179 (15), 160 (15), 155 (33), 154 (29), 142 (16), 141 (17), 129 (19), 128 (20), 124 (16), 115 (16).

Elemental analysis:

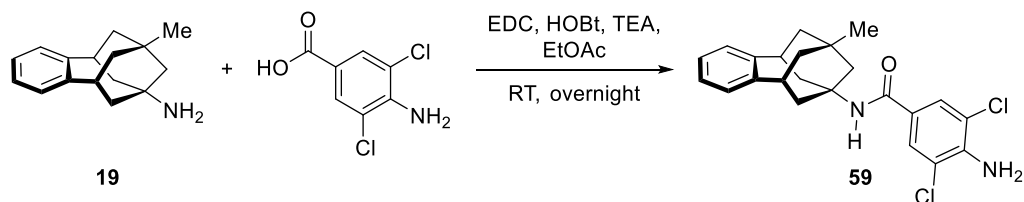
Calculated for C<sub>22</sub>H<sub>22</sub>Cl<sub>2</sub>N<sub>2</sub>O<sub>2</sub>: C 63.32% H 5.31% N 6.71%



Found:

C 63.32% H 5.35% N 6.52%

**Preparation of 4-amino-3,5-dichloro-*N*-(9-methyl-6,7,8,9,10,11-hexahydro-5*H*-9,7,11-dimethanobenzo[9]annulen-7-yl)benzamide, 59**



4-Amino-3,5-dichlorobenzoic acid (165 mg, 0.80 mmol), 1-hydroxybenzotriazole (HOBt) (162 mg, 1.2 mmol), 1-ethyl-3-(3-dimethylaminopropyl)carbodiimide (EDC) (186 mg, 1.2 mmol) and triethylamine (0.25 mL, 1.76 mmol) were added to a solution of amine **19** (200 mg, 0.88 mmol) in ethylacetate (10 mL) and DMF (1 mL) and the reaction mixture was stirred at room temperature for 22 hours. To the resulting suspension was then added water (20 mL) and the phases were separated. The organic phase was washed with 5% aqueous NaHCO<sub>3</sub> solution (15 mL) and brine (15 mL), dried over anh. Na<sub>2</sub>SO<sub>4</sub> and filtered. Evaporation in *vacuo* of the combined organic phases gave an orange solid (320 mg). Column chromatography (Al<sub>2</sub>O<sub>3</sub>, 100% DCM) gave **59** (176.7 mg, 53% yield) as a white solid. The analytical sample was obtained washing the solid with *n*-pentane.

Analytical and spectroscopic data of compound **59**:

Melting point: 173 – 175 °C.

IR (ATR)  $\nu$ : 3460, 3352, 2920, 2852, 1627, 1610, 1532, 1484, 1452, 1322, 1306, 1270, 1232, 1126, 1091, 1049, 1006, 947, 908, 880, 837, 789, 757, 720, 695, 663, 581 cm<sup>-1</sup>.

<sup>1</sup>H-NMR (500 MHz, CDCl<sub>3</sub>)  $\delta$ : 0.95 (s, 3 H, C9-CH<sub>3</sub>), 1.58 [dt,  $J = 13.5$  Hz,  $J' = 1.5$  Hz, 2 H, 10(13)-H<sub>b</sub>], 1.69 [ddm,  $J = 13.5$  Hz,  $J' = 6.5$  Hz, 2 H, 10(13)-H<sub>a</sub>], 1.93 (s, 2 H, 8-H), 2.15 [dt,  $J = 13.0$  Hz,  $J' = 1.5$  Hz, 2 H, 6(12)-H<sub>b</sub>], 2.25 [ddm,  $J = 13.0$  Hz,  $J' = 6.5$  Hz, 2 H, 6(12)-H<sub>a</sub>], 3.11 [tt,  $J = 6.5$  Hz,  $J' = 1.5$  Hz, 2 H, 5(11)-H], 4.71 (broad s, 2 H, NH<sub>2</sub>), 5.68 (broad s, 1 H, NH), 7.04-7.11 [complex signal, 4 H, 1(4)-H, 2(3)-H], 7.54 [s, 2 H, 16(20)].

<sup>13</sup>C-NMR (125.7 MHz, CDCl<sub>3</sub>)  $\delta$ : 32.2 (CH<sub>3</sub>, C9-CH<sub>3</sub>), 33.7 (C, C9), 39.1 [CH<sub>2</sub>, C6(12)], 41.0 [CH, C5(11)], 41.1 [CH<sub>2</sub>, C10(13)], 47.3 (CH<sub>2</sub>, C8), 55.0 (C, C7), 118.8 [C, C17(19)], 125.7 (C, C15), 126.3 [CH, C2(3)], 126.6 [CH, C16(20)], 128.0 [CH, C1(4)], 142.4 (C, C18), 146.1 [d, C, C4a(C11a)], 164.1 (C, CO).

MS (EI),  $m/z$  (%); significant ions: 416 (25), 415 (11), 414 (M<sup>+</sup>, 38), 211 (20), 210 (100), 195 (26), 190 (48), 188 (74), 182 (19), 181 (19), 160 (12), 156 (14), 155 (78), 154 (30), 143 (13), 142 (14), 141 (18), 129 (18), 128 (19), 124 (15), 115 (14).

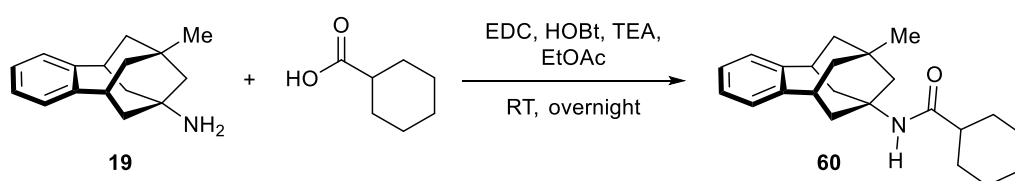
Elemental analysis:

Calculated for  $C_{23}H_{24}Cl_2N_2O_2$ : C 66.51% H 5.82% N 6.74%

Calculated for  $C_{23}H_{24}Cl_2N_2O_2 \cdot 0.1C_5H_{12}$ : C 66.79% H 6.01% N 6.63%

Found: C 66.82% H 6.04% N 6.54%

Preparation of *N*-(9-methyl-6,7,8,9,10,11-hexahydro-5*H*-9,7,11-dimethanobenzo[9]annulen-7-yl)cyclohexanecarboxamide, **60**



Cyclohexanecarboxylic acid (104.9 mg, 0.82 mmol), HOBT (166.1 mg, 1.23 mmol), EDC (190.5 mg, 1.23 mmol) and triethylamine (0.251 mL, 1.80 mmol) were added to a solution of amine **19** (204.8 mg, 0.90 mmol) in EtOAc (15 mL) and the reaction mixture was stirred at room temperature overnight. To the resulting suspension was then added water (15 mL) and the phases were separated. The organic phase was washed with saturated aqueous  $NaHCO_3$  solution (15 mL) and brine (15 mL), dried over anhydrous  $Na_2SO_4$  and filtered. Evaporation in *vacuo* of the combined organic layers gave **60** (265 mg, 96% yield) as a white solid. The analytical sample was obtained by crystallization with EtOAc/pentane.

Analytical and spectroscopic data of compound **60**:

Melting point: 197-198 °C.

IR (ATR)  $\nu$ : 3299, 3060, 2917, 2850, 1645, 1545, 1490, 1447, 1381, 1361, 1335, 1316, 1261, 1214, 1091, 1047, 1005, 960, 942, 894, 753, 675, 665  $cm^{-1}$ .

$^1H$ -NMR (500 MHz,  $CDCl_3$ )  $\delta$ : 0.91 (s, 3 H, 14-H), 1.15-1.27 [complex signal, 4 H, 18-H, 17(19)- $H_a$ ], 1.37 [m, 2 H, 16(20)- $H_a$ ], 1.53 [broad d,  $J = 13.5$  Hz, 2 H, 10(13)- $H_b$ ], 1.65 [m, 2 H, 10(13)- $H_a$ ], 1.72-1.83 [m, complex signal, 4 H, 16(20)- $H_b$ , 17(19)- $H_b$ ], 1.85 (s, 2 H, 8-H), 1.93 (tt,  $J = 11.5$  Hz,  $J' = 3.5$  Hz, 1 H, 15-H), 1.97 [dt,  $J = 13$  Hz,  $J' = 1.5$  Hz, 2 H, 6(12)- $H_b$ ], 2.16 [ddm,  $J = 13.0$  Hz,  $J' = 6.5$  Hz, 2 H, 6(12)- $H_a$ ], 3.06 [tt,  $J = 6.5$  Hz,  $J' = 1.5$  Hz, 2 H, 5(11)-H], 5.14 (broad s, 1 H, NH), 7.02-7.08 [complex signal, 4 H, Ar-H].

$^{13}C$ -NMR (125.7 MHz,  $CDCl_3$ )  $\delta$ : 25.7 [ $CH_2$ , C17(19)], 25.8 ( $CH_2$ , C18), 29.8 [ $CH_2$ , C16(20)], 32.2 ( $CH_3$ , C14), 33.6 (C, C9), 39.1 [ $CH_2$ , C6(12)], 41.0 [CH, C5(11)], 41.1 [ $CH_2$ , C10(13)], 46.4 (CH, C16), 47.2 ( $CH_2$ , C8), 54.0 (C, C7), 126.2 [CH, C2(3)], 127.9 [CH, C1(4)], 146.2 [d, C, C4a(C11a)], 175.3 (C, CO).

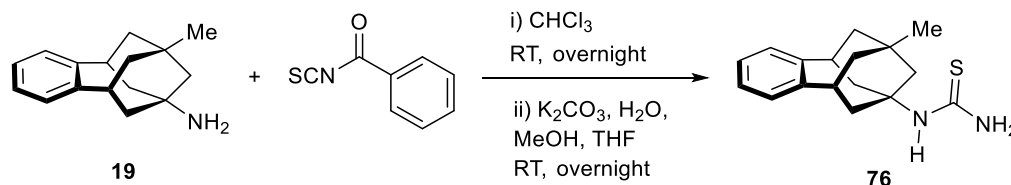
MS (EI),  $m/z$  (%); significant ions: 338 (18), 337 ( $M^+$ , 68), 282 (49), 212 (22), 211 (92), 210 (61), 169 (18), 156 (19), 155 (100), 154 (20), 143 (34), 141 (30), 129 (27), 128 (23), 83 (17), 55 (22).

Elemental analysis:

Calculated for  $C_{23}H_{31}NO$ : C 81.85% H 9.26% N 4.15%

Found: C 81.82% H 9.34% N 4.14%

**Preparation of *N*-(9-methyl-6,7,8,9,10,11-hexahydro-5*H*-5,9:7,11-dimethanobenzo[9]annulen-7-yl)thiourea, **76****



- a) *N*-[(9-methyl-6,7,8,9,10,11-hexahydro-5,9:7,11-dimethano-5*H*-benzocyclononen-7-yl)carbamothioyl]benzamide formation:

Benzoyl isothiocyanate (0.327 mL, 2.43 mmol) was added to a solution of amine **19** (500 mg, 2.21 mmol) in  $CHCl_3$  (20 mL) and the reaction mixture was stirred at room temperature overnight. The resulting solution was concentrated in *vacuo* to give a brown gum (1.11 g).

- b) *N*-[(9-methyl-6,7,8,9,10,11-hexahydro-5,9:7,11-dimethano-5*H*-benzocyclononen-7-yl)thiourea formation:

$K_2CO_3$  (1.97 g, 14.26 mmol) and water (10 mL) were added to a solution of the aforementioned benzamide (1.11 g, approx. 2.85 mmol) in methanol (22 mL) and THF (10 mL), and the mixture was stirred at room temperature overnight. The resulting suspension was filtered and the solids were washed with methanol (15 mL) to give **76** (330.3 mg, 52% overall yield) as a white solid.

Analytical and spectroscopic data of compound **76**:

Melting point: 197-199 °C.

IR (ATR)  $\nu$ : 3481, 3209, 3135, 3097, 3012, 2916, 2840, 1618, 1529, 1491, 1450, 1359, 1302, 1238, 1209, 1134, 1090, 1048, 1022, 941, 815, 799, 758, 719, 708, 643, 611  $cm^{-1}$ .

$^1H$ -RMN (400 MHz,  $DMSO-d_6$ )  $\delta$ : 0.88 (s, 3 H, 14-H), 1.36 [broad d,  $J = 13.0$  Hz, 2 H, 10(13)- $H_b$ ], 1.61 [ddd,  $J = 13.0$  Hz,  $J' = 6.0$  Hz,  $J'' = 1.2$  Hz, 2 H, 10(13)- $H_a$ ], 1.77 (s, 2 H, 8-

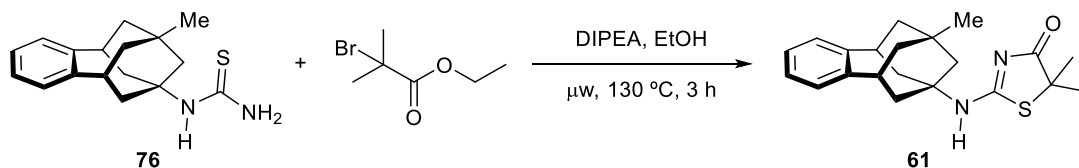
H<sub>2</sub>), 2.06 [ddd,  $J = 12.0$  Hz,  $J' = 5.6$  Hz,  $J'' = 2.0$  Hz, 2 H, 6(12)-H<sub>a</sub>], 3.04 [m, 2 H, 5(11)-H], 6.76 (broad s, 2 H, NH<sub>2</sub>), 7.02-7.09 (complex signal, 4 H, Ar-H), 7.31 (broad s, 1 H, NH).

<sup>13</sup>C-RMN (100.6 MHz, DMSO-d<sub>6</sub>)  $\delta$ : 32.1 (CH<sub>3</sub>, C14), 33.2 [CH<sub>2</sub>, C10(13)], 38.2 [CH, C5(11)], 41.0 [CH<sub>2</sub>, C6(12)], 47.5 (CH<sub>2</sub>, C8), 50.1 (C, C7), 55.0 (C, C9), 126.1 [CH, C2(3)], 127.7 [CH, C1(4)], 146.2 [d, C, C4a(C11a)], 181.2 (C, CS).

MS-DIP (EI),  $m/z$  (%); significant ions: 287 (15), 286 (M<sup>+</sup>, 66), 285 (66), 212 (10), 211 [(C<sub>16</sub>H<sub>19</sub>)<sup>+</sup>, 50], 210 (14), 169 (15), 156 (17), 155 (100), 154 (12), 153 (12), 143 (37), 141 (33), 129 (29), 128 (24), 117 (11), 115 (24).

HRMS-ESI<sup>+</sup>  $m/z$  [M+H]<sup>+</sup> calcd for [C<sub>17</sub>H<sub>22</sub>N<sub>2</sub>S+H<sup>+</sup>]: 287.1576, found: 287.1578.

**Preparation of 5,5-dimethyl-2-[(9-methyl-6,7,8,9,10,11-hexahydro-5*H*-9,9:7,11-dimethanobenzo[9]annulen-7-yl)amino]thiazol-4(5*H*)-one, 61**



Thiourea **76** (300 mg, 1.05 mmol), ethyl 2-bromoisobutyrate (0.29 mL, 1.95 mmol), DIPEA (0.36 mL) and abs. ethanol (3.5 mL) were placed into a microwave vial. The white suspension was heated to 130 °C, 250 psi and 250 W for 3 hours. The solvents were then removed under *vacuo* and the resulting solid was partitioned between DCM (10 mL) and 0.5 N HCl solution (10 mL) and the phases were separated. The aqueous phase was extracted with further DCM (3 x 10 mL), and the combined organic phases were dried over anh. Na<sub>2</sub>SO<sub>4</sub> and filtered. Evaporation in *vacuo* of the combined organic layers gave a white solid (315 mg). Column chromatography (Al<sub>2</sub>O<sub>3</sub>, DCM/methanol mixtures) gave **61** (47 mg, 13% yield) as a white solid. The analytical sample was obtained washing the solid with pentane.

Analytical and spectroscopic data of compound **61**:

Melting point: 294 – 299 °C.

IR (ATR)  $\nu$ : 3223, 2906, 1673, 1586, 1540, 1505, 1458, 1376, 1361, 1293, 1281, 1255, 1235, 1182, 1128, 1091, 1033, 1005, 951, 756, 651, 633, 602, 534 cm<sup>-1</sup>.

<sup>1</sup>H-NMR (500 MHz, CDCl<sub>3</sub>)  $\delta$ : 0.93 (s, 3 H, C-CH<sub>3</sub>), 1.53 [d,  $J = 13.5$  Hz, 2 H, 10(13)-H<sub>b</sub>], 1.62 [s, 6 H, C(CH<sub>3</sub>)<sub>2</sub>], 1.67 [ddm,  $J = 12.5$  Hz,  $J' = 6.5$  Hz, 2 H, 10(13)-H<sub>a</sub>], 1.95 (s, 2 H, 8-H), 2.17 [d,  $J = 12.5$  Hz, 2 H, 6(12)-H<sub>b</sub>], 2.29 [dd,  $J = 12.5$  Hz,  $J' = 6.5$  Hz, 2 H, 6(12)-H<sub>a</sub>],

3.09 [t,  $J = 6.5$  Hz, 2 H, 5(11)-H], 5.75 (broad s, 1 H, NH), 7.04 [m, H, 1(4)-H], 7.08 [m, H, 2(3)-H].

$^{13}\text{C}$ -NMR (125.7 MHz,  $\text{CDCl}_3$ )  $\delta$ : 27.9 [ $\text{CH}_3$ ,  $\text{C}(\underline{\text{C}}\text{H}_3)_2$ ], 32.0 ( $\text{CH}_3$ ,  $\text{C}-\underline{\text{C}}\text{H}_3$ ), 33.9 (C, C9), 38.9 [ $\text{CH}_2$ , C6(12)], 40.8 [ $\text{CH}_2$ , C10(13)], 40.9 [CH, C5(11)], 47.1 ( $\text{CH}_2$ , C8), 59.4 (C, C7), 61.0 [C,  $\underline{\text{C}}(\text{CH}_3)_2$ ], 126.5 [CH, C2(3)], 128.0 [CH, C1(4)], 145.7 [d, C, C4a(C11a)], 176.2 (C, CN), 193.8 (C, CO).

MS (EI),  $m/z$  (%); significant ions: 355 (24), 354 ( $\text{M}^+$ , 100), 285 (34), 211 [ $(\text{C}_{16}\text{H}_{19})^+$ , 35], 210 (11), 169 (14), 156 (15), 155 (100), 154 (10), 143 (35), 141 (29), 129 (27), 128 (21), 117 (11), 115 (18).

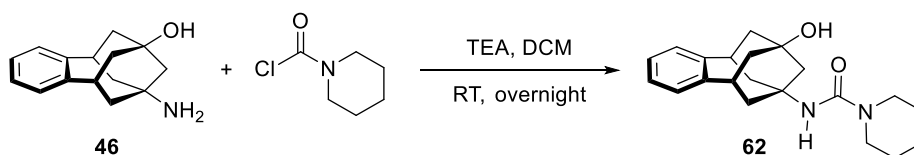
Elemental analysis:

Calculated for  $\text{C}_{21}\text{H}_{26}\text{N}_2\text{OS}$ : C 71.15% H 7.39% N 7.90% S 9.04%

Calculated for  $\text{C}_{21}\text{H}_{26}\text{N}_2\text{OS}\cdot 0.75\text{CH}_3\text{OH}\cdot 0.1\text{DCM}$ : C 67.81% H 7.60% N 7.24% S 8.28%

Found: C 67.98% H 7.22% N 7.29% S 7.88%

#### Preparation of *N*(9-hydroxy-6,7,8,9,10,11-hexahydro-5*H*5,9:7,11-dimethanobenzo[9]annulen-7-yl)piperidine-1-carboxamide, **62**



1-Piperidinecarbonyl chloride (0.162 mL, 1.30 mmol) and triethylamine (0.328 mL, 2.36 mmol) were added to a solution of amine **46** (270 mg, 1.18 mmol) in DCM (10 mL) and the reaction mixture was stirred at room temperature overnight. Saturated aqueous  $\text{NaHCO}_3$  solution (15 mL) was added and the phases were separated. The aqueous phase was extracted with further DCM (2 x 15 mL), and the combined organic phases were dried over anhydrous  $\text{Na}_2\text{SO}_4$ , filtered and concentrated *in vacuo* to give a yellow solid (472 mg). Column chromatography ( $\text{Al}_2\text{O}_3$ , DCM/methanol mixtures) gave **62** (288 mg, 64% overall yield) as a white solid, that was washed with pentane for obtaining an analytical sample.

Analytical and spectroscopic data of compound **62**:

Melting point: 188 – 190 °C.

IR (ATR)  $\nu$ : 3419, 2934, 2899, 2852, 1635, 1502, 1444, 1414, 1375, 1356, 1334, 1291, 1249, 1201, 1161, 1148, 1111, 1067, 1028, 992, 969, 907, 848, 762, 728, 625, 570, 544  $\text{cm}^{-1}$ .

$^1\text{H}$ -RMN (500 MHz,  $\text{CDCl}_3$ )  $\delta$ : 1.48-1.59 [complex signal, 6 H, 16(18)- $\text{H}_2$ , 17- $\text{H}_2$ ], 1.76 [d, J

= 13.0 Hz, 2 H, 10(13)-H<sub>b</sub>], 1.90-2.02 [complex signal, 4 H, 6(12)-H<sub>b</sub>, 10(13)-H<sub>a</sub>], 2.09 (s, 2 H, 8-H<sub>2</sub>), 2.17 [ddd, J = 13.0 Hz, J' = 6.5 Hz, J'' = 1.5 Hz, 2 H, 6(12)-H<sub>a</sub>], 3.16 [tt, J = 6.5 Hz, J' = 1.5 Hz, 2 H, 5(11)-H], 3.23 [m, 4 H, 15(19)-H<sub>2</sub>], 7.05 [m, 2 H, 1(4)-H], 7.09 [m, 2 H, 3(2)-H].

<sup>13</sup>C-RMN (125.7 MHz, CDCl<sub>3</sub>) δ: 24.3 (CH<sub>2</sub>, C17), 25.5 [CH<sub>2</sub>, C16(18)], 39.4 [CH<sub>2</sub>, C6(12)], 40.1 [CH, C5(11)], 42.4 [CH<sub>2</sub>, C10(13)], 44.9 [CH<sub>2</sub>, C15(19)], 49.1 (CH<sub>2</sub>, C8), 56.3 (C, C7), 71.0 (C, C9), 126.5 [CH, C2(3)], 128.0 [CH, C1(4)], 145.4 [d, C, C4a(C11a)], 156.4 (C, CO).

MS-DIP (EI), *m/z* (%); significant ions: 341 (11), 340 (M<sup>+</sup>, 48), 255 (41), 212 (9), 157 (13), 155 (22), 144 (13), 141 (13), 129 (35), 128 (33), 127 (43), 115 (21), 112 (20), 86 (19), 85 (70), 84 (100), 69 (20), 57 (10), 56 (14).

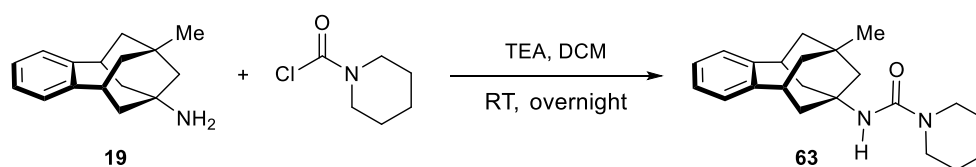
Elemental analysis:

Calculated for C<sub>21</sub>H<sub>28</sub>N<sub>2</sub>O<sub>2</sub>: C 74.08% H 8.29% N 8.23%

Calculated for C<sub>21</sub>H<sub>28</sub>N<sub>2</sub>O<sub>2</sub>·0.45CH<sub>3</sub>OH·0.2C<sub>3</sub>H<sub>12</sub>: C 73.01% H 8.79% N 7.59%

Found: C 73.17% H 8.43% N 7.23%

Preparation of *N*(9-methyl-6,7,8,9,10,11-hexahydro-5*H*-5,9:7,11-dimethanobenzo[9]annulen-7-yl)piperidine-1-carboxamide, **63**



1-Piperidinecarbonyl chloride (0.247 mL, 1.98 mmol) and triethylamine (0.367 mL, 2.64 mmol) were added to a solution of amine **19** (300 mg, 1.32 mmol) in DCM (15 mL). The reaction mixture was stirred at room temperature overnight. To the resulting mixture was added saturated aqueous NaHCO<sub>3</sub> solution (15 mL) and the phases were separated. The aqueous phase was extracted with further DCM (2 x 15 mL), and the combined organic phases were dried over anhydrous Na<sub>2</sub>SO<sub>4</sub>, filtered and concentrated *in vacuo* to give a yellow solid (419 mg). Column chromatography (Al<sub>2</sub>O<sub>3</sub>, DCM/methanol mixtures) gave **63** (265 mg, 59% yield) as a white solid. The analytical sample was obtained washing with pentane.

Analytical and spectroscopic data of compound **63**:

Melting point: 170 – 171 °C.

IR (ATR) *v*: 3361, 2914, 2850, 1617, 1525, 1479, 1439, 1404, 1360, 1343, 1275, 1261, 1228,

1211, 1168, 1022, 978, 949, 852, 758, 576  $\text{cm}^{-1}$ .

$^1\text{H}$ -RMN (500 MHz,  $\text{CDCl}_3$ )  $\delta$ : 0.91 (s, 3 H, C9- $\text{CH}_3$ ), 1.49-1.59 [complex signal, 8 H, 10(13)- $\text{H}_b$ , 16(18)- $\text{H}_2$ , 17- $\text{H}_2$ ], 1.65 [ddm,  $J = 13.5$  Hz,  $J' = 6.5$  Hz, 2 H, 10(13)- $\text{H}_a$ ], 1.84 (s, 2 H, 8-H), 2.00 [d,  $J = 13.0$  Hz, 2 H, 6(12)- $\text{H}_b$ ], 2.16 [ddm,  $J = 13.0$  Hz,  $J' = 6.5$  Hz, 2 H, 6(12)- $\text{H}_a$ ], 3.06 [tt,  $J = 6.5$  Hz,  $J' = 1.5$  Hz, 2 H, 5(11)-H], 3.22-3.25 [complex signal, 4 H, 15(19)-H], 4.25 (s, 1 H, NH), 7.03 [m, 2 H, 1(4)-H], 7.06 [m, 2 H, 3(2)-H].

$^{13}\text{C}$ -RMN (125.7 MHz,  $\text{CDCl}_3$ )  $\delta$ : 24.4 ( $\text{CH}_2$ , C17), 25.6 [ $\text{CH}_2$ , C16(18)], 32.3 ( $\text{CH}_3$ , C9- $\text{CH}_3$ ), 33.7 (C, C9), 39.8 [ $\text{CH}_2$ , C6(12)], 41.2 [ $\text{CH}$ , C5(11)], 41.3 [ $\text{CH}_2$ , C10(13)], 44.9 [ $\text{CH}_2$ , C15(19)], 48.0 ( $\text{CH}_2$ , C8), 53.6 (C, C7), 126.1 [ $\text{CH}$ , C2(3)], 127.9 [ $\text{CH}$ , C1(4)], 146.4 [d, C, C4a(C11a)], 156.6 (C, CO).

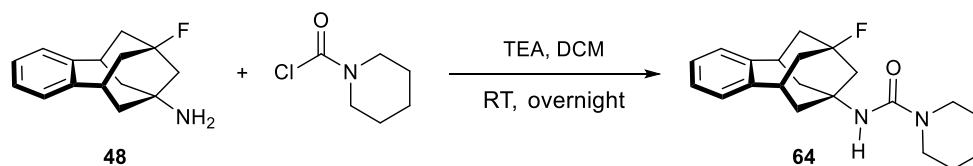
MS-DIP (EI),  $m/z$  (%); significant ions: 254 (18), 253 [(M-C<sub>5</sub>H<sub>11</sub>N)<sup>+</sup>, 100], 238 (25), 195 (10), 182 (14), 155 (32), 143 (13), 141 (15), 129 (17), 128 (15), 115 (15).

Elemental analysis:

Calculated for  $\text{C}_{22}\text{H}_{30}\text{N}_2\text{O}$ : C 78.06% H 8.93% N 8.28%

Found: C 78.05% H 9.11% N 8.06%

Preparation of *N*-(9-fluoro-5,6,8,9,10,11-hexahydro-7*H*-5,9:7,11-dimethanobenzo[9]annulen-7-yl)piperidine-1-carboxamide, **64**



1-Piperidinecarbonyl chloride (0.1 mL, 0.80 mmol) and triethylamine (0.213 mL, 1.54 mmol) were added to a solution of amine **48** (177.5 mg, 0.79 mmol) in DCM (9 mL) and the reaction mixture was stirred at room temperature overnight. To the resulting mixture was added saturated aqueous  $\text{NaHCO}_3$  solution (10 mL) and the phases were separated. The aqueous phase was extracted with further DCM (2 x 10 mL), and the combined organic phases were dried over anhydrous  $\text{Na}_2\text{SO}_4$ , filtered and concentrated in *vacuo* to give a yellow gum (246.3 mg). Column chromatography ( $\text{Al}_2\text{O}_3$ , DCM/methanol mixtures) gave **64** (68 mg, 26% yield) as a white solid. The analytical sample was obtained by crystallization with EtOAc/pentane.

Analytical and spectroscopic data of compound **64**:

Melting point: 178 – 179  $^\circ\text{C}$ .

IR (ATR)  $\nu$ : 3285, 2932, 2856, 1614, 1538, 1470, 1442, 1359, 1278, 1259, 1230, 1088, 1024, 1005, 968, 915, 865, 851, 804, 756, 648, 605, 570  $\text{cm}^{-1}$ .

$^1\text{H}$ -RMN (500 MHz,  $\text{CDCl}_3$ )  $\delta$ : 1.50-1.60 [complex signal, 6 H, 16(18)- $\text{H}_2$ , 17- $\text{H}_2$ ], 1.91 [d,  $J = 12.5$  Hz, 2 H, 10(13)- $\text{H}_b$ ], 2.03 [d,  $J = 13.5$  Hz, 2 H, 6(12)- $\text{H}_b$ ], 2.12-2.22 [complex signal, 4 H, 6(12)- $\text{H}_a$ , 10(13)- $\text{H}_a$ ], 2.25 (d,  $J_{\text{CF}} = 6.5$  Hz, 2 H, 8- $\text{H}_2$ ), 3.20-3.27 [complex signal, 6 H, 5(11)-H, 15(19)- $\text{H}_2$ ], 4.32 (s, 1 H, NH), 7.07 [m, 2 H, 1(4)-H], 7.11 [m, 2 H, 3(2)-H].

$^{13}\text{C}$ -RMN (125.7 MHz,  $\text{CDCl}_3$ )  $\delta$ : 24.4 ( $\text{CH}_2$ , C17), 25.6 [ $\text{CH}_2$ , C16(18)], 39.3 [ $\text{CH}_2$ , C6(12)], 39.6 [CH, d,  $^3J_{\text{CF}} = 13.3$  Hz, C5(11)], 40.1 [ $\text{CH}_2$ , d,  $^2J_{\text{CF}} = 20.1$  Hz, C10(13)], 44.9 [ $\text{CH}_2$ , C15(19)], 46.8 ( $\text{CH}_2$ , d,  $^2J_{\text{CF}} = 17.8$  Hz, C8), 51.1 (C, d,  $^3J_{\text{CF}} = 11.4$  Hz, C7), 95.4 (C, d,  $^1J_{\text{CF}} = 173.2$  Hz, C9), 126.8 [CH, C2(3)], 128.1 [CH, C1(4)], 144.9 [d, C, C4a(C11a)], 156.3 (C, CO).

MS (EI),  $m/z$  (%); significant ions: 258 (17), 257 [ $(\text{C}_{16}\text{H}_{16}\text{FNO})^+$ , 100], 215 (12), 170 (10), 159 (13), 155 (10), 141 (9), 129 (13), 128 (12), 115 (15).

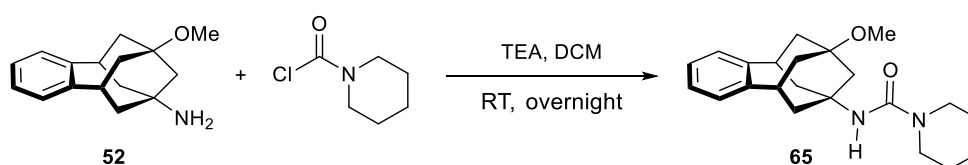
Elemental analysis:

Calculated for  $\text{C}_{21}\text{H}_{27}\text{FN}_2\text{O}$ : C 73.65% H 7.95% N 8.18%

Calculated for  $\text{C}_{21}\text{H}_{27}\text{FN}_2\text{O} \cdot 0.1\text{EtOAc}$ : C 73.17% H 7.98% N 7.97%

Found: C 73.35% H 8.06% N 7.93%

Preparation of *N*-(9-methoxy-5,6,8,9,10,11-hexahydro-7*H*-5,9:7,11-dimethanobenzo[9]annulen-7-yl)piperidine-1-carboxamide, **65**



1-Piperidinecarbonyl chloride (0.04 mL, 0.33 mmol) and triethylamine (0.09 mL, 0.62 mmol) were added to a solution of amine **52** (76 mg, 0.31 mmol) in DCM (3.5 mL) and the reaction mixture was stirred at room temperature overnight. To the resulting mixture was added saturated aqueous  $\text{NaHCO}_3$  solution (5 mL) and the phases were separated. The aqueous phase was extracted with further DCM (2 x 5 mL), and the combined organic phases were dried over anhydrous  $\text{Na}_2\text{SO}_4$ , filtered and concentrated *in vacuo* to give a yellow gum (201.4 mg). Column chromatography ( $\text{Al}_2\text{O}_3$ , DCM/methanol mixtures) gave **65** (42 mg, 38% yield) as a white solid.

Analytical and spectroscopic data of compound **65**:



Melting point: 172 – 173 °C.

IR (ATR)  $\nu$ : 3293, 2926, 2850, 2820, 1616, 1540, 1491, 1441, 1409, 1383, 1360, 1344, 1265, 1256, 1231, 1151, 1080, 1064, 1045, 1025, 994, 984, 969, 914, 848, 756, 638, 602  $\text{cm}^{-1}$ .

$^1\text{H}$ -RMN (500 MHz,  $\text{CDCl}_3$ )  $\delta$ : 1.47-1.57 [complex signal, 6 H, 16(18)- $\text{H}_2$ , 17- $\text{H}_2$ ], 1.43 [d,  $J$  = 13.0 Hz, 2 H, 10(13)- $\text{H}_b$ ], 1.96 [m, 2 H, 10(13)- $\text{H}_a$ ], 2.08 (s, 2 H, 8- $\text{H}_2$ ), 2.07 [d,  $J$  = 13.5 Hz, 2 H, 6(12)- $\text{H}_b$ ], 2.14 [m, 2 H, 6(12)- $\text{H}_a$ ], 3.18 [tt,  $J$  = 6.5 Hz,  $J'$  = 1.5 Hz, 2 H, 5(11)-H], 3.23-3.27 [complex signal, 7 H, 15(19)-H, C9-OCH $_3$ ], 4.31 (s, 1 H, NH), 7.05 [m, 2 H, 1(4)-H], 7.09 [m, 2 H, 3(2)-H].

$^{13}\text{C}$ -RMN (125.7 MHz,  $\text{CDCl}_3$ )  $\delta$ : 24.4 ( $\text{CH}_2$ , C17), 25.5 [ $\text{CH}_2$ , C16(18)], 38.3 [ $\text{CH}_2$ , C6(12)], 39.6 [ $\text{CH}_2$ , C10(13)], 39.9 [CH, C5(11)], 44.9 [ $\text{CH}_2$ , C15(19)], 45.4 ( $\text{CH}_2$ , C8), 48.2 ( $\text{CH}_3$ , OCH $_3$ ), 56.1 (C, C7), 74.8 (C, C9), 126.5 [CH, C2(3)], 128.0 [CH, C1(4)], 145.5 [d, C, C4a(C11a)], 156.5 (C, CO).

MS (EI),  $m/z$  (%); significant ions: 270 (18), 269 [( $\text{C}_{17}\text{H}_{19}\text{NO}_2$ ) $^+$ , 100], 238 (36), 226 (12), 195 (15), 182 (20), 171 (22), 159 (32), 158 (91), 155 (35), 153 (15), 150 (17), 141 (20), 129 (26), 128 (30), 127 (13), 115 (32).

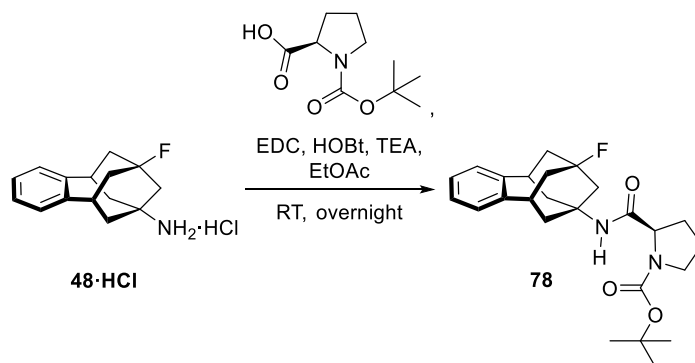
Elemental analysis:

Calculated for  $\text{C}_{22}\text{H}_{30}\text{N}_2\text{O}_2$ : C 74.54% H 8.53% N 7.90%

Calculated for  $\text{C}_{22}\text{H}_{30}\text{N}_2\text{O}_2 \cdot 0.1\text{CH}_3\text{OH}$ : C 74.21% H 8.57% N 7.83%

Found: C 74.11% H 8.54% N 7.67%

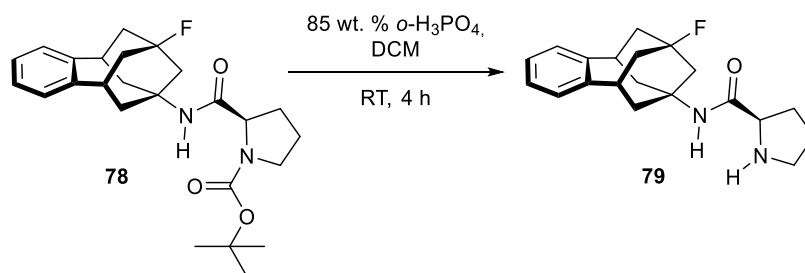
Preparation of (2*R*)-tert-butyl-2-[(9-fluoro-6,7,8,9,10,11-hexahydro-5*H*-9,9:7,11-dimethanobenzo[9]annulen-7-yl)carbamoyl]pyrrolidine-1-carboxylate, 78



Boc-D-proline (55 mg, 0.26 mmol), HOBT (52 mg, 0.38 mmol), EDC (59 mg, 0.38 mmol) and triethylamine (0.14 mL, 1.02 mmol) were added to a solution of amine 48·HCl (75 mg, 0.28 mmol) in EtOAc (4 mL) and the mixture was stirred at room temperature

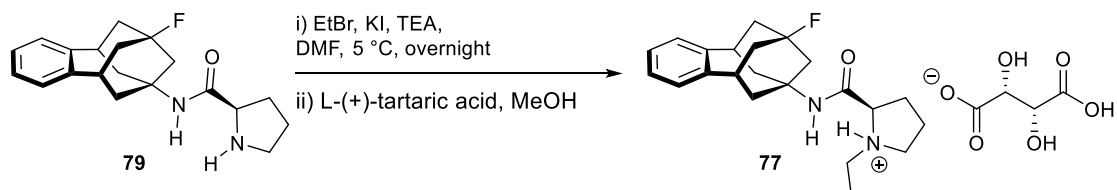
overnight. To the resulting suspension was then added water (5 mL) and the phases were separated. The organic phase was washed with saturated aqueous NaHCO<sub>3</sub> solution (5 mL) and brine (5 mL), dried over anh. Na<sub>2</sub>SO<sub>4</sub> and filtered. Evaporation in *vacuo* of the combined organic layers gave **78** (110 mg, 92% yield) as a beige solid. The product was used in next step without further purification or characterization.

**Preparation of (2*R*)-*N*-(9-fluoro-6,7,8,9,10,11-hexahydro-5*H*-5,9:7,11-dimethanobenzo[9]annulen-7-yl)pyrrolidine-2-carboxamide, **79****



A solution of Boc-protected pyrrolidine **78** (110 mg, 1.26 mmol) in DCM (2 mL) and 85% *o*-phosphoric acid (0.26 mL, 3.90 mmol) was stirred at room temperature for 4 hours. To the reaction mixture was then added water (5 mL) and the aqueous phase was basified until pH ~12 with 5 N NaOH solution. The phases were separated and the aqueous phase was extracted with further DCM (2 x 5 mL). The combined organic layers were dried over anh. Na<sub>2</sub>SO<sub>4</sub>, filtered and evaporated in *vacuo* to give **79** (82 mg, quantitative yield) as a maroon gum. The product was used in next step without further characterization or purification.

**Preparation of (2*R*)-1-ethyl-*N*-(9-fluoro-6,7,8,9,10,11-hexahydro-5*H*-5,9:7,11-dimethanobenzo[9]annulen-7-yl)pyrrolidine-2-carboxamide, **77**·tartrate**



A solution of pyrrolidine **79** (82 mg, 0.25 mmol) in DMF (1.5 mL) was cooled to 5 °C with an ice bath. Then KI (4 mg, 0.03 mmol) and triethylamine (0.14 mL, 1.00 mmol) were added, followed by the dropwise addition of a solution of ethyl bromide (29 mg, 0.26 mmol) in DMF (0.5 mL). The reaction mixture was stirred at room temperature in an ice-water bath overnight. To the resulting solution was added EtOAc (5 mL) and water (5 mL). The phases were separated and the aqueous layer was extracted with further EtOAc (2 x 5 mL). The combined organic phases were washed with saturated aqueous NaHCO<sub>3</sub> solution

(5 mL) and brine (5 mL), dried over anhydrous  $\text{Na}_2\text{SO}_4$ , filtered and concentrated in *vacuo* to give an orange oil (74 mg). Column chromatography ( $\text{SiO}_2$ , DCM/methanol mixtures) gave **77** (33 mg, 35% yield) as a white solid. A solution of L-(+)-tartaric acid (11 mg, 0.07 mmol) in methanol (1 mL) was added to **77** directly. The solvents were removed under *vacuo* to give **77** as its tartrate salt.

Analytical and spectroscopic data of compound **77**·tartrate:

Melting point: 94-96 °C.

IR (ATR)  $\nu$ : 3500-2800 (3432, 3381, 3285, 3063, 2923, 2856), 2553, 2363, 2182, 1962, 1721, 1667, 1563, 1441, 1395, 1358, 1341, 1301, 1235, 1118, 1074, 997, 863, 757, 663  $\text{cm}^{-1}$ .

$^1\text{H}$ -RMN (500 MHz,  $\text{CD}_3\text{OD}$ )  $\delta$ : 1.28 (t,  $J = 7.5$  Hz, 3 H,  $\text{NCH}_2\text{CH}_3$ ), 1.84 [d,  $J = 11.5$  Hz, 2 H, 10(13)- $\text{H}_b$ ], 1.99 (complex signal, 2 H, 16- $\text{H}_a$ , 17- $\text{H}_a$ ), 2.08 [d,  $J = 13$  Hz, 2 H, 6(12)- $\text{H}_b$ ], 2.16 [complex signal, 6 H, 6(12)- $\text{H}_a$ , 10(13)- $\text{H}_a$ , 17- $\text{H}_a$ ], 2.24 (d,  $J = 6.5$  Hz, 2 H, 8-H), 2.50 (m, 1 H, 16- $\text{H}_b$ ), 3.17 (complex signal, 3 H,  $\text{NCH}_2\text{CH}_3$ , 18- $\text{H}_a$ ), 3.27 [m, 2 H, 5(11)-H], 3.68 (m, 1 H, 18- $\text{H}_b$ ), 3.95 (dd,  $J = 8.5$  Hz,  $J' = 7$  Hz, 1 H, 15-H), 4.45 (s, 2 H, tartrate-CH), 7.11 [complex signal, 4 H, Ar-H].

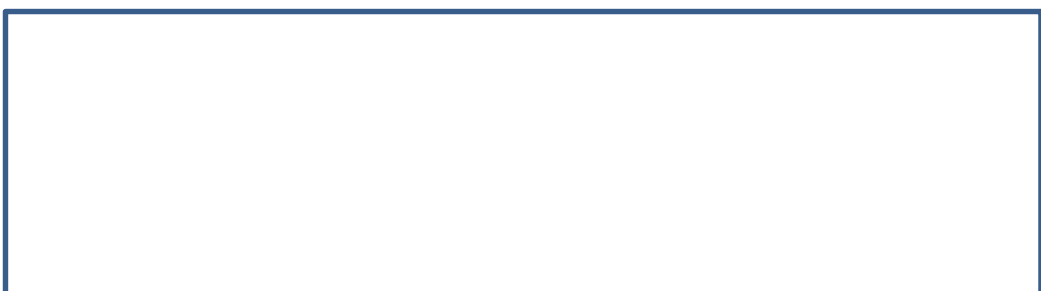
$^{13}\text{C}$ -RMN (125.7 MHz,  $\text{CD}_3\text{OD}$ )  $\delta$ : 11.4 ( $\text{CH}_3$ ,  $\text{NCH}_2\text{CH}_3$ ), 24.0 ( $\text{CH}_2$ , C17), 31.1 ( $\text{CH}_2$ , C16), 39.1 [ $\text{CH}_2$ , d,  $^4J_{\text{CF}} = 7.4$  Hz, C6(12)], 40.9 [CH, d,  $^3J_{\text{CF}} = 12.9$  Hz, C5(11)], 41.2 [ $\text{CH}_2$ , d,  $^2J_{\text{CF}} = 20.1$  Hz, C10(13)], 46.6 ( $\text{CH}_2$ , d,  $^2J_{\text{CF}} = 18.9$  Hz, C8), 51.4 ( $\text{CH}_2$ ,  $\text{NCH}_2\text{CH}_3$ ), 55.6 ( $\text{CH}_2$ , C18), 59.3 (C, d,  $^3J_{\text{CF}} = 11.2$  Hz, C7), 68.6 (CH, C15), 73.8 (CH, tartrate-CH), 94.6 (C, d,  $^1J_{\text{CF}} = 177.6$  Hz, C9), 128.1 [CH, C2(3)], 129.2 [CH, C1(4)], 146.1 [C, C4a(C11a)], 168.4 (C, CO), 176.9 (C, tartrate-CO).

MS (DEPEI),  $m/z$  (%); significant ions: 99 (27), 98 (100), 97 (26), 96 (11), 76 (13), 71 (10), 70 (34), 69 (14), 68 (11).

HRMS-ESI+  $m/z$  [ $\text{M}+\text{H}$ ] $^+$  calcd for  $[\text{C}_{22}\text{H}_{29}\text{FN}_2\text{O}+\text{H}^+]$ : 357.2337, found: 357.2338.

**scaffolds**



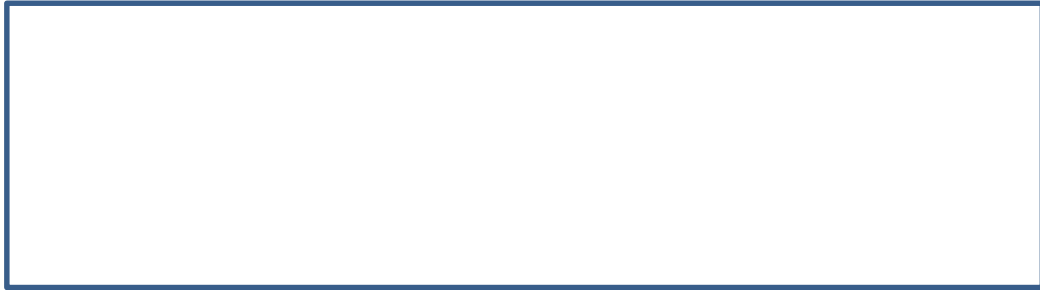


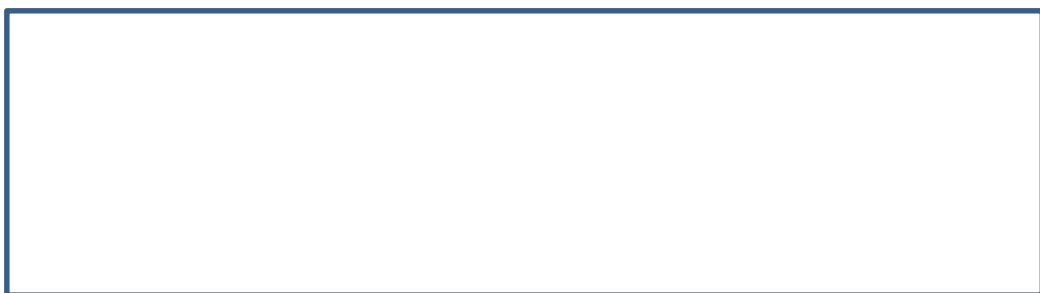




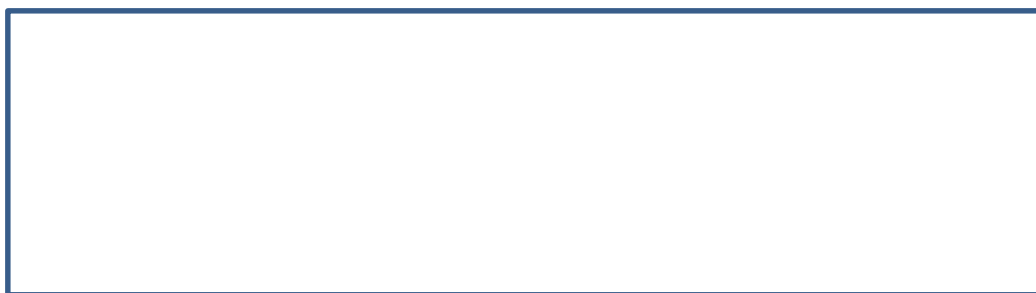




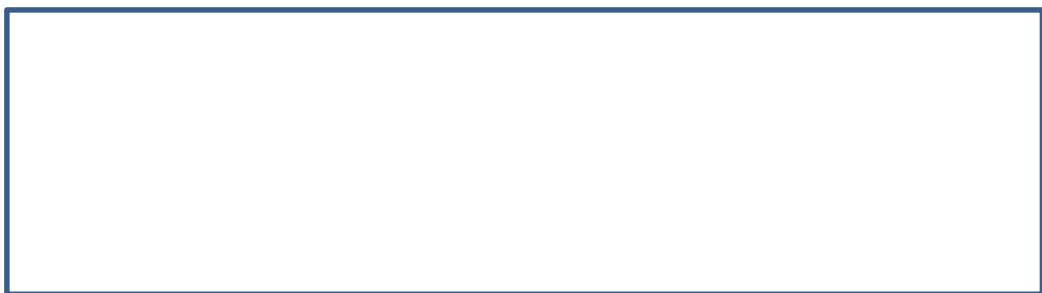


















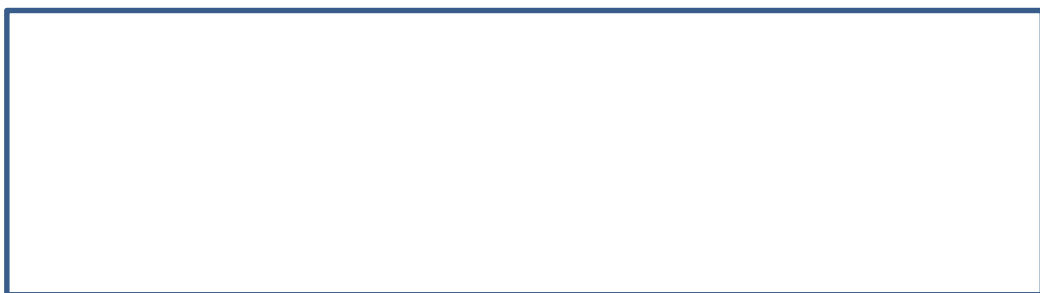
## **Chapter 3**



**Chemistry**

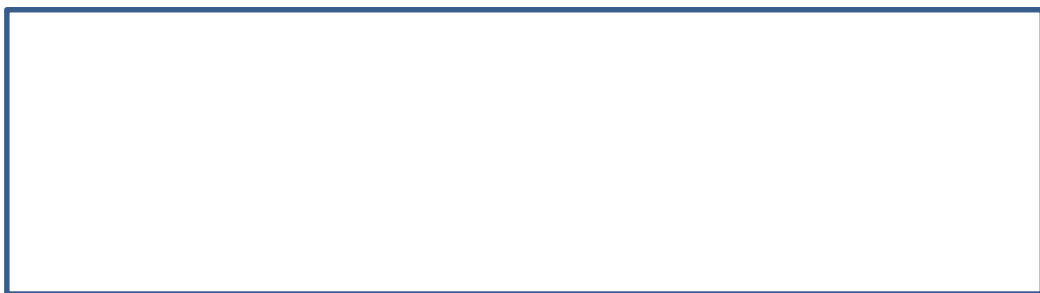






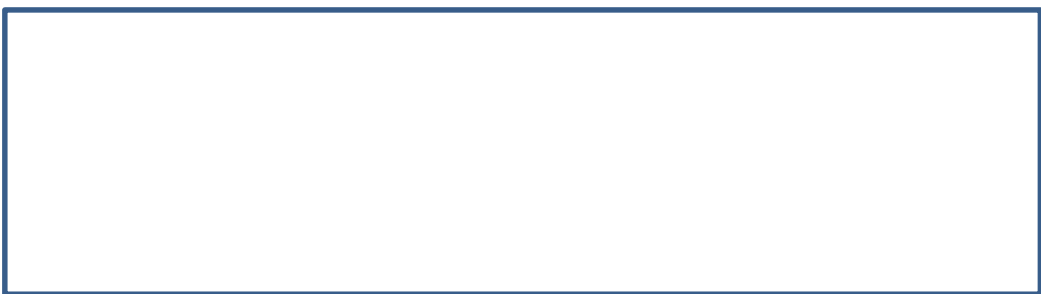


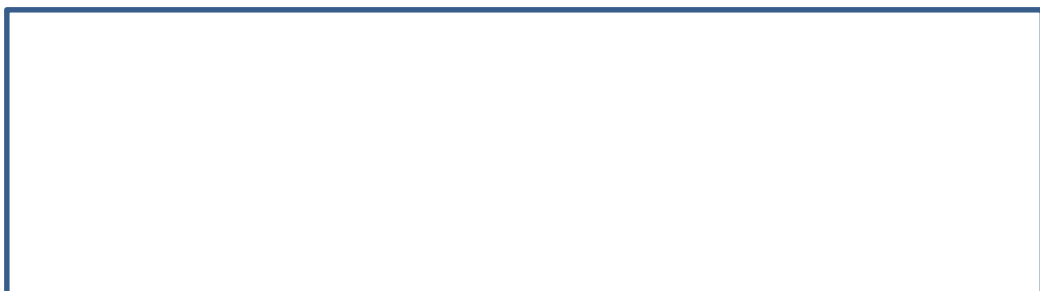


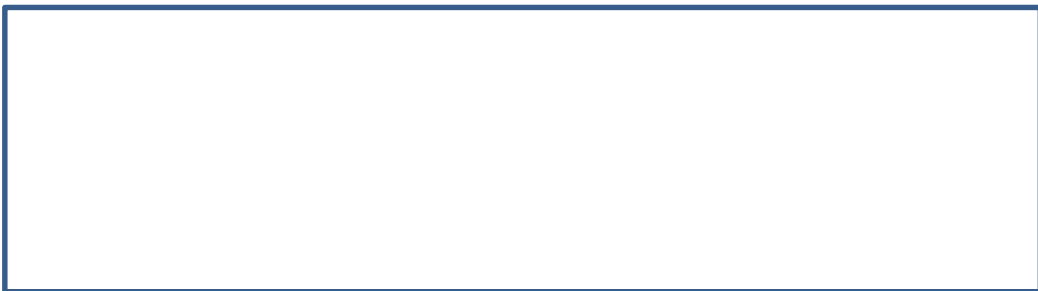


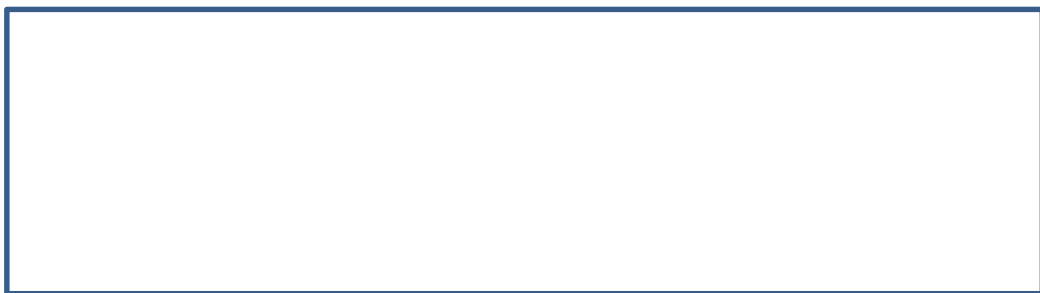


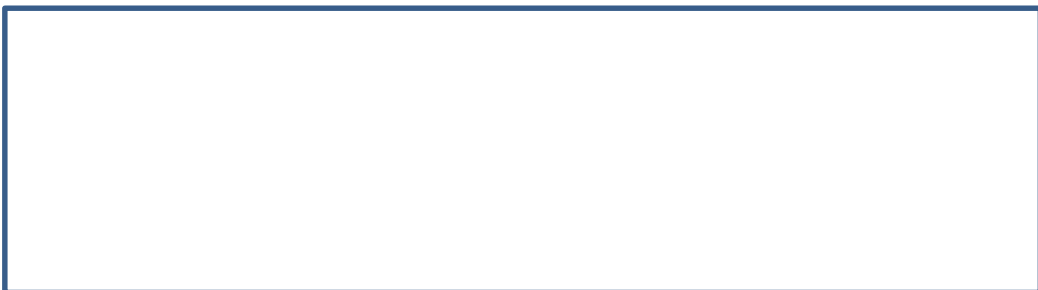




















































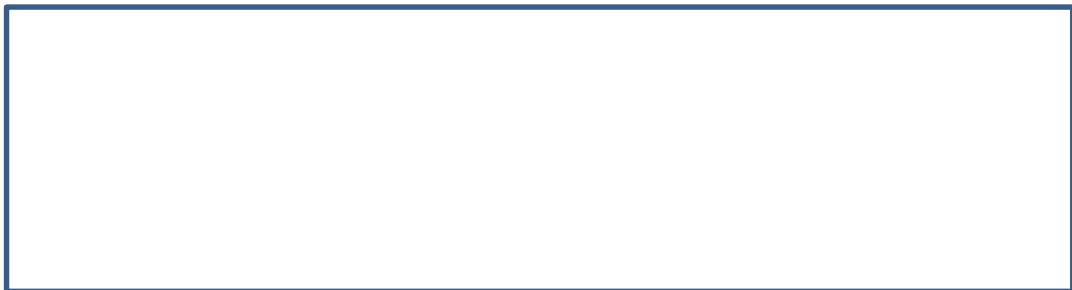
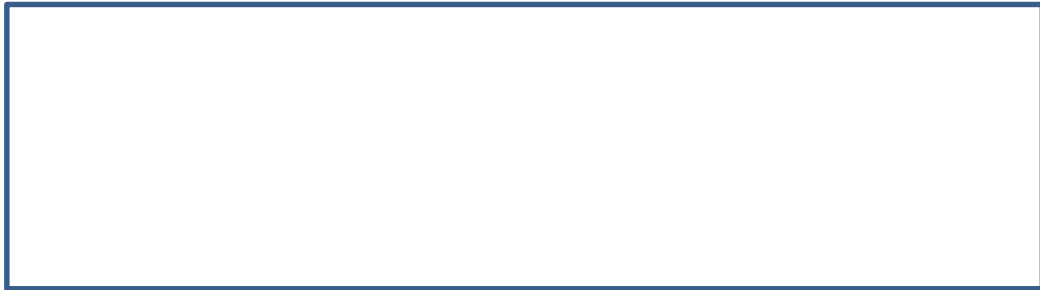


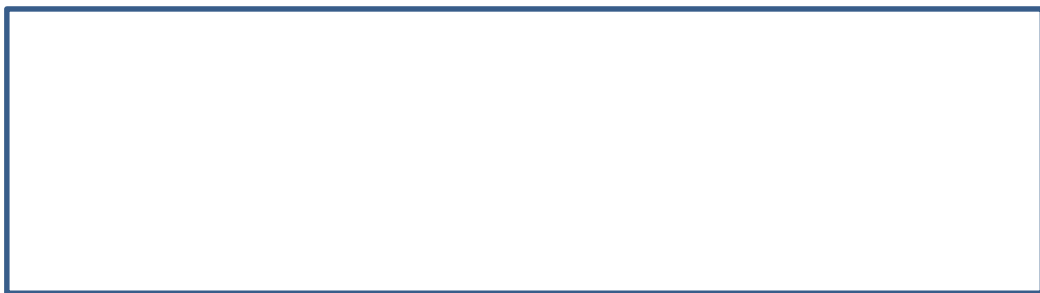












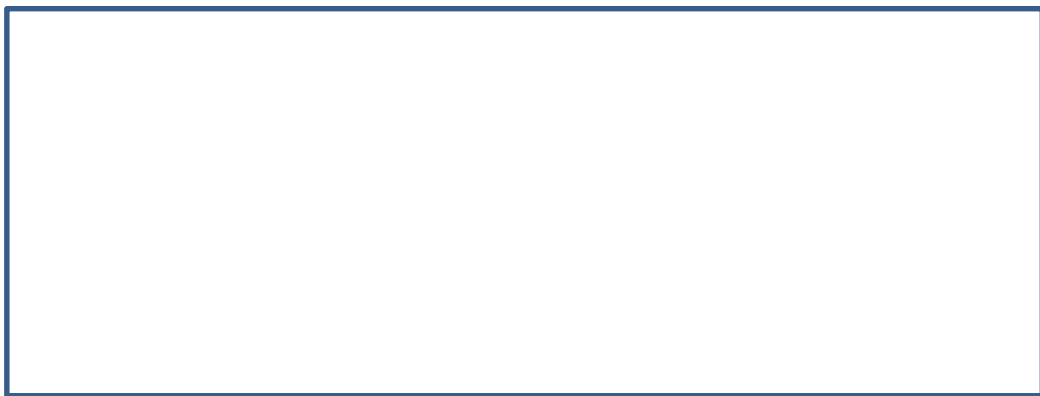






















# **IC<sub>50</sub> determination**



### IC<sub>50</sub> assay determination

a) *Buffer preparation:*

The buffer utilized was *bis*-tris with an ionic strength of 25 mM, supplemented with 0.1 mg BSA fraction V per mL of buffer and prepared with water filtered through a MilliQ reagent water system (Millipore Corp., Bedford, MA, USA). The pH was adjusted to 7.0 with 1 N HCl solution.

b) *Substrate preparation:*

(3-Phenyl-oxiranyl)-acetic acid cyano-(6-methoxy-naphthalen-2-yl)-methyl ester (PHOME, Cayman Chemical, item number 10009134) was employed as a fluorescent substrate at a final concentration of 5  $\mu$ M. As the total volume of the assay is 200  $\mu$ L in all the wells, a 200  $\mu$ M-solution of PHOME in DMSO was prepared *prior* to the assay performance.

c) *Enzyme dilution:*

Beforehand to assaying, human recombinant sEH, purchased by Cayman Chemical, was diluted with cold assay buffer (588  $\mu$ L) and kept on ice during the assay, no longer than 4 hours.

d) *Preparation of inhibitors:*

Each compound was dissolved in DMSO so as to prepare an 800  $\mu$ M-stock solution. Serial dilutions in DMSO were followed in order to have a range of concentrations for the compound testing (from 0.05 to 20 nM). In that the final concentration of the assay is 40x diluted, the compounds were prepared 40 times more concentrated (from 2 to 800 nM). Five different concentrations were used for each compound.

e) *Assay performance:*

For every determination, the 96-well black microplate (Greiner Bio-one, item n° 655900) was designed so to have at least a duplicate of the background and a triplicate of each concentration of inhibitor, as well as a triplicate of 100% activity.

Table 25 discloses the pipetting summary for performing the assay.

**Table 25.** Reagents of the inhibitory assay and addition order.

Well	Assay Buffer	Solvent (DMSO)	Inhibitor	sEH	Assay Buffer + Substrate
Background	90 $\mu$ L	5 $\mu$ L	-	-	100 $\mu$ L + 5 $\mu$ L
Positive control	85 $\mu$ L	5 $\mu$ L	-	5 $\mu$ L	100 $\mu$ L + 5 $\mu$ L
Inhibitor	85 $\mu$ L	-	5 $\mu$ L	5 $\mu$ L	100 $\mu$ L + 5 $\mu$ L
Addition order	1	2	3	4	5

As shown in Table 25, a pre-mixture of the assay buffer and the substrate was prepared for its final addition with a multichannel pipette.

After the addition of the substrate, the microplate was carefully shaken for 10 seconds and incubated for 5 minutes at room temperature. Enzyme activity was measured by means of the fluorescence appearance of the hydrolysed product 6-methoxy-2-naphthaldehyde over 10 min with a FLUOstar OPTIMA microplate reader (BMG) (excitation wavelength: 337 nm; emission wavelength: 460 nm).

f) *Pharmacological results:*

Results were obtained by regression analysis from at least three data points in a linear region of the curve.  $IC_{50}$  values are average of minimum three independent replicates. Results are given as means  $\pm$  standard error.

# **Water solubility**



### Apparent or semi-equilibrium solubility measurements

#### a) Calibration curve of a standard, 109.

Compound 109 was used as a standard for calculating the linear regression of concentration *vs* area. In this manner, the calibration curve was obtained from six standard stock solutions with UV detection at 225 and 254 nm ( $r = 0.99$ ) (Table 26).

**Table 26.** Area values for six standard stock solutions at 225 and 254 nm.

Concentration		Area	
$\mu\text{g/mL}$	$\mu\text{mol/mL}$	225 nm	254 nm
100	0.3042	6056764	965689
50	0.1521	2966801	560875
10	0.0304	503418	125001
5	0.0152	200315	70518
1	0.0030	34244	10530
0,1	0.0003	30309	3147

The measurement was performed by HPLC (Waters), with an Akady ODS-C18 column (250 mm x 4.6 mm, 5  $\mu\text{m}$ ) at room temperature. Ten microliters of the samples were injected into the column. The conditions were the following: flow rate of 0.55 mL/min with an isocratic elution for 25 min (0.1% formic acid in acetonitrile/0.1% formic acid in water, 75:25 (v/v)).

#### b) Sample preparation for solubility measurements:

Solubility samples were prepared according to the method described by Tsai *et al.*<sup>539</sup> Each compound (~1 mg) was added into sodium phosphate buffer (0.1 M sodium phosphate, pH 7.4, 1 mL) to create a suspension, which was equilibrated for 24 h at room temperature. The suspension was then centrifuged (8,000 rpm, 5 min, RT) using centrifuge. The supernatant was transferred to new Falcon™ tube and was diluted 10 times with methanol to precipitate the salts. The solution was centrifuged (8,000 rpm, 5 min, RT) by centrifuge and the supernatant was filtered through PTFE membrane filters (0.22  $\mu\text{m}$ ) to a vial. The samples were kept at -20 °C before being analysed by HPLC, if necessary.

#### c) Solubility determination:

Two different conditions were applied depending on the compound for testing:



• Conditions A: flow rate of 0.55 mL/min with an isocratic elution for 25 min (0.1% formic acid in acetonitrile/0.1% formic acid in water, 75:25 (v/v)).

• Conditions B: flow rate of 0.60 mL/min with an isocratic elution for 15 min (0.1% formic acid in acetonitrile/0.1% formic acid in water, 92:8 (v/v)).

Compounds **170-183** and **192-193** were measured applying conditions A, whereas compounds **184**, **188** and **195** were tested using conditions B, either at 225 nm or at 254 nm.

d) *Correction factor calculation:*

The absorbance of a 1 mM solution of **184**, **188** and **195** in methanol was measured by HPLC, as well as of a 1 mM solution of the standard **109** in methanol. The correction factors were determined for each compound (Table 27).

**Table 27.** Correction factor applied for the determination of the solubility of compounds **184**, **188** and **195**.

Comp.	Correction factor
184	2.28
188	2.81
195	3.27

e) *Results:*

Apparent solubility results are average of minimum two independent replicates in  $\mu\text{g/mL} \pm$  standard deviation.

***In vitro* studies**



### *In vitro* cell cultures

#### a) *Cell culture:*

Human Huh-7 were maintained in a humid atmosphere of 5% CO<sub>2</sub> at 37 °C in high glucose (25 mmol/L) Dulbecco's modified Eagle's medium (DMEM) supplemented with 10% heat-inactivated fetal bovine serum (FBS), 1% of penicillin/streptomycin (10.000 units/mL of penicillin and 10.000 µg/mL of streptomycin) and 1% of amphotericin B (250 µg/mL).

#### b) *Cell treatment:*

Huh-7 cells were serum-starved overnight *prior* to treatment. Lipid-containing media were prepared by conjugation of palmitic acid with fatty acid-free BSA, as previously described.<sup>575</sup> Cells were pre-treated with the inhibitors (final concentration 1 µmol/L) for 1 hour before treatment with palmitate (final concentration 0.5 mmol/L) and inhibitors (final concentration 1 µmol/L). For each condition, at least 3 replicates were performed. Following 48 hours of incubation, RNA or protein were extracted as described below.

#### c) *Immunoblotting:*

To obtain total protein, hepatocytes were homogenized in RIPA lysis buffer (Sigma) with 5 mmol/L NaF, 1 mmol/L phenylmethylsulfonyl fluoride, 10 mmol/L sodium orthovanadate and 5.4 µg/mL aprotinin at 4 °C for 30 min. The homogenate was centrifuged at 10.000 g for 20 min at 4 °C. Protein concentration was measured by the Bradford method. Total proteins (30 µg) were separated by SDS-PAGE on 10% separation gels and transferred to Immun-Blot<sup>®</sup> polyvinylidene difluoride membranes (BioRad). Western blot analysis was performed using antibodies against BiP, CHOP and ATF3 (Cell Signalling Technology or Santa Cruz Biotechnology). Detection was achieved exposing to Hyperfilm-ECL films, and analysed using an imaging system (Alpha Innotech, CA) to obtain densitometric values. The equal loading of proteins was assessed by detection of GAPDH. The size of proteins detected was estimated using protein molecular-mass standards (BioRad).

#### d) *Real-Time PCR:*

Total RNA in hepatocytes was harvested by TRIsure (Bioline) according to the manufacturer's instructions. The extracted RNA was dissolved in RNase-free water and concentrations of total RNA were quantified using a NanoDrop 2000c spectrophotometer (Thermo Scientific). First-stranded cDNA was synthesized from 0.5 µg total RNA (Fermentas Life Science). Primer Express Software (Applied Biosystems, Foster City, CA, USA) was used to design the primers examined with SYBR Green I (Table 28). The PCR reaction contained 10 ng of reverse-transcribed RNA, 2X IQ<sup>™</sup> SYBRGreen Supermix (BioRad, Barcelona, Spain) and 900 nmol/L concentration of each primer. Optical primer amplification efficiency for each primer set was assessed and a dissociation protocol was

carried out to assure a single PCR product. PCR assays were performed on a MiniOpticon™ Real-Time PCR system (BioRad). Thermal cycling conditions were as follows: activation of Taq DNA polymerase at 95 °C for 10 min, followed by 40 cycles of amplification at 95 °C for 15 sec and 60 °C for 1 min. The relative levels of specific mRNA were estimated from the value of the threshold cycle (Ct) of the real-time PCR adjusted by that of GAPDH through the formula  $2^{\Delta C_t}$  ( $\Delta C_t = \text{Gene of interest Ct} - \text{GAPDH Ct}$ ).

**Table 28.** Primer sequences of selected genes for quantitative real-time PCR.

Gene	Primer sequence
<i>hATF3</i>	Forward 5'-AAGAACGAGAAGCAGCATTGAT-3'
	Reverse 5'-TTCTGAGCCCGGACAATACAC-3'
<i>hBIP</i>	Forward 5'-ACTATTGCTGGCCTAAATGTTATGAG-3'
	Reverse 5'-TTATCCAGGCCATAAGCAATAGC-3'
<i>hCHOP</i>	Forward 5'-GGAAATGAAGAGGAAGAATCAAAAAT-3'
	Reverse 5'-GTTCTGGCTCCTCCTCAGTCA-3'
<i>hGAPDH</i>	Forward 5'-GGCCTCCAAGGAGTAAGACC-3'
	Reverse 5'-AGGGGTCTACATGGCAACTG-3'

e) *Statistical analysis:*

Results are expressed as means  $\pm$  SD of 3-6 separate experiments. Significant differences were established by one-way ANOVA using the GraphPad Instat programme (GraphPad Software V5.01; GraphPad Software Inc., San Diego, CA). When significant variations were found, the Tukey-Kramer multiple comparisons test was applied. Differences were considered at  $P < 0.05$ .

## **REFERENCES**



1. Landa, S. *Chem. Listy* **1933**, *27*, 415-418 and **1933**, *27*, 443-448.
2. Fort, R. C., Jr.; Schleyer, P. von R. *Chem. Rev.* **1964**, 277-300.
3. Adcock, W.; Kok, G. B. *J. Org. Chem.* **1987**, *52*, 356-364.
4. Duddeck, H. *Tetrahedron* **1978**, *34*, 247-251.
5. Kaselj, M.; Adcock, J. L.; Luo, H.; Zhang, H.; Li, H.; William, J. le N. *J. Am. Chem. Soc.* **1995**, *117*, 7088-7091.
6. Adcock, W.; Trout, N. A. *Chem. Rev.* **1999**, *99*, 1415-1435.
7. Gleicher, G. J.; Schleyer, P. von R. *J. Am. Chem. Soc.* **1967**, *89*, 582-593.
8. Wishnok, J. J. *Chem. Educ.* **1973**, *50*, 780-781.
9. Wanka, L.; Iqbal, K.; Schreiner, P. R. *Chem. Rev.* **2013**, *113*, 3516-3604.
10. Lamoureux, G.; Artavia, G. *Curr. Med. Chem.* **2010**, *17*, 2967-2978.
11. Dahl, J. E.; Liu, S. G.; Carlson, R. M. K. *Science* **2003**, *299*, 96-99.
12. Senning, A. Elsevier's Dictionary of Chemoetymology; Elsevier: Oxford, **2007**.
13. Mair, B. J.; Shamaingar, M.; Krouskop, N. C.; Rossini, F. D. *Anal. Chem.* **1959**, *31*, 2082-2083.
14. Schreiner, P. R.; Fokina, N. A.; Tkachenko, B. A.; Hausmann, H.; Serafin, M.; Dahl, J. E. P.; Liu, S.; Carlson, R. M. K.; Fokin, A. A. *J. Org. Chem.* **2006**, *71*, 6709-6720.
15. Woodward, R. B.; Gougoutas, J. Z. *J. Am. Chem. Soc.* **1964**, *86*, 5030-5030.
16. Tanner, J. A.; Zheng, B.-J.; Zhou, J.; Watt, R. M.; Jiang, J.-Q.; Wong, K.-L.; Lin, Y.-P.; Lu, L.-Y.; He, M.-L.; Kung, H.-F.; Kesel, A. J.; Huang, J.-D. *Chem. Biol.* **2005**, *12*, 303-311.
17. Hu, L. H.; Sim, K. Y. *Org. Lett.* **1999**, *1*, 879-882.
18. Tanaka, N.; Takaishi, Y.; Shikishima, Y.; Nakanishi, Y.; Bastow, K.; Lee, K.-H.; Honda, G.; Ito, M.; Takeda, Y.; Kodzhimatov, O. K.; Ashurmetov, O. *J. Nat. Prod.* **2004**, *67*, 1870-1875
19. Prelog, V.; Seiwerth, R. *Ber. Dtsch. Chem. Ges.* **1941**, *74*, 1644-1648.
20. Schleyer, P. v. R. *J. Am. Chem. Soc.* **1957**, *79*, 3292-3292.
21. Schleyer, P. v. R.; Donaldson, M. M.; Nicholas, R. D.; Cupas, C. *Org. Synth. Coll. Vol. V* **1973**, 16-19.
22. Morel-Desrosiers, N.; Morel, J.-P. *J. Solution Chem.* **1979**, *8*, 579-592.
23. Leach, A. R. *Compr. Med. Chem. II* **2007**, *4*, 87-118.
24. Kaminski, G. A.; Stern, H. A.; Berne, B. J.; Friesner, R. A. *J. Phys. Chem. A* **2004**, *108*, 621-627.
25. Maple, J. R.; Cao, Y.; Damm, W.; Halgren, T. A.; Kaminski, G. A.; Zhang, L. Y.; Friesner, R. A. *J. Chem. Theory Comput.* **2005**, *1*, 694-715.
26. Lipinski, C. A.; Lombardo, F.; Dominy, B. W.; Feeney, P. J. *Adv. Drug Deliv. Rev.* **1997**, *23*, 3-25.
27. Leeson, P. D.; Springthorpe, B. *Nat. Rev. Drug Discov.* **2007**, *6*, 881-890.
28. Liu, J.; Obando, D.; Liao, V.; Lifa, T.; Codd, R. *Eur. J. Med. Chem.* **2011**, *46*, 1949-1963.
29. Terasaki, T.; Pardridge, W. M. *J. Drug Targets* **2000**, *8*, 353-355.
30. Tsuzuki, N.; Hama, T.; Kawada, M.; Hasui, A.; Konishi, R.; Shiwa, S.; Ochi, Y.; Futaki, S.; Kitagawa, K. *J. Pharm. Sci.* **1994**, *83*, 481-484.
31. Abraham, M. H., Chadha, H. S., Whiting, G. S.; Mitchell, R. C. *J. Pharm. Sci.* **1994**, *83*, 1085-1100.
32. Spyrakakis, F.; Bidon-Chanal, A.; Barril, X.; Luque, F. J. *Curr. Top. Med. Chem.* **2011**, *11*, 192-210.



33. Mansoori, G. A.; George, T. F.; Assoufid, L.; Zhang, G. Molecular building blocks for nanotechnology. From diamondoids to nanoscale materials and applications. Springer: New York, 2007.
34. Raags, R.; Poulos, T. L. *Biochemistry* **1991**, *30*, 2674-2684.
35. Suckow, R. F. *J. Chromatogr. B Biomed. Sci. Appl.* **2001**, *764*, 313-325.
36. Sturm, G.; Schollmeyer, J. D.; Wesemann, W. *IRCS Medical Science: Library Compendium*, **1976**, *4*, 55.
37. Hayden, F. G.; Minocha, A.; Spyker, D. A.; Hoffman, H. E. *Antimicrob. Agents Chemother.* **1985**, *28*, 216-221.
38. Rubio, F. A.; Choma, N.; Fukuda, E. K. *J. Chromatogr.* **1989**, *497*, 147-157.
39. Su, H.; Boulton, D. W.; Barros, A. Jr.; Wang, L.; Cao, K.; Bonacorsi, S. J. Jr.; Iyer, R. A.; Humphreys, W. G.; Christopher, L. J. *Drug Metab. Dispos.* **2012**, *40*, 1345-1356.
40. Fokin, A. A.; Schreiner, P. R. *Chem. Rev.* **2002**, *102*, 1551-1593.
41. Nagasawa, H. T.; Elberling, J. A.; Shiota, F. N. *J. Med. Chem.* **1975**, *18*, 826-830.
42. Davies, W. L.; Grunert, R. R.; Haff, R. F.; McGahen, J. W.; Neumayer, E. M.; Paulshock, N.; Watts, J. C.; Wood, T. R.; Hermann, E. C.; Hoffman, C. E. *Science* **1964**, *144*, 862-863.
43. De Clercq, E. *Nat. Rev. Drug Discov.* **2006**, *5*, 1015-1025.
44. Cady, S. D.; Luo, W.; Hu, F.; Hong, M. *Biochemistry* **2009**, *48*, 7356-7364.
45. Cady, S. D.; Wang, J.; Wu, Y.; DeGrado, W. F.; Hong, M. *J. Am. Chem. Soc.* **2011**, *133*, 4274-4284.
46. Schwab, R. S.; England, A. C. Jr.; Poskanzer, D. C.; Young, R. R. *J. Am. Med. Assoc.* **1969**, *208*, 1168-1170.
47. Kornhuber, J.; Bormann, J.; Hubers, M.; Rusche, K.; Riederer, P. *J. Pharmacol.* **1991**, *206*, 297-300.
48. Blanpied, T. A.; Clarke, R. J.; Johnson, J. W. *J. Neurosci.* **2005**, *25*, 3312-3322.
49. Kelly, J. M.; Miles, M. A.; Skinner, A. C. *Antimicrob. Agents Chemother.* **1999**, *43*, 985-987.
50. Kelly, J. M.; Quack, G.; Miles, M. A. *Antimicrob. Agents Chemother.* **2001**, *45*, 1360-1366.
51. Rammes, G.; Danysz, W.; Parsons, C. G. *Curr. Neuropharmacol.* **2008**, *6*, 55-78.
52. Herrmann, N.; Li, A.; Lanctôt, K. *Expert Opin. Pharmacother.* **2011**, *12*, 787-800.
53. Lipton, S. A. *Nat. Rev. Drug Discov.* **2006**, *5*, 160-170.
54. Tsunoda, A.; Maassab, H. F.; Cochran, K. W.; Eveland, W. C. *Antimicrob. Agents Chemother.* **1965**, *5*, 553-560.
55. Hayden, F. G.; Minocha, A.; Spyker, D. A.; Hoffman, H. E. *Antimicrob. Agents Chemother.* **1985**, *28*, 216-221.
56. Barret, M. P.; Burchmore, R. J. S.; Stich, A.; Lazzari, J. O.; Frasc, A. C.; Cazzulo, J. J.; Krishna, S. *Lancet* **2003**, *362*, 1469-1480.
57. von Geldern, T. W.; Trevillyan, J. M. *Drug Dev. Res.* **2006**, *67*, 627-642.
58. Villhauer, E. B.; Brinkman, J. A.; Naderi, G. B.; Burkey, B. F.; Dunning, B. E.; Prasad, K.; Mangold, B. L.; Russell, M. E.; Hughes, T. E. *J. Med. Chem.* **2003**, *46*, 2774-2789.
59. Augeri, D. J.; Robl, J. A.; Betebenner, D. A.; Magnin, D. R.; Khanna, A.; Robertson, J. G.; Wang, A.; Simpkins, L. M.; Taunk, P.; Huang, Q.; Han, S.-P.; Abboa-Offei, B.; Cap, M.; Xin, L.; Tao, L.; Tozzo, E.; Welzel, G. E.; Egan, D. M.; Marcinkeviciene, J.; Chang, S. Y.; Biller, S. A.; Kirby, M. S.; Parker, R. A.; Hamann, L. G. *J. Med. Chem.* **2005**, *48*, 5025-5037.

60. Metzler, W. J.; Yanchunas, J.; Weigelt, C.; Kish, K.; Klei, H. E.; Xie, D.; Zhang, Y.; Corbett, M.; Tamura, J. K.; He, B.; Hamann, L. G.; Kirby, M. S.; Marcinkeviciene, J. *Protein Sci.* **2008**, *17*, 240-250.
61. Rosenthal, K. S.; Sokol, M. S.; Ingram, R. L.; Subramanian, R.; Fort, R. C. *Antimicrob. Agents Chemother.* **1982**, *22*, 1031-1036.
62. Ickes, D. E.; Venetta, T. M.; Phonphok, Y.; Rosenthal, K. S. *Antiviral Res.* **1990**, *14*, 75-85.
63. Shroot, B.; Michel, S. J. *Am. Acad. Dermatol.* **1997**, *36* (Suppl.), S96-S103.
64. Piérard, G. E.; Piérard-Franchimont, C.; Paquet, P.; Quatresooz, P. *Expert Opin. Drug Metab. Toxicol.* **2009**, *5*, 1565-1575.
65. Wells, T. N.; Alonso, P. L.; Gutteridge, W. E. *Nat. Rev. Drug Discovery* **2009**, *8*, 879-891.
66. Glennon, R. A. *Drug Dev. Res.* **1992**, *26*, 251-274.
67. Imig, J. D.; Zhao, X.; Zaharis, C. Z.; Olearczyk, J. J.; Pollock, D. M.; Newman, J. W.; Kim, I. H.; Watanabe, T.; Hammock, B. D. *Hypertension* **2005**, *46*, 975-981.
68. Fieser, L. F.; Nazer, M. Z.; Archer, S.; Berberian, D. A.; Slighter, R. G. *J. Med. Chem.* **1967**, *10*, 517-521.
69. Wang, X.; Dong, Y.; Wittlin, S.; Creek, D.; Chollet, J.; Charman, S. A.; SantoTomas, J.; Scheurer, C.; Snyder, C.; Vennerstrom, J. L. *J. Med. Chem.* **2007**, *50*, 5840-5847.
70. Protopopova, M.; Hanrahan, C.; Nikonenko, B.; Samala, R.; Chen, P.; Gearhart, J.; Einck, L.; Nacy, C. A. *J. Antimicrob. Chemother.* **2005**, *56*, 968-974.
71. Trivedi, B. K.; Padia, J. K.; Holmes, A.; Rose, S.; Wright, D. S.; Hinton, J. P.; Pritchard, M. C.; Eden, J. M.; Kneen, C.; Webdale, L.; Suman-Chauhan, N.; Boden, P.; Singh, L.; Field, M. J.; Hill, D. *J. Med. Chem.* **1998**, *41*, 38-45.
72. Solaja, B. A.; Opsenica, D.; Smith, K. S.; Milhous, W. K.; Terzic, N.; Opsenica, I.; Burnett, J. C.; Nuss, J.; Gussio, R.; Bavari, S. *J. Med. Chem.* **2008**, *51*, 4388-4391.
73. Moehrle, J. J.; Duparc, S.; Siethoff, C.; van Giersbergen, P. L.; Craft, J. C.; Arbe-Barnes, S.; Charman, S. A.; Gutierrez, M.; Wittlin, S.; Vennertrom, J. L. *Br. J. Clin. Pharmacol.* **2012**, *75*, 524-537.
74. Le, S. B.; Hailer, M. K.; Buhrow, S.; Wang, Q.; Flatten, K.; Padiaditakis, P.; Bible, K. C.; Lewis, L. D.; Sausville, E. A.; Pang, Y. P.; Ames, M. M.; Lemasters, J. J.; Holmuhamedov, E. L.; Kaufmann, S. H. *J. Biol. Chem.* **2007**, *282*, 8860-8872.
75. Kaur, G.; Narayanan, V. L.; Risbood, P. A.; Hollingshead, M. G.; Stinson, S. F.; Varma, R. K.; Sausville, E. A. *Bioorg. Med. Chem.* **2005**, *13*, 1749-1761.
76. Kelland, L. R.; Barnard, F. J.; Evans, I. G.; Murrer, B. A.; Theobald, B. R. C.; Wyer, S. B.; Goddard, P. M.; Jones, M.; Valenti, M.; Bryant, A.; Rogers, P. M.; Harrap, K. R. *J. Med. Chem.* **1995**, *38*, 3016-3024.
77. Guile, S. D.; Alcaraz, L.; Birkinshaw, T. N.; Bowers, K. C.; Ebden, M. R.; Furber, M.; Stocks, M. J. *J. Med. Chem.* **2009**, *52*, 3123-3141.
78. Mehta, N.; Kaur, M.; Singh, M.; Chand, S.; Vyas, B.; Silakari, P.; Bahia, M. S.; Silakari, O. *Bioorg. Med. Chem.* **2014**, *22*, 54-88.
79. Horvat, S.; Varga-Defterdarovic, L.; Horvat, J.; Jukic, R.; Kantoci, D.; Chung, N. N.; Schiller, P. W.; Biesert, L.; Pflutzner, A.; Suhartono, H.; Rubsamen-Waigmann, H. *J. Pept. Sci.* **1995**, *1*, 303-310.
80. Lovekamp, T.; Cooper, P. S.; Hardison, J.; Bryant, S. D.; Guerrini, R.; Balboni, G.; Salvadori, S.; Lazarus, L. H. *Brain Res.* **2001**, *902*, 131-134.

81. Lu, J. J.; Crimin, K.; Goodwin, J. T.; Crivori, P.; Orrenius, C.; Xing, L.; Tandler, P. J.; Vidmar, T. J.; Amore, B. M.; Wilson, A. G. E.; Stouten, P. F. W.; Burton, P. S. *J. Med. Chem.* **2004**, *47*, 6104-6107.
82. Arnott, J. A.; Planey, S. L. *Expert Opin. Drug Discov.* **2012**, *7*, 863-875.
83. (a) Leeson, P. D.; Young, R. J. *ACS Med. Chem. Lett.* **2015**, *6*, 722-725. (b) Waring, M. J.; Arrowsmith, J.; Leach, A. R.; Leeson, P. D.; Mandrell, S.; Owen, R. M.; Pairaudeau, G.; Pennie, W. D.; Pickett, S. D.; Wang, J.; Wallace, O.; Weir, A. *Nat. Rev. Drug Discov.* **2015**, *14*, 475-486.
84. Gleeson, M. P. *J. Med. Chem.* **2008**, *51*, 817-834.
85. Charifson, P. S.; Walters, W. P. *J. Med. Chem.* **2014**, *57*, 9701-9717.
86. Zhang, M.-Q. *Methods Mol. Biol.* **2012**, *803*, 297-307.
87. Jordan, R.; Bailey, T. R.; Rippin, S. R.; Dai, D. WO 2008130348, **2008**.
88. Zoidis, G.; Papanastasiou, I.; Dotsikas, I.; Sandoval, A.; Dos Santos, R. G.; Papadopoulou-Daifoti, Z.; Vamvakides, A.; Kolocouris, N.; Felix, R. *Bioorg. Med. Chem.* **2005**, *13*, 2791-2798.
89. Becker, D. P.; Flynn, D. L.; Shone, R. L.; Gullikson, G. *Bioorg. Med. Chem. Lett.* **2004**, *14*, 5509-5512.
90. Duque, M. D.; Ma, C.; Torres, E.; Wang, J.; Naesens, L.; Juárez-Jiménez, J.; Camps, P.; Luque, F. J.; DeGrado, W. F.; Lamb, R. A.; Pinto, L. H.; Vázquez, S. *J. Med. Chem.* **2011**, *54*, 2646-2657.
91. Rey-Carrizo, M.; Torres, E.; Ma, C.; Barniol-Xicota, M.; Wang, J.; Wu, Y.; Naesens, L.; Degrado, W. F.; Lamb, R. A.; Pinto, L. H.; Vázquez, S. *J. Med. Chem.* **2013**, *56*, 9265-9274.
92. Torres, E.; Leiva, R.; Gazzarrini, S.; Rey-Carrizo, M.; Frigolé-Vivas, M.; Moroni, A.; Naesens, L.; Vázquez, S. *ACS Med. Chem. Lett.* **2014**, *5*, 831-836.
93. Rey-Carrizo, M.; Barniol-Xicota, M.; Ma, C.; Frigolé-Vivas, M.; Torres, E.; Naesens, L.; Llabrés, S.; Juárez-Jiménez, J.; Luque, F. J.; Degrado, W. F.; Lamb, R. A.; Pinto, L. H.; Vázquez, S. *J. Med. Chem.* **2014**, *57*, 5738-5747.
94. Rey-Carrizo, M.; Gazzarrini, S.; Llabrés, S.; Frigolé-Vivas, M.; Juárez-Jiménez, J.; Font-Bardia, M.; Naesens, L.; Moroni, A.; Luque, F. J.; Vázquez, S. *Eur. J. Med. Chem.* **2015**, *96*, 318-329.
95. Camps, P.; Duque, M. D.; Vázquez, S.; Naesens, L.; De Clercq, E.; Sureda, F. X.; López-Querol, M.; Camins, A.; Pallàs, M.; Prathalingam, S. R.; Kelly, J. M.; Romero, V.; Ivorra, D.; Cortés, D. *Bioorg. Med. Chem.* **2008**, *16*, 9925-9936.
96. Duque, M. D.; Camps, P.; Profire, L.; Montaner, S.; Vázquez, S.; Sureda, F. X.; Mallol, J.; López-Querol, M.; Naesens, L.; De Clercq, E.; Prathalingam, S. R.; Kelly, J. M. *Bioorg. Med. Chem.* **2009**, *17*, 3198-3206.
97. Duque, M. D.; Camps, P.; Torres, E.; Valverde, E.; Sureda, F. X.; López-Querol, M.; Camins, A.; Prathalingam, S. R.; Kelly, J. M.; Vázquez, S. *Bioorg. Med. Chem.* **2010**, *18*, 46-57.
98. Torres, E.; Duque, M. D.; López-Querol, M.; Taylor, M. C.; Naesens, L.; Ma, C.; Pinto, L. H.; Sureda, F. X.; Kelly, J. M.; Vázquez, S. *Bioorg. Med. Chem.* **2012**, *20*, 942-948.
99. Gu, R.-X.; Liu, L. A.; Wang, Y.-H.; Xu, Q.; Wei, D.-Q. *J. Phys. Chem. B* **2013**, *117*, 6042-6051.
100. Watkins, J. C.; Evans, R. H. *Annu. Rev. Pharmacol. Toxicol.* **1981**, *21*, 165-204.
101. Danbolt, N. C. *Prog. Neurobiol.* **2001**, *65*, 1-105.

102. Traynelis, S. F.; Wollmuth, L. P.; McBain, C. J.; Menniti, F. S.; Vance, K. M.; Ogden, K. K.; Hansen, K. B.; Yuan, H.; Myers, S. J.; Dingledine, R. *Pharmacol. Rev.* **2010**, *62*, 405-496.
103. Niswender, C. M.; Conn, P. J. *Annu. Rev. Pharmacol. Toxicol.* **2010**, *50*, 295-322.
104. Kleckner, N. W.; Dingledine, R. *Science* **1988**, *241*, 835-837.
105. Chris Parsons web page. Projects: NMDA receptors. <http://www.chrisparsons.de/Chris/nmda.htm> (accessed on 11<sup>th</sup> September 2015).
106. Bleich, S.; Romer, K.; Wiltfang, J.; Kornhuber, J. *Int. J. Geriatr. Psychiatry* **2003**, *18*, S33-S40.
107. Parsons, C. G.; Stöffler, A.; Danysz, W. *Neuropharmacology* **2007**, *53*, 699-723.
108. Karakas, E.; Furukawa, H. *Science* **2014**, *344*, 992-997.
109. Lee, C.-H.; Lü, W.; Michel, J. C.; Goehring, A.; Du, J.; Song, X.; Gouaux, E. *Nature* **2014**, *511*, 191-197.
110. Karakas, E.; Regan, M. C.; Furukawa, H. *Trends Biochem. Sci.* **2015**, *40*, 328-337.
111. Danysz, W.; Parsons, C. G. *Br. J. Pharmacol.* **2012**, *167*, 324-352.
112. Butterfield, D. A.; Pocernich, C. B. *CNS Drugs* **2003**, *17*, 641-652.
113. Lipton, S. A.; Rosenberg, P. A. *N. Engl. J. Med.* **1994**, *330*, 613-622.
114. Lipton, S. A.; Nicoretta, P. *Cell Calcium* **1998**, *23*, 165-171.
115. Lipton, S. A. *Nat. Rev. Drug Discov.* **2006**, *5*, 160-170.
116. Zeevalk, G. D.; Nicklas, W. J. *J. Neurochem.* **1992**, *59*, 1211-1220.
117. Herrmann, N.; Li, A.; Lanctôt, K. *Expert Opin. Pharmacother.* **2011**, *12*, 787-800.
118. Lange, K. W.; Kornhuber, J.; Riederer, P. *Neurosci. Biobehav. Rev.* **1997**, *21*, 393-400.
119. Cioffi, C. L. *Bioorg. Med. Chem. Lett.* **2013**, *23*, 5034-5044.
120. Rammes, G.; Danysz, W.; Parsons, C. G. *Curr. Neuropharmacol.* **2008**, *6*, 55-78.
121. Lipton, S. A. *Nat. Rev. Neurosci.* **2007**, *8*, 803-808.
122. Kemp, J. A.; McKernan, R. M. *Nat. Neurosci.* **2002**, *5* (Suppl.), 1039-1042.
123. Koller, M.; Urwyler, S. *Expert Opin. Ther. Pat.* **2010**, *20*, 1683-1702.
124. Strong, K. L.; Jing, Y.; Prosser, A. R.; Traynelis, S. F.; Liotta, D. C. *Expert Opin. Ther. Pat.* **2014**, *24*, 1349-1366.
125. Abraham, W. C.; Mason, S. E. *Brain Res.* **1988**, *462*, 40-46.
126. Lehmann, J.; Schneider, J.; McPherson, S.; Murphy, D. E.; Bernard, P.; Tsai, C.; Bennett, D. A.; Pastor, G.; Steel, D. J.; Boehm, C. J. *Pharmacol. Exp. Ther.* **1987**, *240*, 737-746.
127. Sveinbjornsdottir, S.; Sander, J. W.; Upton, D.; Thompson, P. J.; Patsalos, P. N.; Hirt, D.; Emre, M.; Lowe, D.; Duncan, J. S. *Epilepsy Res.* **1993**, *16*, 165-174.
128. Davis, S.; Butcher, S. P.; Morris, G. M. *J. Neurosci.* **1992**, *12*, 21-34.
129. Yenari, M. A.; Bell, T. E.; Kotake, A. N.; Powell, M.; Steinberg, G. K. *Clin. Neuropharmacol.* **1998**, *21*, 28-34.
130. Kvist, T.; Greenwood, J. R.; Hansen, K. B.; Traynelis, S. F.; Bräuner-Osborne, H. *Neuropharmacology* **2013**, *75*, 324-336.
131. Sonkusare, S. K.; Kaul, C. L.; Ramarao, P. *Pharmacol. Res.* **2005**, *51*, 1-17.
132. Michaud, M.; Warren, H.; Drian, M. J.; Rambaud, J.; Cerruti, P.; Nicolas, J. P.; Vignon, J.; Privat, A.; Kamenka, J. M. *Eur. J. Med. Chem.* **1994**, *29*, 869-876.
133. White, J. M.; Ryan, C. F. *Drug Alcohol Rev.* **1996**, *15*, 145-155.
134. Dorandeu, F.; Dhote, F.; Barbier, L.; Baccus, B.; Testylier, G. *CNS Neurosci. Ther.* **2013**, *19*, 411-427.
135. Parsons, C. G.; Danysz, W.; Quack, G. *Amino Acids* **2000**, *19*, 157-166.

136. Blanpied, T. A.; Clarke, R. J.; Johnson, J. W. *J. Neurosci.* **2005**, *25*, 3312-3322.
137. Rammes, G. *Expert Rev. Clin. Pharmacol.* **2009**, *2*, 231-238.
138. Mattia, C.; Coluzzi, F. *Drugs* **2007**, *10*, 636-644.
139. Kiewert, C.; Hartmann, J.; Stoll, J.; Thekkumkara, T. J.; Van der Schyf, C. J.; Klein, J. *Neurochem. Res.* **2006**, *31*, 395-399.
140. Rogawski, M. A. *Amino Acids* **2000**, *19*, 133-149.
141. Torres-Gómez, H.; Lehmkuhl, K.; Frehland, B.; Daniliuc, C.; Schepmann, D.; Ehrhardt, C.; Wünsch, B. *Bioorg. Med. Chem.* **2015**, *23*, 4277-4285.
142. Williams, K. *Curr. Drug Targets* **2001**, *2*, 285-298.
143. Parsons, C. G.; Danysz, W.; Quack, G. *Neuropharmacology* **1999**, *38*, 735-767.
144. Gotti, B.; Duverger, D.; Bertin, J.; Carter, C.; Dupont, R.; Frost, J.; Gaudilliere, B.; MacKenzie, E. T.; Rousseau, J.; Scatton, B.; Wick, A. *J. Pharmacol. Exp. Ther.* **1988**, *247*, 1211-1221.
145. Kew, J. N. C.; Trube, G.; Kemp, J. A. *J. Physiol.* **1996**, *497*, 761-772.
146. Gawaskar, S.; Schepmann, D.; Bonifazi, A.; Wünsch, B. *Bioorg. Med. Chem.* **2014**, *22*, 6638-6646.
147. Bettini, E.; Sava, A.; Griffante, C.; Carignani, C.; Buson, A.; Capelli, A. M.; Negri, M.; Andreetta, F.; Senar-Sancho, S. A.; Guiral, L.; Cardullo, F. *J. Pharmacol. Exp. Ther.* **2010**, *335*, 636-644.
148. Regan, M. C.; Romero-Hernandez, A.; Furukawa, H. *Curr. Opin. Struct. Biol.* **2015**, *33*, 68-75.
149. Blanpied, T. A.; Boeckman, F. A.; Aizenman, E.; Johnson, J. W. *J. Neurophysiology* **1997**, *77*, 309-323.
150. Chen, H. S. V.; Lipton, S. A. *J. Pharmacol. Exp. Ther.* **2005**, *314*, 961-971.
151. Johnson, J. W.; Glasgow, N. G.; Povysheva, N. V. *Curr. Opin. Pharmacol.* **2015**, *20*, 54-63.
152. Limapichat, W.; Yu, W. Y.; Branigan, E.; Lester, H. A.; Dougherty, D. A. *ACS Chem. Neurosci.* **2013**, *4*, 255-260.
153. European Medicines Agency, Ebixa (memantine). [http://www.ema.europa.eu/ema/index.jsp?curl=pages/medicines/human/medicines/000463/human\\_med\\_000750.jsp&mid=WC0b01ac058001d124](http://www.ema.europa.eu/ema/index.jsp?curl=pages/medicines/human/medicines/000463/human_med_000750.jsp&mid=WC0b01ac058001d124) (accessed on 21<sup>st</sup> May 2015).
154. FDA approves memantine drug for treating AD. *Am. J. Alzheimers Dis. Other Demen.* **2003**, *18*, 329-330.
155. Alzheimer's association. <http://www.alz.org/> (accessed on 31<sup>st</sup> August 2015).
156. Anand, R.; Gill, K. D.; Mahdi, A. A. *Neuropharmacology* **2014**, *76*, 27-50.
157. Parsons, C. G.; Danysz, W.; Dekundy, A.; Pulte, I. *Neurotox. Res.* **2013**, *24*, 358-369.
158. Herrmann, N.; Cappell, J.; Eryavec, G. M.; Lanctôt, K. L. *CNS Drugs* **2011**, *25*, 425-433.
159. Peng, D.; Yuan, X.; Zhu, R. *J. Clin. Neurosci.* **2013**, *20*, 1482-1485.
160. Brocardo, P. S.; Gil-Mohapel, J. M. *Curr. Physicopharmacol.* **2012**, *1*, 137-154.
161. Dang, Y.-H.; Ma, X.-C.; Zhang, J.-C.; Ren, Q.; Wu, J.; Gao, C.-G.; Hashimoto, K. *Curr. Pharm. Des.* **2014**, *20*, 5151-5159.
162. Costa, A. C. S. *CNS Neurol. Disord. Drug Targets* **2014**, *13*, 16-25.
163. Tomek, S. E.; LaCrosse, L. A.; Nemirovsky, N. E.; Foster Olive, M. *Pharmaceuticals* **2013**, *6*, 251-268.
164. Duque, M. D. Ph.D. Dissertation, University of Barcelona, 2010.

165. Amini; Bishop, R. *Aust. J. Chem.* **1983**, *36*, 2465-2472.
166. Amini; Bishop, R.; Burgess, G.; Craig, D. C.; Dance, I. G.; Scudder, M. L. *Aust. J. Chem.* **1989**, *42*, 1919-1928.
167. Föhlisch, B.; Widmann, E.; Schupp, E. *Tetrahedron Lett.* **1969**, *28*, 2355-2358.
168. Föhlisch, B.; Dukek, U.; Graessle, I.; Novotny, B.; Schupp, E.; Schwaiger, G.; Widmann, E. *Justus Liebigs Ann. Chem.* **1973**, 1839-1850.
169. The previous method used for dehydration of the hydrate was to sublime the mixture at 160 °C and 0.5 Torr.
170. Greenwald, R.; Chaykovsky, M.; Corey, E. J. *J. Org. Chem.* **1963**, *28*, 1128-1129.
171. Coxon, J. M.; Maclagan, R. G. A. R.; McDonald, D. Q.; Steel, P. J. *J. Org. Chem.* **1991**, *56*, 2542-2549.
172. Torres, E. Ph.D. Dissertation, University of Barcelona, 2013.
173. Fokin, A. A.; Merz, A.; Fokina, N. A.; Schwertfeger, H.; Liu, S. L.; Dahl, J. E. P.; Carlson, R. K. M.; Schreiner, P. R. *Synthesis* **2009**, *6*, 909-912.
174. Shimizu, K.-I.; Kanno, S.; Kon, K.; Hakim Siddiki, S. M. A.; Tanaka, H.; Sakata, Y. *Catal. Today* **2014**, *232*, 134-138.
175. Sigl, M.; Heidemann, T. Process for preparing a primary amine with a tertiary alpha carbon atom by reacting a tertiary alcohol with ammonia. WO 2009/053275 A1.
176. Itoh, H.; Kato, I.; Unoura, K.; Senda, Y. *Bull. Chem. Soc. Jpn.* **2001**, *74*, 339-345.
177. Burkhardt, E. R.; Matos, K. *Chem. Rev.* **2006**, *106*, 2617-2650.
178. Fortunato, J. M.; Ganem, B. *J. Org. Chem.* **1976**, *41*, 2194-2200.
179. Martin, H. J.; Drescher, M.; Mulzer, J. *Angew. Chem. Int. Ed.* **2000**, *39*, 581-583.
180. White, D. R. 6'-Alkylspectinomycins. US 4532336 A.
181. Kim, S.; Choon Moon, Y.; Han Ahn, K. *J. Org. Chem.* **1982**, *47*, 3311-3315.
182. Yamashita, M.; Kato, Y.; Suemitsu, R. *Chem. Lett.* **1980**, 847-848.
183. Barton, D. H. R.; Bohé, L.; Lusinch, X. *Tetrahedron* **1990**, *46*, 5273-5284.
184. Yamashita, M.; Tanaka, Y.; Arita, A.; Nishida, M. *J. Org. Chem.* **1994**, *59*, 3500-3502.
185. Marchand, A. P.; LaRoe, W. D.; Sharma, G. V. M.; Suri, S. C.; Reddy, D. S. *J. Org. Chem.* **1986**, *51*, 1622-1625.
186. Jackson, W. R.; Zurqiyar, A. *J. Chem. Soc.* **1965**, 5280-5287.
187. Ishiyama, J.; Senda, Y.; Imaizumi, S. *Chem. Lett.* **1983**, 771-774.
188. Ishiyama, J.; Senda, Y.; Imaizumi, S. *Chem. Lett.* **1983**, 1243-1244.
189. Bishop, R. *Ritter-Type Reactions, Comprehensive Organic Synthesis II*; Elsevier Ltd., 2014.
190. Schwertfeger, H.; Würtele, C.; Sefarin, M.; Hausmann, H.; Carlson, R. M. K.; Dahl, J. E. P.; Schreiner, P. R. *J. Org. Chem.* **2008**, *73*, 7789-7792.
191. Barton, D. H. R.; McCombie, S. W. *J. Chem. Soc., Perkin Trans.* **1975**, *1*, 1574-1585.
192. McCombie, S. W.; Motherwell, W. B.; Tozer, M. *J. Org. React.* **2012**, *77*, 161-591.
193. Zard, S. Z. *Xanthates and Related Derivatives as Radical Precursors*, in *Encyclopedia of Radicals in Chemistry, Biology and Materials*; John Wiley & Sons, Ltd., Chichester, UK, 2012.
194. Kerr, J. A. *Chem. Rev.* **1966**, *66*, 465-500.
195. Chenneberg, L.; Baralle, A.; Daniel, M.; Fensterbank, L.; Goddard, J.-P.; Ollivier, C. *Adv. Synth. Catal.* **2014**, *356*, 2756-2762.
196. Chatgililoglu, C.; Ferreri, C. *Res. Chem. Intermed.* **1993**, *19*, 755-775.
197. Schummer, D.; Hoefle, G. *Synlett* **1990**, *11*, 705-706.
198. Xu, J.; Yadan, J. C. *Tetrahedron Lett.* **1996**, *37*, 2421-2424.
199. Padwa, A.; Haring, S. R.; Semones, M. A. *J. Org. Chem.* **1998**, *63*, 44-54.
200. Marino, J. P.; Osterhout, M. H.; Padwa, A. *J. Org. Chem.* **1995**, *60*, 2704-2713.

201. Boussaguet, P.; Delmond, B.; Dumartin, G.; Pereyre, M. *Tetrahedron Lett.* **2000**, *41*, 3377-3380.
202. Kaneko, S.; Watanabe, T.; Oda, K.; Mohan, R.; Schweiger, E. J.; Martin, R. Fused-ring pyrimidin-4(3H)-one derivatives, processes for the preparation and uses thereof. WO 03/106435 A1.
203. Luzzio, F. A.; Fitch, R. W. *J. Org. Chem.* **1999**, *64*, 5485-5493.
204. Lam, K.; Markó, I. E. *Org. Lett.* **2008**, *10*, 2773-2776.
205. Jang, D. O.; Kim, J.; Cho, D. H.; Chung, C.-M. *Tetrahedron Lett.* **2001**, *42*, 1073-1075.
206. Larson, G. L.; Fry, J. L. *Ionic and organometallic-catalyzed organosilane reductions*, in *Organic Reactions*; John Wiley & Sons, Ltd., Chichester, UK, 2008.
207. Gevorgyan, V.; Rubin, M.; Benson, S.; Liu, J.-X.; Yamamoto, Y. *J. Org. Chem.* **2000**, *65*, 6179-6186.
208. Duddeck, H.; Rosenbaum, D. *J. Org. Chem.* **1991**, *56*, 1707-1713.
209. Banide, E. V.; Molloy, B. C.; Ortin, Y.; Müller-Bunz, H.; McGlinchey, M. J. *Eur. J. Org. Chem.* **2007**, 2611-2622.
210. Ito, M.; Konno, F.; Kunamoto, T.; Suzuki, N.; Kawahata, M.; Yamaguchi, K.; Ishikawa, T. *Tetrahedron* **2011**, *67*, 8041-8049.
211. Ashby, E. C.; Deshpande, A. K. *J. Org. Chem.* **1994**, *59*, 3798-3805.
212. Banister, S. D.; Yoo, D. T.; Chua, S. W.; Cui, J.; Mach, R. H.; Kassiou, M. *Bioorg. Med. Chem. Lett.* **2011**, *21*, 5289-5292.
213. Jang, D. O. *Synth. Commun.* **1997**, *27*, 1023-1027.
214. Sumino, Y.; Harato, N.; Tomisaka, Y.; Ogawa, A. *Tetrahedron* **2003**, *59*, 10499-10508.
215. Rowlands, G. J. *Tetrahedron* **2009**, *65*, 8603-8655.
216. Jirgensons, A.; Kauss, V.; Kalvinsh, I.; Gold, M. R. *Synthesis* **2000**, *12*, 1709-1712.
217. The blue colour is distinctive of samarium(II), whereas the yellow colour of samarium(III).
218. Jasch, H. Heinrich, M. R. *Tin hydrides and functional group transformations*, in *Encyclopedia of Radicals in Chemistry, Biology and Materials*; John Wiley & Sons, Ltd., Chichester, UK, 2012.
219. Renaud, P.; Sibi, M. P. *Radicals in Organic Synthesis Vol. 1*; Wiley-VCH, Weinheim, Germany, 2001.
220. Kumar, K.; Tepper, R. J.; Zeng, Y.; Zimmt, M. B. *J. Org. Chem.* **1995**, *60*, 4051-4066.
221. Marchand, A. P.; Namboothiri, I. N. N. *Heterocycles* **2000**, *52*, 451-457.
222. Borch, R. F.; Bernstein, M. D.; Durst, H. D. *J. Am. Chem. Soc.* **1971**, *93*, 2897-2904.
223. Lane, C. F. *Synthesis* **1975**, *1975*, 135-146.
224. Rohde, J. J.; Pliushchev, M. A.; Sorensen, B. K.; Wodka, D.; Shuai, Q.; Wang, J.; Fung, S.; Monzon, K. M.; Chiou, W. J.; Pan, L.; Deng, X.; Chovan, L. E.; Ramaiya, A.; Mullally, M.; Henry, R. F.; Stolarik, D. F.; Imade, H. M.; Marsh, K. C.; Beno, D. W. A.; Fey, T. A.; Droz, B. A.; Brune, M. E.; Camp, H. S.; Sham, H. L.; Frevert, E. U.; Jacobson, P. B.; Link, J. T. *J. Med. Chem.* **2007**, *50*, 149-164.
225. Jasys, V. J.; Lombardo, F.; Appleton, T. A.; Bordner, J.; Ziliox, M.; Volkmann, R. A. *J. Am. Chem. Soc.* **2000**, *122*, 466-473.
226. Hagmann, W. K. *J. Med. Chem.* **2008**, *51*, 4359-4369.
227. Müller, K.; Faeh, C.; Diederich, F. *Science* **2007**, *317*, 1881-1886.
228. Furuya, T.; Kamlet, A. S.; Ritter, T. *Nature* **2011**, *473*, 470-477.
229. Jeschke, P. *ChemBioChem* **2004**, *5*, 570-589.
230. O'Hagan, D. *Chem. Soc. Rev.* **2008**, *37*, 308-319.

231. *ChemBioChem* **2004**, *5*, 557-726 (special issue: Fluorine in Life Sciences).
232. Meanwell, N. A. *J. Med. Chem.* **2011**, *54*, 2529-2591.
233. Shimizu, M.; Hiyama, T. *Angew. Chem. Int. Ed. Engl.* **2004**, *44*, 214-231.
234. Middleton, W. J. *J. Org. Chem.* **1975**, *40*, 574-578.
235. Lal, G. S.; Pez, G. P.; Pesaresi, R. J.; Prozonic, F. M.; Cheng, H. *J. Org. Chem.* **1999**, *64*, 7048-7054.
236. Lal, G. S.; Pez, G. P.; Syvret, R. G. *Chem. Rev.* **1996**, *96*, 1737-1756.
237. Sodeoka, M. *Science* **2011**, *334*, 1651-1652.
238. Johnson, A. L. *J. Org. Chem.* **1982**, *47*, 5220-5222.
239. Singh, R. P.; Shreeve, J. M. *Synthesis* **2002**, 2561-2578.
240. Yung-Chi, C.; Prusoff, W. H. *Biochem. Pharmacol.* **1973**, *22*, 3099-3108.
241. Verdaguer, E.; García-Jordà, E.; Jiménez, A.; Stranges, A.; Sureda, F. X.; Canudas, A. M.; Escubedo, E.; Camarasa, J.; Pallàs, M.; Camins, A. *Br. J. Pharmacol.* **2002**, *135*, 1297-1307.
242. Gryniewicz, G.; Poenie, M.; Tsien, R. Y. *J. Biol. Chem.* **1985**, *260*, 3440-3450.
243. Life technologies web page. Ion indicators & ionophores: Fura-2. <https://www.lifetechnologies.com/order/catalog/product/F1200> (accessed on 14<sup>th</sup> June 2015).
244. Sakmann, B.; Neher, E. *Ann. Rev. Physiol.* **1984**, *46*, 455-472.
245. Chen, H. S.; Pellegrini, J. W.; Aggarwal, S. K.; Lei, S. Z.; Warach, S.; Jensen, F. E.; Lipton, S. A. *J. Neurosci.* **1992**, *12*, 4427-4436.
246. Parsons, G. R.; Gruner, R.; Rozental, J.; Millar, J.; Lodge, D. *Neuropharmacol.* **1993**, *32*, 1337-1350.
247. Blanpied, T. A.; Clarke, R. J.; Johnson, J. W. *J. Neurosci.* **2005**, *25*, 3312-3322.
248. Gilling, K.; Jatzke, C.; Wollenburg, C.; Vanejevs, M.; Kauss, V.; Jirgensons, A.; Parsons, C. G. *J. Neural Transm.* **2007**, *114*, 1529-1537.
249. Koller, M.; Urwyler, S. *Expert Opin. Ther. Pat.* **2010**, *20*, 1683-1702.
250. Science Lab website. The patch-clamp technique. <http://www.leica-microsystems.com/science-lab/the-patch-clamp-technique/> (accessed on 18<sup>th</sup> September 2015).
251. Dallman, M. F.; Strack, A. M.; Akana, S. F.; Bradbury, M. J.; Hanson, E. S.; Scribner, K. A.; Smith, M. *Front. Neuroendocrinol.* **1993**, *14*, 303-347.
252. Sapolsky, R. M.; Romero, L. M.; Munck, A. U. *Endocr. Rev.* **2000**, *21*, 55-89.
253. Rosen, E. D.; MacDougald, O. A. *Nat. Rev. Mol. Cell Bio.* **2006**, *7*, 885-896.
254. Smoak, K. A.; Cidlowski, J. A. *Mech. Ageing Dev.* **2004**, *125*, 697-706.
255. Arriza, J. L.; Weinberger, C.; Cerelli, G.; Glase, T. M.; Handelin, B. L.; Housman, D. E.; Evans, R. M. *Science* **1987**, *237*, 268-275.
256. Dzykanchuk, A. A.; Balázs, Z.; Nashev, L. G.; Amrein, K. E.; Odermatt, A. *Mol. Cell. Endocrinol.* **2009**, *301*, 137-141.
257. Atanasov, A. G.; Nashev, L. G.; Gelman, L.; Legeza, B.; Sack, R.; Portmann, R.; Odermatt, A. *Biochim. Biophys. Acta* **2008**, *1783*, 1536-1543.
258. Hardy, R. S.; Seibel, M. J.; Cooper, M. S. *Curr. Opin. Pharmacol.* **2013**, *13*, 440-444.
259. Edwards, C. R.; Stewart, P. M.; Burt, D.; Brett, L.; McIntyre, M. A.; Sutanto, W. S. de Kloet, E. R.; Monder, C. *Lancet* **1988**, *2*, 986-989.
260. Hollis, G.; Huber, R. *Diabetes Obes. Metab.* **2011**, *13*, 1-6.
261. Staab, C. A.; Maser, E. *J. Steroid Biochem. Mol. Biol.* **2010**, *119*, 56-72.
262. Odermatt, A.; Nashev, L. G. *J. Steroid Biochem. Mol. Biol.* **2010**, *119*, 1-13.



263. Mitić, T.; Andrew, R.; Walker, B. R.; Hadoke, P. W. F. *Biochimie* **2013**, *95*, 548-555.
264. Odermatt, A.; Klusonova, P. J. *Steroid Biochem. Mol. Biol.* **2015**, *151*, 85-92.
265. Gathercole, L. L.; Lavery, G. G.; Morgan, S. A.; Cooper, M. S.; Sinclair, A. J.; Tomlinson, J. W.; Stewart, P. M. *Endocr. Rev.* **2013**, *34*, 525-555.
266. Klein, T.; Henn, C.; Negri, M.; Frotscher, M. *PLoS One* **2011**, *6*, 1-13.
267. Kotelevtsev, Y.; Brown, R. W.; Fleming, S.; Kenyon, C.; Edwards, C. R.; Seckl, J. R.; Mullins, J. J. *J. Clin. Invest.* **1999**, *103*, 683-689.
268. Bisschop, P. H.; Dekker, M. J. H. J.; Osterthun, W.; Kwakkel, J.; Anink, J. J.; Boelen, A.; Unmehopa, U. A.; Koper, J. W.; Lamberts, S. W. J.; Stewart, P. M.; Swaab, D. F.; Fliers, E. J. *Neuroendocrinol.* **2013**, *25*, 425-432.
269. Kilgour, A. H. M.; Semple, S.; Marshall, I.; Andrews, P.; Andrew, R.; Walker, B. R. J. *Clin. Endocrinol. Metab.* **2015**, *100*, 483-489.
270. Robb, G. R.; Boyd, S.; Davies, C. D.; Dossetter, A. G.; Goldberg, F. W.; Kemmitt, P. D.; Scott, J. S.; Swales, J. G. *Med. Chem. Commun.* **2015**, *6*, 926-934.
271. Wamil, M.; Seckl, J. R. *Drug Discov. Today* **2007**, *12*, 504-520.
272. WHO web page. Diabetes Fact Sheet. <http://www.who.int/mediacentre/factsheets/fs312/en/> (accessed on 26<sup>th</sup> June 2015).
273. European Commission web page. Major and chronic diseases: Diabetes. [http://ec.europa.eu/health/major\\_chronic\\_diseases/diseases/diabetes/index\\_en.htm#fragment7](http://ec.europa.eu/health/major_chronic_diseases/diseases/diabetes/index_en.htm#fragment7) (accessed on 2<sup>nd</sup> July 2015).
274. WHO web page. Obesity and overweight Fact Sheet. <http://www.who.int/mediacentre/factsheets/fs311/en/> (accessed on 26<sup>th</sup> June 2015).
275. Grundy, S. M.; Brewer, H. B.; Cleeman, J. I.; Smith, S. C.; Lenfant, C. *Circulation* **2004**, *109*, 433-438.
276. Huang, P. L. *Dis. Model Mech.* **2009**, *2*, 231-237.
277. Masuzaki, H.; Paterson, J.; Shinyama, H.; Morton, N. M.; Mullins, J. J.; Seckl, J. R.; Flier, J. S. *Science* **2001**, *294*, 2166-2170.
278. Masuzaki, H.; Yamamoto, H.; Kenyon, C. J.; Elmquist, J. K.; Morton, N. M.; Paterson, J. M.; Shinyama, H.; Sharp, M. G. F.; Fleming, S.; Mullins, J. J.; Seckl, J. R.; Flier, J. S. *J. Clin. Invest.* **2003**, *1125*, 83-90.
279. Paterson, J.; Morton, N.; Fievet, C.; Kenyon, C.; Holmes, M.; Staels, B.; Seckl, J. R.; Mullins, J. J. *Proc. Natl. Acad. Sci. USA* **2004**, *101*, 7088-7093.
280. Kotelevtsev, Y.; Holmes, M. C.; Burchell, A.; Houston, P. M.; Schmoll, D.; Jamieson, P.; Best, R.; Brown, R.; Edwards, C. R.; Seckl, J. R.; Mullins, J. J. *Proc. Natl. Acad. Sci. USA* **1997**, *94*, 14924-14929.
281. Morton, N. M.; Paterson, J. M.; Masuzaki, H.; Holmes, M. C.; Staels, B.; Fievet, C.; Walker, B. R.; Flier, J. S.; Mullins, J. J.; Seckl, J. R. *Diabetes* **2004**, *53*, 931-938.
282. Morton, N. M.; Holmes, M. C.; Fievet, C.; Staels, B.; Tailleux, A.; Mullins, J. J.; Seckl, J. R. *J. Biol. Chem.* **2001**, *276*, 41293-41300.
283. Kershaw, E. E.; Morton, N. M.; Dhillon, H.; Ramage, L.; Seckl, J. R.; Flier, J. S. *Diabetes* **2005**, *54*, 1023-1031.
284. Morgan, S. A.; Tomlinson, J. W. *Expert Opin. Investig. Drugs* **2010**, *19*, 1067-1076.
285. Wake, D. J.; Rask, E.; Livingstone, D. E.; Soderberg, S.; Olsson, T.; Walker, B. R. J. *Clin. Endocrinol. Metab.* **2003**, *88*, 3983-3988.
286. Valsamakis, G.; Anwar, A.; Tomlinson, J. W.; Shackleton, C. H. L.; McTernan, P. G.; Chetty, R.; Wood, P. J.; Banerjee, A. K.; Holder, G.; Barnett, A. H.; Stewart, P. M.; Kumar, S. J. *Clin. Endocrinol. Metab.* **2004**, *89*, 4755-4761.

287. Wang, M. *Drug Dev. Res.* **2006**, *67*, 567-569.
288. Cooper, M. S.; Stewart, P. M. *J. Clin. Endocrinol. Metab.* **2009**, *94*, 4645-4654.
289. Morton, N. M. *Mol. Cell. Endocrinol.* **2010**, *316*, 154-164.
290. Joharapurkar, A.; Dhanesha, N.; Shah, G.; Kharul, R.; Jain, M. *Pharmacol. reports* **2012**, *64*, 1055-1065.
291. Anderson, A.; Walker, B. R. *Drugs* **2013**, *73*, 1385-1393.
292. McEwen, B. S.; Biron, C. A.; Brunson, K. W.; Bulloch, K.; Chambers, W. H.; Dhabhar, F. S.; Goldfarb, R. H.; Kitson, R. P.; Miller, A. H.; Spencer, R. L.; Weiss, J. M. *Brain Res. Rev.* **1997**, *23*, 79-133.
293. Sapolsky, R. M.; Romero, L. M.; Munck, A. U. *Endocr. Rev.* **2000**, *21*, 55-89.
294. Yeager, M. P.; Guyre, P. M.; Munck, A. U. *Acta Anaesthesiol. Scand.* **2004**, *48*, 799-813.
295. Chapman, K. E.; Coutinho, A. E.; Gray, M.; Gilmour, J. S.; Savill, J. S.; Seckl, J. R. *Mol. Cell. Endocrinol.* **2009**, *301*, 123-131.
296. Hardy, R. S.; Seibel, M. J.; Cooper, M. S. *Curr. Opin. Pharmacol.* **2013**, *13*, 440-444.
297. Hadoke, P. W. F.; Kipari, T.; Seckl, J. R.; Chapman, K. E. *Curr. Atheroscler. Rep.* **2013**, *15*, 320-330.
298. Jun, Y. J.; Park, S. J.; Hwang, J. W.; Kim, T. H.; Jung, K. J.; Jung, J. Y.; Hwang, G. H.; Lee, S. H.; Lee, S. H. *Clin. Exp. Allergy* **2014**, *44*, 197-211.
299. Chapman, K. E.; Gilmour, J. S.; Coutinho, A. E.; Savill, J. S.; Seckl, J. R. *Mol. Cell. Endocrinol.* **2006**, *248*, 3-8.
300. Chapman, K. E.; Seckl, J. R. *Neurochem. Res.* **2008**, *33*, 624-636.
301. Hotamisligil, G. S. *Nature* **2006**, *444*, 860-867.
302. Squire, L. R. *Psychol. Rev.* **1992**, *99*, 195-231.
303. Sapolsky, R. M.; Pulsinelli, W. A. *Science* **1985**, *229*, 1397-1400.
304. Beraki, S.; Litrus, L.; Soriano, L.; Monbureau, M.; To, L. K.; Braithwaite, S. P.; Nikolich, K.; Urfer, R.; Oksenberg, D.; Shamloo, M. *PLoS One* **2013**, *8*, 1-13.
305. Sandeep, T. C.; Yau, J. L. W.; Maclullich, A. M. J.; Noble, J.; Deary, I. J.; Walker, B. R.; Seckl, J. R. *Proc. Natl. Acad. Sci. USA* **2004**, *101*, 6734-6739.
306. Meaney, M. J.; O'Donnell, D.; Rowe, W.; Tannenbaum, B.; Steverman, A.; Walker, M.; Nair, N. P.; Lupien, S. *Exp. Gerontol.* **1995**, *30*, 229-251.
307. Yau, J. L. W.; Wheelan, N.; Noble, J.; Walker, B. R.; Webster, S. P.; Kenyon, C. J.; Ludwig, M.; Seckl, J. R. *Neurobiol. Aging* **2015**, *36*, 334-343.
308. de Quervain, D. J.-F.; Poirier, R.; Wollmer, M. A.; Grimaldi, L. M. E.; Tsolaki, M.; Streffer, J. R.; Hock, C.; Nitsch, R. M.; Mohajeri, M. H.; Papassotiropoulos, A. *Hum. Mol. Genet.* **2004**, *13*, 47-52.
309. Martocchia, A.; Stefanelli, M.; Falaschi, G. M.; Toussan, L.; Ferri, C.; Falaschi, P. *Aging Clin. Exp. Res.* **2015**, *ahead of print*. DOI: 10.1007/s40520-015-0353-0.
310. Katz, D. A.; Liu, W.; Locke, C.; Jacobson, P.; Barnes, D. M.; Basu, R.; An, G.; Rieser, M. J.; Daszkowski, D.; Groves, F.; Heneghan, G.; Shah, A.; Gevorkyan, H.; Jhee, S. S.; Ereshefsky, L.; Marek, G. J. *Transl. Psychiatry* **2013**, *3*, e295.
311. Yau, J. L. W.; Noble, J.; Seckl, J. R. *J. Neurosci.* **2011**, *31*, 4188-4193.
312. Green, K. N.; Billings, L. M.; Roozendaal, B.; McGaugh, J. L.; LaFerla, F. M. *J. Neurosci.* **2006**, *26*, 9047-9056.
313. Sooy, K.; Noble, J.; McBride, A.; Binnie, M.; Yau, J. L. W.; Seckl, J. R.; Walker, B. R.; Webster, S. P. *Endocrinology* **2015**, *ahead of print*. DOI: 10.1210/en.2015-1395.
314. Yau, J. L. W.; Noble, J.; Kenyon, C. J.; Hibberd, C.; Kotelevtsev, Y.; Mullins, J. J.; Seckl, J. R. *Proc. Natl. Acad. Sci. USA* **2001**, *98*, 4716-4721.

315. Sooy, K.; Webster, S. P.; Noble, J.; Binnie, M.; Walker, B. R.; Seckl, J. R.; Yau, J. L. *W. J. Neurosci.* **2010**, *30*, 13867-13872.
316. Mohler, E. G.; Browman, K. E.; Roderwald, V. A.; Cronin, E. A.; Markosyan, S.; Bitner, R. S.; Strakhova, M. I.; Drescher, K. U.; Hornberger, W.; Rohde, J. J.; Brune, M. E.; Jacobson, P. B.; Rueter, L. E. *J. Neurosci.* **2011**, *31*, 5406-5413.
317. Strachan, M. W. J.; Reynolds, R. M.; Frier, B. M.; Mitchell, R. J.; Price, J. F. *Diabetes Obes. Metab.* **2009**, *11*, 407-414.
318. Anderson, S.; Carreiro, S.; Quenzer, T.; Gale, D.; Xiang, C.; Gukasyan, H.; Lafontaine, J.; Cheng, H.; Krauss, A.; Prasanna, G. *J. Ocul. Pharmacol. Ther.* **2009**, *25*, 215-222.
319. Park, J. S.; Bae, S. J.; Choi, S.-W.; Son, Y. H.; Park, S. B.; Rhee, S. D.; Kim, H. Y.; Jung, W. H.; Kang, S. K.; Ahn, J. H.; Kim, S. H.; Kim, K. Y. *J. Mol. Endocrinol.* **2014**, *52*, 191-202.
320. Tiganescu, A.; Tahrani, A. A.; Morgan, S. A.; Otranto, M.; Desmoulière, A.; Abrahams, L.; Hassan-Smith, Z.; Walker, E. A.; Rabbitt, E. H.; Cooper, M. S.; Amrein, K.; Lavery, G. G.; Stewart, P. M. *J. Clin. Invest.* **2013**, *123*, 3051-3060.
321. Terao, M.; Murota, H.; Kimura, A.; Kato, A.; Ishikawa, A.; Igawa, K.; Miyoshi, E.; Katayama, I. *PLoS One* **2011**, *6*, 1-11.
322. Hench, P. S.; Kendall, E. C.; Slocumb, C. H.; Polley, H. F. *Ann. Rheum. Dis.* **1949**, *8*, 97-104.
323. Sandeep, T. C.; Walker, B. R. *Trends Endocrinol. Metab.* **2001**, *12*, 446-453.
324. Zhang, J.; Osslund, T. D.; Plant, M. H.; Clogston, C. L.; Nybo, R. E.; Xiong, F.; Delaney, J. M.; Jordan, S. R. *Biochemistry* **2005**, *44*, 6948-6957.
325. Schuster, D.; Maurer, E. M.; Laggner, C.; Nashev, L. G.; Wilckens, T.; Langer, T.; Odermatt, A. *J. Med. Chem.* **2006**, *49*, 3454-3466.
326. Wang, H.; Ruan, Z.; Li, J. J.; Simpkins, L. M.; Smirk, R. A.; Wu, S. C.; Hutchins, R. D.; Nirschl, D. S.; Van Kirk, K.; Cooper, C. B.; Sutton, J. C.; Ma, Z.; Golla, R.; Seethala, R.; Salyan, M. E. K.; Nayeem, A.; Krystek, S. R.; Sheriff, S.; Camac, D. M.; Morin, P. E.; Carpenter, B.; Robl, J. A.; Zahler, R.; Gordon, D. A.; Hamann, L. G. *Bioorg. Med. Chem. Lett.* **2008**, *18*, 3168-3172.
327. Hosfield, D. J.; Wu, Y.; Skene, R. J.; Hilgers, M.; Jennings, A.; Snell, G. P.; Aertgeerts, K. *J. Biol. Chem.* **2005**, *280*, 4639-4648.
328. Scott, J. S.; Chooramun, J. *11 $\beta$ -hydroxysteroid dehydrogenase Type 1 (11 $\beta$ -HSD1) inhibitors in development*, in *RSC Drug Discovery Series No. 27*, The Royal Society of Chemistry, 2012.
329. Thomas, M. P.; Potter, B. V. L. *Future Med. Chem.* **2011**, *3*, 367-390.
330. Zhang, J.; Osslund, T. D.; Plant, M. H.; Clogston, C. L.; Nybo, R. E.; Xiong, F.; Delaney, J. M.; Jordan, S. R. *Biochemistry* **2005**, *44*, 6948-6957.
331. Webster, S. P.; Pallin, T. D. *Expert Opin. Ther. Pat.* **2007**, *17*, 1407-1422.
332. Hughes, K. A.; Webster, S. P.; Walker, B. R. *Expert Opin. Investig. Drugs* **2008**, *17*, 481-496.
333. St. Jean Jr., D. J.; Wang, M.; Fotsch, C. *Curr. Top. Med. Chem.* **2008**, *8*, 1508-1523.
334. Boyle, C. D.; Kowalski, T. J. *Expert Opin. Ther. Pat.* **2009**, 801-826.
335. Scott, J. S.; Goldberg, F. W.; Turnbull, A. V. *J. Med. Chem.* **2014**, *57*, 4466-4486.
336. Pavlova, S. I.; Uteshev, B. S.; Sergeev, A. V. *Pharm. Chem. J.* **2003**, *37*, 314-317.
337. Bühler, H.; Perschel, F. H.; Hierholzer, K. *Biochim. Biophys. Acta* **1991**, *1075*, 206-212.
338. Su, X.; Lawrence, H.; Ganeshapillai, D.; Cruttenden, A.; Purohit, A.; Reed, M. J.; Vicker, N.; Potter, B. V. L. *Bioorg. Med. Chem.* **2004**, *12*, 4439-4457.

339. Pandya, K.; Dietrich, D.; Seibert, J.; Vederas, J. C.; Odermatt, A. *Bioorg. Med. Chem.* **2013**, *21*, 6274-6281.
340. Wang, M. *Inhibitors of 11 $\beta$ -hydroxysteroid dehydrogenase type 1 in antidiabetic therapy*, in *Diabetes – Perspectives in Drug Therapy, Handbook of Experimental Pharmacology*, 203, Springer-Verlag Berlin Heidelberg, 2011.
341. Walker, B. R.; Connacher, A. A.; Lindsay, R. M.; Webb, D. J.; Edwards, C. R. *J. Clin. Endocrinol. Metab.* **1995**, *80*, 3155-3159.
342. Andrews, R. C.; Rooyackers, O.; Walker, B. R. *J. Clin. Endocrinol. Metab.* **2003**, *88*, 285-291.
343. Nuotio-Antar, A. M.; Hachey, D. L.; Hasty, A. H. *Am. J. Physiol. Endocrinol. Metab.* **2007**, *293*, E1517-E1528.
344. PDB codes: 2BEL, 3D4N, 3D3E, 2ILT, 3BYZ, 3CZR, 3CH6, among others. See also reference 329 for a detailed analyses of the crystal structures of 11 $\beta$ -HSD1.
345. Stefan, N.; Ramsauer, M.; Jordan, P.; Nowotny, B.; Kantartzis, K.; Machann, J.; Hwang, J.H.; Nowotny, P.; Kahl, S.; Harreiter, J.; Hornemann, S.; Sanyal, A. J.; Stewart, P. M.; Pfeiffer, A. F.; Kautzky-Willer, A.; Roden, M.; Häring, H. U.; Fürst-Recktenwald, S. *Lancet Diabetes Endocrinol.* **2014**, *2*, 406-416.
346. Siu, M.; Johnson, T. O.; Wang, Y.; Nair, S. K.; Taylor, W. D.; Cripps, S. J.; Matthews, J. J.; Edwards, M. P.; Pauly, T. A.; Ermolieff, J.; Castro, A.; Hosea, N. A.; LaPaglia, A.; Fanjul, A. N.; Vogel, J. E. *Bioorg. Med. Chem. Lett.* **2009**, *19*, 3493-3497.
347. Feig, P. U.; Shah, S.; Hermanowski-Vosatka, A.; Plotkin, D.; Springer, M. S.; Donahue, S.; Thach, C.; Klein, E. J.; Lai, E.; Kaufman, K. D. *Diabetes Obes. Metab.* **2011**, *13*, 498-504.
348. Shah, S.; Hermanowski-Vosatka, A.; Gibson, K.; Ruck, R. A.; Jia, G.; Zhang, J.; Hwang, P. M. T.; Ryan, N. W.; Langdon, R. B.; Feig, P. U. *J. Am. Soc. Hypertens.* **2011**, *5*, 166-176.
349. Clinical trials web site. 11 $\beta$ -HSD1. <https://www.clinicaltrials.gov/> (accessed on 28<sup>th</sup> July 2015).
350. Cheng, H.; Hoffman, J.; Le, P.; Nair, S. K.; Cripps, S.; Matthews, J.; Smith, C.; Yang, M.; Kupchinsky, S.; Dress, K.; Edwards, M.; Cole, B.; Walters, E.; Loh, C.; Ermolieff, J.; Fanjul, A.; Bhat, G. B.; Herrera, J.; Pauly, T.; Hosea, N.; Paderes, G.; Rejto, P. *Bioorg. Med. Chem. Lett.* **2010**, *20*, 2897-2902.
351. Johansson, L.; Fotsch, C.; Bartberger, M. D.; Castro, V. M.; Chen, M.; Emery, M.; Gustafsson, S.; Hale, C.; Hickman, D.; Homan, E.; Jordan, S. R.; Komorowski, R.; Li, A.; McRae, K.; Moniz, G.; Matsumoto, G.; Orihuela, C.; Palm, G.; Veniant, M.; Wang, M.; Williams, M.; Zhang, J. *J. Med. Chem.* **2008**, *51*, 2933-2943.
352. Tice, C. M.; Zhao, W.; Xu, Z.; Cacatian, S. T.; Simpson, R. D.; Ye, Y. J.; Singh, S. B.; McKeever, B. M.; Lindblom, P.; Guo, J.; Krosky, P. M.; Kruk, B. A.; Berbaum, J.; Harrison, R. K.; Johnson, J. J.; Bukhtiyarov, Y.; Panemangalore, R.; Scott, B. B.; Zhao, Y.; Bruno, J. G.; Zhuang, L.; McGeehan, G. M.; He, W.; Claremon, D. A. *Bioorg. Med. Chem. Lett.* **2010**, *20*, 881-886.
353. Olson, S.; Aster, S. D.; Brown, K.; Carbin, L.; Graham, D. W.; Hermanowski-Vosatka, A.; LeGrand, C. B.; Mundt, S. S.; Robbins, M. A.; Schaeffer, J. M.; Slossberg, L. H.; Szymonifka, M. J.; Thieringer, R.; Wright, S. D.; Balkovec, J. M. *Bioorg. Med. Chem. Lett.* **2005**, *15*, 4359-4362.
354. Rohde, J. J.; Pliushchev, M. A.; Sorensen, B. K.; Wodka, D.; Shuai, Q.; Wang, J.; Fung, S.; Monzon, K. M.; Chiou, W. J.; Pan, L.; Deng, X.; Chovan, L. E.; Ramaiya, A.; Mullally, M.; Henry, R. F.; Stolarik, D. F.; Imade, H. M.; Marsh, K. C.; Beno, D. W. A.;

- Fey, T. A.; Droz, B. A.; Brune, M. E.; Camp, H. S.; Sham, H. L.; Frevert, E. U.; Jacobson, P. B.; Link, J. T. *J. Med. Chem.* **2007**, *50*, 149-164.
355. Richards, S.; Sorensen, B.; Jae, H.-S.; Winn, M.; Chen, Y.; Wang, J.; Fung, S.; Monzon, K.; Frevert, E. U.; Jacobson, P.; Sham, H.; Link, J. T. *Bioorg. Med. Chem. Lett.* **2006**, *16*, 6241-6245.
356. Venier, O.; Pascal, C.; Braun, A.; Namane, C.; Mougnot, P.; Crespin, O.; Pacquet, F.; Mougnot, C.; Monseau, C.; Onofri, B.; Dadji-Faïhun, R.; Leger, C.; Ben-Hassine, M.; Van-Pham, T.; Ragot, J. L.; Philippo, C.; Farjot, G.; Noah, L.; Maniani, K.; Boutarfa, A.; Nicolai, E.; Guillot, E.; Pruniaux, M. P.; Güssregen, S.; Engel, C.; Coutant, A. L.; de Miguel, B.; Castro, A. *Bioorg. Med. Chem. Lett.* **2013**, *23*, 2414-2421.
357. Webster, S. P.; Ward, P.; Binnie, M.; Craigie, E.; McConnell, K. M. M.; Sooy, K.; Vinter, A.; Seckl, J. R.; Walker, B. R. *Bioorg. Med. Chem. Lett.* **2007**, *17*, 2838-2843.
358. Okazaki, S.; Takahashi, T.; Iwamura, T.; Nakaki, J.; Sekiya, Y.; Yagi, M.; Kumagai, H.; Sato, M.; Sakami, S.; Nitta, A.; Kawai, K. *J. Pharmacol. Exp. Ther.* **2014**, *351*, 181-189.
359. Ryu, J. H.; Kim, S.; Lee, J. A.; Han, H. Y.; Son, H. J.; Lee, H. J.; Kim, Y. H.; Kim, J.-S.; Park, H. *Bioorg. Med. Chem. Lett.* **2015**, *15*, 1679-1683.
360. Kim, Y. H.; Kang, S. K.; Lee, G. Bin; Lee, K. M.; Kumar, J. A.; Kim, K. Y.; Rhee, S. D.; Joo, J.; Bae, M. A.; Lee, W. K.; Ahn, J. H. *Med. Chem. Commun.* **2015**, *6*, 1360-1369.
361. Waddell, S. T.; Balkovec, J. M.; Kevin, N. J.; Gu, X. Preparation of triazoles derivatives as inhibitors of 11 $\beta$ -hydroxysteroid dehydrogenase-1. WO 2007047625.
362. Wang, H.; Robl, J. A.; Hamann, L. G.; Simpkins, L. M.; Golla, R.; Li, X.; Seethala, R.; Zvyaga, T.; Gordon, D. A.; Robl, J. A.; Li, J. L. *Bioorg. Med. Chem. Lett.* **2011**, *21*, 4146-4149.
363. Bauman, D. R.; Whitehead, A.; Contino, L. C.; Cui, J.; Garcia-Calvo, M.; Gu, X.; Kevin, N.; Ma, X.; Pai, L.; Shah, K.; Shen, X.; Stribling, S.; Zokian, H. J.; Metzger, J.; Shevell, D. E.; Waddell, S. T. *Bioorg. Med. Chem. Lett.* **2013**, *23*, 3650-3653.
364. Leiva, R.; Seira, C.; McBride, A.; Binnie, M.; Luque, F. J.; Bidon-Chanal, A.; Webster, S. P.; Vázquez, S. *Bioorg. Med. Chem. Lett.* **2015**, *25*, 4250-4253.
365. Roughley, S. D.; Jordan, A. M. *J. Med. Chem.* **2011**, *54*, 3451-3479.
366. Pattabiraman, V. R.; Bode, J. W. *Nature* **2011**, *480*, 471-479.
367. Montalbetti, C. A. G. N.; Falque, V. *Tetrahedron* **2005**, *61*, 10827-10852.
368. Valeur, E.; Bradley, M. *Chem. Soc. Rev.* **2009**, *38*, 606-631.
369. Sheehan, J. C.; Hess, G. P. *J. Am. Chem. Soc.* **1955**, *77*, 1067-1068.
370. Chan, L. C.; Cox, B. G. *J. Org. Chem.* **2007**, *72*, 8863-8869.
371. Carpino, L. A. *J. Am. Chem. Soc.* **1993**, *115*, 4397-4398.
372. Albericio, F.; Bofill, J. M. El-Faham, A.; Kates, S. A. *J. Org. Chem.* **1998**, *63*, 9678-9683.
373. Carpino, L. A.; Imazumi, H.; El-Faham, A.; Ferrer, F. J.; Zhang, C.; Lee, Y.; Foxman, B. M.; Henklein, P.; Hanay, C.; Mügge, C.; Wenschuh, H.; Klose, J.; Beyermann, M.; Bienert, M. *Angew. Chem. Int. Ed.* **2002**, *41*, 441-445.
374. Li, B.; Bemish, R.; Buzon, R. A.; Chiu, C. K. F.; Colgan, S. T.; Kissel, W.; Le, T.; Leeman, K. R.; Newell, L.; Roth, J. *Tetrahedron Lett.* **2003**, *44*, 8113-8115.
375. Dragovich, P. S.; Prins, T. J.; Zhou, R.; Johnson, T. O.; Hua, Y.; Luu, H. T.; Sakata, S. K.; Brown, E. L.; Maldonado, F. C.; Tuntland, T.; Lee, C. A.; Fuhrman, S. A.; Zalman, L. S.; Patick, A. K.; Matthews, D. A.; Wu, E. Y.; Guo, M.; Borer, B. C.; Nayyar, N. K.; Moran, T.; Chen, L.; Rejto, P. A.; Rose, P. W.; Guzman, M. C.; Doval Santos, E. Z.; Lee, S.;

- McGee, K.; Mohajeri, M.; Liese, A.; Tao, J.; Kosa, M. B.; Liu, B.; Batugo, M. R.; Gleeson, J. P. R.; Wu, Z. P.; Liu, J.; Meador, J. W.; Ferre, R. A. *J. Med. Chem.* **2003**, *46*, 4572-4585.
376. Nikitenko, A.; Alimardanov, A.; Afragola, J.; Schmid, J.; Kristofova, L.; Evrard, D.; Hatzenbuehler, N. T.; Marathias, V.; Stack, G.; Lenicek, S.; Potski, J. *Org. Process Res. Dev.* **2009**, *13*, 91-97.
377. Sasaki, N. A.; Garcia-Álvarez, M. C.; Wang, Q.; Ermolenko, L.; Franck, G.; Nhiri, N.; Martin M. T.; Audic, N.; Potier, P. *Bioorg. Med. Chem.* **2009**, *17*, 2310-2320.
378. Jean, D. J. S.; Yuan, C.; Bercot, E. A.; Cupples, R.; Chen, M.; Fretland, J.; Hale, C.; Hungate, R. W.; Komorowski, R.; Veniant, M.; Wang, M.; Zhang, X.; Fotsch, C. *J. Med. Chem.* **2007**, *50*, 429-432.
379. Johansson, L.; Fotsch, C.; Bartberger, M. D.; Castro, V. M.; Chen, M.; Emery, M.; Gustafsson, S.; Hale, C.; Hickman, D.; Homan, E.; Jordan, S. R.; Komorowski, R.; Li, A.; McRae, K.; Moniz, G.; Matsumoto, G.; Orihuela, C.; Palm, G.; Veniant, M.; Wang, M.; Williams, M.; Zhang, J. *J. Med. Chem.* **2008**, *51*, 2933-2943.
380. Tice, C. M.; Zhao, W.; Xu, Z.; Cacatian, S. T.; Simpson, R. D.; Ye, Y.J.; Singh, S. B.; McKeever, B. M.; Lindblom, P.; Guo, J.; Krosky, P. M.; Kruk, B. A.; Berbaum, J.; Harrison, R. K.; Johnson, J. J.; Bukhtiyarov, Y.; Panemangalore, R.; Scott, B. B.; Zhao, Y.; Bruno, J. G.; Zhuang, L.; McGeehan, G. M.; He, W.; Claremon, D. A. *Bioorg. Med. Chem. Lett.* **2010**, *20*, 881-886.
381. Claremont, D. A.; Zhuang, L.; Ye, Y.; Singh, S. B.; Tice, C. M. Carbamate and urea inhibitors of 11beta-hydroxysteroid dehydrogenase 1. US 2011/0112062 A1.
382. Jimenez, H. N.; Ma, G.; Li, G.; Grenon, M.; Doller, D. Adamantyl amide derivatives and uses of same. WO 2011/087758 A1.
383. Mundt, S.; Solly, K.; Thieringer, R.; Hermanowski-Vosatka, A. *Assay Drug Dev. Technol.* **2005**, *3*, 367-375.
384. Solly, K.; Mundt, S. S.; Zokian, H. J.; Ding, G. J.; Hermanowski-vosatka, A.; Strulovici, B.; Zheng, W. *Assay Drug Dev. Technol.* **2005**, *3*, 377-384.
385. PerkinElmer website. Radiometric assays and detection, SPA bead Technology. [http://www.perkinelmer.com/Resources/TechnicalResources/ApplicationSupportKnowledgebase/radiometric/spa\\_bead.xhtml#top](http://www.perkinelmer.com/Resources/TechnicalResources/ApplicationSupportKnowledgebase/radiometric/spa_bead.xhtml#top) (accessed on 11<sup>th</sup> August 2015).
386. Friesner, R. A.; Murphy, R. B.; Repasky, M. P.; Frye, L. L.; Greenwood, J. R.; Halgren, T. A.; Sanschagrin, P. C.; Mainz, D. T. *J. Med. Chem.* **2006**, *49*, 6177-6196.
387. Curutchet, C.; Orozco, M.; Luque, F. J. *J. Comput. Chem.* **2001**, *22*, 1180-1193.
- 388.
- 389.
- 390.
- 391.
392. For further study on the pyrolysis of urea: Schaber, P. M.; Colson, J.; Higgins, S.; Thielen, D.; Anspach, B.; Brauer, J. *Thermochim. Acta* **2004**, *424*, 131-142.
393. Rey-Carrizo, M. Ph.D. Dissertation, University of Barcelona, 2014.
394. Gugelchuk, M.; Silva, L. F. Jr.; Vasconcelos, R. S.; Quintiliano, S. A. P. *e-EROS* **2007**, 1-8.
395. Data from computational studies is not shown.
396. Kodomari, M.; Suzuki, M.; Tanigawa, K.; Aoyama, T. *Tetrahedron Lett.* **2005**, *46*, 5841-5843.

397.

398. Harizi, H.; Corcuff, J. B.; Gualde, N. *Trends Mol. Med.* **2008**, *14*, 461-469.
399. Funk, C. D. *Science* **2001**, *294*, 1871-1875.
400. Zeldin, D. C. *J. Biol. Chem.* **2001**, *276*, 36059-36062.
401. Node, K.; Huo, Y.; Ruan, X.; Yang, B.; Spiecker, M.; Ley, K.; Zeldin, D. C.; Liao, J. K. *Science* **1999**, *285*, 1276-1279.
402. Morisseau, C.; Hammock, B. D. *Annu. Rev. Pharmacol. Toxicol.* **2013**, *53*, 37-58.
403. Fleming, I. *Circ. Res.* **2001**, *89*, 753-762.
404. El-Sherbeni, A. A.; El-Kadi, A. O. S. *Arch. Toxicol.* **2014**, *88*, 2013-2032.
405. Duflot, T.; Roche, C.; Lamoureux, F.; Guerrot, D.; Bellien, J. *Expert Opin. Drug Discov.* **2014**, *9*, 1-15.
406. Falck, J. R.; Manna, S.; Moltz, J.; Chacos, N.; Capdevila, J. *Biochem. Biophys. Res. Commun.* **1983**, *114*, 743-749.
407. Skepner, J. E.; Shelly, L. D.; Ji, C.; Reidich, B.; Luo, Y. *Prostaglandins Other Lipid Mediat.* **2011**, *94*, 3-8.
408. Imig, J. D.; Hammock, B. D. *Nat. Rev. Drug Discov.* **2009**, *8*, 794-805.
409. Pillarisetti, S. *Inflamm. Allergy - Drug Targets* **2012**, *11*, 143-158.
410. Harris, T. R.; Hammock, B. D. *Gene* **2013**, *526*, 61-74.
411. Morisseau, C.; Hammock, B. D. *Annu. Rev. Pharmacol. Toxicol.* **2005**, *45*, 311-333.
412. Imig, J. D. *Physiol. Rev.* **2012**, *92*, 101-130.
413. Node, K.; Huo, Y.; Ruan, X.; Yang, B.; Spiecker, M.; Ley, K.; Zeldin, D. C.; Liao, J. K. *Science* **1999**, *285*, 1276-1279.
414. Schmelzer, K. R.; Kubala, L.; Newman, J. W.; Kim, I.; Eiserich, J. P.; Hammock, B. D. *Proc. Natl. Acad. Sci. USA* **2005**, *102*, 9772-9777.
415. Deng, Y.; Edin, M. L.; Theken, K. N.; Schuck, R. N.; Flake, G. P.; Kannon, M. A.; DeGraff, L. M.; Lih, F. B.; Foley, J.; Bradbury, J. A.; Graves, J. P.; Tomer, K. B.; Falck, J. R.; Zeldin, D. C.; Lee, C. R. *FASEB J.* **2011**, *25*, 703-713.
416. Liu, Y.; Zhang, Y.; Schmelzer, K.; Lee, T. S.; Fang, X.; Zhu, Y.; Spector, A. A.; Gill, S.; Morisseau, C.; Hammock, B. D.; Shyy, J. Y. J. *Proc. Natl. Acad. Sci. USA* **2005**, *102*, 16747-16752.
417. Ollivier, V.; Parry, G. C. N.; Cobb, R. R.; de Prost, D.; Mackman, N. *J. Biol. Chem.* **1996**, *271*, 20828-20835.
418. Hammock, B. D.; Wagner, K.; Inceoglu, B. *Pain Manag.* **2011**, *1*, 383-386.
419. Wagner, K.; Inceoglu, B.; Dong, H.; Yang, J.; Hwang, S. H.; Jones, P.; Morisseau, C.; Hammock, B. D. *Eur. J. Pharmacol.* **2013**, *700*, 93-101.
420. Sing, K.; Lee, S.; Liu, J.; Wagner, K. M.; Pakhomova, S.; Dong, H.; Morisseau, C.; Fu, S. H.; Yang, J.; Wang, P.; Ulu, A.; Mate, C. A.; Nguyen, L. V.; Hwang, S. H.; Edin, M. L.; Mara, A. A.; Wul, H.; Newcomer, M. E.; Zeldin, D. C.; Hammock, B. D. *J. Med. Chem.* **2014**, *57*, 7016-7030.
421. Pillarisetti, S.; Khanna, I. *Drug Discov. Today* **2015**, *In press*. DOI: 10.1016/j.drudis.2015.07.017.
422. Bettaieb, A.; Nagata, N.; Aboubechara, D.; Chahed, S.; Morisseau, C.; Hammock, B. D.; Haj, F. G. *J. Biol. Chem.* **2013**, *288*, 14189-14199.
423. Inceoglu, B.; Bettaieb, A.; Trindade da Silva, C. A.; Lee, K. S. S.; Haj, F. G.; Hammock, B. D. *Proc. Natl. Acad. Sci. USA* **2015**, *112*, 9082-9087.

424. Schmelzer, K. R.; Inceoglu, B.; Kubala, L.; Kim, I.; Jinks, S. L.; Eiserich, J. P.; Hammock, B. D. *Proc. Natl. Acad. Sci. USA* **2006**, *103*, 13646-13651.
425. Fleming, I.; Rueben, A.; Popp, R.; Fisslthaler, B.; Schrod, S.; Sander, A.; Haendeler, J.; Falck, J. R.; Morisseau, C.; Hammock, B. D.; Busse, R. *Arterioscler. Thromb. Vasc. Biol.* **2007**, *27*, 2612-2618.
426. Imig, J. D. *Am. J. Physiol. Regul. Integr. Comp. Physiol.* **2004**, *287*, R3-5.
427. Loch, D.; Hoey, A.; Morisseau, C.; Hammock, B. O.; Brown, L. *Cell Biochem. Biophys.* **2007**, *47*, 87-98.
428. Ulu, A.; Davis, B. B.; Tsai, H.; Kim, I.; Morisseau, C.; Inceoglu, B.; Fiehn, O.; Hammock, B. D.; Weiss, R. H. *J. Cardiovasc. Pharmacol.* **2008**, *52*, 314-323.
429. Shen, L.; Peng, H.; Peng, R.; Fan, Q.; Zhao, S.; Xu, D.; Morisseau, C.; Chiamvimonvat, N.; Hammock, B. D. *Atherosclerosis* **2015**, *239*, 557-565.
430. Shrestha, A.; Krishnamurthy, P. T.; Thomas, P.; Hammock, B. D.; Hwang, S. H. *J. Pharm. Pharmacol.* **2014**, *66*, 1251-1258.
431. Xu, D.; Davis, B. B.; Wang, Z.; Zhao, S.; Wasti, B.; Liu, Z.; Li, N.; Morisseau, C.; Chiamvimonvat, N.; Hammock, B. D. *Int. J. Cardiol.* **2013**, *167*, 1298-1304.
432. Zhang, W.; Otsuka, T.; Sugo, N.; Ardeshiri, A.; Alhadid, Y. K.; Iliff, J. J.; DeBarber, A. E.; Koop, D. R.; Alkayed, N. J. *Stroke* **2008**, *39*, 2073-2078.
433. Xu, D.; Li, N.; He, Y.; Timofeyev, V.; Lu, L.; Tsai, H.; Kim, I.; Tuteja, D.; Mateo, R. K. P.; Singapuri, A.; Davis, B. B.; Low, R.; Hammock, B. D.; Chiamvimonvat, N. *Proc. Natl. Acad. Sci. USA* **2006**, *103*, 18733-18738.
434. Duflot, T.; Roche, C.; Lamoureux, F.; Guerrot, D.; Bellien, J. *Expert Opin. Drug Discov.* **2014**, *9*, 1-15.
435. Deng, Y.; Thenken, K. N.; Lee, C. R. *J. Mol. Cell. Cardiol.* **2010**, *48*, 331-353.
436. Luo, P.; Chang, H. H.; Zhou, Y.; Zhang, S.; Hwang, S. H.; Morisseau, C.; Wang, C.-Y.; Inscho, E. W.; Hammock, B. D.; Wang, M. H. *J. Pharmacol. Exp. Ther.* **2010**, *334*, 430-438.
437. Luria, A.; Bettaieb, A.; Xi, Y.; Shieh, G.-J.; Liu, H.-C.; Inoue, H.; Tsai, H.-J.; Imig, J. D.; Haj, F. G.; Hammock, B. D. *Proc. Natl. Acad. Sci. USA* **2011**, *108*, 9038-9043.
438. De Taeye, B. M.; Morisseau, C.; Coyle, J.; Covington, J. W.; Luria, A.; Yang, J.; Murphy, S. B.; Friedman, D. B.; Hammock, B. B.; Vaughan, D. E. *Obesity* **2010**, *18*, 489-498.
439. Iyer, A.; Kauter, K.; Alam, M. A.; Hwang, S. H.; Morisseau, C.; Hammock, B. D.; Brown, L. *Exp. Diabetes Res.* **2012**, *2012*, 14-16.
440. Wang, S.; Kaufman, R. J. *J. Cell Biol.* **2012**, *197*, 857-867.
441. Zhao, X.; Yamamoto, T.; Newman, J. W.; Kim, I. H.; Watanabe, T.; Hammock, B. D.; Stewart, J.; Pollock, J. S.; Pollock, D. M.; Imig, J. D. *J. Am. Soc. Nephrol.* **2004**, *15*, 1244-1253.
442. Olearczyk, J. J.; Quigley, J. E.; Mitchell, B. C.; Yamamoto, T.; Kim, I.-H.; Newman, J. W.; Luria, A.; Hammock, B. D.; Imig, J. D. *Clin. Sci.* **2009**, *116*, 61-70.
443. Wang, L.; Yang, J.; Guo, L.; Uyeminami, D.; Dong, H.; Hammock, B. D.; Pinkerton, K. E. *Am. J. Respir. Cell Mol. Biol.* **2012**, *46*, 614-622.
444. Podolin, P. L.; Bolognese, B. J.; Foley, J. F.; Long, E.; Peck, B.; Umbrecht, S.; Zhang, X.; Zhu, P.; Schwartz, B.; Xie, W.; Quinn, C.; Qi, H.; Sweitzer, S.; Chen, S.; Galop, M.; Ding, Y.; Belyanskaya, S. L.; Israel, D. I.; Morgan, B. A.; Behm, D. J.; Marino, J. P.; Kurali, E.; Barnette, M. S.; Mayer, R. J.; Booth-Genthe, C. L.; Callahan, J. F. *Prostaglandins Other Lipid Mediators* **2013**, *104-105*, 25-31.



445. Zhou, Y.; Sun, G. Y.; Liu, T.; Duan, J. X.; Zhou, H. F.; Lee, K. S.; Hammock, B. D.; Fang, X.; Jiang, J. X.; Guan, C. X. *Cell Tissue Res.* **2015**, *Ahead of print*. DOI: 10.1007/s00441-015-2262-0.
446. Wecksler, A. T.; Hwang, S. H.; Wettersten, H. I.; Gilda, J. E.; Patton, A.; Leon, L. J.; Carraway, K. L.; Gomes, A. V.; Baar, K.; Weiss, R. H.; Hammock, B. D. *Anticancer. Drugs* **2014**, *25*, 433-446.
447. Wecksler, A. T.; Hwang, S. H.; Liu, J. Y.; Wettersten, H. I.; Morisseau, C.; Wu, J.; Weiss, R. H.; Hammock, B. D. *Cancer Chemother. Pharmacol.* **2014**, *75*, 161-171.
448. Ma, M.; Ren, Q.; Fujita, Y.; Ishima, T.; Zhang, J. C.; Hashimoto, K. *Pharmacol. Biochem. Behav.* **2013**, *110*, 98-103.
449. Inceoglu, B.; Zolkowska, D.; Yoo, H. J.; Wagner, K. M.; Yang, J.; Hackett, E.; Hwang, S. H.; Lee, K. S. S.; Rogawski, M. A.; Morisseau, C.; Hammock, B. D. *PLoS One* **2013**, *8*, 8-17.
450. Harris, T. R.; Bettaieb, A.; Kodani, S.; Dong, H.; Myers, R.; Chiamvimonvat, N.; Haj, F. G.; Hammock, B. D. *Toxicol. Appl. Pharmacol.* **2015**, *286*, 102-111.
451. Newman, J. W.; Morisseau, C.; Hammock, B. D. *Prog. Lipid Res.* **2005**, *44*, 1-51.
452. Fretland, A. J.; Omiecinski, C. J. *Chem. Biol. Interact.* **2000**, *129*, 41-59.
453. Gomez, G. A.; Morisseau, C.; Hammock, B. D.; Christianson, D. W. *Biochemistry* **2004**, *43*, 4716-4723.
454. Morisseau, C.; Schebb, N. H.; Dong, H.; Ulu, A.; Aronov, P. A.; Hammock, B. D. *Biochem. Biophys. Res. Commun.* **2012**, *419*, 796-800.
455. Gorman, J.; Shapiro, L. *Acta Crystallogr. Sect. D* **2004**, *60*, 1600-1605.
456. Amano, Y.; Yamaguchi, T.; Tanabe, E. *Bioorg. Med. Chem.* **2014**, *22*, 2427-2434.
457. Gill, S. S.; Hammock, B. D. *Biochem. Pharmacol.* **1980**, *29*, 389-395.
458. Enayetallah, A. E.; French, R. A.; Thibodeau, M. S.; Grant, D. F. *J. Histochem. Cytochem.* **2004**, *52*, 447-454.
459. Fang, X.; Hu, S.; Watanabe, T.; Weintraub, N. L.; Snyder, G. D.; Yao, J.; Liu, Y.; Shyy, J. J. Y.; Hammock, B. D.; Spector, A. A. *J. Pharmacol. Exp. Ther.* **2005**, *314*, 260-270.
460. Wong, S. L.; Huang, Y. *Clin. Exp. Pharmacol. Physiol.* **2011**, *38*, 356-357.
461. Ai, D.; Fu, Y.; Guo, D.; Tanaka, H.; Wang, N.; Tang, C.; Hammock, B. D.; Shyy, J. J. Y.; Zhu, Y. *Proc. Natl. Acad. Sci. USA* **2007**, *104*, 9018-9023.
462. Zhang, D.; Xie, X.; Chen, Y.; Hammock, B. D.; Kong, W.; Zhu, Y. *Circ. Res.* **2012**, *110*, 808-817.
463. Shen, H. C. *Expert Opin. Ther. Pat.* **2010**, *20*, 941-956.
464. Shen, H. C.; Hammock, B. D. *J. Med. Chem.* **2012**, *55*, 1789-1808.
465. Morisseau, C.; Du, G.; Newman, J. W.; Hammock, B. D. *Arch. Biochem. Biophys.* **1998**, *356*, 214-228.
466. Dietze, E. C.; Kuwano, E.; Casas, J.; Hammock, B. D. *Biochem. Pharmacol.* **1991**, *42*, 1163-1175.
467. Draper, A. J.; Hammock, B. D. *Toxicol. Sci.* **1999**, *52*, 23-32.
468. Morisseau, C.; Goodrow, M. H.; Dowdy, D.; Zheng, J.; Greene, J. F.; Sanborn, J. R.; Hammock, B. D. *Proc. Natl. Acad. Sci. USA* **1999**, *96*, 8849-8854.
469. Nakagawa, Y.; Wheelock, C. E.; Morisseau, C.; Goodrow, M. H.; Hammock, G.; Hammock, B. D. *Bioorg. Med. Chem.* **2000**, *8*, 2663-2675.
470. McElroy, N. R.; Jurs, P. C.; Morisseau, C.; Hammock, B. D. *J. Med. Chem.* **2003**, *46*, 1066-1080.

471. Anandan, S. K.; Do, Z. N.; Webb, H. K.; Patel, D. V.; Gless, R. D. *Bioorg. Med. Chem. Lett.* **2009**, *19*, 1066-1070.
472. Gomez, G. A.; Morisseau, C.; Hammock, B. D.; Christianson, D. W. *Protein Sci.* **2006**, *15*, 58-64.
473. Kodani, S. D.; Hammock, B. D. *Drug Metab. Dispos.* **2015**, *43*, 788-802.
474. Yu, Z.; Xu, F.; Huse, L. M.; Morisseau, C.; Draper, A. J.; Newman, J. W.; Parker, C.; Graham, L.; Engler, M. M.; Hammock, B. D.; Zeldin, D. C.; Kroetz, D. L. *Circ. Res.* **2000**, *87*, 992-998.
475. Morisseau, C.; Goodrow, M. H.; Newman, J. W.; Wheelock, C. E.; Dowdy, D. L.; Hammock, B. D. *Biochem. Pharmacol.* **2002**, *63*, 1599-1608.
476. Chen, H.; Zhang, Y.; Ye, C.; Feng, T. T.; Han, J. G. *J. Biomol. Struct. Dyn.* **2014**, *32*, 1231-1247.
477. Anandan, S.-K.; Webb, H. K.; Do, Z. N.; Gless, R. D. *Bioorg. Med. Chem. Lett.* **2009**, *19*, 4259-4263.
478. Rose, T. E.; Morisseau, C.; Liu, J.-Y.; Inceoglu, B.; Jones, P. D.; Sanborn, J. R.; Hammock, B. D. *J. Med. Chem.* **2010**, *53*, 7067-7075.
479. Morisseau, C.; Goodrow, M. H.; Newman, J. W.; Wheelock, C. E.; Dowdy, D. L.; Hammock, B. D. *Biochem. Pharmacol.* **2002**, *63*, 1599-1608.
480. Dorrance, A. M.; Rupp, N.; Pollock, D. M.; Newman, J. W.; Hammock, B. D.; Imig, J. D. *J. Cardio. Pharm.* **2005**, *46*, 842-848.
481. Imig, J. D.; Zhao, Z.; Zaharis, C. Z.; Olearczyk, J. J.; Pollock, D. M.; Newman, J. W.; Kim, I. H.; Watanabe, T.; Hammock, B. D. *Hypertension* **2005**, *46*, 975-981.
482. Hammock, B. D.; Kim, I. H.; Morisseau, C.; Watanabe, T.; Newman, J. W. Inhibitors of the soluble epoxide hydrolase. US 2005/0164951 A1.
483. Hwang, S. H.; Tsai, H.; Liu, J.; Morisseau, C.; Hammock, B. D. *J. Med. Chem.* **2007**, *50*, 3825-3840.
484. Jones, P. D.; Tsai, H. J.; Do, Z. N.; Morisseau, C.; Hammock, B. D. *Bioorg. Med. Chem. Lett.* **2006**, *16*, 5212-5216.
485. Kim, I.; Morisseau, C.; Watanabe, T.; Hammock, B. D. *J. Med. Chem.* **2004**, *47*, 2110-2122.
486. Kim, I.; Tsai, H.; Nishi, K.; Kasagami, T.; Morisseau, C.; Hammock, B. D. *J. Med. Chem.* **2007**, *50*, 5217-5226.
487. Kim, I. H.; Heirtzler, F. R.; Morisseau, C.; Nishi, K.; Tsai, H. J.; Hammock, B. D. *J. Med. Chem.* **2005**, *48*, 3621-3629.
488. Kasagami, T.; Kim, I. H.; Tsai, H. J.; Nishi, K.; Hammock, B. D.; Morisseau, C. *Bioorg. Med. Chem. Lett.* **2009**, *19*, 1784-1789.
489. Clinical trials web site. AR9281. <https://www.clinicaltrials.gov/> (accessed on 5<sup>th</sup> September 2015).
490. Bhattachar, S. N.; Deschenes, L. A.; Wesley, J. A. *Drug Discov. Today* **2006**, *11*, 1012-1018.
491. Di, L.; Fish, P. V.; Mano, T. *Drug Discov. Today* **2012**, *17*, 486-495.
492. Leeson, P. D.; Springthorpe, B. *Nat. Rev. Drug Discov.* **2007**, *6*, 881-890.
493. Sun, H.; Tawa, G.; Wallqvist, A. *Drug Discov. Today* **2012**, *17*, 310-324.
- 494.
- 495.

- 496.
497. Brown, J. R.; North, E. J.; Hurdle, J. G.; Morisseau, C.; Scarborough, J. S.; Sun, D.; Korduláková, J.; Scherman, M. S.; Jones, V.; Grzegorzewicz, A.; Crew, R. M.; Jackson, M.; McNeil, M. R.; Lee, R. E. *Bioorg. Med. Chem.* **2011**, *19*, 5585-5595.
498. Scherman, M. S.; North, E. J.; Jones, V.; Hess, T. N.; Grzegorzewicz, A. E.; Kasagami, T.; Kim, I. H.; Merzlikin, O.; Lenaerts, A. J.; Lee, R. E.; Jackson, M.; Morisseau, C.; McNeil, M. R. *Bioorg. Med. Chem.* **2012**, *20*, 3255-3562.
- 499.
- 500.
- 501.
- 502.
- 503.
- 504.
- 505.
- 506.
507. Ivanoff, D.; Spassoff, A. *Bull. Soc. Chim. Fr.* **1935**, *2*, 76-78.
508. Rathke, M. W.; Lindert, A. *J. Am. Chem. Soc.* **1971**, *93*, 4605-4606.
509. Ito, Y.; Konoike, T.; Saegusa, T. *J. Am. Chem. Soc.* **1975**, *97*, 2912-2914.
510. Frazier, R. H. Jr.; Harlow, R. L. *J. Org. Chem.* **1980**, *45*, 5408-5411.
511. Kise, N.; Tokioka, K.; Aoyama, Y.; Matsumura, Y. *J. Org. Chem.* **1995**, *60*, 1100-1101.
512. Paquette, L. A.; Bzowej, E. I.; Branan, B. M.; Stanton, K. J. *J. Org. Chem.* **1995**, *60*, 7277-7283.
513. Baran, P. S.; DeMartino, M. P. *Angew. Chem. Int. Ed. Engl.* **2006**, *45*, 7083-7086.
514. DeMartino, M. P.; Chen, K.; Baran, P. S. *J. Am. Chem. Soc.* **2008**, *130*, 11546-11560.
- 515.
516. Renaud, P.; Fox, M. A. *J. Org. Chem.* **1988**, *53*, 3745-3752.
517. Barton, D. H. R.; Crich, D.; Motherwell, W. B. *J. Chem. Soc. Chem. Commun.* **1983**, 939-941.
518. Barton, D. H. R.; Hervé, Y.; Potier, P.; Thierry, J. *J. Chem. Soc. Chem. Commun.* **1984**, 1298-1299.
519. Barton, D. H. R.; Crich, D.; Motherwell, W. B. *Tetrahedron* **1985**, *41*, 3901-3924.
520. Barton, D. H. R.; Samadi, M. *Tetrahedron* **1992**, *48*, 7083-7090.
521. Ko, E. J.; Savage, G. P.; Williams, C. M.; Tsanaktsidis, J. *Org. Lett.* **2011**, *13*, 1944-1947.
522. Ho, J.; Zheng, J.; Meana-Pañeda, R.; Truhlar, D. G.; Ko, E. J.; Savage, G. P.; Williams, C. M.; Coote, M. L.; Tsanaktsidis, J. *J. Org. Chem.* **2013**, *78*, 6677-6687.
523. Ninomiya, K.; Shioiri, T.; Yamada, S. *Tetrahedron* **1974**, *30*, 2151-2157.

- 524.
525. North, E. J.; Scherman, M. S.; Bruhn, D. F.; Scarborough, J. S.; Maddox, M. M.; Jones, V.; Grzegorzewicz, A.; Yang, L.; Hess, T.; Morisseau, C.; Jackson, M.; McNeil, M. R.; Lee, R. E. *Bioorg. Med. Chem.* **2013**, *21*, 2587-2599.
526. Dietze, E. C.; Kuwano, E.; Hammock, B. D. *Anal. Biochem.* **1974**, *216*, 176-187.
527. Borhan, B.; Mebrahtu, T.; Nazarian, S.; Kurth, M. J.; Hammock, B. D. *Anal. Biochem.* **1995**, *231*, 188-200.
528. Morisseau, C.; Hammock, B. D. *Curr. Protoc. Toxicol.* **2007**, *Suppl. 33*, 4.23.1-4.23.18.
529. Jones, P. D.; Wolf, N. M.; Morisseau, C.; Whetstone, P.; Hock, B.; Hammock, B. D. *Anal. Biochem.* **2005**, *343*, 66-75.
530. Newman, J. W.; Watanabe, T.; Hammock, B. D. *J. Lipid Res.* **2002**, *43*, 1563-1578.
531. Cayman Chemical Company website. Soluble epoxide hydrolase inhibitor screening assay kit. <https://www.caymanchem.com/app/template/Product.vm/catalog/10011671> (accessed on 13<sup>th</sup> September 2015)
532. Zhang, J. H.; Chung, T. D. Y.; Oldenburg, K. R. *J. Biomol. Screen.* **1999**, *4*, 67-73.
533. Wolf, N. M.; Morisseau, C.; Jones, P. D.; Hock, B.; Hammock, B. D. *Anal. Biochem.* **2006**, *355*, 71-80.
534. Reuveni, S.; Urbakh, M.; Klafater, J. *Proc. Natl. Acad. Sci. USA* **2014**, *111*, 4391-4396.
- 535.
536. Sugano, K.; Okazaki, A.; Sugimoto, S.; Tavornvivas, S.; Omura, A.; Mano, T. *Drug Metab. Pharmacokinet.* **2007**, *22*, 225-254.
537. Bhattachar, S. N.; Deschenes, L. A.; Wesley, J. A. *Drug Discov. Today* **2006**, *11*, 1012-1018.
538. Di, L.; Fish, P. V.; Mano, T. *Drug Discov. Today* **2012**, *17*, 486-495.
539. Tsai, H. J.; Hwang, S. H.; Morisseau, C.; Yang, J.; Jones, P. D.; Kasagami, T.; Kim, I. H.; Hammock, B. D. *Eur. J. Pharm. Sci.* **2010**, *40*, 222-238.
540. Alsenz, J.; Kansy, M. *Adv. Drug Deliv. Rev.* **2007**, *59*, 546-567.
541. Morisseau, C.; Newman, J. W.; Tsai, H. J.; Baecker, P. A.; Hammock, B. D. *Bioorg. Med. Chem. Lett.* **2006**, *16*, 5439-5444.
542. Banerjee, S. *Environ. Sci. Technol.* **1980**, *14*, 1227-1229.
543. Meanwell, N. A. *Chem. Res. Toxicol.* **2011**, *24*, 1420-1456.
544. Abad-Zapatero, C.; Champness, E. J.; Segall, M. D. *Future Med. Chem.* **2014**, *6*, 577-593.
545. Hopkins, A. L.; Keserü, G. M.; Leeson, P. D.; Rees, D. C.; Reynolds, C. H. *Nat. Rev. Drug Discov.* **2014**, *13*, 105-121.
546. Kuntz, I. D.; Chen, K.; Sharp, K. A.; Kollman, P. A. *Proc. Natl. Acad. Sci. USA* **1999**, *96*, 9997-10002.
547. Hopkins, A. L.; Groom, C. R.; Alex, A. *Drug Discov. Today* **2004**, *9*, 430-431.
548. Freeman-Cook, K. D.; Hoffman, R. L.; Johnson, T. W. *Future Med. Chem.* **2013**, *5*, 113-115.
549. Hansch, C.; Björkroth, J. P.; Leo, A. *J. Pharm. Sci.* **1987**, *76*, 663-687.
550. Pdiya, K. J.; Gavade, S.; Kardile, B.; Tiwari, M.; Bajare, S.; Mane, M.; Gaware, V.; Varghese, S.; Harel, D.; Kurhade, S. *Org. Lett.* **2012**, *14*, 2814-2817.
551. Sciuto, A. M.; Hurt, H. H. *Inhal. Toxicol.* **2004**, *16*, 565-580.
552. Ichikawa, Y.; Matsukawa, Y.; Nishiyama, T.; Isobe, M. *Eur. J. Org. Chem.* **2004**, *2004*, 586-591.
553. Davis, M. C.; Dahl, J. E. P.; Carlson, R. M. K. *Synth. Commun.* **2008**, *38*, 1153-1158.

554. Rawling, T.; McDonagh, A. M.; Tattam, B.; Murray, M. *Tetrahedron* **2012**, *68*, 6065-6070.
555. Hwang, S. H.; Wecksler, A. T.; Zhang, G.; Morisseau, C.; Nguyen, L. V.; Fu, S. H.; Hammock, B. D. *Bioorg. Med. Chem. Lett.* **2013**, *23*, 3732-3737.
556. Schröder, M.; Kaufman, R. J. *Annu. Rev. Biochem.* **2005**, *74*, 739-789.
557. Ozcan, U.; Cao, Q.; Yilmaz, E.; Lee, A. H.; Iwakoshi, N. N.; Ozdelen, E.; Tuncman, G.; Görgün, C.; Glimcher, L. H.; Hotamisligil, G. S. *Science* **2004**, *306*, 457-461.
558. Sharma, N. K.; Das, S. K.; Mondal, A. K.; Hackney, O. G.; Chu, W. S.; Kern, P. A.; Rasouli, N.; Spencer, H. J.; Yao-Borengasser, A.; Elbein, S. C. *J. Clin. Endocrinol. Metab.* **2008**, *93*, 4532-4541.
559. Hummasti, S.; Hotamisligil, G. S. *Circ. Res.* **2010**, *107*, 579-591.
560. Hotamisligil, G. S. *Int. J. Obs.* **2008**, *32*, S52-S54.
561. Eizirik, D. L.; Cardozo, A. K.; Cnop, M. *Endocr. Rev.* **2008**, *29*, 42-61.
562. Wu, J.; Kaufman, R. J. *Cell Death Differ.* **2006**, *13*, 374-384.
563. Zinszner, H.; Kuroda, M.; Wang, X.; Batchvarova, N.; Lightfoot, R. T.; Remotti, H.; Stevens, J. L.; Ron, D. *Genes Dev.* **1998**, *12*, 982-995.
564. Nishitoh, H.; Matsuzawa, A.; Tobiume, K.; Saegusa, K.; Takeda, K.; Inoue, K.; Hori, S.; Kakizuka, A.; Ichijo, H. *Genes Dev.* **2002**, *16*, 1345-1355.
565. Pluquet, O.; Pourtier, A.; Abbadie, C. *Am. J. Physiol. Cell Physiol.* **2015**, *308*, C415-C425.
566. Ron, D.; Walter, P. *Nat. Rev. Mol. Cell Biol.* **2007**, *8*, 519-529.
567. Hotamisligil, G. S. *Cell* **2010**, *140*, 900-917.
568. Shi, Y.; Vattem, K. M.; Sood, R.; An, J.; Liang, J.; Stramm, L.; Wek, R. C. *Mol. Cell Biol.* **1998**, *18*, 7499-7509.
569. Novoa, I.; Zhang, Y.; Zeng, H.; Jungreis, R.; Harding, H. P.; Ron, D. *EMBO J.* **2003**, *22*, 1180-1187.
570. Harding, H. P.; Zhang, Y.; Zeng, H.; Novoa, P. D.; Lu, M.; Calfon, N.; Sadri, C.; Yun, B.; Popko, R.; Paules Stojdl, D. F.; Bell, J. C.; Hettmann, T.; Leiden, J. M.; Ron, D. *Mol. Cell* **2003**, *11*, 619-633.
571. Hiramatsu, N.; Messah, C.; Han, J.; LaVail, M. M.; Kaufman, R. J.; Lin, J. H. *Mol. Biol. Cell* **2014**, *25*, 1411-1420.
572. Sidrauski, C.; Walter, P. *Cell* **1997**, *90*, 1031-1039.
573. Yoshida, H.; Matsui, T.; Yamamoto, A.; Okada, T.; Mori, K. *Cell* **2001**, *107*, 881-891.
574. Calfon, M.; Zeng, H.; Urano, F.; Till, J. H.; Hubbard, S. R.; Harding, H. P.; Clark, S. G.; Ron, D. *Nature* **2002**, *415*, 92-96.
575. Ye, J.; Rawson, R. B.; Komuro, R.; Chen, X.; Davé, U. P.; Prywes, R.; Brown, M. S.; Goldstein, J. L. *Mol. Cell* **2000**, *6*, 1355-1364.
576. Okada, T.; Yoshida, H.; Akazawa, R.; Negishi, M.; Mori, K. *Biochem. J.* **2002**, *366*, 585-594.
577. Bertolotti, A.; Zhang, Y.; Hendershot, L. M.; Harding, H. P.; Ron, D. *Nat. Cell Biol.* **2000**, *2*, 326-332.
578. Sanderson, T.; Gallaway, M.; Kumar, R. *Int. J. Mol. Sci.* **2015**, *16*, 7133-7142.
579. Shen, J.; Chen, X.; Hendershot, L.; Prywes, R. *Dev. Cell* **2002**, *3*, 99-111.
580. Liu, C. Y.; Wong, H. N.; Schauerte, J. A.; Kaufman, R. J. *J. Biol. Chem.* **2002**, *277*, 18346-18356.
581. Kimata, Y.; Kimata, Y. I.; Shimizu, Y.; Abe, H.; Farcasanu, I. C.; Takeuchi, M.; Rose, M. D.; Kohno, K. *Mol. Biol. Cell* **2003**, *14*, 2559-2569.

582. Ma, Y.; Brewer, J. W.; Diehl, J. A.; Hendershot, L. M. *J. Mol. Biol.* **2002**, *318*, 1351-1365.
583. Rutkowski, D. T.; Arnold, S. M.; Miller, C. N.; Wu, J.; Li, J.; Gunnison, K. M.; Mori, K.; Sadighi Akha, A. A.; Raden, D.; Kaufman, R. J. *PLoS Biol.* **2006**, *4*, e374.
584. Koh, I.; Lim, J. H.; Joe, M. K.; Kim, W. H.; Jung, M. H.; Yoon, J. B.; Song, J. *FEBS J.* **2010**, *277*, 2304-2317.
585. Guo, W.; Wong, S.; Xie, W.; Lei, T.; Luo, Z. *Am. J. Physiol. Endocrinol. Metab.* **2007**, *293*, E576-E586.
586. Gwiazda, K. S.; Yang, T. L.; Lin, Y.; Johnson, J. D. *Am. J. Physiol. Endocrinol. Metab.* **2009**, *296*, E690-701.
587. Wei, Y.; Wang, D.; Gentile, C. L.; Pagliassotti, M. J. *Mol. Cell. Biochem.* **2009**, *331*, 31-40.
588. Srivastava, R. K.; Sollott, S. J.; Khan, L.; Hansford, R.; Lakatta, E. G.; Longo, D. L. *Mol. Cell Biol.* **1999**, *19*, 5659-5674.
589. Sidhu, A.; Miller, J. R.; Tripathi, A.; Garshott, D. M.; Brownell, A. L.; Chiego, D. J.; Arevang, C.-J.; Zeng, Q.; Jackson, L. C.; Bechler, S. A.; Callaghan, M. U.; Yoo, G. H.; Sethi, S.; Lin, H.-S.; Callaghan, J. H.; Tamayo-Castillo, G.; Sherman, D. H.; Kaufman, R. J.; Fribley, A. M. *ACS Med. Chem. Lett.* **2015**, ASAP. DOI: 10.1021/acsmchemlett.5b00133.
590. Salvadó, L.; Coll, T.; Gómez-Foix, A. M.; Salmerón, E.; Barroso, E.; Palomer, X.; Vázquez-Carrera, M. *Diabetologia* **2013**, *56*, 1372-1382.
591. Maruyama, H.; Takahashi, M.; Sekimoto, T.; Shimada, T.; Yokosuka, O. *Lipids Health Dis.* **2014**, *13*, 1-8.
592. Rahman, S. M.; Qadri, I.; Janssen, R. C.; Friedman, J. E. *J. Lipid Res.* **2009**, *50*, 2193-2202.
593. Xiao, C.; Giacca, A. Lewis, L. F. *Diabetes* **2011**, *60*, 918-924.
594. Ozcan, U.; Yilmaz, E.; Ozcan, L.; Furuhashi, M.; Vaillancourt, E.; Smith, R. O.; Görgün, C. Z.; Hotamisligil, G. S. *Science* **2006**, *313*, 1137-1140.
595. Bettaieb, A.; Nagata, N.; Aboubechara, D.; Chahed, S.; Morisseau, C.; Hammock, B. D.; Haj, F. G. *J. Biol. Chem.* **2013**, *288*, 14189-14199.
596. López-Vicario, C.; Alcaraz-Quiles, J.; García-Alonso, V.; Rius, B.; Hwang, S. H.; Titos, E.; Lopategi, A.; Hammock, B. D.; Arroyo, V.; Clària, J. *Proc. Natl. Acad. Sci. USA* **2015**, *112*, 536-541.
597. Inceoglu, B.; Bettaieb, A.; Trindade da Silva, C. A.; Lee, K. S. S.; Haj, F. G.; Hammock, B. D. *Proc. Natl. Acad. Sci. USA* **2015**, *112*, 9082-9087.
598. Salvadó, L.; Palomer, X.; Barroso, E.; Vázquez-Carrera, M. *Trends Endocrinol. Metab.* **2015**, *26*, 438-448.
599. Huh-7 cell line website. <http://huh7.com/> (accessed on 18<sup>th</sup> September 2015).
- 600.

601.

602.